

**Herbivorous large mammals from the late Middle Miocene
Gratkorn locality (Styria, Austria)**

**Taxonomy and Isotopic Tracking of Palaeoecology
($\delta^{18}\text{O}_{\text{CO}_3}$, $\delta^{13}\text{C}$, $^{87}\text{Sr}/^{86}\text{Sr}$)**

Dissertation

der Mathematisch-Naturwissenschaftlichen Fakultät
der Eberhard Karls Universität Tübingen
zur Erlangung des Grades eines
Doktors der Naturwissenschaften
(Dr. rer. nat.)

vorgelegt von
Manuela Aiglstorfer
aus Nördlingen

Tübingen
2014

Tag der mündlichen Qualifikation:

28.05.2014

Dekan:

Prof. Dr. Wolfgang Rosenstiel

1. Berichterstatter:

Prof. Dr. Madelaine Böhme

2. Berichterstatter:

Prof. Dr. Hervé Bocherens

Table of Contents

Abstract

Zusammenfassung

1. Introduction
 - 1.1. Miocene sedimentary succession of the Central Paratethys realm
 - 1.2. Miocene mammal record of Central Europe
 - 1.3. Research history, geographical and geological setting and stratigraphy of the Gratkorn locality
 - 1.4. Lithology of the vertebrate bearing palaeosol and frame conditions during soil formation
2. Methods and abbreviations
3. Taxonomic assignation of herbivorous large mammals
 - 3.1. Proboscidea - *Deinotherium levius* vel *giganteum*
 - 3.2. Perissodactyla
 - 3.3. Artiodactyla - Ruminantia
4. Taphonomical considerations with focus on large mammal taphonomy
5. Ecology, provenance and migration
 - 5.1. Ecology of large mammals
 - 5.2. Provenance and migration of large mammals
6. Summary
7. Acknowledgements
8. References
9. Appendix:
 - 9.1. Aiglstorfer M, Göhlich UB, Böhme M, Gross M. (2014): A partial skeleton of *Deinotherium* (Proboscidea, Mammalia) from the late Middle Miocene Gratkorn locality (Austria). *Palaeobiodiversity and Palaeoenvironments* 94, 49-70. [Publication #1]
 - 9.2. Aiglstorfer M, Heissig K, Böhme M. (2014): Perissodactyla from the late Middle Miocene Gratkorn locality (Austria). *Palaeobiodiversity and Palaeoenvironments* 94, 71-82 [Publication #2]
 - 9.3. Aiglstorfer M, Rössner GE, Böhme M. (2014): *Dorcatherium navi* and pecoran ruminants from the late Middle Miocene Gratkorn locality (Austria). *Palaeobiodiversity and Palaeoenvironments* 94, 83-123. [Publication #3]
 - 9.4. Havlik P, Aiglstorfer M, Beckman A, Gross M, Böhme M. (2014): Taphonomical and ichnological considerations on the late Middle Miocene Gratkorn locality (Styria, Austria) with focus on large mammal taphonomy. *Palaeobiodiversity and Palaeoenvironments* 94, 171-188. [Publication #4]
 - 9.5. Aiglstorfer M, Bocherens H, Böhme M. (2014): Large Mammal Ecology in the late Middle Miocene locality Gratkorn (Austria). *Palaeobiodiversity and Palaeoenvironments* 94, 189-213. [Publication #5]

Abstract

During transition from Middle to Late Miocene strong geographic, climatic, and biotic changes had a strong impact on aquatic and terrestrial ecosystems in Central Europe. Large-scale erosion in the Central Paratethys realm caused a lack of terrestrial sediments from this time period and thus resulted in a remarkable palaeobiological “blackout” for the record on land in this region from late Sarmatian to early Pannonian.

The here presented Gratkorn locality, well dated to an age of 12.2/12.0 Ma (early late Sarmatian) provides a rich vertebrate assemblage (species diversity as well as total number of specimens) with 65 recorded species up to date. It represents a unique window to the terrestrial record of this time period and helps to understand the evolution of vertebrate faunas during the Middle-Late Miocene transition. Remains of herbivorous large mammals were morphologically described and assigned to the following taxa (Suidae not part of this thesis): *Deinotherium levius* vel *giganteum*, *Aceratherium* sp., *Brachypotherium brachypus*, *Lartetotherium sansaniense*, *Chalicotherium goldfussi*, *Anchitherium* sp., *Listriodon splendens*, *Parachleuastochoerus steinheimensis*, *Dorcatherium nauti*, *Micromeryx flourensianus*, *?Hispanomeryx* sp., *Euprox furcatus*, Palaeomerycidae gen. et sp. indet., and *Tethytragus* sp..

Except of *Dorcatherium nauti*, presence and evolutionary stage of the large mammals are well in accordance with a late Middle Miocene assemblage. The records of *Euprox furcatus* and *Micromeryx flourensianus* comprise the first for the Styrian Basin and *Hispanomeryx* has not been recorded for Central Europe so far besides the locality Steinheim a. A.. *Dorcatherium nauti* is considered a typical faunal element of the Late Miocene and has been described only recently from Middle Miocene localities. With the rich material from Gratkorn assignation of this species to a more selenodont phylogenetic lineage together with *Dorcatherium guntianum* and well distinct from *Dorcatherium crassum* can be verified and the descent of the species from the latter thus shown to be unlikely.

The fossil assemblage from Gratkorn is considered an autochthonous taphocoenosis without any significant time averaging or faunal mixing. Most likely the accumulation did not last longer than a few years or decades and local accumulation of large mammal bones was the result of scavenging.

Based on the taxonomic record, morphology of skeletal and dental elements, and especially isotope analyses ($\delta^{18}\text{O}_{\text{CO}_3}$, $\delta^{13}\text{C}$, $^{87}\text{Sr}/^{86}\text{Sr}$), dominance of C3 vegetation, semi-arid and subtropical climate with distinct seasonality, and too little precipitation for closed canopy woodlands can be reconstructed for the wider area around the locality. The landscape provided diversity in plant resources to allow occupation of different niches by herbivorous large mammals: subcanopy browsing, rooting, top canopy browsing, facultative frugivory, and mixed feeding. Comparison with data from other Miocene localities from different areas and time slices showed rather stable niche partitioning for the herbivorous large mammal species. Thus these seem to be affected only to a minor degree by climatic conditions but rather represent a typical partitioning for a Middle Miocene ecosystem.

Zusammenfassung

Starke geographische, klimatologische und biotische Veränderungen während des Übergangs vom Mittleren zum Späten Miozän hatten einschneidende Auswirkungen auf aquatische als auch terrestrische Ökosysteme Zentraleuropas. Durch stark erosive Ereignisse wurden terrestrische Ablagerungen aus diesem Zeitbereich in der zentralen Paratethys abgetragen und führten dort zu einem paläobiologischen "Blackout" im festländischen Raum für spätes Sarmatium bis frühes Pannonium.

Von der hier vorgestellten Lokalität Gratkorn, gut datiert auf 12.2/12.0 Ma (frühes Spätsarmatium), ist eine reiche Wirbeltierfauna (Arten- und Individuenreichtum) mit bisher 65 dokumentierten Arten überliefert. Die Fundstelle stellt ein einzigartiges Fenster in die terrestrischen Ablagerungen dieses Zeitabschnittes dar und ist essentiell für das Verständnis der Faunenentwicklung während des Übergangs vom Mittleren zum Späten Miozän. Reste von herbivoren Großsäugern wurden morphologisch beschrieben und folgenden Taxa zugeordnet (Suidae nicht Teil dieser Arbeit): *Deinotherium levius* vel *giganteum*, *Aceratherium* sp., *Brachypotherium brachypus*, *Lartetotherium sansaniense*, *Chalicotherium goldfussi*, *Anchitherium* sp., *Listriodon splendens*, *Parachleuastochoerus steinheimensis*, *Dorcatherium naui*, *Micromeryx flourensianus*, ?*Hispanomeryx* sp., *Euprox furcatus*, Palaeomerycidae gen. et sp. indet. und *Tethytragus* sp..

Bis auf *Dorcatherium naui* passen alle Großsäuger-Taxa und die jeweilige evolutive Stufe gut in eine spätmittelmiozäne Vergesellschaftung. *Euprox furcatus* und *Micromeryx flourensianus* werden zum ersten Mal aus dem Steirischen Becken beschrieben und für *Hispanomeryx* ist es nach der Fundstelle Steinheim a. A. erst der zweite Nachweis aus Zentraleuropa. *Dorcatherium naui* ist typisch für obermiozäne Faunenvergesellschaftungen und wurde erst vor kurzem aus mittelmiozänen Fundstellen beschrieben. Mit dem reichen Material von Gratkorn konnte die Zuordnung dieser Art zusammen mit *Dorcatherium guntianum* zu einer selenodonteren, deutlich von *Dorcatherium crassum* getrennten phylogenetischen Linie verifiziert werden. Eine Abstammung der Art *Dorcatherium naui* von *Dorcatherium crassum* kann daher nun als unwahrscheinlich eingestuft werden.

Die Fossilvergesellschaftung wird als schnell abgelagerte, autochthone Taphocoenose interpretiert, die vermutlich in nur wenigen Jahren bis Jahrzehnten akkumuliert wurde. Die lokale Anreicherung geht wahrscheinlich zu einem großen Teil auf Aasfresser zurück. Anhand der Faunenvergesellschaftung, morphologischen Untersuchungen und vor allem Isotopenanalysen ($\delta^{18}\text{O}_{\text{CO}_3}$, $\delta^{13}\text{C}$, $^{87}\text{Sr}/^{86}\text{Sr}$) kann für die Gegend um die Fundstelle eine von C3 Pflanzen dominierte Vegetation in einem semi-ariden, subtropischen Klima mit ausgeprägter Saisonalität und zu geringer Niederschlagsmenge für eine geschlossene Waldfläche rekonstruiert werden. Der Lebensraum bot verschiedene ökologische Nischen für herbivore Großsäuger: „subcanopy browsing“, Rhizophagie, „top canopy browsing“, fakultative Frugivorie und „mixed feeding“. Der Vergleich mit Daten von Miozänen Fundstellen anderer Ablagerungsräume und Zeitabschnitte zeigt eine gewisse Konstanz in der Einnischung der Großsäuger. Die in Gratkorn beobachtete jeweilige ökologische Nische scheint daher für ein mittelmiozänes Ökosystem typisch zu sein und weniger stark von klimatischen Rahmenbedingungen abzuhängen.

1. Introduction

For the understanding of climatologic and geodynamic changes and their impact on ecosystems through time and space, a comprehensive data set, including data from marine as well as terrestrial deposits, is indispensable. The Miocene (23.03–5.33 Ma; Cohen et al. 2013) has proven an essential time slice for the decoding of our continent's cenozoic history. Many geodynamic changes (e.g. the uplift of the Alpine mountain chain) took place during this epoch, which strongly influenced and finally led to the modern shape of our continents and landscapes. Furthermore, it is marked as a time of strong climatic turnovers and characterized by the diversification of many mammal groups, as for example Ruminantia, Rhinocerotidae, and Primates (e.g. Rössner 1995; Heissig 1999; Bibi and Güleç 2008; Casanovas-Vilar et al. 2011).

While there is more and often far better information available for aquatic sedimentary sections, investigations on terrestrial deposits lack the necessary frame data in many cases, as for example well-founded stratigraphic dating and especially estimation of the stratigraphic coverage. Furthermore, the more patchy occurrence of localities and the regular lack of any information for certain time slices very often enhance the incorporation of terrestrial data in the "big picture".

The here presented Gratkorn locality can be assigned to such a time slice poor in data so far. It provides besides a rich vertebrate fauna also the necessary frame data to integrate the locality in the stratigraphic, palaeoenvironmental, and palaeoclimatological context of the Central European Miocene sedimentary succession.

1.1. Miocene sedimentary succession of the Central Paratethys realm

During Miocene, Central Europe was influenced by the North Sea in the north, the Mediterranean Sea in the south and to a great extent by the Paratethys Sea (Early to Middle Miocene)/Lake Pannon (Late Miocene to Pliocene) in between (Rasser et al. 2008). The Paratethys realm can be subdivided in Western (Rhône Basin, Alpine Foreland Basins from Switzerland to Austria), Central (Vienna Basin to Carpathian Foreland) and Eastern Paratethys (Fig.1; Steininger and Wessely 2000; Rasser et al. 2008). Its sedimentary succession was controlled by tectonics, sea level fluctuations, and climatic changes, leading to permanently changing and complex seaways and land bridges between the above mentioned marine systems as well as the western Indo-Pacific and causing an alternating sequence of marine and terrestrial deposits (Steininger and Wessely 2000; Harzhauser et al. 2007; ter Borgh et al. 2013). This led to a strong biogeographic differentiation and consequently resulted in the establishment of different chronostratigraphic and lithostratigraphic concepts (Steininger and Wessely 2000; Rasser et al. 2008). The regional stage concept of the Central Paratethys realm (Fig. 2; housing the late Middle Miocene locality Gratkorn), is well established by the combination of litho-, bio-, cyclo-, and magneto-stratigraphy as well as astrochronology and the correlation with eustatic sea level fluctuations (Rögl 1998; Gross et al. 2007a; Gross et al. 2007b; Schreilechner and Sachsenhofer 2007; Gross 2008; Harzhauser et al. 2008; Lirer et al. 2009; Vasiliev et al. 2010; Flügel et al. 2011; Gross et al. 2011; ter Borgh et al. 2013; Gross et al. 2014).

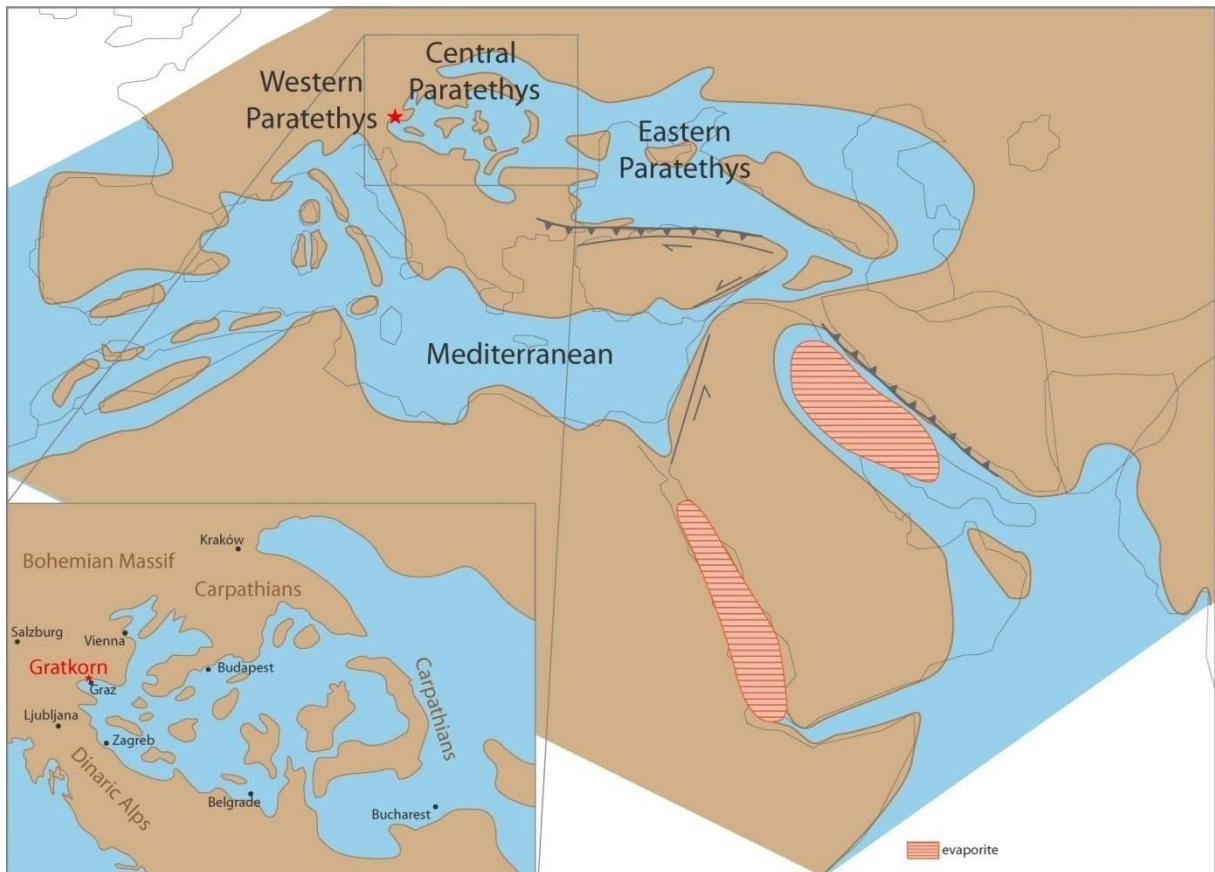


Fig. 1: Palaeogeographic situation in Central Europe at the time of the early Sarmatian with focus on Central Paratethys realm (modified after Rögl 1998; Lukeneder et al. 2011).

1.2. Miocene mammal record of Central Europe

In the earlier Middle Miocene many localities can be found rich in vertebrates and reasonably well dated with methods independent of biochronology and thus enabling a comparison of faunal assemblages and the reconstruction of climatic frame conditions (Abdul Aziz et al. 2008; Gross and Martin 2008; Kälin and Kempf 2009; Abdul Aziz et al. 2010; Sachsenhofer et al. 2010; Reichenbacher et al. 2013). During late Middle and early Late Miocene substantial turnovers strongly affected aquatic as well as terrestrial life in Central Europe [see e.g. decline in species diversity in Tragulidae and Cervidae in Central Europe on Fig. 2 (only localities with well determined material and reliable dating are taken into consideration; influences of sampling biases, as e.g. faunal mixing cannot be completely ruled out but are considered in evaluation of data), or the Sarmatian-Pannonian-extinction-event (Harzhauser and Piller 2007)]. After the warm and humid Miocene climatic optimum (Böhme 2003), the Middle Miocene climatic cooling (14–12 Ma; Shevenell et al. 2004; Anthonissen 2012) and geodynamic changes led to a decrease in the mean annual temperature (MAT), an increase in seasonality as well as generally more pronounced aridity during the late Middle Miocene and early Late Miocene in Central Europe (Böhme et al. 2008; Böhme et al. 2011b). The successive enlargement of the East Antarctica ice shield during the Serravallian can be well observed in the marine record (Zachos et al. 2001; Abels et al. 2005). A cooling of more than 7 °C in MAT is indicated

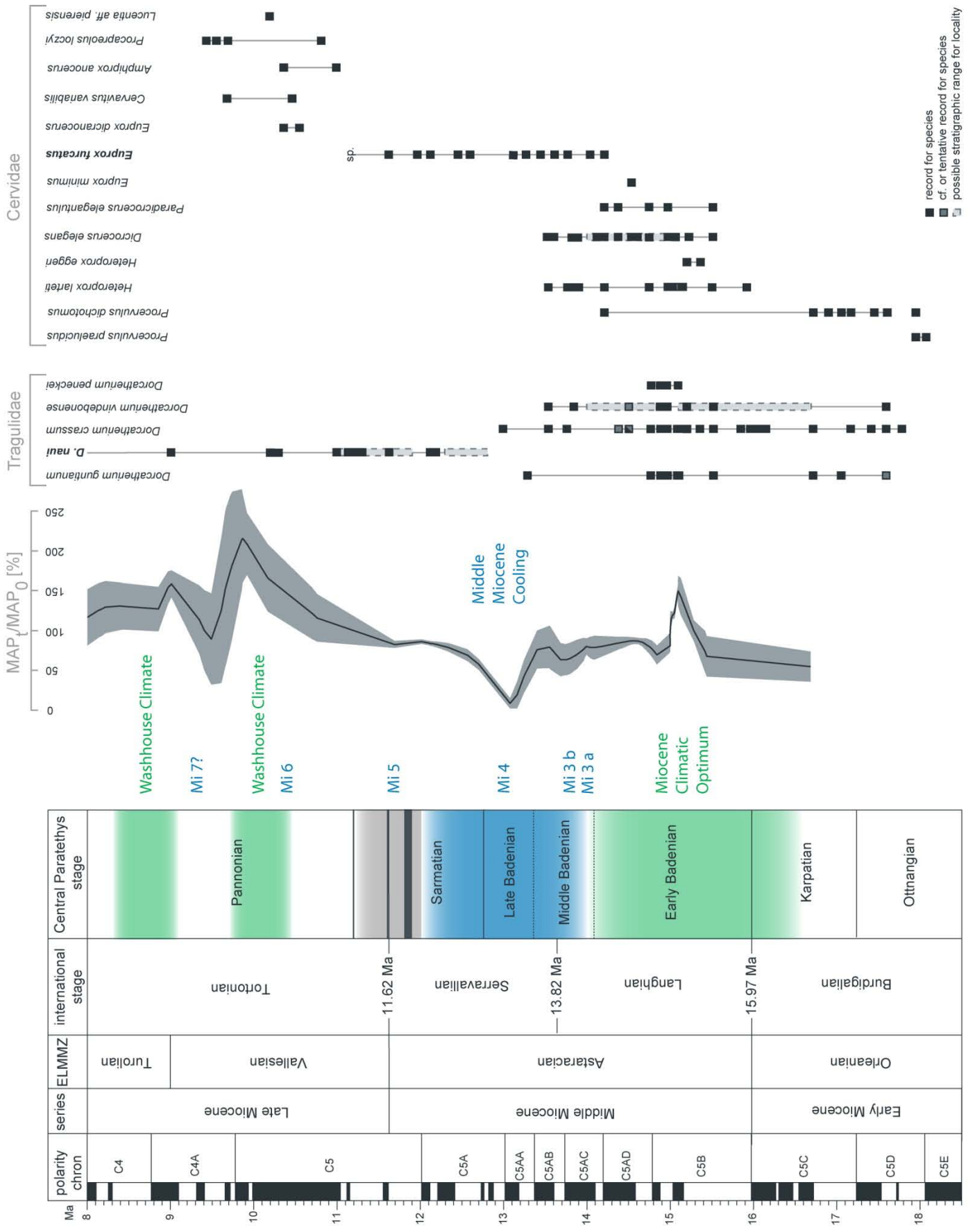
for the terrestrial record of Central Europe by the disappearance of reptiles adapted to warmer temperatures, like e.g. crocodiles and giant tortoises (Böhme 2003), but also short phase intensifications of the hydrologic cycle (more humid and warm; “washhouse-climate phases” *sensu* Böhme et al. 2008) are recorded (Böhme 2003; Böhme et al. 2008).

The isolation of the Pannonian basin at 11.6 Ma triggered maybe by an eustatic sea level drop was sustained by the uplift of the Carpathian Mountains (ter Borgh et al. 2013) and led to large-scale erosion of Upper Sarmatian/Lower Pannonian deposits in the Central Paratethys (Schreilechner and Sachsenhofer 2007; Kováč et al. 2008; Fig. 2). Consequently, terrestrial sediments of this time period are only rarely preserved in the Styrian Basin, which led to a remarkable palaeobiological “blackout” at about the Late Sarmatian to Early Pannonian (~12.5–11.5 Ma; Gross et al. 2011).

For the North Alpine Foreland Basin (NAFB) late Middle Miocene localities delivering a noteworthy large mammal assemblage are rare as well and often comprise only fluvial accumulations providing mainly big sized large mammal remains, such as proboscideans (Eronen and Rössner 2007). This can either be explained by the deficiency of fieldwork (which is rather unlikely considering the strong record of scientific publications dealing with the Neogene sedimentary succession of the NAFB), strong tectonic/orogenic changes (Frisch et al. 1998; Kuhlemann 2007; Ziegler and Dèzes 2007), or climatic changes like the aforementioned global cooling and the formation of open landscapes in temperate zones (Böhme et al. 2008). However, biostratigraphic and lithostratigraphic investigations indicate a continuous sedimentation from 14 to 11 Ma for Western Bavaria in contrast to the deposits from Styria (M. Böhme pers. comm. March 21st 2014).

Other terrestrial records for the terminal Middle Miocene in Central and Western Europe either comprise fissure fillings [e.g. Przeworno (Poland; Glazek et al. 1971) and La Grive (France; Mein and Ginsburg 2002)], for which estimations on stratigraphic age/range and accumulation processes are often limited, or present accumulations most likely biased by a considerable degree of redeposition (overrepresentation of mammals with large body sizes, such as proboscideans and rhinocerotids; see e.g. data from Fortelius (2014)). Recently, the existence of a short time faunal turnover in Spain at about 9.75 Ma (Early/Late Vallesian; “Mid Vallesian Crisis”) has been questioned (at least for small mammals; Casanovas-Vilar et al. 2014). They consider a scenario with a series of extinctions over a longer time span more realistic for the early Late Miocene in this region.

In any case, late Middle Miocene/early Late Miocene localities providing a rich sympatric vertebrate fauna are still rare and thus the detailed chronologic context and response of large mammal communities in Europe to the climatic change during the Middle Miocene Cooling and the late Middle Miocene climax in aridity followed by the “washhouse” phases during the Tortonian (Böhme et al. 2008) remain open questions so far. An interesting point concerning this topic is also the evolution of hominoids. While the first record of hominoids in Europe dates back to about 17 Ma (Böhme et al. 2011a), the quite rich record of late Middle to early Late Miocene hominoid findings points to a diverse and geographically wide spread fauna in Europe (e.g. Abocador de Can Mata (Valles Penedes; Spain), St. Gaudens and La Grive (France), and St. Stephan (Austria); Casanovas-Vilar et al. 2011).



◀ Fig. 2: Stratigraphic chart (including international and regional stratigraphy as well as European Land Mammal Zones (ELMMZ)) with recorded species diversity of Tragulidae and Cervidae (focus on Central Europe) correlated to the mean annual precipitation (MAP) of the Paratethys area (Central and Eastern Europe) and to major climatic events (green = more humid and warm; blue = cooling; Mi 3a–7? = deep sea Miocene isotope events referred to glaciation) and geodynamic events recorded in the Central Paratethys realm (dark grey lines = erosional surfaces and light grey = general increase of erosion) [stratigraphic stages after Gross et al. (2014); absolute ages follow Cohen et al. (2013); climatic events after Böhme (2003), Abels et al. (2005), Böhme et al. (2008), Mourik et al. (2011); erosional surfaces after Schreilechner and Sachsenhofer (2007) and Kováč et al. (2008); MAP (means and $\pm 1\sigma$ confidence intervals (grey shaded area) of the MAP in relation to the modern local value: MAP_t/MAP_0 ($\times 100\%$); age uncertainties not included) modified (following M. Böhme pers. comm. March 17th 2014) after Böhme et al. (2011b); tragulid record after Aiglstorfer et al. (2014d) and cervid record modified after Böhme et al. (2012)].

The here presented terrestrial vertebrate locality Gratkorn closes one of these big gaps in the record of terrestrial environments in Central Europe and provides besides a rich fauna also the necessary frame data. It is stratigraphically well defined and due to lithological and taphonomical analysis can be termed a sympatric large mammal assemblage (Gross et al. 2011; Gross et al. 2014; Havlik et al. 2014). Its faunal content shows strong affinities to other localities of this time slice, like the fissure fillings from La Grive and especially the alluvial deposits of Abocador de Can Mata (Spain), famous for their high diversity in hominoids.

1.3. Research history, geographical and geological setting and stratigraphy of the Gratkorn locality

The term “Gratkorn locality” stands for a late Middle Miocene (Sarmatian *sensu stricto*; 12.2/12.0 Ma) fossil site rich in terrestrial vertebrates (Gross et al. 2011). It is located in the clay pit St. Stefan (15°20'56"E/47°08'14"N) 700 m E of the town Gratkorn (about 10 km NNW of Graz; Fig. 1; Gross et al. 2014). Besides lacustrine sediments yielding mostly plant and invertebrate remains (Meller and Gross 2006; Gross et al. 2007a; Gross et al. 2007b; Klaus and Gross 2007; Gross 2008; Klaus and Gross 2010) the site comprises a fossiliferous layer housing nearly all vertebrate findings from this locality (Gross et al. 2011; Gross et al. 2014). While the first fossil findings from the area around St. Stefan were described more than 160 years ago (Unger 1850, 1852; Gross 1999), the vertebrate comprising palaeosol was detected not until 2005, when the first bones were discovered during geological mapping of the region. So far this has led to 18 scientific publications (Gross et al. 2007b; Harzhauser et al. 2008; Daxner-Höck 2010; Prieto et al. 2010a; Prieto et al. 2010b; Gross et al. 2011; Aiglstorfer et al. 2014a; Aiglstorfer et al. 2014b; Aiglstorfer et al. 2014c; Aiglstorfer et al. 2014d; Angelone et al. 2014; Böhme and Vasilyan 2014; Göhlich and Gross 2014; Gross et al. 2014; Havlik et al. 2014; Prieto et al. 2014a; Prieto et al. 2014b; Made et al. in press; not listed: contributions to scientific congresses).

To avoid confusion, especially with the locality “St. Stefan im Lavanttal” (Carinthia, Austria), famous for its *Dryopithecus*-findings (Mottl 1957), and as “St. Stefan”/“St. Stephan” is quite a common name in Austria, it was decided to name the locality “Gratkorn” instead of “St. Stefan” (Gross et al. 2014).

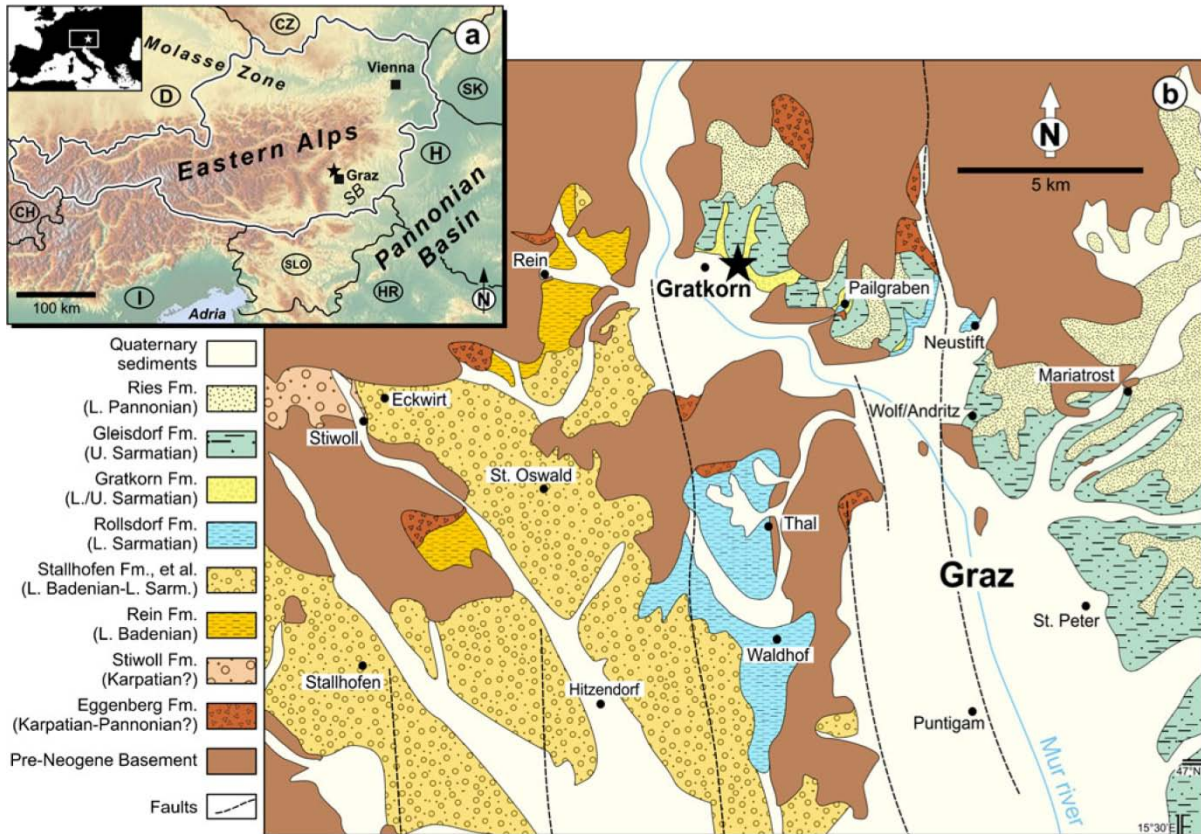


Fig. 3: Geographical and Geological setting of the Gratkorn locality (from Gross et al. 2014).

The locality is situated in the Gratkorn Basin, a satellite basin at the northern margin of the Styrian Basin (Fig. 3). To the North this basin is bordered by Palaeozoic basement (Flügel and Hubmann 2000; Flügel et al. 2011) and to the South most of the Sarmatian strata are covered by Pannonian and younger sediments (Fig. 3). The Styrian Basin as part of the Pannonian Basin System is a N-S striking extensional structure formed in connection with the extrusion of the Eastern Alps (Sachsenhofer 2000; Steininger and Wessely 2000; Gross et al. 2007a). The sedimentary filling of the Basin was initiated in the Early Miocene (syn-rift phase; Gross et al. 2007a). The oldest Neogene sediments can be roughly assigned to the Otnangian, the youngest Miocene sediments are dated as Late Pannonian (Gross et al. 2007a).

The most basal sediments in the eastern Gratkorn basin are interpreted as braided river system with influences of alluvial fans (polymict gravels/conglomerates in alternating sequence with more sand dominated deposits; Gross et al. 2014; Fig. 4). They are assigned to the Gratkorn Formation (Fm) and house the here discussed vertebrate yielding palaeosol (on top of the so called Gratkorn Gravel) (Flügel et al. 2011; Gross et al. 2014). On top of the Gratkorn Fm the up to 25 m thick limnic pelites of the Peterstal Member (Mb; Gleisdorf Formation) comprise the clay, which is mined in Gratkorn. Up section follow the upper part of the Gleisdorf Formation (Lustbühel Mb; alternating sequences of gravel, sand, and pelite) and the fluvial Ries Formation (Gross et al. 2014).

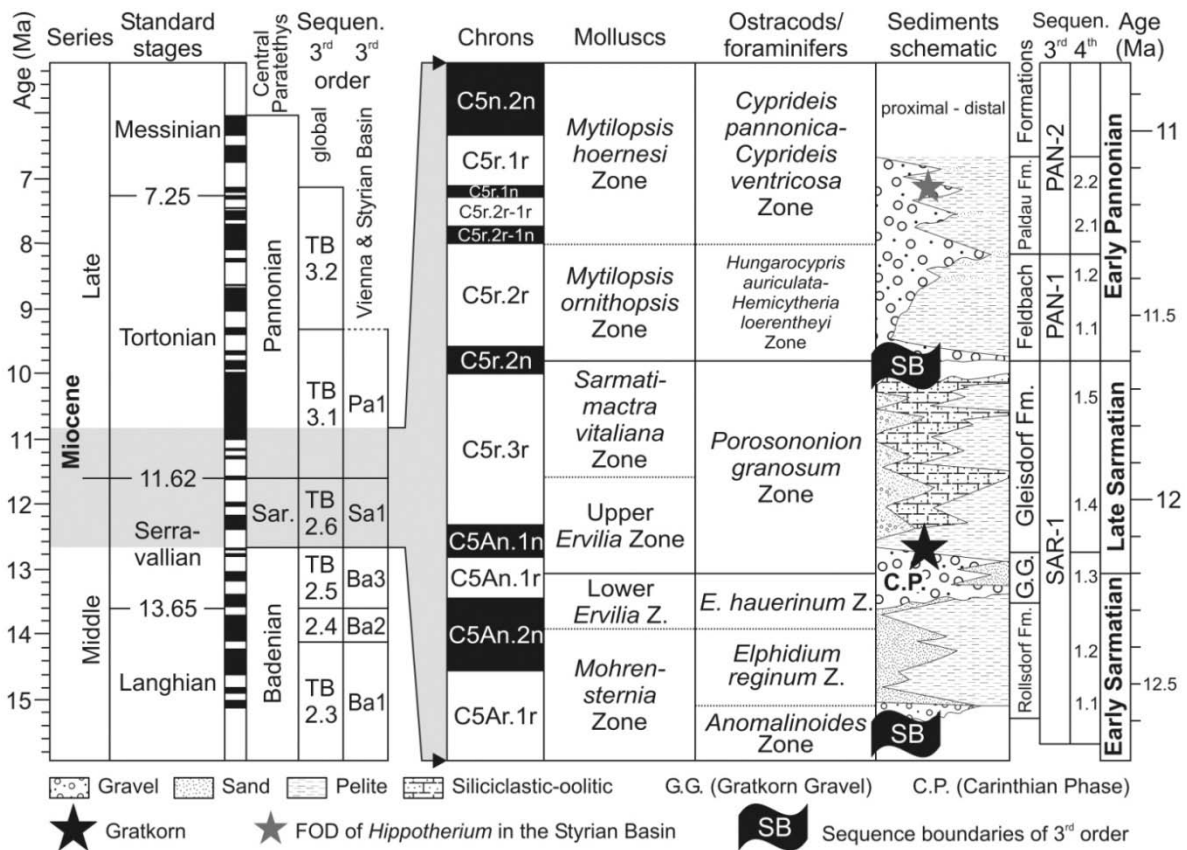


Fig. 4: Stratigraphic position of the Gratkorn locality (from Gross et al. 2011).

The latter is already early Late Miocene (Pannonian) of age (Flügel et al. 2011; for more detailed discussions on lithostratigraphy and lithofacies see Gross et al. (2014) and references therein). The Gratkorn Fm can be traced at least as far as to the northern part of the Styrian Basin, where it is underlain by marine sediments of lower Sarmatian age (Rollsdorf Fm; Flügel et al. 2011; Gross et al. 2014). The overlying Peterstal Mb is likely older than Late Miocene due to the abundance of *Podocarpium podocarpum* and the Lustbühel Mb was biostratigraphically dated in the area around Graz as late Sarmatian (Gross et al. 2014 and references therein). Due to its lithostratigraphic position the Gratkorn Fm can be correlated to the so called “Carinthian Phase”, at the end of the early Sarmatian and thus can be well integrated in the sequence stratigraphical concept of the Styrian Basin (Gross et al. 2014 and references therein). An age of 12.2 Ma has been proposed for the early/late Sarmatian boundary (Lirer et al. 2009). Normal magnetic polarity of the Peterstal Mb at Gratkorn locality imply correlation to Chron C5An.1n (12.174–12.049 Ma; Gross et al. 2014 and references therein).

1.4. Lithology of the vertebrate bearing palaeosol and frame conditions during soil formation

The here described fossil bearing palaeosol is located in the top of a coarse-grained braided-river sequence of the Gratkorn Fm and overlain by marly to pelitic lacustrine sediments of the Peterstal Mb (Fig. 5; Gross et al. 2011; Gross et al. 2014; Havlik et al. 2014). The lithology of the vertebrate bearing palaeosol itself evolves from non-laminated silty fine sand/fine sandy silt (lower part) to weakly

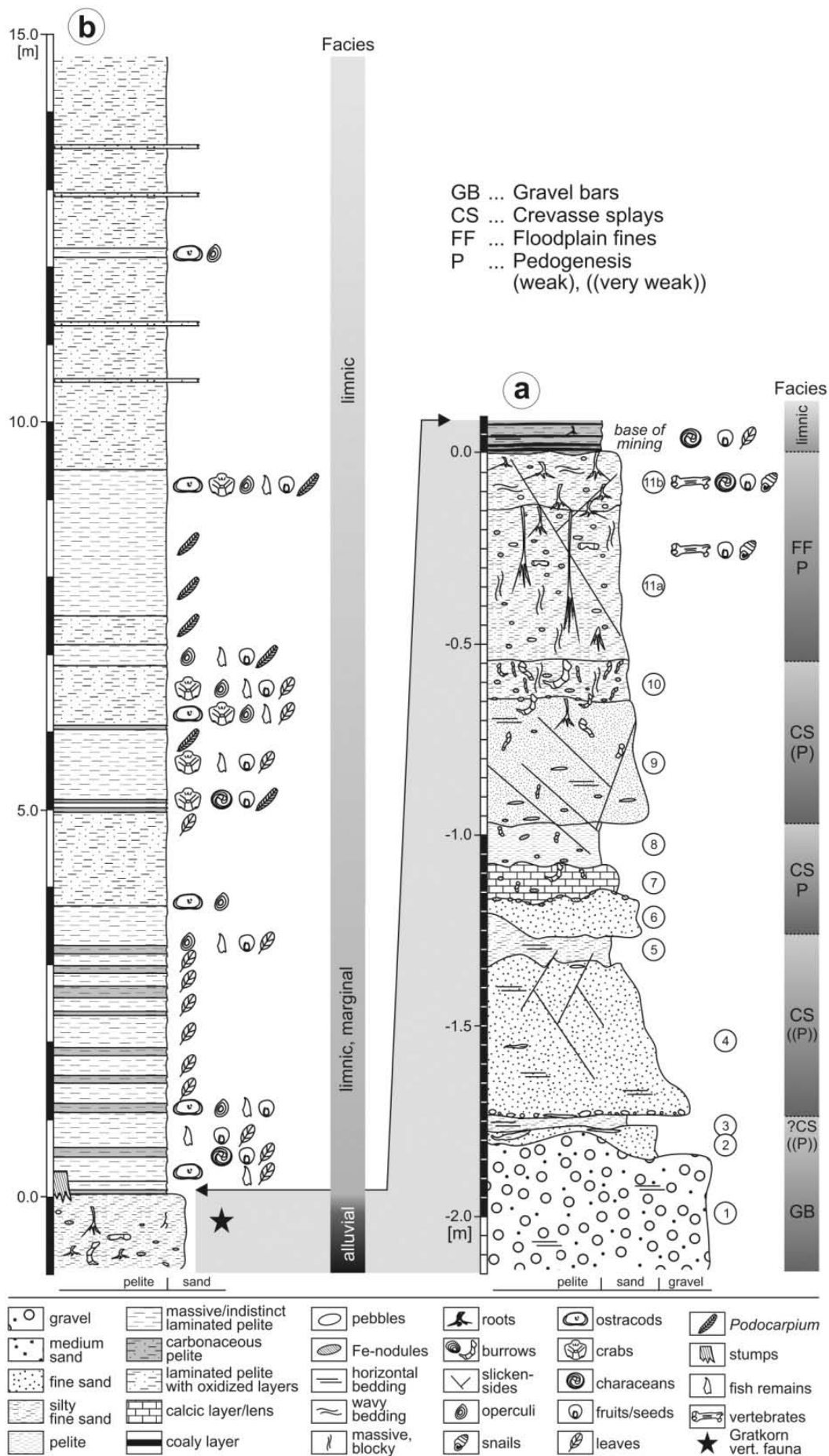


Fig. 5: Lithologic section of the Gratkorn locality (from Gross et al. 2011).

laminated, strongly mottled fine sandy (sometimes more clayey) silt (upper part; Gross et al. 2011; Gross et al. 2014; Havlik et al. 2014). The lower part bears larger oxidized root traces, ferruginous nodules, hackberry fruits (*Celtis*; usually clustered in dozens of specimens), and more rarely septaria like glaeboles, as well as very seldom phosphoric coprolites. Oxidized root traces, *Celtis*-clusters, gastropod remains, as well as sand-filled burrows of different sizes are quite common in the upper part, which houses as well carbonate nodules, interpreted as microbialites (Gross et al. 2011; Gross et al. 2014; Havlik et al. 2014). The layer is interpreted as a pedogenically altered overbank deposit, occasionally influenced by a braided river system (Gross et al. 2014). The lack of distinct soil horizons, the partly articulated or at least associated vertebrate remains, the preservation of bird of prey pellets, and rare coprolite findings indicate a short time span for the soil formation, assumably only a few years or decades (Gross et al. 2011; Aiglstorfer et al. 2014b; Gross et al. 2014; Havlik et al. 2014; Prieto et al. 2014a). Especially the pellets in the upper part of the palaeosol point to rapid burial (less than one year?; Gross et al. 2011; Gross et al. 2014; Prieto et al. 2014a). Sedimentology and faunal content indicate transient water-logging during soil formation and consequently alternating wet and dry periods (Gross et al. 2014). Furthermore, more pronounced hydromorphic conditions and a weaker effect of pedogenic processes can be assumed for the upper part in comparison to the lower part of the palaeosol (Gross et al. 2014). The observed ferric staining and iron oxide/-hydroxide incrustation of the vertebrate remains and early diagenetic iron hydroxide rhizoconcretions are typical features in hydromorphic and weakly to moderately developed soils in warm and seasonal climates (Gross et al. 2014; Havlik et al. 2014; and references therein). However, most likely water-logging varied significantly laterally due to the local topography and variable colours of the fossil content in the palaeosol point to changing moisture conditions (Gross et al. 2014) and/or influences of diagenetic fluids. The common occurrence of root traces indicates plant cover of the palaeosol, although some of the roots might belong to vegetation growing at the time of the following lake formation (Gross et al. 2014; Havlik et al. 2014). Only the mentioned *Celtis* fruits (primarily mineralized and thus offering higher potential for preservation; Aiglstorfer et al. 2014c; Gross et al. 2014) can be clearly assigned to the time of the soil formation and prove that medium-sized hackberry trees have been growing in the area (Gross et al. 2014; Havlik et al. 2014). At least in the upper part of the palaeosol vital infauna is recorded with subterranean gastropods (Harzhauser et al. 2008) and ichnofossils tentatively assigned to insects (Gross et al. 2014; Havlik et al. 2014).

Lithology and ectothermic vertebrates point to semiarid/subhumid climate with clear seasonality (Gross et al. 2011; Böhme and Vasilyan 2014; Gross et al. 2014). Based on the herpetofauna a mean annual precipitation (MAP) of 486 ± 252 mm and a MAT of less than 15 °C can be estimated for the time of the soil formation (Böhme and Vasilyan 2014).

2. Methods and abbreviations

Chapter three to five summarize the content of the publications included in this thesis. To avoid unnecessary iteration the publication(s), which is/are summarized are given at the beginning of the respective chapter and not repeatedly cited in the text.

Morphologic descriptions and measurements were accomplished according to standard procedures and specific terminologies follow the references given in Aiglstorfer et al. (2014b), Aiglstorfer et al. (2014c), and Aiglstorfer et al. (2014d). Linear measures on dental and bone material were taken with a digital calliper (where possible with a precision of 0.1mm) in the way indicated in the respective publication. Methods for taphonomical analyses comprise besides standard procedures like determination of minimum number of individuals (MNI), weathering stages, age classes, body size distribution, and Voorhies analysis also analyses of mineralogy and content and distribution of rare earth elements (REE) (for detailed information see Havlik et al. 2014). $\delta^{18}\text{O}_{\text{CO}_3}$ and $\delta^{13}\text{C}$ values (quoted in reference to Vienna Pee Dee Belemnite (V-PDB)) as well as strontium isotope composition ($^{87}\text{Sr}/^{86}\text{Sr}$ ratio) were analyzed in order to gain information about diet, drinking behaviour, as well as provenance and migration of animals (for detailed information see Aiglstorfer et al. 2014a). Taphonomical and isotope analyses follow the protocols given in Havlik et al. (2014) and Aiglstorfer et al. (2014a).

Institutional abbreviations

GPIT	Paläontologische Sammlung der Universität Tübingen, Tübingen, Germany
HLMD	Hessisches Landesmuseum Darmstadt, Darmstadt, Germany
BMNH	British Museum of Natural History, London, UK
MNHN	Muséum National d'Histoire Naturelle, Paris, France
NHMW	Naturhistorisches Museum Wien, Wien, Austria
SMNS	Staatliches Museum für Naturkunde Stuttgart, Stuttgart, Germany
SNSB-BSPG	Staatliche Naturwissenschaftliche Sammlungen Bayerns-Bayerische Staatssammlung für Paläontologie und Geologie, München, Germany
UMJGP	Universalmuseum Joanneum, Graz, Austria

Anatomical abbreviations

sin.	sinistral/left
dex.	dextral/right
C	upper canine
P2, -3, -4	second, third, fourth upper premolar
M1, -2, -3	first, second, third upper molar
i1, -2, -3	first, second, third lower incisor
p1, -2, -3, -4	first, second, third, fourth lower premolar
m1, -2, -3	first, second, third lower molar

3. Taxonomic assignation of herbivorous large mammals

Up to date 65 vertebrate species have been described from the Gratkorn locality comprising all major vertebrate groups [fishes (2 taxa), amphibians (8 species), reptiles (17 species), birds (4 species), and mammals (34 taxa; excluding carnivores, of which scientific description is still in progress); Gross et al. 2014; Tab. 1]. The locality thus holds the most diverse sympatric vertebrate fauna from stratigraphically well defined sediments in the late Middle Miocene of Europe (Gross et al. 2014).

Class	Order	Family	Taxon		Reference	
Teleostei	Cypriniformes	Cyprinidae	Leuciscinae	indet.	Böhme and Vasilyan 2014	
	Perciformes	Gobiidae	Gobiidae	indet.	Böhme and Vasilyan 2014	
Amphibia	Urodela	Salamandridae	<i>Triturus</i>	aff. <i>vulgaris</i>	Böhme and Vasilyan 2014	
			<i>Chelotriton</i>	aff. <i>paradoxus</i>	Böhme and Vasilyan 2014	
			<i>Salamandra</i>	<i>sansaniensis</i>	Böhme and Vasilyan 2014	
	Anura	Discoglossidae	<i>Litoria</i>	sp.	Böhme and Vasilyan 2014	
			<i>Bufotes</i>	cf. <i>viridis</i>	Böhme and Vasilyan 2014	
		Pelobatidae	<i>Pelobates</i>	<i>sanchizi</i>	Böhme and Vasilyan 2014	
		Ranidae	<i>Pelophylax</i>	sp.	Böhme and Vasilyan 2014	
		<i>Rana</i>	sp.	Böhme and Vasilyan 2014		
Reptilia	Testudines	Emydidae	<i>Clemmysopsis</i>	<i>turnauensis</i>	Böhme and Vasilyan 2014	
			<i>Chelydridae</i>	<i>Chelydropsis</i>	<i>murchisonae</i>	Böhme and Vasilyan 2014
		Testudinidae	<i>Testudo</i>	cf. <i>steinheimensis</i>	Böhme and Vasilyan 2014	
			<i>Testudo</i>	cf. <i>steinheimensis</i>	Böhme and Vasilyan 2014	
	Iguania	Gekkonidae	Gekkonidae	indet.	Böhme and Vasilyan 2014	
	Scincomorpha	Lacertidae	<i>Lacerta</i>	s.l. sp. 1	Böhme and Vasilyan 2014	
			<i>Lacerta</i>	s.l. sp. 2	Böhme and Vasilyan 2014	
			<i>Lacerta</i>	s.l. sp. 3	Böhme and Vasilyan 2014	
			<i>Miolacerta</i>	<i>tenuis</i>	Böhme and Vasilyan 2014	
			<i>Eclartitia</i>	sp.	Böhme and Vasilyan 2014	
		Scincidae	<i>Scincidae</i>	gen. et sp. indet.	Böhme and Vasilyan 2014	
	Anguimorpha	Anguidae	<i>Ophisaurus</i>	<i>spinari</i>	Böhme and Vasilyan 2014	
		Varanidae	<i>Varanus</i>	sp.	Böhme and Vasilyan 2014	
	Serpentes	Colubridae	Colubrinae	sp. 1	Böhme and Vasilyan 2014	
			Colubrinae	sp. 2	Böhme and Vasilyan 2014	
			Natricinae	sp. indet.	Böhme and Vasilyan 2014	
		Elapidae	<i>Naja</i>	sp.	Böhme and Vasilyan 2014	
Aves	Galliformes	Phasianidae	<i>Miogallus</i>	<i>altus</i>	Göhlich and Gross 2014	
			cf. <i>Palaeocryptonyx</i>	<i>edwardsi</i>	Göhlich and Gross 2014	
			cf. <i>Palaeocryptonyx</i>	sp.	Göhlich and Gross 2014	
	Coliiformes	Coliidae	<i>Necornis</i>	cf. <i>palustris</i>	Göhlich and Gross 2014	
Mammalia	Eulipotyphla	Erinaceidae	<i>Schizogalerix</i>	<i>voesendorfensis</i>	Prieto et al. 2010b, 2014a	
			<i>Galericinae</i>	gen. et sp. indet.	Prieto et al. 2010b, 2014a	
		Talpidae	<i>Desmanodon</i>	<i>fluegeli</i>	Prieto et al. 2010b, 2014a	
		Soricidae	<i>Dinosorex</i>	sp.	Prieto et al. 2010b, 2014a	
		Chiroptera	Vespertilionidae	cf. <i>Myotis</i>	sp.	Prieto et al. 2010b, 2014a
			Rodentia	Cricetidae	" <i>Cricetodon</i> "	<i>fandli</i>
				<i>Democricetodon</i>	n.sp.	Prieto et al. 2010a, 2014a
				<i>Megacricetodon</i>	<i>minutus</i>	Prieto et al. 2010a, 2014a
				<i>Eumyarion</i>	sp.	Prieto et al. 2010a, 2014a
			Gliridae	<i>Muscardinus</i>	aff. <i>sansaniensis</i>	Daxner-Höck 2010; Prieto et al. 2014a
				<i>Miodyromys</i>	sp.	Daxner-Höck 2010; Prieto et al. 2014a
			Eomyidae	<i>Keramidomys</i>	sp.	Daxner-Höck 2010; Prieto et al. 2014a
			Sciuridae	<i>Albanensia</i>	<i>albanensis</i>	Daxner-Höck 2010; Prieto et al. 2014a
				<i>Forsythia</i>	<i>gaudryi</i>	Daxner-Höck 2010; Prieto et al. 2014a
				<i>Blackia</i>	sp.	Daxner-Höck 2010; Prieto et al. 2014a
				<i>Spermophilinus</i>	<i>bredai</i>	Daxner-Höck 2010; Prieto et al. 2014a
			Castoridae	<i>Euroxenomys</i>	<i>minutus minutus</i>	Prieto et al. 2014 a,b
	Lagomorpha	Ochotonidae	<i>Prolagus</i>	<i>oeningsensis</i>	Angelone et al. 2014; Prieto et al. 2012, 2014a	
			cf. <i>Eurolagus</i>	<i>fontannes</i>	Angelone et al. 2014; Prieto et al. 2012, 2014a	
		Ochotonidae		gen. et sp. indet.	Angelone et al. 2014; Prieto et al. 2014a	
	Perissodactyla	Chalicotheriidae	<i>Chalicotherium</i>	<i>goldfussi</i>	Aiglstorfer et al. 2014c	
		Rhinocerotidae	<i>Aceratherium</i>	sp.	Aiglstorfer et al. 2014c	
			<i>Brachypotherium</i>	<i>brachypus</i>	Aiglstorfer et al. 2014c	
				<i>Lartetotherium</i>	<i>sansaniense</i>	Aiglstorfer et al. 2014c
	Artiodactyla	Equidae	<i>Anchitherium</i>	sp.	Aiglstorfer et al. 2014c	
			<i>Listriodon</i>	<i>splendens</i>	Made et al. in press	
				<i>Parachleuastochoerus</i>	<i>steinheimensis</i>	Made et al. in press
		Tragulidae	<i>Dorcatherium</i>	<i>nau</i>	Aiglstorfer et al. 2014d	
		Moschidae	<i>Micromeryx</i>	<i>flourensianus</i>	Aiglstorfer et al. 2014d	
			? <i>Hispanomeryx</i>	sp.	Aiglstorfer et al. 2014d	
			Cervidae	<i>Euprox</i>	<i>furcatus</i>	Aiglstorfer et al. 2014d
		Palaeomerycidae	Palaeomerycidae	gen. et sp. indet.	Aiglstorfer et al. 2014d	
		Bovidae	<i>Tethytragus</i>	sp.	Aiglstorfer et al. 2014d	
	Proboscidea	Deinotheriidae	<i>Deinotherium</i>	<i>levius vel giganteum</i>	Aiglstorfer et al. 2014b	

Tab. 1: Fossil vertebrates from the Gratkorn locality (except of Carnivora) with reference to scientific description (after Gross et al. 2014).

The herbivorous large mammals from the Gratkorn locality, excavated so far, are assigned to the following taxa (except of Suidae part of this thesis):

Proboscidea:	<i>Deinotherium levius</i> vel <i>giganteum</i>
Perissodactyla:	<i>Aceratherium</i> sp., <i>Brachypotherium brachypus</i> , <i>Lartetotherium sansaniense</i> <i>Chalicotherium goldfussi</i> , <i>Anchitherium</i> sp.
Artiodactyla - Suidae:	<i>Listriodon splendens</i> , <i>Parachleuastochoerus steinheimensis</i>
Artiodactyla - Ruminantia:	<i>Dorcatherium navi</i> , <i>Micromeryx flourensianus</i> , ? <i>Hispanomeryx</i> sp., <i>Euprox furcatus</i> , Palaeomerycidae gen. et sp. indet., <i>Tethytragus</i> sp.

3.1. Proboscidea - *Deinotherium levius* vel *giganteum*

[Aiglstorfer M, Göhlich UB, Böhme M, Gross M. (2014): A partial skeleton of *Deinotherium* (Proboscidea, Mammalia) from the late Middle Miocene Gratkorn locality (Austria). *Palaeobiodiversity and Palaeoenvironments* 94, 49-70. Publication #1]

Deinotheres remains are frequent findings in the Miocene of Europe and a useful tool for biochronological and biostratigraphical considerations (see, e.g. Dehm 1960; Huttunen 2002a, 2002b; Böhme et al. 2012; Pickford and Pourabrishami 2013). Taxonomy of deinotheres has been in discussion for long (e.g. Gräf 1957; Bergounioux and Crouzel 1962; Harris 1973; Gasparik 1993; Antoine 1994; Huttunen 2000; Gasparik 2001; Ginsburg and Chevrier 2001; Duranthon et al. 2007; Markov 2008b, a; Vergiev and Markov 2010; Böhme et al. 2012; Pickford and Pourabrishami 2013). Besides different opinions on valid genera, the number of species is still in discussion. Some authors accept five valid morpho- (Böhme et al. 2012) or chronospecies (Pickford and Pourabrishami 2013), others only four (Gasparik 1993, 2001; Markov 2008a; Vergiev and Markov 2010) or even only two species (Huttunen 2002a). In this thesis two genera, *Prodeinotherium* Éhik, 1930 and *Deinotherium* Kaup, 1829, and five species, *Prodeinotherium cuvieri* (Kaup, 1832) and *P. bavaricum* (von Meyer, 1831), *Deinotherium levius* Jourdan, 1861, *D. giganteum* Kaup, 1829 and *D. proavum* Eichwald, 1835, are considered valid.

While the genus *Prodeinotherium* is indicative for the Early to middle Middle Miocene, *Deinotherium* first occurs in Europe during the Middle Miocene (Mottl 1969; Svistun 1974) and is recorded up to the terminal Late Miocene (Markov 2008b). Although deinotheres remains are quite common in the fossil record, they often comprise only isolated teeth or bones accumulated in fluvial sediments, like for example in the famous *Dinotheriensande* (Eppelsheim Formation). Skeletons are less common but recorded for the smaller genus *Prodeinotherium* (e.g. Heizmann 1984; Musil 1997; Huttunen and Göhlich 2002; Huttunen 2004) and for the largest species *Deinotherium proavum* (Stefanescu 1894; Tarabukin 1968; Bajgusheva and Titov 2006; Kovachev and Nikolov 2006). Up to now the only well described skeleton of a medium sized deinotheres is the partial *Deinotherium levius* skeleton from Gusyatin (Middle Miocene; Svistun 1974). The assignment of deinotheres remains from Opatov to *Deinotherium levius* (Middle Miocene; Zázvorka 1940; Musil 1997; most likely representing at least two skeletons) could not be fully verified so far. Dental measurements given by Zázvorka (1940) would fit with a medium-sized deinotheres, however (Fig. 7).

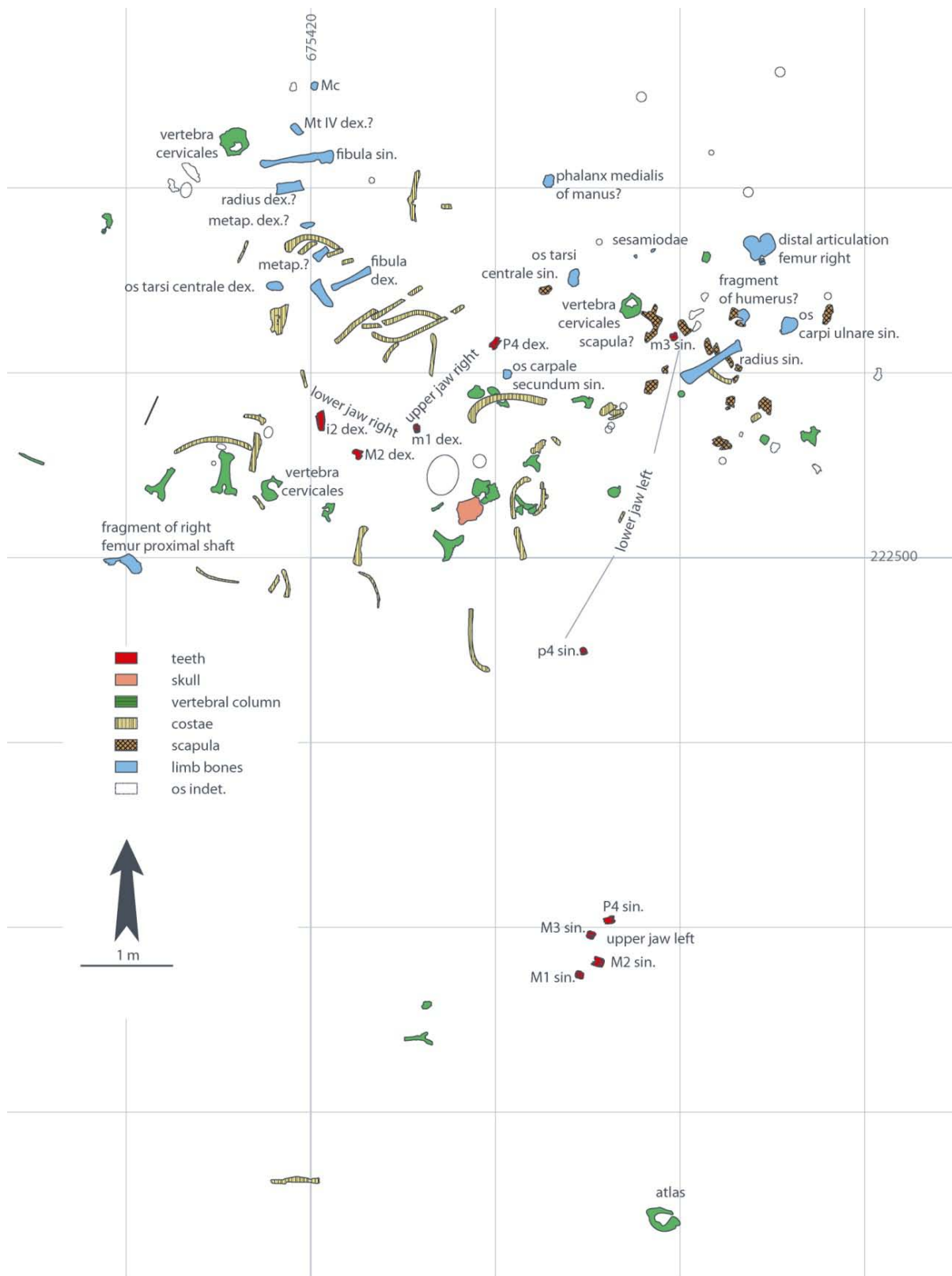


Fig. 6: Excavation plan of the partial *Deinotherium levius vel giganteum* skeleton from Gratkorn with identification of skeletal elements (modified after excavation plan by M. Gross (excavations 2005–2008); coordinates are in Austrian Grid (BMN M34 – GK); from Aiglstorfer et al. 2014b

Order Proboscidea Illiger, 1811
Family Deinotheriidae Bonaparte, 1845
Genus *Deinotherium* Kaup, 1829
Type species: *Deinotherium giganteum* Kaup, 1829

Valid European species: *Deinotherium levius* Jourdan, 1861, *D. giganteum* Kaup, 1829, *D. proavum* Eichwald, 1835

Deinotherium levius vel giganteum

Deinotherium levius Jourdan, 1861

Lectotype: toothrow with P3–M3 (Lyon, Muséum des Sciences Naturelles, Nr. L.Gr. 962)

Type locality: La Grive Saint-Alban, France

Deinotherium giganteum Kaup, 1829

Holotype: left mandibula with tusk, m2–3, right mandibula fragment: symphysis with tusk fragment (HLMD Din. 466)

Type locality: Eppelsheim, Germany

Due to finding position (Fig. 6), tooth wear pattern, degree of ossification and absence of doubled anatomical elements, the deinotherium remains excavated at the Gratkorn locality can be assigned to one individual except of some tooth fragments (sampled for isotope analyses), which were detected 30 m NW of the specimen.

The postcranial material of the Gratkorn specimen confirms well the genus separation of the two genera, *Prodeinotherium* and *Deinotherium*. It can be assigned to the genus *Deinotherium* due to a generally more flattened corpus radii, a mediodorsal-lateropalmar flattened proximal diaphysis and the weaker torsion of the bone, a distal surface on the os carpi ulnare with two concave facets (axes dorsopalmarly) divided by a central convexity, three distal articulation facets and none for the articulation to the metatarsal I in the os tarsi centrale. These characters clearly distinguish it from the smaller genus *Prodeinotherium*.

Dental dimensions point to a medium sized species, *D. levius* or *D. giganteum*. It nests well in the variability observed for *D. levius* and plots for most tooth positions with the lower dimensional range of *D. giganteum* (Fig. 7). The Gratkorn specimen is well in accordance with the gradual size increase observed for European Deinotheriidae and most likely represents *D. levius*. However, due to the lack of a lower p3 (diagnostic for species separation) a distinction from *D. giganteum* cannot be given, and the specimen is determined as *Deinotherium levius vel giganteum*.

Besides the few skeletal remains mentioned above, the skeleton from Gratkorn, though partial, is the only skeleton of a medium-sized deinotherium taxon described so far.

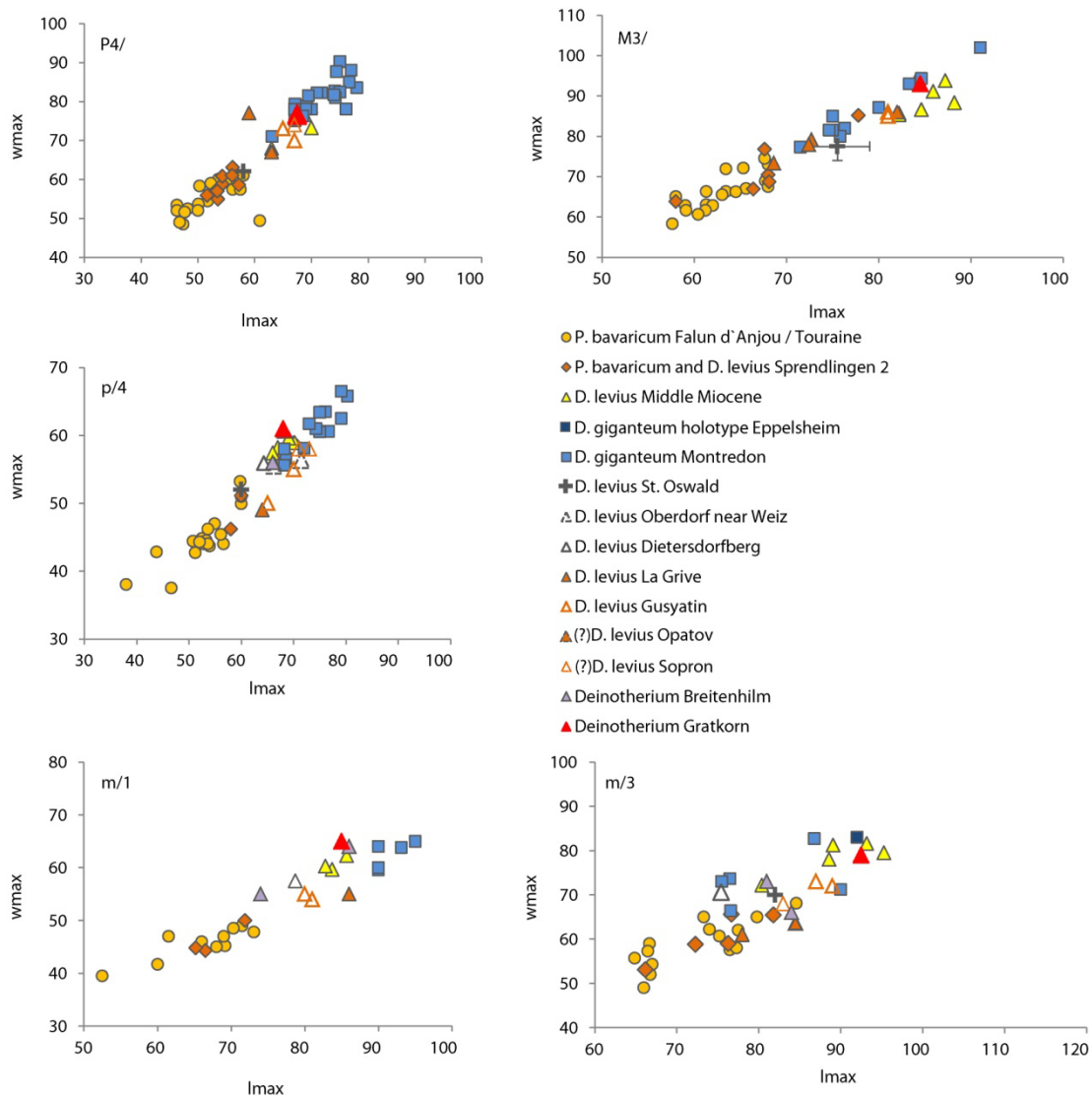


Fig. 7: Bivariate plots [wmax versus lmax (mm)] of dental material of *D. levius vel giganteum* from Gratkorn in comparison to other Deinotheriidae: *Prodeinotherium bavaricum* from Falun de la Touraine and Anjou (both France; early Middle Miocene; Langhian; MN 5; 15 ± 0.5 Ma; data from Ginsburg and Chevrier 2001); *P. bavaricum* and *Deinotherium levius* from Sprendlingen 2 (Germany; Middle Miocene; data from Böhme et al. 2012 and own measurements); *D. levius* from Middle Miocene sites [from France and Germany: St. Gaudens, Tournan (both France; late Middle Miocene; MN 7/8; 13–11.5 Ma); Massenhäusen, Hinterauerbach (both Germany; late Middle Miocene; MN 7/8; 13–11.5 Ma; data from Gräf 1957; Ginsburg and Chevrier 2001); *D. levius* from St. Oswald near Gratwein (Austria; Middle Miocene; early Badenian), Oberdorf near Weiz (Austria; late Middle Miocene; late Sarmatian; 12.2–11.6 Ma) and Dietersdorfberg near Mureck (Austria; late Middle Miocene; Sarmatian; 12.7–11.6 Ma) after Mottl 1969 and own measurements; *D. levius* from La Grive (France; late Middle Miocene; MN 7/8; 13–11.5 Ma; data from Huttunen 2000) and from Gusyatyn (also Husyatyn) (Ukraine; Middle Miocene; early late Badenian; 13.1–13.4 Ma; data from Svistun 1974); *D. levius*(?) from Opatov (formerly Abtsdorf; Czech Republic; Middle Miocene; Badenian; data from Zázvorka 1940); *D. levius*(?) from Sopron (Hungary; Late Miocene; Pannonian B/C; MN 9; data from Huttunen 2000); *Deinotherium* from Breitenhilm near Hausmannstetten (Austria; late Middle Miocene; late Sarmatian; 12.2–11.6 Ma; data from Peters 1871); holotype of *D. giganteum* from Eppelsheim (Germany; Miocene; data from Gräf 1957) and *D. giganteum* from Montredon (France; Late Miocene; late Vallesian; MN 10; 9.5 Ma; data from Tobien 1988; Ginsburg and Chevrier 2001); from Aiglstorfer et al. 2014b

3.2. Perissodactyla

[Aiglstorfer M, Heissig K, Böhme M. (2014): Perissodactyla from the late Middle Miocene Gratkorn locality (Austria). *Palaeobiodiversity and Palaeoenvironments* 94, 71-82. Publication #2]

Although few in findings the Perissodactyla from Gratkorn represent a quite diverse assemblage, with at least 5 different taxa: the chalicotheriid *Chalicotherium goldfussi* Kaup, 1833, three rhinocerotid species (*Aceratherium* sp., *Brachypotherium brachypus* (Lartet, 1837), and *Lartetotherium sansaniense* (Lartet, in Laurillard 1848)), and the equid *Anchitherium* sp..

Order Perissodactyla Owen, 1848

Family Chalicotheriidae Gill, 1872

Subfamily Chalicotheriinae Gill, 1872

Genus *Chalicotherium* Kaup, 1833

Type species: *Chalicotherium goldfussi* Kaup, 1833

Chalicotherium goldfussi

Lectotype: M3 dex. (Kaup 1832-1839, pl. VII, fig. 3; HLMD BIN 3167)

Type locality: Eppelsheim, Rheinhessen, Germany

Following Anquetin et al. (2007) an M3 dex. of a chalicotheriid from Gratkorn (Fig. 8 a-e) must be assigned to the subfamily Chalicotheriinae because of the non-fusion of proto-loph and protocone. As in most Chalicotheriinae (Fahlke et al. 2013), the protocone is posterior to the paracone. Schizotheriinae possess an anteroposteriorly elongated rectangular shape in the upper molars in contrast to the square shape in Chalicotheriinae (Zapfe 1979; Coombs 1989). A square shape can be observed in the specimen from Gratkorn. In size, it is well within the dimensions of both *Chalicotherium goldfussi* and *Anisodon grande* (de Blainville, 1849) (overlap of dimensions also recorded by Zapfe (1979) and Coombs (1989)) and is clearly wider than representatives of the Schizotheriinae. In general shape, it fits best to *Chalicotherium goldfussi*. With this species, the Gratkorn specimen shares the presence of a cingulum at the lingual wall of the protocone (Schaefer and Zapfe 1971), a wide and lingually open central valley (Schaefer and Zapfe 1971; Zapfe 1979), and the course of the labial wall of metacone–metastyle and hypocone (fig. 30 in Schaefer and Zapfe 1971; Anquetin et al. 2007).

Family Rhinocerotidae Gray, 1821

Subfamily Aceratheriinae Dollo, 1885

Tribe Aceratheriini Dollo, 1885

Genus *Aceratherium* Kaup, 1832

Type species: *Aceratherium incisivum* Kaup, 1832

***Aceratherium* sp.**

The taxonomic status of the diverse *Aceratherium*-like Rhinocerotidae in the Early and Middle Miocene of Europe is still in discussion. Geraads and Saraç (2003) stated that most of the Middle Miocene *Aceratherium*-like “genera’ correspond to poorly defined evolutionary grades rather than to clades” (Geraads and Saraç 2003, p. 218). Heissig (2009) observed only a few differences between *Alicornops* and *Aceratherium* in dentition and stated that they may not exceed subgeneric or even specific rank. He included *Alicornops* as a subgenus in the genus *Aceratherium*. Antoine et al. (2010) and Becker et al. (2013) provided cranial, dental, and postcranial characters and observed differences between *Aceratherium incisivum* and *Alicornops simorreense*, thus enabling now a better discrimination between the different *Aceratherium*-like Rhinocerotidae.

A lingual fragment of a D2 sin. (Fig. 8 h, i) from Gratkorn shows most similarities in dimensions and morphology with an *Aceratherium*-like Rhinocerotidae. Unfortunately, the only characteristic feature described by Antoine et al. (2010) and Becker et al. (2013) observable on a D2 cannot be observed on the specimen from Gratkorn due to fragmentation.

Therefore, the genus attribution *Aceratherium* was used *sensu lato* and the specimen left in open nomenclature as *Aceratherium* sp.

Tribe Teleoceratini Hay, 1902

Genus *Brachypotherium* Roger, 1904

Type species: *Brachypotherium brachypus* (Lartet, 1837)

Brachypotherium brachypus

Type: not designated (see also Heissig 2012)

Type locality: Simorre, Gers, France

Two European *Brachypotherium* species are considered valid at the moment, *B. brachypus* and *B. goldfussi* (Kaup, 1834), though synonymy of the two taxa is well possible (Heissig 2012).

The lateral half of an astragalus sin. (Fig. 9 a-d) from Gratkorn and a partial metatarsal II sin. (Fig. 8 j-m) are assigned to the rhinocerotid *Brachypotherium brachypus*. The astragalus is broad and possesses only a shallow trochlear notch as typical for Teleoceratini (Heissig 2012). With *Brachypotherium brachypus* it shares the general shape, a main facet for the articulation with the calcaneum distally more prolonged and less concave than in *Aceratherium*, a longer collum tali than in *Aceratherium*, the separation of all three calcaneum facets in contrast to Rhinocerotinae (distolateral and sustentacular ones are fused in these) (Heissig 1976; Ginsburg and Bulot 1984; Hünemann 1989; Cerdeño 1993; Geraads and Saraç 2003; Heissig 2009; Antoine et al. 2010). The specimen from Gratkorn is smaller than most representatives of the species, but overlaps well with a few specimens from Çandır and Sofca (Turkey; late Middle Miocene; MN 7/8; Heissig 1976; Geraads and Saraç 2003).

Fig. 8: a–e M3 dex. of *Chalicotherium goldfussi* from Gratkorn (UMJGP 204676; a occlusal view, b posterior view, c anterior view, d lingual view, e labial view); f, g m1 sin. of *Lartetotherium sansaniense* from Gratkorn (UMJGP 203459; f occlusal view, g labial view); h, i D2 sin. of *Aceratherium* sp. from Gratkorn (UMJGP 203711; h occlusal view, i lingual view); j–m Mt II sin. of *Brachypotherium brachypus* from Gratkorn (UMJGP 204720; j proximal view, k dorsal view, l plantar view; m lateral view; articulation facets labelled); scale bar 10 mm; from Aiglstorfer et al. 2014c

The metatarsal II sin. is shorter and more massive than that of all rhinoceroses of the Middle Miocene except of *Brachypotherium*. Furthermore, the proximal facet for the mesocuneiform is broader and less concave than in *Aceratherium* (Hünemann 1989) and *Lartetotherium* (Heissig 2012). Like the astragalus it is smaller in dimensions than what is usually observed for the species, but fits well to a metatarsal III of *Brachypotherium brachypus* from Sofca (Heissig 1976).

Subfamily Rhinocerotinae Dollo, 1885

Tribe Rhinocerotini Dollo, 1885

Genus *Lartetotherium* Ginsburg, 1974

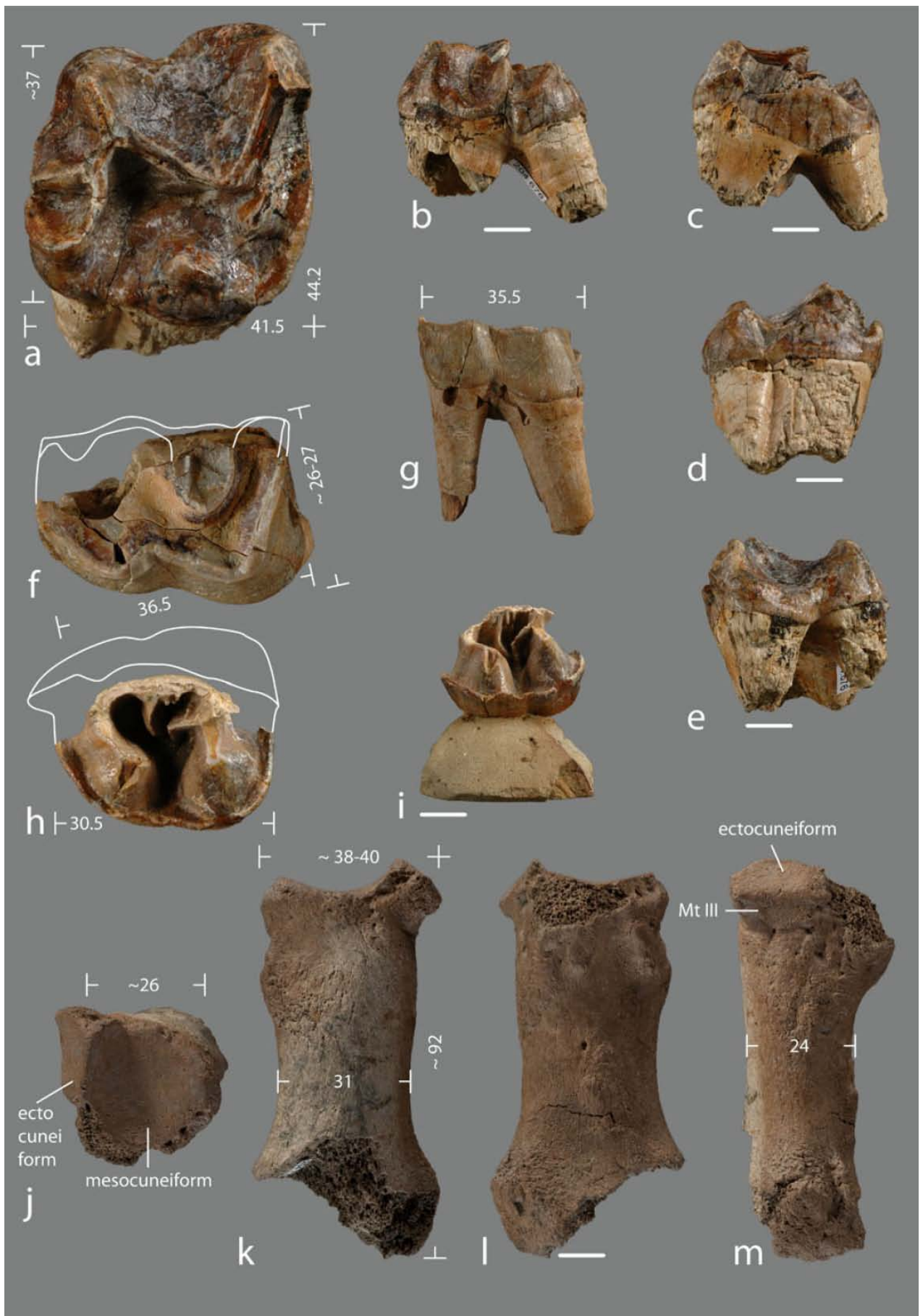
Type and only species: *Lartetotherium sansaniense* (Lartet in Laurillard, 1848)

***Lartetotherium sansaniense* (Lartet in Laurillard, 1848)**

Holotype: skull with mandible MNHN Sa 6478 (monotype)

Type locality: Sansan, France

A m1 sin. (Fig. 8 f, g) and a small fragment of a m2 sin. from the same individual (together with some jaw fragments) are assigned to *Lartetotherium sansaniense*. Tooth dimensions seem to be rather variable inter- but also intraspecific among rhinocerotid species. Thus the use of size as discriminative feature can only give indications for species assignment and is less valuable than in other groups. In any case the m1 from Gratkorn is smaller than teeth assigned to the genus *Brachypotherium* and larger than teeth assigned to "*Dicerorhinus*" *steinheimensis* Jäger, 1839. As the most useful character for the separation of Rhinocerotini and Aceratheriini, the length of the paralophid, is not preserved in the m1, the configuration of the cingulids is used for species determination. Due to the lack of any labial cingulid and the rather short anterior and the posterior cingulids, which do not proceed onto the labial side the assignment to Aceratheriinae can be excluded. The strongly reduced cingulids are very characteristic for *Lartetotherium sansaniense* (Heissig 2012).



Family Equidae Gray, 1821
Subfamily Anchitheriinae Leidy, 1869
Genus *Anchitherium* Meyer, 1844
Type species: *Anchitherium aurelianense* (Cuvier, 1825)

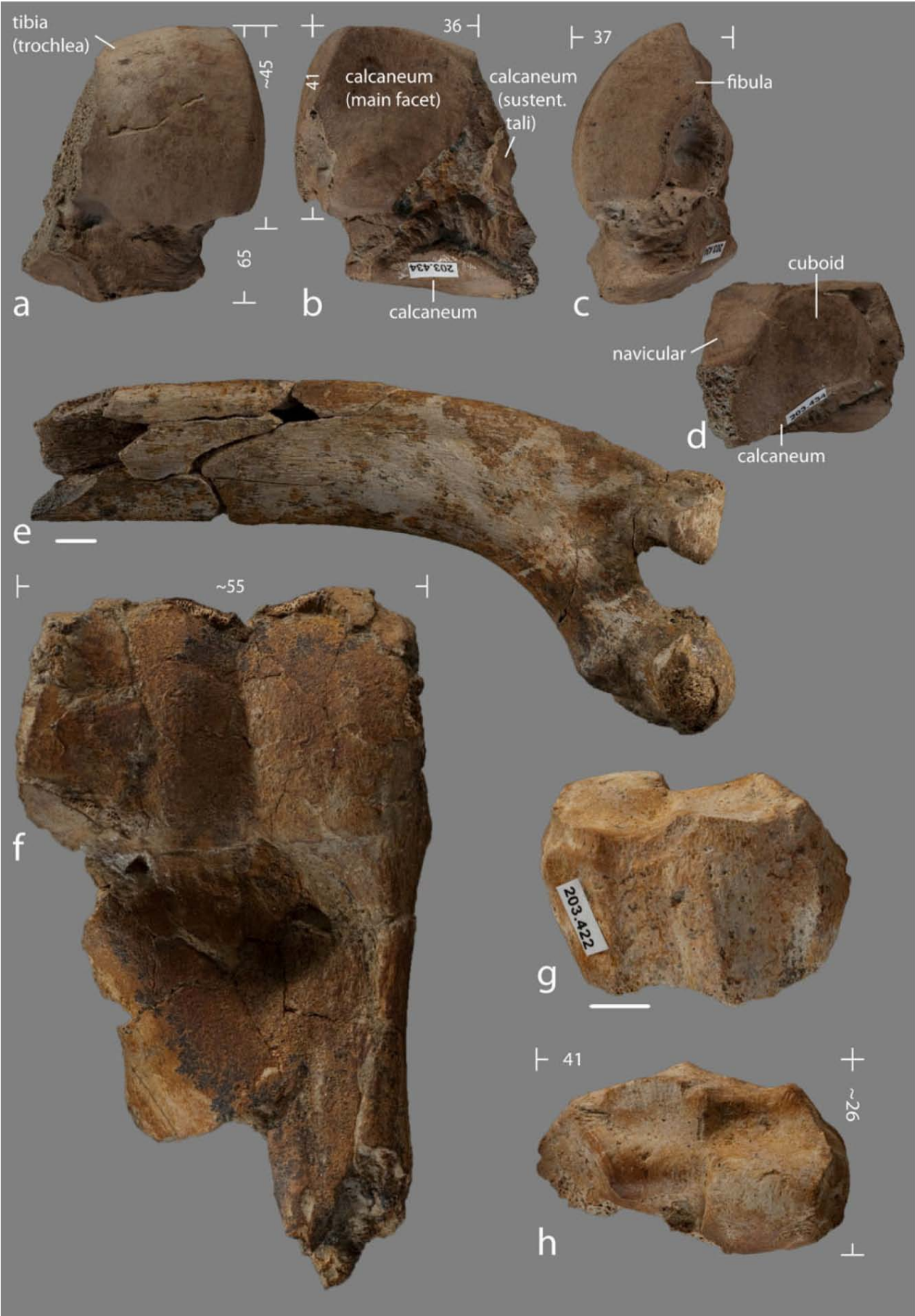
***Anchitherium* sp.**

The distal fragments of a humerus sin. (Fig. 9 f) and a radius dex. (Fig. 9 g, h) from Gratkorn can be assigned to the equid *Anchitherium*. In morphology and dimensions the humerus is well in the variability of *A. aurelianense* from several Middle Miocene localities. Due to the fragmentary nature of the specimen no species diagnostic features can be observed, however.

The radius fragment does not indicate any distal fusion of radius and ulna as typical for *Anchitherium* and distinguishing it from *Hipparion* (Iñigo 1997; Alberdi and Rodríguez 1999; Alberdi et al. 2004). In shape and dimensions it fits well to *A. aurelianense* from Baigneaux (Alberdi et al. 2004), Sansan (Alberdi and Rodríguez 2012), and Sandelzhausen (personal observation), as well as to *A. corcolense* Iñigo, 1997 from Córcoles (Spain; Early Miocene; MN 4; Iñigo 1997), but is smaller than *Sinohippus* Zhai, 1962 (Salesa et al. 2004).

As a clear species assignation is not possible at the moment the two fragments from Gratkorn are left in open nomenclature as *Anchitherium* sp..

Fig. 9: a–d astragalus sin. of *Brachypotherium brachypus* from Gratkorn (UMJGP 203434; a dorsal view, b plantar view, c lateral view; d distal view; articulation facets labelled); e left rib of Rhinocerotidae indet. (GPIT/MA/2400) from Gratkorn; f humerus sin. of *Anchitherium* sp. from Gratkorn (UMJGP 204694); g, h radius dex. of *Anchitherium* sp. from Gratkorn (UMJGP 203422; g dorsal view, h distal view); scale bar 10 mm; from Aiglstorfer et al. 2014c



3.3. Artiodactyla – Ruminantia

[Aiglstorfer M, Rössner GE, Böhme M. (2014) *Dorcatherium nauti* and pecoran ruminants from the late Middle Miocene Gratkorn locality (Austria). *Palaeobiodiversity and Palaeoenvironments* 94, 83-123. Publication #3]

The ruminant fauna from Gratkorn is the most abundant and richest large mammal group recorded from the locality. So far it comprises 6 different taxa, *Dorcatherium nauti*, *Micromeryx flourensianus*, *?Hispanomeryx* sp., *Euprox furcatus*, Palaeomerycidae gen. et sp. indet., and *Tethytragus* sp. and a minimum number of 34 individuals (MNI; Havlik et al. 2014). Size classes of the species range from 4–5 kg (*Micromeryx flourensianus*) up to about 270 kg (Palaeomerycidae gen. et sp. indet.).

Order Artiodactyla Owen, 1848
Suborder Ruminantia Scopoli, 1777
Infraorder Tragulina Flower, 1883
Family Tragulidae Milne Edwards, 1864
Genus *Dorcatherium* Kaup, 1833
Type species: *Dorcatherium nauti* Kaup, 1833

Further European species: *Dorcatherium crassum* (Lartet, 1851), *Dorcatherium vindebonense* von Meyer, 1846, *Dorcatherium guntianum*, von Meyer, 1846, *Dorcatherium penecke* (Hofmann, 1893), *Dorcatherium jourdani* Depéret, 1887, and *Dorcatherium puyhauberti* Arambourg and Piveteau, 1929

***Dorcatherium nauti* Kaup, 1833**

Holotype: mandibula with p3–m3 and alveolae of p1 and p2 described in Kaup 1833 and figured in Kaup (1832-1839, pl. XXIII, fig. 1, 1a, 1b), lost, cast available (BMNH M3714, SNSB-BSPG 1961 XIX 37).

Type locality: Eppelsheim, Germany

Fig. 10: Dental and postcranial material of *Dorcatherium nauti*. a C dex. (UMJGP 204059; 1 labial view, 2 lingual view), b D2 dex. (GPIT/MA/2377; 1 lingual view, 2 occlusal view), c D3 dex. (UMJGP 204675; occlusal view), d D3–4 sin. (UMJGP 204067; occlusal view), e d2 sin. (UMJGP 210956; labial view), f d3 sin. (UMJGP 210696; occlusal view), g d4 sin. (UMJGP 210692; occlusal view), h P4 dex. (GPIT/MA/2379; occlusal view), i M1 sin. (UMJGP 209952; occlusal view), j M2 sin. (UMJGP 210698; occlusal view), k M3 sin. (UMJGP 210697; occlusal view), l mandibula sin. with p4–m3 and alveolae for p1–p3 (GPIT/MA/2734; 1 occlusal view, 2 labial view, 3 m3 in occlusal view), m mandibula sin. with p2–3 (UMJGP 204667; 1 labial view, 2 occlusal view), n fractured mandibula with i1, p2–m3 sin. and dex. (UMJGP 210694; 1 mandibula dex. in lingual view and sin. in labial view, 2 p4–m3 sin. in labial view, 3 p4–m3 sin. in lingual view, 4 p4–m3 sin. in occlusal view, 5 m3 sin. in occlusal view), o humerus sin. (GPIT/MA/2389; 1 cranial view, 2 distal view), p radius sin. (GPIT/MA/2391; 1 dorsal view, 2 proximal view), q cubonavicular sin. (UMJGP 203419; dorsal view), r tibia sin. (UMJGP 203419; 1 dorsal view, 2 lateral view of distal end, 3 distal view), s astragalus dex. (GPIT/MA/2409; 1 dorsal view, 2 palmar view), t fragmented calcaneum dex. (GPIT/MA/2409; medial view); scale bar 10 mm (except n1, 50 mm); from Aiglstorfer et al. 2014d



The five European *Dorcatherium* species generally accepted at the moment differ in dimensions, dental and postcranial morphology and stratigraphic range (Fig. 2): small-sized: *D. guntianum*, medium-sized: *D. naui* and *D. crassum*, larger-sized: *D. vindebonense*, large-sized: *D. penecke*. *D. puyhauberti* and *D. jourdani* possess no unambiguous features distinguishing them from other European species and could be synonymous to *D. guntianum* and *D. naui* (Geraads et al. 2005; Morales et al. 2012), respectively.

In any case, two different phylogenetic lineages can be observed for the Miocene European Tragulidae, at the moment integrated in the genus "*Dorcatherium*": a more bunodont lineage including *D. crassum*, *D. vindebonense*, and *D. penecke* with (1) a tricuspid p2/d2, (2) a more dominant mesolabial conid in the tricuspid p3, (3) a p4 with a more simple morphology of the posterior valley, (4) more bunodont, wider and less high crowned lower molars with a more prominent ectostylid, (5) a more middle position of the third lobe in the lower m3, (6) upper molars more bulky in habitus, and (7) a tibia fused with the malleolus lateralis; and a more selenodont lineage including *D. naui* and *D. guntianum* with (1) a bicuspid p2/d2, (2) a tricuspid p3 with a less dominant mesolabial conid than in *D. crassum*, (3) a p4 with a more complex posterior valley, (4) more selenodont, more slender and higher crowned lower molars, (5) a labially turned third lobe in the lower m3, (6) upper molars with less bulky styles than in *D. crassum*, and (7) a non-fusion of tibia and malleolus lateralis (Kaup 1832-1839; Mottl 1961; Fahlbusch 1985; Sach 1999; Hillenbrand et al. 2009; Rössner 2010; Alba et al. 2011; Sánchez et al. 2011; Morales et al. 2012; Rössner and Heissig 2013; Alba et al. 2014).

The tragulid material from Gratkorn (Fig. 10) nests well within the dimensions of the medium-sized *Dorcatherium* species (Mottl 1961; Moyà-Solà 1979; Fahlbusch 1985; Rössner 2010; Alba et al. 2011; Morales et al. 2012; Alba et al. 2014) and from morphology it clearly belongs to the more selenodont lineage. The material can thus be clearly assigned to the species *Dorcatherium naui*.

The species is considered typical for Late Miocene faunal assemblages, but has been documented with some remains lately for the Middle Miocene (Alba et al. 2011). The material from Gratkorn provides the first abundant Middle Miocene assemblage of the species and due to its morphologic and dimensional accordance with Late Miocene representatives and the type material of the species well underlines the clear separation of the two phylogenetic lineages and negates the evolution of *D. naui* out of *D. crassum*. At the moment we can date back the record of the species *Dorcatherium naui* to the early Sarmatian (Fig. 2).

Infraorder Pecora Linnaeus, 1758

Family Moschidae Gray, 1821

Genus *Micromeryx* Lartet, 1851

Type species: *Micromeryx flourensianus* Lartet, 1851

Further European species considered valid at the moment: *Micromeryx flourensianus* Lartet, 1851, *Micromeryx styriacus* Thenius, 1950, *Micromeryx azanzae* Sánchez and Morales, 2008, *Micromeryx soriae* Sánchez, Domingo and Morales, 2009, and *Micromeryx mirus* Vislobokova, 2007

***Micromeryx flourensianus* Lartet, 1851**

Holotype: hitherto not determined (Ginsburg proposed (letter from 1974): MNHN Sa 2957); type material under revision; partly figured in Filhol (1891, pls. 24, 25); stored at MNHN

Type locality: Sansan, France

The small moschid from Gratkorn shows characteristic dental features for the genus *Micromeryx*: (1) the closed or nearly closed anterior valley in the triangular p4, (2) lower molars with only anterior cingulid, (3) bicuspid third lobe with a high entoconulid in the m3, and (4) non-shortened lower premolar row (Gentry et al. 1999; Rössner 2006; Vislobokova 2007; Sánchez and Morales 2008; Rössner 2010). Dimensions and morphology are well within the range of the type species *M. flourensianus* and show the greatest overlap with specimens from the Middle Miocene of La Grive and Steinheim a. A. (am Albuch) and the Late Miocene of Atzelsdorf. Especially in terms of tooth crown height and reduction of the external postprotocristid the Gratkorn specimens differ from those of the type locality Sansan (Fig. 11) but are well in accordance with the mentioned contemporaneous and slightly younger specimens. The assignment of *Micromeryx* findings from Central Europe clearly younger than the type material to the species *M. flourensianus* cannot be challenged with the scarce material from Gratkorn and the still missing scientific descriptions of the type material from Sansan and from the rich locality Steinheim a. A.. However, a morphological change from early to late records can be observed and might result in assignation of the younger material to a different or even new species.



Fig. 11: Increase in general crown height and the height of the lingual wall at third lobe in m3 of *Micromeryx* from early to late representatives: a m3 dex. of *M. flourensianus* from Sansan (MNHN Sa 2962; mirrored), b m3 dex. of *M. flourensianus* from Steinheim a. A. (SMNS 46077; mirrored), c m3 sin. of *M. flourensianus* from Gratkorn (UMJGP 204685), d m3 sin of *M. mirus* from Kohfidisch (NHMW 2005z0021/0007); specimens become stratigraphically from a to d; from Aiglstorfer et al. 2014d

Genus *Hispanomeryx* Morales, Moyà-Solà and Soria, 1981

Type species: *Hispanomeryx duriensis* Morales, Moyà-Solà and Soria, 1981

Further species: *Hispanomeryx aragonensis* Azanza, 1986, *Hispanomeryx daamsi* Sánchez, Domingo and Morales, 2010, *Hispanomeryx andrewsi* Sánchez, DeMiguel, Quiralte and Morales, 2011

? *Hispanomeryx* sp.

Two fragmented upper molars from Gratkorn, from presumably one tooth row, are intermediate in size between the medium sized Pecora (*Euprox* and *Tethytragus*) and the small-sized *Micromeryx*, but are well within dimensional and morphological range of the genus *Hispanomeryx*. Morphologically the teeth differ from *Dorcatherium* by the lack of a strong lingual cingulum and the presence of well-developed internal and external postprotocrista, from Cervidae by the weak basal cingulum and by the weakly developed rib at the metacone. The latter is shared with Moschidae and Bovidae, however.

Due to the limited material, the advanced stage of wear and the preservation, a determination can only be given with reservations, the specimen is therefore left in open nomenclature as ?*Hispanomeryx* sp.. The record of the genus in Gratkorn is the first for Central Europe besides Steinheim a. A. (indicated in Heizmann and Reiff 2002, but not yet described) and indicates a wider geographic range for the larger moschids than assumed so far.

Family Cervidae Goldfuss, 1820

Genus *Euprox* Stehlin, 1928

Type species: *Euprox furcatus* (Hensel, 1859)

Further species: *Euprox dicranocerus* (Kaup, 1839), *Euprox minimus* (Toula, 1884)

***Euprox furcatus* (Hensel, 1859)**

Holotype: fragmented antler sin. (MB.Ma.42626)

Type locality: Kieferstädel (today: Sośnicowice), Poland

The cervid remains from Gratkorn are assigned to *Euprox furcatus* due the characteristic antler morphology (Fig. 12): (1) the strong inclination of the pedicle to posterior, (2) the anteromedial location of the foramina supraorbitale, (3) the clearly developed suboval and only slightly anteroposterior elongated coronet, (4) the constriction of the shaft above the coronet, (5) the shaft length of 32–38 mm, and (6) the simple bifurcation of the antler into a shorter anterior and a longer posterior branch (Fig. 12). The dental material from Gratkorn is also in accordance with the morphological and dimensional variability of the medium sized brachyoselenodont Miocene cervids *Euprox furcatus* and *Heteroprox larteti*. However, a species differentiation based on dental material between the two taxa is hindered due to the close resemblance of the two species (Stehlin 1928), the co-occurrence in the locality Steinheim a. A. (yielding so far the richest material of both species), and a large intraspecific variability. Differences in the dentition among specimens of *Euprox* vel *Heteroprox* from Steinheim a. A. are small and not considered distinct so far. Comparing the dental material from Steinheim a. A. with *Euprox furcatus* from Gratkorn and literature data for the species (e.g. Czyżewska and Stefaniak 1994; Azanza 2000), it can be observed that some specimens share with specimens determined as *Euprox furcatus* a lingual turn of the third lobe and a lingual depression at the entoconulid in the m3.

Although representing only an indication so far due to the lack of a comprehensive scientific description and evaluation of the rich material from Steinheim a. A., this feature might prove a valuable character for species determination in the future.

So far no indications have been found for a second cervid taxon in Gratkorn. In this location, for the first time, antler and complete upper and lower dentition can be assigned to one individual (young adult male) of *Euprox furcatus*. The locality might thus prove helpful for future evaluation of species characteristics.



Fig. 12: Cranial appendages of *E. furcatus* from Gratkorn in comparison to female *D. elegans* from Sansan: a antler sin. from Gratkorn (lateral view; GPIT/MA/2398), b antler dex. from Gratkorn (medial view; UMJGP 204062), c antler sin. of *D. elegans* from Sansan with reconstructed orientation (MNHN Sa 3451; lateral view), d same as c (anterior view), e same as (a) with reconstructed orientation (anterior view), f reconstruction of *E. furcatus* from Gratkorn in lateral view with orientation of antler (UMJGP 210955) and mandibula and maxilla (GPIT/MA/2736; mirrored); skull drawing after Thenius (1989; *Muntiacus*); from Aiglstorfer et al. 2014d

Family Palaeomerycidae Lydekker, 1883
Type species: *Palaeomeryx kaupi* von Meyer, 1834

Palaeomerycidae gen. et sp. indet.

The largest ruminant from Gratkorn is recorded so far only by a fragmented metacarpal sin. It is assigned to the family Palaeomerycidae due to size and morphology. As typical for the family, the cross-section of the diaphysis is rounded dorsally and palmarly less concave than in Cervidae, but distally more dorsopalmarly flattened than in the latter (Astibia 2012).

Taking into consideration dimensions, morphology, and the record of "*Palaeomeryx* cf. *eminens*" from the early Late Miocene locality of Atzelsdorf (Hillenbrand et al. 2009), the Gratkorn specimen most likely represents "*Palaeomeryx eminens*". However, as so far only one metacarpal has been excavated from Gratkorn, and with ongoing discussion on the taxonomy inside the family (see, e.g. Astibia 2012), a determination as Palaeomerycidae gen. et sp. indet. seems the most reasonable at the present stage.

Family Bovidae Gray, 1821
Genus *Tethytragus* Azanza and Morales, 1994
Type species: *Tethytragus langai* Azanza and Morales, 1994

Further species: *Tethytragus koehlerae* Azanza and Morales, 1994, *Tethytragus stehlini* (Thenius, 1951).

***Tethytragus* sp.**

Some upper cheek teeth (P2-4 and M3 dex., labial wall of M2 dex., M2-3 sin.) of the ruminant material from Gratkorn can be assigned to a single individual of *Tethytragus* sp.

With the steep lingual wall, the more developed crown height, and the simple crown morphology, the teeth clearly differ from the similar-sized cervid teeth from Gratkorn, and justify an attribution to the family Bovidae. In size and morphology, the teeth belong to a small-sized, rather brachyo- to mesodont bovid species, and are smaller than those of most bovid genera recorded from the late Middle Miocene of Central Europe so far. With *Tethytragus koehlerae* Azanza and Morales, 1994 from Çandir (Turkey) the Gratkorn bovid overlaps in dimensions and morphology (Köhler 1987) and shares tooth crown height, clearly developed styles, a pronounced paracone rib, a reduced entostyle, and a planar labial wall at the metacone in the upper molars. However, with a smooth enamel surface, the Gratkorn specimen differs from this species which possesses wrinkled enamel (Köhler 1987; Made 2012). Taxonomy inside the genus is still in discussion and no consensus has been reached concerning the validity of other species (Azanza and Morales 1994; Made 2012). The Gratkorn specimen differs in morphology from other small sized bovids. *Eotragus* possesses a wider P4, the upper molars are lower crowned, the labial wall at the metacone is less plane, and the mesostyle is less slender (Made 1989, 2012). *Pseudoeotragus* possesses a wider P4 as well, but is higher

crowned, shows a parastyle more parallel to the paracone rib, and a more planar labial wall in the upper molars (Made 1989, 2012) than the specimen from Gratkorn.

Morphology and dimensions of the Gratkorn bovid correspond best to those of *Tethytragus koehlerae*. However, due to the smooth enamel surface in the Gratkorn specimens, the lack of any associated horn core remains so far, and as there is no dental material unambiguously assigned to *T. stehlini* available for comparison, the Gratkorn specimen was left in open nomenclature as *Tethytragus* sp.

4. Taphonomical considerations with focus on large mammal taphonomy

[Havlik P, Aiglstorfer M, Beckman A, Gross M, Böhme M. (2014): Taphonomical and ichnological considerations on the late Middle Miocene Gratkorn locality (Styria, Austria) with focus on large mammal taphonomy. *Palaeobiodiversity and Palaeoenvironments* 94, 171-188. Publication #4]

[Aiglstorfer M, Göhlich UB, Böhme M, Gross M. (2014) A partial skeleton of *Deinotherium* (Proboscidea, Mammalia) from the late Middle Miocene Gratkorn locality (Austria). *Palaeobiodiversity and Palaeoenvironments* 94, 49-70. Publication #1]

Analysis of the taphonomy of a fossil assemblage is the base for the evaluation of ecological and diagenetical influences on composition and preservation of the accumulation. First of all depositional mechanisms and time coverage of the deposition have to be considered: analysis of sedimentology, stratigraphic distribution of faunal elements horizontally and vertically and, accumulation mechanisms [analysis of disarticulation, decomposition, disruption and weathering, bioerosion, taxonomic-, body size-, and age-distribution, frequency of different anatomical elements (e.g. Voorhies analysis)]. Furthermore, estimations on diagenetic overprint and recrystallization (like e.g. analysis of mineralogy and content/distribution of REE) are indispensable e.g. for evaluating the informative value of the isotopic composition of mammalian hard tissues in context of ecosystem reconstruction.

Nearly all vertebrate remains described from the locality originate from a single palaeosol layer except of the rare fish remains, which come from the hanging lacustrine pelites (Gross et al. 2011; Gross et al. 2014; Havlik et al. 2014). Field observations showed that locally accumulated pellets (assumably from owls; Gross et al. 2011), as well as articulated/associated fossorial smaller vertebrates (small mammals and ectothermic vertebrates) are restricted to the upper part of the palaeosol and cervid remains are more common here than in the lower part, while suids and heavier large mammals are more common in the lower part. Detailed assignment of the findings to different levels of the palaeosol is enhanced due to gradual change in lithology and strong neotectonic activities. Furthermore, fragments from the same bone were excavated in different horizons of the palaeosol. All large mammal findings should be considered as more or less deposited in a short time span, maximally several decades. Bones and teeth are ferruginous stained, display iron oxide and iron hydroxide coatings, as well as root traces and were gnawed by small and large mammals. Colour ranges from whitish to black (Gross et al. 2011; Gross et al. 2014; Havlik et al. 2014). Fragmentation of bones and teeth can be observed regularly. Diagenetic alteration is low in the fossil assemblage. Gastropod shells are preserved in primary (aragonitic) mineralization.

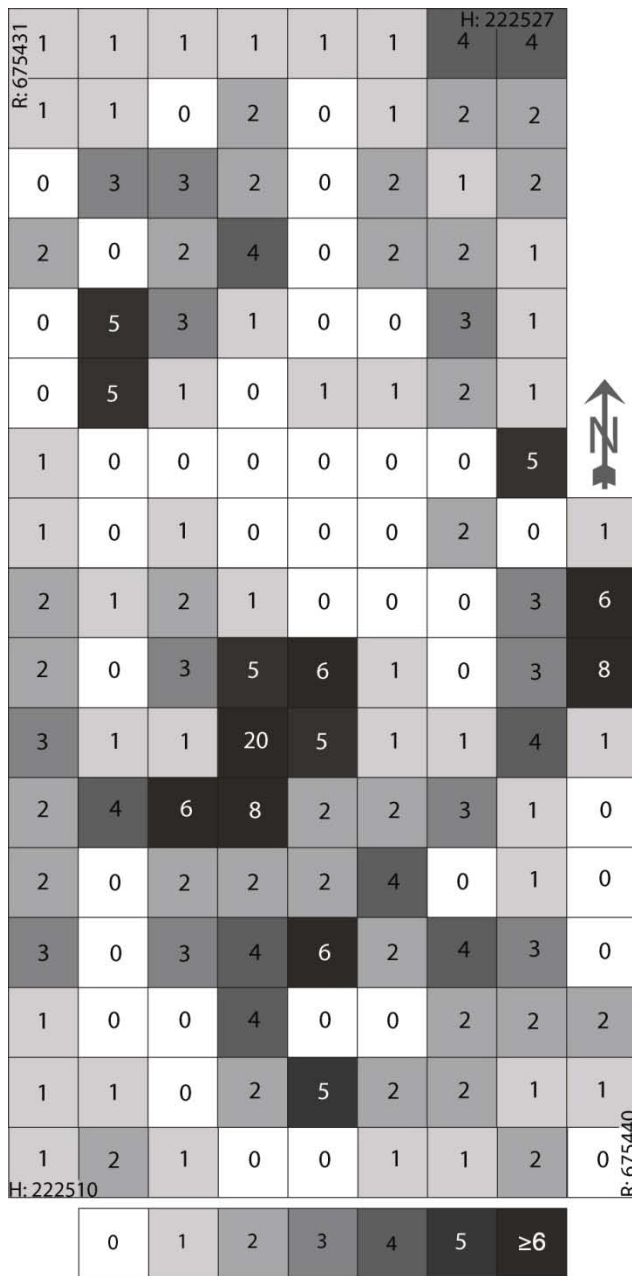


Fig. 13: Excavation map of campaigns 2011 and 2012 with additional data from 2013 showing the heterogeneous concentration of large mammal specimen per square meter. Numbers indicate the number of objects excavated; coordinates are in Austrian Grid (BMN M34–GK); modified after Havlik et al. 2014

Bone, dentine, and especially enamel of large mammals show a relatively low total REE content, indicating low diagenetic alteration. Shapes of REE distribution patterns have been used to evaluate degree and time of diagenetic alteration (Badiola et al. 2009). Although uptake of REE has proven more complex than assumed so far (Kocsis et al. 2010; Herwartz et al. 2013; Trueman 2013), the flat pattern (no considerable enrichment in medium-sized rare earth elements) in the specimens from Gratkorn still indicate a minor degree of recrystallization (Kowal-Linka et al. 2014). Similar values and patterns for tissues from the upper and the lower part are well in accordance with the assumption of a “uniform” diagenetical history and shale-normalised ratios of La/Sm (0.337 to 1.6198) and of La/Yb (0.1302 and 0.9903) are well in the variability for “terrestrial samples” (Trueman et al. 2006; Herwartz et al. 2013).

The large mammal remains are not randomly distributed in the palaeosol but locally concentrated (Fig. 13), in general disarticulated but still roughly associated. No indication for fluvial transportation, as e.g. abrasion, current alignment or size sorting, can be detected on the large mammal remains. Although an expanded Voorhies analysis based on a NISP (number of identified specimens) of 363 from all excavation campaigns up to 2012 shows a clear dominance of Voorhies Group III (elements resistant to prolonged fluvial transportation, such as teeth, jaw fragments, and astragali), a remarkable amount can also be attributed to Voorhies Group I (elements non-resistant to transportation, e.g. vertebra and ribs; Fig. 14 b). The results of the Voorhies analysis object a prolonged fluvial transportation (Badiola et al. 2009), but could be explained by carnivore behavior. Gnawing and scavenging by carnivores is furthermore evidenced by biting and gnawing traces. Taken into consideration the typical consumption sequence (Lyman 1994) strong influence of the assemblage by carnivore behavior furthermore explains the over-representation of teeth (Fig. 14 a).

Carnivores are most likely also responsible for the high percentage of breakage in skeletal elements from Gratkorn. The presence of epiphyses of long bones with biting marks (diaphyses are often missing) indicates extensive marrow consumption. The ratio of vertebrae and ribs versus girdle and limb bones rather points to an accumulation by scavengers than by predators (Palmqvist and Arribas 2001). Trampling and neotectonics must be considered important fracturing mechanisms for large mammal bones and teeth as well and trampling was most likely also an important burial mechanism. The wide distribution of body masses (Fig. 15 a) and high diversity of species is more typical for scavengers than for predators and furthermore makes a fluvial accumulation of the assemblage unlikely (Palmqvist and Arribas 2001).

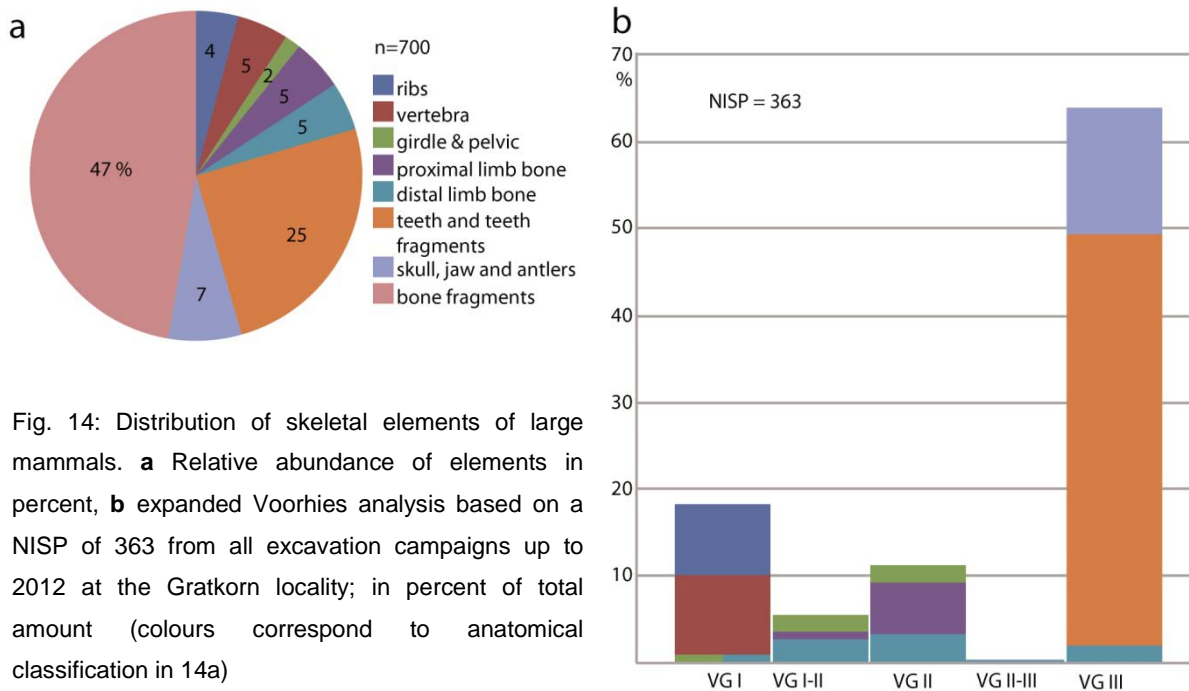


Fig. 14: Distribution of skeletal elements of large mammals. **a** Relative abundance of elements in percent, **b** expanded Voorhies analysis based on a NISP of 363 from all excavation campaigns up to 2012 at the Gratkorn locality; in percent of total amount (colours correspond to anatomical classification in 14a)

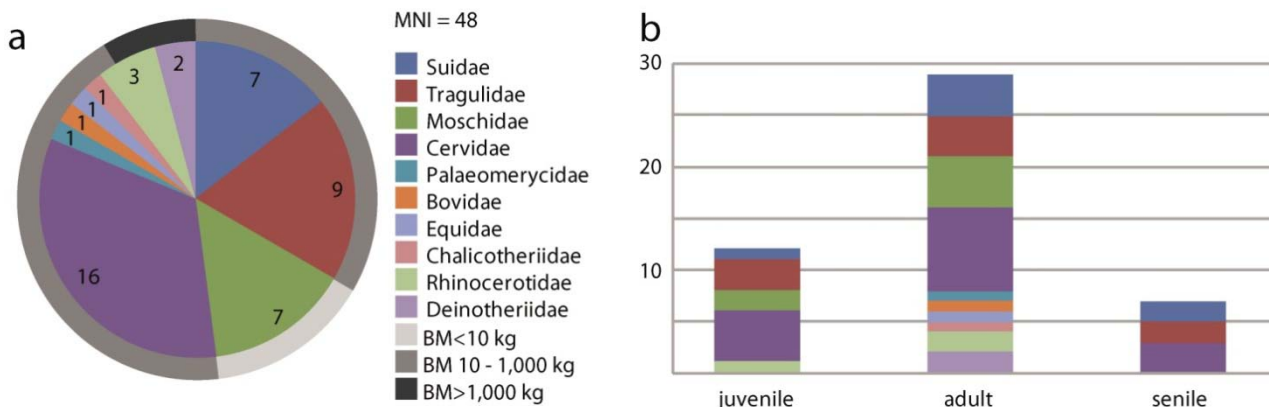


Fig. 15: Faunal composition of the Gratkorn large mammal taphocoenosis: **a** MNI of herbivorous large mammals on family level based on the number of similar anatomical elements and tooth enamel consumption (body mass, BM, follows categories given in Costeur et al. 2013), **b** age model of large mammals based on enamel consumption (juvenile: deciduous dentition; adult: permanent dentition, senile: trigonid of m1 completely worn) and ossification (colours correspond to Fig. 15a)

Although keeping in mind that the data on age profiles from Gratkorn (Fig. 15 b) are not statistically significant, the clear dominance of prime individuals still points to an accumulation either by mass mortality, ambush predators or collection by scavengers (Stiner 1990; Lyman 1994; Palmqvist and Arribas 2001). Due to different weathering stages, anatomical separation and inhomogeneous dispersal of the material, mass mortality can be clearly excluded. Although we cannot exclude the presence of ambush predators like e.g. Felidae, the direct evidence is missing so far and first data on carnivores rather indicates the presence of scavengers (D. Nagel pers. comm. March 2013).

Summing up the large mammal assemblage is considered a more or less autochthonous taphocoenosis. It is contemporaneously deposited (in terms of years or decades), without any significant time averaging (or faunal mixing). It was most likely accumulated to a considerable degree by scavengers.

5. Ecology, provenance and migration

[Aiglstorfer M, Bocherens H, Böhme M. (2014): Large Mammal Ecology in the late Middle Miocene locality Gratkorn (Austria). *Palaeobiodiversity and Palaeoenvironments* 94, 189-213. Publication #5]

[Aiglstorfer M, Göhlich UB, Böhme M, Gross M. (2014): A partial skeleton of *Deinotherium* (Proboscidea, Mammalia) from the late Middle Miocene Gratkorn locality (Austria). *Palaeobiodiversity and Palaeoenvironments* 94, 49-70. Publication #1]

[Aiglstorfer M, Heissig K, Böhme M. (2014): *Perissodactyla* from the late Middle Miocene Gratkorn locality (Austria). *Palaeobiodiversity and Palaeoenvironments* 94, 71-82. Publication #2]

[Aiglstorfer M, Rössner GE, Böhme M. (2014): *Dorcatherium naui* and pecoran ruminants from the late Middle Miocene Gratkorn locality (Austria). *Palaeobiodiversity and Palaeoenvironments* 94, 83-123. Publication #3]

$\delta^{18}\text{O}_{\text{CO}_3}$ and $\delta^{13}\text{C}$ values of mammalian fossil tooth enamel can help to gain information about diet, drinking water and drinking behaviour of the animals, since differences in isotopic compositions of diet and drinking water are incorporated into body tissues (DeNiro and Epstein 1978; Longinelli 1984; Luz et al. 1984; Bocherens et al. 1996; Kohn 1996; Kohn et al. 1996; Levin et al. 2006; Tütken et al. 2006; Clementz et al. 2008; Tütken and Vennemann 2009; Ecker et al. 2013). In general lower values in $\delta^{18}\text{O}_{\text{CO}_3}$ and $\delta^{13}\text{C}$ in herbivores point to feeding in more closed and humid environment, while higher values are indicative for feeding in open and arid environment (Fig. 16). In addition to $\delta^{18}\text{O}_{\text{CO}_3}$ and $\delta^{13}\text{C}$ values, the strontium isotopic composition ($^{87}\text{Sr}/^{86}\text{Sr}$ ratio) of diet and drinking water is incorporated in the skeletal and dental tissues of animals (Hoppe et al. 1999; Maurer et al. 2012). Since this ratio is constant and does not change up the food chain, it reflects the bioavailable $^{87}\text{Sr}/^{86}\text{Sr}$ in the animal's habitat (Blum et al. 2000; Bentley 2006) and is thus a useful tool for provenance analyses.

14 bulk enamel samples of large mammal teeth (*Parachleuastochoerus steinheimensis*, *Listriodon splendens*, *Dorcatherium naui*, *Euprox furcatus*, *Micromeryx flourensianus*, *Tethytragus* sp.), and 21 serial samples of *Deinotherium levius vel giganteum* and *Lartetotherium sansaniense* were gained for stable isotope analysis ($\delta^{18}\text{O}_{\text{CO}_3}$, $\delta^{13}\text{C}$). Strontium isotopic composition ($^{87}\text{Sr}/^{86}\text{Sr}$) was measured on

enamel samples of the large mammals *Listriodon splendens*, *Parachleuastochoerus steinheimensis*, *Dorcatherium navi*, *Euprox furcatus*, *Tethytragus* sp., *Lartetotherium sansaniense*, and *Deinotherium levius* vel *giganteum*. For the taxa *Aceratherium* sp., *Brachypotherium brachypus*, *Chalicotherium goldfussi*, *Anchitherium* sp., *?Hispanomeryx* sp., Palaeomerycidae gen. et sp. indet. material was too scarce or did not comprise any dental material at all. Therefore, ecology of these taxa is not considered specifically in this work.

5.1. Ecology of large mammals

Morphological adaptation and data from stable isotope analyses gained from the large mammalian herbivore record from Gratkorn fit well in a mesic/woodland environment of a pure C3 ecosystem (Fig. 16). None of the taxa derived its diet from closed canopy conditions and different values for $\delta^{18}\text{O}_{\text{CO}_3}$ and $\delta^{13}\text{C}$ indicate that the ecosystem provided enough diversity in plant resources to allow occupation of different niches.

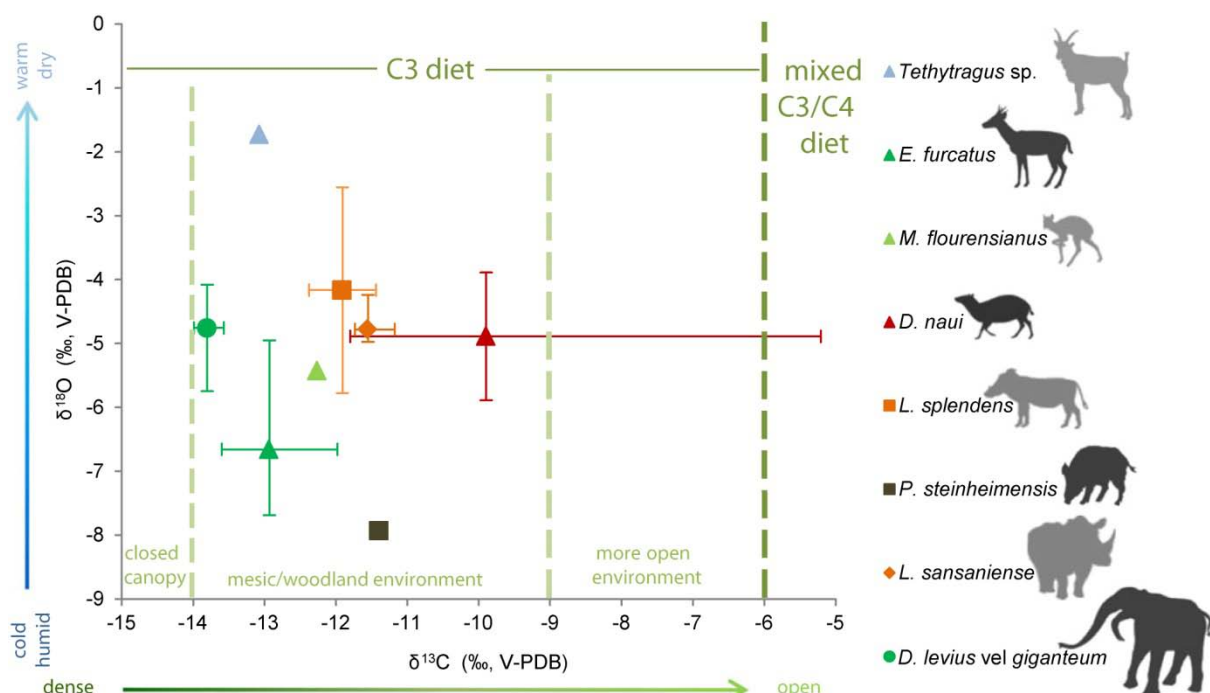


Fig. 16: Mean values with total range of $\delta^{18}\text{O}_{\text{CO}_3}$ (‰V-PDB) versus $\delta^{13}\text{C}$ (‰V-PDB) for large mammals (enamel) from the Gratkorn locality with designated niches (after Domingo et al. 2012) in a predominantly C3 vegetation. Trends from dense and cold/humid environment to more open and warm/dry environment are indicated (*E* *Euprox*, *M* *Micromeryx*, *D* *Dorcatherium*, *L* *Listriodon*, *P* *Parachleuastochoerus*, *L* *Lartetotherium*, *D* *Deinotherium*; from Aiglstorfer et al. 2014a

The data fit well with a late Middle Miocene faunal assemblage from this area and are well in accordance with other Middle Miocene large mammal communities from Europe (see e.g. Tütken et al. 2006; Domingo et al. 2009; Tütken and Vennemann 2009; Domingo et al. 2012). They seem to be affected only to a minor degree by climatic conditions but rather represent a typical niche partitioning of large mammals in a Middle Miocene ecosystem.

Deinotherium levius vel giganteum

The species represents the largest large mammal taxon recorded at the locality. A body mass of 6t was reconstructed for the not fully grown “young” adult from Gratkorn (representing rather a small value for the taxon). Although body size was most likely smaller for the specimen sampled for stable isotope analyses, it was still by way larger than the other large mammals recorded from the locality.

$\delta^{13}\text{C}$ and $\delta^{18}\text{O}_{\text{CO}_3}$ values for *Deinotherium levius vel giganteum* fit well with browsing on top canopy leaves (Bocherens and Sen 1998). In comparison to other measurements on Proboscidea from different Miocene localities of different stratigraphic levels, it can be observed that the Gratkorn specimen nests well among the Deinotheriidae (Fig. 17 d). Representatives of this family (with Tapir-like lophodont dentition) in general show values typical for browsing in a C3 dominated mesic/woodland environment. In contrast, Miocene European Gomphotheres (data from Tütken et al. 2006; Domingo et al. 2009; Tütken and Vennemann 2009; Domingo et al. 2012; more bunodont dentition) usually show higher $\delta^{13}\text{C}$ values, indicating a higher degree of mixed feeding and feeding in a more open environment, though still in C3-dominated vegetation.

Serial measurements along the axis of two fragmented teeth from Gratkorn, of assumably one individual, show seasonal variation in $\delta^{18}\text{O}_{\text{CO}_3}$. Each tooth displays one maximum (summer) and one minimum (winter), a 1-year cycle would be recorded by combining the two patterns, under the assumption that both teeth belong to the same individual. Little variation in $\delta^{13}\text{C}$ and incoherent with $\delta^{18}\text{O}_{\text{CO}_3}$ imply no seasonal diet change for *Deinotherium levius vel giganteum* from Gratkorn but fit to a more generalistic and unselective feeding strategy (Tütken and Vennemann 2009).

Lartetotherium sansaniense

Lartetotherium sansaniense belongs to the second largest mammal group, Rhinocerotidae, in Gratkorn and is the smallest species of rhinocerotids recorded. Its $\delta^{13}\text{C}$ values are slightly higher than in the cervid *Euprox furcatus* or the proboscidean *Deinotherium levius vel giganteum*, though still nesting well within the range expected for feeding in a mesic/woodland C3-dominated environment (Fig. 16).

Comparing different values for Miocene Rhinocerotidae from literature and own measurements (Fig. 17c), it can be observed that, independent of age and climate, *Lartetotherium sansaniense* usually shows higher values for $\delta^{13}\text{C}$ and also frequently for $\delta^{18}\text{O}_{\text{CO}_3}$ than other Rhinocerotidae.

Although more data are needed to reconstruct ecological adaptations for the different rhinocerotid genera and species, the data already indicate different ecological niches with *Brachypotherium* and other teleoceratini feeding in a more closed mesic/woodland environment (also fitting well to the graviportal gait and limb shortening; Heissig 1999), while *Lartetotherium sansaniense* was feeding in more open environment and aceratini occupied niches in between, which is also well in accordance with other considerations on the ecology of the different taxa (Heissig 1999; Bentaleb et al. 2006; Tütken and Vennemann 2009). Due to the morphology of the upper premolars (lack of lingual cingula) *Lartetotherium sansaniense* has often been interpreted as a selective browser (Coombs 1989; Heissig 2012), but this feature does not exclude a considerable amount of low abrasive grasses.

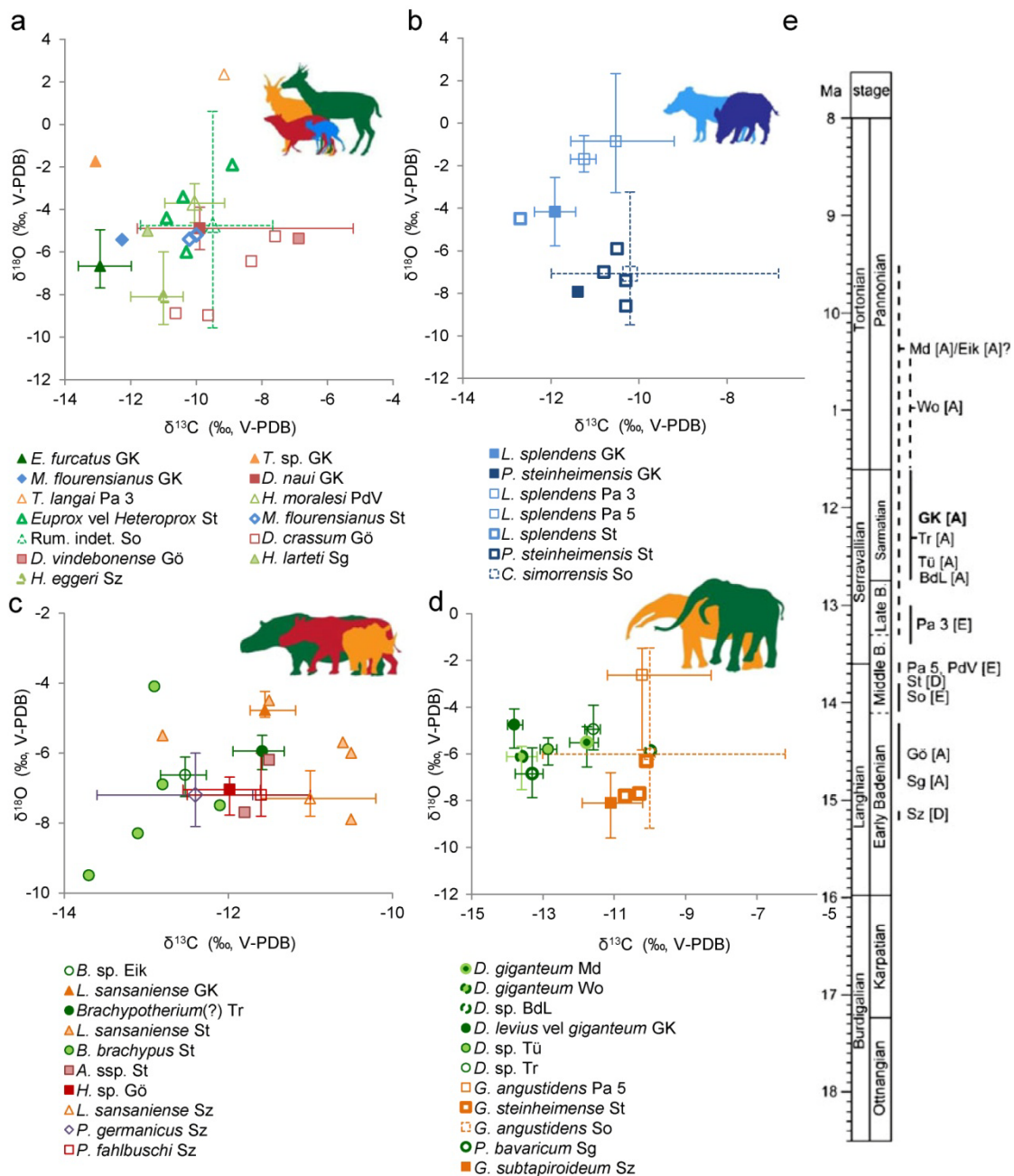


Fig. 17: Mean values with total range of $\delta^{18}\text{O}_{\text{CO}_3}$ (‰V-PDB) versus $\delta^{13}\text{C}$ (‰ V-PDB) for large mammals (enamel) from the Gratkorn locality in comparison with data from other Miocene localities [GK Gratkorn (own measurements); Pa 3 Paracuellos 3 (from Domingo et al. 2012); PdV Puente de Vallecas (from Domingo et al. 2012); St Steinheim a. A. (from Tütken et al. 2006); So Somosaguas (from Domingo et al. 2009); Gö Göriach (own measurements); Sg Seegraben (own measurements); Sz Sandelzhausen (from Tütken and Vennemann 2009); Pa 5 Paracuellos 5 (from Domingo et al. 2012); Eik Eichkogel (own measurement); Tr Trössing (own measurements); Md Mödling (own measurements); Wo Wolfau (own measurements); BdL Bruck an der Leitha (own measurements)].

a Ruminantia (*E. Euprox*; *T. Tethytragus*; *M. Micromeryx*; *D. Dorcatherium*; *H. Heteroprox*; Rum. Ruminantia); **b** Suidae (*L. Listriodon*; *P. Parachleuastochoerus*; *C. Conohyus*); **c** Rhinocerotidae (*B. Brachypotherium*; *L. Lartetotherium*; *A. Aceratherium*; ssp. several species; *H. Hoploaceratherium*; *P. germanicus Prosantorhinus germanicus*; *P. fahlbuschi Plesiaceratherium fahlbuschi*); **d** Proboscidea (*D. Deinotherium*; *G. Gomphotherium*; *P. Prodeinotherium*); **e** Stratigraphic age of different localities (A Austria, D Germany, E Spain, B Badenian); from Aiglstorfer et al. 2014a

Serial sampling of the Gratkorn rhinocerotid tooth did not show significant variations in $\delta^{13}\text{C}$ and $\delta^{18}\text{O}_{\text{CO}_3}$. As seasonality for the region around Gratkorn is indicated by sedimentology, ectothermic vertebrates (Gross et al. 2011), and the serial measurements on *Deinotherium levius vel giganteum*, the height of the rhino tooth fragment might be too short to represent a time interval recording seasonal variation.

Suidae

Listriodon splendens and *Parachleuastochoerus steinheimensis* show similar values for $\delta^{13}\text{C}$ but are quite distinct in $\delta^{18}\text{O}_{\text{CO}_3}$ (Fig. 16). Isotopic measurements of *Listriodon splendens* from Gratkorn fit well within the ecological niche of a specialized folivore and higher values in $\delta^{18}\text{O}_{\text{CO}_3}$ indicate a certain amount of mixed feeding or ingestion of maybe upper canopy fruit, fitting well also to traditional interpretations based on morphology (Made 1996; Made et al. in press).

The distinctly lower $\delta^{18}\text{O}_{\text{CO}_3}$ values, but similar $\delta^{13}\text{C}$ values in *Parachleuastochoerus steinheimensis* from Gratkorn, could be explained by digging for roots, as these are depleted in $\delta^{18}\text{O}_{\text{CO}_3}$ in comparison to leaves, while $\delta^{13}\text{C}$ values are similar (Sponheimer and Lee-Thorp 2001). While incisor and general jaw morphology makes consumption of roots for the genus *Listriodon* unlikely (Made 1996; Made et al. in press and references therein), for the subfamily Tetraconodontinae, to which *Parachleuastochoerus* is assigned, a certain amount of root consumption is assumed due to dental morphology (Hünemann 1999; Made et al. in press).

Combining isotopic measurements from Gratkorn with literature data from other Miocene localities (Tütken et al. 2006; Domingo et al. 2009; Domingo et al. 2012; Fig. 17b) different ecological niches for *Listriodon splendens* and for tetraconodontid suids (*Parachleuastochoerus steinheimense* and *Conohyus simorreensis*) are verified and seem to be rather independent of climate and stratigraphic level.

Dorcatherium nauti

The tragulid, *Dorcatherium nauti*, from Gratkorn had a shoulder height of about 40–50cm and body mass estimates for the Gratkorn specimens are about 28–29kg (min: 26kg, max 30.6kg; n=6), well in accordance with literature data.

Modern Tragulidae inhabit the undergrowth of forested environments (Rössner 2007), and other species of the genus, like *Dorcatherium crassum*, have been considered indicators for wetland conditions. From limb-morphology a low-gear locomotion seems most likely for the species (Leinders 1979; Köhler 1993; Morales et al. 2012) and hind limb morphology indicates an inability of zigzag flight behaviour for the genus (Alba et al. 2011). This led Moyà-Solà (1979) to the assumption that the escaping behaviour in *Dorcatherium* was fleeing straight into the next open water as in the living African tragulid *Hyemoschus* (Dubost 1978) and thus indicating an adaptation to rather more humid environments.

So far, no isotopic measurements have been published on Miocene Tragulidae of Europe. The clearly higher $\delta^{13}\text{C}$ values (Fig. 16) in *Dorcatherium nauti* from Gratkorn in comparison to all other large mammals from the locality were quite unexpected, as one would expect lower values in a taxon adapted to closed and humid undergrowth. $\delta^{18}\text{O}_{\text{CO}_3}$ values are instead only slightly higher than in

cervids. These values can be either explained by a certain amount of mixed feeding (leaves and grass) or by ingestion of a considerable amount of fruit. Modern Tragulidae, for example, feed on fallen fruit, seeds, flowers, leaves, shoots, petioles, stems, and mushrooms in the forest undergrowth (Dubost 1984). On the one hand there is no evidence for the existence of a relevant amount of grass in the vegetation of Gratkorn so far. On the other hand an exclusively frugivore diet for the species cannot be assumed, as the climate makes an all-year fruit supply for the area around Gratkorn most unlikely. Today, the fruit supply is not high enough even in evergreen forests for a strictly frugivore feeding of terrestrial frugivores all year long (Smythe 1986). Measurements on other species of the genus, *D. crassum* and *D. vindebonense*, from an intramontane basin (early Middle Miocene locality of Göriach; Austria; ~14.5 Ma \pm 0.3 Ma) also showed generally slightly higher $\delta^{13}\text{C}$ values than other ruminants (Fig. 17a), which could result as well from an ingestion of a considerable amount of fruits. Based on microwear analyses a frugivore browsing diet was reconstructed for *D. naui* from the Late Miocene locality Atzelsdorf (Austria; 11.1 Ma; Merceron 2009). Furthermore, an ingestion of a certain amount of fruits is also supported by the morphology of the incisor arcade of *D. naui* from Gratkorn. The strongly widened i_1 in comparison to i_2 and i_3 observed in *Dorcatherium naui* and in modern Tragulidae points to a more selective feeding strategy. Although limited in its predictions (Fraser and Theodor 2011), disparity in incisor widths is significantly higher in browsers than in grazers (Janis and Ehrhardt 1988; Clauss et al. 2008). Applying these ecomorphological considerations, a more selective picking of perhaps fruits might explain the higher ratio of i_1 width to i_2 or i_3 width of *Dorcatherium* in comparison to the subcanopy browsing cervid, *Euprox furcatus*, while grazing would not fit with the relative incisor width. On the other hand, a mixed diet was reconstructed for the other more selenodont *Dorcatherium* species, *D. guntianum*, from the NAFB by Kaiser and Rössner (2007). Furthermore, Ungar et al. (2012) observed mixed feeding for Early Miocene Tragulidae from Africa. In addition to different diets, a different digestion system or drinking behaviour in *Dorcatherium* could also explain differences in isotopic ratios in comparison to higher ruminants.

In summary, for the moment, we consider *Dorcatherium naui* from Gratkorn a browser with facultative frugivory, but we cannot completely rule out a certain amount of mixed feeding. In any case, the abundance of *D. naui* at Gratkorn indicates a tolerance to less humid environments for the species than assumed for other species of the genus.

Micromeryx flourensianus

With an estimated body mass of about 4–5kg (min.: 3.8kg, max. 5.0kg; n=6), *M. flourensianus* is the smallest ruminant taxa from Gratkorn and was most likely adapted to a more or less closed environment with sufficient understory, as it can be observed for all modern ruminants of this size class (Köhler 1993; Rössner 2010). A pure C3 browsing diet can be assumed for *M. flourensianus*, possibly with slight enrichment with fruits and seeds, resulting in the slightly higher values for $\delta^{13}\text{C}$ and $\delta^{18}\text{O}_{\text{CO}_3}$ in comparison to most of the cervids (Tütken and Vennemann 2009). Although the data from Gratkorn are based on only one individual, the diet reconstruction seems to be quite stable as it fits to isotopic data, and morphologic and microwear analyses of conspecific material from other localities (Köhler 1993; Tütken et al. 2006; Merceron et al. 2007; Merceron 2009; Fig 17a).

Fig. 18: $^{87}\text{Sr}/^{86}\text{Sr}$ isotope compositions from Gratkorn versus body mass (mammals only). Gastropods, the microbialite and small mammals (complete teeth) represent the local ratio for the locality. Most of the large mammals (enamel), especially with larger body mass, show different values from the local ratio due to migration (maybe provoked by limitation of available biomass at the locality). The values are compared to the modern natural mineral water values from Graz (data from Voerkelius et al. 2010), to the range for marine carbonates in general (data from Tütken 2010) and to ratios from measurements on shark teeth and foraminifera from late Karpatian to early Sarmatian sediments from Austria (Bad Vöslau, Leithakalk, Siebenhirten) and Hungary (Danitzpuszta and Himesháza) (data from Hagmaier 2002; Kocsis et al. 2009; VB Vienna Basin; PB Pannonian Basin). Bodymass estimations follow Aiglstorfer et al. (2014d) for ruminants, Costeur et al. (2012) for *Listriodon splendens* and *Prolagus oeningensis*, Aiglstorfer et al. (2014b) and citations therein for *Deinotherium levius vel giganteum*, and Fortelius (2013) for *Parachleuastochoerus steinheimensis*; and is oriented for *Schizogalerix voesendorfensis* on the value for *Schizogalerix* sp. given by Merceron et al. (2012); from Aiglstorfer et al. 2014a

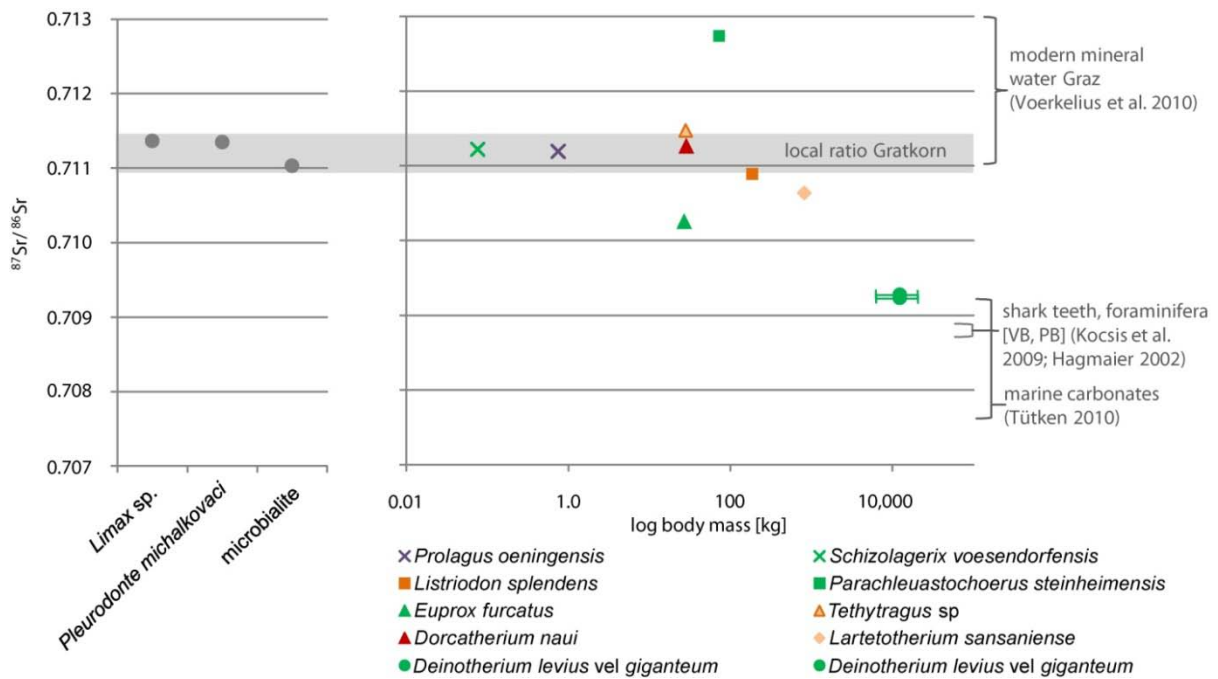
Euprox furcatus

With a body mass of 24–30kg (min: 23.8kg, max: 29.9kg; n=6) and a shoulder height of about 60–70cm, this species was comparable in habitus to the modern red muntjac (*Muntiacus muntjak*; Mattioli 2011). It is assumed that the species possessed the typical sexual dimorphism for cervids with only males displaying cranial appendages (Peters 1871; Heizmann and Reiff 2002) and also indicated by an antlerless articulated *Euprox* vel *Heteroprox* skeleton from Steinheim a. A.. *Euprox furcatus* from Gratkorn generally shows lower values for $\delta^{13}\text{C}$ and $\delta^{18}\text{O}_{\text{CO}_3}$ in comparison to other taxa from Gratkorn (Fig. 16). The lower values in *Euprox furcatus* fit well with an ecological niche comprising mostly subcanopy diet in a more closed, forested C3 environment. The low $\delta^{18}\text{O}_{\text{CO}_3}$ values for *Euprox furcatus* in comparison to other large mammals could also indicate an obligate drinking behaviour (Kohn 1996; Kohn et al. 1996).

Combining literature data with the data from Gratkorn (Fig. 17a) it can be observed that *Euprox furcatus* shows lower values, while *Heteroprox* seems to be more enriched in both $^{18}\text{O}_{\text{CO}_3}$ and ^{13}C . This could be explained by less browsing in subcanopy environment by the latter in comparison to *Euprox furcatus* but a higher degree of mixed feeding. However, occupation of different ecological niches is also dependent on the frame conditions and the number of co-occurring species (DeMiguel et al. 2011) and so far, there is not enough data to define clearly distinct ecological niches for *Euprox furcatus* and *Heteroprox* ssp.. However, the results from Gratkorn and literature data (Tütken et al. 2006; DeMiguel et al. 2011; Domingo et al. 2012) indicate that *Euprox furcatus* rather represents a subcanopy browser and, in the case of co-occurrence with *Heteroprox larteti*, might have displayed a lower degree of mixed feeding than the latter.

Tethytragus sp.

With a body mass of about 27–29kg (min: 27.4kg, max: 29.1kg; n=2), *Tethytragus* sp. from Gratkorn is considered a medium-sized ruminant. It shows the highest value for $\delta^{18}\text{O}_{\text{CO}_3}$ observed in the large mammal fauna of the locality (Fig. 16) well in accordance to literature data on the same genus (Domingo et al. 2012; Fig. 17a). This fits well to feeding on top canopy plants exposed to higher evaporation, as was reconstructed, for example, for *Giraffokeryx* (Giraffidae) from Paşalar by



Bocherens and Sen (1998) and for *Germanomeryx* (Palaeomerycidae) from Sandelzhausen by Tütken and Vennemann (2009). Although smaller in body size than these taxa, a feeding on top canopy plants could have been possible for *Tethytragus* due to a caprine-like postcranial adaptation, which allowed climbing and tree-/rock-jumping to a certain degree (indicated for the Gratkorn specimen due to the morphology of a recorded metatarsal). Adaptation to mountainous areas was shown by Köhler (1993) for *Tethytragus koehlerae* from the Turkish locality of Çandır (Middle Miocene).

5.2. Provenance and migration of large mammals

A detailed migrational history cannot be reconstructed from $^{87}\text{Sr}/^{86}\text{Sr}$ ratios of the large mammals from Gratkorn (Fig. 18). However, it can be observed that *Tethytragus* sp. and *Dorcatherium navi* were more or less local residents and assumably better adapted to the seasonal variations and food supply limitations of the locality. *Parachleuastochoerus steinheimensis* lived at least temporarily in areas with higher $^{87}\text{Sr}/^{86}\text{Sr}$ ratios in bioavailable strontium, as e.g. the Eastern Alpine Mountain Chain. While the other large mammals, *Listriodon splendens* (only to a minor degree), *Lartetotherium sansaniense*, and *Euprox furcatus*, inhabited, at least temporarily, areas with slightly lower $^{87}\text{Sr}/^{86}\text{Sr}$ ratios in bioavailable strontium (early Sarmatian sediments with considerable terrestrial input), *Deinotherium levius vel giganteum* shows the lowest values, fitting well to fully marine early Sarmatian sediments, most likely exposed during the Middle Miocene in the Styrian basin (Fig. 18).

Especially the larger herbivores, such as the proboscidean or the rhinocerotids (see Fig. 18 for bodymasses), were dependent on a large amount of daily food supply and a limitation in the available biomass (at least during some seasons) at the Gratkorn locality might be an explanation for migration of the larger mammals.

6. Summary

The early late Sarmatian Gratkorn locality (12.2/12.0 Ma) yielded a rich large mammal community with so far 14 species of herbivorous large mammals, *Deinotherium levius* vel *giganteum*, *Aceratherium* sp., *Brachypotherium brachypus*, *Lartetotherium sansaniense*, *Chalicotherium goldfussi*, *Anchitherium* sp., *Listriodon splendens*, *Parachleuastochoerus steinheimensis*, *Dorcatherium nauai*, *Micromeryx flourensianus*, *?Hispanomeryx* sp., *Euprox furcatus*, Palaeomerycidae gen. et sp. indet., and *Tethytragus* sp.. The fossil assemblage from Gratkorn is considered to form a more or less autochthonous taphocoenosis without any significant time averaging (or faunal mixing) in terms of geologic resolution (contemporaneously deposited). Most likely the accumulation did not extant a few years or decades and was to a considerable amount the result of scavenging carnivores.

During the late Middle Miocene the Gratkorn locality (bordered by the Eastern Alpine Mountain Chain in the north and the Styrian Basin in the south) was part of an ecosystem with a predominantly C3 vegetation in a semi-arid and subtropical climate with distinct seasonality and too little precipitation (MAP of 486 ± 252 mm and a MAT of less than 15 °C; Böhme and Vasilyan 2014) for a closed canopy woodland. Gastropod, small and large mammal assemblages fit well within such a well-structured, riparian landscape (Gross et al. 2014). It provided enough diversity in plant resources to allow occupation of different niches by herbivorous large mammals (subcanopy browsing, rooting, top canopy browsing, facultative frugivory, and mixed feeding). Niche partitioning among large mammals proved to be stable comparing the data from Gratkorn with data for other localities, distinct in time and space, and seem to reflect a rather typical partitioning in a Middle Miocene faunal assemblage and less dependent on climatic frame conditions.

Most of the large mammals from Gratkorn are typical for a late Middle Miocene faunal assemblage. The presence of the tragulid *Dorcatherium nauai* (more common during the Late Miocene) in contrast is one of the earliest records of this species and the richest assemblage from the Middle Miocene. It provides essential data for an assignation of this species to a more selenodont lineage among Miocene European Tragulidae, well distinct from *D. crassum*, and thus represents a key population for the evaluation of tragulid phylogeny.

Due to the rich record and the well defined frame conditions the Gratkorn locality can be well termed a benchmark locality for the terrestrial deposits from the Sarmatian *sensu stricto* of the Central Paratethys realm (Gross et al. 2011).



Fig. 19: Student excavation at the Gratkorn locality 2012

7. Acknowledgements

First of all I want to thank my supervisors Madelaine Böhme and Hervé Bocherens for giving me the possibility to work on this topic and for their help in excavating, gaining and interpreting the data. Thanks a lot for taking the time for questions or discussions on the thesis or topics reaching far beyond, in getting to know many other scientists from this field, and for supporting me in the participation in conferences, workshops, and all kinds of field excursions.

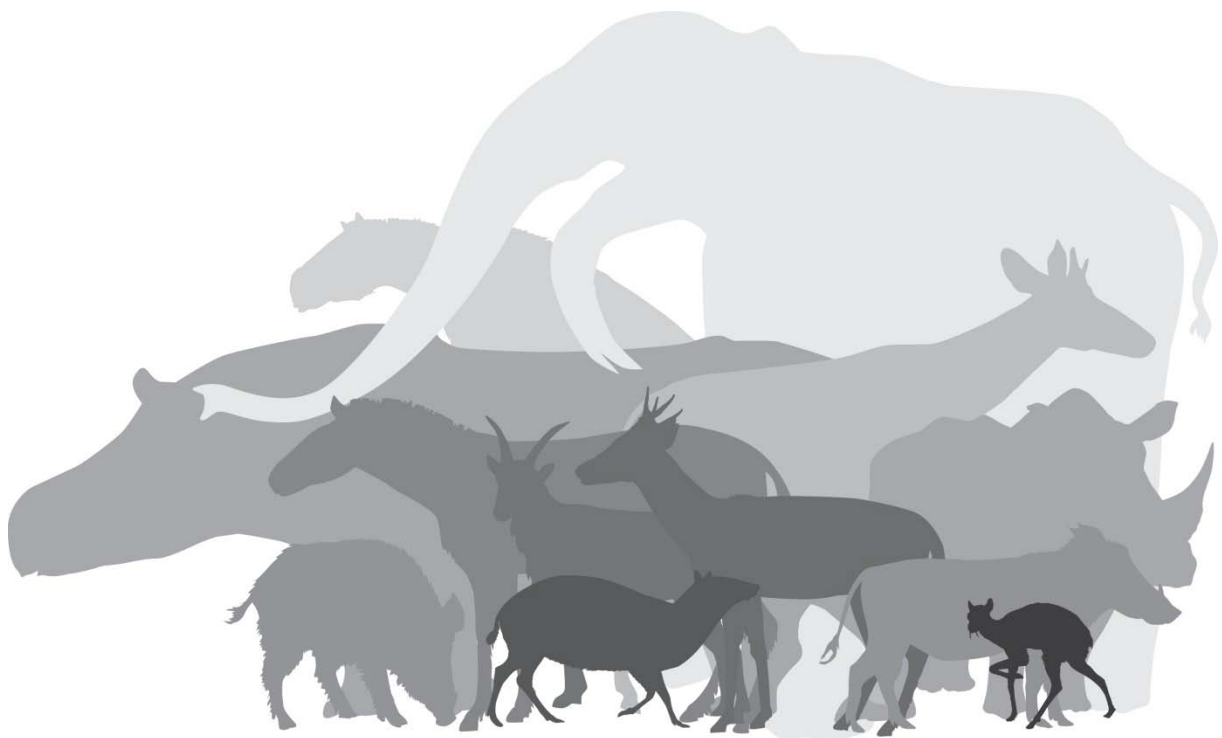
I want to thank both of them for the evaluation of my PhD thesis and Gertrud Rössner and Wilfried Konrad for being members of the defence committee. For the good cooperation I want to thank furthermore my co-authors Ursula Göhlich, Martin Gross, Kurt Heissig, Gertrud Rössner, Philippe Havlik, and Annika Beckmann. It was a pleasure to work with you and I gained and learnt a lot from your experiences. Furthermore, I want to thank the editor-in-chief Peter Königshof and the managing editor Sinje Weber for giving us the possibility to publish our work on the project Gratkorn in the special volume "The Sarmatian vertebrate locality Gratkorn, Styrian Basin" and all the support and endurance during the publication process.

Without our cooperation partner, Universalmuseum Joanneum Graz, this thesis would not have been possible. I want to thank especially Martin Gross, the key person of the Project Gratkorn. Many thanks for the long year excavation prior and during our cooperation, the support with material transport, and the possibility for extended collection visits. Concerning the latter I am greatly indebted also to his colleagues, especially Ingomar Fritz, Reinhold Niederl, Frank Gitter, and Norbert Winkler, for the help during my every year sitting in the UMJGP collection and when I wanted to have a look in the uppermost box on the shelf for the ten-thousandth time. Helmut Reindl assisted substantially during fieldwork and the search for comparison data for isotopic measurements. Excavations at Gratkorn were financially, organisationally and ideally supported by the Marktgemeinde Gratkorn, the fire fighters from Gratkorn, the Land Steiermark, and Universalmuseum Joanneum as well as by many people from Gratkorn. The Wieterdorfer & Peggauer Zementwerke AG enabled access to the pit every year. For the arduous and good work in the field many thanks to all the students and volunteers from Graz, Munich, and Tübingen (Fig. 19). Hans Luginsland, Regina Ellenbracht, Henrik Stöhr, Jochen Fuß, Philippe Havlik, Martin Gross, and especially Norbert Winkler, prepared and/or supported preparation of the specimens. Most of the pictures in the publications related to this thesis were taken by Wolfgang Gerber and Alice Schuhmacher. Many scientists supported this thesis with fruitful discussions and by providing partly unpublished information on diverse topics. Gertrud Rössner (SNSB-BSPG), Günther Scharfe (Montanuniversität Leoben, Leoben, Austria), Reinhard Ziegler (SMNS), Herbert Lutz, Thomas Engel (both (Naturhistorisches Museum Mainz, Mainz, Germany), Harald Stapf (Paläontologisches Museum Nierstein, Nierstein, Germany), Nikolai Spassov, Georgi Markov, Latinka Hristova (all three National Museum of Natural History, Sofia, Bulgaria), Marin Ivanov (Paleontological Museum of Sofia University "St. Kliment Ohridsky", Department of Geology and Paleontology, Sofia, Bulgaria), Michael Rummel (Naturmuseum Augsburg, Augsburg, Germany), Emma Bernard (British Museum of Natural History, London, UK), Doris Nagel (Institut für Paläontologie Universität Wien, Wien, Austria), Loïc Costeur (Naturhistorisches Museum Basel, Basel, Switzerland), Christine Argot (MNHN), David Alba (Institut Català de Paleontologia), Jürgen Rösinger,

Erich Weber (both University Tübingen, Zoological Collection), Philippe Havlik (GPIT), and Martin Gross (UMJGP) are cordially thanked for providing access to collection material. Collection visits were only possible due to the funding of my employer “Senckenberg Gesellschaft für Naturforschung”. Furthermore, I received funding from the SYNTHESYS Project (FR-TAF-1892) which is financed by the European Community Research Infrastructure Action under the FP7 “Capacities” Program. I am greatly indebted to my working group “AG Böhme – Terrestrische Paläoklimatologie” for all the support during the years, from mental support, provision with caffeine products, over help in the search for comparison material, constructive discussions, and tiresome proofreading of the manuscripts. In this context I want to thank especially Annika Beckmann, Sabine Kötter and Adrian Tröscher and above all Philippe Havlik, who had to go through all the mammals from the beginning to the final publications.

I want to thank my friends and colleagues for moral support, their endurance in getting me away from this office at night in many cases. Thanks for all the patience and the help to think of something else sometimes and thanks a lot to Susanne Göb for final proof reading.

And last but not least I want to thank my family, and above all my parents, for all the support literally from the beginning and never questioning the passion of their daughter for non-precious stones. Without you I would never have made it!



“Dang Eich fir ällas!”

8. Reverences

- Abdul Aziz H, Böhme M, Rocholl A, Prieto J, Wijbrans J, Bachtadse V, Ulbig A. (2010): Integrated stratigraphy and $^{40}\text{Ar}/^{39}\text{Ar}$ chronology of the early to middle Miocene Upper Freshwater Molasse in western Bavaria (Germany). *International Journal of Earth Sciences* 99, 1859-1886.
- Abdul Aziz H, Böhme M, Rocholl A, Zwing A, Prieto J, Wijbrans J, Heissig K, Bachtadse V. (2008): Integrated stratigraphy and $^{40}\text{Ar}/^{39}\text{Ar}$ chronology of the Early to Middle Miocene Upper Freshwater Molasse in eastern Bavaria (Germany). *International Journal of Earth Sciences* 97, 115-134.
- Abels HA, Hilgen FJ, Krijgsman W, Kruk RW, Raffi I, Turco E, Zachariasse WJ. (2005): Long-period orbital control on middle Miocene global cooling: Integrated stratigraphy and astronomical tuning of the Blue Clay Formation on Malta. *Paleoceanography* 20, PA4012.
- Aiglstorfer M, Bocherens H, Böhme M. (2014a): Large Mammal Ecology in the late Middle Miocene locality Gratkorn (Austria). *Palaeobiodiversity and Palaeoenvironments* 94, 189-213.
- Aiglstorfer M, Göhlich UB, Böhme M, Gross M. (2014b): A partial skeleton of *Deinotherium* (Proboscidea, Mammalia) from the late Middle Miocene Gratkorn locality (Austria). *Palaeobiodiversity and Palaeoenvironments* 94, 49-70.
- Aiglstorfer M, Heissig K, Böhme M. (2014c): Perissodactyla from the late Middle Miocene Gratkorn locality (Austria). *Palaeobiodiversity and Palaeoenvironments* 94, 71-82.
- Aiglstorfer M, Rössner GE, Böhme M. (2014d): *Dorcatherium naui* and pecoran ruminants from the late Middle Miocene Gratkorn locality (Austria). *Palaeobiodiversity and Palaeoenvironments* 94, 83-123.
- Alba DM, DeMiguel D, Morales J, Sánchez IM, Moyà-Solà S. (2014): New remains of *Dorcatherium crassum* (Artiodactyla: Tragulidae) from the Early Miocene (MN4) of Els Casots (Subirats, Vallès-Penedès Basin). *Comptes Rendus Palevol* 13, 73-86.
- Alba DM, Moyà-Solà S, Robles JM, Casanovas-Vilar I, Rotgers C, Carmona R, Galindo J. (2011): Middle Miocene tragulid remains from Abocador de Can Mata: The earliest record of *Dorcatherium naui* from Western Europe. *Geobios* 44, 135-150.
- Alberdi MT, Ginsburg L, Rodríguez J. (2004): *Anchitherium aurelianense* (Mammalia, Equidae) (Cuvier, 1825) dans l'Orléanien (Miocène) de France. *Geodiversitas* 26, 115-155.
- Alberdi MT, Rodríguez J. (1999): Restos de *Anchitherium* de Lisboa, Portugal. *Ciências da Terra (UNL)* 13, 93-114.
- Alberdi MT, Rodríguez J. (2012): *Anchitherium* Meyer, 1844 (Perissodactyla, Equidae) de Sansan. In: S Peigné and S Sen (Eds), *Mammifères de Sansan*, Mémoires du Muséum national d'Histoire naturelle 203, 487-533.
- Angelone C, Prieto J, Gross M. (2014): Complement to the study of the pikas (Lagomorpha, Ochotonidae) from Gratkorn. *Palaeobiodiversity and Palaeoenvironments* 94, 125-134.
- Anquetin J, Antoine P-O, Tassy P. (2007): Middle Miocene Chalicotheriinae (Mammalia, Perissodactyla) from France, with a discussion on chalicotheriine phylogeny. *Zoological Journal of the Linnean Society* 151, 577-608.

- Anthonissen ED. (2012): A new Miocene biostratigraphy for the northeastern North Atlantic: an integrated foraminiferal, bolboformid, dinoflagellate and diatom zonation. *Newsletters on Stratigraphy* 45, 281-307.
- Antoine P-O, Downing KF, Crochet J-Y, Duranthon F, Flynn LJ, Marivaux L, Métais G, Rajpar AR, Roohi G. (2010): A revision of *Aceratherium blanfordi* Lydekker, 1884 (Mammalia: Rhinocerotidae) from the Early Miocene of Pakistan: postcranials as a key. *Zoological Journal of the Linnean Society* 160, 139-194.
- Antoine PO. (1994): Tendances évolutives de Deinotheriidae (Mammalia, Proboscidea) miocènes du domaine sous-pyrénéen. unpubl. master thesis, Université Paul-Sabatier, Toulouse, 55 p.
- Astibia H. (2012): Les Palaeomerycidae (Artiodactyla) de Sansan. In: S Peigné and S Sen (Eds), *Mammifères de Sansan, Mémoires du Muséum national d'Histoire naturelle* 203, 201-224.
- Azanza B. (2000): Los Cervidae (Artiodactyla, Mammalia) del Mioceno de las cuencas del Duero, Tajo, Calatayud-Teruel y Levante. *Memorias del Museo Paleontológico de la Universidad de Zaragoza* 8, 1-376.
- Azanza B, Morales J. (1994): *Tethytragus* nov. gen. et *Gentrytragus* nov. gen. Deux nouveaux Bovidés (Artiodactyla, Mammalia) du Miocène moyen. Relations phylogénétiques des Bovidés anté-vallésiens. *Proceedings of the Koninklijke Nederlandse Akademie van Wetenschappen Series B* 97, 249-282.
- Badiola A, Berreteaga A, Pereda-Suberbiola X, Elorza J, Astibia H, Etxebarria N. (2009): Taphonomy of vertebrate fossil assemblages from swampy circum-lake environments: An Example from the Late Eocene of Zambrana (Iberian Peninsula). *PALAIOS* 24, 522-534.
- Bajgusheva SV, Titov V. (2006): About teeth of *Deinotherium giganteum* Kaup from eastern Paratethys. *Hellenic Journal of Geosciences* 41, 177-182.
- Becker D, Antoine P-O, Maridet O. (2013): A new genus of Rhinocerotidae (Mammalia, Perissodactyla) from the Oligocene of Europe. *Journal of Systematic Palaeontology* 11, 947-972.
- Bentaleb I, Langlois C, Martin C, Iacumin P, Carré M, Antoine P-O, Duranthon F, Moussa I, Jaeger J-J, Barrett N, Kandorp R. (2006): Rhinocerotid tooth enamel $^{18}\text{O}/^{16}\text{O}$ variability between 23 and 12 Ma in southwestern France. *Comptes Rendus Geoscience* 338, 172-179.
- Bentley AR. (2006): Strontium Isotopes from the Earth to the Archaeological Skeleton: A Review. *Journal of Archaeological Method and Theory* 13, 135-187.
- Bergounioux F-M, Crouzel F. (1962): Les déinothéridés d'Europe. *Annales de Paléontologie* 48, 13-56.
- Bibi F, Güleç ES. (2008): Bovidae (Mammalia: Artiodactyla) from the late Miocene of Sivas, Turkey. *Journal of Vertebrate Paleontology* 28, 501-519.
- Blum JD, Taliaferro EH, Weisse MT, Holmes RT. (2000): Changes in Sr/Ca, Ba/Ca and $^{87}\text{Sr}/^{86}\text{Sr}$ Ratios between Trophic Levels in Two Forest Ecosystems in the Northeastern U.S.A. *Biogeochemistry* 49, 87-101.
- Bocherens H, Koch PL, Mariotti A, Geraads D, Jaeger J-J. (1996): Isotopic biogeochemistry (^{13}C , ^{18}O) of mammalian enamel from African Pleistocene hominid sites. *PALAIOS* 11, 306-318.

- Bocherens H, Sen S. (1998): Pliocene vertebrate locality Calta, Ankara, Turkey. 11. Isotopic investigation. *Geodiversitas* 20, 487-495.
- Böhme M. (2003): The Miocene Climatic Optimum: evidence from ectothermic vertebrates of Central Europe. *Palaeogeography, Palaeoclimatology, Palaeoecology* 195, 389-401.
- Böhme M, Aiglstorfer M, Uhl D, Kullmer O. (2012): The Antiquity of the Rhine River: Stratigraphic Coverage of the *Dinotheriensande* (Eppelsheim Formation) of the Mainz Basin (Germany). *PLoS ONE* 7, e36817.
- Böhme M, Aziz HA, Prieto J, Bachtadse V, Schweigert G. (2011a): Bio-magnetostratigraphy and environment of the oldest Eurasian hominoid from the Early Miocene of Engelswies (Germany). *Journal of Human Evolution* 61, 332-339.
- Böhme M, Ilg A, Winklhofer M. (2008): Late Miocene “washhouse” climate in Europe. *Earth and Planetary Science Letters* 275, 393-401.
- Böhme M, Vasilyan D. (2014): Ectothermic vertebrates from the late Middle Miocene of Gratkorn (Austria, Styria). *Palaeobiodiversity and Palaeoenvironments* 94, 21-40.
- Böhme M, Winklhofer M, Ilg A. (2011b): Miocene precipitation in Europe: Temporal trends and spatial gradients. *Palaeogeography, Palaeoclimatology, Palaeoecology* 304, 212-218.
- Casanovas-Vilar I, Alba DM, Garcés M, Robles JM, Moyà-Solà S. (2011): Updated chronology for the Miocene hominoid radiation in Western Eurasia. *Proceedings of the National Academy of Sciences* 108, 5554-5560.
- Casanovas-Vilar I, Hoek Ostende van den L, Furió M, Madern PA. (2014): The range and extent of the Vallesian Crisis (Late Miocene): new prospects based on the micromammal record from the Vallès-Penedès basin (Catalonia, Spain). *Journal of Iberian Geology* 40, 29-48.
- Cerdeño E. (1993): Étude sur *Diaceratherium aurelianense* et *Brachypotherium brachypus* (Rhinocerotidae, Mammalia) du Miocène moyen de France. *Bulletin du Muséum National d'Histoire Naturelle* 4, 25-77.
- Clauss M, Kaiser T, Hummel J. (2008): The Morphophysiological Adaptations of Browsing and Grazing Mammals. In: I Gordon and HT Prins (Eds), *The Ecology of Browsing and Grazing*, Ecological Studies Springer Berlin Heidelberg, 47-88.
- Clementz MT, Holroyd PA, Koch PL. (2008): Identifying Aquatic Habits Of Herbivorous Mammals Through Stable Isotope Analysis. *PALAIOS* 23, 574-585.
- Cohen KM, Finney SM, Gibbard PL, Fan J-X. (2013): The ICS International Chronostratigraphic Chart. *Episodes* 36, 199-204.
- Coombs MC. (1989): Interrelationships and Diversity in the Chalicotheriidae. In: DR Prothero and RM Schoch (Eds), *The Evolution of Perissodactyls*, New York Oxford, Clarendon Press Oxford University Press, 438-457.
- Costeur L, Guérin C, Maridet O. (2012): Paléoécologie et paléoenvironnement du site miocène de Sansan. In: S Peigné and S Sen (Eds), *Mammifères de Sansan*, Mémoires du Muséum national d'Histoire naturelle 203, 661-693.
- Costeur L, Maridet O, Montuire S, Legendre S. (2013): Evidence of northern Turolian savanna-woodland from the Dorn-Dürkheim 1 fauna (Germany). *Palaeobiodiversity and Palaeoenvironments* 93, 259-275.

- Czyżewska T, Stefaniak K. (1994): *Euprox furcatus* (HENSEL, 1859) (Cervidae, Mammalia) from Przeworno (Middle Miocene, Lower Silesia, Poland). *Acta zoologica cracoviensia* 37, 55-74.
- Daxner-Höck G. (2010): Sciuridae, Gliridae and Eomyidae (Rodentia, Mammalia) from the Middle Miocene of St. Stefan in the Gratkorn Basin (Styria, Austria). *Annalen des Naturhistorischen Museums in Wien* 112A, 507-536.
- Dehm. (1960): Zur Frage der Gleichaltrigkeit bei fossilen Säugerfaunen. *Geologische Rundschau* (now: *International Journal of Earth Sciences*) 49, 36-40.
- DeMiguel D, Azanza B, Morales J. (2011): Paleoenvironments and paleoclimate of the Middle Miocene of central Spain: A reconstruction from dental wear of ruminants. *Palaeogeography, Palaeoclimatology, Palaeoecology* 302, 452-463.
- DeNiro MJ, Epstein S. (1978): Influence of diet on the distribution of carbon isotopes in animals. *Geochimica et Cosmochimica Acta* 42, 495–506.
- Domingo L, Cuevas-González J, Grimes ST, Hernández Fernández M, López-Martínez N. (2009): Multiproxy reconstruction of the palaeoclimate and palaeoenvironment of the Middle Miocene Somosaguas site (Madrid, Spain) using herbivore dental enamel. *Palaeogeography, Palaeoclimatology, Palaeoecology* 272, 53-68.
- Domingo L, Koch PL, Grimes ST, Morales J, López-Martínez N. (2012): Isotopic paleoecology of mammals and the Middle Miocene Cooling event in the Madrid Basin (Spain). *Palaeogeography, Palaeoclimatology, Palaeoecology* 339–341, 98-113.
- Dubost G. (1978): Un aperçu sur l'écologie du chevrotain africain *Hyemoschus aquaticus* Ogilby, Artiodactyle Tragulidé. *Mammalia* 42, 1-61.
- Dubost G. (1984): Comparison of the diets of frugivorous forest ruminants of Gabon. *Journal of Mammalogy* 65, 298-316.
- Duranthon F, Antoine PO, Laffont D, Bilotte M. (2007): Contemporanéité de *Prodeinotherium* et *Deinotherium* (Mammalia, Proboscidea) à Castelnaud-Magnoac (Hautes Pyrénées, France). *Revue de Paléobiologie* 26, 403–411.
- Ecker M, Bocherens H, Julien M-A, Rivals F, Raynal J-P, Moncel M-H. (2013): Middle Pleistocene ecology and Neanderthal subsistence: Insights from stable isotope analyses in Payre (Ardèche, southeastern France). *Journal of Human Evolution* 65, 363-373.
- Eronen JT, Rössner GE. (2007): Wetland paradise lost: Miocene community dynamics in large herbivorous mammals from the German Molasse Basin. *Evolutionary Ecology Research* 9, 471-494.
- Fahlbusch V. (1985): Säugetierreste (*Dorcatherium*, *Steneofiber*) aus der miozänen Braunkohle von Wackersdorf/Oberpfalz. *Mitteilungen der Bayerischen Staatssammlung für Paläontologie und historische Geologie* 25, 81-94.
- Fahlke J, Coombs M, Semprebon G. (2013): *Anisodon* sp. (Mammalia, Perissodactyla, Chalicotheriidae) from the Turolian of Dorn-Dürkheim 1 (Rheinessen, Germany): morphology, phylogeny, and palaeoecology of the latest chalicothere in Central Europe. *Palaeobiodiversity and Palaeoenvironments* 93, 151-170.

- Flügel HW, Hubmann B. (2000): Das Paläozoikum von Graz: Stratigraphie und Bibliographie. Österreichische Akademie der Wissenschaften, Schriftenreihe der erdwissenschaftlichen Kommissionen 13, 1-118.
- Flügel HW, Nowotny A, Gross M. (2011): Geologische Karte der Republik Österreich 1:50000. Blatt 164 Graz.
- Fortelius M. (2013): New and Old Worlds Database of Fossil Mammals (NOW). dataset downloaded September 22, 2013. University of Helsinki. <http://www.helsinki.fi/science/now/>.
- Fortelius M. (2014): New and Old Worlds Database of Fossil Mammals (NOW). dataset downloaded March 6, 2014. University of Helsinki. <http://www.helsinki.fi/science/now/>.
- Fraser D, Theodor JM. (2011): Anterior dentary shape as an indicator of diet in ruminant artiodactyls. *Journal of Vertebrate Paleontology* 31, 1366-1375.
- Frisch W, Kuhlemann J, Dunkl I, Brügel A. (1998): Palinspastic reconstruction and topographic evolution of the Eastern Alps during the late Tertiary extrusion. *Tectonophysics* 297, 1-15.
- Gasparik M. (1993): Deinotheres (Proboscidea, Mammalia) of Hungary. *Annales Historico-Naturales Musei Nationalis Hungarici* 85, 3-17.
- Gasparik M. (2001): Neogene proboscidean remains from Hungary; an overview. *Fragmenta Palaeontologica Hungarica* 19, 61-77.
- Gentry AW, Rössner G, Heizmann EPJ. (1999): Suborder Ruminantia. In: G Rössner and K Heissig (Eds), *The Miocene land mammals of Europe*, München, Verlag Dr. Friedrich Pfeil, 225-253.
- Geraads D, Kaya T, Mayda S. (2005): Late Miocene large mammals from Yulafli, Thrace region, Turkey, and their biogeographic implications. *Acta Palaeontologica Polonica* 50, 523-544.
- Geraads D, Saraç G. (2003): Rhinocerotidae from the Middle Miocene Hominoid Locality of Çandır (Turkey). *Courier Forschungsinstitut Senckenberg* 240, 217-231.
- Ginsburg L, Bulot C. (1984): Les Rhinocerotidae (Perissodactyla, Mammalia) du Miocène de Bézian à La Romieu (Gers). *Bulletin du Muséum National d'Histoire Naturelle* 6, 353-377.
- Ginsburg L, Chevrier F. (2001): Les Dinotheres du bassin de la Loire et l'évolution du genre *Deinotherium* en France. *Symbioses* 5, 9-24.
- Glazek J, Oberc J, Sulimski A. (1971): Miocene vertebrate faunas from Przeworno (Lower Silesia) and their geological setting. *Acta Geologica Polonica* 21, 473-516.
- Göhlich UB, Gross M. (2014): The Sarmatian (late Middle Miocene) avian Fauna from Gratkorn, Austria. *Palaeobiodiversity and Palaeoenvironments* 94, 41-48.
- Gräf IE. (1957): Die Prinzipien der Artbestimmung bei *Deinotherium*. *Palaeontographica A* 108, 131-185.
- Gross M. (1999): Die phytopaläontologische Sammlung Franz Unger am Landesmuseum Joanneum. *Joannea* 1, 5-26.
- Gross M. (2008): A limnic ostracod fauna from the surroundings of the Central Paratethys (Late Middle Miocene/Early Late Miocene; Styrian Basin; Austria). *Palaeogeography, Palaeoclimatology, Palaeoecology* 264, 263-276.
- Gross M, Böhme M, Havlik P, Aiglstorfer M. (2014): The late Middle Miocene (Sarmatian s.str.) Fossilagerstätte Gratkorn – First decade of research, geology, stratigraphy and vertebrate fauna. *Palaeobiodiversity and Palaeoenvironments* 94, 5-20.

- Gross M, Böhme M, Prieto J. (2011): Gratkorn: A benchmark locality for the continental Sarmatian s.str. of the Central Paratethys. *International Journal of Earth Sciences* 100, 1895-1913.
- Gross M, Fritz I, Piller WE, Soliman A, Harzhauser M, Hubmann B, Moser B, Scholger R, Suttner T, Bojar H-P. (2007a): The Neogene of the Styrian Basin - Guide to Excursions. *Joannea* 9, 117-193.
- Gross M, Harzhauser M, Mandic O, Piller WE, Rögl F. (2007b): A Stratigraphic Enigma: The age of the Neogene deposits of Graz (Styrian Basin; Austria). *Joannea* 9, 195–220.
- Gross M, Martin J. (2008): From the Palaeontological Collection of the Provincial Museum Joanneum - The fossil Crocodylians (Crocodylia). *Joannea* 10, 91-125.
- Hagmaier M. (2002): Isotopie (C, O und Sr) von Foraminiferen der zentralen nördlichen Paratethys (Bayerische Molasse, Wiener Becken) im Miozän als paläozeanographische Proxies. Diploma Thesis, Eberhard Karls Universität Tübingen, Tübingen, 69 p.
- Harris JM. (1973): *Prodeinotherium* from Gebel Zelten, Libya. *Bulletin of the British Museum (Natural History), Geology* 23, 285-350.
- Harzhauser M, Gross M, Binder H. (2008): Biostratigraphy of Middle Miocene (Sarmatian) wetland systems in an Eastern Alpine intramontane basin (Gratkorn Basin, Austria): the terrestrial gastropod approach. *Geologica Carpathica* 59, 45-58.
- Harzhauser M, Kroh A, Mandic O, Piller WE, Göhlich U, Reuter M, Berning B. (2007): Biogeographic responses to geodynamics: A key study all around the Oligo–Miocene Tethyan Seaway. *Zoologischer Anzeiger - A Journal of Comparative Zoology* 246, 241-256.
- Harzhauser M, Piller WE. (2007): Benchmark data of a changing sea — Palaeogeography, Palaeobiogeography and events in the Central Paratethys during the Miocene. *Palaeogeography, Palaeoclimatology, Palaeoecology* 253, 8-31.
- Havlik P, Aiglstorfer M, Beckman A, Gross M, Böhme M. (2014): Taphonomical and ichnological considerations on the late Middle Miocene Gratkorn locality (Styria, Austria) with focus on large mammal taphonomy. *Palaeobiodiversity and Palaeoenvironments* 94, 171-188.
- Heissig K. (1976): Rhinocerotidae (Mammalia) aus der *Anchitherium*-Fauna Anatoliens. *Geologisches Jahrbuch B* 19, 3-121.
- Heissig K. (1999): Family Rhinocerotidae. In: GE Rössner and K Heissig (Eds), *The Miocene Land Mammals of Europe*, Munich, Verlag Dr. Friedrich Pfeil, 175-188.
- Heissig K. (2009): The early Vallesian vertebrates of Atzelsdorf (Late Miocene, Austria) 11. Rhinocerotidae and Chalicotheriidae (Perissodactyla). *Annalen des Naturhistorischen Museums in Wien* 111 A, 619-634.
- Heissig K. (2012): Les Rhinocerotidae (Perissodactyla) de Sansan. In: S Peigné and S Sen (Eds), *Mammifères de Sansan, Mémoires du Muséum national d'Histoire naturelle* 203, 317-485.
- Heizmann EPJ. (1984): *Deinotherium* im Unter-Miozän von Langenau und seine Bedeutung für die Untergliederung der Molasse. In: H-J Gregor (Eds), *August-Wetzler-Gedenkband Molasseforschung '84, Günzburg, Historischer Verein Günzburg e.V.*, 36-39.
- Heizmann EPJ, Reiff W. (2002): *Der Steinheimer Meteorkrater*. München, Verlag Dr. Friedrich Pfeil, 160 p.

- Herwartz D, Tütken T, Jochum KP, Sander PM. (2013): Rare earth element systematics of fossil bone revealed by LA-ICPMS analysis. *Geochimica et Cosmochimica Acta* 103, 161-183.
- Hillenbrand V, Göhlich UB, Rössner GE. (2009): The early Vallesian vertebrates of Atzelsdorf (Late Miocene, Austria) 7. Ruminantia. *Annalen des Naturhistorischen Museums in Wien* 111A, 519-556.
- Hoppe KA, Koch PL, Carlson RW, Webb SD. (1999): Tracking mammoths and mastodons: Reconstruction of migratory behavior using strontium isotope ratios. *Geology* 27, 439-442.
- Hünemann KA. (1989): Die Nashornskelette (*Aceratherium incisivum* Kaup 1832) aus dem Jungtertiär vom Höwenegg im Hegau (Südwestdeutschland). *andrias* 6, 5-116.
- Hünemann KA. (1999): Superfamily Suidea. In: GE Rössner and K Heissig (Eds), *Land Mammals of Europe*, München, Fritz Pfeil Verlag, 209-216.
- Huttunen KJ. (2000): Deinotheriidae (Proboscidea, Mammalia) of the Miocene of Lower Austria, Burgenland and Czech Republic: Systematics, Odontology and Osteology. unpubl. PhD thesis, Universität Wien, Wien, 98 p.
- Huttunen KJ. (2002a): Systematics and Taxonomy of the European Deinotheriidae (Proboscidea, Mammalia). *Annalen des Naturhistorischen Museums Wien* 103A, 237-250.
- Huttunen KJ. (2002b): Deinotheriidae (Proboscidea, Mammalia) dental remains from the Miocene of Lower Austria and Burgenland. *Annalen des Naturhistorischen Museums Wien* 103A, 251-285.
- Huttunen KJ. (2004): On a *Prodeinotherium bavaricum* (Proboscidea, Mammalia) skeleton from Franzensbad, Czech Republic. *Annalen des Naturhistorischen Museums Wien* 105A, 333-361.
- Huttunen KJ, Göhlich UB. (2002): A partial skeleton of *Prodeinotherium bavaricum* (Proboscidea, Mammalia) from the Middle Miocene of Unterzolling (Upper Freshwater Molasse, Germany). *Geobios* 35 489–514.
- Iñigo C. (1997): *Anchitherium corcolense* nov. sp., a new anchitherine (Equidae, Mammalia) from the Early Aragonian site of Córcoles (Guadalajara, Spain). *Geobios* 30, 849-869.
- Janis CM, Ehrhardt D. (1988): Correlation of relative muzzle width and relative incisor width with dietary preference in ungulates. *Zoological Journal of the Linnean Society* 92, 267-284.
- Kaiser TM, Rössner GE. (2007): Dietary resource partitioning in ruminant communities of Miocene wetland and karst palaeoenvironments in Southern Germany. *Palaeogeography, Palaeoclimatology, Palaeoecology* 252, 424-439.
- Kälin D, Kempf O. (2009): High-resolution stratigraphy from the continental record of the Middle Miocene Northern Alpine Foreland Basin of Switzerland. *Neues Jahrbuch für Geologie und Paläontologie - Abhandlungen* 254, 177-235.
- Kaup JJ. (1832-1839): Description d'ossements fossiles de Mammifères inconnus jusqu'à présent, qui se trouvent au Muséum grand-ducal de Darmstadt, cinquième cahier. Darmstadt, J.P. Diehl, 119 p.
- Kaup JJ. (1833): Darmstadt, 2. Juli 1833 [letter to Bronn]. *Neues Jahrbuch für Mineralogie, Geognosie, Geologie und Petrefaktenkunde* 419–420.
- Klaus S, Gross M. (2007): The Neogene Freshwater Crabs of Europe. *Joannea* 9, 45-46.

- Klaus S, Gross M. (2010): Synopsis of the fossil freshwater crabs of Europe (Brachyura: Potamoidea: Potamidae). *Neues Jahrbuch für Geologie und Paläontologie - Abhandlungen* 256, 39-59.
- Kocsis L, Trueman CN, Palmer MR. (2010): Protracted diagenetic alteration of REE contents in fossil bioapatites: Direct evidence from Lu–Hf isotope systematics. *Geochimica et Cosmochimica Acta* 74, 6077-6092.
- Kocsis L, Vennemann TW, Hegner E, Fontignie D, Tütken T. (2009): Constraints on Miocene oceanography and climate in the Western and Central Paratethys: O-, Sr-, and Nd-isotope compositions of marine fish and mammal remains. *Palaeogeography, Palaeoclimatology, Palaeoecology* 271, 117-129.
- Köhler M. (1987): Boviden des türkischen Miozäns (Känozoikum und Braunkohlen der Türkei. 28). *Paleontologia i Evolució* 21, 133-246.
- Köhler M. (1993): Skeleton and Habitat of recent and fossil Ruminants. *Münchner Geowissenschaftliche Abhandlungen* 25, 1-87.
- Kohn MJ. (1996): Predicting animal $\delta^{18}\text{O}$: Accounting for diet and physiological adaptation. *Geochimica et Cosmochimica Acta* 60, 4811-4829.
- Kohn MJ, Schoeninger MJ, Valley JW. (1996): Herbivore tooth oxygen isotope compositions: Effects of diet and physiology. *Geochimica et Cosmochimica Acta* 60, 3889-3896.
- Kováč M, Sliva Lu, Sopková B, Hlavatá J, Škulová A. (2008): Serravallian sequence stratigraphy of the northern Vienna Basin: high frequency cycles in the Sarmatian sedimentary record. *Geologica Carpathica* 59, 545-561.
- Kovachev D, Nikolov I. (2006): *Deinotherium thraceiense* sp. nov. from the Miocene near Ezerovo, Plovdiv District. *Geologica Balcanica* 35, 5-40.
- Kowal-Linka M, Jochum KP, Surmik D. (2014): LA-ICP-MS analysis of rare earth elements in marine reptile bones from the Middle Triassic bonebed (Upper Silesia, S Poland): Impact of long-lasting diagenesis, and factors controlling the uptake. *Chemical Geology* 363, 213-228.
- Kuhlemann J. (2007): Paleogeographic and paleotopographic evolution of the Swiss and Eastern Alps since the Oligocene. *Global and Planetary Change* 58, 224-236.
- Leinders JJM. (1979): On the osteology and function of the digits of some ruminants and their bearing on taxonomy. *Zeitschrift für Säugetierkunde - International Journal of Mammalian Biology* 44, 305-318.
- Levin NE, Cerling TE, Passey BH, Harris JM, Ehleringer JR. (2006): A stable isotope aridity index for terrestrial environments. *Proceedings of the National Academy of Sciences* 103, 11201-11205.
- Lirer F, Harzhauser M, Pelosi N, Piller WE, Schmid HP, Sprovieri M. (2009): Astronomically forced teleconnection between Paratethyan and Mediterranean sediments during the Middle and Late Miocene. *Palaeogeography, Palaeoclimatology, Palaeoecology* 275, 1-13.
- Longinelli A. (1984): Oxygen isotopes in mammal bone phosphate: A new tool for paleohydrological and paleoclimatological research? *Geochimica et Cosmochimica Acta* 48, 385-390.
- Lukeneder S, Zuschin M, Harzhauser M, Mandic O. (2011): Spatiotemporal signals and palaeoenvironments of endemic molluscan assemblages in the marine system of the Sarmatian Paratethys. *Acta Palaeontologica Polonica* 56, 767-784.

- Luz B, Kolodny Y, Horowitz M. (1984): Fractionation of oxygen isotopes between mammalian bone-phosphate and environmental drinking water. *Geochimica et Cosmochimica Acta* 48, 1689-1693.
- Lyman RL. (1994): *Vertebrate Taphonomy*. Cambridge, University Press, 524 p.
- Made Jvd. (1989): The bovid *Pseudoeotragus seegrabensis* nov. gen., nov. sp. from the Aragonian (Miocene) of Seegraben near Leoben (Austria). *Proceedings of the Koninklijke Nederlandse Akademie van Wetenschappen Series B* 92, 215-240.
- Made Jvd. (1996): Listriodontinae (Suidae, Mammalia), their evolution, systematics and distribution in time and space. *Contributions to Tertiary and Quaternary geology* 33, 1-160.
- Made Jvd. (2012): *Eotragus clavatus* (Artiodactyla, Bovidae, Boselaphini) de Sansan. In: S Peigné and S Sen (Eds), *Mammifères de Sansan, Mémoires du Muséum national d'Histoire naturelle* 203, 145-199.
- Made Jvd, Prieto J, Aiglstorfer M, Böhme M, Gross M. (in press): Taxonomic study of the pigs (Suidae, Mammalia) from the late Middle Miocene of Gratkorn (Austria, Styria). *Palaeobiodiversity and Palaeoenvironments*
- Markov GN. (2008a): Fossil proboscideans (Mammalia) from the vicinities of Varna: a rare indication of middle Miocene vertebrate fauna in Bulgaria. *Historia naturalis bulgarica* 19, 137-152.
- Markov GN. (2008b): The Turolian proboscideans (Mammalia) of Europe: preliminary observations. . *Historia naturalis bulgarica* 19, 153–178.
- Mattioli S. (2011): Cervidae. In: DE Wilson and R Mittermeier (Eds), *Handbook of the Mammals of the World*, Madrid, Lynx Edicions, 350-443.
- Maurer A-F, Galer SJG, Knipper C, Beierlein L, Nunn EV, Peters D, Tütken T, Alt KW, Schöne BR. (2012): Bioavailable $^{87}\text{Sr}/^{86}\text{Sr}$ in different environmental samples — Effects of anthropogenic contamination and implications for isoscapes in past migration studies. *Science of The Total Environment* 433, 216-229.
- Mein P, Ginsburg L. (2002): Sur l'âge relatif des différents dépôts karstiques miocènes de la Grive-Saint-Alban (Isère). *2/2002*, 7-41.
- Meller B, Gross M. (2006): An important piece of stratigraphic puzzle? *Podocarpium podocarpum* (A. Braun) Herendeen from the Styrian Basin (Miocene). *Pangeo Austria*. 194-195. Innsbruck University Press.
- Merceron G. (2009): The early Vallesian vertebrates of Atzelsdorf (Late Miocene, Austria) 13. Dental wear patterns of herbivorous ungulates as ecological indicators. *Annalen des Naturhistorischen Museums Wien* 111A, 647-660.
- Merceron G, Costeur L, Maridet O, Ramdarshan A, Göhlich UB. (2012): Multi-proxy approach detects heterogeneous habitats for primates during the Miocene climatic optimum in Central Europe. *Journal of Human Evolution* 63, 150-161.
- Merceron G, Schulz E, Kordos L, Kaiser TM. (2007): Paleoenvironment of *Dryopithecus brancoi* at Rudabánya, Hungary: evidence from dental meso- and micro-wear analyses of large vegetarian mammals. *Journal of Human Evolution* 53, 331-349.

- Morales J, Sánchez IM, Quiralte V. (2012): Les Tragulidae (Artiodactyla) de Sansan. In: S Peigné and S Sen (Eds), Mammifères de Sansan, Mémoires du Muséum national d'Histoire naturelle 203, 225-247.
- Mottl M. (1957): Bericht über die neuen Menschenaffenfunde aus Österreich, von St. Stefan im Lavanttal, Kärnten. Carinthia II, 39-84.
- Mottl M. (1961): Die Dorcatherien der Steiermark. Mitteilungen des Museums für Bergbau, Geologie und Technik, Landesmuseum Joanneum Graz 22, 21–71.
- Mottl M. (1969): Die Säugetierfunde von St. Oswald bei Gratwein, westlich von Graz in der Steiermark. In: B Sutter (Eds), Festschrift 150 Jahre Joanneum, 1811-1961, Graz, 299-320.
- Mourik AA, Abels HA, Hilgen FJ, Di Stefano A, Zachariasse WJ. (2011): Improved astronomical age constraints for the middle Miocene climate transition based on high-resolution stable isotope records from the central Mediterranean Maltese Islands. *Paleoceanography* 26, PA1210.
- Moyà-Solà S. (1979): Estudio de *Dorcatherium naui* Kaup 1833, de las cuencas del Vallés (Barcelona) y de la Seu d'Urgell (Lleida), y su esqueleto locomotor. Interpretación ecológico-funcional. unpubl. master thesis, Universidad de Barcelona, Barcelona, 227 p.
- Musil R. (1997): A *Dinotherium* Skeleton from Česká Třebová. *Acta Musei Moraviae Scientiae Geologicae* 82, 105-122.
- Palmqvist P, Arribas A. (2001): Taphonomic decoding of the paleobiological information locked in a lower Pleistocene assemblage of large mammals. *Paleobiology* 27, 512-530.
- Peters KF. (1871): Über Reste von *Dinotherium* aus der obersten Miozänstufe der südlichen Steiermark. Mitteilungen des Naturwissenschaftlichen Vereins für Steiermark 2, 367-399.
- Pickford M, Pourabrishami Z. (2013): Deciphering Dinotheriensande deinotheriid diversity. *Palaeobiodiversity and Palaeoenvironments* 93, 121-150.
- Prieto J, Angelone C, Casanovas-Vilar I, Gross M, Hír J, Hoek Ostende van den L, Maul LC, Vasilyan D. (2014a): The small mammals from Gratkorn: an overview. *Palaeobiodiversity and Palaeoenvironments* 94, 135-162.
- Prieto J, Böhme M, Gross M. (2010a): The cricetid rodents from Gratkorn (Austria, Styria): a benchmark locality for the continental Sarmatian *sensu stricto* (late Middle Miocene) in the Central Paratethys. *Geologica Carpathica* 61, 419-436.
- Prieto J, Casanovas-Vilar I, Gross M. (2014b): *Euroxenomys minutus minutus* (Rodentia, Castoridae) from Gratkorn (Austria, Styria). *Palaeobiodiversity and Palaeoenvironments* 94, 163-170.
- Prieto J, Gross M, Böhmer C, Böhme M. (2010b): Insectivores and bat (Mammalia) from the late Middle Miocene of Gratkorn (Austria): biostratigraphic and ecologic implications. *Neues Jahrbuch für Geologie und Paläontologie, Abhandlungen* 258, 107-119.
- Rasser MW, Harzhauser M, Anistratenko OY, Anistratenko VV, Bassi D, Belak M, Berger J-P, Bianchini G, Čičić S, Ćosović V, Doláková N, Drobne K, Filipescu S, Gürs K, Hladilová Š, Hrvatović H, Jelen B, Kasiński JR, Kováč M, Kralj P, Marjanac T, Márton E, Mietto P, Moro A, Nagymarosy A, Nebelsick JH, Nehyba S, Ogorelec B, Oszczypko N, Pavelić D, Pavlovec R, Pavšič J, Petrova P, Piwocki M, Poljak M, Pugliese N, Redžepović R, Rifelj H, Roetzel R, Skaberne D, Sliva Lu, Standke G, Tunis G, Vass D, Wagreich M, Wesselingh F. (2008): 17 Palaeogene and Neogene. In: T McCann (Eds), *The Geology of Central Europe Volume 2*:

Mesozoic and Cenozoic, The Geology of Central Europe London, The Geological Society, 1031-1139.

- Reichenbacher B, Krijgsman W, Lataster Y, Pippèrr M, Van Baak C, G. C. , Chang L, Kälin D, Jost J, Doppler G, Jung D, Prieto J, Aziz HA, Böhme M, Garnish J, Kirscher U, Bachtadse V. (2013): A new magnetostratigraphic framework for the Lower Miocene (Burdigalian/Ottnangian, Karpatian) in the North Alpine Foreland Basin. *Swiss Journal of Geosciences* 106, 309-334.
- Rögl F. (1998): Palaeogeographic Considerations for Mediterranean and Paratethys Seaways (Oligocene to Miocene). *Annalen des Naturhistorischen Museums in Wien* 99A, 279-310.
- Rössner G, Heissig K. (2013): New records of *Dorcatherium guntianum* (Tragulidae), stratigraphical framework, and diphyletic origin of European tragulids. *Swiss Journal of Geosciences (SJG)* 106, 335-347.
- Rössner GE. (1995): Odontologische und schädelanatomische Untersuchungen an *Procervulus* (Cervidae, Mammalia). *Münchner Geowissenschaftliche Abhandlungen A* 29, 127.
- Rössner GE. (2006): A community of Middle Miocene Ruminantia (Mammalia, Artiodactyla) from the German Molasse Basin. *Palaeontographica A* 277, 103-112.
- Rössner GE. (2007): Family Tragulidae. In: DR Prothero and SE Foss (Eds), *The evolution of artiodactyls*, Baltimore, The Johns Hopkins University Press, 213-220.
- Rössner GE. (2010): Systematics and palaeoecology of Ruminantia (Artiodactyla, Mammalia) from the Miocene of Sandelzhausen (southern Germany, Northern Alpine Foreland Basin). *Paläontologische Zeitschrift* 84, 123-162.
- Sach VJ. (1999): Litho- und biostratigraphische Untersuchungen in der Oberen Süßwassermolasse des Landkreises Biberach a. d. Riß (Oberschwaben). *Stuttgarter Beiträge zur Naturkunde Serie B (Geologie und Paläontologie)* 276, 1-167.
- Sachsenhofer RF. (2000): Geodynamic Controls on Deposition and Maturation of Coal in the Eastern Alps. *Mitteilungen der Österreichischen Geologischen Gesellschaft* 92 (1999), 185-194.
- Sachsenhofer RF, Gruber W, Dunkl I. (2010): Das Miozän der Becken von Leoben und Fohnsdorf - The Miocene Leoben and Fohnsdorf Basins. *Journal of Alpine Geology* 53, 9-38.
- Salesa MJ, Sánchez IM, Morales J. (2004): Presence of the Asian horse *Sinohippus* in the Miocene of Europe. *Acta Palaeontologica Polonica* 49, 189-196.
- Sánchez IM, Morales J. (2008): *Micromeryx azanzae* sp. nov. (Ruminantia: Moschidae) from the middle-upper Miocene of Spain, and the first description of the cranium of *Micromeryx*. *Journal of Vertebrate Paleontology* 28, 873-885.
- Sánchez IM, Quiralte V, Morales J. (2011): Solving an old dispute: Anatomical differences between the European Miocene Chevrotains *Dorcatherium crassum* LARTET, 1839 and *Dorcatherium nauti* KAUP & SCHOLL, 1834 (Mammalia, Ruminantia, Tragulidae). *Paleontologia i Evolució, Mem Espec* 5, 343-347.
- Schaefer H, Zapfe H. (1971): *Chalicotherium grande* Blainv. und *Chalicotherium goldfussi* Kaup. Odontologische und osteologische Unterschiede. *Verhandlungen der Naturforschenden Gesellschaft in Basel* 81, 157-199.

- Schreilechner MG, Sachsenhofer RF. (2007): High Resolution Sequence Stratigraphy in the Eastern Styrian Basin (Miocene, Austria). *Austrian Journal of Earth Sciences* 100, 164-184.
- Shevenell AE, Kennett JP, Lea DW. (2004): Middle Miocene Southern Ocean Cooling and Antarctic Cryosphere Expansion. *Science* 305, 1766-1770.
- Smythe N. (1986): Competition and Resource Partitioning in the Guild of Neotropical Terrestrial Frugivorous Mammals. *Annual Review of Ecology and Systematics* 17, 169-188.
- Sponheimer M, Lee-Thorp J. (2001): The oxygen isotope composition of mammalian enamel carbonate from Morea Estate, South Africa. *Oecologia* 126, 153-157.
- Stefanescu G. (1894): *Dinotherium gigantissimum*. *Annuarulu Museului de Geologia si de Paleontologia* 1894, 126-199.
- Stehlin HG. (1928): Bemerkungen über die Hirsche von Steinheim am Albuch. *Eclogae geologicae Helvetiae* 21, 245-256.
- Steininger FF, Wessely G. (2000): From the Tethyan Ocean to the Paratethys Sea: Oligocene to Neogene Stratigraphy, Paleogeography and Paleobiogeography of the circum-Mediterranean region and the Oligocene to Neogene Basin evolution in Austria. *Mitteilungen der Österreichischen Geologischen Gesellschaft* 92 (1999), 95-116.
- Stiner MC. (1990): The use of mortality patterns in archaeological studies of hominid predatory adaptations. *Journal of Anthropological Archaeology* 9, 305-351.
- Svistun VI. (1974): *Dinotheriums* of Ukraine [in Russian]. 50 p.
- Tarabukin BA. (1968): Excavation of a deinothere skeleton in the Rezech-Area of the Moldavian Republic [in Russian]. *Izvestia Akad. Nauk Moldavska, SSR, Ser. Bid. Chim. Nauk.* 3, 37-42.
- ter Borgh M, Vasiliev I, Stoica M, Knežević S, Matenco L, Krijgsman W, Rundić L, Cloetingh S. (2013): The isolation of the Pannonian basin (Central Paratethys): New constraints from magnetostratigraphy and biostratigraphy. *Global and Planetary Change* 103, 99-118.
- Thenius E. (1989): Zähne und Gebiß der Säugetiere. In: J Niethammer, H Schliemann and D Starck (Eds), Vol. 8 Mammalia, *Handbuch der Zoologie Handbook of Zoology* Berlin, New York, Walter de Gruyter, 513 p.
- Tobien H. (1988): Contributions a l'étude du gisement miocène supérieur de Montredon (Herault). Les grands Mammifères. 7 - Les proboscidiens Deinotheriidae. *Palaeovertebrata, Mémoire Extraordinaire* 135-175.
- Trueman CN. (2013): Chemical taphonomy of biomineralized tissues. *Palaeontology* 56, 475-486.
- Trueman CN, Behrensmeyer AK, Potts R, Tuross N. (2006): High-resolution records of location and stratigraphic provenance from the rare earth element composition of fossil bones. *Geochimica et Cosmochimica Acta* 70, 4343-4355.
- Tütken T. (2010): Die Isotopenanalyse fossiler Skelettreste – Bestimmung der Herkunft und Mobilität von Menschen und Tieren. In: H Meller and KW Alt (Eds), *Anthropologie, Isotopie und DNA – biografische Annäherung an namenlose vorgeschichtliche Skelette*. Tagungsband 2. Mitteldeutscher Archäologentag, Tagungen des Landesmuseums für Vorgeschichte Halle, 33–51.
- Tütken T, Vennemann T. (2009): Stable isotope ecology of Miocene large mammals from Sandelzhausen, southern Germany. *Paläontologische Zeitschrift* 83, 207-226.

- Tütken T, Vennemann TW, Janz H, Heizmann EPJ. (2006): Palaeoenvironment and palaeoclimate of the Middle Miocene lake in the Steinheim basin, SW Germany: A reconstruction from C, O, and Sr isotopes of fossil remains. *Palaeogeography, Palaeoclimatology, Palaeoecology* 241, 457-491.
- Ungar PS, Scott JR, Curran SC, Dunsworth HM, Harcourt-Smith WEH, Lehmann T, Manthi FK, McNulty KP. (2012): Early Neogene environments in East Africa: Evidence from dental microwear of tragulids. *Palaeogeography, Palaeoclimatology, Palaeoecology* 342–343, 84-96.
- Unger F. (1850): Localflora der Tertiärzeit. Berichte über die Mitteilungen von Freunden der Naturwissenschaften in Wien 6, 2-3.
- Unger F. (1852): *Iconographia plantarum fossilium*. Denkschriften der Kaiserlichen Akademie der Wissenschaften in Wien. Mathematisch-naturwissenschaftliche Klasse 4, 73-118.
- Vasiliev I, de Leeuw A, Filipescu S, Krijgsman W, Kuiper K, Stoica M, Briceag A. (2010): The age of the Sarmatian–Pannonian transition in the Transylvanian Basin (Central Paratethys). *Palaeogeography, Palaeoclimatology, Palaeoecology* 297, 54-69.
- Vergiev S, Markov GN. (2010): A mandible of *Deinotherium* (Mammalia: Proboscidea) from Aksakovo near Varna, Northeast Bulgaria. *Palaeodiversity* 3, 241–247.
- Vislobokova IA. (2007): New Data on Late Miocene Mammals of Kohfidisch, Austria. *Paleontological Journal* 41, 451-460.
- Voerkelius S, Lorenz GD, Rummel S, Quézel CR, Heiss G, Baxter M, Brach-Papa C, Deters-Itzelsberger P, Hoelzl S, Hoogewerff J, Ponzevera E, Van Bocxstaele M, Ueckermann H. (2010): Strontium isotopic signatures of natural mineral waters, the reference to a simple geological map and its potential for authentication of food. *Food Chemistry* 118, 933-940.
- Zachos J, Pagani M, Sloan L, Thomas E, Billups K. (2001): Trends, Rhythms, and Aberrations in Global Climate 65 Ma to Present. *Science* 292, 686-693.
- Zapfe H. (1979): *Chalicotherium grande* (BLAINV.) aus der miozänen Spaltenfüllung von Neudorf an der March (Děvinská Nová Ves), Tschechoslowakei. Wien, Verlag Ferdinand Berger & Söhne, 282 p.
- Zázvorka V. (1940): *Deinotherium levius* Jourdan a jeho stratigrafický význam [in Czech and English]. *Acta Musei Nationalis Pragae IIB*, 191-214.
- Ziegler PA, Dèzes P. (2007): Cenozoic uplift of Variscan Massifs in the Alpine foreland: Timing and controlling mechanisms. *Global and Planetary Change* 58, 237-269.

9. Appendix

9.1. Aiglstorfer M, Göhlich UB, Böhme M, Gross M. (2014): A partial skeleton of *Deinotherium* (Proboscidea, Mammalia) from the late Middle Miocene Gratkorn locality (Austria). *Palaeobiodiversity and Palaeoenvironments* 94, 49-70. [Publication #1]

9.2. Aiglstorfer M, Heissig K, Böhme M. (2014): Perissodactyla from the late Middle Miocene Gratkorn locality (Austria). *Palaeobiodiversity and Palaeoenvironments* 94, 71-82 [Publication #2]

9.3. Aiglstorfer M, Rössner GE, Böhme M. (2014): *Dorcatherium naui* and pecoran ruminants from the late Middle Miocene Gratkorn locality (Austria). *Palaeobiodiversity and Palaeoenvironments* 94, 83-123. [Publication #3]

9.4. Havlik P, Aiglstorfer M, Beckman A, Gross M, Böhme M. (2014): Taphonomical and ichnological considerations on the late Middle Miocene Gratkorn locality (Styria, Austria) with focus on large mammal taphonomy. *Palaeobiodiversity and Palaeoenvironments* 94, 171-188. [Publication #4]

9.5. Aiglstorfer M, Bocherens H, Böhme M. (2014): Large Mammal Ecology in the late Middle Miocene locality Gratkorn (Austria). *Palaeobiodiversity and Palaeoenvironments* 94, 189-213. [Publication #5]

Publication #1

Aiglstorfer M, Göhlich UB, Böhme M, Gross M. (2014) A partial skeleton of *Deinotherium* (Proboscidea, Mammalia) from the late Middle Miocene Gratkorn locality (Austria). *Palaeobiodiversity and Palaeoenvironments* 94, 49-70.

Own contribution:

Scientific ideas (%)	80
Data generation (%)	90
Analysis and Interpretation (%)	80
Paper writing (%)	95

A partial skeleton of *Deinotherium* (Proboscidea, Mammalia) from the late Middle Miocene Gratkorn locality (Austria)

Manuela Aiglstorfer · Ursula B. Göhlich ·
Madelaine Böhme · Martin Gross

Received: 26 September 2013 / Revised: 11 November 2013 / Accepted: 28 November 2013 / Published online: 11 February 2014
© Senckenberg Gesellschaft für Naturforschung and Springer-Verlag Berlin Heidelberg 2014

Abstract A disarticulated, though still roughly associated partial *Deinotherium* skeleton from the late Middle Miocene (late Sarmatian sensu stricto; 12.2–12.0 Ma) Gratkorn locality (Austria) is described. Based on dimensions and morphology of the material it can be determined as a medium-sized taxon of Deinotheriidae and definitively assigned to the genus *Deinotherium*. This specimen from Gratkorn confirms the osteological differences in the postcrania between *Prodeinotherium* and *Deinotherium*. As the diagnostically important p/3 is missing on the specimen it can only be assigned to *Deinotherium levius* vel *giganteum*. The Gratkorn specimen is one of not many skeletons of a medium-sized taxon of Deinotheriidae and one of only a few well-dated late Middle Miocene occurrences in Central Europe with associated dental and postcranial material.

Keywords Biostratigraphy · Biochronology · Styria · Sarmatian · Central Europe · *Deinotherium levius* · *Deinotherium giganteum*

Introduction

Deinothere remains are frequent findings in the Miocene of Europe and a useful tool for biochronological and biostratigraphical considerations (see, e.g. Dehm 1960; Huttunen 2002a, b; Böhme et al. 2012; Pickford and Pourabrishami 2013). Following recent works (Böhme et al. 2012; Pickford and Pourabrishami 2013) on the stratigraphic range of the different species, the genus *Prodeinotherium* Éhik, 1930 can be considered as indicative for the Early to middle Middle Miocene, while *Deinotherium* Kaup, 1829 first occurs in Europe during the Middle Miocene (Mottl 1969; Svistun 1974) and is recorded up to the terminal Late Miocene (Markov 2008b). Unfortunately, in most cases the findings comprise only isolated remains, and very often only isolated teeth [e.g. abundant tooth material from the famous Eppelsheim Formation (Eppelsheim Fm)]. In contrast to this, a fairly well preserved, disarticulated, partial *Deinotherium* skeleton (Fig. 1) of late Sarmatian age (12.2–12.0 Ma) was discovered in the clay pit St. Stefan near Gratkorn (Styria, Austria; Gross et al. 2011; 2014, this issue) during geological mapping of the region in 2005. It is one of very few skeleton findings of a medium-sized deinothere taxon described so far. The remains were excavated by the Universalmuseum Joanneum, Graz, from 2005 to 2008. All elements could be assigned to one individual except for some tooth remains detected about 30 m NW of the skeleton that represent a second individual. The fragmentary preservation of the latter allowed stable isotope analyses ($\delta^{18}\text{O}_{\text{CO}_3}$, $\delta^{13}\text{C}$; see Aiglstorfer et al. 2014, this issue). The excavation of the *Deinotherium* skeleton led to the discovery of an abundant

This article is a contribution to the special issue “The Sarmatian vertebrate locality Gratkorn, Styrian Basin.”

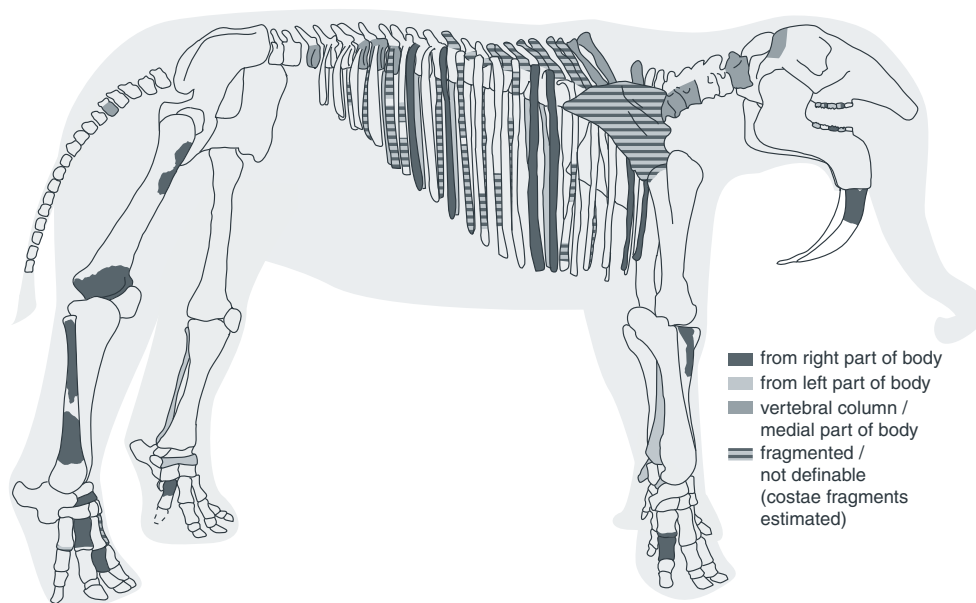
M. Aiglstorfer · M. Böhme
Department for Geosciences, Eberhard Karls Universität Tübingen,
Sigwartstraße 10, 72076 Tübingen, Germany

M. Aiglstorfer (✉) · M. Böhme
Senckenberg Center for Human Evolution and Palaeoenvironment
(HEP), Sigwartstraße 10, 72076 Tübingen, Germany
e-mail: manuela.aiglstorfer@senckenberg.de

U. B. Göhlich
Geologisch-Paläontologische Abteilung, Naturhistorisches Museum
Wien, Burgring 7, 1010 Vienna, Austria

M. Gross
Universalmuseum Joanneum, Graz, Weinzöttlstraße 16,
8045 Graz, Austria

Fig. 1 Sketch of the partial skeleton of *Deinotherium levius* vel *giganteum* from the Middle Miocene of Gratkorn indicating preserved remains [reconstructed after *D. proavum* from Ezerovo (Late Miocene) mounted at PMSU (modified after Huttunen 2000; Markov 2008b)]



and rich vertebrate fauna, which has been excavated in continuous campaigns in a cooperative project of the Universalmuseum Joanneum, Graz, the Eberhard Karls Universität Tübingen and the Ludwig-Maximilians-Universität München (see other publications in this special issue).

Taxonomy of European Deinotheriidae

Taxonomy of Deinotheriidae has been under discussion for long (see, e.g. Gräf 1957; Bergounioux and Crouzel 1962; Harris 1973; Gasparik 1993, 2001; Antoine 1994; Huttunen 2000; Ginsburg and Chevrier 2001; Duranthon et al. 2007; Markov 2008a, b; Vergiev and Markov 2010; Böhme et al. 2012; Pickford and Pourabrishami 2013). At the moment, one, *Deinotherium* (Ginsburg and Chevrier 2001; Pickford and Pourabrishami 2013), respectively two genera, *Prodeinotherium* and *Deinotherium* (Gasparik 1993; Antoine 1994; Huttunen 2000; Duranthon et al. 2007; Vergiev and Markov 2010), are considered valid. While a gradual size increase within Deinotheriidae from the Early to the Late Miocene is generally accepted, Antoine (1994), Huttunen (2000), Vergiev and Markov (2010) and others argue that *Prodeinotherium* and *Deinotherium* do not only differ in size but also in dental and postcranial morphology. Huttunen (2000) gives an overview of distinguishing characters between the smaller genus *Prodeinotherium* and the larger genus *Deinotherium*, discussing and evaluating the characters given by Harris (1973) and others on specimens from Central Europe. As noted by Huttunen and also observed in this study (see Discussion below), genus diagnostic characters can indeed be identified in the postcranial material and therefore support the separation of two genera *Prodeinotherium* and *Deinotherium* as proposed by Éhik

(1930). In addition to the on-going discussion on valid genera, different concepts concerning species validity are also held at the moment. While some authors accept five valid morphospecies (Böhme et al. 2012) or chronospecies (Pickford and Pourabrishami 2013), others tend to reduce the number to four (Gasparik 1993, 2001; Markov 2008a; Vergiev and Markov 2010) or even only two species (Huttunen 2002a). Species determination is hindered considerably by the difficulty in identifying stratigraphically mixed faunas, the great dimensional and morphological overlap between the species and the impossibility to evaluate intraspecific variation (Huttunen 2000). Huttunen (2002a), for example, synonymized *Deinotherium levius* Jourdan, 1861 with *Deinotherium giganteum* Kaup, 1829 due to the assumed contemporaneous occurrence of *D. giganteum* and *D. levius* morphotypes in the Eppelsheim Fm. Furthermore, the mentioned gradual size increase (Gasparik 1993; Böhme et al. 2012; Pickford and Pourabrishami 2013) and the stepwise morphological modification of the characteristic features (Antoine 1994; Gasparik 2001) aggravate a clear species differentiation. Huttunen (2002a), like others before her, considered *Deinotherium gigantissimum* Stefanescu, 1892 only “a large variety of *D. giganteum*” (Huttunen 2002a, p. 244). Dating of deinothere findings and identification of stratigraphically mixed faunas are the keys for evaluation of inter- and intraspecific variations and for determination of the role of sexual dimorphism or the sympatric occurrence of different species. In the modern *Loxodonta africana* Blumenbach, 1797, for example, the average weight of females (about 2.8 t) reaches only about 56 % of the males’ average weight (5 t; Joger 2010). Such a scope would include specimens from *Prodeinotherium bavaricum* von Meyer, 1831 to *D. giganteum*. The large dimensional and morphological variability in *D. giganteum* observed by Huttunen (2000) that led

her to a supposed synonymy with *D. levius* could thus be a consequence of faunal mixing or uncertainty in stratigraphic positions of localities, and also biased by a certain degree of sexual dimorphism (Huttunen 2000, 2002b). The mixed and time-averaged faunal assemblage from the “Dinotheriensande” (Eppelsheim Fm; at that time considered stratigraphically uniform) in particular has biased her observations and those of others for a long time. Böhme et al. (2012) and Pickford and Pourabrishami (2013) were able to show, however, that the Eppelsheim Fm also covers a considerable amount of the Middle Miocene and therefore comprises several non-co-occurring *Deinotherium* species. In contrast to the observations of Huttunen (2000, 2002a, b), Gräf (1957) gives a morphospecies differentiation of *D. giganteum* and *D. levius* based on differences in dental material. She already observed variability concerning dental features but as her comparison material was limited (Pickford and Pourabrishami 2013) some of her features were found to be more variable than she considered (see, for example, Huttunen 2000 for discussion), while others show a smaller variability than she estimated due to mixed faunal assemblages (see, for example, Pickford and Pourabrishami 2013 for discussion). Gräf (1957) further underestimated the dimensional range sometimes (Pickford and Pourabrishami 2013). Pickford and Pourabrishami (2013) based their work on a large number of deinotherid dental material and tried to focus their considerations on well-dated material and to avoid faunal assemblages likely to result from a considerable extent of faunal mixing, such as fluvial deposits. These researchers classify different size groups in combination with their stratigraphic range while being well aware that these groups cannot be strictly separated due to a gradual size increase. Böhme et al. (2012) mention *D. bavaricum*, *D. levius* and *D. giganteum* as morphospecies recorded from the Eppelsheim Fm based on comparisons with dental material from rich and well-documented localities from Europe.

We follow the morphospecies concept of Böhme et al. (2012) with five European species, which differs from other concepts, such as those of Gasparik (1993, 2001) and Vergiev and Markov (2010) in the acceptance of the species *D. levius*, based on the diagnostic features in the p/3 described by Gräf (1957) and referred to, for example, by Mottl (1969) and Böhme et al. (2012). We could observe the generic differences on the postcranial material from Gratkorn in comparison to *Prodeinotherium* from several localities, and therefore follow the two genera concept as proposed by Éhik (1930) and used by Gasparik (1993, 2001), Huttunen (2000, 2002a, b), Duranthon et al. (2007), Vergiev and Markov (2010) and others, in contrast to Böhme et al. (2012) and Pickford and Pourabrishami (2013). In this work, we therefore consider the following European morphospecies to be valid: *Prodeinotherium cuvieri*, *P. bavaricum*, *Deinotherium levius*, *D. giganteum* and *D. proavum* Eichwald, 1831. Codrea (1994), Gasparik (2001)

and Pickford and Pourabrishami (2013) stated that *D. proavum* should have priority over *D. giganteum* Stefanescu, 1892 and that the latter should be considered a junior synonym.

Nomenclature

The terminology for dentition used here (Fig. 2) is modified after Gräf (1957), Tassy (1996), Harris (1973), Tobien (1988), Huttunen (2000), Pickford and Pourabrishami (2013). Postcranial terminology follows that of Göhlich (1998).

Institutional abbreviations

GPIT	Paläontologische Sammlung der Universität Tübingen, Tübingen, Germany
IGM	Montanuniversität Leoben, Leoben, Austria
MNHN	Muséum National d’Histoire Naturelle, Paris, France
NHMM	Naturhistorisches Museum Mainz, Mainz, Germany
NHMW	Naturhistorisches Museum Wien, Vienna, Austria
NMNHS	National Museum of Natural History, Sofia, Bulgaria
PMSU	Paleontological Museum of Sofia University “St. Kliment Ohridsky”, Department of Geology and Paleontology, Sofia, Bulgaria
SMNS	Staatliches Museum für Naturkunde Stuttgart, Stuttgart, Germany
SNSB-BSPG	Staatliche Naturwissenschaftliche Sammlungen Bayerns Bayerische Staatssammlung für Paläontologie und Geologie, Munich, Germany
SSN	Paläontologisches Museum Nierstein, Nierstein, Germany
UMJGP	Universalmuseum Joanneum, Graz, Austria

Anatomical abbreviations

prc/prcd	protocone/protoconid
pac	paracone
mc/mcd	metacone/metaconid
hyc/hycd	hypocone/hypoconid
ecd	entoconid
Mc	metacarpal
Mt	metatarsal
sin.	sinistral
dex.	dextral
lmax	maximal length
wmax	maximal width

Material

Dental and cranial material

UMJGP 204078 (P4/ sin.); UMJGP 203690 (P4/ dex.); UMJGP 204081 (M1/ sin.); UMJGP 204079 (M2/ sin.); UMJGP 203628 (M2/ dex.); UMJGP 204080 (M3/ sin.); UMJGP 203624 (i/2 dex.?); UMJGP 203670 (p/4 sin.); UMJGP 203669 (m/1 dex.); UMJGP 203689 (m/3 sin.); UMJGP 203654 (fragment of skull ?); UMJGP 203435 (p/4 sin.); 203460 (tooth fragment, buccal wall of 203435?); UMJGP203420–21 (tooth fragments).

Postcranial material

Vertebral column and ribs

UMJGP 204654 (atlas); UMJGP 203623, 204111, 203605 (vertebrae cervicales); 203638, 203653, 203659, 203680 (vertebrae thoracicae or lumbales); UMJGP 203663 (fragment of vertebra caudalis?); UMJGP 204681 (processus spinosus of vertebra cervicalis 6 or 7); UMJGP 203693 (fragment of processus spinosus of vertebra cervicalis 7 or vertebra thoracica 1); UMJGP 203642 (processus spinosus of vertebrae thoracicae 1 or 2); UMJGP 203655, 203649, 203647, 203602, 203694 and 203603 (processus spinosi of cranial series of vertebrae thoracicae); UMJGP 203687 (fragments of processus spinosus (?)); UMJGP 203681 (?), UMJGP 204684 (?), UMJGP 203716, UMJGP 203646 (?), UMJGP 203675(?) (fragments of arcus vertebrarum); UMJGP 203604, 203608, 203610 (two crushed costa fragments ?), 203634, 203643, 203644, 203648 (with fragment 203645), 203660(?), 203687, 203696, 203692, 203697, 203703, 203717, 203666, 203658, 203629, 203630, 203635, 203617, 204673(?) (fragments of costae); UMJGP 203657 (costa 1/2? dex.); UMJGP 203606 (costa 2/3? dex.); UMJGP 203639, 203650, 203695, 203633 (costae dex. of central to caudal series of the thorax); UMJGP 204110, 203618 and 203614–5 (fragment of the same costa?), 203631, 203632, 203607 (costae sin. of central to caudal series of the thorax).

Limb elements

UMJGP 203662, 203664, 203667, 203668, 203671, 203672, 203676, 203677, 203678(?), 203679, 203691, 204103 (fragments of scapula?); UMJGP 203674 (humerus dex.? with part of scapula?); UMJGP 203665 (radius sin.); UMJGP 203621 (fragment of radius dex.); UMJGP 203688 (os carpi ulnare sin.); UMJGP 203640 (os carpale secundum sin.); UMJGP 203685 (distal epiphysis of metacarpal II or III sin. or IV dex.); UMJGP 203684 (phalanx proximalis of manus?); UMJGP 204112 (femur dex., distal epiphysis); UMJGP

203601 (femur dex., fragment of proximal shaft); UMJGP 203612, 203613 (fragments of fibula dex.); UMJGP 203622 (fibula sin.); UMJGP 203611 (os tarsi centrale sin.); UMJGP 203683 (os tarsi centrale dex.); UMJGP 204696 (distal trochlea of metatarsal II?); UMJGP 203625 (? metatarsal IV dex.); UMJGP 203708 (phalanx proximalis II, III, IV dex. of pes?); UMJGP 203709 (os sesamoideum); UMJGP 203710 (os sesamoideum); UMJGP 203620 (lateral fragment of metacarpal I or metatarsal I dex.?); UMJGP 203616 (metapodial?).

Methods

For comparison of postcranial material we used the *Prodeinotherium* skeleton from Langenau (SMNS 41562; Germany; Early Miocene; MN 4; 17.2–17.1 Ma), the partial *Prodeinotherium* skeletons from Franzensbad (NHMW2000z0047/0001; Czech Republic; Early Miocene; MN 5; 16.9 Ma) and Unterzolling (SNSB-BSPG 1977 I 229; Germany; early Middle Miocene; 15–14.5 Ma) described by Huttunen (2000, 2004) and Huttunen and Göhlich (2002), the partial skeleton of *D. levius* from Gussyatin (also Husyatyn) (Ukraine; Middle Miocene; early late Badenian; 13.1–13.4 Ma; marine sediments dated with foraminifera by Didkovsk in Svistun 1974) described by Svistun (1974) and the skeleton of *Deinotherium proavum* from Ezerovo (Bulgaria; Late Miocene; MN 12; Kovachev and Nikolov 2006) mounted at the PMSU, as well as descriptions of postcranial elements by Huttunen (2000).

Comparison material for teeth comprises *Prodeinotherium* remains from Falun de la Touraine and Anjou (both France; early Middle Miocene; Langhian; MN 5; 15 ± 0.5 Ma), Unterzolling, Sprendlingen 2 (Germany; Middle Miocene), the Eppelsheim Formation and localities from the North Alpine Foreland Basin (NAFB) described by Antoine (1994), Ginsburg and Chevri er (2001), Huttunen and G ohlich (2002), Huttunen (2004), Duranthon et al. (2007) and B ohme et al. (2012). For *Deinotherium*, dental material from the Middle Miocene sites La Grive, St. Gaudens, Tournan (all France; late Middle Miocene; MN 7/8; 13–11.5 Ma), Massenhausen, Hinterauerbach, Sprendlingen 2 (all Germany; late Middle Miocene; MN 7/8; 13–11.5 Ma), St. Oswald near Gratwein (Austria; Middle Miocene; early Badenian), Oberdorf near Weiz (Austria; late Middle Miocene; late Sarmatian; 12.2–11.6 Ma), Breitenhilm near Hausmannstetten (Austria; late Middle Miocene; late Sarmatian; 12.2–11.6 Ma) and Dietersdorfberg near Mureck (Austria; late Middle Miocene; Sarmatian; 12.7–11.6 Ma) described by Peters (1871), Dep erit (1887), Gr af (1957), Mottl (1969, 1970), Ginsburg and Chevri er (2001) and B ohme et al. (2012) was compared with the Gratkorn specimen. Furthermore, we considered *Deinotherium giganteum* specimens described by Gr af (1957) and Tobien (1988) from Montredon (France; Late Miocene; late

Vallesian; MN 10; 9.5 Ma) and Frohnstetten (Germany; Late Miocene), as well as the type of *D. giganteum* from Eppelsheim (HLMD Din. 466), described by Kaup (1829, 1832). Due to the stratigraphic mixture of the rich *Deinotherium* material from the Eppelsheim Formation, it is excluded besides the type of *D. giganteum*. *Deinotherium* remains from Austria described or referred to by Mottl (1969), Hilber (1914) and Huttunen (2000) and general observations on dental material by Tobien (1988), Antoine (1994), Ginsburg and Chevrier (2001) and Duranthon et al. (2007) on deinothere material from France are included in the discussion. As unfortunately no description on the dental material of *D. levius* from Gussyatin is given in Svistun (1974), we only took the tooth metrics into consideration here. Furthermore, tooth metrics of (?)*D. levius* from Opatov (formerly Abtsdorf; Czech Republic; Middle Miocene; Badenian) given by Zázvorka (1940) are considered.

Measurements were accomplished with a calliper (precision if possible 0.1 mm in teeth; 1 mm in postcranial material) and are modified after Göhlich (1998).

Systematic palaeontology

Order Proboscidea Illiger, 1811
Family Deinotheriidae Bonaparte, 1845
Genus *Deinotherium* Kaup, 1829

Type species: *Deinotherium giganteum* Kaup, 1829

Valid European species: *Deinotherium levius* Jourdan, 1861, *D. giganteum* Kaup, 1829, *D. proavum* Eichwald, 1835

Deinotherium levius vel *giganteum*
Deinotherium levius Jourdan, 1861

Lectotype: tooththrow with P3/ to M3/ (Lyon, Muséum des Sciences Naturelles, Nr. L.Gr. 962)

Type locality: La Grive Saint-Alban, France (late Middle Miocene)

Deinotherium giganteum Kaup, 1829

Holotype: Left mandible with tusk, m/2 - 3, right mandible fragment: symphysis with tusk fragment (HLMD Din. 466)

Type locality: Eppelsheim, Germany (Miocene)

Measurements

The measurements of *Deinotherium levius* vel *giganteum* from Gratkorn are presented in Table 1. Sections of measurements are modified after Göhlich (1998)

Description

The partial deinothere skeleton from Gratkorn (Fig. 1), which is preserved in a disarticulated but roughly associated situation, consists of elements of the vertebral column, of the anterior and posterior limbs, and of some teeth. Most of the bones are fragmentary. This partial skeleton represents one individual, while a second individual can be identified by some additional cheek teeth fragments found 30 m NW of the skeleton.

With not fully fused epiphyses in longbones and permanent, lightly worn dentition, the partial skeleton represents a not fully grown “young” adult. It could already have reached sexual maturity. A delayed fusion of the longbones and continuation of growth beyond sexual maturity has been observed in the modern *Loxodonta africana* (Poole 1996; in males even till the age of 30–45 years).

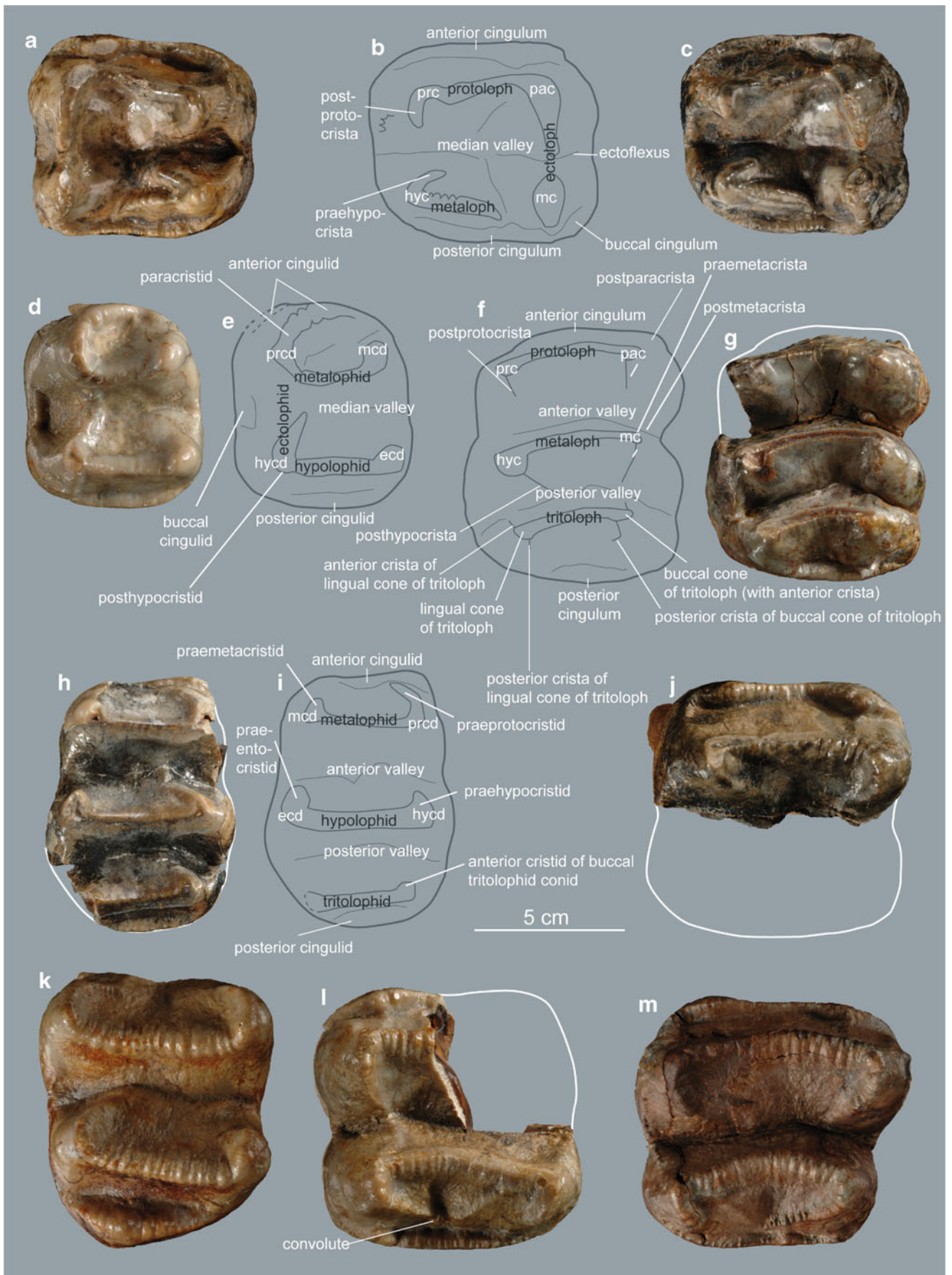
Dentition and cranial material

Dental remains comprise ten teeth of one individual (P4/ sin., P4/ dex., M1/ sin., M2/ sin., M2/ dex., M3/ sin., i/2 dex.?, p/4 sin., m/1 dex., m/3 sin.) and one p/4 sin., with some cheek teeth fragments (UMJGP 203420, 203421, 203460) of a second individual. A poorly preserved fragment of a pneumatized (?) bone (UMJGP 203654) of the skull cannot be described in detail due to limitations of preservation.

Upper dentition

P4/ (P4/ sin.: UMJGP 204078; P4/ dex.: UMJGP 203690; Fig. 2a–c): P4/ sin. enamel damaged anterobuccally, P4/ dex. enamel damaged posterobuccally, both slightly worn. Subrectangular in occlusal view being wider than long; bilophodont; protoloph complete (reaching paracone); metaloph incomplete (no contact with metacone); ectoloph complete with moderate ectoflexus; blunt postprotocrista weak and short; praehypocrista moderate and crenulated; median valley open lingually; anterior cingulum strong ascending at paracone and forming a well-developed cone; posterior cingulum strong, ascending both to hypo- and metacone (fusion with ectoloph posterior to metacone); small posterobuccal cingulum present at metacone; three roots.

Comparison: After Gräf (1957) a P4/ with fused metaloph and ectoloph is typical for *D. levius*. In the Gratkorn specimen, metaloph and ectoloph are not fully fused, but with a fused protoloph and a clearly developed praehypocrista they show a similar pattern as described by Huttunen (2000) for *D. giganteum* from Mannersdorf near Angern (NHMW2000z0013/000; Austria; Late Miocene; Pannonian H/F), which is slightly larger in dimensions than the latter or than the range for *D. levius* given by Gräf (1957) or Pickford and Pourabrishami (2013). *D. levius* from St. Oswald near Gratwein (Middle Miocene) described by Mottl (1969,



◀ **Fig. 2** Cheek teeth of *D. levius* vel *giganteum* from Gratkorn in occlusal view and with dental terminology. **a** P4/ dex. (UMJGP 203690), **b** sketch of **c** with terminology used for upper premolars, **c** P4/ sin. (UMJGP 204078), **d** p/4 sin. (UMJGP 203670), **e** sketch of **d** with terminology used for lower premolars, **f** sketch of **g** with terminology used for upper molars, **g** M1/ sin. (UMJGP 204081), **h** m/1 dex. (UMJGP 203669), **i** sketch of **h** with terminology used for lower molars, **j** M2/ sin. (UMJGP 204079), **k** m/3 sin. (UMJGP 203689), **l** M2/ dex. (UMJGP 203628), **m** M3/ sin. (UMJGP 204080)

fig. 3) is heavily worn, but shows a metaloph not fully fused with the ectoloph as well. It is smaller in dimensions than generally observed for *D. levius*. Meta- and ectoloph are also not fully fused in a Middle Miocene *Deinotherium* specimen from Massenhausen (SNSB-BSPG 1951 I 47), which should be *D. levius* following Gräf (1957), and not in all figures for *D. levius* given by Depéret [1887; see, for example, *D. levius* from La Grive (late Middle Miocene) figured on pl. 20, fig. 3]. Tobien (1988) observed fusion and non fusion of ecto- and metaloph, as well as variability in the presence of a well-developed praehypocrista for *D. giganteum* from Montredon (Late Miocene). Antoine (1994) and Ginsburg and Chevrier (2001) describe a rectangular shape and a weak ectoflexus as being typical for *P. bavaricum*, a trapezoid shape and a strong ectoflexus for “*D. giganteum*” (including *D. levius*). As shape and ectoflexus vary in *D. giganteum* from Montredon (Tobien 1988) and as, for example, a P4/ of *P. bavaricum* from Sprendlingen 2 (SSN12SP10; Middle Miocene) shows a stronger ectoflexus than the specimens from Montredon figured by Tobien (1988), this feature is considered variable as well. Therefore, we agree with Huttunen (2000) that a certain variability concerning the fusion of lophs in the P4/ exists and that the morphology of the P4/ does not provide a significant feature for species separation.

M1/ (M1/ sin.: UMJGP 204081; Fig. 2f–g): slightly worn, incomplete, missing anterior and lingual wall of protoloph, buccal cone of tritoloph damaged posterobuccally. Subrectangular shape and longer than wide; trilophodont; all three lophs complete and concave posteriorly; tritoloph linguobuccally less wide than protoloph and metatoloph; buccal posterior cristae (postparacrista, postmetacrista and posterior crista of the buccal cone of the tritoloph) short and pointing posteriorly; blunt lingual posterior cristae (postprotocrista, posthypocrista and posterior crista of the lingual cone of the tritoloph) pointing posteromedian; praecrista only present at metacone (very weak) and at buccal cone of tritoloph, running anteriorly and contacting postmetacrista at its base; anterior valley anteroposteriorly wider than the posterior and with a small tubercle at its buccal side; buccal cingulum present ascending occlusally at cones; posterior cingulum descends from lingual to buccal ascending at buccal cone of tritoloph.

Comparison: Due to fragmentation it cannot be verified whether the metaloph in M1/ is wider than the protoloph on the Gratkorn specimen, which would be characteristic for

D. levius after Gräf (1957), but seems to be more variable following the observations of Tobien (1988) and Huttunen (2000). Comparable to the specimen from Gratkorn, for a specimen from St. Oswald near Gratwein (Middle Miocene) Mottl (1969) observed a stronger incision on the buccal wall between protoloph and metaloph than between metaloph and tritoloph, which she states as common for *D. levius* from La Grive (late Middle Miocene) but less common in *D. giganteum*. Indeed, the incision is more pronounced in figures of *D. levius* from La Grive (Depéret 1887, pls. 18–20), and can be observed as strong only in one single specimen of *D. giganteum* figured by Tobien (1988, pl. 2, fig. 9) from Montredon (Late Miocene), but comparably strong in specimens from Massenhausen (SNSB-BSPG 1951 I 47; late Middle Miocene) and Hinterauerbach (SNSB-BSPG 1951 I 90; late Middle Miocene). The more developed incision between proto- and metaloph seems to be more common in *D. levius*, but is variable in its extent as well in *D. levius* [see, for example, SSN12SP15 and 16 from Sprendlingen 2 (Middle Miocene)]. The morphology of the M1/ thus makes an assignation to *D. levius* more likely but does not exclude a determination as *D. giganteum*.

M2/(anterior part of M2/ sin.: UMJGP 204079; M2/ dex.: UMJGP 203628; Fig. 2j, l): both slightly worn, M2/ sin. incomplete (only anterior half preserved), M2/ dex. incomplete (anterolingual quarter missing). Subquadratic shape in occlusal view; bilophodont; lophs complete and concave posteriorly; postparacrista pointing posterior and crenulated; postmetacrista long and pointing posteromedially, crenulated as well; weak praemetacrista present, connected to postparacrista at its base; blunt postprotocrista long and pointing posteromedially; posthypocrista short and pointing posteriorly; weak ridge present posterior to metaloph at lingual side on top of large but weak elevation pointing posterobuccally and fusing with postmetacrista by forming a small convolute and enclosing a clear depression anterior to it; anterior and posterior cingula strong; anterior cingulum ascends slightly at protocone forming a small elevation, but ascends strongly at paracone forming a pronounced apex; posterior cingulum descends from lingual to buccal ascending at metacone forming a small apex; posterior cingulum ascends lingual at hypocone; weak lingual cingulum.

Comparison: The postmetaloph morphology of the M2/ dex. from Gratkorn fits well in the description of Gräf (1957) for *D. levius* and to *D. levius* from Sprendlingen 2 (MNHM PW2013/29-LS; Middle Miocene). With a clearly present (though small) convolute and the stronger postmetaloph incision it clearly differs from the specimen assigned to *D. giganteum* by Gräf (1957) from Frohnstetten (GPIT/1035; Late Miocene). Mottl (1969) describes as well the presence of a convolute in specimens from St. Oswald near Gratwein (Middle Miocene), but the posthypocrista in the specimens she figures (Mottl 1969, pl. 3, fig.2) is more strongly developed than in the specimen from Gratkorn. Huttunen (2000) showed that the

Table 1 Measurements of *Deinotherium levius* vel *giganteum* from Gratkorn (sections of measurements modified after Göhlich 1998)Measurements of *Deinotherium levius* vel *giganteum* from Gratkorn^{a, b}**Dentition**

Location	Tooth	lmax	wmax	want	wpost	w third lobe	bas dm max	Remarks
Upper jaw								
UMJGP 204078	P4/ sin.	67.5	76.9	76.9	76			
UMJGP 203690	P4/ dex.	67.5	76.5	76.5	[75]			Missing enamel
UMJGP 204081	M1/ sin.	[83.3-90]	[74]	/	74	[67]		Missing anterior part
UMJGP 203628	M2/ dex.	[85]	/	/	[86]			Missing anterolingual quarter
UMJGP 204079	M2/ sin.	/	/	86	/			Only anterior half preserved
UMJGP 204080	M3/ sin.	84.5	93	93	79			
Lower jaw								
UMJGP 203624	i/2 dex?						[90-100]	Measured at most preserved basal part
UMJGP 203670	p/4 sin.	68	61	59	61			
UMJGP 203435	p/4 sin.	[[65]]	/	/	/			
UMJGP 203669	m/1 dex.	85	[65]	/	[65]	/		
UMJGP 203689	m/3 sin.	92.5	79	79	73.5			

lmax = maximal length; wmax = maximal width; want = anterior width; wpost = posterior width; bas dm max = maximal basal diameter

Postcranial material (measurements modified after Göhlich (1998)^b)

Vertebra	HFr	BFr	BPcr	DT pres cv	Remarks
UMJGP 204654					Maximal BFr preserved: 130mm; maximal width preserved at foveae articulares craniales: 230-240mm
UMJGP 203623	[55-57]	[105]	[235]	260	
UMJGP 204111	[75]	[110-115]		245	
UMJGP 203605	[60-70]			240	
UMJGP 203638				~150	
UMJGP 203659				~125	
UMJGP 203680				~110	
UMJGP 203653				~130	

HFr = cranial height of foramen vertebrae; BFr = cranial width of foramen vertebrae; BPcr = width at processus articulares craniales; DT pres cv = preserved transversal width of corpus vertebra (note: is not anatomical width!)

Processus spinosus	HFr	BFr	BPcr	DT dorsal Fr	L dorsal Fr	Remarks
UMJGP 204681			[40]	[85]	[30-40]	Preserved distal width: 30mm; preserved proximodistal length: 200mm;
UMJGP 203642						Minimal distal width: 30mm
UMJGP 203603	[100-105]	65-70	[30-40]	137	[40]	

HFr = cranial height of foramen vertebrae; BFr = cranial width of foramen vertebrae; BPcr = width at processus articulares craniales; DT dorsal Fr = width at dorsal rim of foramen vertebrae; L dorsal Fr = craniocaudal length at dorsal rim of foramen vertebrae

Radius		BD	GL	TD	UD	Bp	Tp
UMJGP 203665	sin.	32	>720	77	188	112	84

BD = smallest mediadorsal width of diaphysis; GL = maximal length; TD = smallest lateropalmar width of diaphysis; UD = smallest circumference of diaphysis; Bp = mediadorsal width at caput radii; Tp = lateropalmar width at caput radii

Os carpi ulnare		TFd	Tfp	BFp	GT
UMJGP 203688	sin.	120	107	115	~127

TFd = dorsopalmar width of the articulation facet with carpale quartum; Tfp = dorsopalmar width of the articulation facet with the ulna; BFp = mediolateral width of the articulation facet with the ulna; GT = maximal dorsopalmar width parallel to medial plane

Os carpale secundum		GB	GH
UMJGP 203640	sin.	75	72

GB = maximal mediolateral width rectangular to medial plane; GH = maximal proximodistal width

Table 1 (continued)Measurements of *Deinotherium levius* vel *giganteum* from Gratkorn^{a, b}

Femur		DT troch min	BTr					
UMJGP 203601 and UMJGP 204112	dex.	~60	[[230]]					
DT troch min = mediolateral width at base of trochanter minor; BTr = width of trochlea								
Fibula		UD						
UMJGP 203622	sin.	115					Preserved maximal length: 670mm; preserved mediolateral width distally: 120mm	
UMJGP 203612-3	dex.	~120						
UD = minimal circumference of diaphysis								
Os tarsi centrale		BFp	GH	Hph				
UMJGP 203683	dex.	[[130]]; > 125	[57]	39				
UMJGP 203611	sin.		[58]	40				
BFp = width of articulation facet for astragalus; GH = maximal proximodistal width; Hph = central proximodistal width								
Metapodial		BTr	TD	Tp				
UMJGP 203685		[70]						
UMJGP 203620			45	55.7				
BTr = mediolateral width of trochlea; TD = minimal dorsovolar width of diaphysis; Tp = maximal dorsovolar width								
Phalanx proximalis?		Bp	GL	BD	Bd	Tp	TD	Td
UMJGP 203684	manus ?	[75]						
UMJGP 203708	pes ?	>68	[79]	60	70.5	56.5	35	37
Bp = proximal mediolateral width; GL = maximal proximodistal length; BD = minimal mediolateral width of diaphysis; Bd = distal mediolateral width; Tp = proximal dorsovolar width; TD = minimal dorsovolar width of diaphysis; Td = dorsovolar width of trochlea								

^aAll measurements are in millimetres. Square brackets ([]) = estimated; double set of square brackets [[]] = higher degree of estimation; / = no measurement possible

^b ~ = approximately)

morphology of the postmetaloph is highly variable, that it does not significantly change with tooth size and that all morphological variations are recorded in teeth of lengths 59–88 mm. Tobien (1988) even observed an intraindividual variation for *D. giganteum* from Montredon (Late Miocene) concerning this feature (see, for example, Tobien 1988, pl. 4). Thus, the morphology of M2/ cannot be used at the moment for species determination of the Gratkorn specimen.

M3/ (M3/ sin.: UMJGP 204080; Fig. 2m): not worn (tooth germ), enamel missing at protocone. Trapezoid (widening anteriorly) shape in occlusal view, wider than long; bilophodont; loph complete and concave posteriorly; protoloph linguobuccally wider than metaloph; postparacrista long, crenulated, and pointing posteriorly; postmetacrista long, crenulated, pointing posteromedially, and terminating at midline of tooth; postprotocrista and posthypocrista short, crenulated and pointing posteriorly; lingual half of posterior wall of protoloph and metaloph with blunt elevation; anterior and posterior cingulum present (anterior more strongly developed); anterior cingulum slightly ascending at protocone forming a small elevation but stronger at paracone forming a pronounced apex; anterior cingulum ascending lingually at protocone; posterior

cingulum descending from lingual to buccal ascending at metacone twice forming two small peaks; weak lingual cingulum.

Comparison: The M3/ from Gratkorn strongly resembles *D. giganteum* from Frohnstetten (GPIT/1035; Late Miocene) but also *D. levius* from Sprendlingen 2 (SSN12SP22; late Middle Miocene). It differs from the specimen from St. Oswald near Gratwein (Middle Miocene) by a less strongly developed posthypocrista (see e.g. Mottl 1969, pl. 3, fig. 3). Gräf (1957) described a long postmetacrista turning to anterior at midline and tapering in the postmetaloph valley parallel to the posthypocrista as typical for *D. levius*. Tobien (1988) did not observe such a long postmetacrista for *D. giganteum* from Montredon (Late Miocene) and considered it a typical feature for *D. levius* as well. In any case, the specimens of *D. giganteum* figured by him (Tobien 1988, pl. 4 and 5) resemble more closely *D. levius* from Hinterauerbach (SNSB-BSPG 1951 I 90; late Middle Miocene) than the specimen from Gratkorn. In Depéret (1887) the extension and morphology of the postmetacrista seem to vary as well (see, for example, *D. levius* from La Grive (late Middle Miocene; Depéret 1887, pl. 18, fig. 1 and pl. 20, fig. 3)). We thus consider the

development of the postmetacrista not useful as a diagnostic feature for the determination of the Gratkorn specimen.

Lower dentition

tusk (i/2 dex.?: UMJGP 203624; Fig. 3): basal part of lower tusk including deep pulpa, very fragmentary, missing tip and complete caudal wall. Basal ovoid cross section [maximal diameter (DAP) of 90–100 mm reconstructed) with a shallow longitudinal furrow along the lateral side; flattened medial side; no enamel band; no “guillochage”.

Comparison: As typical for Deinotheriidae the tusk does not possess an enamel band and no “guillochage” (Göhlich 1999; Duranthon et al. 2007). In terms of its size it fits well with *D. levius* or *giganteum* (see, for example, values in Duranthon et al. 2007). As it is only a fragment of a young adult and diameters of tusks are highly variable among the two genera [for comparison, see, for example, diameter for *P. bavaricum* from Unterzolling (early Middle Miocene) in Huttunen and Göhlich (2002)], the assignation is mainly based on the association with the specimen.

p/4 (p/4 sin.: UMJGP 203670; Fig. 2d–e): slightly worn. Subrectangular shape longer than wide; bilophodont; metalophid and hypolophid complete and concave anteriorly, the latter being more straight and slightly longer than the first; ectolophid low and descending anteriorly; strongly crenulated paracristid ascending lingually and ending in anterior cingulid; cingulid present anterobuccal of paracristid; posterior cingulid straight and low and fusing with weak posthypocristid; low buccal cingulid at median valley; two roots.

p/4 sin.: UMJGP 203435 (isolated tooth from different specimen): very fragmentary, smaller and stronger worn than UMJGP 203670.



Fig. 3 Lower tusk (i/2 dex.?) (UMJGP 203624) in caudal (a) and rostral view (b). Scale bar 20 mm

Comparison: In the p/4, the reduced metalophid compared to the hypolophid is used as a character by Gräf (1957) to distinguish *D. giganteum* from *D. levius* [although her values for *D. giganteum* vary between 87.9 and 98.9 % and therefore overlap with *D. levius* (99.4–103.2 %)]. The *Deinotherium* from Gratkorn fits well in morphology with *D. levius* from Spredlingen 2 (MNHM PW2013/28-LS, SSN12SP34; Middle Miocene) and to the specimen from Dietersdorfberg near Mureck (UMJGP 3699; late Middle Miocene; see also description in Mottl 1969) but differs from the specimen from St. Oswald near Gratwein (Middle Miocene; Mottl 1969, pl. 4, fig. 1) by a less wide hypolophid and from one specimen from Oberdorf near Weiz (UMJGP 9641; late Middle Miocene) by a less wide metalophid. *D. giganteum* from Montredon (Late Miocene; Tobien 1988) shows a relatively wide metalophid in the p/4 of some specimens. Duranthon et al. 2007 observed that a trapezoid shape is more frequent in *D. giganteum* than in *P. bavaricum*. Comparing different specimens of *P. bavaricum* (e.g. SNSB-BSPG 1952 I 36; SNSB-BSPG 1959 XIII 12; GPIT/1035-34 and 37) and *D. levius* (SNSB-BSPG 1951 I 90) with specimens of *D. giganteum* figured by Tobien (1988), it can be observed that the ratio of meta-/hypolophid width is variable and does not show any significant differences between the species. Furthermore, Tobien (1988) showed a more or less constant ratio between metalophid and hypolophid width (with higher variability for *D. giganteum*; Tobien 1988, fig. 6). We therefore agree with Huttunen (2000), who observed no morphological change for this tooth position.

m/1 (m/1 dex.: UMJGP 203669; Fig. 2h–i): slightly worn, damaged anterobuccal wall of metalophid and posterolingual wall of tritolophid. Trilophodont; elongated anteroposterior in occlusal view with maximal width at second lophid; all three lophids concave anteriorly; blunt praeprotocristid, praehypocristid and anterior cristid of buccal tritolophid conid pointing anteromedially; praehypocristid ending in small tubercle; anterior cingulid weak; posterior cingulid well pronounced; both valleys open on both sides, deeper at buccal sides; two roots.

Comparison: The feature on m/1 for distinguishing *D. levius* and *D. giganteum* given by Gräf (1957; length of posterior cristid/length of tritolophid) cannot be verified on the specimen from Gratkorn as the latter misses the posterior cristid. Taking into consideration the observations of Tobien (1988) for *D. giganteum* and of Huttunen (2000) for *Deinotherium* from Lower Austria, the ratios seem to show a greater overlap than expected by Gräf. Duranthon et al. (2007) observed a tendency of tritolophid enlargement from *P. bavaricum* to *D. giganteum*. Though varying as well, a general tendency can be observed upon comparison of the different specimens of the species with the specimen from Gratkorn (though fragmented), fitting well with *D. levius* from Hinterauerbach (SNSB-BSPG 1951 I 90; late Middle Miocene) and Massenhausen (late Middle Miocene).

m/3 (m/3 sin.: UMJGP 203689; Fig. 2k): not worn (tooth germ). Elongated widening anteriorly in occlusal view being longer than wide; bilophodont; loph complete and concave anteriorly; metalophid linguobuccally wider than hypolophid; praeprotocristid and praehypocristid crenulated, long, and pointing anteromedially; praehypocristid longer than praeprotocristid; praemetacristid and praeprotocristid pronounced, mirror-inverted, both descending in a curve pointing medially recurring anteriorly to lingual and buccal side, respectively; praentocristid pronounced but short pointing anteriorly; median valley deeper at buccal side; anterior cingulid low and very weak with small peak at buccal side; posterior cingulid (positioned buccally) strongly developed with a strong apex.

Comparison: In the type of *D. giganteum* (Kaup 1832; add. pl. I, figs. 3, 5 and pl. IV) the posterior cingulid is wider and not positioned buccally as it is in the Gratkorn specimen. However, based on the figures and observations in Tobien (1988; pl. 3, fig. 20, pl. 5, figs. 23–25) for *D. giganteum* from Montredon (Late Miocene), the width and position of the posterior cingulid is variable. In comparison to other material from Styria, the m/3 from Gratkorn is similar to the specimen from St. Oswald near Gratwein (Middle Miocene; Mottl 1969, pl. 4, fig. 1), differing only in its less wide hypolophid. The m/3 in the *Deinotherium* from Breitenhilm near Hausmannstetten (UMJGP 1756; late Middle Miocene) is also similar in morphology to the Gratkorn specimen. UMJGP 1756

was assigned to *D. giganteum* by Mottl (1969). However, due to the strong wear of the p/3 in the specimen an assignment to *D. levius* cannot be excluded, and based on its dimensions the specimen is well in accordance with this species as well [see Fig. 6; furthermore, the well-developed anterior cingulid of the p/3 in the specimen points rather to a more primitive evolutionary stage, as it is the case in *D. levius* (Gräf 1957; Böhme et al. 2012)]. In the specimen from Dietersdorf near Mureck (UMJGP 3699; late Middle Miocene) the posterior cingulid is more set off than in the specimen from Gratkorn. As the morphology of the m/3 thus seems to be quite variable, no distinguishing characters can be recognised for species differentiation at the moment, as also observed by Huttunen (2000) and Duranthon et al. (2007).

Postcranial material

Columna vertebralis: Of the vertebral column the atlas, eight fragmentary vertebrae and 12 processus spinosi/arcus vertebrarum are preserved (Fig. 4).

Atlas (UMJGP 204654; Fig. 4a): poorly preserved; relatively wide arcus vertebrae; on cranial side two suboval foveae articulares craniales for the articulation with the occipital condyles still visible; dorsal of articulation facets depression on each side; lateral median walls of foramina transversaria still observable.

Comparison: The atlas from Gratkorn is similar in dimensions to *D. giganteum* from Brunn-Vösendorf (Austria; Late

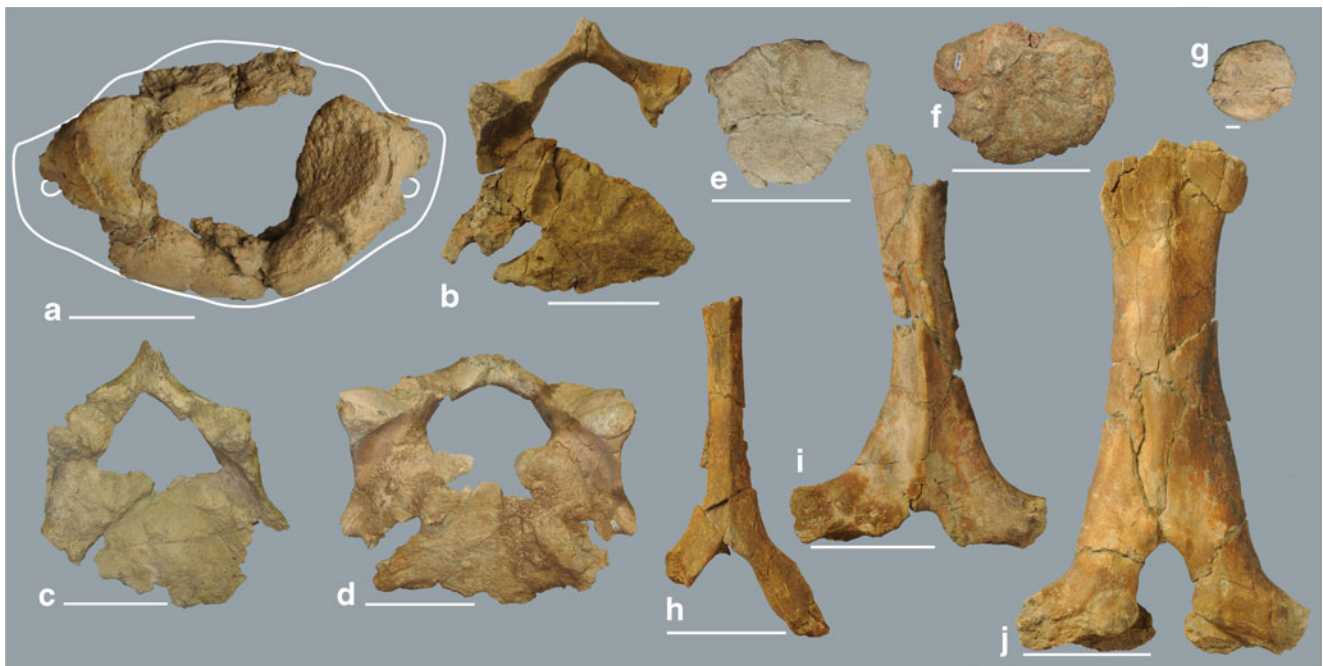


Fig. 4 Elements of vertebral column of *D. levius* vel *giganteum* from Gratkorn. **a** Atlas in cranial view (UMJGP204654), **b** vertebra cervicalis in cranial view (UMJGP 203605), **c** vertebra cervicalis in cranial view (UMJGP 204111), **d** vertebra cervicalis in cranial view (UMJGP 203623), **e** vertebra thoracica or lumbalis (UMJGP 203659), **f** vertebra

thoracica or lumbalis (UMJGP 203653), **g** fragment of vertebra caudalis? (UMJGP 203663), **h** processus spinosus of vertebra cervicalis 6 or 7 (UMJGP 204681), **i** processus spinosus of vertebra thoracica from cranial series (UMJGP 203602), **j** processus spinosus of vertebra thoracica from cranial series (UMJGP 203603). Scale bar 10 cm (**a–f**, **h–j**), 1 cm (**g**)

Miocene; Pannonian E; MN 9) described by Huttunen (2000), to *D. levius* from Gusyatin (Middle Miocene; Svistun 1974) and to the specimen from Holzmannsdorfberg (UMJGP 61634; Austria; Late Miocene; Pannonian C/D; MN 9), but it is clearly larger than *Prodeinotherium* from Langenau (Early Miocene). Due to poor preservation, a morphological comparison is not possible.

In addition to the atlas, eight further vertebrae (more or less badly preserved) could be identified. Following comparisons with the skeletons of *Prodeinotherium* from Franzensbad and Langenau (both Early Miocene) and the descriptions of Göhlich (1998) and Huttunen and Göhlich (2002), these vertebrae remains were tentatively identified as cervicales, thoracicae or lumbales. UMJGP 203623, 204111, 203605 comprise **vertebrae cervicales** (Fig. 4b–d): corpora vertebrarum relatively large and craniocaudally flat (enhanced flattening likely due to sediment compaction) as typical for vertebrae cervicales, comprising more or less preserved arcus vertebrarum; UMJGP 203605 still showing convex right cranial articulation facet, concave, kidney-shaped and caudoventrally facing right caudal articulation facet, and a nearly complete arcus vertebrae; basal part of processus spinosus recognisable as being cranially convex and caudally concave; UMJGP 204111 more poorly preserved, slightly larger than UMJGP 203605, with complete arcus vertebrae and both kidney-shaped caudal articulation facets still preserved; foramen vertebrae possibly slightly higher dorsoventrally than in UMJGP 203605; concave base of processus spinosus inclined cranially; UMJGP 203623 largest and best preserved vertebra cervicalis with both the convex cranial articulation facets facing craniomedially (axis inclined medially) and concave caudal articulation facets facing laterally; UMJGP 203638, 203653 (with small bone fragment), 203659, 203680 represent **vertebrae thoracicae** or **lumbales** (Fig. 4e–f): smaller corpus vertebrae than in vertebrae cervicales with a subtriangular (UMJGP 203638, 203659, 203680) to transverse-oval shape (UMJGP 203653) and less flattened craniocaudally than vertebrae cervicales; UMJGP 203663 badly preserved and quite small, but due to its transversal subrounded shape and its small cranial caudal width it could be a fragment of a **vertebra caudalis** (non-fused extremitas; Fig. 4g).

Several more or less fragmented **processus spinosi** (Fig. 4h–j) could be tentatively assigned to certain parts of the vertebral column: processus spinosus of vertebra cervicalis 6 or 7 (UMJGP 204681; Fig. 4h): slender processus spinosus [assigned to caudal part of cervical vertebral column due to length and slender habitus and based on comparison with the skeleton of *Prodeinotherium* from Langenau (Early Miocene) and figures in Huttunen and Göhlich (2002)]; in cross section triangular (pointing anterior); only slight cranial inclination (nearly vertical); fragment of processus spinosus of vertebra cervicalis 7 or vertebra thoracica 1 (UMJGP 203693): slender and similar in dimensions to UMJGP 204681 but with stronger developed triangular cross section, more pronounced cranial

crest and more concave caudal side [following Huttunen and Göhlich (2002) the processus spinosi become more concave from caudal part of cervical vertebrae to cranial part of thoracic vertebrae]; processus spinosi of vertebrae thoracicae from cranial series {UMJGP 203642, 203655, 203649 [with fragment of arcus vertebrae (? UMJGP 203646)], 203647, 203602, 203694 and 203603}: mediolaterally wider than processus spinosi of vertebrae cervicales; ordered from cranial to caudal due to increase in mediolateral width [in accordance with the skeleton of *Prodeinotherium* from Langenau (Early Miocene)]: processus spinosus of vertebra thoracica 1 or 2 (UMJGP 203642): with small fragment of right arcus and fragmented right processus lateralis; processus spinosus with triangular cross section, caudally slightly concave and decreasing in mediolateral width from proximal to distal (minimum preserved width distally: 30 mm); other processus spinosi of vertebrae thoracicae from cranial series {UMJGP 203655, 203649 [with fragment of arcus vertebralis (? UMJGP 203646)], 203647, 203602, 203694 and 203603} strongly increase in mediolateral width; craniocaudally flattened; longitudinal crest along the midline on the cranial surface opposed by a concave caudal surface; cranial crest more pronounced in UMJGP 203655 and 203602; mediolateral width and dorsoventral height of arcus vertebrae increases from UMJGP 203602 (Fig. 4i) to 203603 (Fig. 4j); UMJGP 203603 caudally not concave but with crest; fragment of one processus spinosus with clear bite mark (UMJGP 203694). Further fragments of processus spinosi [UMJGP 203687(?) and arcus vertebrarum [UMJGP 203681 (?), UMJGP 204684(?), UMJGP 203716, UMJGP 203675(?)] are preserved but cannot be assigned to specific vertebrae due to fragmentary preservation and do not allow any detailed description.

Costae: Most costae are fragmentary and allow no specific diagnosis [UMJGP 203604, 203608, 203610 (two crushed fragments?), 203634, 203643, 203644, 203648 (with fragment 203645), 203660 (?), 203687, 203696, 203692, 203697, 203703, 203717, 203666, 203658, 203629, 203630, 203635, 203617, 204673 (?)]. They were assigned to the *Deinotherium* skeleton due to their large dimensions and their finding position. Eleven costae were more complete and could be determined as elements of the cranial [UMJGP 203657 (costa 1/2? dex.), UMJGP 203606 (costa 2/3? dex.), and central-caudal part of the thorax (costae dex.: UMJGP 203639, 203650, 203695, 203633; costae sin.: 204110, 203631, 203618 and 203614–5 (fragment of the same rib), 203632, 203607]. Costae 1/2? and 2/3? in contrast to more caudal costae less curved but straight and shorter, craniocaudally flattened (stronger distal than proximal) and mediolaterally expanded, widening distally; cross section of costa 1/2? (UMJGP 203657) proximally ovoid (pointing caudolaterally) to distally strongly flattened and more acute caudolaterally; costae of central to caudal part of thorax

decrease in mediolateral width from cranial to caudal (UMJGP 203639 mediolaterally wider than UMJGP 203695) and gain a more rounded cross section from cranial to caudal; on the proximal part of corpus costae more or less developed sulcus costae on the cranial side and crest on caudal side; on craniolateral side ellipsoid shaped plane surface developed; sulcus costae more pronounced along distal part of corpus on caudal plane; costae mediolaterally flattened distally.

Scapula: represented by several blade-like bone fragments, the largest being 100–200 mm [UMJGP 203662, 203664, 203667, 203668, 203671, 203672, 203676, 203677, 203678(?), 203679, 203691, 204103]. The affiliation to the scapula is due to the flatness and rather constant thickness (5–25 mm) of the bone-blades and due to their finding position (Fig. 7). All fragments are supposed to represent a single scapula, although completely compressed and fractured. No anatomical details or diagnostic characters are preserved. An additional, small blade-like bone fragment, probably also belonging to the scapula, is attached to the humerus fragment (UMJGP 203674). On fragment UMJGP 204103 chewing marks are preserved.

Fragment of **humerus dex.?** (UMJGP 203674): very fragmentary, with plane surface on one side and convex one on the other; epiphyseal surface on plane side; in size and morphology the convex bone fits best to a proximal articulation surface of a humerus; due to poor preservation a more detailed description and reasonable affiliation not possible.

Radius (radius sin. missing distal end (UMJGP 203665; Fig. 5d); radius dex. proximal fragment with articulation facet for humerus (UMJGP 203621)): slender, tapering proximally and bent concave laterally; distal half of corpus radii mediolaterally flattened; cross-section at level of collum subtriangular; torsion of radius not very pronounced; caput radii subtriangular in proximal view; collum radii with pronounced incision dorsally; proximal articular facet for humerus subdivided in two slightly concave facets, facing proximolaterally and proximomedially, and enclosing an obtuse angle (Fig. 5d1); lateropalmar on caput radii large triangular facet for articulation with ulna (Fig. 5d1); due to preservation no detailed description can be given, though) distally bordered by a ridge running from lateroproximal to mediolateral; medial and lateral tuberosity on collum radii; distal to facet for the ulna on the lateropalmar side of the diaphysis longitudinal depression extending distally, becoming less deep in the middle part of the bone but deepening and widening again more distally; minimum width of the corpus radii in dorsal view in its middle part, broadening both distally and proximally.

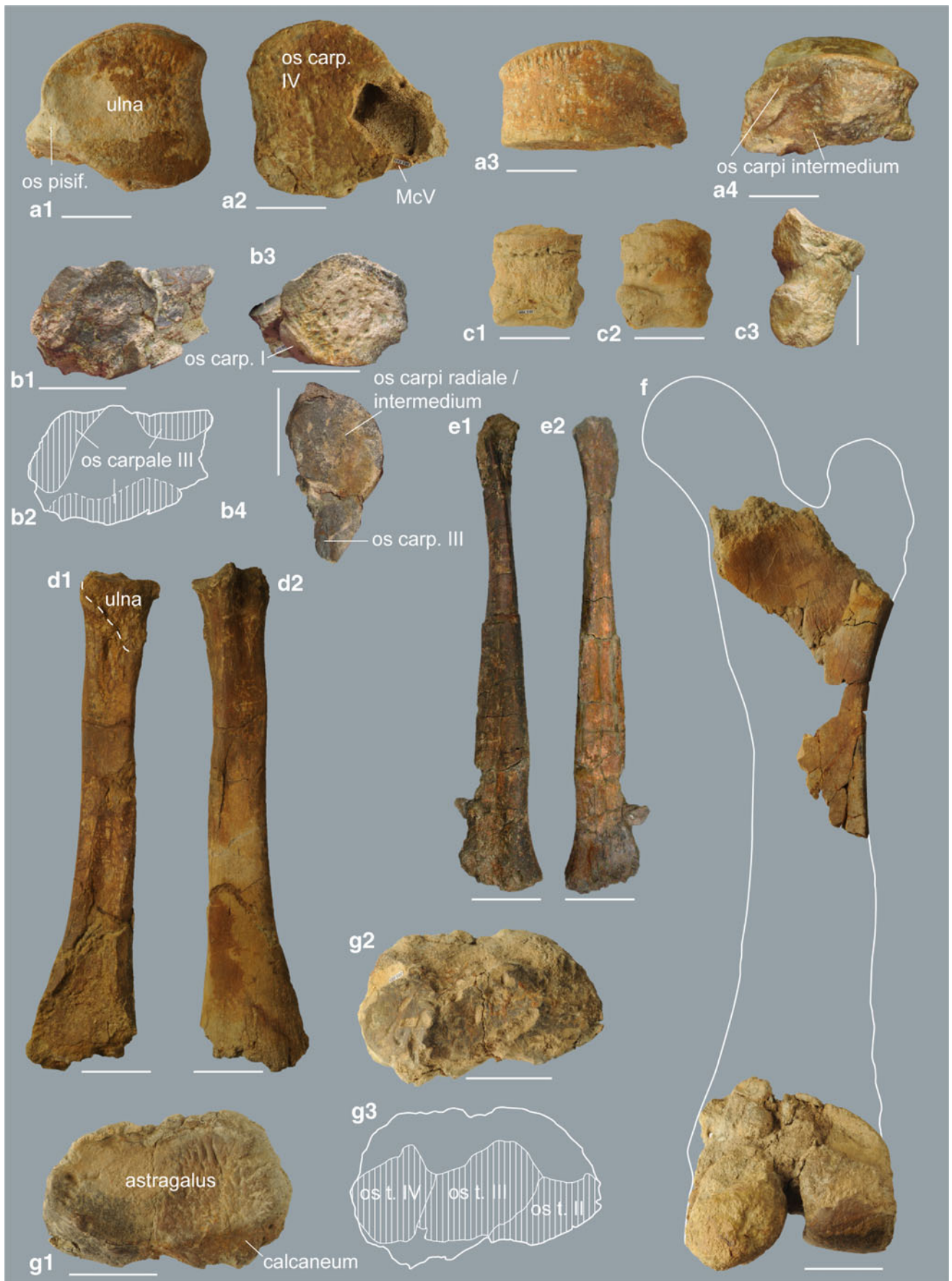
Comparison: The radius sin. (UMJGP 203665) is mediodorsal-lateropalmar more flattened at the proximal diaphysis than in *P. bavaricum* from Franzensbad (Early Miocene) or Unterzolling (early Middle Miocene; Huttunen and Göhlich 2002) which show a more triangular proximal

diaphysis. In overall shape, the radius from Gratkorn stronger resembles that of *D. proavum* from Ezerovo (Late Miocene) mounted at the University of Sofia. With the latter it also shares the generally more flattened corpus radii and the reduced torsion. Svistun (1974) unfortunately does not give any information concerning the degree of the torsion of the radius in comparison to other species. Though varying in its extent [in the specimen from Langenau (Early Miocene) it is more weakly developed than in the specimens from Unterzolling and Franzensbad] the torsion of the radius in the genus *Prodeinotherium* is stronger than in the Gratkorn specimen and in other specimens of *Deinotherium*.

Os carpi ulnare sin. (UMJGP 203688; Fig. 5a): quite large with pronounced lateropalmar processus (mostly broken off); proximal articulation surface for ulna large, subtriangular (pointing palmar) and dorsopalmar concave with a slightly convex medial half and a slightly concave lateral half (Fig. 5a1); triangular articulation facet for os pisiforme located at the lateral half of palmar surface and extending on lateral processus, facing lateropalmar forming a right angle with the proximal facet and tapering off medially (Fig. 5a1); distal articulation facet for articulation with os carpale quartum (damaged laterally) comprising two concave facets (axes dorsopalmarly) divided by central convexity (Fig. 5a2); due to fragmentariness of lateral processus only small part of articulation facet for Mc V preserved distally on the process, separated from distal facet by a distinct ridge; medial surface with a proximal and a distal longitudinal facet for articulation with os carpi intermedium (Fig. 5a4).

Comparison: The distal surface of the os carpi ulnare comprises two concave facets (axes dorsopalmarly) divided by central convexity as observed in *Deinotherium* from Paasdorf near Mistelbach (NHMW; Austria; Late Miocene) and described by Svistun (1974) for *D. levius* from Gusyatin (Middle Miocene). Following Huttunen (2000) this is typical for the genus. It can be distinguished from the concavo-convex or concave distal surface in *Prodeinotherium* (Huttunen 2000; Huttunen and Göhlich 2002).

Os carpale secundum sin. (UMJGP 203640; Fig. 5b): triangular shaped in proximal and distal view, narrowing palmarly (here damaged); proximal articulation facet for os carpi radiale and intermedium large and triangular, concave and tapering palmarly; facet for carpi radiale and intermedium enclosing an obtuse angle with facet for os carpale tertium; distal articulation facet for Mc II slightly convex (preserved only medially, damaged laterally); medial side damaged palmarly; round (three-quarters of circle), and slightly convex facet for articulation with os carpale primum on dorsodistal quarter of medial side (enclosing a nearly right angle with distal articulation facet); on lateral side three facets for articulation with the os carpale tertium not well preserved but still recognisable (Fig. 5b1, b2): large facet located proximodorsally,



◀ **Fig. 5** Elements of anterior and posterior limbs of *D. levius vel giganteum* from Gratkorn with affiliation of articulation facets: **a** os carpi ulnare sin. [UMJGP 203688; 1 proximal view (os pisif. = os pisiforme), 2 distal view, 3 dorsal view, 4 medial view], **b** os carpale secundum sin. [UMJGP 203640; 1 lateral view, 2 sketch of lateral view with identified articulation facets for os carpale tertium (III), 3 dorsal view (articulation facet for os carpale primum on medial side)], 4 proximal view with articulation facet for ossa carpi radiale and intermedium, **c** phalanx proximalis of pes? (UMJGP 203708; 1 dorsal view, 2 plantar view, 3 lateral/medial view), **d** radius sin. (UMJGP 203665; 1 lateropalmar view, 2 mediodorsal view); **e** fibula sin. (UMJGP 203622; 1 lateroplantar view, 2 mediodorsal view), **f** fragments of femur dex. in caudal view with sketch of outline (fragment of proximal shaft: UMJGP 203601; distal epiphysis: UMJGP 204112), **g** os tarsi centrale dex. [UMJGP 203683; 1 proximal view, 2 distal view, 3 sketch of distal view with identified articulation facets for os tarsale secundum (II), tertium (III) and quartum (IV)]. *Scale bar* 5 cm (**a–c, g**), 10 cm (**d–f**)

semicircular facet in proximopalmar part, only a small portion of the elongated distal facet preserved.

Comparison: Comparison material for the os carpale secundum consisted of one specimen of *D. cf. giganteum* from Wien XII Oswaldgasse (NHMW SK 2810; Austria; Late Miocene; Pannonian E; 10.4–10 Ma), which is larger and differs morphologically from the Gratkorn specimen by a less rounded dorsal side and the facet for articulation with os carpale primum, which comprises only a semi circle in the specimen from Wien XII Oswaldgasse. Following the description by Svistun (1974) the os carpale secundum of *D. levius* is in general of similar shape as the Gratkorn specimen but differs from the latter as it seems to possess only two facets for the articulation to the os carpale tertium.

Distal epiphysis with articulation facet of **Mc II** or **III** sin. or **IV** dex. (UMJGP 203685): due to its relatively large size it can be assigned to the manus rather than to the pes; due to fragmentary preservation most of the articulation facet missing; distal articulation facet dorsopalmar convex with small oblique ridge slightly shifted from the central line on palmar part of the trochlea, but not as asymmetric as it would be expected for Mc V.

Phalanx proximalis? of manus (UMJGP 203684) of unidentified digit: dorsal surface not preserved and phalanx missing its distal part; epiphysis not entirely closed proximally; proximal facet for articulation with metacarpal dorsopalmarly concave with a general inclination to proximopalmar; palmar side convex.

Comparison: Morphology alone does not allow affiliation to manus or pes, but dimensions in comparison with UMJGP 203708 render a determination as phalanx proximalis of manus more likely.

Femur dex. (distal epiphysis (UMJGP 204112), fragment of proximal shaft (UMJGP 203601); Fig. 5f): portion of proximal femur shaft with basis of trochanter minor (distinct depression on shaft caudal of trochanter minor); caudolateral edge of shaft subrectangular at base of trochanter minor; both

condyles on distal epiphysis damaged, the articulation surface of the condylus lateralis femoris damaged, except for its caudalmost part; only distal part of the trochlea ossis femoris preserved and showing a deep distal incision between the two condyles widening caudally; pronounced mediolateral depressions proximal to both condyles.

Comparison: Due to fragmentary preservation of the Gratkorn femur no comparison to other specimens can be given.

Fibula sin. (UMJGP 203622; Fig. 5e) and dex. (UMJGP 203613 (proximal portion of shaft without facet) 203612 (distal portion of shaft)): fibula sin. almost complete though lacking proximal and distal articulation facets; corpus fibulae triangular proximally (here smallest circumference); distal half mediolaterally flattened with slightly concave medial side; diagonal crest running from smallest circumference proximodorsally along the lateral side of the proximal fourth of the shaft.

Comparison: The morphological difference concerning the fibula between *Prodeinotherium* and *Deinotherium* as observed by Huttunen [“form of shaft proximally flattened in dorsoplantar direction” in *Deinotherium* (Huttunen 2000, p. 91)] cannot be confirmed based on the specimen from Gratkorn, as the cross section of the proximal shaft is triangular. The proximal cross section of both Gratkorn specimens is not more dorsoplantarly flattened than in *Prodeinotherium* from Langenau (Early Miocene), but its distal shaft seems to be more flattened mediolaterally than the latter.

Os tarsi centrale sin. (UMJGP 203611) and dex. (UMJGP 203683; Fig. 5g): both ossa tarsorum centralia badly preserved and missing most of dorsal, medial and plantar surfaces; proximal articulation facet for astragalus large, concave and oval shaped (mediolaterally elongated); small, proximoplantar oriented facet for articulation with the calcaneum located in the lateral half of the plantar side forming an obtuse angle with proximal articulation facet; on distal surface three articulation facets for the tarsals II–IV identified (from lateral to medial for os tarsale quartum (oriented distoplantolateral); os tarsale tertium; os tarsale secundum); most medial distal facet for Mt I not traceable, all preserved distal facets slightly concave separated by dorsomedial-plantolateral oriented ridges diverging in dorsomedial direction; no plantomedial process.

Comparison: With only three distal facets and no articulation facet for the Mt I the os tarsi centrale differs from that of *Prodeinotherium* (which shows four facets) but fits well with the situation in *Deinotherium* (Huttunen 2000). Furthermore, the os tarsi centrale differs from that of *P. bavaricum* from Unterzolling (early Middle Miocene) in the lack of a plantomedial process (Huttunen and Göhlich 2002).

Distal trochlea of **Mt II?** (UMJGP 204696): due to its smaller size in comparison to the Mc described above

(UMJGP 203685) trochlea assigned to a metatarsal; allocation of trochlea to digit II based on only slightly asymmetric shape.

? **Mt IV** dex. (UMJGP 203625): fragmentary assumed metatarsal missing most of the proximal and the complete distal end; elongated rectangular shape in dorsal view; cross section of diaphysis subtriangular widening medially; large trapezoid proximal articulation facet slightly declining laterally and smaller proximal facet (due to preservation shape cannot be reconstructed) declining medially; two facets enclosing an obtuse angle of about 130°; lateral side of shaft with pronounced proximodistal elongated sulcus weakening distally.

Comparison: identification as Mt IV dex. with uncertainty due to fragmentary preservation; overall shape of fragment also fitting to morphology of Mc II and III sin., but comparing dimensions with anterior and posterior metapodials of *P. bavaricum* from Franzensbad (Early Miocene), determination as Mt IV dex. is more likely.

Lateral fragment of **Mc I** or **Mt I** dex.? (UMJGP 203620): missing distal end; proximal articulation facet slightly dorsopalmarly concave and distinctly declining dorsally.

Phalanx proximalis II, III or IV? of pes (UMJGP 203708; Fig. 5c): subquadratic shape in dorsal view with proximal epiphyseal suture not entirely closed; proximal facet for articulation with metatarsal oval and dorsoplantar concave; distal trochlea slightly concave on plantar side; plantar surface concave; dorsal surface more plane.

Comparison: Quite symmetric shape of the phalanx indicates assignment to central digits II, III or IV, affiliation to pes is due to dimension in comparison with UMJGP 203684.

Os sesamoideum (UMJGP 203709 (almost complete; hmax = 61 mm); UMJGP 203710 (only distal half): morphology does not permit affiliation to manus or pes nor to any digit.

An additional small shaft fragment (UMJGP 203616) might represent another metapodial, which is similar in its dimension to UMJGP 203625; shaft with rectangular cross-section and slight concavity on lateral side;

Discussion

In terms of size and morphology, the teeth of the Gratkorn specimen fit well with both medium-sized species *D. giganteum* and *D. levius* from the type localities and other well-documented sites (Fig. 6). Differentiation between the two species *D. levius* and *D. giganteum* has been in discussion for a considerable time, and the validity of *D. levius* is often questioned, due to aforementioned supposed morphological, dimensional and stratigraphic overlap with *D. giganteum* (Huttunen 2002a). Gräf (1957) provided a comprehensive description and comparison of dental material of *D. levius* and *D. giganteum*. However, most of the species characteristics for *D. levius* described by her were shown to be more variable

(see also discussions in Bergounioux and Crouzel 1962; Tobien 1988; Huttunen 2000; Pickford and Pourabrishami 2013). Unfortunately, a p/3, so far “the only tooth that has clearly differential morphology in different size classes and different MN Zones” (Huttunen 2000, p. 42; see also discussion in Gasparik 2001), is not preserved from the Gratkorn specimen. This tooth is generally accepted to be species specific (Mottl 1969; Gasparik 2001; Huttunen and Göhlich 2002; Duranthon et al. 2007; Böhme et al. 2012) and distinguishes *D. levius* (proto- and metaconid separated) and *D. giganteum* (proto- and metaconid fused) (Gräf 1957; Mottl 1969; Böhme et al. 2012). Gasparik (2001) described in detail the morphology of the p/3 and especially the degree of fusion for proto- and metaconid in the species differentiation he gave for the material from Hungary. He figured a p/3 of “*D. giganteum*” from Sopron (Hungary; Late Miocene; Pannonian B; MN 9), which shows not fully fused proto- and metaconid (which would be typical for *D. levius*). Furthermore, measurements for this tooth given by Huttunen (2000) would not contradict an assignation to *D. levius*. The specimen from Sopron would thus be the youngest representative of the species *D. levius*, as the locality Sopron, Boór’s sandpit, can be correlated to Pannonian B, based on the occurrence of *Melanopsis impressa* (Vendl 1930 cited in Thenius 1948). The assumption of Huttunen and Göhlich (2002) that the separation of proto- and metaconid in the p/3 is a typical feature in *Prodeinotherium* distinguishing it from *Deinotherium* cannot be confirmed, taking into consideration the p/3s from Massenhausen (e.g. SNSB-BSPG 1955 I 43 and 47; late Middle Miocene), Hinterauerbach (SNSB-BSPG 1951 I 90; late Middle Miocene) and Sprendlingen 2 (Middle Miocene; Böhme et al. 2012), which all show separated proto- and metaconid, but are not in the dimensional variability of *Prodeinotherium* and should be assigned to *D. levius*. The separation of proto- and metaconid in the p/3 has thus to be considered a primitive dental character, still present in the oldest representative of the genus *Deinotherium*, *D. levius*, but lost in the younger representatives, such as *D. giganteum*.

The skeletal deinotherere elements from Gratkorn fit with the larger genus *Deinotherium* in size and morphology and show some distinct differences from the smaller genus *Prodeinotherium*. The specimen therefore corresponds well with the genus separation proposed by Éhik (1930). The weak torsion of the radius, a mediadorsal-lateropalmar flattened proximal diaphysis and the generally more flattened corpus radii are typical of *Deinotherium* and distinguish the radius from that of *Prodeinotherium* (Huttunen 2000 and personal observation). The distal articulation facet of the os carpi ulnare comprises two concave facets (axes dorsopalmarly) divided by a central convexity in the Gratkorn specimen and is not flat concave like in *Prodeinotherium* (Huttunen 2000). Furthermore, the Gratkorn specimen shares an os tarsi centrale with only three distal articulation facets and no facet for

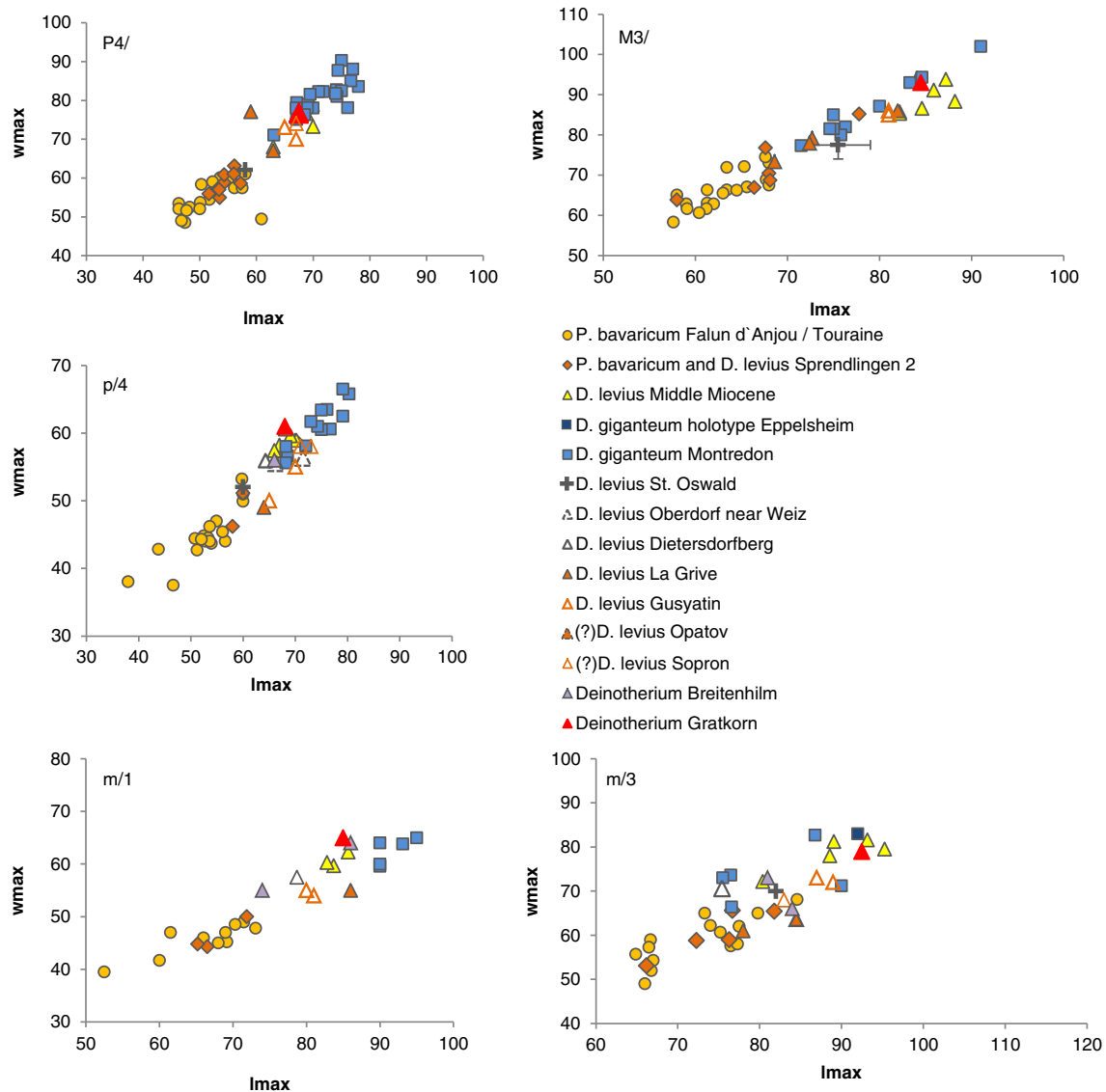


Fig. 6 Bivariate plots [wmax versus lmax (mm)] of dental material of *D. levius* vel *giganteum* from Gratkorn in comparison to other Deinotheriidae: *Prodeinotherium bavaricum* from Falun de la Touraine and Anjou (both France; early Middle Miocene; Langhian; MN 5; 15 ± 0.5 Ma; data from Ginsburg and Chevrier 2001); *P. bavaricum* and *Deinotherium levius* from Sprendlingen 2 (Germany; Middle Miocene; data from Böhme et al. 2012 and own measurements); *D. levius* from Middle Miocene sites [from France and Germany: St. Gaudens, Tournan (both France; late Middle Miocene; MN 7/8; 13–11.5 Ma); Massenhausen, Hinterauerbach (both Germany; late Middle Miocene; MN 7/8; 13–11.5 Ma; data from Gräf 1957; Ginsburg and Chevrier 2001); *D. levius* from St. Oswald near Gratwein (Austria; Middle Miocene; early Badenian), Oberdorf near Weiz (Austria; late Middle Miocene; late Sarmatian; 12.2–11.6 Ma) and Dietersdorfberg near Mureck

(Austria; late Middle Miocene; Sarmatian; 12.7–11.6 Ma) after Mottl 1969 and own measurements; *D. levius* from La Grive (France; late Middle Miocene; MN 7/8; 13–11.5 Ma; data from Huttunen 2000) and from Gussyatin (also Husyatyn) (Ukraine; Middle Miocene; early late Badenian; 13.1–13.4 Ma; data from Svistun 1974); *D. levius*(?) from Opatov (formerly Abtsdorf; Czech Republic; Middle Miocene; Badenian; data from Zázvorka 1940); *D. levius*(?) from Sopron (Hungary; Late Miocene; Pannonian B/C; MN 9; data from Huttunen 2000); *Deinotherium* from Breitenhilm near Hausmannstetten (Austria; late Middle Miocene; late Sarmatian; 12.2–11.6 Ma; data from Peters 1871); holotype of *D. giganteum* from Eppelsheim (Germany; Miocene; data from Gräf 1957) and *D. giganteum* from Montredon (France; Late Miocene; late Vallesian; MN 10; 9.5 Ma; data from Tobien 1988; Ginsburg and Chevrier 2001)

the articulation with the Mt I with *Deinotherium*, whereas *Prodeinotherium* shows four distal articulation facets (Huttunen 2000).

Summing up, from size and dimensions of the postcranial elements the specimen from Gratkorn fits well to the larger genus *Deinotherium*. As the teeth show most

dimensional and morphological overlap with *D. levius*, which is described from other localities of the same age, it most likely represents this species. However, it cannot be clearly distinguished from *D. giganteum* due to the absence of the diagnostic p/3 and it is thus determined as *Deinotherium levius* vel *giganteum*.

Ecology

In contrast to the bunodont gomphotheres, deinotheriids with their more primitive lophodont dentition, are considered to represent typical browsers (Harris 1975) well adapted to the consumption of soft foliage (Göhlich 1999). Calandra et al. (2008) showed that in comparison to two different *Gomphotherium* species, *D. giganteum* fed on less abrasive food. Harris (1975) observed only slight striation on the molar wear facets, which he interpreted as an indication for feeding on soft vegetation, while Calandra et al. (2008) found a higher scratch density on grinding than on shearing facets and therefore assume that each facet had two different functions during mastication. Harris (1996) observed a strict feeding on C₃-plants for deinotheres through their evolutionary history, while Miocene gomphotheres in Africa switched from a C₃ to a C₄-diet (Harris 1996; Huttunen 2000; Lister 2013). Stable isotope analyses ($\delta^{18}\text{O}_{\text{CO}_3}$, $\delta^{13}\text{C}$) from Gratkorn (Aiglstorfer et al. 2014, this issue) show a C₃-diet for *D. levius* vel *giganteum* as well and indicate canopy browsing.

The Gratkorn specimen was a not fully grown “young” adult, but could have reached sexual maturity. Due to the fact that most deinotheres occur as isolated finds or in fluvialite accumulated (and often stratigraphically mixed) assemblages, estimations on sexual dimorphism in terms of general size and tusk dimensions cannot be given so far (see also Huttunen 2000 for discussion). Therefore, gender determination for the partial skeleton from Gratkorn cannot be assessed.

Following estimations of Christiansen (2004) a body mass of about 6 t was calculated for the Gratkorn specimen based on the minimal circumference of the radius. As the animal was not fully grown lower values than for a fully grown specimen would be expected. However, this weight estimation has to be considered rather as a minimum value as it is based on modern elephants and following Christiansen (2007) can be applied to primitive proboscideans with reservations only [with more elongate bodies they could have reached higher body masses with the same shoulder height than the more compact modern elephants (Christiansen 2007)]. Other body mass estimations for *Deinotherium giganteum* vary between 11 t [Fortelius 2013 (NOW database)] and 19 t (representing an assumed fully-grown specimen; Merceron et al. 2012). In any case, *Deinotherium levius* vel *giganteum* was by far the largest herbivorous mammal at the Gratkorn locality.

The significantly different Sr⁸⁷/Sr⁸⁶ values in *D. levius* vel *giganteum* from Gratkorn in comparison to the local mammal fauna indicate that it was not a permanent resident of the locality but had a different habitat, such as the Styrian Basin, at least during tooth enamel formation (Aiglstorfer et al. 2014, this issue). Migration was most likely necessary for the animal as the environs around the Gratkorn locality presumably could not provide enough biomass during all seasons to support

such a large animal. Comparable to modern elephants (Galanti et al. 2006), the *Deinotherium* from Gratkorn thus presumably had a large habitat range.

Taphonomy

The partial skeleton of *Deinotherium levius* vel *giganteum* is spread over an area of about 140 m², with most of the material concentrated in the northern 50 m² (Fig. 7). Rough anatomical associations are preserved in some cases, such as the assemblage of posterior extremities comprising both fibulae, os tarsi centrale dex. and metatarsals in the western part of the excavation. Most costae are accumulated in the central part, and fragments of scapula, humerus, radius and os carpi ulnare sin. are deposited in the eastern part. Teeth of the sinistral upper jaw (though dislocated from the rest) or dextral part of the skull and mandible are still roughly associated as well, while the sinistral lower jaw is torn apart, as is the dextral femur, of which two parts have been excavated more than 6 m apart. Besides the sinistral upper jaw, the atlas is dislocated from the rest of the skeleton by more than 6 m. The rough association of the specimen and the lack of long bone or rib alignment indicate no significant water transport of the carcass after death and decomposition, but rather fragmentation, disintegration and finally burial at the actual place of death. Havlik et al. (2014, this issue) were able to show that the large mammal assemblage from Gratkorn was a preferred feeding place for scavengers. Scavenging by carnivores or trampling by large herbivorous mammals (such as, for example, Rhinocerotidae or Deinotheriidae) could explain dislocation and breakage of some skeletal parts. In studies on death and deposition of modern elephants in Africa, dislocation of the long bones of more than 100 m by lions, hyenas or even other elephants was observed (Haynes 1988). Furthermore, African elephants show a high degree of interest in skulls of their kin, touching them with trunks or feet, turning them over or even carrying them away (McComb et al. 2006). The strong demolition and dislocation of the dextral femur could thus simply result from such a treatment through other deinotheres, similar to what has also been described for modern elephants in Shabi Shabi (Zimbabwe; Conybeare and Haynes 1984). The strong breakage of most deinotheres bones and biting and chewing marks of carnivores on several bones [e.g. costa fragment with bite marks at distal part (UMJGP 203630), radius sin. with bite marks at lateral tuberosity of collum radii (UMJGP 203665) and chewing marks on fragment of scapula (UMJGP 204103)] fit well with an intense feeding by scavengers on the carcass. The general preservation of most bones of this partial skeleton is rather bad and very fragmentary and shows traits of weathering (see, for example, os tarsi centrale), which indicates no fast burial of the carcass but exposure on the surface for a considerable amount of time.

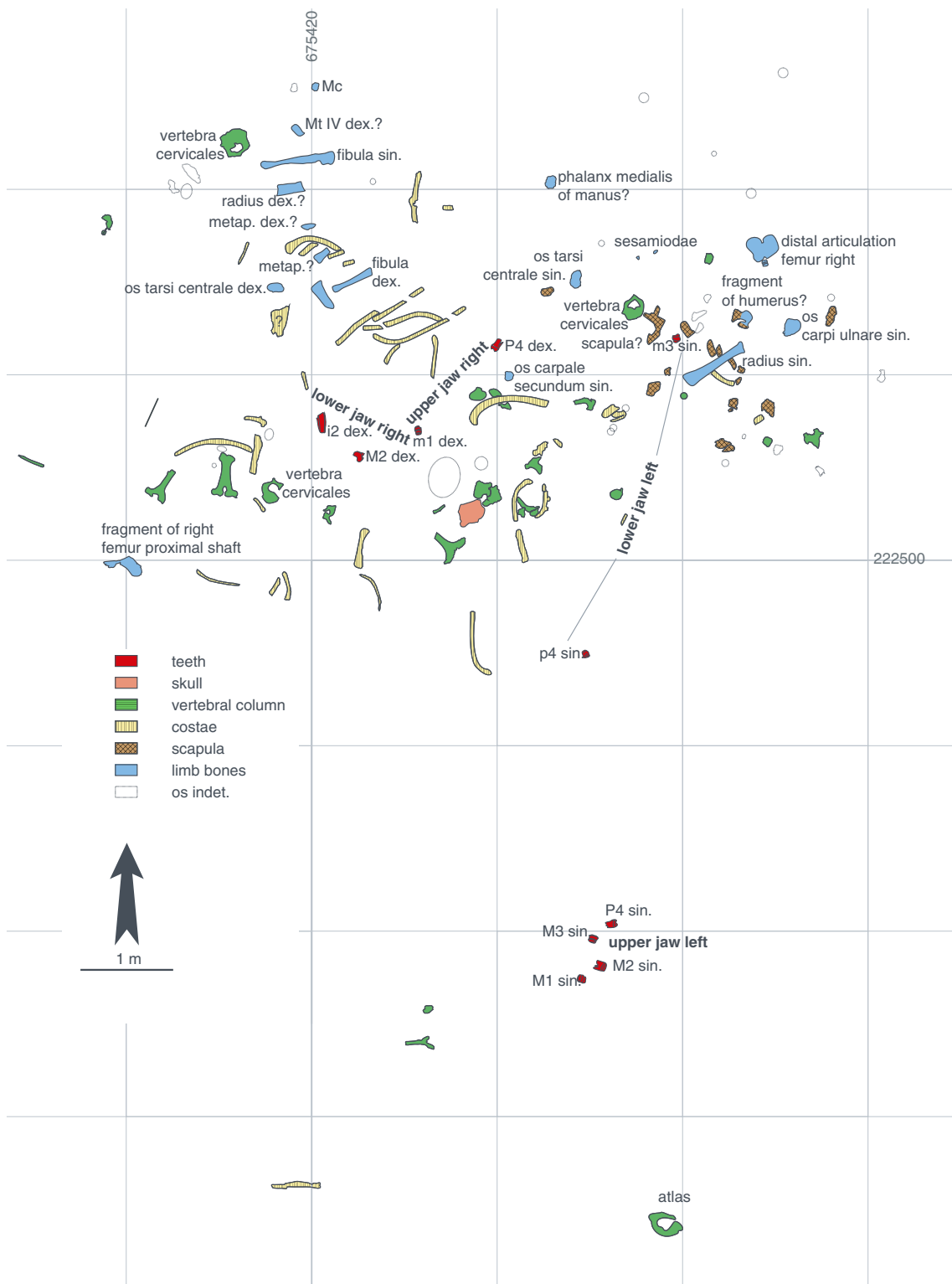


Fig. 7 Excavation plan of the partial *Deinotherium* skeleton from Gratkorn with identification of skeletal elements (modified after excavation plan by M. Gross (excavations 2005–2008); coordinates are in Austrian Grid (BMN M34 – GK)

One p/4 sin. (UMJGP 203435) and some tooth fragments from lower and/or upper molars (UMJGP 203420, 203421, 203460) were found on the surface about 30 m NW of the partial skeleton. As there is a p/4 sin. preserved from the

partial skeleton described above, the second p/4 sin. has to be assigned to a second specimen. Due to the position in the field and the general taphonomic situation (see, for example, Havlik et al. 2014, this issue) it is most likely that the

tooth fragments belong to the same individual like the p/4. The tooth remains differ from the teeth assigned to the skeleton by smaller dimensions, and stronger tooth wear (see Table 1 for different lengths of p/4). Sampling for isotopic measurements was done on this second specimen (see Aiglstorfer et al. 2014, this issue).

Conclusions

Besides the partial skeleton from Gusyatin (Middle Miocene; Svistun 1974) the specimen from Gratkorn, though partial, is the only one of a medium-sized deinother taxon described so far. Other deinother skeletons recorded are the mentioned *Prodeinotherium* skeletons from Langenau (Germany; Early Miocene), Franzensbad (Czech Republic; Early Miocene) and Unterzolling (Germany; early Middle Miocene) (Huttunen 2000, 2004; Huttunen and Göhlich 2002), the *Prodeinotherium* skeleton from Česká Třebová (Czech Republic; Middle Miocene; Badenian; Musil 1997) and the *Deinotherium proavum* skeletons from Ezerovo (Bulgaria; Late Miocene; Kovachev and Nikolov 2006), from Obuhovka (Russia; Late Miocene; Turolian; pre-Pontian; Bajgusheva and Titov 2006), from Pripiceni (Moldava; Late Miocene; Turolian; post-Bessarabian; Tarabukin 1968) and from Mânzați (Romania; Late Miocene; Stefanescu 1894). The assignment of deinother remains from Opatov (Middle Miocene; Zázvorka 1940; Musil 1997; most likely representing at least two skeletons) to *D. levius* could not be verified during the investigation for this publication. However, the dental measurements (Zázvorka 1940), fit with a medium-sized deinother.

With a generally more flattened corpus radii, a mediadorsal-lateralopalmar flattened proximal diaphysis and the weaker torsion of the bone, a distal surface on the os carpi ulnare with two concave facets (axes dorsopalmarly) divided by a central convexity, three distal articulation facets and none for the articulation to the Mt I in the os tarsi centrale, the deinother from Gratkorn fits well in postcranial morphology to the larger genus *Deinotherium* and clearly differs from the smaller genus *Prodeinotherium*. It thus confirms well to the genus separation. In dental dimensions the specimen fits with the medium-sized species *D. levius* and *D. giganteum*. For most tooth positions it overlaps with the lower dimensional range of *D. giganteum* and for all positions it nests well in the variability observed for *D. levius* (Fig. 6). The Gratkorn specimen is thus well in accordance with the gradual size increase observed for European Deinotheriidae mentioned above and most likely represents *D. levius*. However, due to the lack of a p/3 a distinction from *D. giganteum* cannot be given, and the specimen is determined as *Deinotherium levius* vel *giganteum*. Although the specimen cannot be clearly assigned to a certain

species, it is of scientific value. It possesses a clearly defined stratigraphic age and represents one of the rare records of associated postcranial and dental material of a medium sized deinother taxon.

Acknowledgements The authors are indebted to P. Havlik (GPIT) for fruitful discussions and correction of the manuscript. G. Rössner (SNSB-BSPG), G. Scharfe (IGM), R. Ziegler (SMNS), H. Lutz (NHMM), T. Engel (NHMM), H. Stapf (SSN), N. Spassov (NMNHS), G. Markov (NMNHS), L. Hristova (NMNHS), M. Ivanov (PMSU) and P. Havlik (GPIT) are thanked for the help and access to comparison material. D. Vasilyan (University Tübingen) is thanked for the help with the Russian literature. W. Gerber (University Tübingen) and A. Schumacher (NHMW) are thanked for taking pictures. N. Winkler (UMJGP) is thanked for preparation of the material. Many thanks go to the reviewers, G. Markov (NMNHS) and M. Pickford (MNHN), who greatly supported the improvement of the manuscript with their careful comments and correction of the English. For improvement of the English we want to thank as well A. Beckmann (University Tübingen). And last but not least the authors want to thank the students and volunteers from Graz, Munich and Tübingen for the good work in the excavations from 2005 to 2013.

References

- Aiglstorfer M, Bocherens H, Böhme M (2014) Large mammal ecology from the late Middle Miocene locality Gratkorn (Austria). In: Böhme M, Gross M, Prieto J (eds) The Sarmatian vertebrate locality Gratkorn, Styrian Basin. Palaeobio Palaeoenv 94(1). doi 10.1007/s12549-013-0145-5
- Antoine PO (1994) Tendances évolutives de Deinotheriidae (Mammalia, Proboscidea) miocènes du domaine sous-pyrénéen. Master thesis. Université Paul-Sabatier, Toulouse
- Bajgusheva SV, Titov V (2006) About teeth of *Deinotherium giganteum* Kaup from eastern paratethys. Hellenic J Geosci 41:177–182
- Bergounioux F-M, Cruzel F (1962) Les déinothéridés d'Europe. Ann Paléontol 48:13–56
- Böhme M, Aiglstorfer M, Uhl D, Kullmer O (2012) The antiquity of the Rhine river: stratigraphic coverage of the Deinotheriensande (Eppelsheim Formation) of the Mainz basin (Germany). PLoS ONE 7(5):e36817
- Calandra I, Göhlich UB, Merceron G (2008) How could sympatric megaherbivores coexist? Example of niche partitioning within a proboscidean community from the Miocene of Europe. Naturwissenschaften 95(9):831–838. doi:10.1007/s00114-008-0391-y
- Christiansen P (2004) Body size in proboscideans, with notes on elephant metabolism. Zool J Linn Soc 140(4):523–549. doi:10.1111/j.1096-3642.2004.00113.x
- Christiansen P (2007) Long-bone geometry in columnar-limbed animals: allometry of the proboscidean appendicular skeleton. Zool J Linn Soc 149(3):423–436. doi:10.1111/j.1096-3642.2007.00249.x
- Codrea V (1994) A priority issue: *Deinotherium proavum* Eichwald or *Deinotherium gigantissimum* Stefanescu? In: Petersen (ed) The Miocene from the Transylvanian Basin. Cluj-Napoca, Romania, pp 105–110
- Conybeare A, Haynes G (1984) Observations on elephant mortality and bones in water holes. Quat Res 22(2):189–200. doi:10.1016/0033-5894(84)90039-5

- Dehm R (1960) Zur Frage der Gleichaltrigkeit bei fossilen Säugerfaunen. *Int J Earth Sci* 49(1):36–40
- Depéret C (1887) Recherches sur la succession des faunes des vertèbres miocènes de la vallée du Rhône. *Arch Mus Natl Hist Nat (Lyon)* 4: 45–133
- Duranthon F, Antoine PO, Laffont D, Bilotte M (2007) Contemporanéité de *Prodeinotherium* et *Deinotherium* (Mammalia, Proboscidea) à Castelnau-Magnoac (Hautes Pyrénées, France). *Rev Paléobiol* 26(2):403–411
- Éhik J (1930) *Prodeinotherium hungaricum* n.g., n.sp. *Institutum Regni Hungariae Geologicum* 6:1–21
- Fortelius M (2013) New and Old Worlds database of fossil mammals (NOW). University of Helsinki. Available at: <http://www.helsinki.fi/science/now/>. Accessed 2 Sept 2013
- Galanti V, Preatoni D, Martinoli A, Wauters LA, Tosi G (2006) Space and habitat use of the African elephant in the Tarangire–Manyara ecosystem, Tanzania: Implications for conservation. *Mamm Biol* 71(2): 99–114. doi:10.1016/j.mambio.2005.10.001
- Gasparik M (1993) *Deinotheres* (Proboscidea, Mammalia) of Hungary. *Ann Hist-Nat Mus Natl Hung* 85:3–17
- Gasparik M (2001) Neogene proboscidean remains from Hungary; an overview. *Fragm Pal Hung* 19:61–77
- Ginsburg L, Chevrier F (2001) Les Dinotheres du bassin de la Loire et l'évolution du genre *Deinotherium* en France. *Symbioses* 5:9–24
- Göhlich UB (1998) Elephantoida (Proboscidea, Mammalia) aus dem Mittel- und Obermiozän der oberen Süßwassermolasse Süddeutschlands: Odontologie und Osteologie. *Münchner Geowiss Abh A* 36:1–245
- Göhlich UB (1999) Order Proboscidea. In: Rössner G, Heissig K (eds) *The Miocene land mammals of Europe*. Verlag Dr. Friedrich Pfeil, München, pp 157–168
- Gräf IE (1957) Die Prinzipien der Artbestimmung bei *Dinotherium*. *Palaeontogr Abt A Palaeozool-Stratigr* 108(5/6):131–185
- Gross M, Böhme M, Prieto J (2011) Gratkorn: A benchmark locality for the continental Sarmatian s.str. of the Central Paratethys. *Int J Earth Sci (Geol Rundsch)* 100(8):1895–1913. doi:10.1007/s00531-010-0615-1
- Gross M, Böhme M, Havlik P, Aiglstorfer M, (2014) The late Middle Miocene (Sarmatian s.str.) fossil site Gratkorn - the first decade of research, geology, stratigraphy and vertebrate fauna. In: Böhme M, Gross M, Prieto J (eds) *The Sarmatian vertebrate locality Gratkorn, Styrian Basin*. *Palaeobio Palaeoenv* 94(1). doi:10.1007/s12549-013-0149-1
- Harris JM (1973) *Prodeinotherium* from Gebel Zelten, Libya. *Bull Br Mus (Nat Hist) Geol* 23:285–350
- Harris JM (1975) Evolution of feeding mechanisms in the family Deinotheriidae (Mammalia: Proboscidea). *Zool J Linn Soc* 56: 331–362
- Harris JM (1996) Isotopic changes in the diet of African Proboscideans. *J Vertebr Paleontol* 16(40A)
- Havlik P, Aiglstorfer M, Beckman A, Gross M, Böhme M (2014) Taphonomical and ichnological considerations on the late Middle Miocene Gratkorn locality (Styria, Austria) with focus on large mammal taphonomy. In: Böhme M, Gross M, Prieto J (eds) *The Sarmatian vertebrate locality Gratkorn, Styrian Basin*. *Palaeobio Palaeoenv* 94(1). doi 10.1007/s12549-013-0142-8
- Haynes G (1988) Longitudinal studies of African elephant death and bone deposits. *J Archaeol Sci* 15(2):131–157. doi:10.1016/0305-4403(88)90003-9
- Hilber V (1914) Steirische Dinotherien. *Mitt Naturwiss Ver Steiermark* 51:111–132
- Huttunen KJ (2000) *Deinotheriidae* (Proboscidea, Mammalia) of the Miocene of Lower Austria, Burgenland and Czech Republic: Systematics, Odontology and Osteology. PhD thesis. Universität Wien, Vienna
- Huttunen KJ (2002a) Systematics and Taxonomy of the European Deinotheriidae (Proboscidea, Mammalia). *Ann Naturhist Mus Wien A* 103A:237–250
- Huttunen KJ (2002b) *Deinotheriidae* (Proboscidea, Mammalia) dental remains from the Miocene of Lower Austria and Burgenland. *Ann Naturhist Mus Wien A* 103A:251–285
- Huttunen KJ (2004) On a *Prodeinotherium bavaricum* (Proboscidea, Mammalia) skeleton from Franzensbad, Czech Republic. *Ann Naturhist Mus Wien A* 105A:333–361
- Huttunen KJ, Göhlich UB (2002) A partial skeleton of *Prodeinotherium bavaricum* (Proboscidea, Mammalia) from the Middle Miocene of Unterzolling (Upper Freshwater Molasse, Germany). *Geobios* 35: 489–514
- Joger U (2010) The way of life and ecology of modern elephants: Are conclusions about straight-tusked elephants and their habitat possible? [in German]. In: Meller H (ed) *Elefantenreich. Eine Fossilwelt in Europa*. Landesamt für Denkmalpflege und Archäologie Sachsen-Anhalt. Landesmuseum für Vorgeschichte, Halle, pp 314–321
- Kaup JJ (1829) Neues Säugethier, *Deinotherium: Deinotherium giganteum*. *Isis* 22(4):401–404
- Kaup JJ (1832) Description d'ossements fossiles de Mammifères inconnus jusqu'à présent, qui se trouvent au Muséum grand ducal de Darmstadt. C. Stahl, Darmstadt
- Kovachev D, Nikolov I (2006) *Deinotherium thraceiense* sp. nov. from the Miocene near Ezerovo, Plovdiv District. *Geol Balc* 35(3–4): 5–40
- Lister AM (2013) The role of behaviour in adaptive morphological evolution of African proboscideans. *Nature* 500:331–334. doi:10.1038/nature12275
- Markov GN (2008a) Fossil proboscideans (Mammalia) from the vicinities of Varna: a rare indication of middle Miocene vertebrate fauna in Bulgaria. *Hist Nat Bulg* 19:137–152
- Markov GN (2008b) The Turolian proboscideans (Mammalia) of Europe: preliminary observations. *Hist Nat Bulg* 19:153–178
- McComb K, Baker L, Moss C (2006) African elephants show high levels of interest in the skulls and ivory of their own species. *Biol Lett* 2(1): 26–28. doi:10.1098/rsbl.2005.0400
- Merceron G, Costeur L, Maridet O, Ramdarshan A, Göhlich UB (2012) Multi-proxy approach detects heterogeneous habitats for primates during the Miocene climatic optimum in Central Europe. *J Hum Evol* 63(1):150–161. doi:10.1016/j.jhevol.2012.04.006
- Mottl M (1969) Die Säugetierfunde von St. Oswald bei Gratwein, westlich von Graz in der Steiermark. *Festschrift des Landesmuseums Joanneum Graz*:299–320
- Mottl M (1970) Die jungtertiären Säugetierfaunen der Steiermark, Südost-Österreichs. *Mitt Mus Bergbau Geol Tech* 31:3–92
- Musil R (1997) A *Deinotherium* Skeleton from Česká Třebová. *Acta Mus Moraviae Sci Geol* 82:105–122
- Peters KF (1871) Über Reste von *Dinotherium* aus der obersten Miozänstufe der südlichen Steiermark. *Mitt Naturwiss Ver Steiermark* 2:367–399
- Pickford M, Pourabrishami Z (2013) Deciphering *Dinotheriidae* diversity. *Palaeobio Palaeoenv* 93(2):121–150. doi:10.1007/s12549-013-0115-y
- Poole JH (1996) The African elephant. In: Kangwana K (ed) *Studying elephants*. African Wildlife Foundation Technical Handbook Series vol 7. African Wildlife Foundation, Nairobi, pp 1–8
- Stefanescu G (1894) *Dinotherium gigantissimum*. *Annu Mus Geologia Paleontol* 1894:126–199
- Svistun VI (1974) *Dinotheriums* of Ukraine [in Russian]. *Naukovka dumka*, Kiev
- Tarabukin BA (1968) Excavation of a deinotherium skeleton in the Rezesh-Area of the Moldavian Republic [in Russian]. *Proc Acad Sci Mold SSR, Biol Chem Sci* 3:37–42

- Tassy P (1996) Dental homologies and nomenclature in the Proboscidea. In: Shoshani J, Tassy P (eds) *The Proboscidea—Evolution and palaeoecology of elephants and their relatives*. Oxford University Press, Oxford, pp 21–25
- Thenius E (1948) Über die Entwicklung des Hornzapfens von *Miotragocerus*. *Oesterr Akad Wiss Math-Natwiss Kl Sitzungsber* 157: 203–221
- Tobien H (1988) Contributions a l'étude du gisement miocène supérieur de Montredon (Herauld). *Les grands Mammifères*. 7—
Les proboscidiens Deinotheriidae. *Palaeovertebrata, Mémoire Extraordinaire* 1988:135-175
- Vendl M (1930) Die Geologie der Umgebung von Sopron II. *Erdeszeti Kiserletek* 32
- Vergiev S, Markov GN (2010) A mandible of *Deinotherium* (Mammalia: Proboscidea) from Aksakovo near Varna, Northeast Bulgaria. *Palaeodiversity* 3:241–247
- Zázvorka V (1940) *Deinotherium levius* Jourdan a jeho stratigrafický význam (in Czech and English). *Acta Mus Nat Pragae IIB* 7:191–214

Publication #2

Aiglstorfer M, Heissig K, Böhme M. (2014) Perissodactyla from the late Middle Miocene Gratkorn locality (Austria). *Palaeobiodiversity and Palaeoenvironments* 94, 71-82.

Own contribution:

Scientific ideas (%)	80
Data generation (%)	100
Analysis and Interpretation (%)	80
Paper writing (%)	85

Perissodactyla from the late Middle Miocene Gratkorn locality (Austria)

Manuela Aiglstorfer · Kurt Heissig · Madelaine Böhme

Received: 30 August 2013 / Revised: 5 November 2013 / Accepted: 20 November 2013 / Published online: 24 January 2014
© Senckenberg Gesellschaft für Naturforschung and Springer-Verlag Berlin Heidelberg 2014

Abstract Although quite rare in comparison to other large mammal groups, the Perissodactyla from Gratkorn show a diverse assemblage. Besides the three rhinocerotid species, *Aceratherium* sp., *Brachypotherium brachypus* (Lartet, 1837), and *Lartetotherium sansaniense* (Lartet, in Laurillard 1848), the families Chalicotheriidae and Equidae are represented by *Chalicotherium goldfussi* Kaup, 1833 and *Anchitherium* sp., respectively. The perissodactyl assemblage fits well in a late Middle Miocene (Sarmatian) riparian woodland with diverse habitats from active rivers to drier more open environments, as were present at the Gratkorn locality.

Keywords *Chalicotherium* · *Aceratherium* · *Brachypotherium* · *Lartetotherium* · *Anchitherium* · late Middle Miocene · Sarmatian · Central Europe

Introduction

The Gratkorn locality (clay pit St. Stefan) is located 10 km NNW of Graz (Styria, Austria). The fossil-bearing palaeosol of late Middle Miocene age (late Sarmatian sensu stricto;

12.2–12.0 Ma; Gross et al. 2011) comprises abundant small and large vertebrate fossils and is one of very few qualitatively and quantitatively rich vertebrate localities of this time period of the Paratethys realm. While artiodactyls are abundant within the large mammals from Gratkorn, perissodactyl remains are rare and comprise only some isolated teeth and some fragmented bones. Taxonomic determination is therefore limited for the material and cannot supply much information on general taxonomic and phylogenetic questions. For palaeoenvironmental considerations on the Gratkorn locality, the perissodactyls are essential elements. In contrast to many other, though richer, localities, they can furthermore provide confidently dated material for stratigraphic range estimations.

Materials and methods

Rhinocerotidae vel Chalicotheriidae: UMJGP 204701 (distal fragment of humerus sin.), UMJGP 204719 (petrosium)
Rhinocerotidae indet: UMJGP 203705 (distal fragment of tibia dex.), GPIT/MA/2400 (costa sin.?; proximal fragment)
Chalicotherium goldfussi: UMJGP 204676 (M3 dex.)
Aceratherium sp.: UMJGP 203711 (fragment of D2 sin.)
Brachypotherium brachypus: UMJGP 203434 (lateral half of astragalus sin.), UMJGP 204720 (Mt II sin.)
Lartetotherium sansaniense: UMJGP 203459 (m1 sin.; fragment of m2 sin.)
Anchitherium sp.: UMJGP 204694 (distal articulation of humerus sin.), UMJGP 203422 (distal articulation of radius dex.)
Terminology for dental material of Chalicotheriidae follows Fahlke et al. (2013; except for the term ectoloph, which is understood sensu Zapfe 1979; postfossette is understood sensu Butler 1965; and labial is used instead of buccal). For Rhinocerotidae, it is modified after Heissig (1969, 1972), and Heissig and Fejfar (2007). For postcranial

This article is a contribution to the special issue “The Sarmatian vertebrate locality Gratkorn, Styrian Basin.”

M. Aiglstorfer (✉) · M. Böhme
Fachbereich Geowissenschaften, Eberhard Karls Universität
Tübingen, Sigwartstraße 10, 72076 Tübingen, Germany
e-mail: manuela.aiglstorfer@senckenberg.de

M. Aiglstorfer · M. Böhme
Senckenberg Center for Human Evolution and Palaeoenvironment
(HEP), Sigwartstraße 10, 72076 Tübingen, Germany

K. Heissig
SNSB – Bayerische Staatssammlung für Paläontologie und
Geologie, Richard-Wagner-Str. 10, 80333 München, Germany

elements, current anatomical terms are used. Measurements are taken with a digital calliper (where possible with a precision of 0.1 mm) in the way indicated on Figs. 2 and 3. The way of measurement follows modified Heissig (1969), Zapfe (1979), Hünemann (1989) and Antoine (2002).

Institutional abbreviations

BMNH	British Museum of Natural History, London, Great Britain
GPIT	Paläontologische Sammlung der Universität Tübingen, Tübingen, Germany
SNSB-BSPG	Staatliche Naturwissenschaftliche Sammlungen Bayerns - Bayerische Staatssammlung für Paläontologie und Geologie, München, Germany
NHMW	Naturhistorisches Museum Wien, Wien, Austria
NMA	Naturmuseum Augsburg, Augsburg, Germany
UMJGP	Universalmuseum Joanneum, Graz, Austria

Anatomical abbreviations

L	Anteroposterior length of tooth
l max	Maximum anteroposterior length of tooth
l basally	Basal length of tooth at the base of the tooth crown (sensu Heissig 1969)
l ling	Lingual anteroposterior length of tooth
w ant	Anterior linguolabial width of tooth
w post	Posterior linguolabial width of tooth

Systematic palaeontology

Order Perissodactyla Owen, 1848
Rhinocerotidae vel Chalicotheriidae

Description and comparison

In size and morphology, specimen UMJGP 204701 fits well to the distal articulation of a left humerus from a large perissodactyl. It resembles *Anisodon grande* (see, e.g. Zapfe 1979, fig. 69, and Guérin 2012, fig. 1), but differs from it in the stronger distal concavity of the trochlea and the more rounded medial condyle. Furthermore it is slightly larger than *Anisodon grande*, which would fit well to *Chalicotherium goldfussi* (Zapfe 1989). However the morphology also resembles the humeri of Rhinocerotidae [see, e.g. Heissig 2012, figs. 65–67, *Brachypotherium* from Petersbuch (SNSB-BSPG 1969; Germany; Miocene), or Rhinocerotidae indet. from Mering (SNSB-BSPG 1960 I 121; Germany; Middle Miocene)]. In

comparison to the Gratkorn specimen, the concavity in the distal trochlea is even stronger in the two rhinocerotid humeri (personal observation). As no humerus of *Chalicotherium goldfussi* was available for comparison and as the fragment resembles both large perissodactyl families recorded from Gratkorn but slightly differs from both and cannot be assigned with certainty, it is assigned only to Rhinocerotidae vel Chalicotheriidae.

The size of an isolated petrosal fragment (UMJGP 204719) also corresponds with a rather large mammal. It is smaller than a proboscidean and larger than *Anchitherium* and all occurring Artiodactyla from Gratkorn. Whether it represents a chalicothere or a large rhinocerotid cannot be determined. It is therefore also assigned to Rhinocerotidae vel Chalicotheriidae.

Family Chalicotheriidae Gill, 1872

Subfamily Chalicotheriinae Gill, 1872

Genus *Chalicotherium* Kaup, 1833

Type species: *Chalicotherium goldfussi* Kaup, 1833

Chalicotherium goldfussi Kaup, 1833

Lectotype: M3 dex. (Kaup 1833, tab. VII, fig. 3)

Type locality: Eppelsheim, Rheinhessen, Germany

Description and comparison

The M3 dex. (UMJGP 204676; l: 41.5 mm, w ant: 44.2 mm, w post: ~37 mm; Figs. 1, 2a–e) is well preserved. It is low crowned and possesses a trapezoid shape decreasing in width posteriorly. Paracone, protocone, metacone, and hypocone are well developed. The paracone is the dominant cusp with a strongly inclined labial wall. The protocone is large and as strong as the hypocone. It is located slightly more posterior than the paracone. Para- and mesostyle are distinct, the metastyle is little developed and nearly fused with the metacone. The ectoloph is triconcave with a small depression anterior to the parastyle; its largest depression is at the labial wall of the paracone. A protoloph and paraconule are present and are connected to the paracone but only by a faint basal ridge to the protocone. The protoloph is short and the paraconule is lower than the protocone. The anterior valley is shallow, while the central valley is strongly developed, lingually open, and deeply incised into the lingual wall of the mesostyle. The posterior part of the ectoloph, comprising the metacone and metastyle, is directed posterolingually. The short metastyle is bent to the rear becoming almost longitudinal at its end. The posterior crest of the hypocone turns labially. Basally, it is connected to the metastyle forming a short posterior cingulum enclosing with the metacone a basally narrow and occlusally more open postfossette. A strong anterior and a weak lingual cingulum are present, while labially no cingulum is developed. At the protocone, the lingual cingulum rises and is less distinct, but is clearly still present.

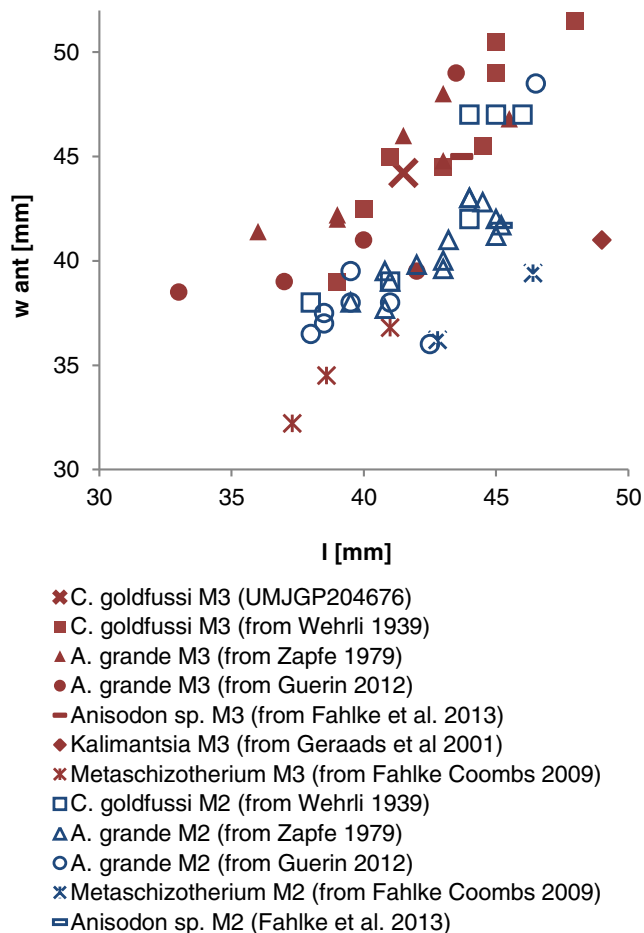


Fig. 1 Bivariate plot of length (l [mm]) versus anterior width (w_{ant} [mm]) of M3 of *Chalicotherium goldfussi* from Gratkorn (UMJGP 204676) in comparison to M2 and M3 of other Chalicotheriidae (references given in parentheses)

Following Anquetin et al. (2007), the upper M3 of Gratkorn must be assigned to the subfamily Chalicotheriinae because of the nonfusion of protoloph and protocone. A weak ridge connecting the paraconule and protocone very basally, which is observed in the specimen from Gratkorn, is not considered a fusion sensu Anquetin et al. (2007), as it can also be observed in the type specimen of *Chalicotherium goldfussi* (Schaefer and Zapfe 1971; Zapfe 1979). As in most Chalicotheriinae (Fahlke et al. 2013), the protocone is posterior to the paracone. Furthermore, Schizotheriinae possess an anteroposteriorly elongated rectangular shape in the upper molars in contrast to the square shape in Chalicotheriinae (Zapfe 1979; Coombs 1989), as observed in UMJGP 204676. In size, the Gratkorn specimen is well within the dimensions of both *Chalicotherium goldfussi* and *Anisodon grande* (de Blainville, 1849) (overlap of dimensions also recorded by Zapfe 1979; Coombs 1989) and is clearly wider than representatives of the Schizotheriinae (Fig. 1). In general shape, it fits best to *Chalicotherium goldfussi*. With this species, the specimen shares the presence of a cingulum at the lingual wall of the protocone (Schaefer and Zapfe 1971), a

wide and lingually open central valley (Schaefer and Zapfe 1971; Zapfe 1979), and the course of the labial wall of metacone–metastyle and hypocone (fig. 30 in Schaefer and Zapfe 1971; Anquetin et al. 2007). In *A. grande*, the metacone and metastyle are differently shaped and aligned to the anteroposterior axis of the tooth (see, e.g. fig. 31 in Schaefer and Zapfe 1971; Anquetin et al. 2007) and the central valley is narrower and lingually closed (Schaefer and Zapfe 1971; Zapfe 1979). In the M3 of *Anisodon* sp. from Dorn-Dürkheim 1 (Germany; Late Miocene; MN 11), which possesses a wider central valley than observed in *A. grande* (Fahlke et al. 2013), the central valley is still narrower than in the specimen from Gratkorn. From the M3 of *Kalimantsia* Geraads et al., 2001, the specimen differs by a more subsquare shape and the pattern and morphology of meta-, hypocone, and metastyle (Geraads et al. 2001).

Family Rhinocerotidae Gray, 1821

Rhinocerotidae indet.

Description and comparison

The dorsal half of a broad distal articular facet of a tibia dex. (UMJGP 203705) shows two grooves, a wider and deeper lateral one and a shallower and narrower medial one. A rather low ridge separating the grooves is oblique to the mediolateral axis. The articulation is very small in comparison to *Anisodon grande* (see, e.g. Zapfe 1979) and may, therefore, represent a large rhinocerotid.

The proximal part of a left rib (GPIT/MA/2400; Fig. 3e) has a large caput costae and a smaller tuberculum costae. In cross-section, the sulcus costae is not clearly set off, the cross-section of the corpus costae is drop-shaped, pointed anteriorly. This bone is far too small to represent a chalicothere and is therefore taken to be a rhinocerotid.

Subfamily Aceratheriinae Dollo, 1885

Tribe Aceratheriini Dollo, 1885

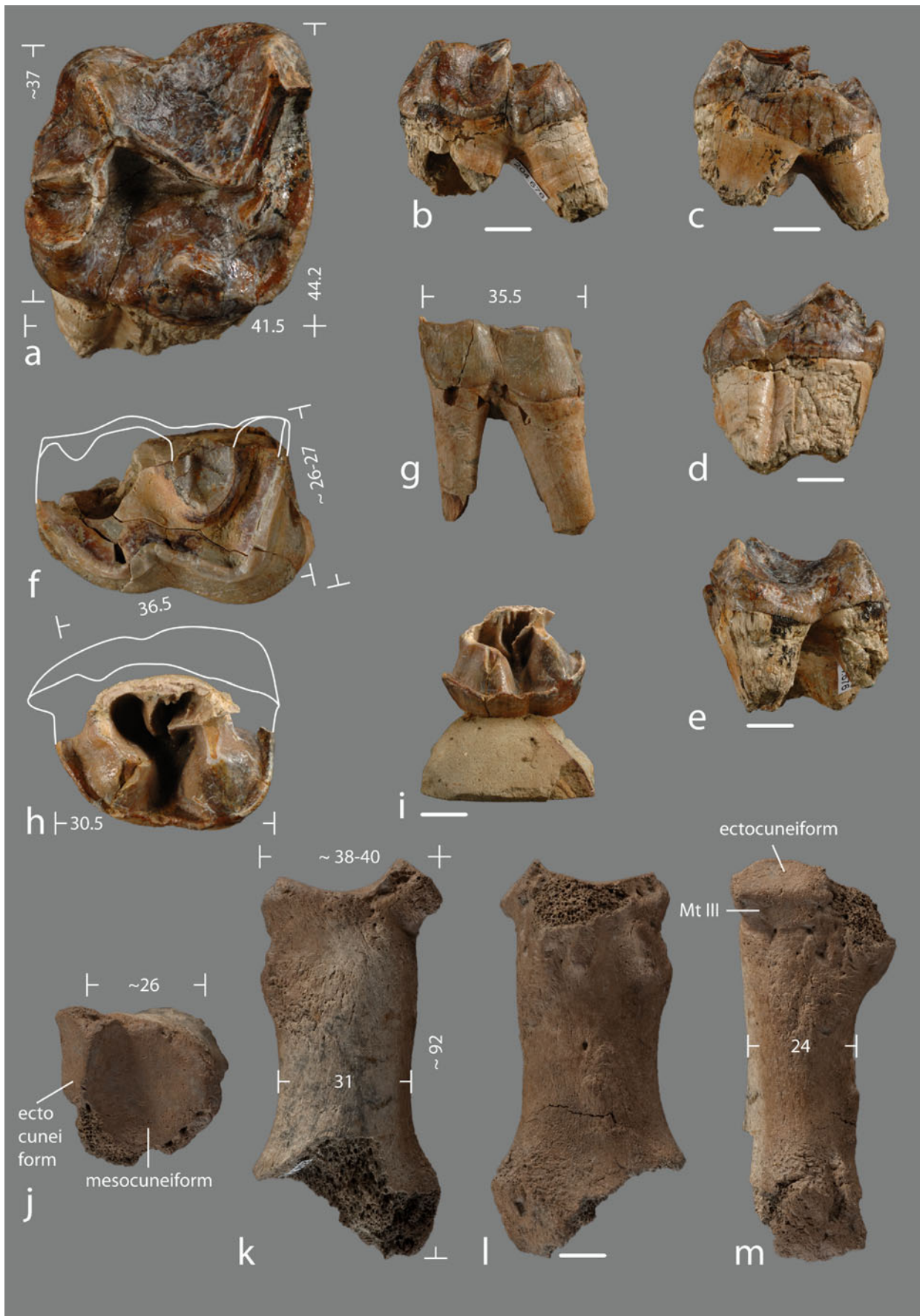
Genus *Aceratherium* Kaup, 1832

Type species: *Aceratherium incisivum* Kaup, 1832

Lectotype: Skull fragment, HLMD DIN 1927

Type locality: Eppelsheim, Rheinhessen, Germany

Remarks: So far, no general consensus has been reached concerning the taxonomic status of the diverse *Aceratherium*-like Rhinocerotidae in the Early and Middle Miocene of Europe. Geraads and Saraç (2003) even stated that most of the Middle Miocene *Aceratherium*-like “genera” correspond to poorly defined evolutionary grades rather than to clades” (Geraads and Saraç 2003, p. 218). Heissig (2009) observed only a few differences between *Alicornops* and *Aceratherium* in dentition and stated that they may not exceed



◀ **Fig. 2** a–e M3 dex. of *Chalicotherium goldfussi* from Gratkorn (UMJGP 204676; **a** occlusal view, **b** posterior view, **c** anterior view, **d** lingual view, **e** labial view); **f**, **g** m1 sin. of *Lartetotherium sansaniense* from Gratkorn (UMJGP 203459; **f** occlusal view, **g** labial view); **h**, **i** D2 sin. of *Aceratherium* sp. from Gratkorn (UMJGP 203711; **h** occlusal view, **i** lingual view); **j–m** Mt II sin. of *Brachypotherium brachypus* from Gratkorn (UMJGP 204720; **j** proximal view, **k** dorsal view, **l** plantar view; **m** lateral view; articulation facets labelled); *scale bar* 10 mm

subgeneric or even specific rank. He included *Alicornops* as a subgenus in the genus *Aceratherium*. Antoine et al. (2010) and Becker et al. (2013) provided cranial, dental, and postcranial characters and observed many differences between *Aceratherium incisivum* and *Alicornops simorreense*, thus enabling now a better discrimination between the different *Aceratherium*-like Rhinocerotidae. Unfortunately, the only characteristic feature observable on the D2 cannot be observed on the specimen from Gratkorn described below due to fragmentation. Therefore, we can only use the genus attribution *Aceratherium* here sensu lato.

Aceratherium sp.

Description and comparison

The lingual fragment of a D2 sin. (UMJGP 203711; 1 ling: 30.5 mm; Fig. 2h, i) could be assigned to *Aceratherium* sp.. It is little worn, low crowned, and possesses a subrounded lingual wall. The protoloph and metaloph are well developed, and oriented obliquely, respectively perpendicular to the anteroposterior axis of the tooth. The crista is fused with the ectoloph. The crochet arises anteriorly from the metaloph near its connection to the ectoloph. On the lingual wall of the ectoloph anteriorly and posteriorly to the crista, one and two additional small folds, respectively, are developed. The crista is oriented perpendicular to the length axis of the tooth, the crochet subparallel. They are not fused and the medifossette is not closed. The tooth possesses a weak anterior protocone groove and a strong postfossette. Due to breakage, the shape of the prefossette cannot be reconstructed. A strong basal cingulum reaches lingually from anterior to posterior interrupted briefly only at the hypocone.

In dimensions and morphology, the tooth strongly resembles D2 of *Aceratherium incisivum* described by Kaya and Heissig (2001) from Yulafli (Turkey; Late Miocene; Vallesian) and of *Aceratherium* sp. from Çandır (Turkey; Middle Miocene; MN 6; Geraads and Saraç 2003), differing only in the lingually open medifossette and the lack of a sharp incision of the lingual cingulum at the medisinus. *Aceratherium* sp. from Çandır possesses furthermore an additional fossette anterior to the medifossette, absent in the specimen from Yulafli as well as in the specimen from Gratkorn. From the similar-sized *Hoploaceratherium tetradactylum* (Lartet, 1836), the tooth from Gratkorn differs in the straight unbending protoloph, the lingually open medifossette, a less pronounced lingual cingulum and in a

shorter lingual length (Heissig 2012). The D2 of *Lartetotherium sansaniense* (Lartet in Laurillard, 1848) differs from the Gratkorn specimen in a smaller size, the reduced crista and a smaller postfossette (Heissig 2012). Dimensions of D1 of *Brachypotherium brachypus* (Lartet, 1837) (Heissig 2012) indicated a larger size for the D2 in this species than in the specimen from Gratkorn. At the moment, three genera (*Aceratherium*, *Alicornops*, *Hoploaceratherium*) are considered valid for the aceratheres from the Middle and Late Miocene of Western Europe (MN6 –MN13; Giaourtsakis 2003). Heissig (2009) explained that the only dental difference between *Alicornops* and *Aceratherium* is the size of the big incisors. Generally, teeth are very similar within the tribe (Heissig 2004) and differentiation based on teeth is difficult even between genera such as *Hoploaceratherium* and *Aceratherium*, due to the similarity in “cheek tooth characters” (Heissig 2004, p. 228). Giaourtsakis (2003) also stated that an assignment of isolated teeth to one of these genera is difficult and that the type locality of *Aceratherium incisivum* might contain more than one species as also indicated by Heissig (1972, 1996). The tooth from Gratkorn described here shows most similarities in dimensions and morphology with the genus *Aceratherium* s. l., but cannot be assigned to a species and is therefore left in open nomenclature as *Aceratherium* sp.

Tribe Teleoceratini Hay, 1902

Genus *Brachypotherium* Roger, 1904

Type species: *Brachypotherium brachypus* (Lartet, 1837)

Remarks: At the moment, two European *Brachypotherium* species are considered valid, *B. brachypus* and *B. goldfussi* (Kaup, 1834), though synonymy of the two taxa is possible (Heissig 2012).

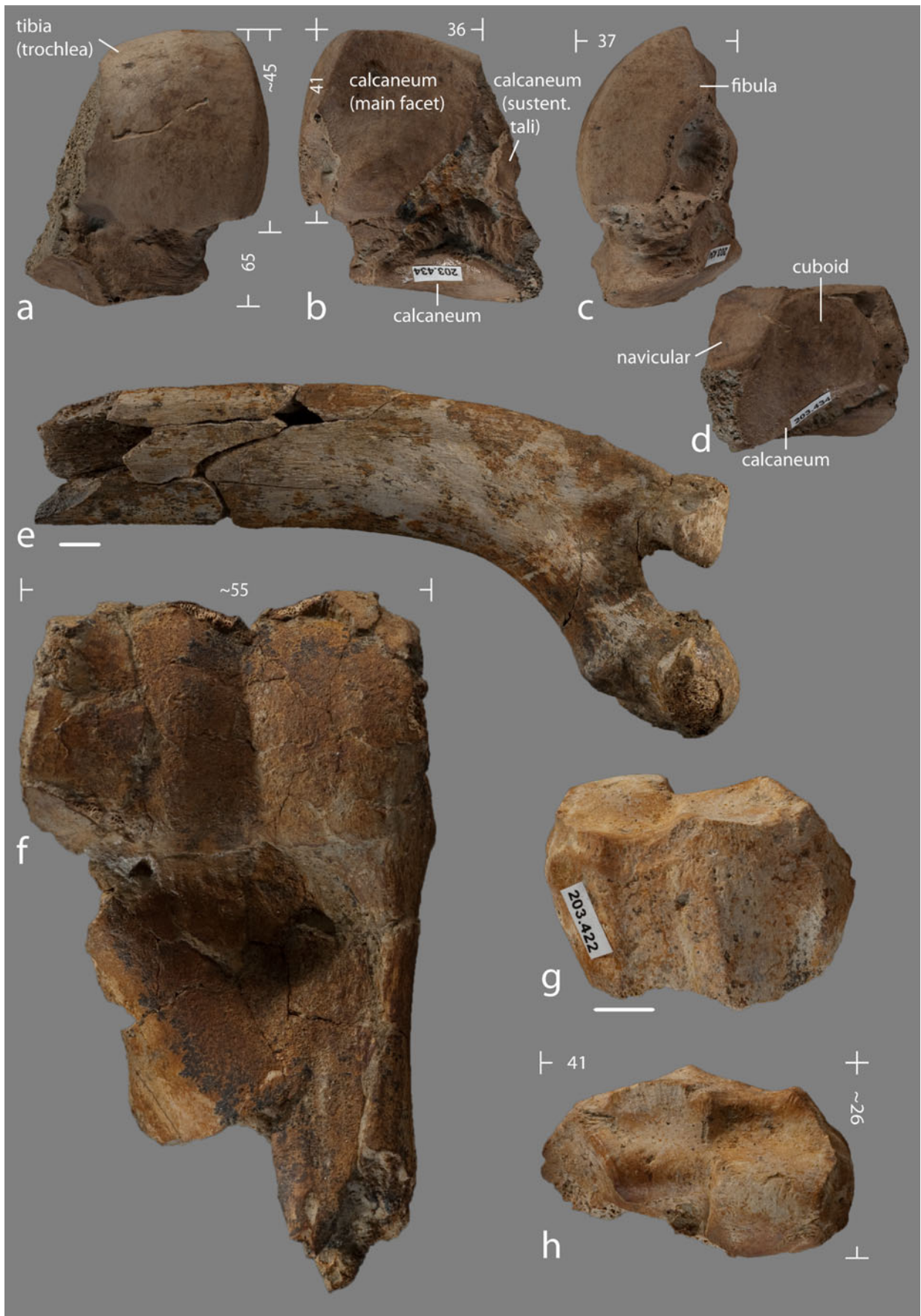
Brachypotherium brachypus

Type: not designated (see also Heissig 2012)

Type locality: Simorre, Gers, France

Description and comparison

Of an astragalus sin. the lateral half is preserved (UMJGP 203434; lateral proximodistal length: about 65 mm; lateral dorsoplantar width of trochlea: 37 mm; lateral proximodistal length of trochlea: ~45 mm; proximodistal length of main (=ectal) facet for calcaneum: 41 mm; mediolateral width of main facet for calcaneum: 36 mm; Fig. 3a–d). The astragalus is proximodistally shorter than it is in Equidae (see, e.g. Alberdi et al. 2004), but longer than in Chalicotheriidae (see, e.g. Zapfe 1979) as it is typical in Rhinocerotidae (Heissig 2012). On the dorsal side, it still shows the convex lateral part of the trochlea with a shallow trochlear notch indicated medially. In lateral view, the narrow radius of the trochlea can be observed. The trochlea proximally meets the large



◀ **Fig. 3** **a–d** Astragalus sin. of *Brachypotherium brachypus* from Gratkorn (UMJGP 203434; **a** dorsal view, **b** plantar view, **c** lateral view; **d** distal view; articulation facets labelled); **e** left rib of Rhinocerotidae indet. (GPIT/MA/2400) from Gratkorn; **f** humerus sin. of *Anchitherium* sp. from Gratkorn (UMJGP 204694); **g, h** radius dex. of *Anchitherium* sp. from Gratkorn (UMJGP 203422; **g** dorsal view, **h** distal view); scale bar 10 mm

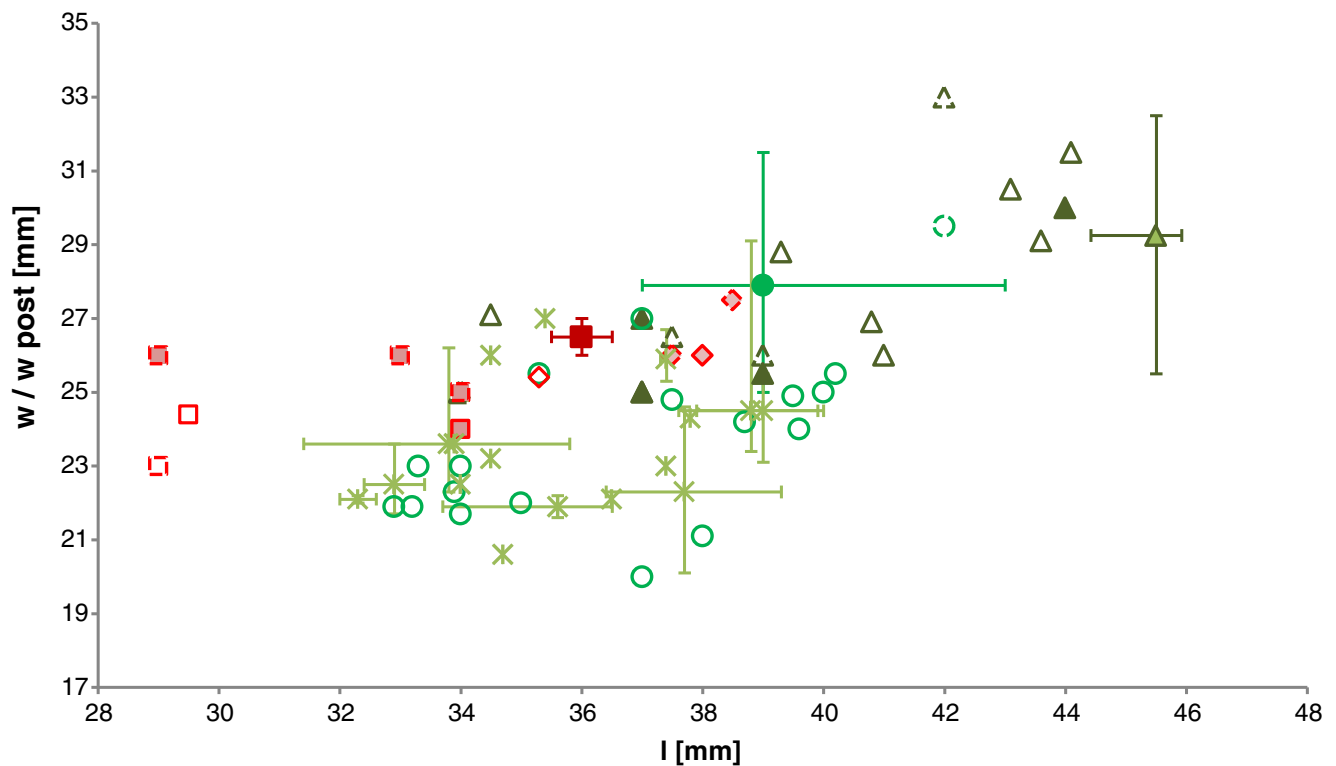
lateroproximal main facet for the articulation with the calcaneum at an acute angle. The latter possesses the typical “saddle-structure” of rhinoceroses, but is only slightly concave proximally and increasingly convex distally. It meets the facet for the articulation to the fibula to form an obtuse angle. The fibula facet is broad and convex. The narrow distal articular facet with the calcaneum is transversely elongated and meets the facet for articulation with the cuboid at an obtuse angle, while only a small part of the sustentaculum tali facet is preserved. The three calcaneum facets are separated by wide grooves. The cuboid facet is large, oval to subtriangular, and slightly convex along its short axis (dorsomedial to lateroplantar). Along its length axis, it changes from convex laterally to faintly concave medioplantarily. Of the facet for the articulation with the navicular, only the lateral-most part is preserved which is concave in both directions. It meets the cuboid facet at a rectangular to obtuse angle and is inclined laterally. The collum tali separating the articular facets for navicular and cuboid from the trochlea by a shallow depression is about 16 mm high laterally.

The astragalus from Gratkorn is most similar to that of *Brachypotherium brachypus*. As is typical for the Teleoceratini, it is broad and possesses only a shallow trochlear notch (Heissig 2012). With *Brachypotherium brachypus*, the specimen shares, besides the general shape, the distal prolongation of the main facet for the articulation with the calcaneum (Heissig 1976; Ginsburg and Bulot 1984; Cerdeño 1993; Geraads and Saraç 2003). While this is a constant feature in the species, dimensions seem to vary over time (Geraads and Saraç 2003). *Brachypotherium brachypus* from Bézian à La Romieu (Gers, France; Early Miocene; MN 4; Ginsburg and Bulot 1984), from Middle Miocene localities from France (Cerdeño 1993), and from Çandır (Turkey; Heissig 1976) are generally larger. A few smaller specimens are recorded from Çandır and Sofca (Turkey; late Middle Miocene; MN 7/8; Geraads and Saraç 2003; Heissig 1976). The astragalus from Gratkorn differs from those of representatives of the Rhinocerotinae by the separation of all the three calcaneum facets, whereas the distolateral one is fused to the sustentacular facet in this subfamily (Heissig 2009). In dimensions, the astragalus from Gratkorn would also fit well with *Aceratherium incisivum* from Höwenegg (Germany; Late Miocene; MN 9; Hünemann 1989), Rudabánya (Hungary; Late Miocene; MN 9; Heissig 2004) and Atzelsdorf (Austria; Late Miocene; MN 9; Heissig 2009), but differs in general morphology. In *Aceratherium*, the main facet for the articulation with the

calcaneum is more strongly concave and distally not prolonged (Hünemann 1989; Heissig 2009; Antoine et al. 2010), the collum tali is shorter (Hünemann 1989), the trochlea is less bent in lateral view (Heissig 2009), the trochlear notch is deeper (see figs. in Hünemann 1989 and Heissig 2004), and in dorsal view, the distal rim of the trochlea rises more strongly proximally in the medial direction (see figs. in Heissig 2009). The latter two features and the non-elongated main calcaneum facet also distinguish the astragalus of *Hoploaceratherium tetradactylum* from the Gratkorn specimen (see figs. in Heissig 2004, 2012). In *A. (Alicornops) simorreense*, the main calcaneum articulation is also more strongly convex (Antoine et al. 2010). Based on size and morphology, UMJGP 203434 can be assigned to *Brachypotherium brachypus*.

A partial metatarsal II sin. (UMJGP 204720; Fig. 2j–m), missing the distal part, is preserved (preserved length: 92 mm; preserved proximal mediolateral width: ~38–40 mm; mediolateral width of facet for mesocuneiform: ~26 mm; smallest mediolateral width of diaphysis: 31 mm; smallest dorsoplantar width of diaphysis: 24 mm). The distal articulation and the lateroplantar part of the articulations for the ectocuneiform and metatarsal III are broken. In proximal view, the plantar half of the medial rim possesses at least three large foramina. The subtriangular articular surface for the mesocuneiform is large and mediolaterally moderately concave. Laterally, it borders the articular surface for the ectocuneiform. The latter is inclined to the proximal surface and abuts the articular surface for metatarsal III. These two dorsolateral facets meet at an angle of about 130–140°. Only the dorsolateral facets are preserved. The further presence of plantolateral facets is not proved but probable. In the space between the preserved dorsal and the missing plantar facets, there is a foramen near the margin of the proximal facet.

The Gratkorn second metatarsal is shorter and more massive than that of all rhinoceroses of the Middle Miocene except *Brachypotherium*. Further, the proximal facet for the mesocuneiform is broader and less concave than in *Aceratherium* (Hünemann 1989) and *Lartetotherium* (Heissig 2012). The inclination of the articular facet for the ectocuneiform is a typical sign of shortened metapodials and also occurs in other rhinocerotids with short metapodials. As for the astragalus, the metatarsal II differs from most specimens of *Brachypotherium brachypus* in its smaller size. Great size variability, as, e.g. observed above for the astragalus, can also be observed for the distal elements of the hind limb. A high variability has also been noticed for carpal elements of Late Miocene *Teleoceras* from Florida (Harrison and Manning 1983). A *Brachypotherium* metatarsal III from Sofca (Heissig 1976) fits well to the Gratkorn metatarsal II described here. UMJGP 204720 can therefore be readily assigned to *Brachypotherium brachypus*.



- ✱ *A. simorreense* m1 (Cerdeño and Sánchez 2000 l/w)
- △ *A. incisivum* m1 (Teppner 1915 l/wpost)
- ▲ *A. incisivum* m1 (Cerdeño and Sánchez 1998 l/w)
- *H. tetradactylum* m1 (Santafe-Llopis et al. 1982 l/w)
- ◐ *H. belvederense* m1 (Heissig 2004 l/w)
- ◇ *L. aff. sansaniense* m2 (Heissig 2004 l/w)
- ◊ *L. sans.* Hofkirchen m2 (pers obs l/wpost)
- ◻ *L. aff. sansaniense* m1 (Heissig 2004 l/w)
- ◻ *L. sans.* Hofkirchen m1 (pers obs l/wpost)
- ▲ *A. incisivum* m1 (Kaup 1832 l/w)
- ▲ *A. incisivum* m1 (Guérin 1980 l/w)
- ▲ *A. incisivum* m1 (Heissig 2004 l/w)
- *H. tetradactylum* m1 (Heissig 2012 l/wpost)
- ◇ *L. sansaniense* m2 (Heissig 2012 l/wpost)
- ◇ *L. sansaniense* m2 (Heissig 1972 l/w)
- ◻ *L. sansaniense* m1 (Heissig 2012 l/wpost)
- ◻ *L. sansaniense* m1 (Heissig 1972 l/w)
- *L. sansaniense* m1 Gratkorn (UMJGP 203459)

Fig. 4 Bivariate plot of length (l [mm]) versus width of m1 of *Lartetotherium sansaniense* from Gratkorn (UMJGP 203459) in comparison to m1 and m2 of other Rhinocerotidae of similar dimensions (if given posterior width was used, [mm]); for the Gratkorn specimen, the

mean and the range from l basally to l max is given). References for measurements are given in parentheses (*L. sansaniense* from Hofkirchen (SNSB-BSPG 1958 I 170; Germany; Early/Middle Miocene)

Subfamily Rhinocerotinae Dollo, 1885

Tribe Rhinocerotini Dollo, 1885

Genus *Lartetotherium* Ginsburg, 1974

Type and only species: *Lartetotherium sansaniense* (Lartet in Laurillard, 1848)

Lartetotherium sansaniense (Lartet in Laurillard, 1848)

Holotype: Skull with mandible MNHN Sa 6478 (monotype)

Type locality: Sansan, France

Remarks: For a long time, there have been doubts whether this genus was single- or double-horned. After the determination that there was no trace of a second horn (Heissig 2012), the separation of *Lartetotherium* from the double-horned

Dicerorhinus was fully justified. This is also well in accordance with Antoine et al. (2010), who reconstructed a phylogenetic position for *Lartetotherium* remote from *Dicerorhinus sumatrensis* (Fischer, 1814), and observed a sister group relationship with the one-horned *Gaindatherium*.

Description and comparison

A lower m1 sin. and a small fragment of a m2 sin. (UMJGP 203459; l max m1: 36.5 mm, l basally m1: 35.5, w post m1: ~26–27 mm; Fig. 2f, g) are preserved with some jaw fragments. The m2 fragment exhibits no usable characters. The m1 is fragmented lacking most of the trigonid, of which only the labial wall is preserved. The length of the parolophid and

the width of the trigonid cannot be estimated therefore. The lingual wall of the talonid is also missing. The tooth is strongly worn (maximal preserved height at hypoconid: 15 mm). It possesses a short anterior and posterior, but lacks a labial cingulid. The labial wall is steep and forms an angle of about 120° with the occlusal surface at the hypoconid. The metalophid and hypolophid are united by wear. The trigonid and talonid are angular. The ectoflexid is distinct but not deep. It is inclined posteriorly. The incision of the talonid groove is not deep. The enamel is weakly wrinkled.

Tooth dimensions are quite variable between and among rhinocerotid species (compare, e.g. dimensions in Kaup 1832; Teppner 1915; Heissig 1972; Guérin 1980; Sántafe-Llopis et al. 1982; Cerdeño 1993; Cerdeño and Sánchez 1998, 2000; Heissig 2004, 2012; Fig. 4). Even if p4 and m1 cannot be distinguished by size (Heissig 2012), the rather open angulation of the hypolophid excludes the determination as a premolar. Many characters, such as a basally inclined labial wall and a moderately deep ectoflexid, are common to a lot of rhinoceros species. Because the most striking character for the separation of Rhinocerotini and Aceratheriini, the length of the paralophid, is not preserved, the only valuable character is the configuration of the cingulids. There is absolutely no labial cingulid and the anterior and the posterior cingulid are short and do not proceed onto the labial side. This configuration excludes the Aceratheriinae, which have longer terminal cingulids, mainly on the posterior side, and often short cingular ridges or cusps below the ectoflexid. “*Dicerorhinus*” *steinheimensis* Jäger, 1839, which also has strongly reduced cingulids, differs from the Gratkorn specimen by a clearly smaller size. The strongly reduced cingulids are very characteristic for *Lartetotherium sansaniense* (Heissig 2012). So the tooth proves the presence of this third species, which is widespread in Middle Miocene faunas.

Family Equidae Gray, 1821

Subfamily Anchitheriinae Leidy, 1869

Genus *Anchitherium* Meyer, 1844

Type species: *Anchitherium aurelianense* (Cuvier, 1825)

Lectotype: Left upper jaw with P2-M3 (Sa 5154; Abusch-Siewert 1983; pl. 16, fig. 1)

Type locality: Sansan, France

Anchitherium sp.

Description and comparison

The distal fragment of the humerus sin. (UMJGP 204694; Fig. 3f) is compressed, but the biconcave equine condylus humeri can still be recognised. It comprises a stronger medial and a shallower lateral depression. In size (distal lateromedial

width of articulation: ~55 mm) it fits well in the variability of *A. aurelianense* from Baigneaux (France; Early Miocene; MN 4; Alberdi et al. 2004), Sansan (France; Middle Miocene; MN 6; Alberdi and Rodríguez 2012) and Sandelzhausen (Germany; Middle Miocene; MN 5; personal observation).

Although the distal articulation of a right radius (UMJGP 203422; Fig. 3g, h) is fragmented, lacks most of the processus styloideus radii, and shows intense small mammal gnawing, its typical equine morphology can still be observed. The trochlea radii is bipartite, the medial condyle being larger than the lateral and shifted more in the palmar direction along the sagittal plane. Anterior to the two condyles of the trochlea radii is a depression, which is only slightly biconcave. Distally the radius is not fused with the ulna, as is typical for *Anchitherium* (see, e.g. *A. aurelianense*, Alberdi et al. 2004, and *A. corcolense*, Iñigo 1997) in contrast to *Hipparion* (Alberdi and Rodríguez 1999), where the ulna and radius are fused distally. The distal part of the concavity for the articulation to the ulna is preserved.

The distal fragment from Gratkorn fits well in shape and dimensions (distal lateromedial width of articulation: 41 mm; distal dorsopalmar width of articulation: ~26 mm) to *A. aurelianense* from Baigneaux (Alberdi et al. 2004), Sansan (Alberdi and Rodríguez 2012), and Sandelzhausen (personal observation, material SNSB-BSPG), as well as to *A. corcolense* Iñigo, 1997 from Córcoles (Spain; Early Miocene; MN 4; Iñigo 1997), but is smaller than in the larger genus *Sinohippus* Zhai, 1962 (Salesa et al. 2004). As the taxonomic status of late Middle Miocene to Late Miocene *Anchitherium* species is still unresolved (Abusch-Siewert 1983), and the two fragments from Gratkorn do not show any species diagnostic features, they are left in open nomenclature as *Anchitherium* sp..

Stratigraphic and ecological considerations

The perissodactyl fauna from Gratkorn fits well as a Middle Miocene mammal assemblage. Although *C. goldfussi* was defined by Kaup (1833) on material from the Dinotheriensande from Eppelsheim, so far considered to be of Late Miocene age, its occurrence was not restricted to Upper Miocene sediments, but it is also known from late Middle Miocene localities, such as Saint-Gaudens and La Grive (both France; MN 7/8; Anquetin et al. 2007). Böhme et al. (2012) showed, furthermore, that the Dinotheriensande (Eppelsheim Fm) are not restricted to the Upper Miocene but also include faunal elements of strictly Middle Miocene age. *Brachypotherium*, *Aceratherium* and *Lartetotherium* are part of phylogenetic lineages ranging from Early to Late Miocene (Heissig 2009, 2012). Though Late Miocene occurrences of *Anchitherium* are recorded in some European localities (see, e.g. Villalta and Crusafont 1945; Thenius 1950; Alberdi 1974;

Sondaar 1971; Abusch-Siewert 1983; Hernández Fernández et al. 2003; Daxner-Höck and Bernor 2009), the species is common mainly in the Early and Middle Miocene (Abusch-Siewert 1983). In association with the other large mammal remains, it fits well in a late Middle Miocene assemblage. A general size increase in the Eurasian Anchitheriinae was observed during the Miocene by Mayet (1908), Wehrli (1938), Abusch-Siewert (1983) and Alberdi and Rodríguez (2012), while Salesa et al. (2004) noted co-occurrence of different size classes in some localities. A late Middle Miocene age could not be verified by the increased size of *Anchitherium* remains from Gratkorn, however, because of the scarcity of the material and especially due to the total absence of dental material, in which a size increase can be much better observed than in postcranial elements (Alberdi and Rodríguez 2012).

The fossil assemblage from Gratkorn is preserved in a palaeosol and shows no signs of reworking (Gross et al. 2011; Havlik et al. 2014, this issue). The composition of the fossil assemblage was most likely strongly controlled by ecological factors. Secondary accumulation of very large mammals, due to a higher preservation potential of their robust hard tissues, as, e.g. observed in fluvial sediments, was thus not the case at the locality (for further discussion, see Havlik et al. 2014, this issue). The wider landscape around Gratkorn supplied a great range of habitats, such as active and abandoned channels, riparian woodland, floodplain soils, and ephemeral ponds as well as nearby drier, open areas (Gross et al. 2011; Böhme and Vasilyan 2014, this issue). For the locality itself and the nearer surroundings, it can be assumed that only a limited amount of biomass was available. Perissodactyls with larger body sizes and thus a higher amount of daily food intake, such as Rhinocerotidae and Chalicotheriidae, were therefore most likely rarer in Gratkorn than the artiodactyls with their smaller body sizes (for further discussion, see Aiglstorfer et al. 2014a, this issue). The few records of the equid *Anchitherium* sp. might be explained by ecological adaptation to more open environments than, e.g. in ruminants, which are the most common large mammals in Gratkorn (for further discussion, see Aiglstorfer et al. 2014b, this issue). Generally considered to be non-selective browsers, *B. brachypus* and *A. incisivum* (Heissig 2009) would fit well in this ecosystem with a wide range of habitats. Stable isotope ($\delta^{18}\text{O}_{\text{CO}_3}$, $\delta^{13}\text{C}$) analyses on the enamel of *Lartetotherium sansaniense* from Gratkorn even indicate a certain amount of feeding in a more open environment (see Aiglstorfer et al. 2014a, this issue). Because of the lack of lingual cingula on the upper premolars, this species has often been interpreted as a selective browser (Heissig 2012), but this feature does not exclude a considerable amount of low abrasive grasses. Kaiser (2009) recorded a mixed feeding strategy for *A. aurelianense* from Sandelzhausen, terming it a “dirty” browser. Hernández Fernández et al. (2003) considered *Anchitherium* to be generally a browser. Semperebon et al. (2011) assigned *C. goldfussi*

to the browsing guild by microwear analysis, but, because of the higher enamel abrasion, reconstructed a certain amount of hard fruits, seeds or nuts in their diet. Referring to observations by Zapfe (1979) on the fissure fillings from Devínska Nová Ves (Slovakia; Middle Miocene; MN 6), Semperebon et al. (2011) have suggested that *Celtis* fruits, as a possible diet source, could produce microwear patterns, such as those observed for European Chalicotheriinae in their study. Microwear studies have so far not been accomplished for Gratkorn, but could help to verify the hypothesis of Semperebon et al. (2011) with *Celtis* being a common element of the flora in Gratkorn and therefore a potential food source for *C. goldfussi*. However, the higher potential for preservation of this fruit in comparison to other flora has of course to be taken into consideration. As is common in Central and Western Europe during that time, grazing as a dominant feeding strategy is not indicated in the perissodactyl large mammals from Gratkorn.

Acknowledgments For fruitful discussions, helpful comments and access to the collection, we want to thank Philippe Havlik (GPIT). For access to collections and the possibility to see material for comparison, we want to thank Martin Gross (UMJGP), Gertrud Rössner (SNSB-BSPG), Ursula Göhlich (NHMW), Michael Rummel (NMA), and Emma Bernard (BMNH). For finding, excavating and giving us the possibility to work on the material, many thanks to Martin Gross (UMJGP). For preparation of specimens, many thanks to Norbert Winkler (UMJGP), and, for taking pictures, to Wolfgang Gerber (GPIT). Many thanks to Pierre Olivier Antoine and Margery C. Coombs, who greatly helped to improve the manuscript with their careful reviews and correction of our English. And last but not least, many thanks to all the students and voluntary helpers from Graz, Munich and Tübingen for their good work during the excavations.

References

- Abusch-Siewert S (1983) Gebißmorphologische Untersuchungen an eurasiatischen Anchitherien (Equidae, Mammalia) unter besonderer Berücksichtigung der Fundstelle Sandelzhausen. *Cour Forsch-Inst Senckenberg* 62:1–361
- Aiglstorfer M, Bocherens H, Böhme M (2014a) Large mammal ecology in the late Middle Miocene Gratkorn locality (Austria). In: Böhme M, Gross M, Prieto J (eds) The Sarmatian vertebrate locality Gratkorn, Styrian Basin. *Palaeobio Palaeoenv* 94(1). doi:10.1007/s12549-013-0145-5
- Aiglstorfer M, Rössner GE, Böhme M (2014b) *Dorcatherium nauii* and pecoran ruminants from the late Middle Miocene Gratkorn locality (Austria). In: Böhme M, Gross M, Prieto J (eds) The Sarmatian vertebrate locality Gratkorn, Styrian Basin. *Palaeobio Palaeoenv* 94(1). doi: 10.1007/s12549-013-0141-9
- Alberdi MT (1974) Las “faunas de Hipparion” de los yacimientos españoles. *Estud Geol* 30:189–212
- Alberdi MT, Rodríguez J (1999) Restos de *Anchitherium* de Lisboa, Portugal. *Ciências da Terra (UNL)* 13:93–114
- Alberdi MT, Rodríguez J (2012) *Anchitherium* Meyer, 1844 (Perissodactyla, Equidae) de Sansan. In: Peigné S, Sen S (eds) Mammifères de Sansan. *Mem Mus Natl Hist Nat* 203: 487–533

- Alberdi MT, Ginsburg L, Rodríguez J (2004) *Anchitherium aurelianense* (Mammalia, Equidae) (Cuvier, 1825) dans l'Orléanien (Miocène) de France. *Geodiversitas* 26(1):115–155
- Anquetin J, Antoine P-O, Tassy P (2007) Middle Miocene Chalicotheriinae (Mammalia, Perissodactyla) from France, with a discussion on chalicotheriine phylogeny. *Zool J Linn Soc* 151(3): 577–608. doi:10.1111/j.1096-3642.2007.00327.x
- Antoine P-O (2002) Phylogénie et évolution des Elasmotheriina (Mammalia, Rhinocerotidae). *Mem Mus Natl Hist Nat* 188:1–359
- Antoine P-O, Downing KF, Crochet J-Y, Duranthon F, Flynn LJ, Marivaux L, Métais G, Rajpar AR, Roohi G (2010) A revision of *Aceratherium blanfordi* Lydekker, 1884 (Mammalia: Rhinocerotidae) from the Early Miocene of Pakistan: Postcranials as a key. *Zool J Linn Soc* 160(1):139–194. doi:10.1111/j.1096-3642.2009.00597.x
- Becker D, Antoine P-O, Maridet O (2013) A new genus of Rhinocerotidae (Mammalia, Perissodactyla) from the Oligocene of Europe. *J Syst Palaeontol*. doi:10.1080/14772019.2012.699007
- Böhme M, Vasilyan D (2014) Ectothermic vertebrates from the late Middle Miocene of Gratkorn (Austria, Styria). In: Böhme M, Gross M, Prieto J (eds) The Sarmatian vertebrate locality Gratkorn, Styrian Basin. *Palaeobio Palaeoenv* 94(1). doi:10.1007/s12549-013-0143-7
- Böhme M, Aiglstorfer M, Uhl D, Kullmer O (2012) The Antiquity of the Rhine River: Stratigraphic Coverage of the *Dinotheriensande* (Eppelsheim Formation) of the Mainz Basin (Germany). *PLoS ONE* 7(5):e36817
- Butler PM (1965) East African Miocene and Pleistocene chalicotheres. *Bull Br Mus Nat Hist* 10:163–237
- Cerdeño E (1993) Étude sur *Diaceratherium aurelianense* et *Brachypotherium brachypus* (Rhinocerotidae, Mammalia) du Miocène moyen de France. *Bull Mus Natl Hist Nat* 4(15):25–77
- Cerdeño E, Sánchez B (1998) *Aceratherium incisivum* (Rhinocerotidae) en el Mioceno Superior de Cerro de Los Batallones (Madrid). *Rev Esp Paleontol* 13(1):51–60
- Cerdeño E, Sánchez B (2000) Intraspecific variation and evolutionary trends of *Alicornops simorreense* (Rhinocerotidae) in Spain. *Zool Scr* 29(4):275–305. doi:10.1046/j.1463-6409.2000.00047.x
- Coombs MC (1989) Interrelationships and Diversity in the Chalicotheriidae. In: Prothero DR, Schoch RM (eds) The Evolution of Perissodactyls. Clarendon Oxford University press, New York, pp 438–457
- Daxner-Höck G, Bernor RL (2009) The early Vallesian vertebrates of Atzelsdorf (Late Miocene, Austria) 8. *Anchitherium*, Suidae and Castoridae (Mammalia). *Ann Nathist Mus Wien A* 111 A:557–584
- Fahlke JM, Coombs MC (2009) Dentition and first postcranial description of *Metaschizotherium fraasi* KOENIGSWALD, 1932 (Perissodactyla: Chalicotheriidae) and its occurrence on a karstic plateau - new insights into schizotheriine morphology, relationships, and ecology. *Palaeontographica* 290(1–3):65–129
- Fahlke J, Coombs M, Semperebon G (2013) *Anisodon* sp. (Mammalia, Perissodactyla, Chalicotheriidae) from the Turolian of Dorn-Dürkheim I (Rheinhessen, Germany): morphology, phylogeny, and palaeoecology of the latest chalicothere in Central Europe. *Palaeobio Palaeoenv* 93(2):151–170. doi:10.1007/s12549-013-0119-7
- Geraads D, Saraç G (2003) Rhinocerotidae from the Middle Miocene Hominoid Locality of Çandir (Turkey). *Cour Forsch-Inst Senckenberg* 240:217–231
- Geraads D, Spassov N, Kovachev D (2001) New Chalicotheriidae (Perissodactyla, Mammalia) from the Late Miocene of Bulgaria. *J Vertebr Paleontol* 21(3):596–606. doi:10.1671/0272-4634(2001)021[0596:ncpmft]2.0.co;2
- Giaourtsakis IX (2003) Late Neogene Rhinocerotidae of Greece: distribution, diversity and stratigraphical range. In: Reumer JWF, Wessels W (eds) Distribution and migration of tertiary mammals in Eurasia. A volume in Honour of Hans de Bruijn, vol 10. *Deinsea*. pp 235–253
- Ginsburg L, Bulot C (1984) Les Rhinocerotidae (Perissodactyla, Mammalia) du Miocène de Bézian à La Romieu (Gers). *Bull Mus Natl Hist Nat* 6:353–377
- Gross M, Böhme M, Prieto J (2011) Gratkorn: A benchmark locality for the continental Sarmatian s.str. of the Central Paratethys. *Int J Earth Sci* 100(8):1895–1913. doi:10.1007/s00531-010-0615-1
- Guérin C (1980) Les Rhinocéros (Mammalia, Perissodactyla) du Miocène Terminal au Pleistocène Supérieur en Europe Occidentale Comparaison avec les espèces actuelles. *Doc Labo Géol Fac Sci Lyon* 79(1):1–1185
- Guérin C (2012) *Anisodon grande* (Perissodactyla, Chalicotheriidae) de Sansan. In: Peigné S, Sen S (eds) Mammifères de Sansan. *Mem Mus Natl Hist Nat* 203: 279–315
- Harrison JA, Manning EM (1983) Extreme Carpal Variability in Teleoceras (Rhinocerotidae, Mammalia). *J Vertebr Paleontol* 31(1): 58–64
- Havlik P, Aiglstorfer M, Beckmann AK, Gross M, Böhme M (2014) Taphonomical and ichnological considerations on the late Middle Miocene Gratkorn locality (Styria, Austria) with focus on large mammal taphonomy. In: Böhme M, Gross M, Prieto J (eds) The Sarmatian vertebrate locality Gratkorn, Styrian Basin. *Palaeobio Palaeoenv* 94(1). doi:10.1007/s12549-013-0142-8
- Heissig K (1969) Die Rhinocerotidae (Mammalia) aus der oberoligozänen Spaltenfüllung von Gaimersheim bei Ingolstadt in Bayern und ihre phylogenetische Stellung. *Bayer Akad Wiss Math-Natur Kl Abh (NF)* 138:1–133
- Heissig K (1972) Paläontologische und geologische Untersuchungen im Tertiär von Pakistan 5. Rhinocerotidae (Mamm.) aus den unteren und mittleren Siwalik-Schichten. *Bayer Akad Wiss Math-Natur Kl Abh (NF)* 152:1–112
- Heissig K (1976) Rhinocerotidae (Mammalia) aus der Anchitherium-Fauna Anatoliens. *Geol Jahrb B* 19:3–121
- Heissig K (1996) Ein Schädel von *Hoploaceratherium* aus dem Obermiozän Bayerns. *Mitt Bayer Staatsslg Paläont Hist Geol* 36: 145–156
- Heissig K (2004) The fossil Rhinoceroses of Rudabánya. *Palaeontogr Ital* 90:217–258
- Heissig K (2009) The early Vallesian vertebrates of Atzelsdorf (Late Miocene, Austria) 11. Rhinocerotidae and Chalicotheriidae (Perissodactyla). *Ann Nathist Mus Wien A* 111 A:619–634
- Heissig K (2012) Les Rhinocerotidae (Perissodactyla) de Sansan. In: Peigné S, Sen S (eds) Mammifères de Sansan. *Mem Mus Natl Hist Nat* 203:317–485
- Heissig K, Fejfar O (2007) Die fossilen Nashörner (Mammalia, Rhinocerotidae) aus dem Untermiozän von Tuchořice in Nordwestböhmen. *Acta Mus Natl Prague B* 63(1):19–64
- Hernández Fernández M, Salesa MJ, Sánchez IM, Morales J (2003) Paleoeología del género *Anchitherium* von Meyer, 1834 (Equidae, Perissodactyla, Mammalia) en España: evidencias a partir de las faunas de macromamíferos Paleoeología of the genus *Anchitherium* von Meyer, 1834 (Equidae, Perissodactyla, Mammalia) in Spain: evidence from macromammal faunas. *Coloq Paleontol* 1:253–280
- Hünemann KA (1989) Die Nashornskelette (*Aceratherium incisivum* Kaup 1832) aus dem Jungtertiär vom Höwenegg im Hegau (Südwestdeutschland). *Andrias* 6:5–116
- Iñigo C (1997) *Anchitherium corcolense* nov. sp., a new anchitheriine (Equidae, Mammalia) from the Early Aragonian site of Córcoles (Guadalajara, Spain). *Geobios* 30(6):849–869
- Kaiser T (2009) *Anchitherium aurelianense* (Equidae, Mammalia): a brachydont “dirty browser” in the community of herbivorous large mammals from Sandelzhausen (Miocene, Germany). *Paläontol Z* 83(1):131–140. doi:10.1007/s12542-009-0002-z
- Kaup JJ (1832) Über *Rhinoceros incisivus* Cuv., und eine neue Art, *Rhinoceros schleiermacheri*. *Isis von Oken*:898–904

- Kaup JJ (1833) Description d'ossements fossiles de Mammifères inconnus jusqu'à-présent, qui se trouvent au Muséum grand-ducal de Darmstadt, vol 2. Heyer, Darmstadt
- Kaya T, Heissig K (2001) Late Miocene Rhinocerotids (Mammalia) from Yulafli (Çorlu-Thrace/Turkey). *Geobios* 34(4):457–467
- Mayet L (1908) Etudes des mammifères Miocènes des sables de l'Orléanais et des faluns de la Touraine. *Ann Univ Lyon NV* 1(24):1–336
- Salesa MJ, Sánchez IM, Morales J (2004) Presence of the Asian horse *Sinohippus* in the Miocene of Europe. *Acta Palaeontol Pol* 49(2): 189–196
- Sántafe-Llopis JV, Casanovas-Cladellas ML, Alférez Delgado F (1982) Presencia de *Aceratherium tetradactylum* (Lart, et, 1837) y *A (Alicornops) simorrense* (Lartet, 1851) (*Mamm. Perissodactyla*) en el Vallesiense inferior de Nombrevilla (Daroca, Teruel). *Acta Geol Hisp* 17(1–2):63–76
- Schaefer H, Zapfe H (1971) *Chalicotherium grande* Blainv. und *Chalicotherium goldfussi* Kaup. Odontologische und osteologische Unterschiede. *Verh Naturforsch Ges Basel* 81:157–199
- Semprebon G, Sise P, Coombs M (2011) Potential Bark and Fruit Browsing as Revealed by Stereomicrowear Analysis of the Peculiar Clawed Herbivores Known as Chalicotheres (*Perissodactyla*, *Chalicotherioidea*). *J Mamm Evol* 18(1):33–55. doi:10.1007/s10914-010-9149-3
- Sondaar PY (1971) An *Anchitherium* from the Vallesian of Soblay (Ain, France). *Mémoires du BRGM V° Congrès du Néogène Méditerranéen* 1(78):247–253
- Teppner W (1915) Ein Beitrag zur Kenntnis der neogenen Rhinocerotiden der Steiermark. *Mitt Naturwiss Ver Steiermark* 51:133–160
- Thenius E (1950) Über den Nachweis von *Anchitherium aurelianense* im Pannon des Wiener Beckens. *Anz Österr Akad Wiss Math-Nat wiss Kl* 8:174–181
- Villalta JF, Crusafont M (1945) Un *Anchitherium* en el Pontense español. *Anchitherium sampelayoi*, nov. sp. *Notas Com Inst Geol Min Esp* 14:51–82
- Wehrli H (1938) *Anchitherium aurelianense* Cuv. von Steinheim a. Albuch und seine Stellung im Rahmen der übrigen anchitherien Pferde. *Palaeontogr Suppl* 8(7):1–57
- Wehrli H (1939) Die Chalicotherien aus den Dinotheriensanden Rhein Hessens. *Notizbl Hess Geol L-Amt* 20:26–33
- Zapfe H (1979) *Chalicotherium grande* (BLAINV.) aus der miozänen Spaltenfüllung von Neudorf an der March (Děvinská Nová Ves), Tschechoslowakei, vol 2. *Neue Denkschr Nathist Mus Wien*. Verlag Ferdinand Berger & Söhne, Wien
- Zapfe H (1989) *Chalicotherium goldfussi* KAUP aus dem Vallesian vom Höwenegg im Hegau (Südwestdeutschland). *Andrias* 6: 117–126

Publication #3

Aiglstorfer M, Rössner GE, Böhme M. (2014) *Dorcatherium navi* and pecoran ruminants from the late Middle Miocene Gratkorn locality (Austria). *Palaeobiodiversity and Palaeoenvironments* 94, 83-123.

Own contribution:

Scientific ideas (%)	80
Data generation (%)	100
Analysis and Interpretation (%)	90
Paper writing (%)	95

Dorcatherium navi and pecoran ruminants from the late Middle Miocene Gratkorn locality (Austria)

Manuela Aiglstorfer · Gertrud E. Rössner · Madelaine Böhme

Received: 30 September 2013 / Revised: 1 December 2013 / Accepted: 12 December 2013 / Published online: 21 February 2014
© Senckenberg Gesellschaft für Naturforschung and Springer-Verlag Berlin Heidelberg 2014

Abstract One of the rare records of a rich ruminant fauna of late Middle Miocene age (Sarmatian sensu stricto; 12.2–12.0 Ma) was discovered at the Gratkorn locality (Styria, Austria). It comprises, besides *Micromeryx flourensianus*, *?Hispanomeryx* sp., *Euprox furcatus*, Palaeomerycidae gen. et sp. indet., and *Tethytragus* sp., one of the oldest records of *Dorcatherium navi*. Gratkorn specimens of the latter species are in metric and morphologic accordance (e.g. selenodont teeth, bicuspid p2, non-fusion of malleolus lateralis and tibia) with type material from Eppelsheim (Germany) and conspecific material from Atzelsdorf (Austria), and do not show an intermediate morphology between Late Miocene *Dorcatherium navi* and Middle Miocene *Dorcatherium*

crassum, thus enforcing the clear separation of the two species. It furthermore confirms the assignation of *Dorcatherium navi* to a selenodont lineage (together with *Dorcatherium guntianum*) distinct from a bunoselenodont lineage (including *Dorcatherium crassum*). The record of *?Hispanomeryx* sp. is the first of this genus in Central Europe. While *Tethytragus* sp. could also be a new bovid representative for the Sarmatian of Central Europe, *Micromeryx flourensianus* and *Euprox furcatus* are well-known taxa in the Middle Miocene of Central Europe, but comprise their first records from Styria. Morphological data from this work in combination with isotopic measurements ($\delta^{18}\text{O}_{\text{CO}_3}$, $\delta^{13}\text{C}$; Aiglstorfer et al. 2014a, this issue) indicate a niche partitioning for the ruminants from Gratkorn with subcanopy browsing (*Euprox furcatus*), top canopy browsing (*Tethytragus* sp.) and even a certain amount of frugivory (*Dorcatherium navi* and *Micromeryx flourensianus*).

This article is a contribution to the special issue “The Sarmatian vertebrate locality Gratkorn, Styrian Basin.”

Electronic supplementary material The online version of this article (doi:10.1007/s12549-013-0141-9) contains supplementary material, which is available to authorized users.

M. Aiglstorfer (✉) · M. Böhme
Fachbereich Geowissenschaften, Eberhard Karls Universität
Tübingen, Sigwartstraße 10, 72076 Tübingen, Germany
e-mail: manuela.aiglstorfer@senckenberg.de

M. Aiglstorfer · M. Böhme
Senckenberg Center for Human Evolution and Palaeoenvironment
(HEP), Sigwartstraße 10, 72076 Tübingen, Germany

G. E. Rössner
SNSB—Bayerische Staatssammlung für Paläontologie und
Geologie, Richard-Wagner-Str. 10, 80333 München, Germany

G. E. Rössner
Department für Geo-und Umweltwissenschaften, Paläontologie &
Geobiologie, Ludwig-Maximilians-Universität München,
Richard-Wagner-Str. 10, 80333 München, Germany

G. E. Rössner
GeoBio-Center LMU, Richard-Wagner-Str. 10, 80333 München,
Germany

Keywords *Euprox furcatus* · *Micromeryx flourensianus* ·
Tethytragus · *Hispanomeryx* · Palaeomerycidae · Sarmatian ·
Central Europe · Styrian Basin · Paratethys

Introduction

The Gratkorn locality (claypit St. Stefan; 10 km NNW of Graz, Styria, Austria) is one of the richest vertebrate localities of the late Middle Miocene (late Sarmatian sensu stricto; 12.2–12.0 Ma) in the Central Paratethys realm (Gross et al. 2011, 2014, this issue). Besides a rich and diverse ectothermic vertebrate (Böhme and Vasilyan 2014, this issue) and small mammal fauna (Prieto et al. 2014, this issue), and some birds (Göhhlich and Gross 2014, this issue), a diverse large mammal fauna was excavated, comprising the proboscidean *Deinotherium levius* vel *giganteum* (Aiglstorfer et al. 2014b, this issue), the rhinocerotids *Brachypotherium brachypus*, *Aceratherium* sp., and *Lartetotherium sansaniense*, the chalicothere

Chalicotherium goldfussi, the equid *Anchitherium* sp. (Aiglstorfer et al. 2014c, this issue), the suids *Listriodon splendens* and *Parachleuastochoerus steinheimensis* (van der Made et al. 2014), several carnivores (not yet described), and a rich ruminant fauna, described here.

All vertebrate fossils originate from a single fine-clastic soil layer (55 cm in total thickness; Gross et al. 2011, 2014, this issue), interpreted as a floodplain palaeosol (Gross et al. 2011, 2014, this issue). The uniformity of the palaeosol, the good preservation of the fossils, as well as the preservation of coprolites and pellets, point to a rather rapid accumulation and short time of soil formation (10^1 – 10^2 years; Gross et al. 2011, 2014, this issue; Havlik et al. 2014, this issue) and therefore confirm the assumption of a contemporaneous and stratigraphically not mixed mammal assemblage. The environment of the wider area around Gratkorn at the time of its deposition was reconstructed as a mosaic of a wide range of habitats, comprising, e.g. active and abandoned river channels, riparian woodland, floodplains, and ephemeral ponds as well as drier and more open areas (Gross et al. 2011).

During the Early and earlier Middle Miocene, a great number of Central European localities (see, e.g. Fig. 1) provided rich and diverse ruminant faunas (e.g. five contemporaneous cervid species at about 14.2 Ma; Böhme et al. 2012). Of course, sampling biases, such as fluvial reworking, have to be taken into consideration, but it is still remarkable that late Middle Miocene ruminant findings are rare in Central Europe and usually only provide isolated dental material or cranial appendages (only one cervid species recorded at about 12 Ma; Böhme et al. 2012). Ruminant assemblages from the Late Miocene (though not as rich in total numbers as the Middle Miocene) again comprise a more diverse fauna (with at least four contemporaneous cervid species at about 10.5 Ma, Böhme et al. 2012; or three sympatric species at the locality of Dorn-Dürkheim 1, Azanza et al. 2013), but differ from the Middle Miocene assemblages in their different taxonomic composition. The rich ruminant assemblage from Gratkorn closes a gap in Central Europe between the well-documented record from the Early to middle Middle Miocene and the Late Miocene.

Especially remarkable in this context is the record of *Dorcatherium nauti* Kaup 1833, which represents one of the oldest records of this species so far described. Usually, the species is a rare faunal element in fossil assemblages (see, e.g. Alba et al. 2011). In contrast to this, *D. nauti* is the second most frequent large mammal species at Gratkorn, and one of the most extensive materials recorded besides Eppelsheim (Kaup 1839) and Atzelsdorf (early Late Miocene; Hillenbrand et al. 2009).

Therefore, it adds to a more complete insight into the skeletodental morphology and intraspecific variability of this insufficiently known species. With the first rich record for the early representatives of the species, it gives new insights into its phylogenetic relationships.

Fig. 1 Stratigraphic range for different *Dorcatherium* species in Central Europe (focus is on localities from the North Alpine Foreland Basin (NAFB) and Austria; only localities with reliable species identification have been taken into consideration). Type localities for species highlighted in black. For some localities, only stratigraphic ranges can be given due to lack of good dating or a considerable amount of stratigraphic mixing (e.g. Gaweinstal; Harzhauser et al. 2011). The Eppelsheim Formation (Fm) housing the type locality of *D. nauti* has been recently shown to cover a wide stratigraphic range from Middle Miocene to Late Miocene and is therefore not taken into consideration here (Böhme et al. 2012). *Lassnitz*. Lassnitztunnel, *Holzmannsdorfb.* Holzmannsdorfberg, *Breitenf.* Breitenfeld, *Brunn n. Nestelb.* Brunn near Nestelbach, *Thannh.* Thannhausen, *Wawato 2* Wannenwaldtobel 2, *Stätzl.* Stätzling, *Laim. 3a* Laimering 3a, *Griesb. 1a* Griesbeckerzell 1a, *Ziem. 1b* Ziemetshausen 1b, *Hohenr.* Hohenraunau, *Derch.* Derching, *Pfaff.* Pfaffenzenzell, *Seegr.* Seegraben, *Lab.* Labitschberg near Gamlitz, *Münz.* Münzenberg near Leoben, *Edelbeuren-M.+S.* Edelbeuren-Maurerkopf and Schlachtberg, *Hamb. 6c* Hambach 6c (references for records; online resource 1).

Materials and methods

The material described here was excavated in cooperation of the Universalmuseum Joanneum, Graz (Graz, Austria), the Eberhard Karls Universität Tübingen (Tübingen, Germany) and the Ludwig-Maximilians-Universität München (München, Germany) from 2005 to 2013. It is housed at the Universalmuseum Joanneum (UMJGP) and at the Paläontologische Sammlung der Universität Tübingen (GPIT).

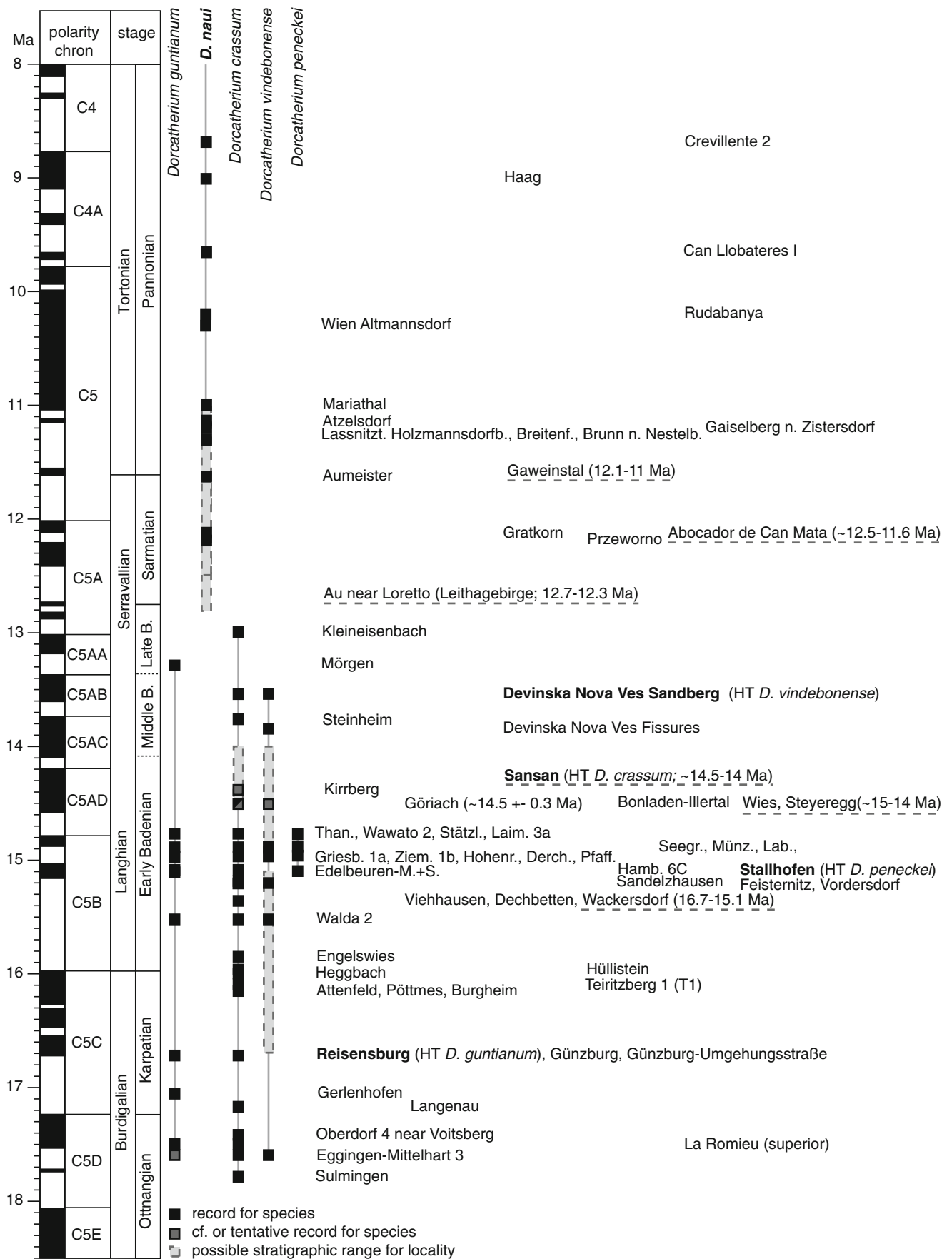
Due to the general taphonomic situation (for further details, see Havlik et al. 2014, this issue), teeth and mandibular fragments are more abundant than postcranial elements in the ruminant material from Gratkorn. Postcrania often only comprise distal or proximal epiphyses, while diaphysis have suffered from intense scavenging (Havlik et al. 2014, this issue).

Metric and morphologic comparison of the material was accomplished by personal observation on collection material (BMNH, SNSB-BSPG, GPIT, IGM, IPS, MNHN, NMB, NHMM, NHMW, NMNHS, IPUW, SMNS, UMJGP) and literature data.

Measurements were done with digital calipers and follow modified van der Made (1996) (for postcrania), Azanza et al. (2013) (for antlers) and Rössner (1995) (for dental material).

Material personally observed for comparison comprises:

***Dorcatherium nauti*:** *D. nauti* from Eppelsheim (NHMM, BMNH, SNSB-BSPG, GPIT), Atzelsdorf (NHMW), Abocador de CanMata (IPS), Holzmannsdorfberg (UMJGP), Lassnitztunnel (UMJGP), Brunn near Nestelbach (UMJGP), Strumyani (NMNHS); *D. guntianum* from Wannenwaldtobel 2 (SMNS), Günzburg/Reisensburg (SNSB-BSPG), Stätzling (SNSB-BSPG, NMA), Thannhausen (SNS-BSPG), Walda 2



(SNSB-BSPG); *D. crassum* from Sansan (MNHN, SNSB-BSPG), Sandelzhausen (SNSB-BSPG), Engelswies (GPIT), Viehhausen (SNSB-BSPG), Göriach (UMJGP, IGM), Vordersdorf (UMJGP, IGM), Feisternitz near Eibiswald (UMJGP), Steyeregg (UMJGP), Piberstein (UMJGP), Steinheim a. A. (am Albuch; SMNS), Münzenberg near Leoben (UMJGP), Labitschberg near Gamlitz (UMGP), Walda 2 (SNSB-BSPG); *D. vindebonense* from Labitschberg near Gamlitz (UMJGP), Wackersdorf (SNSB-BSPG), Seegraben (UMJGP, IGM); *D. penecke* from Stallhofen near Voitsberg (UMJGP); Stätzling (SNSB-BSPG, NMA), Seegraben (UMJGP, IGM), Walda 2 (SNSB-BSPG);

Micromeryx flourensianus: *M. flourensianus* from Sansan (MNHN), Steinheim a. A. (GPIT, NMB, SMNS), Atzelsdorf (NHMW); *M. styriacus* from Göriach (UMJGP); *M. mirus* from Kohfidisch (NHMW); *M. sp.* from Dorn-Dürkheim 1 (SMF); *Lagomeryx ruetimeyeri* from Langenau 1 (SMNS); *Lagomeryx parvulus* from Göriach (UMJGP), Sandelzhausen (SNSB-BSPG); *Lagomeryx pumilio* from Sandelzhausen (SNSB-BSPG);

Euprox furcatus: *Euprox furcatus* from Steinheim a. A. (GPIT, NMB, SMNS); *Euprox minimus* from Göriach (UMJGP); *Euprox sp.* from Atzelsdorf (NHMS); *Euprox vel Heteroprox* from Steinheim a. A. (GPIT, NMB, SMNS); *Heteroprox larteti* from Sansan (MNHN), Steinheim a. A. (GPIT, NMB, SMNS), Göriach (UMJGP), Seegraben (UMJGP); *Heteroprox eggeri* from Sandelzhausen (SNSB-BSPG); *Dicrocerus elegans* from Sansan (MNHN), Göriach (UMJGP, IGM), Seegraben (UMJGP), Stätzling (NMA), Sprendlingen 2 (NHMM, SSN); *Procervulus dichotomus* from Viehhausen (SNSB-BSPG); *Paradicrocerus elegantulus* from Stätzling (NMA), Sprendlingen 2 (NHMM, SSN);

Palaeomerycidae gen. et sp. indet.: *Palaeomeryx eminens* from Steinheim a. A. (GPIT, SMNS); *Germanomeryx* from Sandelzhausen (SNSB-BSPG);

Tethyragus sp.: *Miotragocerus monacensis* from Aumeister (SNSB-BSPG); *Miotragocerus vel Tethyragus* from Atzelsdorf (NHMW); *Eotragus clavatus* from Sansan (MNHN) and Göriach (UMJGP); *Eotragus artenensis* from Artenay (MNHN); *Pseudoeotragus seegrabensis* from Seegraben (UMJGP); as well as other records/isolated findings from the North Alpine Foreland Basin (NAFB) and Austria.

For plots material described by Kaup (1833, 1839), von Meyer (1846), Hofmann (1893), Schlosser (1886), Thenius (1950), Rinnert (1956), Mottl (1954, 1961, 1966, 1970), Ginsburg and Crouzel (1976), Fahlbusch (1985), van der Made (1989), Ginsburg and Azanza (1991), Sach (1999), Azanza (2000), Vislobokova (2007), Hillenbrand et al. (2009), Rössner (2010), Alba et al. (2011), Morales et al. (2012), van der Made (2012), Aiglstorfer and Costeur (2013) was personally measured, to minimise bias due to different measurement standards.

Furthermore, literature data were included (see figure captions for references).

Nomenclature for dental material follows Bärmann and Rössner (2011). To avoid confusion, the term ‘*Dorcatherium*-fold’ is not used in this work, as proposed by Bärmann and Rössner. The term has been under discussion since Mottl (1961; Alba et al. 2011). While some authors prefer to apply the term ‘*Dorcatherium*-fold’ to the whole Σ -like structure (e.g. Janis and Scott 1987; Hillenbrand et al. 2009; Rössner 2010), according to the definition by Mottl (1961), others use the term only for the folded structure posterior of the metaconid (Métais et al. 2001; Sánchez et al. 2010b; Alba et al. 2011; see also discussions in Métais et al. 2001 and Alba et al. 2011). In this publication, the terms ‘internal’ and ‘external postmetacristid’ and ‘internal’ and ‘external postprotocristid’ (sensu Bärmann and Rössner 2011) or the term ‘ Σ -structure’ are used. Postcranial terminology mainly follows Nickel et al. (1968) and König and Liebich (2008), and for antler terminology, Azanza et al. (2013).

Body mass estimations (kg) given here follow, if possible, the equations of Janis (1990), and are based on length of m2 (SLML, mm) and length of the lower molar row (LMRL, mm): *Dorcatherium naui*: equation “ruminants only” [$\log(\text{BM}) = 3.337 \times \log(\text{SLML}/10) + 1.118$], [$\log(\text{BM}) = 3.352 \times \log(\text{LMRL}/10) - 0.604$]; *Micromeryx flourensianus*: equations “ruminants only” (for equation, see above) and “bovids only” [$\log(\text{BM}) = 3.375 \times \log(\text{SLML}/10) + 1.119$], [$\log(\text{BM}) = 3.335 \times \log(\text{LMRL}/10) - 0.581$]; *Euprox furcatus*: equations “cervids only” [$\log(\text{BM}) = 3.106 \times \log(\text{SLML}/10) + 1.119$], [$\log(\text{BM}) = 3.209 \times \log(\text{LMRL}/10) - 0.524$].

Due to limited dental material, the equations of Damuth (1990) based on the length of M2 (mm) “all selenodonts” { $[\log(\text{BM}) = 3.15 \times \log(\text{M2 length}) - 0.94]/1,000$ }, “selenodont browsers” { $[\log(\text{BM}) = 3.34 \times \log(\text{M2 length}) - 0.73]/1,000$ } are used for *Tethyragus* sp. and one of Scott (1990) based on the length of the metacarpal (Mc1, mm) “ruminants” [$\log(\text{BM}) = 2.4722 \times \log(\text{Mc1}) - 1.237$] for the Palaeomerycidae gen. et sp. indet. Body mass estimations based on dental measurements are considered less reliable than those based on postcranial material (Mendoza et al. 2006). However, taking into consideration the tragulid *D. naui*, the equations of Janis (1990) based on dental material of extant ruminants are preferred here to the equations based on postcranial material of extant ruminants by Scott (1990). On the one hand, Janis (1990) also included Tragulidae in her “ruminants only” data matrix, and on the other hand, for tragulids with their peculiar “intermediate suid/ruminant postcranial anatomy”, the equations of Scott (1990) cannot be applied properly.

Anatomical abbreviations

C	upper canine
P 2, -3, -4	second, third, fourth upper premolar
M1, -2, -3	first, second, third upper molar
i1, -2, -3	first, second, third lower incisor
p 1, -2, -3, -4	first, second, third, fourth lower premolar
m1, -2, -3	first, second, third lower molar
sin.	sinistral/left
dex.	dextral/right
l (max)	maximal length of tooth
w (max)	maximal width of tooth
want (max)	maximal anterior width of tooth
h (max)	maximal height
L	length
Lint	internal length in astragalus
Lext	external length in astragalus
wint	internal dorsoplantar width of astragalus
wext	external dorsoplantar width of astragalus
DAPp	proximal anteroposterior/dorsovolar diameter
DAPps	maximal proximal dorsovolar diameter of phalanx
DTp	proximal transversal diameter
DAPd	distal anteroposterior/dorsovolar diameter
DTd	distal transversal diameter
DTn	minimal transversal width in calcaneum
Dtdf	transversal diameter of the trochlea humeri

Institutional abbreviations

BMNH	British Museum of Natural History, London, UK
GPIT	Paläontologische Sammlung der Universität Tübingen, Tübingen, Germany
IGM	Montanuniversität Leoben, Leoben, Austria
IPS	Collections of the Institut Català de Paleontologia, Barcelona, Spain
IPUW	Institut für Paläontologie Universität Wien, Wien, Austria
MB.Ma	Museum für Naturkunde—Leibniz-Institut für Evolutions-und Biodiversitätsforschung an der Humboldt-Universität zu Berlin, Mammal Collection, Berlin, Germany
MNHN	Muséum National d'Histoire Naturelle, Paris, France
NMA	Naturmuseum Augsburg, Augsburg, Germany
NMB	Naturhistorisches Museum Basel, Basel, Switzerland
NHMM	Naturhistorisches Museum Mainz, Mainz, Germany
NHMW	Naturhistorisches Museum Wien, Wien, Austria
NMNHS	National Museum of Natural History, Sofia, Bulgaria
SMF	Senckenberg Museum Frankfurt, Frankfurt, Germany

SMNS	Staatliches Museum für Naturkunde Stuttgart, Stuttgart, Germany
SNSB-BSPG	Staatliche Naturwissenschaftliche Sammlungen Bayerns-Bayerische Staatssammlung für Paläontologie und Geologie, München, Germany
SSN	Paläontologisches Museum Nierstein, Nierstein, Germany
UMJGP	Universalmuseum Joanneum, Graz, Austria

Systematic Palaeontology

Class Mammalia Linnaeus, 1758
 Order Artiodactyla Owen, 1848
 Suborder Ruminantia Scopoli, 1777
 Infraorder Tragulina Flower, 1883
 Family Tragulidae Milne Edwards, 1864
 Genus *Dorcatherium* Kaup, 1833

Type species: *Dorcatherium nauii* Kaup, 1833

Further European species: *Dorcatherium crassum* (Lartet, 1851); *Dorcatherium vindebonense* von Meyer, 1846; *Dorcatherium guntianum*, von Meyer, 1846; *Dorcatherium peneckeii* (Hofmann, 1893); *Dorcatherium jourdani* Depéret, 1887; and *Dorcatherium puyhauberti* Arambourg and Piveteau, 1929.

The genus *Dorcatherium*, erected by Kaup in 1833, comprises five species generally accepted from the Miocene of Europe, differing in dimensions, dental and postcranial morphology and stratigraphic range (Fig. 1): the small-sized *D. guntianum*, the medium-sized *D. nauii* and *D. crassum*, the larger-sized *D. vindebonense*, and the large-sized *D. peneckeii*.

D. puyhauberti and *D. jourdani* are rarely documented, with only a few specimens, which possess no unambiguous features distinguishing them from other European species and could be synonymous to *D. guntianum* and *D. nauii* respectively. Morales et al. (2012), also referring to Geraads et al. (2005), accordingly propose that both species could be included in *D. nauii*, but need to be revised in more detail. *D. puyhauberti* is smaller in dimensions than *D. nauii*, being in the size variability of *D. guntianum* (Hillenbrand et al. 2009; Rössner and Heissig 2013). Hillenbrand et al. (2009) found a character distinguishing the species from all other *Dorcatherium* species: smaller M3 in comparison to M2. The *D. puyhauberti* type material was not available for study during comparative investigations for this paper, but, as could be recognised on photographs recently taken from the type material at the MNHN, the feature, correctly extracted by Hillenbrand et al. (2009) from the original description of Arambourg and Piveteau (1929), cannot be verified on the original material. M2 and M3 are not articulated in the maxilla but fixed together with a gypsum bed, and the two teeth are now fixed in inverse order compared with the original description. The different colours of the enamel furthermore

indicate that the two teeth might originate from different individuals (for further information on the historical context of the genus and discussion on species validity, see Appendix 1).

The Miocene tragulid genus *Dorcabune* Pilgrim, 1910, is known with several species but so far only from Asia (Rössner 2007). As *Dorcabune* and *Dorcatherium* overlap in morphological key features, a revision of the two genera would probably result in two morphotypes/lineages of Miocene tragulids with a differentiation into more bunodont (including *D. crassum*, *vindebonense* and *peneckeri*) and more selenodont forms (including *D. naui* and *guntianum*) (Rössner 2007, referring also to Mottl 1961, Fahlbusch 1985, Qui and Gu 1991).

To get a better idea about relationships of and faunal exchanges between Asian, African and European Miocene tragulids, a revision of the different taxa and lineages, as also proposed by Sánchez et al. 2010b, is surely needed.

Dorcatherium naui Kaup, 1833

Holotype: Mandibula with p3–m3 and alveolae of p1 and p2 described in Kaup (1833) and figured in Kaup (1839, pl. XXIII, fig. 1, 1a, 1b), lost, cast available (BMNH M3714, SNSB-BSPG 1961 XIX 37).

Type locality: Eppelsheim (Germany)

Dentition and mandibulae (Fig. 2a–n)

Material: UMJGP 204059 (C dex.), GPIT/MA/2377 (D2 dex.), UMJGP 204675 (D3 dex.), UMJGP 204064 (D3 dex.), GPIT/MA/2375 (D4–M1 sin.), GPIT/MA/2379 (P4 dex.), GPIT/MA/2376 (M1? dex.), UMJGP 210956 (d2 sin.), UMJGP 210694 (fractured mandibula with i1, p2–m3 sin. and dex.), GPIT/MA/2734 [mandibula sin. with i2 or 3 sin. (isolated), alveolae for p1–p3, and p4–m3], GPIT/MA/2401 (m1 sin.), UMJGP 204109 (fragment of mandibula sin. with fragments of m2–3), GPIT/MA/2756 (m2 sin.), UMJGP 203714 (fragment of labial side of mx).

Finding position, preservation, and degree of dental wear allow for deducing GPIT/MA/2741 (i1 dex.), GPIT/MA/2741 (i2 or 3 dex.), GPIT/MA/2741 (i2 or 3 sin.), GPIT/MA/02741 (p2 sin.) and GPIT/MA/2741 (mandibula sin. with p3–m3) as belonging to one individual, as do UMJGP 204667 (mandibula sin. with p2–3), UMJGP 204661 (mandibula dex. with p2–3), UMJGP 204664 (fragment of mandibula sin. with p4–m1), UMJGP 204663 (fragment of mandibula dex. with m1–2), UMJGP 204662 (fragments of mandibulae with m2 sin., m3 dex.) and UMJGP 204665 (m3 sin. with fragment of mandibula). UMJGP 210696 (d3 sin.), UMJGP 210692 (d4 sin.), and UMJGP 210693 (m1 sin.) most likely belong to one individual.

UMJGP 204067 (D3–4 sin.) and UMJGP 209952 (M1 sin.) also fit together. From finding position and degree of

wear, GPIT/MA/2732 (M1? dex.), UMJGP 210698 (M2 sin.), and UMJGP 210697 (M3 sin.) are also assigned to one individual.

Description and comparison

From dimensions, all teeth are well within the variability of the medium-sized *Dorcatherium naui* and *D. crassum* (Fig. 3; for detailed information and measurements, see online resource 2).

Only isolated teeth and incomplete deciduous tooth rows are preserved of the **upper dentition**. Therefore, characters based on tooth row length, or size increases from M1 to M3, etc., cannot be verified. Only one fragmentary sabrelike **C dex.** (UMJGP 204059; Fig. 2a) is preserved. It is curved with the tip directed to posteriad and a drop-shaped cross-section (rounded anteriorly and with a sharp angle posterior). The anteroposterior diameter of the tooth does not decrease continuously from base to tip as is the case in canines of *Euprox* and *Micromeryx*, but is more constant and the sharp tip has been produced by lingual wear on the tooth. Enamel covers only the labial side. Strong wear during lifetime is indicated by a large wear surface on the lingual side of the tip. The growth striation is more distinct than it is in Cervidae or Moschidae. In size and shape, the canine is in accordance with those of *D. crassum* and *D. naui*. The only **D2** (GPIT/MA/2377; Fig. 2b) preserved is fragmented and missing the posterolabial cone. The tooth is anteroposteriorly elongated and has a strong lingual cingulum, comparable to specimens of *D. crassum* from Sansan. The anterolabial cone is larger than the anterior style. So far, a D2 of *D. naui* has only been described from the localities Ballestar and Can Petit in Spain by Moyà-Solà (1979), but not figured. His description is

Fig. 2 Dental and postcranial material of *Dorcatherium naui*. **a** C dex. (UMJGP 204059; 1 labial view, 2 lingual view), **b** D2 dex. (GPIT/MA/2377; 1 lingual view, 2 occlusal view), **c** D3 dex. (UMJGP 204675; occlusal view), **d** D3–4 sin. (UMJGP 204067; occlusal view), **e** d2 sin. (UMJGP 210956; labial view), **f** d3 sin. (UMJGP 210696; occlusal view), **g** d4 sin. (UMJGP 210692; occlusal view), **h** P4 dex. (GPIT/MA/2379; occlusal view), **i** M1 sin. (UMJGP 209952; occlusal view), **j** M2 sin. (UMJGP 210698; occlusal view), **k** M3 sin. (UMJGP 210697; occlusal view), **l** mandibula sin. with p4–m3 and alveolae for p1–p3 (GPIT/MA/2734; 1 occlusal view, 2 labial view, 3 m3 in occlusal view), **m** mandibula sin. with p2–3 (UMJGP 204667; 1 labial view, 2 occlusal view), **n** fractured mandibula with i1, p2–m3 sin. and dex. (UMJGP 210694; 1 mandibula dex. in lingual view and sin. in labial view, 2 p4–m3 sin. in labial view, 3 p4–m3 sin. in lingual view, 4 p4–m3 sin. in occlusal view, 5 m3 sin. in occlusal view), **o** humerus sin. (GPIT/MA/2389; 1 cranial view, 2 distal view), **p** radius sin. (GPIT/MA/2391; 1 dorsal view, 2 proximal view), **q** cubonavicular sin. (UMJGP 203419; dorsal view), **r** tibia sin. (UMJGP 203419; 1 dorsal view, 2 lateral view of distal end, 3 distal view), **s** astragalus dex. (GPIT/MA/2409; 1 dorsal view, 2 palmar view), **t** fragmented calcaneum dex. (GPIT/MA/2409; medial view); *scale bar* 10 mm (except **n/l**, 50 mm)



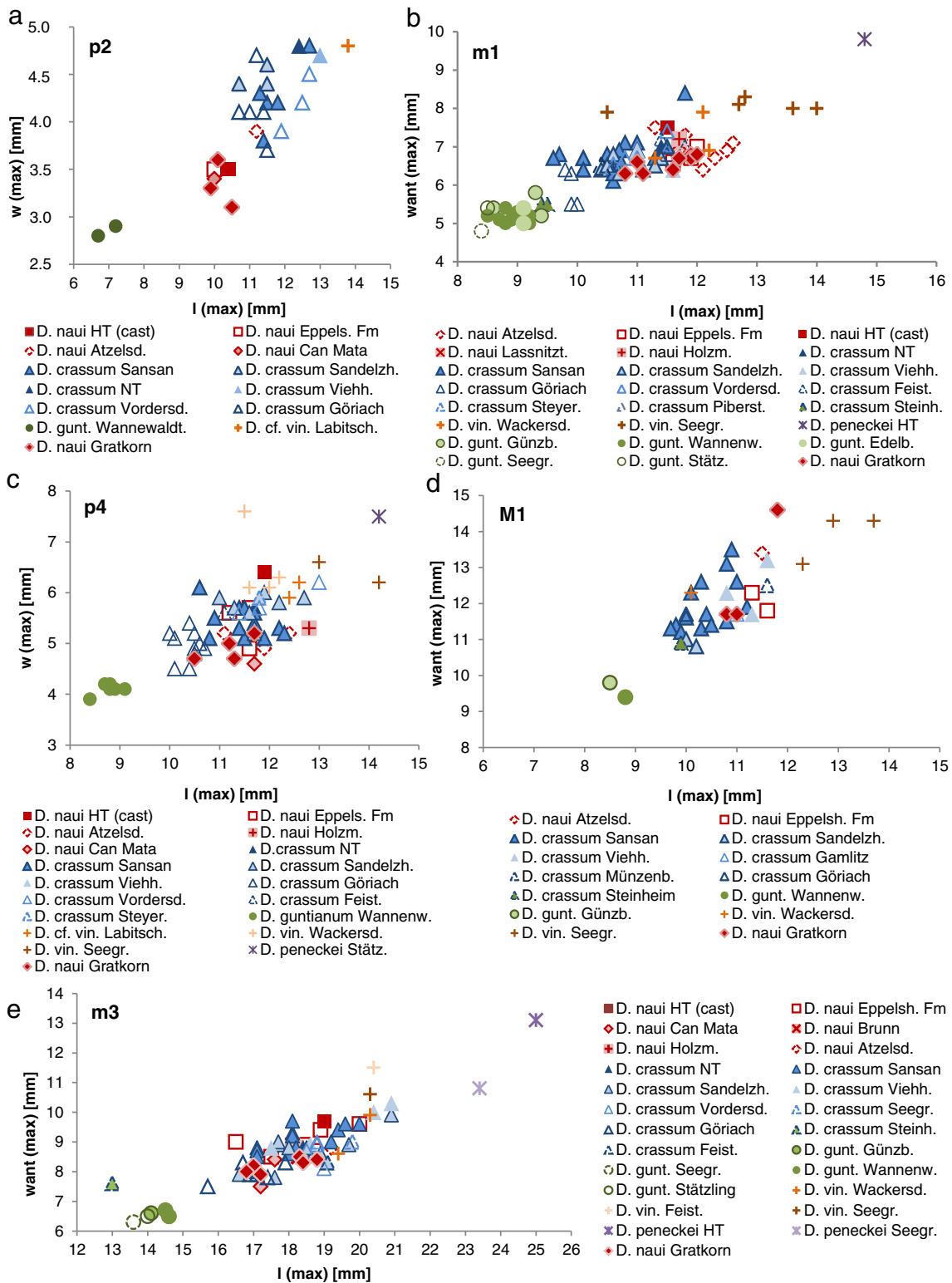


Fig. 3 Bivariate plots for p2 (a), p4 (c), m1 (b), m3 (e) and M1 (d) of *Dorcatherium nawi* from Gratkorn in comparison to other Central European *Dorcatherium* species (all own measurements, mm), with the focus on type material and Styrian localities; HT holotype, NT neotype, gunt. guntianum, vin. vindebonense, Eppelsh. Fm Eppelsheim Fm, Atzelsd. Atzelsdorf, Sandelzh. Sandelzhausen, Viehh. Viehhausen, Vordersd.

Vordersdorf, Wannewaldt. Wannewaldtobel 2, Labitsch. Labitschberg, Lassnitz. Lassnitztunnel near Graz, Holz. Holzmannsdorfberg, Feist. Feisternitz near Eibiswald, Steyer. Steyereg, Piberst. Piberstein, Steinh. Steinheim a. A., Edelb. Edelbeuren-Schlachtberg, Wackersd. Wackersdorf, Seegr. Seegraben, Günzb. Günzburg/Reisensburg, Stätz. Stätzling, Münzenb. Münzenberg

generally in congruence with the specimen from Gratkorn. In occlusal view, the **D3** (Fig. 2c) exhibits a triangular shape and an anterior cone with a well-pronounced anterior crista. Para- and metacone are the dominant cones. The metaconule is well developed, while the protocone is small and positioned at a more anterior level than the paracone. The premetaconulecrista is split into one external and two internal premetacunulecristae; of the latter, the posterior one terminates in a small tubercle. The postmetaconulecrista fuses posterolabially with the posterior cingulum. While the parastyle is weak and attached to a small labial cingulum, the mesostyle is strong and clearly set off from the metacone. The metastyle is tiny. With a weaker cingulum, the specimens from Gratkorn differ from *D. crassum* from Sansan. A D3 of *D. naui* has so far only been described by Moyà-Solà (1979), but not figured. He states a similar size for D3 in *D. naui* and *D. crassum*. The **D4** shows a trapezoid molar-like shape (Fig. 2d) with enlarged and antieriad protruding parastyle and well-pronounced mesostyle. Both D4 specimens from Gratkorn show a crest at the posterolingual wall of the paracone, comparable to a small tubercle lingual to the postprotocrista in *D. naui* from Can Mata and from Atzelsdorf. Comparable to *D. guntianum* and *D. naui*, the mesostyle is not as bulky in the Gratkorn specimens as it is in *D. crassum* from Sansan and Sandelzhausen. Typical for Tragulidae (Milne Edwards 1864, pl. IX fig. 9, pl. X fig. 3; Rössner 2007, fig. 16.3 B), the **P4** (GPIT/MA/2379; Fig. 2h) is triangular in shape and thus differs from Pecora, which have a lingually rounded P4. The labial cone is dominant, and anterior and posterior styles are well developed. The first is more set off than the latter. There is no central fold, but the posterolingual crista is instead shifted anteriorly and not fused with the posterolingual cingulum, but terminates inbetween the lingual cone and posterior style. The anterolingual cingulum is short and weak.

As common in the genus, the five subrectangular to trapezoid **upper molars** (Fig. 2i–k) show no clearly developed splitting of the postprotocrista (Fahlbusch 1985). Only in one specimen (UMJGP 210698) a splitting is developed, resulting in short external and internal postprotocristae. This can also be observed in some specimens of the type series of *D. crassum* from Sansan and was recently described for Early Miocene *D. crassum* from Spain (Alba et al. 2013), indicating that this feature, even if rarer, can occur. As is typical in tragulids, the premetaconulecrista is longer in all specimens than the postprotocrista and reaches the posterolingual wall of the paracone. Only one specimen (UMJGP 210698) exhibits a more complex morphology with small tubercles at its anterior end. All specimens have prominent para- and mesostyles, a clear lingual rib at the paracone and a pronounced lingual cingulum reaching from the anterior side of the protocone to the posterior side of the hypocone. A distinct entostyle is not present in any of the specimens; only in GPIT/MA/2375 is it indicated by a thickening of the cingulum. While in all M1

(UMJGP 210698, GPIT/MA/2375, GPIT/MA/2376; Fig. 3d) the metastyle is very small, it increases in size in the M2 (UMJGP 210698), and is further enlarged in the M3 (UMJGP 210697). Although M2 and M3 are less slender in habitus than M1 and possess a clearly more inflated mesostyle, all teeth are selenodont and differ clearly from the bunoselenodont *D. crassum* from Sansan and Sandelzhausen with its more bulky styles (Morales et al. 2012; Rössner 2010).

The **mandibulae** from Gratkorn show a slender corpus mandibulae (Fig. 2e–g, l–n), nesting in the lower part of the morphological variability of *D. crassum* from Sansan and Sandelzhausen (Morales et al. 2012; Rössner 2010), and are in accordance with dimensions of *D. naui* from Atzelsdorf (Hillenbrand et al. 2009), Abocador de Can Mata (Alba et al. 2011), Eppelsheim (skull with both mandibulae, BMNH M 40632; cast GPIT/MA/3653), and the cast of the holotype (BMNH M 3714, BSPG 1961 XIX 37). In all specimens with a preserved rostral part of the mandibula, an alveola for the p1 is present (Fig. 2l, n). There are two foramina mentalis on the lateral side of the corpus mandibulae (Fig. 2l, n), of which the rostral one is enlarged and elongated reaching from the caudal rim of the symphysis to the alveola of the p1. The interspace between anterior premolars and caudal rim of the symphysis is short, as it is also in *D. naui* from Atzelsdorf (Hillenbrand et al. 2009, pl. 2, fig. 9) and Abocador de Can Mata. In the cast of the holotype of *D. naui* (BMNH M 3714, BSPG 1961 XIX 37), the caudal rim of the symphysis is even at the level of the rostral alveola for the p2. The interspace is also small in *D. crassum* from Sansan. The length of premolar and molar tooth rows from Gratkorn (online resource 2) are within the variability of *D. naui* from Eppelsheim, Atzelsdorf and Abocador de Can Mata, *D. crassum* from Sansan and Sandelzhausen, and *D. “cf. puyhauberti”* from Strumyani (Bulgaria; Geraads et al. 2011; which could very likely be *D. naui*). They are clearly larger than in *D. guntianum* (e.g. from Wannenwaldtobel 2; see also Sach 1999). The holotype of *D. penecke* from Stallhofen (UMJGP 1601; length of m1–3: 54 mm) is larger. In UMJGP 210694, the angulus mandibulae is clearly set off from the corpus mandibulae by a ventral depression (Fig. 2n), which is weak in *D. naui* from Atzelsdorf (Hillenbrand et al. 2009, pl. 2, fig. 9) and not present in a *D. naui* from Eppelsheim (BMNH M 40632). In *D. crassum* from Sansan (e.g. MNHN Sa 10852), it is generally less pronounced. While the processus coronoideus is not preserved in any specimen from Gratkorn, a rounded incisura mandibulae (50 mm dorsal of the ventral rim of the angulus mandibulae) and the caput mandibulae of the processus condylaris, are documented in UMJGP 210694 (Fig. 2n). The caput mandibulae is slightly less high than in the mandibula of *D. naui* from Atzelsdorf (Hillenbrand et al. 2009, pl. 2, fig. 9). The reconstructed length of the symphysis at roughly about 20 mm and the height at about 10 mm

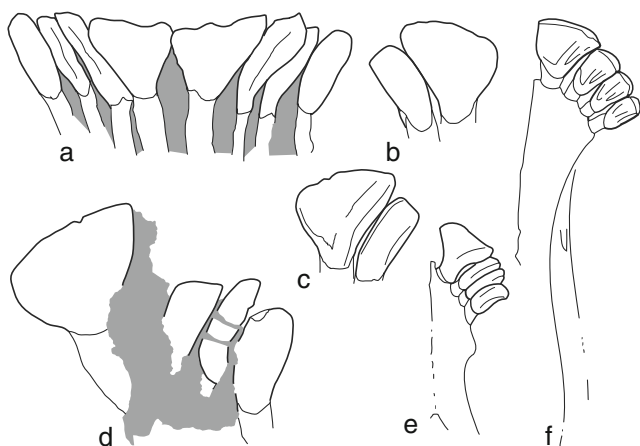


Fig. 4 Schematic drawing of different ruminant incisor arcs: **a** *Dorcatherium naui* (redrawn from Kaup 1839), **b** i1 (UMJGP 210694) and i2 (GPIT/MA/2741) of *D. naui* from Gratkorn in labial view, **c** i1 (UMJGP 210694) and i2 (GPIT/MA/2741) of *D. naui* from Gratkorn in lingual view, **d** i1–c1 of *Dorcatherium* cf. *puyhauberti* in labial view (presumably *nau*) from Strumyani, Bulgaria (NMNHS FM-2741), **e** i1–c1 of *Tragulus javanicus* (modified from Thenius 1989), **f** *Cervus elaphus* (modified from Thenius 1989)

correspond well to the medium-sized *Dorcatherium* species, *D. crassum* and *D. naui*. The **i1** is of spade-like shape (Fig. 4b), widening from base to tip more than in cervids (Fig. 4f). The tooth shape is lingually concave and occlusally bent to the posterior. On the lingual plane, it shows a thin anterior vertical crest and a strong groove at the posterior rim. Three isolated **i2 or 3** are preserved from Gratkorn. They are pen-like, lingually concave, bent to the posterior, and bear a small anterior crest on the lingual plane and a deep groove close to the posterior rim, like in the i1. In contrast to the latter, the anteroposterior diameter is more constant from base to tip, and the posterior groove is not as distinct. Modern tragulids show a similar morphology pattern with an extensively occlusoposteriorly widened i1 and more pen-like i2–c (Fig. 4e), as do *D. naui* from Eppelsheim (BMNH M 40632 and Kaup (1839, tab 23B, fig. 4); Fig. 4a) and *D.* “cf. *puyhauberti*” from Strumyani, Bulgaria (Geraads et al. 2011; Fig. 4d). The only preserved **d2** (UMJGP 210956; Fig. 2e) is posteriorly strongly worn, biradicate, and bicuspid. Its general morphology does not differ from the p2, except for the lower tooth crown height. Only one **d3** (UMJGP 210696; Fig. 2f), with a missing labial half of the posterolabial conid, is recorded. It has an elongate, anterolingually bent shape with anterior, mesolabial and posterolabial conids and a more or less isolated posterolingual conid. The mesolabial conid is the dominant cusp. There is a weak anterior cingulid. From the mesolabial conid, the transverse cristid and posterolabial cristid proceed posteriorly enclosing an acute angle, the latter turning to lingual posteriorly. In *D. crassum*, especially from the type locality Sansan, an anterior stylid is often present, while it is absent in the specimen from Gratkorn as well as in

D. guntianum (e.g. from Thannhausen and Wannwaldtobel 2). One fragmented **d4** (UMJGP 210692 Fig. 2g) is preserved, missing the labial part. It is triradicate, and has three lingual conids, higher than the labial elements. The anterolingual conid is positioned more anterior than the anterolabial conid, similar to a d4-fragment from Atzelsdorf. This seems to be less common in *D. crassum* (personal observation, Sansan), in contrast to *D. guntianum*, where it can be observed more often (e.g. Günzburg-Umgehungsstrasse and Wannwaldtobel 2), but is usually not as pronounced as in the specimen from Gratkorn. On the grounds that there is quite a range of intra-specific variability, that only one d4 from Gratkorn has been recorded so far, and that the comparison material for this tooth position of *D. naui* is also limited, the value of this character as a taxonomic feature cannot be estimated. The entostylid is well pronounced. Postmeta- and postprotocristid are split into external and internal cristids, forming the Σ -structure characteristic for the family, while the preentocristid is short and fused with internal postmeta- and postprotocristids basally. The postentocristid is short and connects with the entostylid at its base, while the posthypocristid is longer and fused with the entostylid. Anterior and posterior cingulid are well pronounced. Although no **p1** is preserved, in both specimens where the rostral part of the mandibula is preserved, one alveola for the p1 was observed. This applies to all specimens of *D. naui* with the rostral part of a mandibula preserved, except for one specimen from Can Petit, where the p1 is lacking (Spain; Moyà-Solà 1979). Though rare in *D. crassum* from the type locality Sansan, a p1 more frequently occurs in *D. crassum* and *D. vindebonense* from the NAFB and Austria and in the Early Miocene record from Spain (Mottl 1961; Rössner 2010; Alba et al. 2013). The presence of a p1 is thus optional in *D. crassum* and *D. vindebonense* and cannot be used as a distinct diagnostic feature for *D. naui*, as proposed, e.g. by Ginsburg (1967; see also discussion in Moyà-Solà 1979; Fahlbusch 1985; Alba et al. 2011). All **p2** from Gratkorn are bicuspid and biradicate (Fig. 2m). The mesolabial conid is dominant, while the posterolabial conid is smaller. While the anterolabial cristid turns slightly lingually at the anterior part and forms a weakly pronounced anterior stylid, the posterolabial cristid bends stronger lingually, forming the posterior wall of the back valley. A posterior cingulid is present. Although the p2 is not preserved in the holotype of *D. naui*, in other specimens from Eppelsheim (e.g. MNHM PW2012/9-LS; BMNH M 40632; cast GPIT/MA/3653), the p2 is bicuspid, as it is in *D. naui* from Can Mata (Alba et al. 2011). In Hillenbrand et al. (2009), the p2 of *D. naui* from Atzelsdorf was described as tricuspid, and is longer than the specimens from Gratkorn. But due to strong wear in the specimen, the morphology of the tooth is difficult to describe and the anterior stylid might give the impression of an anterior conid. In *D. crassum*, the p2 shows a clearly developed anterior conid and a more pointed mesolabial

conid. It is clearly tricuspid in this species (Rössner 2010; Morales et al. 2012; Alba et al. 2013) as it is in *D. vindebonense* (Mottl 1961). *D. guntianum* also possesses a biscuspid p2 (e.g. Sach 1999; Mottl 1961; Rössner and Heissig 2013), but clearly differs by its smaller size from *D. naui* and the Gratkorn *Dorcatherium*. Dimensions of the Gratkorn specimens fall within the variability of *D. naui* from Eppelsheim and Spain and are clearly distinct from *D. crassum*, while the specimen from Atzelsdorf lies within the variability of the latter (Fig. 3). With a small anterior conid, the p3 is tricuspid and longer than the p2. The mesolabial conid is clearly dominant, while the anterior conid is slightly turned lingually, and the posterolabial cristid forms the posterior wall of the back valley and is rectangular to the length axis of the tooth. The back valley is narrow and incises clearly in the posterior wall of the posterolabial conid. A weak anterior and a strong posterior cingulid are present. The preserved shape in the casts of the holotype of *D. naui* (BMNH M 3714, BSPG 1961 XIX 37) indicates a tricuspid p3. It is tricuspid and similar in shape to the Gratkorn specimens and *D. naui* from Eppelsheim (e.g. MNHM PW2012/9-LS; BMNH M 40632), from Atzelsdorf, and from Can Mata (Hillenbrand et al. 2009; see figs. in Alba et al. 2011). In *D. crassum*, the p3 is also tricuspid, but possesses a more dominant mesolabial conid, and a less strongly incised posterior valley (Rössner 2010; Morales et al. 2012). The smaller *D. guntianum* also shows a tricuspid p3 with a less dominant mesolabial conid (e.g. Wannenwaldtobel 2), but differs by a smaller size from *D. naui* and the Gratkorn specimens. The p4 is shorter than the p3, and quite variable in morphology. The mesolabial conid is always dominant. The anterior valley strongly cuts in the anterolabial cristid forming a sharp groove. Anterior and posterior cingulid are present. In contrast to Pecora, only two cristids branch of the posterior part of the mesolabial conid, the lingual one comprising the fusion of transverse cristid, mesolingual conid and posterolingual conid (Rössner 2010), the labial one the posterolabial cristid to posterior stylid. The two cristids enclose the posterior valley, which has a quite complex morphology as it comprises small additional transverse crests, which are varying in size and morphology. Development of the mesolingual, posterolabial and posterolingual conid, as well as of the posterior stylid, is variable (Figs. 2l, n, 5). In the casts of the holotype of *D. naui* (BMNH M 3714, BSPG 1961 XIX 37), as well as in the specimen from Abocador de Can Mata, the p4 possesses a complex posterior valley (see also Alba et al. 2011; Fig. 5). In Atzelsdorf the morphology is more variable. The more bunodont *D. crassum* and *D. vindebonense* are usually simpler in structures (Fig. 5), which is also described by Moyà-Solà (1979) when comparing *D. crassum* and *naui*. *D. guntianum* (e.g. from Wannenwaldtobel 2; Sach 1999) shows the same tendency towards a complex structure in the posterior valley, but is smaller than the specimens from Gratkorn (Fig. 3c).

The **lower molars** in the specimens from Gratkorn are less wide and slightly higher crowned than in the similar sized *D. crassum* but well in accordance with the more slender and higher crowned *D. naui* and *D. guntianum* (Figs. 2l, n, 3b, e). The lower molars from Gratkorn differ by a larger size from *D. guntianum*, and by a smaller size (Fig. 3b, e) and a more selenodont, slender and higher crowned morphology from *D. vindebonense* and *penecke*. The size increases from m1 to m2. The postmetacristid and postprotocristid are both split into internal and external cristids, giving the posterior aspect of the anterior lobus the typical Σ -structure. No lingual stylids are present. The ectostylid is largest in m1 and decreases in size to m3, as in *D. naui* from Atzelsdorf and Abocador de Can Mata (Hillenbrand et al. 2009; Alba et al. 2011). In *D. crassum*, although also decreasing in size from m1 to m3, usually the ectostylid is still more pronounced in m2 and m3 (see, e.g. Morales et al. 2012, fig. 23). The length of the external postmetacristid in ratio to the internal is variable in the specimens from Gratkorn, as it is in other assemblages of *D. naui* (e.g. Eppelsheim and Atzelsdorf) and *D. crassum* from Sansan and Sandelzhausen. The postentocristid in specimens from Gratkorn is short and accentuated and does not reach the posterior cingulid, as is typical for *D. naui* (Morales et al. 2012), whereas the posthypocristid is longer and turns lingually enclosing posterior fossa and postentocristid posteriorly. Although there is also some variability in this feature, generally the postentocristid is blunter and less accentuated in *D. crassum* than in *D. naui* (Morales et al. 2012) and in the specimens observed for this study. A very small additional enamel fold is present at the posterior wall of the posthypocristid in some specimens (GPIT/MA/2741, GPIT/MA/2756, UMJGP 210694, 210693; probably also in GPIT/MA/2734 and UMJGP 204109), which cannot be verified or rejected as a crest due to preservation, while it is lacking in others (UMJGP 204662, 204663, 204664, and GPIT/MA/2401). Anterior and posterior cingulid are present, but less distinct and weaker than in *D. crassum*.

In m3, trigonid and talonid are similar to m1 and m2. At the posterior wall of the entoconid, a small crest-like entostylid is aligned to the postentocristid. In all specimens, the posthypocristid is split into a longer internal posthypocristid fusing with the entostylid closing the posterior fossa and a very short accessory external posthypocristid fusing with preentoconulidcristid and prehypococonulidcristid closing the back fossa of m3 anteriorly almost completely. The hypoconulid is the dominant conid in the third lobe. The postentoconulidcristid is reduced, while the posthypococonulidcristid is very dominant and closes the back fossa posteriorly by fusion with the entoconulid. Some specimens possess a very small posterior ectostylid (UMJGP 204662, 204665 and 210694). In all specimens, the third lobe is clearly set off from the talonid, and turned to labial by a shift of the hypoconulid to anterolabial (Fig. 2l3, n5). This feature is characteristic for the more selenodont *D. guntianum*

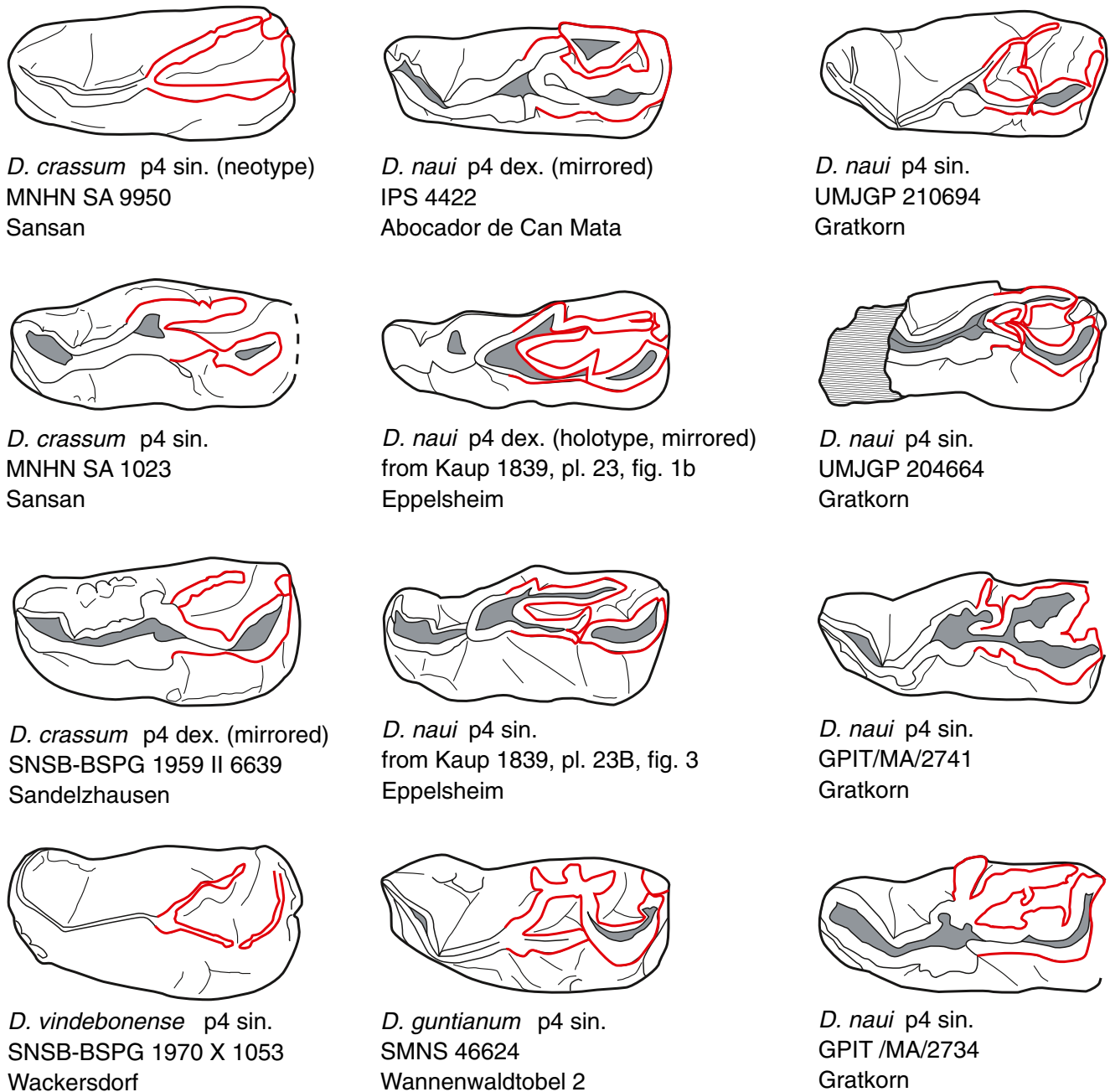


Fig. 5 Different p4 morphotypes for the genus *Dorcatherium*: More bunodont lineage (including *D. crassum* and *D. vindebonense*) with simple posterior valley, more selenodont lineage (including *D. guntianum*

and *D. nauti*) with more complex posterior valley, in terms of additional crests (red lines indicate crests of interest; dimensions not to scale; drawings based on original material or reference given)

and *D. nauti*, while in the more bunodont species *D. crassum*, *D. vindebonense*, and *D. penecke*, the third lobe is not turned to labial (Mottl 1961; Rössner 2010; Alba et al. 2013).

Postcrania (Fig. 20–t)

Material: UMJGP 210792 (proximal part of radius dex.), GPIT/MA/2391 (proximal part of radius sin.), UMJGP 203419 (tibia sin. missing proximal part and cubonavicular sin.), UMJGP 203718 (distal half of tibia sin.), GPIT/MA/2759 (distal

epiphysis of tibia sin.), UMJGP 210205 (cubonavicular dex. and os indet.), GPIT/MA/2745 (phalanx medialis).

As an astragalus dex. and a fragmented calcaneum dex. (GPIT/MA/2409) were found in close vicinity and articulate well, they are considered as part of the same individual.

A radius sin. (GPIT/MA/2420) articulates well with the distal fragment of a humerus sin. (GPIT/MA/2389) and, considering the finding position and general taphonomy of the locality, the affiliation to the same individual seems most reasonable.

Description and comparison

Only a few postcranial ruminant remains found at Gratkorn can be assigned to Tragulidae. Measurements correspond well to the medium-sized *Dorcatherium crassum* and *D. naui* (for measurements, see online resource 2). The distal articulation facet of a **humerus** sin. (GPIT/MA/2389; Fig. 2o) is similar in morphology to extant and extinct tragulids. The epicondylus medialis is short and knob-like, similar to *D. crassum* from Sansan (Morales et al. 2012, figs. 32–36; personal observation), to *D. naui* from Atzelsdorf (Hillenbrand et al. 2009, pl. I, fig. 11), and to modern genera, *Tragulus* and *Hyemoschus* (Gailer 2007, Abb. 4 AII, BII). In contrast, in Pecora, it is caudally more extended. The fossa olecrani is closed. In cranial view, the trochlea humeri is trapezoid in shape with a proximodistal diameter decreasing more strongly from medial to lateral than in Pecora and according to what is described for *D. naui* from Atzelsdorf by Hillenbrand et al. (2009). The distal surface of the trochlea humeri ascends from medial to lateral. The lateral crest is less distinct than in Pecora. In cranial view, the trochlea is less rounded than in Cervidae. In shape, it resembles *D. naui* (Kaup 1839, pl. 23C, fig. 2). Three fragmented **radii** (Fig. 2p) with proximal articulation surfaces are preserved. Although they are slightly varying in size (online resource 2), their morphology and dimensions are within the variability of *D. crassum* from Sansan (Morales et al. 2012), being slightly wider dorsopalmarly than *D. naui* from Abocador de Can Mata (Alba et al. 2011). A plane articulation facet on the palmar plane is present in all specimens for the articulation with the ulna. In proximal view, the proximal articulation surface is biconcave with a roughly trapezoid shape, with the lateral fossa in dorsopalmar extension less wide than the medial fossa in accordance with the shape of the trochlea humeri. The lateral part of the articulation surface reaches further proximally than in cervids and bovids. Two distal **tibia** fragments (Fig. 2r) show a transition from a proximal triangular cross-section to a more trapezoid distal one. A pronounced malleolus medialis is characteristic for Artiodactyla (Schmid 1972; not observable in UMJGP 203178 as mostly lost due to rodent gnawing). Typical for tragulids, it is not the longest distal projection, as it would be in Pecora (Hillenbrand et al. 2009). Medially, the sulcus malleolaris is clearly developed. The biconcave cochlea tibiae reflects the shape of the proximal trochlea of the astragalus. It comprises a narrow, dorsoplantarily extended and stronger plantarily tapering medial concavity and a wider, but less deep and dorsoplantarily clearly shorter, lateral concavity. Following Hillenbrand et al. (2009), this is characteristic for tragulids. The distal fibula, reduced to the malleolus lateralis, is not fused with the laterodistal surface of the tibia in the Gratkorn specimen, as is the case in *D. naui* from Eppelsheim (Kaup 1839, pl. 23 C, fig. 4) and Atzelsdorf (Hillenbrand et al. 2009), in *D. guntianum* from Günzburg (personal

observation), and also in the modern genus *Hyemoschus* (Milne Edwards 1864, pl.11, fig. 1c; Gailer 2007). The tibia of *D. guntianum* differs by its smaller size from the Gratkorn specimens. In *D. crassum*, the malleolus lateralis is fused with the tibia (Milne Edwards 1864, pl.12, fig. 1b, 1c; Filhol 1891, pl. 13, fig. 4; Carlsson 1926; Hillenbrand et al. 2009; Rössner 2010). Two **cubonaviculars** are well within the size variability of the medium-sized *Dorcatherium* species (Fig. 2q). As in all ruminants (Janis and Scott 1987; Vislobokova 2001), they represent fused cuboids and naviculars. Typically for tragulids, they show a fusion with the ectocuneiform (Gentry et al. 1999; Rössner 2007). In comparison to cervids, the articulation surface to the calcaneum is steeper and lacks a central canal at the plantar plane (Gailer 2007; Sánchez et al. 2010a). Furthermore, the proximoplantomedial process is short, while it is more developed in Pecora (Sánchez et al. 2010a). In the **astragalus** dex. (Fig. 2s), the plantar trochlea covers most of the plantar plane, and is not longish triangular as in suids (Schmid 1972), as typical for ruminants (Morales et al. 2012). Like in modern Tragulidae and in *D. crassum*, the proximal trochlea, trochlea tali, encloses medially an obtuse angle with the caput tali, comparable to suids, but different to Pecora, where the two axes are parallel (Schlosser 1916; Gailer 2007; Morales et al. 2012). The lateral condyle of the caput tali is set off and mediolaterally wider than the medial condyle. The lateral border of the lateral condyle possesses a strong notch, as in *D. crassum*, distinguishing it from cervids and bovids, which possess a straight lateral border in the lateral condyle of the distal trochlea. In shape, it agrees with the astragalus of *D. naui* figured in Kaup (1839, pl. 23C, fig. 6). The fragment of a **calcaneum** dex. (GPIT/MA/2409; Fig. 2t) comprises more or less just the sustentaculum tali and a part of the processus calcanei. In comparison to cervids, the sustentaculum tali in the calcaneum is more strongly inclined plantarily (see, e.g., fig. 25 in Gailer 2007; *Euprox* vel *Heteroprox* from Steinheim a. A., GPIT/MA/2984). A badly preserved **phalanx medialis** could be assigned to *D. naui* (GPIT/MA/2745). In dimensions it is smaller than specimens of *Euprox* vel *Heteroprox* (diverse specimens SMNS and GPIT) but within the variability of *Dorcatherium* (Sansan, Sandelzhausen and Viehhausen; see also Rinnert 1956). Due to preservation, the morphology cannot be clearly defined, but the shape of the proximal articulation surface is mediolateral wide, shallow and triangular, similar to *D. crassum* from Sansan (Morales et al. 2012; personal observation) and Sandelzhausen, while it is dorsovolarly elongated and dorsally more rounded in *Euprox* vel *Heteroprox* from Steinheim a. A. (specimens in SMNS and GPIT). Furthermore, the distal articulation is not as large and distinct as it is in *Euprox* vel *Heteroprox* from Steinheim a. A., but more similar in shape to *Dorcatherium* (specimens in SMNS and GPIT). In contrast

to modern Tragulidae, where the proximal tuberosity for the attachment of the tendon is not as marked as in Cervidae (Gailer 2007), it is well pronounced in the specimen from Gratkorn, as it is in other *Dorcatherium* specimens.

Discussion

In size, *Dorcatherium* teeth from Gratkorn nest well within the dimensions (Fig. 3) given by Mottl (1961), Moyà-Solà (1979), Fahlbusch (1985), Rössner (2010), Alba et al. (2011), Morales et al. (2012), and Alba et al. (2013) for the medium-sized *Dorcatherium crassum* and *nauï* (Fig. 3). They are larger than *D. guntianum* (Mottl 1961; Alba et al. 2011) and smaller than *D. vindebonense* (Mottl 1961; Fahlbusch 1985; Rössner 2010; Alba et al. 2011) and *D. peneckeï* (Mottl 1961; Rössner and Heissig 2013).

In morphology, *Dorcatherium* from Gratkorn is in accordance with *D. nauï* and *D. guntianum* (Hillenbrand et al. 2009; Rössner 2010; Alba et al. 2011; Rössner and Heissig 2013) because of: (1) a bicuspid p2/d2, (2) a tricuspid p3 with a less dominant mesolabial conid than in *D. crassum*, (3) a p4 with a more complex posterior valley, (4) more selenodont, more slender and higher crowned lower molars, (5) a labially turned third lobe in the lower m3, (6) upper molars with less bulky styles than in *D. crassum*, and (7) a non-fusion of tibia and malleolus lateralis (Kaup 1839; Mottl 1961; Sach 1999; Hillenbrand et al. 2009; Rössner 2010; Alba et al. 2011; Rössner and Heissig 2013). In contrast to this, *D. crassum*, *D. vindebonense*, and *D. peneckeï* possess (1) a tricuspid p2/d2, (2) a more dominant mesolabial conid in the tricuspid p3, (3) a p4 with a more simple morphology of the posterior valley, (4) more bunodont, wider and less high crowned lower molars with a more prominent ectostylid, (5) a more middle position of the third lobe in the lower m3, (6) upper molars more bulky in habitus, and (7) a tibia fused with the malleolus lateralis (not all characters described in *D. vindebonense* and *D. peneckeï*, as they are more rare and not all dental and skeletal elements have so far been recorded; Fahlbusch 1985; Rössner 2010; Morales et al. 2012; Alba et al. 2013).

Furthermore, the Gratkorn specimens share with *D. nauï* the proportionally short and accentuated postentocristid (Morales et al. 2012). Although this character is variable in *D. crassum*, it seems to be more common in *D. nauï* and is given as a diagnostic feature by Morales et al. (2012) to distinguish the two species. Following Morales et al. (2012), a remarkably shorter external than internal postmetacristid should be characteristic for *D. nauï*, while in *D. crassum* the external postmetacristid should be more equal in length to the internal postmetacristid (see also figs. 81–82 in Morales et al. 2012). As in Gratkorn and in the rich *D. crassum* material from Sandelzhausen and other localities, a certain variability concerning this feature can be observed, it is not taken into

consideration here. The erection of the subspecies *D. nauï meini* on the basis of characters common in *D. crassum* and distinct from *D. nauï* (Alba et al. 2011) cannot be followed, as the characters given (external postmetacristid shorter than internal one and shorter and less developed entocristid) are either more characteristic for *D. nauï* than for *D. crassum*, and/or, as mentioned, variable to a certain degree (Morales et al. 2012; personal observation).

As mentioned above, all specimens with a preserved anterior part of the mandibula possess an alveola for p1, as is the case in all representatives of *D. nauï* except for one specimen from Can Petit (Spain; Moyà-Solà 1979). Although the presence of a p1 cannot be used as a diagnostic feature to differentiate *D. crassum* and *D. nauï*, as it is variable (see also discussion in Moyà-Solà 1979; Alba et al. 2011, 2013; Morales et al. 2012), it seems to be far more common in *D. nauï* than in *D. crassum* from the type locality Sansan (Morales et al. 2012). In recently described *D. crassum* specimens from Lower Miocene sediments of Spain, the p1 is present in all specimens, which are complete enough to show this feature (Alba et al. 2013), while in *D. crassum* from Sandelzhausen, the presence of a p1 is also more common than in the type locality Sansan. As the results of Alba et al. (2013) were published during the review process of our publication, we could not fully take them into consideration. However, we think that the presence of a p1 in early representatives of *D. crassum* and the loss of it in later records should be included in our discussion. The observation by Alba et al. (2013) furthermore underlines that *D. crassum* and *D. nauï* should be considered as belonging to different phylogenetic lineages, as the loss of the p1 is a derived feature in a lineage (see, e.g. discussions in Janis and Scott 1987). Thus, the withholding of p1 in *D. nauï* is one of the arguments that it cannot be considered a direct descendant from *D. crassum* and supports, as mentioned, the suggestion of Moyà-Solà (1979) that the two species should be considered members of two different evolutionary lineages.

Stratigraphic range and phylogenetic relationship of *Dorcatherium nauï*

As pointed out by Alba et al. (2011) and Rössner and Heissig (2013), the supposed synonymy of *D. crassum* and *D. nauï* has produced confusion on the stratigraphic ranges of the different species for more than 100 years. Nevertheless, *D. nauï* has also been considered a valid species distinct from *D. crassum* (Mottl 1961; Moyà-Solà 1979; Morales et al. 2003, 2012; Montoya and Morales 2004; Rössner 2007, 2010; Hillenbrand et al. 2009; Alba et al. 2011; Sánchez et al. 2011b). Its stratigraphic range has so far been considered to be restricted to the Late Miocene (Rössner 2007, 2010; Hillenbrand et al. 2009), while reliable records of *D. peneckeï*, *D. vindebonense*, *D. crassum* and *D. guntianum* are only known from the Early and Middle Miocene (Fig. 1; Rössner 2007, 2010; Alba et al. 2011).

With the description of *D. nauti* from Abocador de Can Mata (Spain, MN8), and the assignment of the tragulid material from Przewomo (Poland, MN7/8) to the same species, Alba et al. (2011) have already documented the first records for the occurrence of *D. nauti* in the late Middle Miocene. For our work, we reevaluated the taxonomic affiliation and the stratigraphic ages for Central and Western European localities with records of *Dorcatherium* to gain a more detailed view of stratigraphic ranges of the different species (Fig. 1; note that this list is far from complete, that the focus is on localities from the NAFB and Austria, and that only localities with reliable species identification have been taken into consideration). Besides the integration of *D. nauti* from Gratkorn in the stratigraphic range, we could date back the oldest record of the species at least as far as the early Sarmatian (12.7–12.3 Ma; Fig. 1).

In general, late Middle Miocene *Dorcatherium* material is quite scarce. It thus gives only limited insight into character variability of Middle Miocene *D. nauti* and possible differences from the Late Miocene representatives of the species. With *D. nauti* from Gratkorn, we present abundant material from the late Middle Miocene and can thus for the first time estimate variability among the early representatives of this species. The specimens from Gratkorn clearly show that there is no significant difference between the Middle Miocene representatives of *D. nauti* and the abundant *D. nauti* material from the Late Miocene Atzelsdorf locality (Hillenbrand et al. 2009). Furthermore, it is well in accordance with the type material from Eppelsheim (Kaup 1839). Thus, morphology of the Gratkorn *D. nauti* does not indicate an intermediate position inbetween *D. crassum* and *D. nauti*, and does not support the idea (e.g. Fahlbusch 1985) of *D. nauti* evolving out of *D. crassum*. On the contrary, *D. nauti* has to be considered part of a selenodont lineage, together with *D. guntianum*, but distinct from the bunoselenodont lineage including *D. crassum*, *D. penecke*, and *D. vindebonense* (see also Rössner and Heissig 2013 and others) due to the characteristic features described above. As no common ancestor has so far been recorded, and as both lineages appear at about the same time (Fig. 1) and are already distinctly different in morphology in the first records, a divergence of both lineages after the immigration of a common ancestor to Europe is evaluated as unlikely, while an immigration of representatives of both lineages during the Early Miocene (Fig. 1) seems more plausible.

Palaeoecological characterisation

Dorcatherium nauti had a shoulder height of about 40–50 cm. Body mass estimates for the Gratkorn specimens are about 28–29 kg (min: 26 kg, max 30.6 kg; $n=6$) and are well in accordance with body mass estimates for *D. nauti* from Abocador de Can Mata by Alba et al. (2011). In weight, the species is therefore comparable to the modern roe deer, though smaller in height. Modern tragulids are exclusively small-sized

ruminants, with a shoulder height of about 20–40 cm (Rössner 2007) and body masses of 7–16 kg for *Hyemoschus aquaticus*, and of 1.5–2.5 kg for *Tragulus kanchil* (Meijaard 2011).

The ecology of Miocene Tragulidae, especially habitat and feeding strategy adaptations, is often discussed but still not fully understood, and presumably was more diverse than in modern members of the family (see, e.g. Kaiser and Rössner 2007; Ungar et al. 2012). In contrast to modern Tragulidae, which are restricted to disjunct areas in tropical Asia and Africa (Meijaard 2011), tragulids were a common faunal element in Europe, Asia and Africa during the Miocene (Vislobokova 2001; Rössner 2010; Rössner and Heissig 2013). Due to an overall morphological similarity of *Dorcatherium* with modern Tragulidae, a wet, forested habitat with dense underwood has always been assumed for the genus (Köhler 1993; Rössner 2010; Alba et al. 2011). The short metapodials and the morphology of the phalanges indicate low-gear locomotion (Leinders 1979; Köhler 1993; Morales et al. 2012). The rigidity in the hindlimb caused by the fusion of ectocuneiform and cubonavicular indicates an inability of a zigzag flight behaviour (Alba et al. 2011). Based on the latter, Moyà-Solà (1979) assumed a similar escaping behaviour in *Dorcatherium* as in the living African *Hyemoschus*, which is documented by Dubost (1978) as fleeing straight into the next open water when threatened. Whether the fusion of malleolus lateralis and tibia in *Tragulus* and *D. crassum* or the nonfusion in *D. nauti* and *Hyemoschus* are convergent adaptations to the same habitat or environment, respectively, can only be verified by ecological investigations of the modern taxa. Morales et al. (2012) observed that *D. nauti* and *crassum* differ furthermore in the articulation of MC III and IV (from Gratkorn this element is not recorded so far). While *D. crassum* may have been enabled to a greater mobility, *D. nauti* would have had more stability in the joint due to an interlocking mechanism, comparable to but not as derived as in the modern *Hyemoschus aquaticus* (Alba et al. 2011; Morales et al. 2003). Whether this feature is indicative of an adaptation in *D. crassum* to soft and humid ground cannot be verified due to only a little material and lack of further investigations, but it is questioned by the similar morphology in *D. nauti* and *Hyemoschus*. The latter is adapted to very humid environments (Dubost 1965).

Although Matsubayashi et al. (2003) observed daytime activity in *Tragulus javanicus*, a nocturnal or crepuscular way of life has been documented for *Hyemoschus* (Dubost 1975). The large size of the orbits in the *D. nauti* skull from Eppelsheim (Kaup 1839, pl. 23A) might also be an indication for a possible nocturnal behaviour of this extinct species (Rössner 2010).

By lancing the sabre-like elongate upper canines at each other, primitive territorial fighting among males can be observed in recent Tragulidae (Dubost 1965), which most likely was not different in the Miocene species, with upper canines being proportionally even larger.

Modern Tragulidae feed on fallen fruit, seeds, flowers, leaves, shoots, petioles, stems, and mushrooms in the forest undergrowth (Dubost 1984). *Hyemoschus* is even known to casually feed on invertebrates, fishes, small mammals and carrion (Dubost 1964). Although diet reconstruction is limited for fossil taxa, different feeding strategies could be observed in fossil tragulids, ranging from browsing to grazing (for further discussion, see Aiglstorfer et al. 2014a, this issue). The only available isotopic measurements ($\delta^{13}\text{C}$ and $\delta^{18}\text{O}$) for *D. naui* published so far were done on the specimens from Gratkorn described here and point to the ingestion of a considerable amount of fruit or grass besides a browsing diet (Aiglstorfer et al. 2014a, this issue). The reconstruction of a diet with a certain amount of fruits is also supported by the incisor arcade of *D. naui* from Gratkorn. In accordance with Janis and Ehrhardt (1988) and Clauss et al. (2008), the architecture of the incisor arcade in *Dorcatherium naui* and modern Tragulidae (Fig. 4; strongly widened i1 in comparison to i2 and i3) points to a more selective feeding strategy. Although limited in its predictions (Fraser and Theodor 2011), disparity in incisor widths is significantly higher in browsers than in grazers, assumedly due to a more selective picking (Janis and Ehrhardt 1988; Clauss et al. 2008). Applying these ecomorphological considerations to the Gratkorn locality, *Euprox furcatus* (Hensel, 1859) with a typical isotopic composition of a subcanopy browser (feeding in the more closed, lower part of the vegetation; Aiglstorfer et al. 2014a, this issue) should have a higher ratio in i1 width to i2 or i3 width than *D. naui*, if the latter were more grazing. This is not the case. Assuming a more selective picking of perhaps fruits, the higher ratio of i1 width to i2 or i3 width of *Dorcatherium* in comparison to the subcanopy browsing cervid could be explained. Thus, combining tooth morphology and isotopic measurements, a significant amount of fruits is most likely to have been part of the diet of *D. naui*.

Although ecological differences between the different *Dorcatherium* species are indicated, a general adaptation to a forested environment or at least one with enough undergrowth, can be assumed for the fossil genus. In general, it is associated with dominantly browsing taxa in the fossil record (Kaiser and Rössner 2007; Hillenbrand et al. 2009; Rössner 2010; Alba et al. 2011; Gross et al. 2011). A dependency of *D. naui* on a forested environment and at least not fully arid conditions is suggested by the restricted occurrence during the late Middle Miocene in Spain. So far, it has only been described from Abocador de Can Mata (Vallès-Penedès Basin, Catalonia, Spain; co-occurring with beavers and arboreal primates there; Alba et al. 2011), which was less arid and more forested than the localities from the inner Iberian basins (less than 400 mm MAP for the Calatayud-Daroca and the Teruel basin between 12.5 and 11.5 Ma; Böhme et al. 2011). However, the abundance of *D. naui* at Gratkorn (MAP of 486 ± 252 mm according to Gross et al. 2011) indicates a tolerance to less humid environments in comparison to

D. crassum. The presence of the “genus” as an indicator for humid environments has thus to be considered with care. Isotopic measurements ($^{87}\text{Sr}/^{86}\text{Sr}$) indicate that *D. naui* was a permanent resident of the locality, and thus could cope with seasonal variations in its diet (for further discussion, see Aiglstorfer et al. 2014a, this issue).

Infraorder Pecora Linnaeus, 1758

Family Moschidae Gray, 1821

Genus *Micromeryx* Lartet, 1851

Type species: *Micromeryx flourensianus* Lartet, 1851

Micromeryx flourensianus Lartet, 1851

Holotype: hitherto not determined (Ginsburg proposed (letter from 1974): MNHN Sa 2957); type material from Sansan (France, MN6) under revision; partly figured in Filhol (1891, pls. 24, 25); stored at MNHN.

For the genus *Micromeryx*, five European species are considered valid at the moment: *Micromeryx flourensianus* Lartet, 1851, *Micromeryx styriacus* Thenius, 1950, *Micromeryx azanzae* Sánchez and Morales, 2008, *Micromeryx soriae* Sánchez, Domingo and Morales, 2009, and *Micromeryx mirus* Vislobokova, 2007.

Material: UMJGP 204058 (C sin.), UMJGP 204678 (sin. maxilla fragment with D2–M3), GPIT/MA/02387 (sin. maxilla fragment with D4–M1), UMJGP 204688 (dex. maxilla fragment with P3–M1, fragment of M2; P2 dex.), GPIT/MA/02388 (sin. maxilla fragment with P2–M3), UMJGP 204718 (M1? sin.), UMJGP 210972 (P4 sin.), UMJGP 210971 (mandibula sin. with d4–m1), UMJGP 204685 (mandibula sin. with m1–3), GPIT/MA/2751 (fragmented mandibula sin. with d3, d4–m3), UMJGP 204068 (mandibula dex. with p2–m3), UMJGP 204710 (mandibula dex. with p3–4; alveola for p2), UMJGP 204709 (mandibula dex. with p4–m3), UMJGP 204715 (m3 sin.; indet. tooth fragment).

Description (for detailed information and measurements, see online resource 3)

Upper toothrow: (Fig. 6a–d): On the sabre-like C sin. (UMJGP 204058; Fig. 6a), enamel covers the labial part of the anterior side and the labial side. The tooth is curved to posteriad and is linguolabially flattened with a triangular to drop-shaped cross-section (posterior edge sharp) and decreases gradually in anteroposterior width from base to tip like in Cervidae but distinct from Tragulidae (Rössner 2010). A slight undulation due to growth striation can be observed on the enamel. The tooth possesses no wear pattern lingually as can be observed in Tragulidae (Rössner 2010). Only one D2 has so far been excavated (UMJGP 204678; Fig. 6b). Due to



Fig. 6 Dental and postcranial material of Moschidae: **a** *Micromeryx flourensianus* C sin. (UMJGP 204058), **b** *M. flourensianus* maxilla sin. with D2–M3 (UMJGP 204678; 1 occlusal view, 2 labial view), **c** *M. flourensianus* maxilla sin. with P2–M3 (GPIT/MA/2388; 1 P2–P4, 2 M1–M3), **d** *M. flourensianus* maxilla dex. with P3–M1 (UMJGP 204688; 1 occlusal view, 2 labial view), **e** *M. flourensianus* mandibula sin. with d3–m3 (GPIT/MA/2751; 1 d3 sin., 2 d4–m3 sin.), **f** *M. flourensianus*

mandibula sin. with m1–3 sin. (UMJGP 204685; 1 labial view, 2 occlusal view), **g** *M. flourensianus* mandibula dex. with p2–m3 (UMJGP 204068; 1 labial view, 2 lingual view, 3 occlusal view), **h** *M. flourensianus* mandibula dex. with p4–m3 (UMJGP 204709; 1 labial view, 2 lingual view, 3 occlusal view), **i** *Hispanomeryx* sp. M1–2? sin. (UMJGP 204666), **j** Moschidae gen. et. sp. indet. distal tibia sin. (UMJGP 204100; 1 dorsal view, 2 distal view); scale bar 10 mm (except e, 5 mm)

strong wear, only the elongated triangular shape can be described. The only **D3** (UMJGP 204678; Fig. 6b) is badly damaged. The **D4** (Fig. 6b) is trapezoid in shape with the typically enlarged parastyle, more pronounced than can be

observed in the cervid from the same locality. The mesostyle is developed while the metastyle is reduced and wing-like. Internal postprotocrista and metaconule fold are present, as are the entostyle and the basal cingulum. The latter is more clearly

developed at the protocone. The **P2** (Fig. 6c) is elongate triangular in shape and lingually more rounded. The lingual cone is located more posteriorly than the labial cone. Anterior and posterior styles are present, and the first encloses a narrow incision with a well-pronounced rib at the labial cone, while the posterolabial depression is wider. At the lingual wall, a depression is clearly developed anterior to the lingual cone. The tooth possesses no clearly developed cingulum. The **P3** (Fig. 6c) is similar in shape to the P2 but linguolabially wider due to a more pronounced lingual cone. A small central fold is present. In comparison to the anterior premolars, the **P4** (Fig. 6c) is anteroposteriorly shortened and linguolabially widened. The lingual side is rounded. The labial wall is concave with a moderately pronounced rib at the labial cone and a strong anterior style. The posterior style is reduced and more wing-like. The anterolingual crista is only slightly shorter than the posterolingual one. There is no cingulum, but a clearly developed central fold, in some cases even split. The **upper molars** (Fig. 6b–d) are trapezoid to subquadratic in shape with four main cusps. Size increases from M1 to M3. Para- and mesostyle are distinct, while the metastyle is reduced and wing-like in shape. The latter increases in size from M1 to M3. The rib at the paracone is well pronounced, enclosing a distinct but narrow incision with the parastyle. The entostyle is clearly developed, increasing in size from M1 to M3. All upper molars show an internal postprotocrista. The premetaconulecrista is developed more or less pronounced and sometimes split anteriorly with one or two small anterior branches fusing with the internal postprotocrista. The premetaconulecrista itself is long and intruding wide labially inbetween paracone and metacone. The metaconule fold is present but varying in size. Anterior and posterior basal lingual cingula are present, usually more strongly anteriorly. The M3 differs from the anterior molars by stronger linguolabially width decrease posteriorly and the more developed metastyle. The **mandibula** (for detailed information and measurements, see online resource 3; Fig. 6e–h) possesses a slender corpus mandibulae, a longer premolar row than observed in *Hispanomeryx* (online resource 3) and no indication for the presence of a p1. Two foramina mentalia are developed, a smaller caudal one and a larger rostral one. The caudal rim of the symphysis is more distant from the toothrow than in Tragulidae due to an elongated rostrum in comparison to the latter. The **d3** (GPIT/MA/2751; Fig. 6 e1) is elongated with well-pronounced anterior conid and stylid. The mesolabial conid is dominant. The posterolingual conid closes the back valley lingually by fusion with the posterior stylid. The transverse cristid is directed slightly posterolingually not reaching the posterolingual conid. There is no mesolingual conid. The posterior and back valleys are oriented obliquely to the length axis of tooth. The first is wider than the latter and open lingually. A slight depression anterior to the posterolabial conid on the labial wall is present but no cingulid. The **d4**

(Fig. 6 e2) is elongated with three lingual and three labial conids. The lingual conids are higher than the labial ones. Anterior stylid and metastylid are slightly stronger than mesostylid and entostylid. Internal and external postprotocristid are well developed forming a v-structure, usually termed *Palaeomeryx*-fold. Preprotocristid and premetacristid are fused with posterior cristids of anterolingual and anterolabial conids, respectively. The internal postprotocristid and metaconid are connected with the preentocristid, while the prehypocristid does not reach the preentocristid. The posthypocristid tapers wide lingually and is fused with the entostylid. Anterior ectostylid and ectostylid are well pronounced, the latter very large. An anterior cingulid is clearly present. The only preserved **p2** (UMJGP 204068; Fig. 6g) is elongated rectangular, with a small anterior conid and no anterior stylid. The mesolabial conid is dominant, the transverse cristid shifted posteriorly and enlarged posteriorly forming the mesolingual conid. The posterior valley is oriented obliquely to the length axis of the tooth and posteriorly open. The back valley is enclosed by posterolabial and -lingual conid and posterior cristid and stylid. It is oriented more perpendicularly to the length axis of tooth, but also open lingually. The incision on the labial wall anterior of the posterolabial conid is small. The **p3** (Fig. 6g) is more elongated rectangular than the p2, with more pronounced anterior conid and stylid (fused lingually in UMJGP 204710). The mesolabial conid is dominant, the transverse cristid is shifted posteriorly to different degrees, while the mesolingual conid is not strongly developed. The posterior valley is oriented obliquely to the length axis of the tooth, while the back valley is oriented more rectangularly and nearly (UMJGP 204068) or fully closed (UMJGP 204710) due to the posterior elongation of the posterior cristid. The incision on the labial wall anterior of the posterolabial conid is very weak. There is no clearly developed cingulid. In the triangular **p4** (Fig. 6g, h), the anterior stylid and conid are clearly separated. By fusion with the well-pronounced mesolingual conid, the latter closes or nearly closes the anterior valley. In contrast to the anterior premolars, the mesolingual conid is the dominant conid and slightly higher than the mesolabial conid. The transverse cristid is slightly shifted posteriorly and fused with the posterolingual cristid. The posterior valley is therefore very narrow, oriented obliquely to the length axis of the tooth and nearly closed. The back valley is also oriented obliquely and closed or nearly closed by elongation of the posterior cristid. The incision between mesolabial and posterolabial conid and the rib at posterolabial conid are stronger than in the preceding premolars. The tooth possesses a weak anterior cingulid.

The **lower molars** are brachyoselenodont (Fig. 6e–h). The main axis of the lingual conids is slightly oblique to the length axis of tooth but not as strong as in Cervidae. The metastylid is well pronounced, while meso- and entostylid are not really distinct. The postprotocristid is split into internal and external cristid forming a moderately developed v-structure (*Palaeomeryx*-fold; less visible with higher degree of wear).

The preprotocristid is long, reaching the lingual side anteriorly and fused with the shorter premetacristid. The preentocristid is short and connected with the longer postprotocristid. The prehypocristid is not fused with preentocristid and postprotocristid. The ectostylid is strong and a strong anterior cingulid is present. From m1 to m2, the size increases, the ectostylid becomes more slender, and the external postprotocristid as well as the anterior cingulid decrease in strength. In the **m3** ectostylid, external postprotocristid and anterior cingulid are further decreased in size. The third lobe is two-coned with a clearly developed entoconulid as the dominant cone. The posthypocristid is connected with the long prehyoconulidcristid closing the back fossa of m3 anteriorly. By the fusion of posthyoconulidcristid with a shorter entoconulidcristid, the back fossa is closed posteriorly and lingually by a quite high entoconulid. The posterior ectostylid is very small to not present.

Comparison and discussion

The small moschid from Gratkorn shows characteristic dental features for the genus *Micromeryx*: (1) the closed or nearly closed anterior valley in the triangular p4, (2) lower molars with only anterior cingulid, (3) bicuspid third lobe with a high entoconulid in the m3, and (4) non-shortened lower premolar row (Gentry et al. 1999; Rössner 2006, 2010; Vislobokova 2007; Sánchez and Morales 2008). It thus differs from the similarly sized cervid *Lagomeryx* (stratigraphic occurrence: late Early Miocene to middle Middle Miocene; Rössner 2010) which has lower crowned teeth, a lower lingual wall/cuspid in the third lobe of the m3 and an open anterior valley in the p4 (Rössner 2010). From the other European Miocene moschid genus, *Hispanomeryx* Morales, Moyà-Solà and Soria, 1981, the specimens from Gratkorn differ by a longer lower premolar row in comparison to the molar row, by the presence of the external postprotocristid, and by a generally smaller size (small overlap in some tooth positions and some specimens; Fig. 7; online resource 3; Sánchez et al. 2010a).

Dimensions of the dentition are well within the range of the type species *M. flourensianus* and show the greatest overlap with *M. flourensianus* from the Middle Miocene of La Grive and Steinheim a. A. and the Late Miocene of Atzelsdorf (Fig. 7). They are in the upper size range of *M. flourensianus* from the type locality, Sansan. In morphology, *Micromeryx* from Gratkorn is similar to *M. flourensianus* from Steinheim a. A. and La Grive and shows the greatest resemblance with *M. flourensianus* from Atzelsdorf (Hillenbrand et al. 2009), e.g. in terms of tooth crown height and reduction of the external postprotocristid with some specimens still showing a more developed cristid and others a more reduced one. It thus differs from the specimens of the type locality, which generally display a more pronounced external

postprotocristid and a slightly lower tooth crown height (Fig. 8).

The validity of *M. styriacus* is still unclear (Sánchez and Morales 2008; Aiglstorfer and Costeur 2013). However, the Gratkorn specimens differ from the only tooth row and holotype of *M. styriacus* by a generally smaller size, a not fully closed posterior valley in the p4, and a less strongly developed external postprotocristid in the lower molars. *Micromeryx* from Gratkorn differs from *M. azanzae* by a general smaller size, a more compressed p4, and the presence of an external postprotocristid in the lower molars (Sánchez and Morales 2008). *M. soriae* is similar in size to the Gratkorn *Micromeryx* but possesses a broader external postprotocristid, so far unique in the genus (Sánchez et al. 2009). With *M. mirus* and *Micromeryx* sp. from Dorn-Dürkheim 1, the Gratkorn specimens share the labial incision anterior of the posterolabial conid in the p4 (in one specimen, UMJGP 204709, even as strong as in *M. mirus* (Vislobokova 2007; Aiglstorfer and Costeur 2013). With a generally smaller size (especially in the molars; not in p4 of *Micromeryx* sp. from Dorn-Dürkheim 1), *M. mirus* from Kohfidisch and *Micromeryx* sp. from Dorn-Dürkheim 1 differ from the Gratkorn specimens, and also by a generally further increased tooth crown height in the lower molars and a strongly reduced to non-existent external postprotocristid (Vislobokova 2007; Aiglstorfer and Costeur 2013). For the species *M. flourensianus*, the observed gradual change in morphology, in terms of the increase in tooth crown height and reduction for the external postprotocristid, could thus be well extended to the stratigraphically much younger *M. mirus* (Vislobokova 2007; Aiglstorfer and Costeur 2013). This trend has also been observed in other ruminant lineages (Janis and Scott 1987). However, in the Iberian Peninsula, it cannot be observed taking into consideration the morphology of the mainly Middle Miocene *M. azanzae* (no external postprotocristid) and the Late Miocene *M. soriae* (strong external postprotocristid; Sánchez et al. 2009).

In summary, the specimens from Gratkorn are well within the morphological and dimensional variability of the species *Micromeryx flourensianus*. They differ from specimens from the type locality, Sansan (early Middle Miocene), by an increase in the tooth crown height and a reduction of the external postprotocristid, and are more similar to the specimens from Steinheim a. A. and La Grive (Middle Miocene) and show the greatest overlap with the early Late Miocene representatives from Atzelsdorf (Hillenbrand et al. 2009). The specimens from Gratkorn are therefore attributed to the species *Micromeryx flourensianus*.

Stratigraphic range

The type species *Micromeryx flourensianus* is recorded from the early Middle Miocene to the Late Miocene (MN 5–9 (11?); Gentry et al. 1999; Bernor et al. 2004; Sánchez and

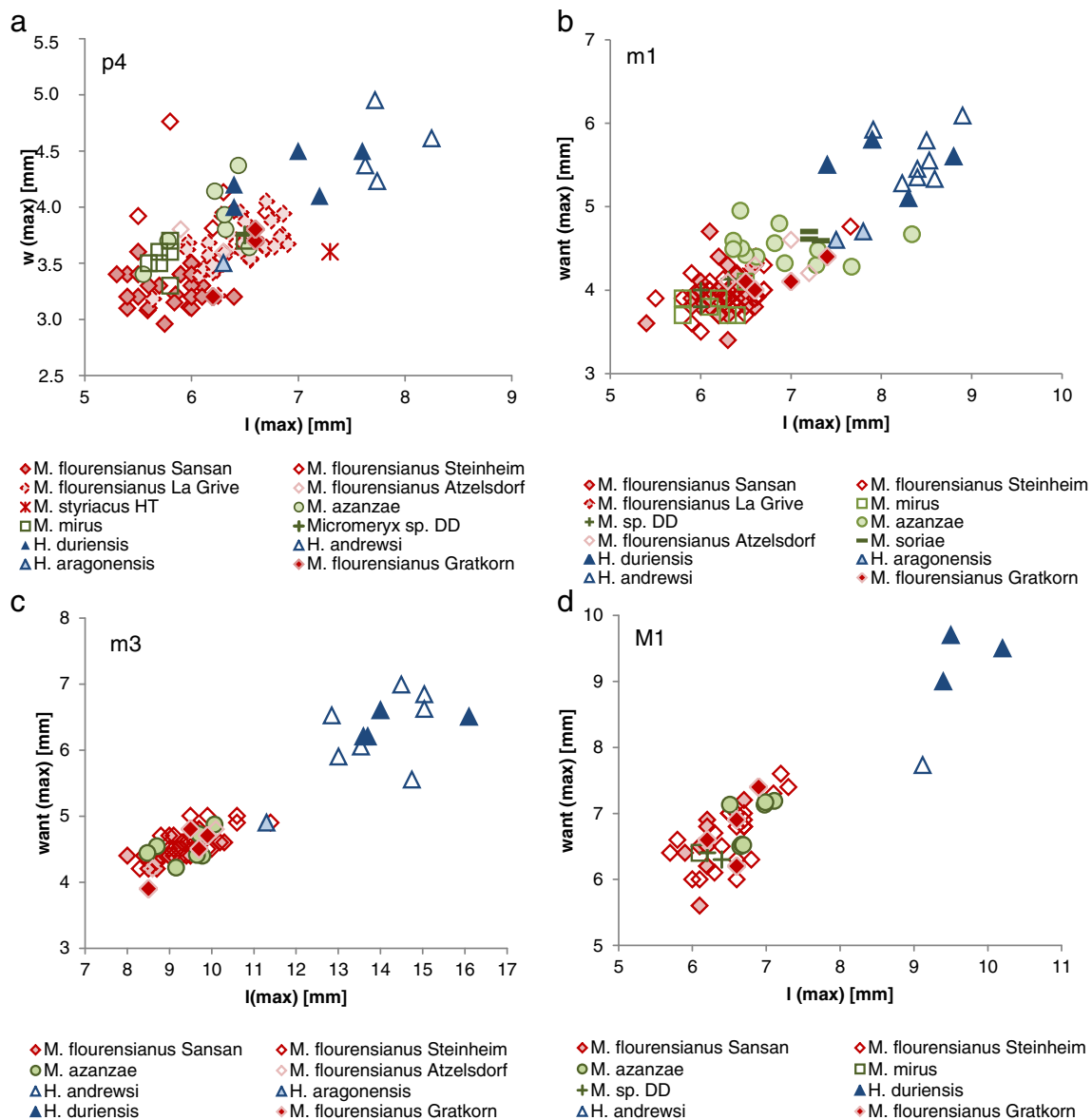


Fig. 7 Bivariate plots for p4 (a), m1 (b), m3 (c), and M1 (d) of *Micromeryx flourensianus* from Gratkorn in comparison to other Miocene Moschidae (data for *M. styriacus* from Göriach, *M. flourensianus* from Gratkorn, Sansan, Steinheim a. A., La Grive, *M. mirus* and *M. sp.* from DD (Dom-Dürkheim 1) personal observation and from Aiglstorfer and

Costeur 2013; *M. flourensianus* from Atzelsdorf from Hillenbrand et al. 2009; *M. azanzae* from Sánchez and Morales 2008; *M. soriae* from Sánchez et al. 2009; *Hispanomeryx duriensis* from Morales et al. 1981; *H. andrewsi* from Sánchez et al. 2011a; *H. aragonensis* from Azanza 1986)

Morales 2008; Seehuber 2008). *Micromeryx styriacus* is so far only known from the locality Göriach (Austria; early Middle Miocene; MN 5/6; $\sim 14.5 \pm 0.3$ Ma). *Micromeryx azanzae* (Middle Miocene to the early Late Miocene; MN6–9; Sánchez and Morales 2008) and *Micromeryx soriae* (Late Miocene; MN10; Sánchez et al. 2009) are recorded from Spain. Together with *Micromeryx sp.* from Dom-Dürkheim 1 (DD; Germany; Late Miocene; Aiglstorfer and Costeur 2013), *Micromeryx mirus* from Kohfidisch (Austria; Late Miocene; MN11) represents the last occurrence of the genus in Europe.

The type species *M. flourensianus* shows a long species duration (at least 5 Ma) and gradual changes

in morphology can be observed from the early representatives (e.g. Sansan; ~ 14.5 – 14.0 Ma) to later representatives [e.g. Gratkorn (12.2–12.0 Ma) and Atzelsdorf (11.1 Ma)], such as, e.g. an increase in tooth crown height (Fig. 8) and the reduction of the external postprotocristid. Well in accordance with a gradual morphological change, the locality Steinheim a. A. (~ 13.8 – 13.7 Ma; Böhme et al. 2012), stratigraphically intermediate between the first and the last records, also shows an intermediate position in morphology for *M. flourensianus*. As the type material from Sansan, as well as the rich material from Steinheim a. A., has



Fig. 8 Increase in general crown height and the height of the lingual wall at third lobe in m3 of *Micromeryx* of different ages: **a** m3 dex. of *M. flourensianus* from Sansan (MNHNS Sa 2962; mirrored), **b** m3 dex.

of *M. flourensianus* from Steinheim a. A. (SMNS 46077; mirrored), **c** m3 sin. of *M. flourensianus* from Gratkorn (UMJGP 204685), **d** m3 sin of *M. mirus* from Kohfidisch (NHMW 2005z0021/0007)

never been described in detail, a challenging of the assignation of younger *Micromeryx* findings from Central Europe to the species *M. flourensianus* cannot be accomplished at the moment. However, it may be that a comprehensive description and comparison of records so far assigned to *Micromeryx flourensianus* might result in a revised specific diagnosis of the younger material. Furthermore, a mixing with the small-sized cervid *Lagomeryx* Roger, 1904 cannot yet be excluded for the undescribed material of *M. flourensianus* from the type locality Sansan. A possible mixing is indicated for example by an open anterior valley in the p4, and a lower tooth crown height in the m3 of one specimen of *M. flourensianus* from Sansan (MNHN Sa 2965), comparable with the morphology of *Lagomeryx pumilio* (Roger, 1896) (Rössner 2006, 2010). This might also bias the present-day species diagnosis of *M. flourensianus*.

Genus *Hispanomeryx* Morales, Moyà-Solà and Soria, 1981

Type species: *Hispanomeryx duriensis* Morales, Moyà-Solà and Soria, 1981.

Further species: *Hispanomeryx aragonensis* Azanza, 1986; *Hispanomeryx daamsi* Sánchez, Domingo and Morales, 2010; *Hispanomeryx andrewsi* Sánchez, DeMiguel, Quiralte and Morales, 2011

? *Hispanomeryx* sp.

Material: UMJGP 204666 (M1–2? sin.; Fig. 6i)

Description and comparison

Two fragmented upper molars from presumably one tooth row (UMJGP 204666) are intermediate in size between the medium-sized Pecora, *Euprox* and *Tethytragus*, and the small-sized *Micromeryx*, but fall well within the variability of the genus *Hispanomeryx* (Fig. 9). One tooth is more complete, lacking only the posterior wall, while only the labial wall is preserved of the second and larger molar. The first tooth is cautiously assigned to an M1?, the larger an M2?, due to a weak metastyle in both (the

M3 has a more pronounced metastyle in the other Moschidae from Gratkorn) and the moderately developed entostyle (which also increases from M1 to M3 in the other Moschidae from Gratkorn; as morphology is variable to a certain degree (see e.g. Sánchez et al. 2010a), the assignation is given with reservations only). In any case, a determination as M3 can be excluded for the more complete tooth due to the only slightly reduced labiolingual width of the posterior part of the tooth. Besides the moderately developed entostyle and the reduced metastyle, the more complete molar shows clearly developed internal and external postprotocrista, an anterior cingulum, and, as far as can be reconstructed, also a posterior one. With the lack of a strong lingual cingulum and the presence of well-developed internal and external postprotocrista, an affiliation to *Dorcatherium* can be excluded. The specimen also differs from Cervidae by the weak basal cingulum and by the weakly developed rib at the metacone. The latter is shared with Moschidae

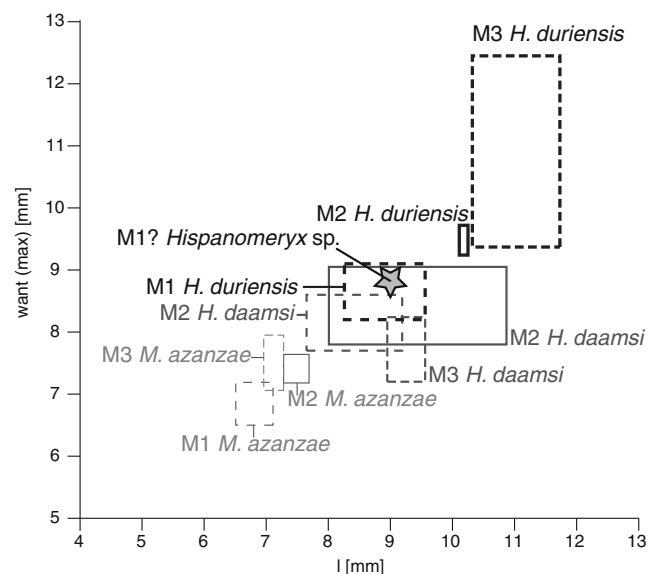


Fig. 9 Bivariate plot of M1? of *Hispanomeryx* sp. from Gratkorn (UMJGP 204666) in comparison to larger-sized Miocene Moschidae (data for *M. azanzae* from Sánchez and Morales 2008, for *H. daamsi* from Sánchez et al. 2010a, for *H. duriensis* from Morales et al. 1981)

and Bovidae, though. Due to strong wear, the degree of hypsodonty cannot be estimated.

As the teeth differ in size and morphology from the other ruminants recorded from the Gratkorn locality, but are well within dimensional and morphological range of the genus *Hispanomeryx*, they are tentatively assigned to this genus. As we are well aware that, due to limited material, the stage of wear and the preservation, a determination can only be given with reservations, we leave the specimens in open nomenclature as ?*Hispanomeryx* sp. The occurrence of *Hispanomeryx* in Gratkorn is the first record of the genus in Central Europe besides Steinheim a. A. (indicated in Heizmann and Reiff 2002, but not yet described) and indicates a wider geographic range than assumed so far.

Stratigraphic range

The genus *Hispanomeryx* first occurred in Europe in the middle Middle Miocene with *H. aragonensis* (MN6–7/8; Sánchez et al. 2010a) and *H. daamsi* (MN6–7/8; Sánchez et al. 2010a), while *H. duriensis* is only recorded from the Late Miocene (MN9–10; Sánchez et al. 2010a). To date, the last representative has been reported from the Late Miocene (one tooth of *Hispanomeryx* sp. from Puente Minero; 7.8 Ma; MN11; Sánchez et al. 2009). *Hispanomeryx andrewsi* has not been recorded from Europe so far (Sánchez et al. 2011a).

Moschidae gen. et sp. indet.

Material: UMJGP 204100 (tibia sin.; Fig. 6j)

Description and comparison

A fragmentary **tibia** sin. shows intense small mammal gnawing at the distal articulation. Its cross-section is trapezoid. There is no fusion of the malleolus lateralis and the tibia. A pronounced malleolus medialis can still be recognised, though its length in ratio to the central projection cannot be observed due to the small mammal gnawing. The sulcus malleolaris is clearly developed. The biconcave cochlea tibiae comprises a narrow, dorsoplantarily extended medial concavity and a wider, but a less deep and dorsoplantarily clearly shorter, lateral concavity. In contrast to Tragulidae, the first does not taper more widely plantarily than the latter. In size (preserved DAPd=10.7 mm and DTd=13.9 mm) the specimen is smaller than *D. naui* and *E. furcatus*, but larger than *M. flourensianus*. It overlaps in size with the larger moschids *M. azanzae* (Sánchez and Morales 2008) and *Hispanomeryx daamsi* (Sánchez et al. 2010a). Sánchez and Morales (2008) describe an anterodistal process of the tibia with a clear step in its lateral border in

Micromeryx, distinguishing it from *Hispanomeryx*. Due to small mammal gnawing, the existence of such a step can neither be verified nor rejected for the Gratkorn material. Furthermore, a sexual size dimorphism for *Micromeryx* has been observed by Sánchez and Morales (2008) in *M. azanzae*, being more pronounced in dental material but also significant in the DAPd of the tibia. A certain size variation in the dental material of *M. flourensianus* from Gratkorn can be observed (Fig. 7). However, the small amount of material does not allow a reasonable differentiation into larger and smaller forms, or, following Sánchez and Morales (2008), into females and males. As both genera, *Micromeryx* and *Hispanomeryx*, seem to be present in the fauna from Gratkorn and a sexual dimorphism cannot be excluded, the tibia is left in open nomenclature as Moschidae gen. et sp. indet.

Palaeoecological characterisation for Moschidae from Gratkorn

With an estimated body mass of about 4 to 5 kg (min.: 3.8 kg, max. 5.0 kg; $n=6$), *M. flourensianus* is by far smaller than all other ruminant taxa from Gratkorn (excluding *Hispanomeryx*) and indicates an adaptation to a more or less closed environment with sufficient understory, as can be observed for all modern ruminants of this size class (Köhler 1993; Rössner 2010). Köhler (1993) reconstructs a diet of soft plants and fruits, but also some degree of omnivory in terms of, e.g. larvae and carrion for the genus, and a solitary or living in small groups lifestyle. Isotopic data ($\delta^{13}\text{C}$ and $\delta^{18}\text{O}$; Tütken et al. 2006; Aiglstorfer et al. 2014a, this issue) and microwear analyses (Merceron et al. 2007; Merceron 2009) reconstruct a browsing diet with considerable intake of fruits or seeds and occasional grazing for the small moschid *Micromeryx flourensianus*. *Hispanomeryx* is also described by Köhler (1993) as an animal adapted to wood or bush with understory. Sánchez et al. (2010a) highlight the sympatric occurrence of either two species of *Micromeryx* or of *Micromeryx* and *Hispanomeryx* as common in the Miocene of Spain, and tentatively assign differences in body size and dentition as a result of the sympatry, meaning their occupation of different ecological niches. At the moment, due to the scarce remains of ?*Hispanomeryx*, a distinctive ecological niche recorded in different isotopic signals of the tooth enamel cannot be verified for Gratkorn.

Family Cervidae Goldfuss, 1820

Genus *Euprox* Stehlin, 1928

Type species: *Euprox furcatus* (Hensel, 1859)

Further species: *Euprox dicranocerus* (Kaup, 1839), *Euprox minimus* (Toula, 1884)

Euprox furcatus (Hensel, 1859)

Holotype: fragmented antler sin. (MB.Ma.42626) from Kieferstädel (today: Sośnicowice; Poland).

Dentition, maxillae and mandibulae

Material: GPIT/MA/2739 (fragments of maxillae with P2–M3 dex. and P3–M3 sin.; mandibula sin. with p2–m3), GPIT/MA/2737 (fragment of maxilla sin. with D2–M1; labial wall M2 (not erupted)), GPIT/MA/2738 (fragment of maxilla dex. with D3–M1), UMJGP 204695 (fragment of maxilla sin. with P2–M3), GPIT/MA/2386 (M1–3 sin.), UMJGP 204063 (M2–3 sin.; P3 sin.; labial wall of P2 sin.), UMJGP 204716 (D2 sin.), GPIT/MA/2749 (fragment of P3 or P4 sin?), UMJGP 204066 (Mx sin.), UMJGP 204065 (M3? sin.), GPIT/MA/2374 (M1 or 2? dex.), UMJGP 210690 (M1 or 2? sin.), UMJGP 204717 (Mx dex.), UMJGP 203445 (M3? sin.), GPIT/MA/2415 (Mx dex. fragment), GPIT/MA/2394 (Mx dex fragment), UMJGP

203686 (mandibula dex. with d2–m1 and mandibula sin. with d2, d3–m2), UMJGP 203737 (sin. and dex. mandibula with p2–m3; i2 or 3? dex, UMJGP 210691 (mandibula sin. and dex. with p2–m3, i1 sin. and two fragmented ix), GPIT/MA/2390 (mandibula dex. with p2–m3), GPIT/MA/2393 (dex. mandibula fragment with m1–m3), UMJGP 204686 (mandibula dex. with p3–m3), GPIT/MA/2399 (mandibula sin. with p4–m3), UMJGP 204711 (mandibula sin. with m2–3; fragments of m1; p4), UMJGP 204674 (p2 dex., p3 sin.), UMJGP 210957 (i1 dex.), GPIT/MA/2384 (i1 dex.), UMJGP 204669 (d4 sin.), UMJGP 204713 (m3 dex.); GPIT/MA/2755 (m3 dex.).

From the finding position, preservation, and degree of dental wear, GPIT/MA/2403 (D3 sin.), GPIT/MA/2378 (D4 sin.), GPIT/MA/2404 (M1? sin. fragment), GPIT/MA/2406 (M2? sin. fragment), GPIT/MA/2382 (D4 dex.), GPIT/MA/2402 (M1–2 dex.), GPIT/MA/2408 (M3? fragment, not erupted), GPIT/MA/2405 (Px? fragment, not erupted), GPIT/MA/2407 (fractured and fragmented longbone) and maybe GPIT/MA/2411 (fragment of phalanx proximalis), and GPIT/MA/2412

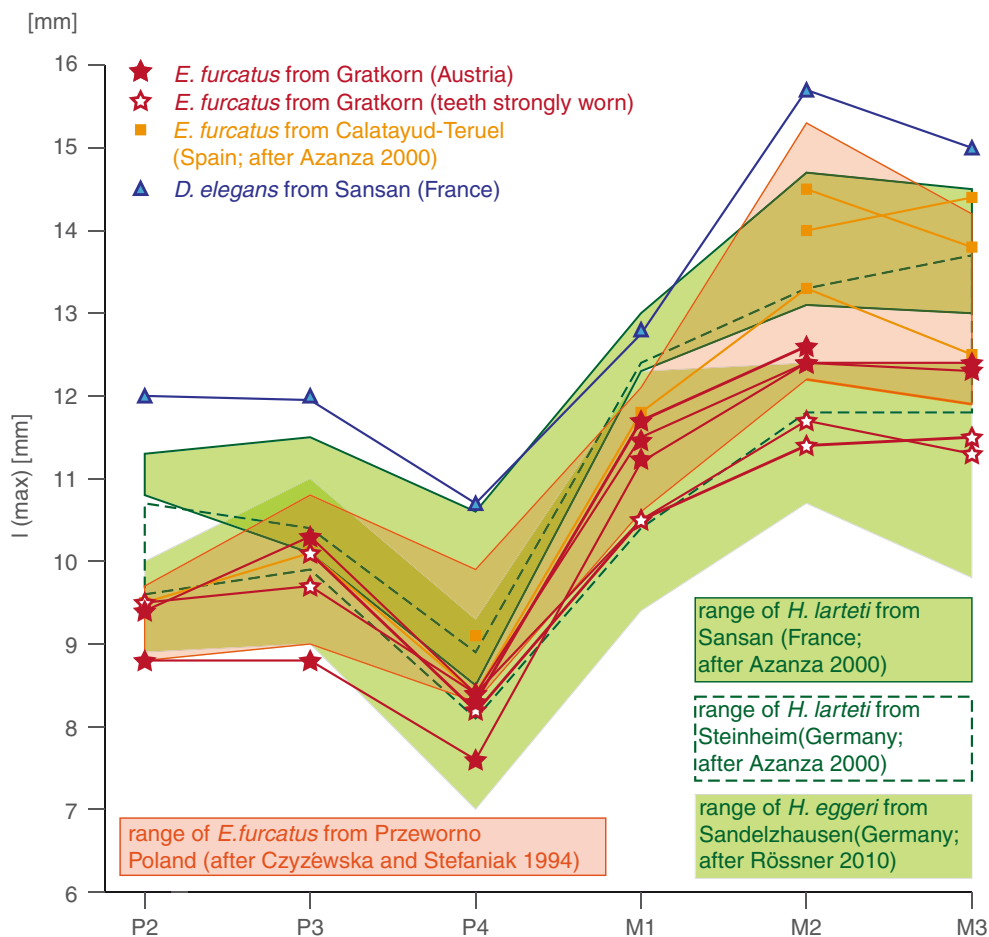


Fig. 10 Upper tooth rows (P2–M3) of *Euprox furcatus* from Gratkorn in comparison to other Miocene Cervidae (note: *E. furcatus* from Gratkorn with strongly worn teeth shows lower values): *E. furcatus* from Calatayud-Teruel (after Azanza 2000) and from Przeworno (after Czyżewska and

Stefaniak 1994), *D. elegans* from Sansan (own measurements), range of *H. eggeri* (after Rössner 2010), range of *H. larteti* from Steinheim a. A. (after Azanza 2000), range of *H. larteti* from Sansan (after Azanza 2000)



◀ **Fig. 11** Dental and postcranial material of *Euprox furcatus*, *Tethytragus* sp., and Ruminantia gen. et sp. indet.: **a** *E. furcatus* C sin. (GPIT/MA/2736; 1 labial view, 2 posterior view), **b** *E. furcatus* mandibula dex. with d2–m1 (UMJGP 203686; 1 labial view, 2 lingual view, 3 occlusal view), **c** *E. furcatus* i1 dex. (GPIT/MA/2736; 1 lingual view, 2 labial view, 3 posterior view), **d** *Euprox furcatus* maxilla sin. with D2–M1 (GPIT/MA/2737), **e** *E. furcatus* maxilla sin. with P2–M3 (UMJGP 204695; 1 occlusal view 2 labial view), **f** *E. furcatus* mandibula sin. with p2–m3 (GPIT/MA/2733; 1 occlusal view, 2 labial view, 3 lingual view), **g** *E. furcatus* mandibula dex. with p3–m3 (UMJGP 204686; 1 occlusal view, 2 lingual view), **h** *E. furcatus* Mc dex. (UMJGP 204722; 1 proximal view, 2 dorsal view), **i** *E. furcatus* humerus sin. (GPIT/MA/2418; 1 lateral view, 2 caudal view), **j** *Tethytragus* sp. P2–4 dex. (GPIT/MA/2753; 1 occlusal view, 2 labial view), **k** *Tethytragus* sp. M2–3 sin. (GPIT/MA/2392; 1 occlusal view, 2 labial view), **l** *Tethytragus* sp. Mt sin. (GPIT/MA/4143; 1 proximal view, 2 lateral view of distal part, 3 distal view, 4 dorsal view, 5 plantar view), **m** Ruminantia gen. et sp. indet. humerus sin. in cranial view (UMJGP 204721), **n** Ruminantia gen. et sp. indet. femur dex. (UMJGP 210695 1 lateral view; 2 distal view); scale bar 10 mm

(fragment of humerus dex.) most likely represent one individual. For the same reasons, GPIT/MA/2383 (d4–m1 sin.), GPIT/MA/2385 (d4–m1 dex.), GPIT/MA/2413 (Mx fragment) and GPIT/MA/2414 (Mx fragment) most likely represent one individual, as do GPIT/MA/2381 (p3 dex.), GPIT/MA/2748 (m1 dex.), GPIT/MA/2750 (m2 dex.), and GPIT/MA/2380 (m3 dex.).

From dental features, finding position, preservation, and degree of dental wear, GPIT/MA/2736 (C sin. and dex.; fragments of maxillae with P2–M3 dex. and P3–M3 sin.; fragmented ix; i1 dex.; fractured mandibula dex. with p2–m3), GPIT/MA/2733 (mandibula sin. with p2–m3) and UMJGP 210955 (antler sin. with part of frontal) belong to one young adult male.

Description

The dentition is brachyoselenodont, and medium sized (Figs. 10, 11; online resource 4).

Maxilla and dentition (Figs. 10, 11): Sabre-like canines are recorded (Figs. 11a, 12f). They are curved posteriad, have a triangular to drop-shaped, laterally compressed cross-section, and are covered by enamel anteriorly and labially. A slight undulation of the enamel is due to growth striation. In contrast to the tragulid canine from Gratkorn (Fig. 2a), the teeth do not possess a wear pattern at their tips and are slightly sinuous-shaped in anterior view. The **D2** (Fig. 11d) is two-rooted and has an elongate, lingually rounded, moderately triangular shape. The labial cone is dominant, anterior and posterior styles are present and the posterolabial crista is longer than the anterolabial crista. In labial view, a well-pronounced rib at the labial cone is well developed, decreasing in width towards occlusal. One dominant crest from the labial cone and smaller additional crests posterior of it cross the fossa. There is no distinct cingulum. With its more triangular shape, the **D3** (Fig. 11d) differs from the D2. Besides a very small anterior cone, a clearly present paracone and a

strongly developed metacone form the labial wall. Meso- and metastyle are prominent, the rib at the paracone is not as developed as in D2, but a clear rib is present at the metacone. The incision between anterolingual crista and protocone is quite weak, while an additional crest connects para- and protocone. At the dominant lingual cone, the metaconule, external and internal premetaconulecrista originate. There is an anterolingual cingulum. The **D4** (Fig. 11d) is typically trapezoid-shaped with an enlarged parastyle (less strong than in tragulids). It possesses the selenodont crown pattern of the upper molars with higher labial than lingual cones, an internal postprotocrista, developed ento- and mesostyle, wing-like metastyle, and a lingual cingulum. Labial ribs at the labial cones are not strongly developed. The **P2** (Fig. 11e) is three-rooted and triangular in shape. Besides the total size, the rounding of the lingual wall is variable, ranging from more acute (GPIT/MA/2739) to strongly rounded (GPIT/MA/2736). The labial cone is dominant with a narrow anterior and wider posterior incision at the labial wall, producing a well-pronounced labial rib. Anterolingually, a weak depression sets off the anterolingual cingulum from the lingual cone. Anterior and posterior styles are present, of which the latter is wing-like and enlarged, elongating the posterolabial crista in ratio to the anterolabial one, which is short. Additional crests cross the fossa, including the central fold. The tooth has no clear cingulum. The **P3** (Fig. 11e) is similar in shape to the P2, but labiolingually wider and lingually more rounded, with a lingual cingulum of varying strength, and a narrower anterior incision on the labial wall. The **P4** (Fig. 11e) is horseshoe-shaped with a rounded lingual side. The labial cone is dominant, with a more developed labial rib than in P2 and P3. The posterior style is weaker than in P2 and P3, and only as strong as the anterior style with the anterolingual crista being only slightly shorter than posterolingual one. The lingual cingulum is pronounced. The **upper molars** (Fig. 11d, e) are selenodont with a rectangular to trapezoid shape, widening towards labial with higher labial cones. The mesostyle is distinct, while the metastyle is reduced and wing-like. The size of para- and entostyle varies, but usually increase from M1 to M3 (entostyle sometimes included in the cingulum in M1; Fig. 11e1). The labial rib at the paracone is distinct enclosing a narrow incision with the parastyle. In all specimens, the internal postprotocrista is well developed with occasionally small additional crests. Sometimes, the premetaconulecrista is split at its anterior end into two or three small anterior branches fusing with the postprotocrista. It is long, intruding inbetween paracone and metacone. The presence of a metaconule fold is variable and sometimes not more than a thickening of the postmetaconulecrista. The lingual cingulum reaches from anterior to posterior, usually disappearing at the lingual aspects of protocone and metaconule (more pronounced in M2). The M3 differs from the anterior molars by a smaller labiolingual width posteriorly. The size increase from M1 to M3 is less distinct than in Tragulidae.

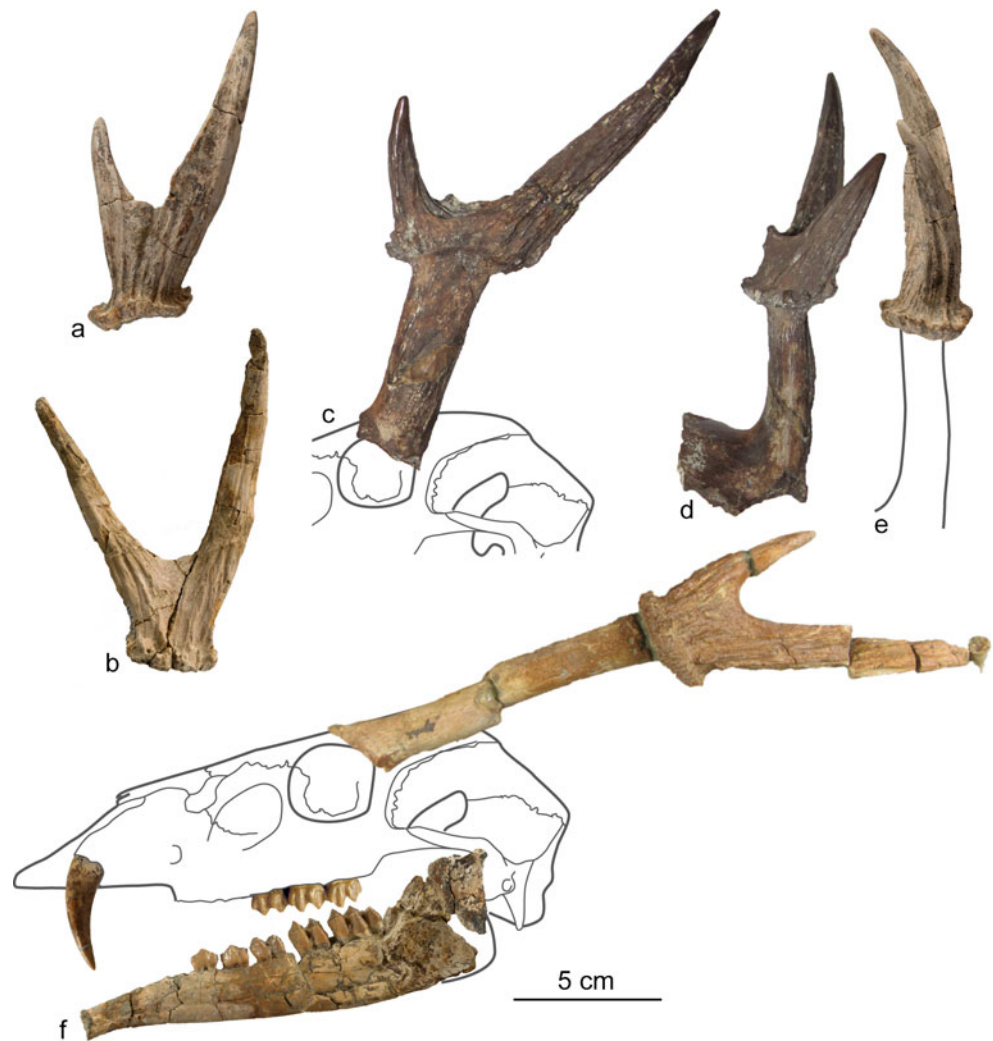
The **mandibulae** (Figs. 11b, f, g, 12f) from Gratkorn show a slender corpus mandibulae (for detailed information and measurements see online resource 4) and nest well in the size variability of *Euprox* vel *Heteroprox* from Steinheim a. A. for the height of the corpus. Where observed, one foramen mentalis is positioned underneath the anterior alveola of p2. The premolar tooth row is shorter than the molar tooth row (online resource 4). The **i1** (Fig. 11c) is of spate-like shape and widens from base to tip, but less than in Tragulidae. It is lingually concave and curved posteriad. The lingual plane has a strong groove along the posterior rim. The i2/3 and the incisiform c(?) are pen-like, lingually concave, bend posteriad, with a small anterior crest on the lingual plane and a deep groove close to the posterior rim as in the i1, but are not increasing in anteroposterior width occlusally as the latter. Only one **d2** (Fig. 11b) is preserved fragmentarily. It is elongate with one anterior conid, a dominant mesolabial conid, and a posterolabial conid. The posterolingual conid and the posterior styloid are present. The transverse cristid is directed posterolingually, but does not reach the posterolingual conid. The posterolabial cristid fuses with the posterolabial conid. The latter nearly closes the back valley (oriented perpendicularly to the longitudinal axis of the tooth) by connecting with the posterolingual conid and posterior styloid. The posterior valley is oriented obliquely to the length axis of the tooth, but wider than the back valley and open lingually with a labial wall less high than in the back valley. The **d3** (Fig. 11b) is longer than the d2, but otherwise similar in morphology. It clearly possesses an anterior conid and styloid, and a small tubercle at the lingual side in the anterior valley. It differs from the d2 by a stronger posteriorly rotated transverse cristid, and a more closed posterior valley. The back valley is closed lingually. The **d4** (Fig. 11b) is elongate with three lingual and three labial conids. The lingual conids are higher than the labial ones. The metastyloid is stronger than mesostyloid and entostyloid. Internal and external postprotocristid are present and form a v-structure, often termed as *Palaeomeryx*-fold. The postmetacristid is short, while the well-pronounced internal postprotocristid turns lingually before reaching the prehypocristid. The latter are only fused at the base, as are the posthypocristid and entostyloid. Anterior ectostyloid and ectostyloid are large, and anterior and posterior cingulid are present. The **p2** (Fig. 11f) is similar in morphology to the d2, but wider. Size and morphology also vary among the different specimens. Except for GPIT/MA/2390 (fragmented p2 with open posterior valley), in all specimens the transverse cristid is directed more posteriad than in the deciduous tooth, more or less closing the oblique posterior valley. The anterior conid is pronounced and basally fused with the lingual cingulid. There is no anterior styloid. A posterior thickening is considered the homologue of the mesolingual conid. As in the d2, the back valley is oriented perpendicularly to the longitudinal axis of tooth, but not always closed. The incision on the labial wall

anterior of the posterolabial conid is present in all specimens, but the strength varies. The **p3** (Fig. 11f, g) is similar in shape to the p2, but wider, and the meso- and posterolingual conid are more developed. The posterior valley is usually closed (not in GPIT/MA/2390 and UMJGP 204674). The back valley is very narrow and in some cases completely closed. The strength of the incision on the labial wall anterior of the posterolabial conid is variable. The shape of the **p4** (Fig. 11f, g) is similar to p3, but the mesolingual conid is as pronounced as the mesolabial conid and clearly better developed than in the preceding premolars. The transverse cristid is positioned more posterior and fused with the posterolingual cristid or with the anterolingual cristid, which is bent to the posterior. The posterior valley is nearly or fully closed and separated from the back valley by the fusion of posterolingual and posterolabial conid (only in UMJGP 204686 the posterolingual conid is isolated and the posterior and back valleys are fused). The back valley is narrow and obliquely to perpendicularly aligned. Only an anterolingual cingulid is present. In the selenodont **lower molars** (Fig. 11b, f, g), the axes of the lingual conids are oblique to the length axis of the tooth. The metastyloid is strongly pronounced and the entostyloid present. The postprotocristid is split into internal and external cristid forming a v-structure often termed the *Palaeomeryx*-fold (with increasing wear, this feature becomes less apparent). The preprotocristid is long and fused with the shorter premetacristid only basally. The prehypocristid is long and fuses with the posterior wall of the postprotocristid, as does the short preentocristid, which is fused with the postprotocristid in specimens with higher degrees of attrition. The postentocristid is short and fused with the posthypocristid only basally. The anterior cingulid is stronger than the posterior one. The ectostyloid is pronounced, slightly decreasing in size from m1 to m3. Size increases significantly from m1 to m2. In m3, the hypoconulid is pronounced and is clearly set off from the talonid. The posthypocristid is usually split posteriorly (length of branches variable). By the fusion with the preentocristid (in GPIT/MA/2399 with the prehypocristid), it closes the back fossa anteriorly (only in GPIT/MA/2755 the back fossa opens anteriorly), while the fusion of posthypocristid and entoconulid closes the back fossa posteriorly. In general, the entoconulid is small, and thus the third lobe appears more or less monocuspidate. The hypoconulid is moved posterolingually giving the third lobe a lingually turned and elongated shape with a lingual depression at the entoconulid. The presence and size of the posterior ectostyloid is variable.

Antlers

Material: GPIT/MA/02398 (antler sin.), UMJGP 204062 (antler dex.), UMJGP 210955 (antler sin. with part of frontal), UMJGP 204670 (pedicle sin. with antlerbase lost due to gnawing), UMJGP 203443 (fragment of pedicle sin.)

Fig. 12 Cranial appendages of *E. furcatus* from Gratkorn in comparison to female *D. elegans* from Sansan: **a** antler sin. from Gratkorn (lateral view; GPIT/MA/2398), **b** antler dex. from Gratkorn (medial view; UMJGP 204062), **c** antler sin. of *D. elegans* from Sansan with reconstructed orientation (MNHN Sa 3451; lateral view), **d** same as c (anterior view), **e** same as (a) with reconstructed orientation (anterior view), **f** reconstruction of *E. furcatus* from Gratkorn in lateral view with orientation of antler (UMJGP 210955) and GPIT/MA/2736 (mandibula and maxilla mirrored); skull drawing after Thenius (1989; *Muntiacus*)



Description

All three complete antlers (Fig. 12; for detailed information and measurements, see online resource 4) are bifurcated, comprising a short anterior and a long posterior branch. Two of the complete ones are shed antlers, while one specimen is still attached to the pedicle and a fragment of the frontal (UMJGP 210955). Two foramina supraorbitale are recorded on the frontal anteromedially of the pedicle. The latter is slightly convex laterally and clearly set off from the coronet. Its cross-section changes from triangular to subcircular from proximal to distal. The surface of the pedicle is smooth, and has a slightly elongated and narrow groove running anteroproximally to mediolaterally ending about 20 mm proximally of the antler's base on specimen UMJGP 204670. The antler's base is a clear coronet with pearls, showing an anteroposterior suboval shape. The coronet is inclined to the anterior with different degrees and encloses with the length axis of the pedicle angles ranging from 45° to nearly 90°. A distinct lateral inclination is absent. There is a constriction above the coronet and the length of the antler shaft ranges from 32 to

38 mm. Both branches are curved distally pointing to median. The cross-section of the branches is variable from triangular to subrounded (in GPIT/MA/2398, the posterior branch is medially concave). Tapering of the branches can be gradual but also with a clear incision from where the branch incurves concavely. All preserved antlers show a well-ornamentation in terms of longitudinal ridges along the shaft and the branches.

Postcrania

Material: GPIT/MA/2418 (humerus sin.), UMJGP 210699 (distal part of humerus dex.), UMJGP 204722 (metacarpal dex.), GPIT/MA/2407 (fractured and fragmented longbone), GPIT/MA/2411 (fragment of phalanx proximalis too fragmentary to allow description), GPIT/MA/2412 (fragment of humerus dex. too fragmentary to allow description)

Description (Fig. 11; for detailed information and measurements, see online resource 4):

A **humerus** sin of *E. furcatus* (GPIT/MA/2418; Fig. 11i) is fairly well preserved, showing the distal articulation and a part of the caput humeri. In contrast to the distal part, most of the proximal part is compressed and fragmented. The preserved length from epicondylus lateralis to the caput humeri is about 155 mm. The distal part and some fragments of the shaft of a humerus dex. (UMJGP 210699) show the same morphology and dimensions. In both humeri, the cross-section of the distal shaft is rounded with a clear edge terminating in the epicondylus medialis. The fossa olecranii is deep but not open as in Suidae. The trochlea humeri is trapezoid in cranial view. The external crest is clearly set off from the trochlea laterally as is typical for Cervidae (Heintz 1970) and also observed in *Euprox* vel *Heteroprox* from Steinheim a. A. (e.g. SMNS 42698, GPIT/MA/3011 and 3007), in contrast to a less marked crest in Bovidae (Heintz 1970). Heintz noted a different ratio of proximodistal width of the medial depression versus transversal width of the trochlea for Cervidae (0.55–0.64) and Bovidae (0.45–0.55). With a height/width ratio of 0.61 (UMJGP 210699: 14.5/23.7) and 0.59 (GPIT/MA/2418: 14.4/24.9), the two humeri would clearly fall into the range of Cervidae, as do *Euprox* vel *Heteroprox* from Steinheim a. A. [five distal humeri dex. (GPIT/MA/3007); four distal humeri sin. (GPIT/MA/3011)] ranging from 0.57 to 0.60. Also, the two humeri correspond in size to *E. furcatus* from Przeworno (Czyzewska and Stefaniak 1994). Both humeri differ from Tragulidae by a less pronounced decrease in the proximodistal width of the trochlea from medial to lateral, the more pronounced external condyle on the trochlea and a strongly developed epicondylus medialis (Gailer 2007; Hillenbrand et al. 2009; Morales et al. 2012).

Metacarpal III and IV are fused to a cannonbone (UMJGP 204722; Fig. 11h). As this is not the case in Tragulidae, the metacarpal can be assigned to Pecora. It is quite slender with a delicate proximal articulation. The cross-section of the shaft is rounded dorsally and palmarily concave. A weak sulcus longitudinalis dorsalis on the dorsal surface runs from the midline distally to the junction of medial and lateral articulation facet. The proximal articulation facet is rounded triangular in cross-section with a larger medial facet for the articulation of os carpale secundum and tertium. The size and shape of the fossa between the facets is unknown due to fragmentation. With a dorsopalmar width of 14.8 mm and a mediolateral width of 20.5 mm, the metacarpal is within the morphological and size range of *Euprox* vel *Heteroprox* from Steinheim a. A. (e.g. SMNS 4801, GPIT/MA/3020), and fits well to *E. furcatus* from Przeworno (Czyzewska and Stefaniak 1994). The specimen differs from *Miotragocerus* vel *Tethytragus* (Atzelsdorf, Austria; Hillenbrand et al. 2009) by a smaller size and the more filigree habitus of the proximal articulation surface. Due to fragmentation, the existence of a longitudinal groove on the palmar side of

the proximal articulation surface, as would be typical for Bovidae (Heintz 1970), cannot be rejected nor verified, but the well-pronounced incision on the dorsolateral aspect (a typical character for cervids, following Heintz 1970) argues for an assignment to *E. furcatus*.

Comparison

The type series of *Euprox furcatus* comprises an isolated antler (holotype), a second antler and a canine from Kieferstadel (today: Sonicowice, Poland). Size and morphology of the antlers from Gratkorn exhibit a great resemblance with the holotype and other specimens assigned to the species (online resource 4; Fig. 12; Hensel 1859; Stehlin 1928; Czyzewska and Stefaniak 1994; Azanza 2000). In detail, the characteristics are (1) the strong inclination of the pedicle to posterior, (2) the anteromedial location of the foramina supraorbitale, (3) the clearly developed suboval and only slightly anteroposterior elongated coronet, (4) the constriction of the shaft above the coronet, (5) the shaft length of 32–38 mm, and (6) the simple bifurcation of the antler into a shorter anterior and a longer posterior branch (Fig. 12). In addition, Hensel (1859) described an anterior inclination of the antler base relative to the antler pedicle and a strong surface ornamentation of the holotype comparable to the specimens from Gratkorn. The narrow groove running anteroproximally to mediolaterally on specimen UMJGP 204670 is shared with one paratype of the species (Hensel 1859; p. 263). Presumably, it represents the course of a branch of the superficial temporal artery (observed to provide the blood support for the antler in modern Cervidae; Suttie and Fennessey 1990). All antlers from Gratkorn show a clearly shorter anterior branch than the holotype, but as the length of the branches is variable and increasing in size during the lifetime of the animal (Stehlin 1928), the length of anterior and posterior branches are not considered diagnostic here. Furthermore, the dimensions of the Gratkorn specimens are in the size range of *E. furcatus* from Przeworno (Poland), Arroyo del Val (Spain) and Steinheim a. A. (Germany; Czyzewska and Stefaniak 1994; Azanza 2000; personal observation).

The cervid from Gratkorn differs from Miocene cervids, such as *Procervulus ginsburgi* Azanza, 1993, *Lagomeryx* Roger, 1904, *Paradicrocerus* Gabunia, 1959, *Palaeoplatyceras* Hernandez-Pacheco, 1913, and *Heteroprox moralesi* Azanza, 2000, by a clear and simple dichotomy in the antlers (Stehlin 1937; Azanza and Ginsburg 1997; Azanza 2000; Rossner 2010). It differs from other Miocene taxa possessing a bifurcated antler like *Procervulus dichotomus* (Gervais, 1859), *Heteroprox larteti* (Filhol, 1890), *Heteroprox eggeri* Rossner, 2010, and *Dicrocerus* Lartet, 1837 by a modern coronet (Stehlin 1928, 1939; Ginsburg and Crouzel 1976; Ginsburg and Azanza 1991; Rossner 1995; Azanza 2000). *Heteroprox* and *Procervulus* differ

from the Gratkorn specimen furthermore by a less inclined pedicle and the lack of a clear distinction between pedicle and antler (Stehlin 1928; Haupt 1935; Azanza 2000; Rössner 2010). Additionally, *Heteroprox* shows an “antlerbase” mediolaterally less wide than in the Gratkorn specimens and *E. furcatus*, and a medial instead of an anteromedial position of the foramen supraorbitale (Stehlin 1928; Rössner 2010). The Gratkorn specimen differs from *Dicrocerus* by a longer and less steeply inclined pedicle, a smaller lateral expansion of the antler, and smaller dimensions in dentition and antlers (Haupt 1935; Stehlin 1939; Thenius 1948, 1950; Ginsburg and Azanza 1991; Azanza 1993; Rössner 2010; Fig. 12). Only female *Dicrocerus* individuals and more gracile males overlap with the specimens from Gratkorn, e.g. in dimensions of the antler plate, but clearly differ in the morphological features described. The specimen from Gratkorn is distinct from the stratigraphically younger *Euprox dicranocerus* (Kaup, 1839) and *Amphiprox anocerus* (Kaup, 1833) by a clearly shorter antler shaft (Haupt 1935; Azanza 2000). *Euprox minimus* (Toula, 1884) (Thenius 1950) is smaller than the cervid from Gratkorn. In Late Miocene Cervidae, such as, e.g. *Cervavitus*, *Pliocervus*, and *Procapreolus*, the antlers are monopodial with three or more tines (Azanza et al. 2013). From antler morphology, the cervids from Gratkorn can thus be clearly assigned to *Euprox furcatus*.

The dental material from Gratkorn is also in accordance with the morphological and dimensional variability of the medium-sized brachyoselenodont Miocene cervids *Euprox furcatus* and *Heteroprox larteti* (Figs. 10, 11; online resource 4; also note here interindividual variation due to different degrees of wear: GPIT/MA/2739 is from a rather old individual with stronger worn teeth). Like *E. furcatus*, *Heteroprox larteti* (Filhol, 1890) is defined on an isolated antler (antler dex. from Sansan (MNHN 3371)). A species differentiation based on dental material between *E. furcatus* and *H. larteti* is hindered due to the close resemblance of the two species (Stehlin 1928), the co-occurrence in the locality Steinheim a. A., yielding so far the richest material of both species (unfortunately, lower dentition and postcranial material of *E. furcatus* associated with the diagnostic antlers of the male have never been described from Steinheim a. A.; in both taxa, females do not possess cranial appendages), and a large intraspecific variability. Differences in the dentition among specimens of *Euprox* vel *Heteroprox* from Steinheim a. A. are small and not really distinct. In the Gratkorn specimens, the external postprotocristid in the lower molars is not strongly developed in general. Czyzewska and Stefaniak (1994) describe a reduced external postprotocristid in *E. furcatus* from the late Middle Miocene locality Przeworno, thus fitting well to the specimens from Gratkorn. Azanza (2000), in contrast, describes a more pronounced external postprotocristid in *E. furcatus* from the Middle Miocene of Spain in comparison to *H. larteti*. Furthermore, she notes a more parallel alignment of the lingual lobes in the lower molars of *E. furcatus* (in contrast to *Heteroprox*, where they should be

more oblique), as well as a weak metastylid for *E. furcatus*. The specimens from Gratkorn show an oblique alignment of the lingual conids and a clearly developed metastylid, as also does, e.g. *Euprox* sp. described from the Late Miocene locality Atzelsdorf (Hillenbrand et al. 2009). Azanza (2000) observes a more inner position of the entoconulid and a distinct concavity for the inner wall of the third lobe of the lower m3. This observation could be well in accordance with the lingual turn of the third lobe and a lingual depression at the entoconulid observed in the m3 of the Gratkorn specimens. These features are also present with moderations in a few mandibulae of *Euprox* vel *Heteroprox* from Steinheim a. A. A mandibula associated with *H. larteti* from Sansan described by Ginsburg and Crouzel (1976; MNHN Sa 3399), is unfortunately strongly worn and does not allow a clear observation concerning these characters. However, as far as can be reconstructed on MNHN Sa 3399, it had a less elongated third lobe and a more pronounced entoconulid than the specimens from Gratkorn. In the description of *E. furcatus* from Przeworno (Czyzewska and Stefaniak 1994), neither a lingual turn of the third lobe nor a lingual depression at the entoconulid in the m3 is mentioned or figured, but the sentence “there is a labial cusp and this lobe has well-developed anterior and posterior wings” (Czyzewska and Stefaniak 1994, p. 61.) indicates a monocuspidate third lobe in accordance with *E. furcatus* from Gratkorn. Thus, the morphology of the third lobe may prove a useful tool for species differentiation in the future.

Azanza (2000) also included dental material from Steinheim a. A. in her description and observed less significant stages for her characters in *E. furcatus* from Steinheim a. A. in comparison with the Spanish material. She thus concluded that it could also be an indication that the Spanish material represents a different species, which could explain the differences observed in the Spanish material to *E. furcatus* from Gratkorn and Przeworno.

Concerning postcranial material, a large size variability can be observed for *Euprox* vel *Heteroprox* from Steinheim a. A. (specimens at SMNS and GPIT; Stehlin 1928). The Gratkorn postcranial material assigned to *E. furcatus* mostly nests in the smaller size ranges of the variability from Steinheim a. A. This could be due to the smaller postcranial dimensions of *E. furcatus* compared to *H. larteti*. However, to verify this assumption, an intensive study of the material from Steinheim a. A. would be necessary.

In summary, the cervid remains from Gratkorn are assigned to *Euprox furcatus* as they show most dimensional and morphological overlap with this species. No indications have so far been found for a second cervid taxon at Gratkorn. In contrast to the still richer assemblage from Steinheim a. A., at Gratkorn antler and complete upper and lower dentition (GPIT/MA/2736, GPIT/2733, UMJGP 210955) can for the first time be assigned to one individual (young adult male) of

Euprox furcatus and might thus be helpful for the evaluation of species characteristics.

Stratigraphic range

The genus *Euprox* is present in the Central Paratethys realm from the middle Middle Miocene with the first representative *E. minimus* from Göriach (Austria; 14.5 ± 0.3 Ma; Thenius 1950), to the Late Miocene with *E. dicranocerus* from Wien III (Austria; 10.5 Ma; Thenius 1948). As Late Miocene two-tined muntiacines and three-tined cervids can easily be misclassified, and as the taxonomic status of *Cervavitus/Euprox sarmaticus* Korotkevich, 1970 and *Cervavitus/Euprox bessarabiensis* Lungu, 1967 seems still to be in discussion (Azanza et al. 2013), they are not taken into consideration here. The record from Kohfidisch (Austria; Late Miocene; Turolian; *Euprox* sp.; Vislobokova 2007) is not included for the same reason, and because it so far comprises only scarce material and no antlers (Vislobokova 2007; Azanza et al. 2013). The species *E. furcatus* first appears at about 14.2 Ma (Klein-Hadersdorf, Austria; Böhme et al. 2012) and is currently recorded only in the Middle Miocene, with abundant findings from, e.g. Steinheim a. A., Przeworno, and Arroyo del Val (Czyzewska and Stefaniak 1994; Azanza 2000). The rich assemblage from Gratkorn is the first record of the species in the Styrian Basin.

Palaeoecological characterisation

The body mass of *Euprox furcatus* from Gratkorn is estimated to have been 24–30 kg (min: 23.8 kg, max: 29.9 kg; $n=6$; specimens with a higher degree of wear were not included in the equations). With a shoulder height of about 60–70 cm (articulated female *Euprox* vel *Heteroprox* from Steinheim a. A.; on exhibition at the SMNS), *E. furcatus* is therefore comparable in habitus to the modern red muntjac (*Muntiacus muntjak*; Mattioli 2011). In contrast to *D. elegans*, in which frontal appendages are recorded for both genders (Ginsburg and Azanza 1991), it is assumed for *E. furcatus* that only males were bearing antlers (Heizmann and Reiff 2002), as also indicated by an antler-less articulated *Euprox* vel *Heteroprox* skeleton from Steinheim a. A.

Thenius (1950) described *E. furcatus* as adapted to dry environments in contrast to the more humid adapted *H. larteti*, while Czyzewska and Stefaniak (1994) interpreted *E. furcatus* as a mobile species between more open and arid biotopes and more wooded areas due to dental and postcranial morphology. Isotopic measurements on well-defined material of *E. furcatus* are so far rare. Stable isotope analyses ($\delta^{13}\text{C}$ and $\delta^{18}\text{O}$) on the material from Gratkorn described here do not support feeding in open and dry environments, but rather point to subcanopy browsing (Aiglstorfer et al. 2014a, this issue).

Isotopic measurements ($^{87}\text{Sr}/^{86}\text{Sr}$) indicate that *E. furcatus* from Gratkorn was not a permanent resident of the locality but temporarily inhabited different areas (maybe in the Styrian Basin; Aiglstorfer et al. 2014a, this issue).

Infraorder Pecora Linnaeus, 1758

Family Palaeomerycidae Lydekker, 1883

Type species: *Palaeomeryx kaupi* von Meyer, 1834

Palaeomerycidae gen. et sp. indet.

Material: UMJGP 203441 (Mc sin.)

Description and comparison

So far, the largest ruminant from Gratkorn is recorded only by a fragmented metacarpal sin. It is assigned to the family *Palaeomerycidae* (Fig. 13). Dimensions (L=305 mm, DAPp preserved=36.7, DTp preserved=58 mm; DAPd (estimated) about 30 mm; DTd (estimated) about 60 mm) overlap with “*Palaeomeryx eminens*” Meyer, 1851 from Steinheim a. A. It is slightly larger than cf. *Ampelomeryx magnus* (Lartet, 1851) (Astibia 2012). As typical in *Palaeomerycidae*, the cross-section of the diaphysis is rounded dorsally and palmarily less concave than in *Cervidae*, but distally more dorsopalmarily flattened than in the latter (Astibia 2012). As in cervids, a weak sulcus longitudinalis dorsalis can be observed on the dorsal surface running from the junction of medial and lateral articulation facet proximally to the midline distally (ending about 50–60 mm proximal of the distal end in a deeper fossa). Proximal articulation facets are not preserved. Morphology of the specimen from Gratkorn is well in accordance with “*Palaeomeryx eminens*” from Steinheim a. A. (Fraas 1870, tab. 7, fig. 7). As in “*Palaeomeryx eminens*” from Steinheim a. A. the sagittal crests on the distal condyles are not strongly set off from the central part of the condyles in dorsal view, comparable to *Cervidae*, but different from *Bovidae* (see, e.g. Leinders 1979). It differs from *Germanomeryx* Rössner, 2010 by the closure of the sulcus longitudinalis dorsalis (Köhler 1993). The metacarpal from Gratkorn differs from *Giraffidae* of similar dimensions by the less concave palmar depression (see, e.g. Bohlin 1926; Solounias 2007). From dimensions and morphology, and taking into consideration the record of “*Palaeomeryx* cf. *eminens*” from the early Late Miocene locality of Atzelsdorf (Hillenbrand et al. 2009), the Gratkorn specimen most likely represents “*Palaeomeryx eminens*”. However, as only one metacarpal has so far been excavated from Gratkorn, and the taxonomy inside the family is still in discussion (see, e.g. Astibia 2012), a determination as *Palaeomerycidae* gen. et sp. indet. is the most reasonable for the moment.

Fig. 13 Mc sin. of *Palaeomerycidae* gen. et sp. indet.: **a** proximal view, **b** dorsal view, **c** distal view; scale bar 2 cm



Stratigraphic range

Palaeomerycidae are typical representatives of European Middle Miocene faunal assemblages. The family is recorded from the Early Miocene (Gentry et al. 1999; Astibia 2012) until the Late Miocene (Astibia 1987; Hillenbrand et al. 2009). Late Miocene findings are so far restricted to the early Late Miocene with the localities of Atzelsdorf (Austria; 11.1 Ma; Hillenbrand et al. 2009) and Carrilanga 1 (Spain; Astibia 1987), which is older than the first record of *Hipparion* from Nombrevilla (López-Guerrero et al. 2011). The record of “*P. eminens*” from the Eppelsheim Fm (Tobien 1961) is not taken into consideration here as a Late Miocene representative, as the Eppelsheim Fm comprises a stratigraphically mixed fauna from Middle and Late Miocene and the specimens thus also could, and most likely do, comprise Middle Miocene elements (Böhme et al. 2012). A continuous size increase in *Palaeomerycidae* has been hypothesised, with the largest representative being “*Palaeomeryx eminens*”, e.g. from the middle Middle Miocene of Steinheim a. A. (Gentry et al. 1999; Ginsburg 1999). However, findings of the large-sized *Germanomeryx* (Rössner 2010) in the early Middle Miocene indicate a more differentiated size evolution among palaeomerycids. Anyhow, the size of the *Palaeomerycidae* gen. et sp. indet. from Gratkorn described here is well in accordance with “*Palaeomeryx eminens*” from Steinheim a. A. (Fraas 1870) and thus fits well into a late Middle Miocene assemblage. The youngest record of “*Palaeomeryx cf. eminens*” described so far is from the early Late Miocene locality Atzelsdorf (Hillenbrand et al. 2009).

Palaeoecological characterisation

Köhler (1993) classifies “*Palaeomeryx eminens*” as a browser of soft, juicy leaves, or aquatic plants, solitary or living in small groups, with slow-gear adapted locomotion (she also included in this description *Germanomeryx* from Sandelzhausen). As there is only one metacarpal of a palaeomerycid so far recorded from Gratkorn, no further information on ecological adaptations can be gained. Rössner (2010) states that, at least for *Germanomeryx* from Sandelzhausen, feeding on aquatic plants can be excluded, and Tütken and Vennemann (2009) reconstructed *Germanomeryx* as a canopy folivore.

In any case, with an estimated bodymass of 270 kg, large territories would be necessary to supply enough plant material for this palaeomerycid from Gratkorn.

Family Bovidae Gray, 1821

Genus *Tethyragus* Azanza and Morales, 1994

Type species: *Tethytragus langai* Azanza and Morales, 1994

Holotype: skull roof with horn cores (MNCN BAR-73).

Type locality: Arroyo de Val-Barranca (Zaragoza, Spain).

Further species: *Tethytragus koehlerae* Azanza and Morales, 1994, *Tethytragus stehlini* (Thenius, 1951).

Tethytragus sp.

Dentition

Material: GPIT/MA/2753 (P2–4, M3 dex., labial wall of M2 dex.), GPIT/MA/2392 (M2–3 sin.)

Description (for measurements, see online resource 5)

Some upper teeth of the ruminant material from Gratkorn can be assigned to the family Bovidae. Due to field position, preservation and wear, the teeth are assigned to one individual.

Dentition (Fig. 11j, k): The **P2** is of elongated trapezoid to rectangular shape. The anterolabial cone is dominant, while the posterolabial cone is not really distinct and in addition strongly worn. Although not distinct, an anterolingual cone is set off from the more dominant posterolingual cone by an incision on the lingual wall. A deep incision (not reaching the base of the tooth crown) on the anterolabial wall separates a pronounced anterior style from the anterolabial cone, while a posterior style is not developed. Due to a depression posterior to the anterolabial cone, a distinct rib can be observed on the labial wall of the cone. Several crests cross the fossa. The **P3** is similar in wear and morphology to the P2, but of more triangular shape. The labial incision is narrower than in the P2, the incision on the lingual wall is stronger, and the tooth crown is higher. The **P4**, which is also worn, is of triangular, lingually rounded shape with one labial and one lingual cone. The anterior incision on the labial wall is shallower than in the anterior premolars, but the rib at the labial cone is well pronounced. Besides, a distinct anterior style, a clearly developed posterior style is present. In the fossa, a small central fold can be observed. The **M2** shows a typical ruminant selenodont dentition with higher labial than lingual cusps. The labial wall at the paracone is missing. The tooth is brachyo- to mesodont and the lingual tooth crown elements are separated from the labial elements. The parastyle is clearly developed and encloses an incision with the distinct labial rib at the paracone. The mesostyle is the strongest style and possesses a distinct rib, while the metastyle is weak and wing-like. On the lingual side, a small entostyle is developed attached to the posterolingual wall of the protocone. The labial wall of the metacone is planar and nearly vertically inclined. The lingual wall encloses an angle of about 55° with the basal plane of the tooth crown in anterior view and of 50° in posterior view. The tooth possesses no internal postprotocrista and only a slight indication for a metaconule fold, but a short

anterior cingulum. The **M3** is similar in shape to the M2. The incision enclosed by parastyle and the rib at the paracone is shallower and the mesostyle more column-like than in the M2, while the labial wall of the metacone is more vertical and planar and the metastyle is more reduced. Both M3 show a splitting into internal and external postprotocrista, weakly developed or only indicated anterior cingulum, and no entostyle.

Postcrania

Material: GPIT/MA/4143 (Mt and cuneiforme sin.)

Description

Metatarsals III and IV are fused to a slender **cannonbone** (GPIT/MA/4143; Fig. 11i; online resource 5). The cross-section of the shaft is rounded dorsally and concave palmarily (flattening distally). A strong sulcus longitudinalis dorsalis runs on the dorsal surface from the junction of the proximal medial and lateral articulation facets distally ending between the two distal condyles. It is not closed distally. The proximal plane is subrounded in cross-section with an elongate dorso-lateral to medioplantar facet for the articulation with the cuneiforme on the mediadorsal side. There are three facets for articulation with the cubonavicular (large on the lateral side, slender mediolaterally elongated on the plantar side, and a small oval in the medioplantar corner). In dorsal view, the transversal width gradually increases distally. The area for the extensor tendon on the dorsal surface is distinct, but not long, though it is more strongly developed than in the modern *Capreolus capreolus*. Distally, two condyles exhibit clearly defined and dorsally and plantarily set off sagittal crests. In dorsal view, they are set off especially externally. The external part of the condyles has a more triangular shape in dorsal view, while the internal is more rectangular. The intertrochlear incision forms a “v”. Directly proximal of the lateral condyle, the metatarsal shows a biting mark on the dorsal surface. The **cuneiforme** sin. (GPIT/MA/4143) articulates well with the metatarsal. It possesses a concave proximal facet for articulation with the cubonavicular and distally a dorsally convex and plantarily concave facet for articulation with the metatarsal. In proximal view, a planar lateral wall for articulation with the cubonavicular and a rounded medial wall are visible.

Comparison

With the steep lingual wall, the more developed crown height and the simple crown morphology, the teeth clearly differ

from the similar-sized cervid teeth from Gratkorn, and justify assigning to the family Bovidae. Taxonomy in Bovidae is based to a great extent on horn cores (see, e.g. Köhler 1987; Gentry 1994). As horn cores have not been recorded from Gratkorn so far, only a tentative species assignment can be given here. According to size and morphology, the teeth belong to a small-sized, rather brachyo- to mesodont species. Most bovid genera so far recorded from the late Middle Miocene of Central Europe [*Protragocerus* Depéret, 1887, *Austroportax* (Sickenberg, 1929), *Miotragocerus* Stromer, 1928 and *Tethytragus* Azanza and Morales, 1994 (Gentry et al. 1999; van der Made 2012)] are larger than the bovid from Gratkorn (Fig. 14a). Only *Tethytragus koehlerae* Azanza and Morales 1994 from Çandir (Turkey) overlaps in dimensions (Köhler 1987). Besides dimensions, the Gratkorn specimen shares with *Tethytragus koehlerae* the tooth crown height, the clearly developed styles, a pronounced paracone rib at the upper molars, the reduced entostyle, and a planar labial wall at the metacone. However, with a smooth enamel surface, the Gratkorn specimen differs from this species which possesses wrinkled enamel (Köhler 1987; van der Made 2012). *Tethytragus langai* possesses a smooth enamel surface, but differs from the Gratkorn specimen by a larger size (Azanza and Morales 1994; Fig. 14b). Azanza and Morales (1994) assigned three species to the genus: *T. langai*, *T. koehlerae*, and *Tethytragus stehlini*. Until today, no dental material is unambiguously referred to *T. stehlini* (Thenius 1951), which was described on the basis of isolated horn cores from the Middle Miocene localities of Mikulov (=Nikolsburg, Czech Republic) and Klein-Hadersdorf (Austria). Its taxonomic status is still in discussion. Some authors consider it to be synonymous with *T. langai* due to features in dentition from Klein-Hadersdorf (Austria), in which case it would have priority over *T. langai* (van der Made 2012; van der Made, personal communication). Others regard both species as valid due to differences in the size and shape of the horn cores (Azanza and Morales 1994). In any case, other teeth so far assigned to the genus than *T. koehlerae* are larger in dimensions than the Gratkorn specimen. Size and morphology of the metatarsal from Gratkorn are in accordance with *Tethytragus koehlerae* from Çandir, figured by Köhler (1993), being only slightly shorter (however, the specimen from Çandir looks fragmented and completed with an at least 10-mm cast). The metatarsal differs from cervids by the clearly open metatarsal sulcus, typical for Bovidae (Leinders 1979). *Turcocerus gracilis* Köhler, 1987 differs from the Gratkorn specimens by a larger size, higher crowned molars and stronger styles (Köhler 1987; van der Made 2012). Besides size, the Gratkorn specimen differs in morphology from *Miotragocerus* sp. vel *Tethytragus* from Atzelsdorf (see, e.g. 2008z0051/0014) by a more developed rib at the paracone, a more planar labial wall at the metacone in M3 and a less pronounced metastyle in upper molars (see, e.g. 2008z0051/0002, 14, 15). An isolated P4

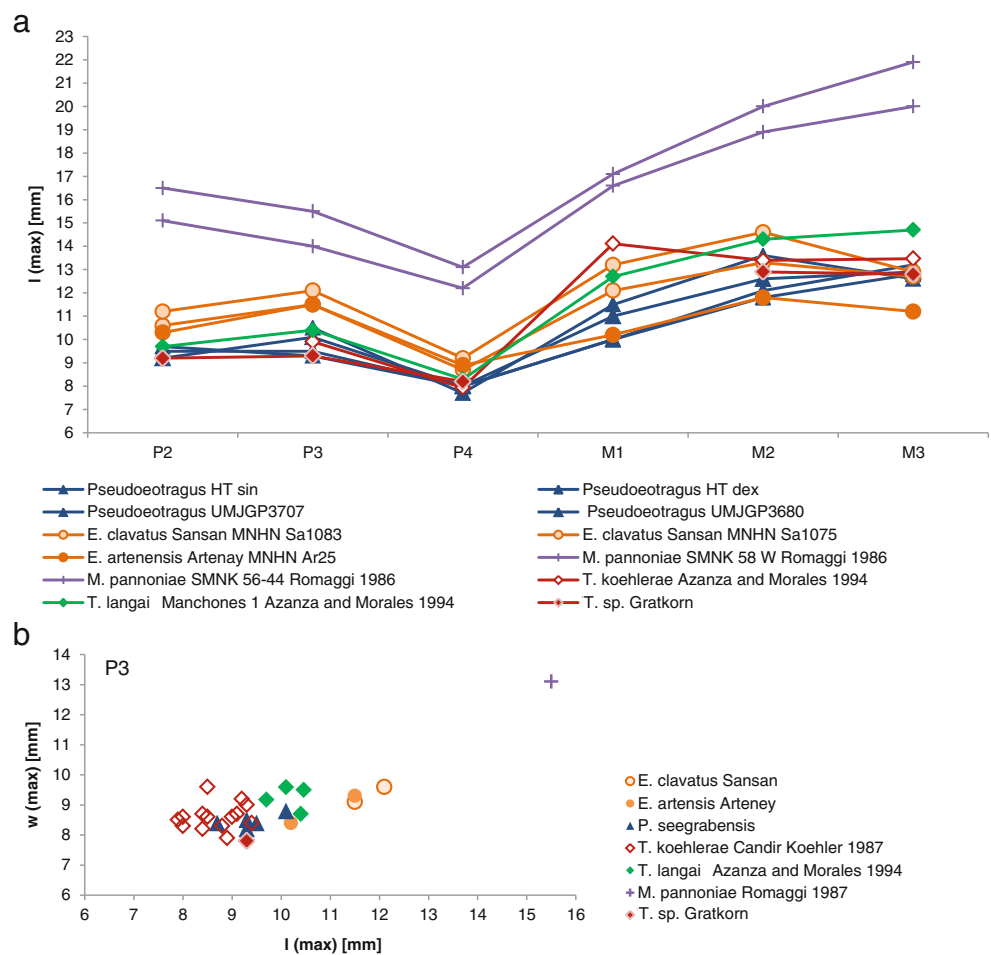
(BSPG/1926/V/34) assigned to *Miotragocerus? monacensis* by Stromer (1928) from the late Middle Miocene locality Aumeister (Munich, Germany) is slightly larger than the specimen from Gratkorn and differs in a more strongly developed central folding. A more planar labial wall at the metacone and a less pronounced metastyle than in *Miotragocerus* has been described for M3 in *Eotragus* and *Protragocerus* by Romaggi (1987). With the simple molar morphology, the separated lingual walls and its small size, the bovid from Gratkorn is in the range of the Early and Middle Miocene taxa *Eotragus* and *Pseudoeotragus* (Figs. 11, 14). However, the Gratkorn bovid differs from *Eotragus* (van der Made 1989 and 2012) in a P4 being less wide, in upper molars being higher crowned with a more planar labial wall at the metacone, and in a more slender and column-like mesostyle. In *Eotragus* (van der Made 1989, 2012), the incision between anterior style and anterolabial cone in P2–4 is not as developed as in the specimen from Gratkorn. *Pseudoeotragus* (van der Made 1989, 2012) possesses a wider P4 and is higher crowned, shows a parastyle more parallel to the paracone rib, and possesses a more planar labial wall in the upper molars than the specimen from Gratkorn.

Conclusively, the entity of morphological and metrical dentition characters of the Gratkorn bovid corresponds best to those of *Tethytragus koehlerae*. However, due to the smooth enamel surface in the Gratkorn specimens, the lack of any associated horn core remains so far, and as there is no dental material unambiguously assigned to *T. stehlini* for comparison, the Gratkorn specimen is left in open nomenclature as *Tethytragus* sp.

Stratigraphic range

The genus *Tethytragus* is a typical Bovidae for the Middle Miocene of Europe (including Turkey; Azanza and Morales 1994; Bibi and Güleç 2008; van der Made et al. 2013). First records are noted from the Middle Miocene localities İnönü I and Paşalar (*Tethytragus* sp.; van der Made 2012). Late Miocene findings are rare and have so far only been recorded from Turkey, described as *T. koehlerae* and *Tethytragus* cf. *T. koehlerae* (Gentry 2003; Bibi and Güleç 2008). The authors of both publications remarked on the unlikelihood that it actually represents the same species as the Middle Miocene *T. koehlerae*, and van der Made et al. (2013) alluded to morphological differences of systematic value between the Middle and the Late Miocene occurrences. In Western Europe, *T. koehlerae* is so far recorded from the late Middle Miocene locality La Grive, which is similar in age to the Gratkorn locality, and, with reservations, from Castelnau Barbarens, Gers, and Arrajegats (both Middle Miocene), as well as from the middle Middle Miocene Crêt-du-Loche (van der Made 2012). *Tethytragus* sp. is recorded from the Spanish

Fig. 14 Upper tooth row of *Tethytragus* sp. from Gratkorn in comparison to other Miocene Bovidae: **a** length of teeth in upper tooth row (data own measurement or after reference given), **b** bivariate plot of P3 (own measurement or after citation given)



locality Abocador de Can Mata (DeMiguel et al. 2012), which is contemporaneous with the Gratkorn locality and could represent the same species. The record of *Tethytragus* sp. is therefore well in accordance with the stratigraphic range of the species.

Palaeoecological characterisation

With a body mass of about 27–29 kg (min: 27.4 kg, max: 29.1 kg; $n=2$), *Tethytragus* sp. from Gratkorn is one of the medium-sized ruminants from the locality. *Tethytragus koehlerae* from the locality Çandir is classified as adapted to humid shrubland, feeding on a wide variability of soft plants, and maybe even sometimes showing an omnivore diet (Köhler 1987, 1993). Following Köhler (1993), most postcranial characters point to an open habitat, but she also notes indications for a wooded or even mountainous habitat, thus defining a more generalistic species. However, the metatarsal of *Tethytragus koehlerae* from Çandir is classified by her as typical for wooded or more open environment. The strongly developed sulcus dorsalis and the gradual and not abruptly distal width increase in the specimen from Gratkorn would fit well with this reconstruction. Some

features observed on the metatarsal of *Tethytragus* sp. from Gratkorn, such as the “v” shaped intertrochlear incision, the dorsally and plantarily set off condyles and the moderately developed area for the extensor tendon, would be in contrast more characteristic for more mountainous habitats (Köhler 1993). As we so far lack further postcranial material of the species, a more precise locomotional adaptation cannot be given, and we thus assume a certain degree of variability in the locomotion of *Tethytragus* sp. from Gratkorn, comparable to the specimens from Çandir, and tentatively assume that it possessed some adaptations to mountainous environments. Stable isotope analysis ($\delta^{13}\text{C}$ and $\delta^{18}\text{O}$; Aiglstorfer et al. 2014a, this issue) reconstruct canopy feeding (feeding in the upper part of the forest, where evaporation is higher) for *Tethytragus* sp. This could be accomplished for a medium-sized ruminant species with the capability of climbing and jumping, as known also for caprine bovids in mountainous regions (Leinders 1979), enabling it to reach vegetation in higher levels of a wooded environment. With the close vicinity of the Alpine mountain chain, the adaptation of one ruminant species to a more mountainous habitat is not unlikely. With a $^{87}\text{Sr}/^{86}\text{Sr}$ value very close to the local ratio, *Tethytragus* aff. *koehlerae* can be considered as

a permanent resident of the locality, and thus was most likely able to cope with seasonal variations in its diet (for further discussion, see Aiglstorfer et al. 2014a, this issue).

Ruminantia gen. et sp. indet.

Material : UMJGP 204721 (fragment of a humerus sin.), UMJGP 210695 (distal half of a femur dex.)

Description and comparison

Most of the unidentified postcranial elements from Gratkorn do not allow a proper description and assignment due to fragmentary preservation (furthermore, some specimens are not so far sufficiently prepared to allow an affiliation) and are therefore not described here. Two specimens, either assignable to *E. furcatus* or *Tethytragus* sp., are displayed, and with further comparison material they might be assigned to one of these species.

A fragment of a **humerus** sin. (UMJGP 204721; Fig. 11m; Dtdf = 27.5; Dtd ~31) is similar to the humeri of *E. furcatus* described above, but mediolaterally wider mainly due to the widening and shallowing of the medial, larger condyle. Furthermore, the fossa at the mediodistal rim of the medial condyle is more pronounced and deeper than in *E. furcatus*. Following Heintz (1970), the ratio of 0.55 [proximodistal width (15 mm) of the medial trochlear depression versus transversal width of the trochlea (27.5 mm)] can be observed both in Cervidae and Bovidae (for details, see discussion above). Morphological features allowing a distinction from Cervidae and assignment to Bovidae for post-Miocene species (medial depression in distal view not more caudally than the epicondylus lateralis and the external crest of the trochlea not as distinct as in Cervidae; Heintz 1970) are not as distinct in the Miocene species. Both characters can be observed in one of the humeri of *E. furcatus* from Gratkorn. As the humerus (UMJGP 204721) described here is different in morphology from the humeri assigned to *E. furcatus*, but cannot be assigned to Bovidae without reservations, it is left at the moment in open nomenclature as Ruminantia gen. et sp. indet.

The distal half of a **femur** dex. with strong biting marks on the medial and lateral sides of the trochlea patellaris (UMJGP 210695; Fig. 11n) is weathered and fractured. Both condyles are well developed, the fossa intercondylica is moderately deep and less pronounced than in modern Cervidae (see, e.g. Gailer 2007, fig. 20). The specimen shares with Cervidae [e.g. *Euprox* vel *Heteroprox* from Steinheim a. A. (GPIT/MA/3005 and 3006)] a depression on the proximal edge of the condylus lateralis and a cavity on the proximolateral edge of the condylus medialis. With DTd between 35 and 36 mm and a DAPd larger than 38 mm, the specimen is in the lower range of variability of *Euprox* vel *Heteroprox* from Steinheim a. A. (GPIT/MA/3005 and 3006) and larger

than *D. crassum* from Sansan (Morales et al. 2012) and Steinheim a. A. (SMNS 4950), but smaller than *E. furcatus* from Przeworno (Czyzewska and Stefaniak 1994). As no femur of *Tethytragus* sp. was available for comparison, and as we cannot estimate the degree of sexual dimorphism in the dimensions of limb bones for *Euprox furcatus*, UMJGP 210695 is left in open nomenclature as Ruminantia gen et sp. indet.

Summary

With a minimum number of 34 individuals (Havlik et al. 2014, this issue), ruminants comprise the most abundant large mammal group from the Late Middle Miocene Gratkorn locality. As, up to now, only isolated and rare remains have been recorded in Central Europe from the late Middle Miocene, the locality fills a gap between the records from the earlier Middle Miocene and the Late Miocene. *Euprox furcatus* is the most abundant large mammal found at the locality, while *Dorcatherium navi* is the second most frequent species. Moschids are represented by some remains of *Micromeryx flourensianus*, and the first hints are given for a Central European occurrence of *Hispanomeryx*. In addition, sparse remains confirm the presence of Palaeomerycidae gen. et sp. indet. and the bovid *Tethytragus* sp. Besides the record of *D. navi*, the ruminants from Gratkorn fit well into a typical late Middle Miocene assemblage. The specimens from Gratkorn comprise the first evidence for *E. furcatus* and *M. flourensianus* from the Styrian Basin. *E. furcatus* is well in accordance with the Middle Miocene records from Steinheim a. A. (Germany) and Przeworno (Poland), and no unambiguous features could be found in the dentition to distinguish it from the early to middle Middle Miocene species *Heteroprox larteti*. *M. flourensianus* from Gratkorn is most similar in morphology to conspecific material from Atzelsdorf (~11.1 Ma), and distinct from the type material from Sansan (~14.5–14.0 Ma) by a less-pronounced external postprotocristid and a slightly higher tooth crown height. Although the assignment of younger *Micromeryx* findings from Central Europe to the species *M. flourensianus* cannot be challenged with the scarce material from Gratkorn and the so far missing scientific descriptions of the type material from Sansan and from the rich locality Steinheim a. A., the morphological change from early to late records inside the species can be mentioned.

The record of *D. navi* from Gratkorn is one of the stratigraphic oldest described so far, but well in accordance in morphology and dimensions with Late Miocene representatives of the species. The record of *D. navi* from Gratkorn thus does not support the idea of

D. nauti evolving out of *D. crassum*. In comparison with other tragulid records from the Miocene of Europe, it rather enforces the assumption that *D. nauti* has to be considered part of a phylogenetic lineage, together with *D. guntianum*, characterised by (1) a bicuspid p2/d2, (2) a tricuspid p3 with a less dominant mesolabial conid than in *D. crassum*, (3) a p4 with a more complex posterior valley, (4) more selenodont, more slender and higher crowned lower molars, (5) a labially turned third lobe in the lower m3, as well as (6) upper molars with less bulky styles than in *D. crassum*, and (7) a non-fusion of tibia and malleolus lateralis. This lineage is distinct from the lineage including *D. crassum*, *D. peneckeii*, and *D. vindebonense* (see also Rössner and Heissig 2013 and others), which show, e.g. more bunoselenodont and lower crowned dentition, a tricuspid p3 with a dominant mesolabial conid, and a fusion of tibia and malleolus lateralis.

Since ruminants are the most abundant large mammals in Gratkorn, they are important for ecological considerations of the respective ecosystem. While the mostly subcanopy browsing *E. furcatus* was not a permanent resident of the locality and temporarily inhabited areas in the South (perhaps the Styrian Basin), isotopic measurements indicate that the probably browsing and facultative frugivore *D. nauti* and the canopy browser *Tethytragus* sp. (Aiglstorfer et al. 2014a, this issue) were more or less permanent residents at the locality and thus most likely were able to cope with seasonal variation of the diet. A caprine-like postcranial adaptation could have enabled *Tethytragus* sp. to canopy browsing and furthermore to greater flexibility concerning food supply in comparison to the cervid *E. furcatus*. The small moschid *M. flourensianus* assumably was a browser with a considerable intake of fruits or seeds and occasional grazing. Due to the scarce remains of *?Hispanomeryx*, a distinctive ecological niche cannot be reconstructed. Most likely, it exhibited a similar ecology as *M. flourensianus*, but, as indicated by the different body sizes (Sánchez et al. 2010a), the two sympatric moschids probably occupied different niches. Due to limited material, no ecological niche can be reconstructed for the Palaeomerycidae gen. et sp. indet. from Gratkorn, but taking into consideration data for other members of the family (e.g. Köhler 1993; Tütken and Vennemann 2009; Rössner 2010), it might represent a canopy browser, which, due to its large size and the possible limitation of available biomass at the locality, was not a permanent resident at Gratkorn but must have displayed a wider habitat range.

Acknowledgements The authors are indebted to P. Havlik for fruitful discussions and correction of the manuscript. M.A. wants to thank S. Kötter, A. Tröscher and A. Beckmann for their help in the search for

comparison material. J van der Made, J. Morales, I. Sánchez (Museo Nacional de Ciencias Naturales, Madrid), E. Heizmann (SMNS), B. Azanza (Universidad de Zaragoza), N. Spassov (NMNHS), N. Heckeberg (SNSB-BSPG and LMU München, Department of Zoology Cambridge), F. Fack, G. Metais, B. Mennecart, M. Pickford (MNHN) and T. Wiedl (University of Graz) are thanked for help and fruitful discussions. D. Vasilyan, J. Prieto (both University Tübingen) and F. Witzmann (Museum für Naturkunde Berlin) are thanked for taking pictures of specimens for comparison. M. Gross (UMJGP), U. Göhlich (NHMW), D. Nagel (IPUW), L. Costeur (NMB), C. Argot (MNHN), G. Scharfe (IGM), D. Alba (ICP), R. Ziegler (SMNS), M. Rummel (NMA), H. Lutz (NHMM), T. Engel (NHMM), H. Stapf (SSN), J. Rösinger and E. Weber (both University Tübingen, Zoological Collection), N. Spassov and L. Hristova (NMNHS), E. Bernard (BMNH), and P. Havlik (GPIT) are thanked for access to comparison material. W. Gerber (University Tübingen) is thanked for taking pictures, P. Havlik, M. Gross, H. Luginland (GPIT), R. Ellenbracht (GPIT), H. Stöhr (GPIT) N. Winkler (UMJGP), J. Fuß (GPIT) are furthermore thanked for preparation or great support in preparation of the material. This research received support from the SYNTHESYS Project (FR-TAF-1892) which is financed by the European Community Research Infrastructure Action under the FP7 “Capacities” Program. B. Azanza and L. Costeur greatly helped to improve the manuscript with careful reviews and helpful advice. And last but not least the authors want to thank students and volunteers from Graz, Munich and Tübingen for their help in excavations from 2005 to 2013.

Appendix: Historical context for the description of the species *Dorcatherium nauti* and considerations on species validity of different *Dorcatherium* species

The genus *Dorcatherium* was erected by Kaup in 1833 in a letter to Prof. Bronn (published in *Neues Jahrbuch für Mineralogie, Geognosie und Petrefaktenkunde*, 1833, p. 419), on a ruminant mandibula with p3–m3 (and alveolae for p1–2) from Eppelsheim (Rheinland-Pfalz, Germany), based on the presence of four premolars, and the rostral extension of the premolar to the level of the symphysis. Due to the resemblance of tooth morphology to that of a deer, he chose the name *Dorcatherium* (ἡ δορκάς greek for gazella, deer). In the same letter, he erected the type species, which he named *nauti* after his friend, Geheimrat von Nau. The catalogue of gypsum casts of the Palaeontological Collection in Darmstadt (Kaup and Scholl 1834) refers to the mandibula, described in 1833, and a fragment of a maxilla with P4–M3. Casts of both were sent to Berlin, Bonn, Frankfurt, London, Lyon, Paris, Strasburg, Stuttgart, and Zürich (Kaup and Scholl 1834).

The other medium-sized *Dorcatherium* species besides *D. nauti*, *Dorcatherium crassum*, is more common in the Miocene of Europe. It was erected by Lartet (1851) as *?Dicrocerus crassus* and he had already noticed the similarity of the upper canines with those in chevrotains (at that time seen as close relatives of *Moschus* and *Moschus* as a cervid genus; Milne Edwards erected the family Tragulidae in 1864). The first description is often cited as *D. crassum* (Lartet, 1839), but no indication can be found in any of the works of Lartet published in 1839 for the species name “*Dorcatherium*

crassum” nor in the first mentioning of remains of the species by Blainville (1837): “Des dents canines supérieures d’un petit ruminant sans bois ou à bois pédonculé des sous-genres moschus ou cervulus;” (Blainville 1837, p. 425) (for detailed discussion of the scientific history concerning the species, see Morales et al. 2012). With *D. crassum*, Milne Edwards (1864) included a fossil species in his newly erected family Tragulidae, together with the modern genera *Hyemoschus*, and *Tragulus* (including *T. meminna* which is considered today to represent a third tragulid genus, *Moschiola*), but affiliated it to the genus *Hyemoschus*. Although he observed the similarity between his *Hyemoschus crassus* and *Dorcatherium naui*, he did not include the latter in the Tragulidae due to the presence of a p1, which is completely reduced in the modern representatives of the family. Finally, Schlosser (1916) found sufficient morphological accordance of both species to affiliate *Hyemoschus crassus* to the genus *Dorcatherium*.

Today, five *Dorcatherium* species are generally accepted from the Miocene of Europe, differing in dimensions, dental and postcranial morphology and stratigraphic range (Fig. 1): the small-sized *D. guntianum* von Meyer, 1846 (late Early to Middle Miocene; MN 4–7/8; Seehuber 2008; Sach and Heizmann 2001; Rössner and Heissig 2013), the medium-sized *D. naui* (late Middle to Late Miocene; MN 7/8–11; Czyzewska and Stefaniak 1994; Rössner 2007, 2010; Alba et al. 2011; this publication) and *D. crassum* (Lartet, 1851) (late Early to Middle Miocene; MN 4–7/8; Eronen and Rössner 2007; Alba et al. 2011; Rössner and Heissig 2013), the larger-sized *D. vindebonense* von Meyer, 1846 (late Early to Middle Miocene; MN 4–6; Thenius 1952; Sach and Heizmann 2001; Rössner 2007, 2010; Rössner and Heissig 2013), and the large-sized *D. penecke* (Hofmann 1893) (early Middle Miocene; MN 5–6; Rössner 2007, 2010; Rössner and Heissig 2013).

D. puyhauberti, Arambourg and Piveteau, 1929 (Late Miocene; MN 9–13; Gentry et al. 1999; Rössner and Heissig 2013) and *D. jourdani* (Déperet, 1887) (Late Miocene; MN 9–11; Gentry et al. 1999; Rössner and Heissig 2013) have been documented only rarely, with only a few specimens, which possess no unambiguous features distinguishing them from other European species and could be synonymous to *D. guntianum* and *D. naui*, respectively (for further information, see discussion in the section on *Dorcatherium naui* of this publication).

D. rogeri, erected by Hofmann in 1909 due to a misunderstanding in von Meyer (1846), must be considered synonymous with *D. vindebonense* (Thenius 1952). The quite small *D. bulgaricum* Bakalov and Nikolov, 1962 from the West-Mariza-Basin (?Pliocene, Bulgaria; Rössner 2007) was erected on two mandibulae with m1–3. Although both specimens show clearly developed internal postmeta- and postprotocristids, the assignation to the genus *Dorcatherium* is ambiguous. As far as it could be observed on the figures in Bakalov and Nikolov (1962; originals supposed to be lost),

the specimens possess a strongly split posthypocristid, especially in the m3. This has so far been described only in the m3 of *Dorcatherium* cf. *pigotti* from Arrisdrift (basal Middle Miocene; Morales et al. 2003). In any case, the splitting of the posthypocristid is much stronger in *D. bulgaricum* than the minor splitting observed in *D. crassum* (Alba et al. 2013) and in *D. naui* from Gratkorn. Furthermore, *D. bulgaricum* possesses a rudimentary paraconid. “A small accessory cusplet” is described by Pickford (2002, p. 97) only in the Early Miocene *D. iririensis* from Africa. However, with a small hypoconulid in m2 and a rounded lingual wall in P4, the latter also differs significantly from other *Dorcatherium* species. A clearly developed paraconid can be observed, for example, in the lophiomerycid *Zhailimeryx* (Guo et al. 2000). Morales et al. (2012) also observed more similarities in *D. bulgaricum* to the Oligocene genera *Lophiomeryx* Pomel, 1853 and *Cryptomeryx* Schlosser 1886 (synonymised with *Iberomeryx*; Métais et al. 2001; Mennecart et al. 2011) than to other *Dorcatherium* species. The stratigraphic age of *D. bulgaricum* is furthermore ambiguous and could also be Paleogene (M. Böhme, personal opinion). We thus did not consider the species *Dorcatherium bulgaricum* in our discussions.

The Miocene tragulid genus *Dorcabune* Pilgrim, 1910 is so far only known, but with several species, from Asia (Rössner 2007). As *Dorcatherium* and *Dorcabune* overlap in morphological key features, a revision of the two genera would probably result in at least two morphotypes of Miocene tragulids with a differentiation into more bunodont (including *D. crassum*, *vindebonense* and *penecke*) and more selenodont forms (including *D. naui* and *guntianum*; Rössner 2007 referring also to Mottl 1961; Fahlbusch 1985; Qui and Gu 1991). Other Miocene tragulid genera described from Asia are *Siamotragulus* Thomas et al., 1990 and *Yunnanotherium* Han, 1986.

Five *Dorcatherium* species have been recorded from the Miocene of Africa: *D. songhorensis* Whitworth, 1958, *D. pigotti* Whitworth, 1958, *D. iririensis* Pickford 2002 and *D. chappuisi* Arambourg, 1933, as well as a second tragulid genus, *Afrotragulus*, with the species *A. parvus* (Witworth, 1958) and *A. moruorotensis* (Witworth, 1958) (Sánchez et al. 2010b).

To get a better idea about the relationships of and faunal exchanges between Asian, African and European Miocene tragulids, a revision of the different taxa and lineages as also proposed in the section on *Dorcatherium naui* in this publication and by Sánchez et al. 2010b is surely needed.

References

- Aiglstorfer M, Costeur L (2013) The Moschidae of Dorn-Dürkheim 1 (Germany). *Palaeobio Palaeoenv* 93(2):207–215. doi:10.1007/s12549-013-0117-9

- Aiglstorfer M, Bocherens H, Böhme M (2014a) Large mammal ecology in the late Middle Miocene Gratkorn locality (Austria). In: Böhme M, Gross M, Prieto J (eds) The Sarmatian vertebrate locality Gratkorn, Styrian Basin. *Palaeobio Palaeoenv* 94(1). doi:10.1007/s12549-013-0145-5
- Aiglstorfer M, Göhlich UB, Böhme M, Gross M (2014b) A partial skeleton of *Deinotherium* (Proboscidea, Mammalia) from the late Middle Miocene Gratkorn locality (Austria). In: Böhme M, Gross M, Prieto J (eds) The Sarmatian vertebrate locality Gratkorn, Styrian Basin. *Palaeobio Palaeoenv* 94(1). doi:10.1007/s12549-013-0140-x
- Aiglstorfer M, Heissig K, Böhme M (2014c) Perissodactyla from the late Middle Miocene Gratkorn locality (Austria). In: Böhme M, Gross M, Prieto J (eds) The Sarmatian vertebrate locality Gratkorn, Styrian Basin. *Palaeobio Palaeoenv* 94(1). doi:10.1007/s12549-013-0138-4
- Alba DM, Moyà-Solà S, Robles JM, Casanovas-Vilar I, Rotgers C, Carmona R, Galindo J (2011) Middle Miocene tragulid remains from Abocador de Can Mata: the earliest record of *Dorcatherium naui* from Western Europe. *Geobios* 44(2–3):135–150. doi:10.1016/j.geobios.2010.10.003
- Alba DM, DeMiguel D, Morales J, Sánchez IM, Moyà-Solà S (2013) New remains of *Dorcatherium crassum* (Artiodactyla: Tragulidae) from the Early Miocene (MN4) of Els Casots (Subirats, Vallès-Penedès Basin). *CR Palevol*. doi:10.1016/j.crpv.2013.09.003
- Arambourg C, Piveteau J (1929) Les Vertébrés du Pontien de Salonique. *Ann Paleontol* 18:57–140
- Astibia H (1987) First data on the presence of Palaeomerycidae (Artiodactyla, Mammalia) in the European Upper Miocene. *Geobios* 20(6):833–836. doi:10.1016/S0016-6995(87)80007-4
- Astibia H (2012) Les Palaeomerycidae (Artiodactyla) de Sansan. In: Peigné S, Sen S (eds) Mammifères de Sansan. *Mem Mus Natl Hist Nat* 203:201–224
- Azanza B (1986) Estudio geológico y paleontológico del Mioceno del sector oeste de la Comarca de Borja. *Cuad Estud Borjanos XVII–XVIII*:63–126
- Azanza B (1993) Sur la nature des appendices frontaux des cervidés (Artiodactyla, Mammalia) du Miocène inférieur et moyen. Remarques sur leur systématique et leur phylogénie. On the nature of the frontal appendages in Lower-Middle Miocene deer (Artiodactyla, Mammalia). Contribution to their systematics and phylogeny. *CR Acad Sci II* 316(8):1163–1169
- Azanza B (2000) Los Cervidae (Artiodactyla, Mammalia) del Mioceno de las cuencas del Duero, Tajo, Calatayud-Teruel y Levante. *Mem Mus Pal Univ Zarag* 8:1–376
- Azanza B, Ginsburg L (1997) A revision of the large lagomerycid artiodactyls of Europe. *Palaeontology* 40(2):461–485
- Azanza B, Morales J (1994) *Tethytragus* nov. gen. et *Gentrytragus* nov. gen. Deux nouveaux Bovidés (Artiodactyla, Mammalia) du Miocène moyen. Relations phylogénétiques des Bovidés anté-vallésiens. *Proc K Ned Akad Wet B* 97(3):249–282
- Azanza B, Rössner GE, Ortiz-Jaureguizar E (2013) The early Turolian (late Miocene) Cervidae (Artiodactyla, Mammalia) from the fossil site of Dorn-Dürkheim 1 (Germany) and implications on the origin of crown cervids. *Palaeobio Palaeoenv* 93(2):217–258. doi:10.1007/s12549-013-0118-8
- Bakalov P, Nikolov I (1962) Mammifères Tertiaires. In: Tzankov V (ed) *Les Fossiles de Bulgarie [In Bulgarian with French summary]*, vol 10. Académie des Sciences de Bulgarie, Sofia, pp 1–162
- Bärmann EV, Rössner GE (2011) Dental nomenclature in Ruminantia: towards a standard terminological framework. *Mamm Biol* 76(6):762–768
- Bernor RL, Kordos L, Rook L, Agustí J, Andrews P, Armour-Chelu M, Begun DR, Cameron DW, Damuth J, Daxner-Höck G, De Bonis L, Fejfar O, Fessaha N, Fortelius M, Franzen J, Gasparik M, Gentry A, Heissig K, Hernyak G, Kaiser T, Koufos GD, Krolopp E, Jánossy D, Llenas M, Meszáros L, Müller P, Renne P, Roček Z, Sen S, Scott R, Szyndlar Z, Topál G, Ungar PS, Utescher T, Van Dam JA, Werdelin L, Ziegler R (2004) Recent advances on multidisciplinary research at Rudabánya, Late Miocene (MN9), Hungary: a compendium. *Palaeontogr Ital* 89:3–36
- Bibi F, Güleş ES (2008) Bovidae (Mammalia: Artiodactyla) from the late Miocene of Sivas, Turkey. *J Vertebr Paleontol* 28(2):501–519. doi:10.1671/0272-4634(2008)28[501:bmaftl]2.0.co;2
- Blainville M (1837) Rapport sur un nouvel envoi de fossiles provenant du dépôt de Sansan. *C R Acad Sci* 12:418–427
- Bohlin B (1926) Die Familie Giraffidae. *Pal Sin C* 4(1):1–178
- Böhme M, Vasilyan D (2014) Ectothermic vertebrates from the late Middle Miocene of Gratkorn (Austria, Styria). In: Böhme M, Gross M, Prieto J (eds) The Sarmatian vertebrate locality Gratkorn, Styrian Basin. *Palaeobio Palaeoenv* 94(1). doi:10.1007/s12549-013-0143-7
- Böhme M, Winkhofer M, Ilg A (2011) Miocene precipitation in Europe: temporal trends and spatial gradients. *Palaeogeogr Palaeoclimatol Palaeoecol* 304(3–4):212–218. doi:10.1016/j.palaeo.2010.09.028
- Böhme M, Aiglstorfer M, Uhl D, Kullmer O (2012) The antiquity of the Rhine River: stratigraphic coverage of the *Dinotheriensande* (Eppelsheim Formation) of the Mainz Basin (Germany). *PLoS ONE* 7(5):e36817
- Carlsson A (1926) Über die Tragulidae und ihre Beziehungen zu den übrigen Artiodactyla. *Acta Zool* 7:69–100
- Clauss M, Kaiser T, Hummel J (2008) The morphophysiological adaptations of browsing and grazing mammals. In: Gordon I, Prins HT (eds) *The ecology of browsing and grazing*. Ecological Studies, vol 195. Springer, Berlin, pp 47–88. doi:10.1007/978-3-540-72422-3_3
- Czyżewska T, Stefaniak K (1994) Tragulidae (Artiodactyla, Mammalia) from the Middle Miocene of Przeworno (Lower Silesia, Poland). *Acta Zool Cracov* 37:47–53
- Damuth J (1990) Problems in estimating body masses of archaic ungulates using dental measurements. In: Damuth J, MacFadden B (eds) *Body size in mammalian paleobiology estimations and biological implications*. Cambridge University Press, Cambridge, pp 229–254
- DeMiguel D, Sánchez IM, Alba DM, Galindo J, Robles JM, Moyà-Solà S (2012) First evidence of *Tethytragus* Azanza and Morales, 1994 (Ruminantia, Bovidae), in the Miocene of the Vallès-Penedès Basin (Spain). *J Vertebr Paleontol* 32(6):1457–1462. doi:10.1080/02724634.2012.696082
- Dubost G (1964) Un ruminant à régime alimentaire partiellement carne: le chevrotaine aquatique (*Hyemoschus aquaticus* Ogilby). *Biol Gab* 1:21–23
- Dubost G (1965) Quelques traits remarquables du compartement de *Hyemoschus aquaticus* (Tragulidae, Ruminantia, Artiodactyla). *Biol Gab* 1:282–287
- Dubost G (1975) Le comportement du Chevrotain africain, *Hyemoschus aquaticus* Ogilby (Artiodactyla, Ruminantia). *Z Tierpsychol* 37:403–448
- Dubost G (1978) Un aperçu sur l'écologie du Chevrotain africain *Hyemoschus aquaticus* Ogilby, Artiodactyle Tragulidé. *Mammalia* 42:1–61
- Dubost G (1984) Comparison of the diets of frugivorous forest ruminants of Gabon. *J Mammal* 65:298–316
- Eronen JT, Rössner GE (2007) Wetland paradise lost: Miocene community dynamics in large herbivore mammals from the German Molasse Basin. *Evol Ecol Res* 9:471–494
- Fahlbusch V (1985) Säugetierreste (*Dorcatherium*, *Steneofiber*) aus der miozänen Braunkohle von Wackersdorf/Oberpfalz. *Mitt Bayer Staetssamml Paläontol Hist Geol* 25:81–94
- Filhol H (1891) Études sur les mammifères fossiles de Sansan. Librairie de l'Académie de Médecine. G. Masson, Paris

- Fraas O (1870) Die Fauna von Steinheim. Mit Rücksicht auf die miocenen Säugethier und Vogelreste des Steinheimer Beckens. Jahresh Ges Natkd Wuerth 26:230–244
- Fraser D, Theodor JM (2011) Anterior dentary shape as an indicator of diet in ruminant artiodactyls. *J Vertebr Paleontol* 31(6):1366–1375. doi:10.1080/02724634.2011.605404
- Gailer JP (2007) Vergleichende Funktionsmorphologie der Extremitäten der Tragulidae (Mammalia) mit *Sus* (Suidae, Mammalia) und *Capreolus* (Cervidae, Mammalia). Unpubl. Diploma Thesis. Ludwig-Maximilians-Universität München, München
- Gentry A (1994) The Miocene differentiation of old world Pecora (Mammalia). *Hist Biol* 7:115–158
- Gentry A (2003) Ruminantia (Artiodactyla). In: Fortelius M, Kappelman J, Bernor RL (eds) *Geology and paleontology of the Miocene Sinap Formation, Turkey*. Columbia University Press, New York
- Gentry AW, Rössner GE, Heizmann EPJ (1999) Suborder Ruminantia. In: Rössner GE, Heissig K (eds) *The Miocene land mammals of Europe*. Verlag Dr. Friedrich Pfeil, München, pp 225–253
- Geraads D, Kaya T, Mayda S (2005) Late Miocene large mammals from Yulafli, Thrace region, Turkey, and their biogeographic implications. *Acta Palaeontol Pol* 50(3):523–544
- Geraads D, Spassov N, Hristova L, Markov GN, Tzankov V (2011) Upper Miocene mammals from Strumyani, South-Western Bulgaria. *Geodiversitas* 33(3):451–484
- Ginsburg L (1967) Une faune de Mammifères dans l’Helvétien marin des Sos (Lot-et-Garonne) et de Rimbez (Landes). *Bull Soc Geol Fr* 7(IX):5–18
- Ginsburg L (1999) Remarques sur la systématique des Palaeomerycidae (Cervoidea, Artiodactyla, Mammalia) d’Europe. *CR Acad Sci II* 329:757–762
- Ginsburg L, Azanza B (1991) Présence de bois chez les femelles du cervidé miocène *Dicrocerus elegans* et remarques sur le problème de l’origine du dimorphisme sexuel sur les appendices frontaux des cervidés. Antlers in females of the Miocene deer *Dicrocerus elegans* and some remarks on the origin of the sexual dimorphism in the deer cranial appendices. *CR Acad Sci II* 313(1):121–126
- Ginsburg L, Crouzel F (1976) Contribution à la connaissance d’*Heteroprox larteti* (Filhol): Cervidé du Miocène européen. *Bull Mus Natl Hist Nat Sc Terr* 58:345–357
- Göhlich UB, Gross M (2014) The Sarmatian (late Middle Miocene) avian fauna from Gratkorn, Austria. In: Böhme M, Gross M, Prieto J (eds) *The Sarmatian vertebrate locality Gratkorn, Styrian Basin*. *Palaeobio Palaeoenv* 94(1). doi:10.1007/s12549-013-0139-3
- Gross M, Böhme M, Prieto J (2011) Gratkorn: a benchmark locality for the continental Sarmatian s.str. of the Central Paratethys. *Int J Earth Sci* 100(8):1895–1913. doi:10.1007/s00531-010-0615-1
- Gross M, Böhme M, Havlik P, Aiglstorfer M (2014) The late Middle Miocene (Sarmatian s.str.) fossil site Gratkorn – the first decade of research, geology, stratigraphy and vertebrate fauna. *Palaeobio Palaeoenv*. doi:10.1007/s12549-013-0149-1
- Guo J, Dawson MR, Beard KC (2000) *Zhailimeryx*, a new Lophiomerycid artiodactyl (Mammalia) from the late Middle Eocene of Central China and the early evolution of ruminants. *J Mamm Evol* 7(4):239–258
- Harzhauser M, Daxner-Höck G, Göhlich UB, Nagel D (2011) Complex faunal mixing in the early Pannonian palaeo-Danube Delta (Late Miocene, Gaweinstal, Lower Austria). *Ann Naturhist Mus Wien A* 113:167–208
- Haupt O (1935) Bemerkungen über die Hirsche aus dem Dinotheriensand Rheinhessens. *Notizbl Hess Geol La* 5 (16)
- Havlik P, Aiglstorfer M, Beckman A, Gross M, Böhme M (2014) Taphonomical and ichnological considerations on the late Middle Miocene Gratkorn locality (Styria, Austria) with focus on large mammal taphonomy. In: Böhme M, Gross M, Prieto J (eds) *The Sarmatian vertebrate locality Gratkorn, Styrian Basin*. *Palaeobio Palaeoenv* 94(1). doi:10.1007/s12549-013-0142-8
- Heintz E (1970) Les cervidés villafranchiens de France et d’Espagne, Vol. I-II. *Mem Mus Natl Hist Nat C22 special volume I and II*: I: 1-303 II: 301-206
- Heizmann EPJ, Reiff W (2002) *Der Steinheimer Meteorkrater*. Verlag Dr. Friedrich Pfeil, München
- Hensel R (1859) Ueber einen fossilen Muntjac aus Schlesien. *Z Dtsch Geol Ges* 11(2):251–279
- Hillenbrand V, Göhlich UB, Rössner GE (2009) The early Vallesian vertebrates of Atzelsdorf (Late Miocene, Austria) 7. Ruminantia. *Ann Naturhist Mus Wien A* 111:519–556
- Hofmann A (1893) Die Fauna von Görtschitz. *Abh K-K Geol Reichsanst* 15:1–87
- Hofmann A (1909) Säugetierreste aus einigen Braunkohleablagerungen Bosniens und der Herzegovina. *Wiss Mitt Bos Herz* 11 (1)
- Janis CM (1990) Correlation of cranial and dental variables with body size in ungulates and macropodoids. In: Damuth J, MacFadden B (eds) *Body size in mammalian paleobiology estimations and biological implications*. Cambridge University Press, Cambridge, pp 225–300
- Janis CM, Ehrhardt D (1988) Correlation of relative muzzle width and relative incisor width with dietary preference in ungulates. *Zool J Linn Soc* 92:267–284
- Janis CM, Scott KM (1987) The interrelationships of higher ruminant families with special emphasis on the members of the Cervoidea. *Am Mus Novit* 2893:1–85
- Kaiser TM, Rössner GE (2007) Dietary resource partitioning in ruminant communities of Miocene wetland and karst palaeoenvironments in Southern Germany. *Palaeogeogr Palaeoclimatol Palaeoecol* 252(3–4): 424–439. doi:10.1016/j.palaeo.2007.04.013
- Kaup JJ (1833) Darmstadt, 2. Juli 1833 [letter to Bronn]. *Neues Jahrb Geol* 419–420
- Kaup JJ (1839) Description d’ossements fossiles de Mammifères inconnus jusqu’à présent, qui se trouvent au Muséum grand-ducal de Darmstadt, cinquième cahier. J.P. Diehl, Darmstadt
- Kaup JJ, Scholl JB (1834) Verzeichniss der Gypsabgüsse von den ausgezeichnetsten urweltlichen Thierresten des Grossherzoglichen Museums zu Darmstadt. J.P. Diehl, Darmstadt
- Köhler M (1987) Boviden des türkischen Miozäns (Känozoikum und Braunkohlen der Türkei. 28). *Pal i Evol* 21:133–246
- Köhler M (1993) Skeleton and habitat of recent and fossil ruminants. *Münchner Geowiss Abh* 25:87
- König HE, Liebich HG (2008) *Anatomie der Haussäugetiere*. Lehrbuch und Farbatlas für Studium und Praxis. Schattauer, Stuttgart
- Lartet È (1851) Notice sur la colline de Sansan. Suivie d’une récapitulation de diverses espèces d’animaux vertébrés fossiles trouvés soit à Sansan, soit dans d’autres gisements du terrain tertiaire mioce’ne dans le bassin sous-pyrénéen. Auch (Portes)
- Leinders JJM (1979) On the osteology and function of the digits of some ruminants and their bearing on taxonomy. *Z Säugetierkd* 44:305–318
- López-Guerrero P, García-Paredes I, Hoek Ostende LW van den, van Dam JA, Álvarez-Sierra MÁ, Hernández-Ballarín V, Meulen AJ van der, Oliver A, Paláez-Campomanes P (2011) Cañada: a new micromammal succession from the lower Vallesian and Turolian of the Daroca area (Calatayud-Montalbán basin, Spain). *Estud Geol* 67(2):443–453
- Made J van der (1989) The bovid *Pseudoeotragus seegrabensis* nov. gen., nov. sp. from the Aragonian (Miocene) of Seegraben near Leoben (Austria). *Proc K Ned Akad Wet B* 92(3):215–240
- Made J van der (1996) Listriodontinae (Suidae, Mammalia), their evolution, systematics and distribution in time and space. *Contrib Tert Quatern Geol* 33(1–4):3–254

- Made J van der (2012) *Eotragus clavatus* (Artiodactyla, Bovidae, Boselaphini) de Sansan. In: Peigné S, Sen S (eds) Mammifères de Sansan. Mem Mus Natl Hist Nat 203:145–199
- Made J van der, Güleç ES, Erkman AC (2013) *Microstonyx* (Suidae, Artiodactyla) from the upper Miocene of Hayranlı-Haliminhani, Turkey. Turk J Zool 37:106–122
- Made J van der, Prieto J, Aiglstorfer M, Böhme M, Gross M (2014) Taxonomic study of the pigs (Suidae, Mammalia) from the late Middle Miocene of Gratkorn (Austria, Styria). In: Böhme M, Gross M, Prieto J (eds) The Sarmatian vertebrate locality Gratkorn, Styrian Basin. Palaeobio Palaeoenv 94(1). doi:10.1007/s12549-014-0152-1
- Matsubayashi H, Bosi E, Kohshima S (2003) Activity and habitat use of lesser mouse-deer (*Tragulus javanicus*). J Mammal 84(1):234–242
- Mattioli S (2011) Cervidae. In: Wilson DE, Mittermeier R (eds) Handbook of the mammals of the world. Lynx, Madrid, pp 350–443
- Meijaard E (2011) Tragulidae. In: Wilson DE, Mittermeier R (eds) Handbook of the mammals of the world, vol 2. Hoofed mammals. Lynx, Madrid, pp 320–336
- Mendoza M, Janis CM, Palmqvist P (2006) Estimating the body mass of extinct ungulates: a study on the use of multiple regression. J Zool 270:90–101
- Mennecart B, Becker D, Berger J-P (2011) *Iberomyx minor* (Mammalia, Artiodactyla) from the Early Oligocene of Soule (Canton Jura, NW Switzerland): systematics and palaeodiet. Swiss J Geosci (SJG) 104(Suppl. 1):S115–S132
- Merceron G (2009) The early Vallesian vertebrates of Atzelsdorf (Late Miocene, Austria) 13. Dental wear patterns of herbivorous ungulates as ecological indicators. Ann Naturhist Mus Wien A 111:647–660
- Merceron G, Schulz E, Kordos L, Kaiser TM (2007) Palaeoenvironment of *Dryopithecus brancoi* at Rudabánya, Hungary: evidence from dental meso- and micro-wear analyses of large vegetarian mammals. J Hum Evol 53(4):331–349. doi:10.1016/j.jhevol.2007.04.008
- Métais G, Chaimanee Y, Jaeger J-J, Ducrocq S (2001) New remains of primitive ruminants from Thailand: evidence of the early evolution of the Ruminantia in Asia. Zool Scr 30:231–248
- Meyer H von (1846) Säugethiere in Molasse zu Günzburg an der Donau. Neues Jahrb Min Geogn Geol und Petref:472–473
- Milne Edwards A (1864) Recherches anatomiques, zoologiques et paléontologiques sur la famille des Chevrotains. Martinet, Paris
- Montoya P, Morales J (2004) Los últimos tragúlidos (Artiodactyla, Mammalia) del registro fósil español: *Dorcatherium nauti* Kaup, 1833 del Turolense inferior de Crevillente 2 (Alicante). Zona Arqueológica, 4. Miscelánea en homenaje a Emiliano Aguirre 2: 328–335
- Morales J, Moyà-Solà S, Soria D (1981) Presencia de la familia Moschidae (Artiodactyla, Mammalia) en el Vallesiense de España: *Hispanomyx duriensis* novo gen. nova sp. Estud Geol 37:467–475
- Morales J, Soria D, Sánchez IM, Quirarte V, Pickford M (2003) Tragulidae from Arrisdrift, basal Middle Miocene, Southern Namibia. Mem Geol Sur Namibia 19:359–369
- Morales J, Sánchez IM, Quirarte V (2012) Les Tragulidae (Artiodactyla) de Sansan. In: Peigné S, Sen S (eds) Mammifères de Sansan. Mem Mus Natl Hist Nat 203:225–247
- Mottl M (1954) *Dorcatherium* im Unterpliozän der Steiermark. Mitteilungen Des Museums Für Bergbau Geologie Und Technik Am Landesmuseum “Joanneum”, Graz 13:72–75
- Mottl M (1961) Die Dorcatherien der Steiermark. Mitt Mus Bergbaustud Geol Tech Landesmus Joanneum Graz 22:21–71
- Mottl M (1966) VIII. Eine neue unterpliozäne Säugetierfauna aus der Steiermark, SO-Österreich. Mitt Mus Bergbaustud Geol Tech Landesmus Joanneum Graz 28:33–62
- Mottl M (1970) Die jungtertiären Säugetierfaunen der Steiermark, Südost-Österreichs. Mitt Mus Bergbaustud Geol Tech Landesmus Joanneum Graz 31:3–92
- Moyà-Solà S (1979) Estudio de *Dorcatherium nauti* Kaup 1833, de las cuencas del Vallés (Barcelona) y de la Seu d’Urgell (Lleida), y su esqueleto locomotor. Interpretación ecológico-funcional. Unpubl. Master Thesis. Universidad de Barcelona, Barcelona
- Nickel R, Schummer A, Seiferle E (1968) Bewegungsapparat, vol 1. Lehrbuch der Anatomie der Haustiere. Paul Parey, Berlin
- Pickford M (2002) Ruminants from the early Miocene of Napak, Uganda. Ann Paleontol 88:85–113
- Prieto J, Angelone C, Casanovas-Vilar I, Gross M, Hir J, Hoek Ostende L van der, Maul LC, Vasilyan D (2014) The small mammals from Gratkorn: an overview. In: Böhme M, Gross M, Prieto J (eds) The Sarmatian vertebrate locality Gratkorn, Styrian Basin. Palaeobio Palaeoenv 94(1). doi:10.1007/s12549-013-0147-3
- Qui Z, Gu Y (1991) The Aragonian vertebrate fauna of Xiacaowan—8. *Dorcatherium* (Tragulidae, Artiodactyla). Vert Palas 29(1):21–37
- Rinnert P (1956) Die Huftiere aus dem Braunkohlenmiozän der Oberpfalz. Palaeontogr A 107(1–2):1–65
- Romaggi J-P (1987) Les Antilopes du Miocene Supérieur du Coiron (Ardeche, France). Université Claude Bernard Lyon 1, Lyon
- Rössner GE (1995) Odontologische und schädelanatomische Untersuchungen an *Procervulus* (Cervidae, Mammalia). Münchner Geowiss Abh A 29:127
- Rössner GE (2006) A community of middle Miocene Ruminantia (Mammalia, Artiodactyla) from the German Molasse Basin. Palaeontogr A 277(1–6):103–112
- Rössner GE (2007) Family Tragulidae. In: Prothero DR, Foss SE (eds) The evolution of artiodactyls. The Johns Hopkins University Press, Baltimore, pp 213–220
- Rössner GE (2010) Systematics and palaeoecology of Ruminantia (Artiodactyla, Mammalia) from the Miocene of Sandelzhausen (southern Germany, Northern Alpine Foreland Basin). Paläontol Z 84(1):123–162. doi:10.1007/s12542-010-0052-2
- Rössner GE, Heissig K (2013) New records of *Dorcatherium guntianum* (Tragulidae), stratigraphical framework, and diphyletic origin of European tragulids. Swiss J Geosci 106:335–347. doi:10.1007/s00015-013-0132-x
- Sach VJ (1999) Litho- und biostratigraphische Untersuchungen in der Oberen Süßwassermolasse des Landkreises Biberach a. d. Riß (Oberschwaben). Stuttg Beitr Naturk B 276:1–167
- Sach VJ, Heizmann EPJ (2001) Stratigraphie und Säugetierfaunen der Brackwassermolasse in der Umgebung von Ulm (Südwestdeutschland). Stuttg Beitr Naturk B 310:1–95
- Sánchez IM, Morales J (2008) *Micromeryx azanzae* sp. nov. (Ruminantia: Moschidae) from the middle-upper Miocene of Spain, and the first description of the cranium of *Micromeryx*. J Vertebr Paleontol 28(3): 873–885. doi:10.1671/0272-4634(2008)28[873:masnrm]2.0.co;2
- Sánchez IM, Domingo MS, Morales J (2009) New data on the Moschidae (Mammalia, Ruminantia) from the upper Miocene of Spain (Mn 10–Mn 11). J Vertebr Paleontol 29(2):567–575. doi:10.1671/039.029.0223
- Sánchez IM, Domingo MS, Morales J (2010a) The genus *Hispanomyx* (Mammalia, Ruminantia, Moschidae) and its bearing on musk deer phylogeny and systematics. Palaeontology 53(5):1023–1047. doi: 10.1111/j.1475-4983.2010.00992.x
- Sánchez IM, Quirarte V, Morales J, Pickford M (2010b) A new genus of tragulid ruminant from the early Miocene of Kenya. Acta Paleontol Pol 55(2):177–187
- Sánchez IM, DeMiguel D, Quirarte V, Morales J (2011a) The first known Asian *Hispanomyx* (Mammalia, Ruminantia, Moschidae). J Vertebr Paleontol 31(6):1397–1403. doi:10.1080/02724634.2011.618155
- Sánchez IM, Quirarte V, Morales J (2011b) Solving an old dispute: Anatomical differences between the European Miocene Chevrotains *Dorcatherium crassum* LARTET, 1839 and *Dorcatherium nauti* KAUP & SCHOLL, 1834 (Mammalia, Ruminantia, Tragulidae) Pal i Evol, Mem Espec 5:343–347

- Schlosser M (1886) Beiträge zur Kenntnis der Stammesgeschichte der Huftiere und Versuch einer Systematik der Paar- und Unpaarhufer. *Morphol Jahrb* 12:1–136
- Schlosser M (1916) Neue Funde fossiler Säugetiere in der Eichstätter Gegend. *Bayer Akad Wiss Math-Natur Kl Abh* 28:1–78
- Schmid E (1972) *Atlas of animal bones for prehistorians, archaeologists and quaternary geologists*. Elsevier, Amsterdam
- Scott KM (1990) Postcranial dimensions of ungulates as predictors of body mass. In: Damuth J, MacFadden B (eds) *Body size in mammalian paleobiology: estimations and biological implications*. Cambridge University Press, Cambridge, pp 301–336
- Seehuber U (2008) Litho- und biostratigraphische Untersuchungen in der Oberen Süßwassermolasse in der Umgebung von Kirchheim in Schwaben. Ludwig-Maximilians-Universität München, München
- Solounias N (2007) Family Giraffidae. In: Prothero DR, Foss SE (eds) *The evolution of artiodactyls*. The Johns Hopkins University Press, Baltimore, pp 257–291
- Stehlin HG (1928) Bemerkungen über die Hirsche von Steinheim am Albuch. *Eclogae Geol Helv* 21:245–256
- Stehlin HG (1937) Bemerkungen über die miocaenen Hirschgenera *Stephanocemas* und *Lagomeryx*. *Verh Naturforsch Ges Basel* 48: 193–214
- Stehlin HG (1939) *Dicrocerus elegans* LARTET und sein Geweihwechsel. *Eclogae Geol Helv* 32(2):162–179
- Stromer E (1928) Wirbeltiere im obermiocänen Flinz Münchens. *Bayer Akad Wiss Math-Natur Kl Abh* 32(1):1–71
- Suttie JM, Fennessey PF (1990) Antler regeneration: studies with antler removal, axial tomography, and angiography. In: Bubenik GA, Bubenik AB (eds) *Horns, pronghorns, and antlers*. Springer, New York, pp 313–338
- Thenius E (1948) Zur Kenntnis der fossilen Hirsche des Wiener Beckens, unter besonderer Berücksichtigung ihrer stratigraphischen Bedeutung. *Ann Naturhist Mus Wien* 56:262–308
- Thenius E (1950) Die tertiären Lagomeryciden und Cerviden der Steiermark. *Oesterr Akad Wiss Math-Natwiss Kl Sitzungsber Abt I Biol Wiss Erdwiss* 159:219–254
- Thenius E (1951) *Gazella* cf. *deperdita* aus dem mitteleuropäischen Vindobonien und das Auftreten der Hipparionfauna. *Eclogae Geol Helv* 44(2):381–394
- Thenius E (1952) Die Säugetierfauna aus dem Torton von Neudorf an der March (CSR). *N Jb Geol Paläont, Abh* 96(1):27–136
- Thenius E (1989) *Mammalia*, vol 8. *Handbuch der Zoologie Handbook of Zoology*. Walter de Gruyter, Berlin
- Tobien H (1961) *Palaeomeryx eminens* H. v. M. (Cervoidea, Mamm.) aus dem unterpliozänen Dinotheriensanden Rheinhessens. *N Jb Geol Paläont, Mh* 9:483–489
- Tütken T, Vennemann T (2009) Stable isotope ecology of Miocene large mammals from Sandelzhausen, southern Germany. *Paläontol Z* 83(1):207–226. doi:10.1007/s12542-009-0011-y
- Tütken T, Vennemann TW, Janz H, Heizmann EPJ (2006) Palaeoenvironment and palaeoclimate of the Middle Miocene lake in the Steinheim basin, SW Germany: A reconstruction from C, O, and Sr isotopes of fossil remains. *Palaeogeogr Palaeoclimatol Palaeoecol* 241(3–4):457–491. doi:10.1016/j.palaeo.2006.04.007
- Ungar PS, Scott JR, Curran SC, Dunsworth HM, Harcourt-Smith WEH, Lehmann T, Manthi FK, McNulty KP (2012) Early Neogene environments in East Africa: Evidence from dental microwear of tragulids. *Palaeogeogr Palaeoclimatol Palaeoecol* 342–343(0):84–96. doi:10.1016/j.palaeo.2012.05.005
- Vislobokova IA (2001) Evolution and classification of *Tragulina* (Ruminantia, Artiodactyla). *Paleontol J* 35(Suppl. 2):S69–S145
- Vislobokova IA (2007) New data on late Miocene Mammals of Kohfidisch, Austria. *Pal J* 41(4):451–460

online resource 1
for Aiglstorfer, M., Rössner, G.E., Böhme, M.: *Dorcatherium nauï* and pecoran ruminants from the late Middle Miocene
Gratkorn locality (Austria):
Stratigraphic range of different *Dorcatherium* species from Central Europe and reference localities
corresponding author: manuela.aiglstorfer@senckenberg.de

Stratigraphic range of *Dorcatherium* species in Central Europe and reference localities
[**bold** = personal observation of material]

locality	genus	species	reference
Abocador de Can Mata	<i>Dorcatherium</i>	<i>nauï</i>	Alba et al. (2011)
Attenfeld	<i>Dorcatherium</i>	<i>crassum</i>	Eronen and Rössner (2007)
Atzelsdorf	<i>Dorcatherium</i>	<i>nauï</i>	Hillenbrand et al. (2009)
Au bei Loretto am Leithagebirge	<i>Dorcatherium</i>	<i>nauï</i>	Kittl (1882); Sohs (1963); Rohatsch (1996)
Aumeister near Munich	<i>Dorcatherium</i>	<i>nauï</i>	Rössner and Heissig (2013)
Bonlanden-Iltertal	<i>Dorcatherium</i>	cf. <i>crassum</i>	Sach (1999)
Breitenfeld	cf. <i>Dorcatherium</i>	<i>nauï</i>	Mottl 1970; Gross et al. (2011); pers. com M. Gross
Brunn near Nestelbach	<i>Dorcatherium</i>	<i>nauï</i>	Mottl (1961); Gross et al. (2011); pers. com M. Gross
Burghheim	<i>Dorcatherium</i>	<i>crassum</i>	Eronen and Rössner (2007)
Can Llobateres I	<i>Dorcatherium</i>	<i>nauï</i>	Agusti et al. (1996)
Crevillente 2	<i>Dorcatherium</i>	<i>nauï</i>	Montoya and Morales (2004)
Dechbetten	<i>Dorcatherium</i>	<i>crassum</i>	Rinnert (1956)
Derching	<i>Dorcatherium</i> <i>Dorcatherium</i>	<i>crassum</i> <i>peneckeï</i>	Eronen and Rössner (2007); Rössner and Heissig (2013)
Devínská Nová Ves - Sandberg	<i>Dorcatherium</i>	<i>crassum</i> <i>vindebonense</i>	Thenius (1952a); Sabol and Holec (2002)
Devínská Nová Ves - Fissures	<i>Dorcatherium</i>	<i>vindebonense</i>	Zapfe (1949)
Edelbeuren-Maurerkopf	<i>Dorcatherium</i>	<i>guntianum</i>	Sach (1999)
Edelbeuren-Schlachtberg	<i>Dorcatherium</i>	<i>guntianum</i>	Sach (1999)
Eggingen-Mittelhart 3	<i>Dorcatherium</i>	cf. <i>guntianum</i> <i>crassum</i> <i>vindebonense</i>	Sach and Heizmann (2001)
Engelswies	<i>Dorcatherium</i>	<i>crassum</i>	Rössner and Heissig (2013)
Feisternitz near Eibiswald	<i>Dorcatherium</i>	<i>crassum</i> <i>vindebonense</i>	Mottl (1961); Gross and Martin (2008)
Gaiselberg near Zistersdorf	<i>Dorcatherium</i>	<i>nauï</i>	Mottl (1961)
Gaweinstal	<i>Dorcatherium</i>	<i>nauï</i>	Harzhauser et al. (2011)
Gerlenhofen	<i>Dorcatherium</i>	<i>guntianum</i>	Rössner and Heissig (2013)
Göriach	<i>Dorcatherium</i>	<i>crassum</i> cf. <i>vindebonense</i>	Mottl (1961)
Gratkorn	<i>Dorcatherium</i>	<i>nauï</i>	this work
Griesbeckerzell 1a	<i>Dorcatherium</i>	<i>crassum</i> <i>guntianum</i> <i>peneckeï</i>	Eronen and Rössner (2007)
Günzburg	<i>Dorcatherium</i>	<i>guntianum</i>	Schlosser (1886); Rössner and Heissig (2013)
Günzburg- Umgehungsstrasse	<i>Dorcatherium</i>	<i>guntianum</i>	Rössner and Heissig (2013)
Haag	<i>Dorcatherium</i>	<i>nauï</i>	Thenius (1952b)
Hambach 6C	<i>Dorcatherium</i>	<i>guntianum</i> <i>crassum</i>	Mörs et al. (2000); Rössner and Heissig (2013)

Heggbach	<i>Dorcatherium</i>	<i>crassum</i>	Rössner and Heissig (2013)
Hohenraunau	<i>Dorcatherium</i>	<i>guntianum peneckeii</i>	Eronen and Rössner (2007); Seehuber (2008)
Holzmannsdorfberg	<i>Dorcatherium</i>	<i>nauii</i>	Mottl (1966) ; Gross et al. (2011); pers. com M. Gross
Hüllistein	<i>Dorcatherium</i>	<i>crassum</i>	Bürgisser et al. (1983)
Kirrbach near Balzhausen	<i>Dorcatherium</i>	<i>crassum?</i>	Eronen and Rössner (2007)
Kleineisenbach	<i>Dorcatherium</i>	<i>crassum</i>	Eronen and Rössner (2007)
La Romieu superior	<i>Dorcatherium</i>	<i>crassum guntianum</i>	Ginsburg and Bulot (1987)
Labitschberg near Gamlitz	<i>Dorcatherium</i>	<i>crassum vindebonense</i>	Mottl (1961)
Laimering 3a	<i>Dorcatherium</i>	<i>crassum</i>	Rössner (2006)
Langenau	<i>Dorcatherium</i>	<i>crassum</i>	Eronen and Rössner (2007)
Lassnitzunnel near Graz	<i>Dorcatherium</i>	<i>nauii</i>	Mottl (1961) ; Gross et al. (2011); pers. com M. Gross
Mariathal	<i>Dorcatherium</i>	<i>nauii</i>	Thenius (1982)
Mörzen	<i>Dorcatherium</i>	<i>guntianum</i>	Rössner and Heissig (2013)
Münzenberg near Leoben, NW-Stmk.	<i>Dorcatherium</i>	<i>vindebonense crassum</i>	Mottl (1961); Sachsenhofer et al. (2010)
Oberdorf 4 near Voitsberg	<i>Dorcatherium</i>	<i>crassum</i>	Rössner (1998)
Pfaffenzell	<i>Dorcatherium</i>	<i>guntianum</i>	Eronen and Rössner (2007)
Pöttmes, Gemeinde-Kiesgrube	<i>Dorcatherium</i>	<i>crassum</i>	Eronen and Rössner (2007)
Przeworno	<i>Dorcatherium</i>	<i>nauii</i>	Czyzewska and Stefaniak (1994)
Reisensburg (Günzburg)	<i>Dorcatherium</i>	<i>crassum guntianum</i>	Eronen and Rössner (2007); Rössner and Heissig (2013)
Rudabanya	<i>Dorcatherium</i>	<i>nauii</i>	Gentry (2005); Bernor et al. (2004)
Sandelzhausen	<i>Dorcatherium</i>	<i>crassum</i>	Rössner (1997) (listed as <i>nauii</i>); Rössner (2010)
Sansan	<i>Dorcatherium</i>	<i>crassum</i>	Morales et al. (2012)
Seegraben near Leoben	<i>Dorcatherium</i>	<i>guntianum vindebonense crassum peneckeii</i>	Mottl (1961); Sachsenhofer et al. (2010)
Stallhofen near Voitsberg	<i>Dorcatherium</i>	<i>peneckeii</i>	Mottl (1961)
Stätzling	<i>Dorcatherium</i>	<i>crassum peneckeii guntianum</i>	Rössner and Heissig (2013)
Steinheim	<i>Dorcatherium</i>	<i>crassum</i>	Heizmann and Reiff (2002)
Steyeregg near Wies	<i>Dorcatherium</i>	<i>crassum</i>	Mottl (1961); Gross and Martin (2008)
Sulmingen	<i>Dorcatherium</i>	<i>crassum</i>	
Teiritzberg 1 (T1)	<i>Dorcatherium</i>	<i>crassum</i>	Rössner (1998)
Thannhausen	<i>Dorcatherium</i>	<i>guntianum crassum (peneckeii)</i>	Rössner and Heissig (2013)
Viehhausen	<i>Dorcatherium</i>	<i>crassum</i>	Rinnert (1956)
Vordersdorf	<i>Dorcatherium</i>	<i>crassum</i>	Mottl (1961); Gross and Martin (2008)
Wackersdorf	<i>Dorcatherium</i>	<i>vindobonense</i>	Fahlbusch (1985)

Walda 2	<i>Dorcatherium</i>	<i>crassum guntianum vindebonense</i>	Rössner and Heissig (2013)
Wannenwaldtobel 2	<i>Dorcatherium</i>	<i>guntianum</i>	Sach (1999)
Wien-Altmanndorf	<i>Dorcatherium</i>	<i>naii</i>	
Wies	<i>Dorcatherium</i>	<i>crassum</i>	Mottl (1961); Gross an Martin (2008)
Ziemetshausen 1b	<i>Dorcatherium</i>	<i>guntianum vindebonense peneckeii</i>	Rössner and Heissig (2013)

References:

- Agusti, J, Köhler M, Moyà-Solà S, Cabrera L, Garcés M, Parés JM (1996) Can Llobateres: the pattern and timing of the Vallesian hominoid radiation reconsidered. *Journal of Human Evolution* 31 (2):143-155.
doi:http://dx.doi.org/10.1006/jhev.1996.0055
- Alba DM, Moyà-Solà S, Robles JM, Casanovas-Vilar I, Rotgers C, Carmona R, Galindo J (2011) Middle Miocene tragulid remains from Abocador de Can Mata: The earliest record of *Dorcatherium naii* from Western Europe. *Geobios* 44 (2–3):135-150.
- Bernor RL, Kordos L, Rook L, Agustí J, Andrews P, Armour-Chelu M, Begun DR, Cameron DW, Damuth J, Daxner-Höck G, De Bonis L, Fejfar O, Fessaha N, Fortelius M, Franzen J, Gasparik M, Gentry A, Heissig K, Hernyak G, Kaiser T, Koufos GD, Krolopp E, Jánossy D, Llenas M, Meszáros L, Müller P, Renne P, Roček Z, Sen S, Scott R, Szyndlar Z, Topál G, Ungar PS, Utescher T, Van Dam JA, Werdelin L, Ziegler R (2004) Recent Advances on Multidisciplinary Research at Rudabánya, Late Miocene (MN9), Hungary: a compendium. *Paleontographia Italica* 89:3-36.
- Bürgisser HM, Furrer H, Hünermann KA (1983) Stratigraphie und Säugetierfaunen der mittelmiozänen Fossilfundstellen Hüllistein und Martinsbrünneli (Obere Süßwassermolasse, Nordostschweiz). *Eclogae Geologicae Helveticae* 76 (3):733–762
- Czyżewska T, Stefaniak K (1994) Tragulidae (Artiodactyla, Mammalia) from the Middle Miocene of Przeworno (Lower Silesia, Poland). *Acta zoologica cracoviensia* 37:47-53
- Eronen JT, Rössner GE (2007) Wetland Paradise Lost: Miocene Community Dynamics in Large Herbivore Mammals from the German Molasse Basin. *Ecology and Evolutionary Research* 9:471-494
- Fahlbusch V (1985) Säugetierreste (*Dorcatherium*, *Steneofiber*) aus der miozänen Braunkohle von Wackersdorf/Oberpfalz. *Mitteilungen der Bayerischen Staatssammlung für Paläontologie und historische Geologie* 25:81-94
- Gentry AW (2005) Ruminants of Rudabánya. *Palaeontographica Italica* 90:283-302
- Ginsburg Lo, Bulot C (1987) Les Artiodactyles sélénodontes du Miocène de Bézian à La Romieu (Gers). *Bulletin du Muséum National d'Histoire Naturelle 4e Serie Section C Sciences de la Terre Paleontologie, Geologie, Mineralogie* 9 (1):63-95
- Gross M, Martin J (2008) From the Palaeontological Collection of the Provincial Museum Joanneum - The fossil Crocodylians (Crocodylia). *Joannea Geol. Paläont.* 10: 91-125
- Gross M, Piller W, Scholger R, Gitter F (2011) Biotic and abiotic response to palaeoenvironmental changes at Lake Pannons' western margin (Central Europe, Late Miocene). *Palaeogeogr Palaeoclimatol Palaeoecol* 312 (1-2): 181-193
- Harzhauser M, Daxner-Höck G, Göhlich UB, Nagel D (2011) Complex faunal mixing in the early Pannonian palaeo-Danube Delta (Late Miocene, Gaweinstal, Lower Austria). *Annalen des Naturhistorischen Museum Wien A* 113:167-208
- Heizmann EPJ, Reiff W (2002) *Der Steinheimer Meteorkrater*. Verlag Dr. Friedrich Pfeil, München
- Hillenbrand V, Göhlich U, Rössner G (2009) The early Vallesian vertebrates of Atzelsdorf (Late Miocene, Austria) 7. Ruminantia. *Annalen des Naturhistorischen Museums in Wien, Serie A* 111:519-556
- Kittl E (1882) *Geologische Beobachtungen im Leithagebirge*. Kaiserlich-Königliche Reichsanstalt Verhandlungen 15-16:292-300
- Montoya P, Morales J (2004) Los últimos tragúlidos (Artiodactyla, Mammalia) del registro fósil español: *Dorcatherium naii* Kaup, 1833 del Turoliense inferior de Crevillente 2 (Alicante). *Zona Arqueológica*, 4 Miscelánea en homenaje a Emiliano Aguirre 2:328-335
- Morales J, Sánchez IM, Quirarte V (2012) Les Tragulidae (Artiodactyla) de Sansan. In: Peigné S, Sen S (eds) *Mammifères de Sansan*. Mémoires du Muséum national d'Histoire naturelle, vol 203. pp 225-247

- Mottl M (1961) Die Dorcatherien der Steiermark. Mitteilungen des Museums für Bergbau, Geologie und Technik, Landesmuseum Joanneum Graz 22:21–71
- Mottl M (1966) VIII. Eine neue unterpliozäne Säugetierfauna aus der Steiermark, SO-Österreich. Mitteilung des Museums für Bergbau, Geologie und Technik am Landesmuseum "Joanneum" Graz 28:33-62
- Mottl M (1970) Die jungtertiären Säugetierfaunen der Steiermark, Südost-Österreichs. Mitteilung des Museums für Bergbau, Geologie und Technik am Landesmuseum "Joanneum" Graz 31:3-92
- Rinnert P (1956) Die Huftiere aus dem Braunkohlenmiozän der Oberpfalz. *Palaeontographica A* 107 (1-2):1-65
- Rohatsch A (1996) Ökologische Aspekte bei Foraminiferenfaunen der kalkigen Randfazies des Wiener Beckens. *Mitt Ges Geol Bergbaustud Österr* 39:55-63
- Rössner GE (1997) Biochronology of Ruminant Assemblages in the Lower Miocene of Southern Germany. In: Aguilar JP, Legendre S, Michaux J (eds) *Actes du Congrès BiochroM'97. Mémoires et Travaux de l'E.P.H.E., Institut de Montpellier* 21:609-618; Montpellier
- Rössner GE (1998) Wirbeltiere aus dem Unter-Miozän des Lignit-Tagebaues Oberdorf (Weststeirisches Becken, Österreich): 9. Ruminantia (Mammalia). *Annalen des Naturhistorischen Museums in Wien (A)* 99: 169-193
- Rössner GE (2006) A community of middle Miocene Ruminantia (Mammalia, Artiodactyla) from the German Molasse Basin. *Palaeontogr A* 277(1–6):103–112
- Rössner GE (2010) Systematics and palaeoecology of Ruminantia (Artiodactyla, Mammalia) from the Miocene of Sandelzhausen (southern Germany, Northern Alpine Foreland Basin). *Palaeontol Z* 84(1):123–162. doi:10.1007/s12542-010-0052-2
- Rössner GE, Heissig K (2013) New records of *Dorcatherium guntianum* (Tragulidae), stratigraphical framework, and diphyletic origin of European tragulids. *Swiss Journal of Geosciences (SJG)* 106 (2): 335-347
- Sabol M, Holec P (2002) Temporal and Spatial Distribution of Miocene Mammals in the Western Carpathians (Slovakia). *Geologica Carpathica* 53 (4):269-279
- Sach VJ (1999) Litho- und biostratigraphische Untersuchungen in der Oberen Süßwassermolasse des Landkreises Biberach a. d. Riß (Oberschwaben). *Stuttgarter Beiträge zur Naturkunde Serie B (Geologie und Paläontologie)* 276:1-167
- Sach VJ, Heizmann EPJ (2001) Stratigraphie und Säugetierfaunen der Brackwassermolasse in der Umgebung von Ulm (Südwestdeutschland). *Stuttgarter Beiträge zur Naturkunde Serie B (Geologie und Paläontologie)* 310:1-95
- Sachsenhofer RF, Gruber W, Dunkl I (2010) Das Miozän der Becken von Leoben und Fohnsdorf The Miocene Leoben and Fohnsdorf Basins. *Journal of Applied Geology* 53:9-38
- Seehuber U (2008) Litho- und biostratigraphische Untersuchungen in der Oberen Süßwassermolasse in der Umgebung von Kirchheim in Schwaben. Ludwig-Maximilians-Universität München, München
- Sohs F (1963) Das Neogen am Westrande des Leithagebirges (zwischen Hornstein und Sommerein) Unpubl. PhD-Thesis Vienna
- Thenius E (1952) Die Säugetierfauna aus dem Torton von Neudorf an der March (CSR). *Neues Jahrbuch für Geologie und Paläontologie, Abhandlungen* 96 (1):27-136
- Thenius E (1982) Ein Menschenaffenfund (Primates: Pongidae) aus dem Pannon (Jung-Miozän) von Niederösterreich. *Folia Primatologica* 39:187-200
- Zapfe H (1949) Eine miozäne Säugetierfauna aus einer Spaltenfüllung bei Neudorf a. d. March (CSR.). *Anz österr Akad Wiss mathem-nat Kl* 86 (7):173-181

online resource 2-1

for Aiglstorfer, M., Rössner, G.E., Böhme, M.: *Dorcatherium nauti* and pecoran ruminants from the late Middle Miocene Gratkorn locality (Austria)
corresponding author: manuela.aiglstorfer@senckenberg.de

D. nauti: measurements of mandibulae from Gratkorn [/ = no measurement possible]

measurements [mm]	GPIT/MA/2734	UMJGP 210694	GPIT/MA/2741
lingual height of corpus mandibulae at m1	18-19	18-19	~ 20 (laterally compressed)
lingual height of corpus mandibulae at m2	/	19-20	~ 22-23
distance of caudal rim of symphysis from p2	10 (2 from p1)	5	/
length of premolar row (p2-4)	/	35	/
length of molar row (m1-3)	~ 40	41.6	42

online resource 2-2

for Aiglstorfer, M., Rössner, G.E., Böhme, M.: *Dorcatherium nauti* and pecoran ruminants from the late Middle Miocene Gratkorn locality (Austria)
corresponding author: manuela.aiglstorfer@senckenberg.de

D. nauti: dental measurements from Gratkorn [/ = no measurement possible]

specimen	tooth	l (max) [mm]	w (max) [mm]	want (max) [mm]	h (max) [mm] at entoconid / paracone
UMJGP 204059	C				
GPIT/MA/2377	D2	/	5.2		
UMJGP 204675	D3	13.4	8.0		
UMJGP 204064	D3	15.6	8.9		
UMJGP 204067	D3	12.9	8.0		
UMJGP 204067	D4	10.7	9.5	9.7	
GPIT/MA/2375	D4	10.9	10.5	9.8	
GPIT/MA/2379	P4	10.2	10.1		
GPIT/MA/2732	M1?	11.8		14.6	
GPIT/MA/2375	M1	10.8		11.7	
UMJGP 209952	M1	11.0		11.7	

UMJGP 210698	M2	12.9		13.8	
UMJGP 210697	M3	13.9		14.4	
UMJGP 210956	d2	8.9	3.3		
UMJGP 210696	d3	13.7	/		
UMJGP 210692	d4	15.0	/		
UMJGP 204661	p2	10.1	3.6		
UMJGP 204667	p2	10.1	3.6		
UMJGP 210694	p2	10.2	/		
UMJGP 210694	p2	10.5	3.1		
GPIT/MA/2741	p2	9.9	3.3		
UMJGP 210694	p3	13.2	/		
UMJGP 204667	p3	12.8	4.5		
UMJGP 204661	p3	12.5	4.5		
UMJGP 210694	p3	12.7	4.2		
GPIT/MA/2741	p3	13.0	4.4		
UMJGP 210694	p4	11.7	5.2		
UMJGP 210694	p4	11.3	4.7		
GPIT/MA/2741	p4	11.2	5.0		
GPIT/MA/2734	p4	10.5	4.7		
UMJGP 210694	m1	11.9		6.8	
UMJGP 204664	m1	10.8		6.3	
UMJGP 204663	m1	11.6		6.4	7.4
UMJGP 210694	m1	11.1		6.3	
UMJGP 210693	m1	11.9		6.7	
GPIT/MA/2741	m1	11.7		6.7	
GPIT/MA/2734	m1	11.0		6.6	

GPIT/MA/2401	m1	12.0	6.8	
UMJGP 204663	m2	12.6	7.8	
UMJGP 204662	m2	12.6	7.5	
UMJGP 210694	m2	13.2	7.8	
UMJGP 210694	m2	13.1	7.5	
GPIT/MA/2741	m2	12.8	7.8	
GPIT/MA/2734	m2	12.4	7.4	
GPIT/MA/2756	m2	13.0	8.0	
UMJGP 204662	m3	18.3	8.5	
UMJGP 204665	m3	18.8	8.4	
UMJGP 204109	m3	17.0	8.2	
UMJGP 210694	m3	17.2	7.9	> 8.5
UMJGP 210694	m3	17.2	/	
GPIT/MA/2741	m3	18.4	8.3	
GPIT/MA/2734	m3	16.8	8.0	

online resource 2-3

for Aiglstorfer, M., Rössner, G.E., Böhme, M.: *Dorcatherium navi* and pecoran ruminants from the late Middle Miocene Gratkorn locality (Austria)

corresponding author: manuela.aiglstorfer@senckenberg.de

***D. navi*: postcranial measurements from Gratkorn** [/ = no measurement possible; [] = approximate value]

specimen	bone	measurements [mm]		
		DAPd	Dtdf	DTd
GPIT/MA/2389	sin.	[20]	[21]	[25]
	radius	DAPp	DTp	
UMJGP 210792	dex.	13.6	19.7	
GPIT/MA/2420	sin.	13.5	[21]	

GPIT/MA/2391	sin.	14.5	[22]						
	tibia	DAPd	DTd						
UMJGP 203718	sin.	[17]	[22]						
UMJGP 203419	sin.	18.2	[22.5-23]						
	cubonavicular	length (anteroposterior)	width (transversal)	height (dorsoventral)					
UMJGP 203419	sin.	[19]	[22]	[20]					
	calcaneum	DTn							
GPIT/MA/2409	dex.	9							
	astragalus	DTp	DTd	Lint	Lm	Lext	wint	wext	
GPIT/MA/2409	dex.	17.4	16.5	29.4	24.9	31.7	16.8	17.2	
	phalanx medialis	DTp	DAPps						
GPIT/MA/2745		9.7	9.8						

online resource 3-1

for Aiglstorfer, M., Rössner, G.E., Böhme, M.: *Dorcatherium navi* and pecoran ruminants from the late Middle Miocene Gratkorn locality (Austria)
corresponding author: manuela.aiglstorfer@senckenberg.de

Micromeryx flourensianus: measurements of maxillae and mandibulae from Gratkorn [/ = no measurement possible]

measurements maxillae [mm]	GPIT/MA/2388	UMJGP 204678
length of premolar row (P2-4)	16.3	/
length of molar row (M1-3)	~ 20	19.7
length of cheek teeth row (P2-M3)	~ 35	/

measurements mandibulae [mm]	UMJGP 204068
lingual height of corpus mandibulae at m1	11.9
lingual height of corpus mandibulae at m2	12.4
number and position of foramina mentalia	two, small one about 1 mm rostral of p2, larger one about 19 mm rostral of p2
length of foramina mentalia	caudal one: < 1 mm; rostral one: ~ 3.5 mm
distance of caudal rim of symphysis from p2	~ 30
length of cheek teeth row (p2-m3)	37.6

online resource 3-2

for Aiglstorfer, M., Rössner, G.E., Böhme, M.: *Dorcatherium navi* and pecoran ruminants from the late Middle Miocene Gratkorn locality (Austria)
corresponding author: manuela.aiglstorfer@senckenberg.de

Micromeryx flourensianus: tooth row lengths from Gratkorn in comparison to other specimens and literature data [/ = no measurement possible]

measurements maxillae [mm]

species	specimen	locality	source	I P2-4 [mm]	I M1-3 [mm]	I P2-M13
<i>M. flourensianus</i>	GPIT/MA/2388	Gratkorn	pers. obs.	16.3	~ 20	0.8
<i>M. flourensianus</i>	UMJGP 204678	Gratkorn	pers. obs.	/	19.7	/

measurements mandibulae [mm]

species	specimen	locality	source	l p2-4 [mm]	l m1-3 [mm]	l p2-m3
<i>M. flourensianus</i>	MNHN Sa 2957	Sansan	pers. obs.	14.5	20.5	0.7
<i>M. flourensianus</i>	MNHN Sa 2954	Sansan	pers. obs.	14.7	21.5	0.7
<i>M. flourensianus</i>	MNHN Sa 10963	Sansan	pers. obs.	15.0	21.0	0.7
<i>M. flourensianus</i>	MNHN Sa 2966	Sansan	pers. obs.	14.5	19.0	0.8
<i>M. flourensianus</i>	MNHN Sa 9773	Sansan	pers. obs.	15.0	22.0	0.7
<i>M. flourensianus</i>	MNHN Sa 2952	Sansan	pers. obs.	16.0	21.0	0.8
<i>M. flourensianus</i>	GPIT/MA/2155	Steinheim	pers. obs.	17.0	25.0	0.7
<i>M. flourensianus</i>		La Grive	Azanza 1986	15.6	20.7	0.8
<i>M. flourensianus</i>	UMJGP 204685	Gratkorn	pers. obs.	/	~ 24	/
<i>M. flourensianus</i>	UMJGP 204709	Gratkorn	pers. obs.	/	22.8	/
<i>M. flourensianus</i>	UMJGP 204068	Gratkorn	pers. obs.	15.5	22.9	0.7
<i>M. mirus</i>	minimum	Kohfidisch	Vislobokova 2007	14.0	21.8	0.6
<i>M. mirus</i>	maximum	Kohfidisch	Vislobokova 2007	15.2	21.8	0.7
<i>H. aragonensis</i>		La Ciesma	Azanza 1986	17.8	27.0	0.7
<i>H. daamsi</i>	minimum	Toril-3, Manschones-1, -2	Sánchez et al. 2010	16.6	27.7	0.6
<i>H. daamsi</i>	medium	Toril-3, Manschones-1, -2	Sánchez et al. 2010	17.5	30.0	0.6
<i>H. daamsi</i>	maximum	Toril-3, Manschones-1, -2	Sánchez et al. 2010	18.9	31.2	0.6
<i>H. duriensis</i>	EL-1	El Lugarejo	Morales et al. 1981	17.5	30.6	0.6
<i>H. duriensis</i>	EL-4-5	El Lugarejo	Morales et al. 1981	18.2	31.1	0.6
<i>H. andrewsi</i>	medium	Wolf Camp	Sánchez et al. 2011	19.5	31.7	0.6

References:

Azanza B (1986) Estudio geológico y paleontológico del Mioceno del sector oeste de la Comarca de Borja. Cuadernos de Estudios Borjanos XVII–XVIII:63-126

Morales J, Moyà-Solà S, Soria D (1981) Presencia de la familia Moschidae (Artiodactyla, Mammalia) en el Vallesiense de España: *Hispanomeryx duriensis* novo gen. nova sp. Estudios Geológicos 37:467-475

Sánchez IM, Domingo MS, Morales J (2010) The genus *Hispanomeryx* (Mammalia, Ruminantia, Moschidae) and its bearing on musk deer phylogeny and systematics. Palaeontology 53 (5):1023-1047. doi:10.1111/j.1475-4983.2010.00992.x

Sánchez IM, DeMiguel D, Quiralte V, Morales J (2011) The first known Asian *Hispanomeryx* (Mammalia, Ruminantia, Moschidae). Journal of Vertebrate Paleontology 31 (6):1397-1403. doi:10.1080/02724634.2011.618155

Vislobokova IA (2007) New Data on Late Miocene Mammals of Kohfidisch, Austria. Paleontological Journal 41 (4):451-460

online resource 3-3

**for Aiglstorfer, M., Rössner, G.E., Böhme, M.: Dorcatherium naui and pecoran ruminants from the late Middle Miocene locality Gratkorn (Austria)
corresponding author: manuela.aiglstorfer@senckenberg.de**

Moschidae: dental measurements from Gratkorn [/ = no measurement possible; [] = approximate value]

species	specimen	tooth	l (max) [mm]	w (max) [mm]	want (max) [mm]	h (max) [mm] at entoconid / paracone
<i>Micromeryx flourensianus</i>	UMJGP 204058	C				
<i>Micromeryx flourensianus</i>	UMJGP 204678	D4	6.8		5.6	
<i>Micromeryx flourensianus</i>	GPIT/MA/2387	D4	6.7		[5.5]	
<i>Micromeryx flourensianus</i>	UMJGP 204688	P2	6.3	4.0		
<i>Micromeryx flourensianus</i>	GPIT/MA/2388	P2	5.8	4.1		
<i>Micromeryx flourensianus</i>	UMJGP 204688	P3	5.1	4.9		
<i>Micromeryx flourensianus</i>	GPIT/MA/2388	P3	5.8	5.1		
<i>Micromeryx flourensianus</i>	UMJGP 204688	P4	5.2	6.0		
<i>Micromeryx flourensianus</i>	UMJGP 210972	P4	5.3	6.4		
<i>Micromeryx flourensianus</i>	GPIT/MA/2388	P4	4.5	6.1		
<i>Micromeryx flourensianus</i>	UMJGP 204688	M1	6.6		6.2	
<i>Micromeryx flourensianus</i>	UMJGP 204718	M1?	6.9		7.4	
<i>Micromeryx flourensianus</i>	UMJGP 204678	M1	6.6		6.9	> 5.1

<i>Micromeryx flourensianus</i>	GPIT/MA/2388	M1	6.2		6.6
<i>Micromeryx flourensianus</i>	GPIT/MA/2387	M1	[6.9]	[7]	/
<i>Micromeryx flourensianus</i>	UMJGP 204678	M2	7.1		7.5
<i>Micromeryx flourensianus</i>	GPIT/MA/2388	M2	7.2		7.3
<i>Micromeryx flourensianus</i>	UMJGP 204678	M3	7.2		7.5
<i>Micromeryx flourensianus</i>	GPIT/MA/2388	M3	6.8		7.5
<i>Micromeryx flourensianus</i>	GPIT/MA/2751	d3	5.5	2.4	
<i>Micromeryx flourensianus</i>	UMJGP 210971	d4	9.3	3.6	
<i>Micromeryx flourensianus</i>	GPIT/MA/2751	d4	8.6	3.9	
<i>Micromeryx flourensianus</i>	UMJGP 204068	p2	3.4	2.0	
<i>Micromeryx flourensianus</i>	UMJGP 204710	p3	5.8	2.7	
<i>Micromeryx flourensianus</i>	UMJGP 204068	p3	6.1	3.3	
<i>Micromeryx flourensianus</i>	UMJGP 204709	p4	6.6	3.8	
<i>Micromeryx flourensianus</i>	UMJGP 204710	p4	6.2	3.2	
<i>Micromeryx flourensianus</i>	UMJGP 204068	p4	6.6	3.7	
<i>Micromeryx flourensianus</i>	UMJGP 204709	m1	6.6		4.0
<i>Micromeryx flourensianus</i>	UMJGP 204685	m1	7.0		4.1
<i>Micromeryx flourensianus</i>	UMJGP 210971	m1	7.4		4.4
<i>Micromeryx flourensianus</i>	UMJGP 204068	m1	6.5		4.1
<i>Micromeryx flourensianus</i>	GPIT/MA/2751	m1	6.6		/
<i>Micromeryx flourensianus</i>	UMJGP 204709	m2	7.3		4.6
<i>Micromeryx flourensianus</i>	UMJGP 204685	m2	7.5		4.4
<i>Micromeryx flourensianus</i>	UMJGP 204068	m2	6.9		4.9
<i>Micromeryx flourensianus</i>	GPIT/MA/2751	m2	7.1		[4.8]
<i>Micromeryx flourensianus</i>	UMJGP 204709	m3	9.7		4.5
<i>Micromeryx flourensianus</i>	UMJGP 204715	m3	8.5		3.9

<i>Micromeryx flourensianus</i>	UMJGP 204685	m3	9.9	4.7	5.1
<i>Micromeryx flourensianus</i>	UMJGP 204068	m3	9.5	4.8	
<i>?Hispanomeryx</i> sp.	UMJGP 204666	M1?	> 9	8.8	

online resource 4-1

for Aiglstorfer, M., Rössner, G.E., Böhme, M.: *Dorcatherium navi* and pecoran ruminants from the late Middle Miocene Gratkorn locality (Austria)
corresponding author: manuela.aiglstorfer@senckenberg.de

Euprox furcatus: measurements of maxillae and mandibulae from Gratkorn [/ = no measurement possible]

measurements maxillae [mm]	UMJGP 204695	GPIT/MA/2736					
length of premolar row (P2-4)	26	/					
length of molar row (M1-3)	34	~ 35					
length of cheek teeth row (P2-M3)	59	/					
measurements mandibulae [mm]	UMJGP 203737	GPIT/MA/2736	GPIT/MA/2733	UMJGP 210691	GPIT/MA/2739	UMJGP 204686	GPIT/MA/2399
lingual height of corpus mandibulae at m1	21	21	20-21	22	/	/	/
lingual height of corpus mandibulae at m2	23	24	22	23	/	/	/
number and position of foramina mentalia	/	? one underneath	one underneath	one underneath	one underneath	/	/
		anterior alveola p2	anterior alveola p2	anterior alveola p2	anterior alveola p2		
size of foramina mentalia (l, h)	/	/	3, 1.5	3, 1.5	2, 1	/	/
distance of caudal rim of symphysis from p2	/	/	/	30	/	/	/
length of premolar row (p2-4)	~ 28 (lower jaw fractured)	/	26-27	27	29	/	/
length of molar row (m1-3)	42	/	41	38-40 (lower jaw fractured)	38	~ 40	~ 41
length of cheek teeth row (p2-m3)	~ 70 (lower jaw fractured)	/	68	60-65 (lower jaw fractured)	65	/	/

online resource 4-2

for Aiglstorfer, M., Rössner, G.E., Böhme, M.: *Dorcatherium navi* and pecoran ruminants from the late Middle Miocene Gratkorn locality (Austria)
corresponding author: manuela.aiglstorfer@senckenberg.de

Euprox furcatus: dental measurements from Gratkorn [/ = no measurement possible; [] = approximate value]

specimen	tooth	l (max) [mm]	w (max) [mm]	want (max) [mm]	h (max) [mm] at entoconid / paracone
GPIT/MA/2737	D2	8.8	5.1		

UMJGP 204716	D2	9.8	6.2	
GPIT/MA/2403	D3	11.5	8.0	
GPIT/MA/2738	D3	11.7	8.5	
GPIT/MA/2737	D3	10.6	7.4	
GPIT/MA/2378	D4	10.1		9.9
GPIT/MA/2382	D4	10.6	[10]	/
GPIT/MA/2738	D4	10.3		10.8
GPIT/MA/2737	D4	10.4		/
GPIT/MA/2739	P2	9.5	8.8	
GPIT/MA/2736	P2	9.4	7.5	
UMJGP 204695	P2	8.8	9.1	
GPIT/MA/2739	P3	9.7	10.5	
GPIT/MA/2739	P3	10.1	10.4	
GPIT/MA/2736	P3	10.3	10.0	
UMJGP 204695	P3	8.8	10.5	
UMJGP 204063	P3	9.3	9.7	
GPIT/MA/2739	P4	8.4	11.1	
GPIT/MA/2739	P4	8.2	11.1	
GPIT/MA/2736	P4	8.4	10.8	
GPIT/MA/2736	P4	8.3	10.9	
UMJGP 204695	P4	7.6	11.3	
GPIT/MA/2739	M1	10.5		12.7
GPIT/MA/2739	M1	10.5		12.6
GPIT/MA/2738	M1	12.2		14.2
GPIT/MA/2737	M1	12.5		12.2
GPIT/MA/2736	M1	11.5		12.8

[8.1]

GPIT/MA/2736	M1	11.7		12.6	
UMJGP 204695	M1	11.2		13.1	
GPIT/MA/2386	M1	12.3		13.4	
UMJGP 204063	M2	12.4		13.6	
GPIT/MA/2402	M2	12.7		13.7	
GPIT/MA/2739	M2	11.7		14.6	
GPIT/MA/2739	M2	11.4		14.6	
GPIT/MA/2736	M2	12.4		14.3	
GPIT/MA/2736	M2	12.6		14.1	
UMJGP 204695	M2	12.4		15.2	
UMJGP 204065	M3?	12.9		14.6	9.7
UMJGP 203445	M3?	12.2		13.8	
UMJGP 204063	M3	12.0		13.5	
GPIT/MA/2739	M3	11.3		14.4	
GPIT/MA/2739	M3	11.5		14.1	
GPIT/MA/2736	M3	12.4		13.8	
GPIT/MA/2736	M3	/		13.9	
UMJGP 204695	M3	12.3		14.5	
GPIT/MA/2386	M3	13.2		15.2	
GPIT/MA/2415	Mx	12.5		/	
UMJGP 204717	Mx	12.1		/	
UMJGP 204066	Mx	12.2		13.1	
UMJGP 210690	M1 or 2?	12.5		13.7	9.2
GPIT/MA/2374	M1 or 2?	13.3		14.8	9.2
UMJGP 203686	d2	7.9	3.3		
UMJGP 203686	d2	/	3.6		

UMJGP 203686	d3	10.0	4.4
UMJGP 203686	d3	10.0	4.2

GPIT/MA/2383	d4	14.6	7.0
GPIT/MA/2385	d4	14.2	[6.7-7]
UMJGP 204669	d4	13.4	6.4
UMJGP 203686	d4	13.1	6.0
UMJGP 203686	d4	13.1	6.4

GPIT/MA/2739	p2	8.4	4.2
GPIT/MA/2736	p2	7.5	3.7
GPIT/MA/2733	p2	7.3	3.9
UMJGP 204674	p2	8.1	4.3
UMJGP 210691	p2	7.5	3.8
UMJGP 210691	p2	7.5	4.2
UMJGP 203737	p2	7.9	4.3
UMJGP 203737	p2	8.2	[3.8]

GPIT/MA/2739	p3	9.6	5.5
GPIT/MA/2736	p3	9.7	5.1
GPIT/MA/2390	p3	10.5	5.6
GPIT/MA/2381	p3	/	5.6
GPIT/MA/2733	p3	9.6	5.2
UMJGP 204686	p3	9.9	5.3
UMJGP 204674	p3	> 9.6	5.3
UMJGP 210691	p3	8.9	4.8
UMJGP 210691	p3	9.5	5.3
UMJGP 203737	p3	9.4	5.4
UMJGP 203737	p3	9.5	4.6

GPIT/MA/2739	p4	10.5	6.0	
GPIT/MA/2736	p4	10.4	5.9	
GPIT/MA/2390	p4	10.8	6.0	
UMJGP 204711	p4	10.8	6.2	
GPIT/MA/2733	p4	10.0	5.9	
UMJGP 204686	p4	10.2	6.3	
GPIT/MA/2399	p4	11.3	6.4	
UMJGP 210691	p4	9.5	5.8	
UMJGP 210691	p4	9.9	6.2	
UMJGP 203737	p4	9.9	6.2	
UMJGP 203737	p4	10.1	[5.9]	

GPIT/MA/2739	m1	9.5		7.4
GPIT/MA/2736	m1	11.5		7.8
GPIT/MA/2385	m1	/		8.5
GPIT/MA/2390	m1	11.6		[8.2]
GPIT/MA/2748	m1	12.1		9.9
GPIT/MA/2733	m1	11.8		7.6
UMJGP 204686	m1	11.3		7.6
GPIT/MA/2399	m1	11.0		8.2
GPIT/MA/2393	m1	11.8		7.8
UMJGP 203686	m1	11.7		[7.2]
UMJGP 203686	m1	11.7		7.5
UMJGP 210691	m1	10.0		6.9
UMJGP 210691	m1	11.0		[8.1]
UMJGP 203737	m1	11.4		8.2
UMJGP 203737	m1	11.9		8.4

7.7

GPIT/MA/2739	m2	11.5	8.6
GPIT/MA/2736	m2	12.5	8.7
GPIT/MA/2390	m2	12.7	[9.2]
GPIT/MA/2750	m2	12.1	9.9
UMJGP 204711	m2	12.8	8.7
GPIT/MA/2733	m2	12.5	8.8
UMJGP 204686	m2	12.1	9.4
GPIT/MA/2399	m2	12.8	9.8
GPIT/MA/2393	m2	12.6	8.7
UMJGP 210691	m2	11.5	8.8
UMJGP 210691	m2	12.0	[9.6]
UMJGP 203737	m2	12.4	8.9

GPIT/MA/2739	m3	17.2	8.4
GPIT/MA/2736	m3	17.5	8.5
GPIT/MA/2390	m3	17.8	[9.2]
GPIT/MA/2380	m3	17.8	9.5
GPIT/MA/2755	m3	18.5	9.2
UMJGP 204711	m3	18.5	8.5
GPIT/MA/2733	m3	18.2	8.6
UMJGP 204713	m3	17.1	8.3
UMJGP 204686	m3	16.8	8.8
GPIT/MA/2399	m3	17.8	9.5
GPIT/MA/2393	m3	17.8	8.3
UMJGP 210691	m3	16.4	[8]
UMJGP 210691	m3	/	[9.2]
UMJGP 203737	m3	17.5	8.9

online resource 4-3for Aiglstorfer, M., Rössner, G.E., Böhme, M.: *Dorcatherium naui* and pecoran ruminants from the late Middle Miocene Gratkorn locality (Austria)

corresponding author: manuela.aiglstorfer@senckenberg.de

***Euprox furcatus*: antler measurements from Gratkorn** [/ = no measurement possible; [] = approximate value]

measurement (lengths in mm, angle in °)	UMJGP 204062	GPIT/MA/2398	UMJGP 210955	UMJGP 204670	UMJGP 203443
medial length of pedicle	/	/	75	60	/
distance from frontal plane to bifurcation of antler	/	/	105	/	/
anteroposterior width of pedicle at base	/	/	16-17	18	18
anteroposterior width of pedicle below the antler base	~ 22	~ 18	18.6	19	/
mediolateral width of pedicle below the antler base	~ 17	~ 17	/	~ 18	/
anteroposterior width of coronet	31	36	37.5		/
transversal width of coronet	24	32	[30]	/	/
anteroposterior width of antler immediately above coronet	27	24	32	/	/
mediolateral width of antler immediately above coronet	~ 20	~ 20	/	/	/
length of the antler shaft	35	37-38	32	/	/
length of anterior prong (measured in straight line from anterior edge of antler base to tip)	~ 90	~ 70	~ 70	/	/
length of anterior prong (measured in straight line from bifurcation of antler base to tip)	68	[40]	~ 35	/	/
length of posterior prong (measured in straight line from posterior edge of antler base to tip)	~ 115	110-115	~ 125	/	/
length of posterior prong (measured in straight line from bifurcation of antler base to tip)	80	[80]	~ 95	/	/
angle enclosed by frontal plane and posterior rim of pedicle	/	/	20-30	~ 20	/
angle enclosed by antler plane and length axis of pedicle	/	/	nearly 90	~ 45	/

online resource 4-4

for Aiglstorfer, M., Rössner, G.E., Böhme, M.: *Dorcatherium navi* and pecoran ruminants from the late Middle Miocene Gratkorn locality (Austria)

corresponding author: manuela.aiglstorfer@senckenberg.de

Euprox furcatus: postcranial measurements from Gratkorn [/ = no measurement possible; [] = approximate value]

specimen	bone	measurements [mm]			
	humerus	DAPd	Dtdf	DTd	L
GPIT/MA/2418	sin.	[25-26]	24.90	[27.6]	[155] from caput humeri to epicondylus lateralis
UMJGP 210699	dex.	[24-24.5]	23.70	[26]	
	MC	DAPp	DTp		
UMJGP 204722	dex.	14.8	20.5		

online resource 5-1

for Aiglstorfer, M., Rössner, G.E., Böhme, M.: *Dorcatherium navi* and pecoran ruminants from the late Middle Miocene Gratkorn locality (Austria)
corresponding author: manuela.aiglstorfer@senckenberg.de

Tethyragus sp.: dental measurements from Gratkorn [/ = no measurement possible]

specimen	tooth	l (max) [mm]	w (max) [mm]	antw (max) [mm]
GPIT / MA / 2753	P2	9.2	6.3	
GPIT / MA / 2753	P3	9.3	7.8	
GPIT / MA / 2753	P4	8.2	9.2	
GPIT / MA / 2753	M2	13.0		
GPIT / MA / 2392	M2	12.9		> 11.6
GPIT / MA / 2753	M3	12.8		12.0
GPIT / MA / 2392	M3	12.9		11.9

online resource 5-2

for Aiglstorfer, M., Rössner, G.E., Böhme, M.: *Dorcatherium navi* and pecoran ruminants from the late Middle Miocene Gratkorn locality (Austria)
corresponding author: manuela.aiglstorfer@senckenberg.de

Tethyragus sp.: postcranial measurements from Gratkorn [/ = no measurement possible; [] = approximate value]

specimen	bone	measurements [mm]				
	MC	DAPp	DTp	DTd	DAPd	L
GPIT/MA/4143-1	sin.	21.3	21.8	22.5	15.8	172
	cuneiform	DAP	DT			
GPIT/MA/4143-2	sin.	[12]	8.4			

Publication #4

Havlik P, **Aiglstorfer M**, Beckman A, Gross M, Böhme M. (2014) Taphonomical and ichnological considerations on the late Middle Miocene Gratkorn locality (Styria, Austria) with focus on large mammal taphonomy. *Palaeobiodiversity and Palaeoenvironments* 94, 171-188.

Own contribution:

Scientific ideas (%)	40
Data generation (%)	40
Analysis and Interpretation (%)	40
Paper writing (%)	40

Taphonomical and ichnological considerations on the late Middle Miocene Gratkorn locality (Styria, Austria) with focus on large mammal taphonomy

Philippe Havlik · Manuela Aiglstorfer ·
Annika K. Beckmann · Martin Gross · Madelaine Böhme

Received: 29 September 2013 / Revised: 25 November 2013 / Accepted: 12 December 2013 / Published online: 11 February 2014
© Senckenberg Gesellschaft für Naturforschung and Springer-Verlag Berlin Heidelberg 2014

Abstract At the Gratkorn locality (Styria, Austria), a highly diverse, late Middle Miocene (late Sarmatian *sensu stricto*; 12.2–12.0 Ma) faunal assemblage is preserved in a palaeosol. It represents the first systematically excavated and well-documented continental Sarmatian site in Central Europe. Taphonomical analysis of the 700 large mammal specimen excavated so far has led to the following conclusions: (1) the level of diagenetic alteration is low, as primary (aragonitic) mineralisation in gastropod shells is preserved and teeth and bones of large mammals in general show a relatively low total REE content; (2) the high degree of disarticulation and fragmentation in large mammal bones is induced by hunting, scavenging, trampling, and neotectonics; (3) there are no signs for fluvial transportation due to the general preservation features of the bones (e.g. no record of abrasion) and the still roughly associated fragments of individual bones and skeletons; and (4) local accumulation of large mammal bones is the result of scavenging. The fossil assemblage is considered to form a more or less autochthonous taphocoenosis without any

significant time averaging (or faunal mixing) in terms of geologic resolution (contemporaneously deposited).

Keywords Vertebrate taphonomy · REE-pattern · Middle Miocene · Scavenging · Palaeosol

Introduction

Taphonomical analysis is the fundamental tool for estimations on the role of ecological and sedimentological (e.g. diagenetic) influences on a fossil assemblage and its preservation. Circumstances of deposition, erosion, and diagenesis have a reasonable impact on the fossil record available for the reconstruction of ancient ecosystems (see e.g. Lyman 1994; Martin 1999). Invertebrate and vertebrate taphonomy in terrestrial sites is mainly influenced by disarticulation, fracturing, and transportation of shell or bone elements (by biotic as well as abiotic processes; for details, see discussions in Behrensmeyer and Kidwell 1985; Behrensmeyer 1988, 1991; Lyman 1994; Martin 1999). Estimations on the degree of diagenesis and recrystallisation in bones, teeth, and invertebrate shells are indispensable for the application of analytical methods, like e.g. isotopic measurements (Rink and Schwarcz 1995; Kohn et al. 1999). The site Gratkorn (Styria, Austria; Middle Miocene, Sarmatian *sensu stricto*, 12.2–12.0 Ma) must be considered a particular site for taphonomic analysis as it houses a mostly contemporaneous, autochthonous community (see Gross et al. 2011). Since 2005, more than 1,000 vertebrate remains (700 attributed to large mammals) have been recovered in excavations from one single layer by the Universalmuseum Joanneum Graz and the Eberhard Karls Universität Tübingen at the clay pit St. Stefan near Gratkorn. This community was investigated by classical taphonomical/palaeoecological methods (Voorhies-Analysis; estimations of completeness, weathering, disarticulation, fracturing, and

This article is a contribution to the special issue “The Sarmatian vertebrate locality Gratkorn, Styrian Basin.”

Electronic supplementary material The online version of this article (doi:10.1007/s12549-013-0142-8) contains supplementary material, which is available to authorized users.

P. Havlik (✉) · M. Aiglstorfer · A. K. Beckmann · M. Böhme
Fachbereich Geowissenschaften, Eberhard Karls Universität
Tübingen, Sigwartstraße 10, 72076 Tübingen, Germany
e-mail: philipe.havlik@senckenberg.de

P. Havlik · M. Aiglstorfer · M. Böhme
Senckenberg Center of Human Evolution and Palaeoenvironment,
Sigwartstraße 10, 72076 Tübingen, Germany

M. Gross
Universalmuseum Joanneum, Graz, Weinzöttlstraße 16, 8045 Graz,
Austria

degree of scavenging; taxonomic, body-mass, and age distribution) and geochemical/mineralogical methods (REE-content and patterns, stable isotope analysis, XRD carbonate analysis). Additionally, ecological circumstances, sedimentology of the host sediment, and the geographic position in the context of regional geology have been taken into consideration.

Geologic overview

The site Gratkorn is situated at the southern rim of the Eastern Alps (Fig. 1; Gross et al. 2014, this issue). A Neogene clastic sedimentary section (“Gratkorn Formation” according to Flügel et al. 2011) is lying discordantly on top of Palaeozoic carbonates and siliciclastics from the “Grazer Paläozoikum” (see Flügel et al. 2011). The fossil-bearing palaeosol on top of a coarse-grained braided river sequence (see Gross et al. 2011; layer 11 a and b in Gross et al. 2014, this issue) was discovered by M. Gross in 2005, during geological mapping of the area. It reaches a thickness of up to 55 cm and lithology consists of a green-grey (sometimes brownish oxidized), moderately solidified, silty-sandy clay to clayey silt/fine sand with very low primary carbonate content (for detailed information, see Gross et al. 2011, 2014, this issue), and is interpreted as a floodplain palaeosol, influenced sporadically by a braided river system during floods (Gross et al. 2011). From base (lower part of palaeosol) to top (upper part of palaeosol), a gradual decrease in grain size and slight enrichment in the carbonate content can be observed. Gravels (generally scarce; most frequent in the lower part) in the palaeosol show a predominance of igneous and metamorphic rocks in the source area (Gross et al. 2014, this issue), which crop out abundantly in today’s hinterland of the locality (Gleinalpe 20 km NW of Gratkorn; Flügel et al. 2011). Maturity of the

sediment is high (low carbonate content, well-rounded grains), grain size sorting well (fine to medium sand with small gravels). Maturity of the palaeosol is low and stratification is missing (particularly in the lower part). The upper part of the palaeosol displays more hydromorphic conditions than the lower part. The soil is overlain by marly lacustrine sediments (Peterstal Member of Gleisdorf Formation with a total thickness of at least 25 m; Gross et al. 2011).

Palaeosol formation

The palaeosol can be subdivided in an upper, clayey part (10 cm), and a lower, more sandy part (45 cm). Pedogenic carbonate glaebules are rarely observed in the lower part of the palaeosol, while microbialites up to few centimetres in diameter have been sporadically detected in the uppermost part. The time span for deposition of the primary sediment of the palaeosol was supposedly very short and is interpreted as sedimentation of a crevasse splay on a flood plain (Gross et al. 2011; 2014, this issue). The time span for soil formation was suggested to be in the range of 10^1 – 10^2 years, more likely lasting only a few decades (Gross et al. 2011). Pedogenic features (mottling, carbonate concretions, stratification, lessification, and clay cutanes) are weakly developed. This would indicate either less intense soil-forming processes or a shorter time span for formation. Since the climate during the late Sarmatian (Böhme et al. 2008, 2011), especially as recorded in Gratkorn (Gross et al. 2011; Böhme and Vasilyan 2014, this issue; based on estimations by ectothermic vertebrates) was warm-temperate to subtropical, with sub-humid conditions (seasonal changes in precipitation), the latter explanation is more plausible. Autochthonous horizontal rhizoms and roots up to several metres in length and 10 cm in thickness are preserved. Gross et al. (2011) mentioned still vertical, xyloid lignitic, partially silicified stumps of trees excavated during active mining. They are attributed to the family Cupressaceae (*Taxodioxylon*; A. Selmeier, personal communication). Those trees were most likely just rooting in the palaeosol and represent vegetation growing at the time of the lake formation. Otherwise, plant remains in the soil layer are more scarce, comprising smaller roots and rootlets, rhizomes, and *Celtis* fruits. Up to now, there have been no sedimentological signs for desiccation or flooding in the palaeosol, but, above it, laminated, calcareous, silty marls rich in leaves (“leaf layer”) comprise the basal 3 m of the lake deposits (for detailed section, see Gross et al. 2011). Only at the northern part of the outcrop on top of the palaeosol, a matrix supported gravel was observed, which is missing completely in other parts (debris flow; see Gross et al. 2011; 2014, this issue). Between 20 and 300 cm above the palaeosol, leaves associated with characean oogonia are most abundant (see Gross et al. 2014, this issue). Invertebrate remains in the palaeosol are

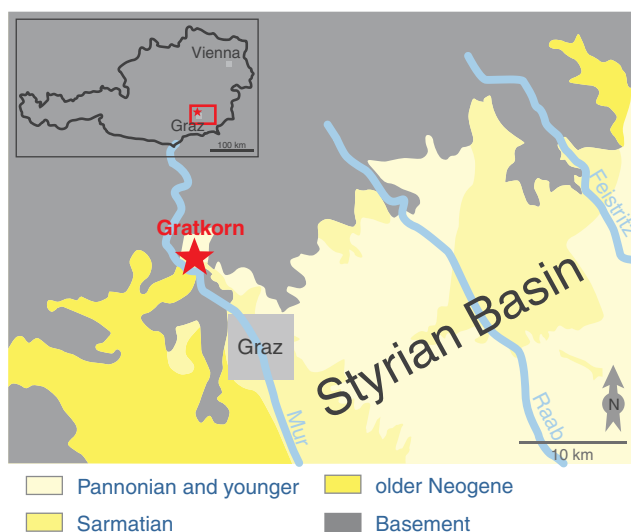


Fig. 1 Geographic position of Gratkorn and geological overview of the surroundings of the site

predominantly terrestrial gastropod shells (including slugs; Harzhauser et al. 2008), while articulated arthropods have only been detected in the lacustrine marls above (see Gross 2008; Klaus and Gross 2010; Gross et al. 2014, this issue). Vertebrate findings are restricted to the

palaeosol itself and only occur very sporadically in the lacustrine marls (these were not considered for taphonomical analysis). The most important taphonomic, ecologic and sedimentologic features of the Gratkorn locality are summarised in Table 1.

Table 1 Main taphonomic, ecologic and sedimentologic features of the Gratkorn locality (Styria, Austria)

Variable	Features observed at Gratkorn locality
Outcrop informations	
Sample size	1,000 vertebrate specimens (700 large mammals)
Surface excavated	220 m ² (2011–2013 continuous surface) and 120 m ² (2006–2010 on different sites)
Bone distribution	Grouped, no current alignment, no size separation
Articulated elements	Small mammals, one cervid vertebral column, proboscidian partial skeleton
Large mammal assemblage	
Number of species	13 (excluding carnivores)
Percentage of indeterminable bone fragments	47 %
MNI	48
NISP	363
Age profile (exluding carnivores)	
Juvenile specimen	25 % (MNI=12)
Adult specimen	60 % (MNI=29)
Senile specimen	15 % (MNI=7)
Predominant taxonomic groups	Cervidae, Tragulidae, Moschidae, Suidae
Predominant skeletal elements	Teeth, jaws, antlers
Predominant Voorhies Groups (VG)	VG III (63 %), VG I (18 %)
Pedological/sedimentological information	
Grain size	Fine clastic (silt, fine sand)
Sorting	Good (except of isolated gravels)
Redox conditions	Predominantly not oxydised, except of fossil roots and rhizomes
Carbonate content	Low (less than 10 %)
Pedogenic carbonates	Present, but only sporadically dispersed up to a few centimetres in size
Roots/rootlets/rhizoms	Frequent, up to several metres long
Bioturbation	Different kinds of presumably insect bio-turbation are frequent
Maturity	Of sediment high, of pedogenesis low
Interpretation	Palaeosol in crevasse splay on flood plain
Bone/shell biostratinomic information	
Breakage	Very common, most long bones crushed, many islated teeth
Weathering	WS 0–5
Abration	No
Diagenetic corrosion/incrustation	Iron hydroxide incrustations, different colour pattern in long bones
Bioerosion	Very common, insects, small mammal gnawing, large mammal bite marks
Bone/shell diagenetic information	
Gastropod shell mineralisation	Original aragonitic/calcitic composition
REE content	Low with no enrichment in mREE
Stabel isotope investigations	Biogenic values (Aiglstorfer et al. 2014a)
Palaeoenvironment	
Palaeoprecipitation	486±252 mm/ year(Gross et al. 2011, Böhme and Vasilyan 2014)
Climate	Temperate subtropical, (MAT=15 °C; Böhme and Vasilyan 2014)
Palaeogeography	At the rim of Eastern Alps; northern border of Styrian Basin

MNI minimum number of individuals, *NISP* number of identified specimen, *WS* weathering stage, after Behrensmeier (1978)

Materials and methods

Excavation technique

The excavation technique chosen for documentation of the faunal assemblage consist in systematic open area excavations recording the exact position of each finding by drawings and digital photography. Vertebrate findings larger than 1 cm were documented in detail (centimetre scale) in excavation plans based on a 1-m-square grid (scale 1:20) and photographed. Since 2011, it has been possible to excavate a continuous area (see overview in Gross et al. 2014, this issue) which was extended up to 2013 on a surface of 220 m². As the palaeosol is solidified to a certain degree, only the uppermost 10–20 cm could be excavated every year, while deeper strata were dug in the following year after surface weathering. For taphonomic analysis, results of excavation campaigns 2005–2012 were considered, while first data from campaign 2013 were only partially available. The exact stratigraphic position of specimens (basal lacustrine marls, and upper and lower parts of palaeosol; see section in Gross et al. 2014, this issue) was documented and considered, if possible. Due to considerable amounts of neotectonics (faults), a gradual lithofacial change along the section from base to top, and biotic influences on the deposition of vertebrate remains, the subdivision of an upper and a lower part of the soil can only be given approximately in many cases.

Coordinates given in figures follow Austrian Grid (BMN M34–GK) without using abbreviations.

Large mammal taphonomy

The terms ‘small mammals’ and ‘large mammals’ are used in different ways in the literature (body mass or taxonomically). We used a taxonomical definition and thus distinguish the groups of rodents, insectivores, and lagomorphs (small mammals) from perissodactyla, artiodactyla, proboscidea, and carnivora (large mammals). Expanded Voorhies analysis of vertebrate remains follows Behrensmeyer (1975). Minimum numbers of individuals (MNI) have been reconstructed for large mammals following the concept by Lyman (1994, p. 100 ff.). Besides the singularity of every anatomical element, attrition of teeth was also taken into consideration. Body mass estimations follow Merceron et al. (2012), Costeur et al. (2013), and Aiglstorfer et al. (2014b, d, this issue).

Age classes were defined as follows: juvenile (deciduous dentition), adult (permanent dentition), and senile (trigonid of m1 completely worn). Due to the clear abundance of tooth remains and the scarcity of well-preserved postcranial material or articulated skeletons, a more detailed subdivision considering tooth wear combined with fusion of postcranial long bones is not realistic for the Gratkorn material. Young adult specimens, such as, e.g. a *Deinotherium levius* vel *giganteum*

partial skeleton, with not fully fused epiphyses, are therefore not disclosed separately but included in adult specimens. A delayed fusion of the long bones and continuation of growth beyond sexual maturity has been observed in modern proboscideans (Poole 1996; in males even up to the age of 30–45 years; see discussion in Aiglstorfer et al. 2014b, this issue). Specimens only documented by postcranial elements are considered adult in all cases, if fusion of long bones is completed and no signs of attrition indicate a senile age.

REE analysis with LA-ICP-MS

Analysis of powder only delivers an average composition of bone or tooth (Trueman 2007) and is more at risk of contamination by filling of microcracks or haversian canals. Laser ablation-inductively coupled plasma-mass spectrometry (LA-ICP-MS) in contrast is distinguished by minimum sample preparation (and the possible contamination during this process) and allows a precise space-resolved sampling, helping to reduce the degree of contamination and allowing to exactly sample the desired tissue (see, e.g. Rogers et al. 2010 for discussion and references). As pointed out by Rogers et al. (2010), LA-ICP-MS has so far only rarely been applied in palaeontological research, but as it has proved to be an ideal analytical tool in work with complex materials such as fossil bones and teeth, it has been used more in recent years (see, e.g. Herwartz et al. 2013). A total of 23 samples, including 11 bone fragments and 12 tooth fragments, were analysed for REE-composition and Sr-content using LA-ICP-MS. Of the tooth fragments, 12 samples were gained from dentine, and 9 from enamel. Specimens were set in epoxy blocks, ground, and polished with agglomerated alpha alumina suspension in order to prepare a plane surface. Blocks were cleaned with distilled H₂O and placed directly in the sample chamber of the LA-ICP-MS system (resonetics RESolution M-50, coupled with a Thermo Scientific iCAP Q ICP-MS). The samples were analysed with a spot size of 33 µm, a repetition rate of 5 Hz and an energy density of 3.5 J/cm². Time per measurement was scheduled as 120 s. Measured lines were positioned in an area of less than 2 mm distance from the outer bone rim. The course of the line scans was visually controlled to avoid contamination due to, e.g. Haversian canal fillings and fractures or microcracks, where possible. Time-resolved ICP-MS spectra showed variations of REE content related to heterogeneous composition and microcracks. In these cases, scans were reduced to areas with stable REE contents. Measurement conditions in the Thermo Scientific iCAP Q ICP-MS were: rF Power 1,550 W, carrier gas flow (He) 0.6 l/min+0.003 l/min N₂, makeup gas (Ar) 0.88 l/min. For calibration, the following standards were used: NIST 611 and NIST 613 (The National Institute of Standards and Technology), as well as T1-G (MPI-DING reference glass, MPI Mainz) for control of quality. For bones and teeth, ⁴³Ca was used as an internal standard to calculate absolute element concentrations from signal intensities. Following Herwartz

et al. (2013), calcium content was assumed to be 36 wt% based on typical Ca contents measured for fossil bones. Most bone samples are assumed to have a Ca content within 2–3 % (Herwartz et al. 2013). Therefore, these 2–3 % need to be added to the external precision of the LA-ICP-MS element concentrations, which is typically better than 5–10 % (Herwartz et al. 2013). Detection limits for the dataset are generally 0.1–0.5 ppm for REE. All samples were standardised with Post-Archaean Australian Shale (PAAS) values of Taylor and McLennan (1985).

Mineralogical analysis

For a non-invasive determination between calcite and aragonite in the gastropod shells, X-ray μ -diffraction analysis was performed using a BRUKER D8 Discover θ/θ GADDS microdiffractometer with a beam diameter of app. 300 μm , due to the used monochromator optic and a large VÅNTEC-500 two-dimensional detector (μ -XRD²) covering 40° in the 2 θ and chi range (Berthold et al. 2009).

Material repository

Material is stored at the Universalmuseum Joanneum, Graz, section for geology and palaeontology (UMJGP), and at the Palaeontological Collection of Eberhard Karls Universität Tübingen (GPIT).

Results and discussion

Plant preservation

The various parts of the soil and the lacustrine marls display different kinds of plant tissue preservation. In the whole palaeosol, calcitic fructifications of *Celtis* are locally abundant, frequently preserved in groups of dozens of specimens. In the lower, more sandy part of the palaeosol roots and rhizomes up to several metres long and 10 cm in diameter were excavated. While the roots and rhizoms themselves are preserved as oxidized organic material or completely decomposed, early diagenetic, brownish iron hydroxide concretions grew around them, preserving the course of the root and its uncompacted cast. Adherent sediment is frequently oxidized up to 50 cm around roots. Noteworthy pyrite or coal layers, indicating anoxic conditions, were not detected. In the upper part of the palaeosol, rhizomes are preserved as oxidized organic material, but without any iron hydroxide concretions (GPIT/IC/253; Fig. 2d, black arrow). With the typical alignment of nodes and rootlets, the rhizomes (Fig. 2f) are attributable to Poales (D. Uhl, personal communication), comprising grasses and sedges. Because of their size (diameters up to 5 cm), giant forms must be assumed, similar to extant *Arundo*,

which reaches several metres in height. They are interpreted as deeper rhizomes of plants growing at the time of deposition of lacustrine marls above the palaeosol. In the uppermost part of the palaeosol, only rootlets, up to 2 mm in diameter, are preserved as brownish impressions. Above the palaeosol, leaves occur frequently, comprising both terrestrial and aquatic species and related fructifications (*Potamogeton*, Characeae, *Salix*, *Alnus*, and other taxa). But cuticular preservation is largely missing, especially in the southern part of the pit. In the uppermost part of the palaeosol, several carbonate nodules have been excavated, ranging in diameter from 10 to 25 cm and showing a clearly flattened, suboval shape with an irregular, cauliflower-like surface (GPIT/LI/731; Fig. 2a). In thin sections (Fig. 2b), internal lamination was observed, but no pillar-structures, as expected, e.g. in freshwater stromatolites or laminated cyanobacterial mats in general (see classification in Gerdes 2007). Therefore, the structures were identified as non-cyanobacterial biomats, or generically as microbialites. Isotopic composition of the microbialites compared to the sediment in the upper part of the palaeosol shows a depletion in ¹³C from $\delta^{13}\text{C} = -7.7\text{‰}$ (sediment) to $\delta^{13}\text{C} = -12.6\text{‰}$ VPDB (microbialite), which may be interpreted as a biological fractionation, whereas the $\delta^{18}\text{O}$ -values are very similar [7.2‰ (sediment), 7.7‰ VPDB (microbialite); values from Aiglstorfer et al. 2014a, this issue]. Carbonate content in nodules is high (85 %), whereas it is very low in the sediment (0.1 %; values from Aiglstorfer et al. 2014a, this issue). Charophytes of the species cf. *Nitellopsis meriani* are documented as abundant from a layer 50 cm above the palaeosol, in the laminated lake sediments. After interpretation in Bhatia et al. (1998), this taxon is indicating water depths of 4–12 m.

Invertebrate taphonomy and ichnology

Gastropods

Gastropod shells are abundant, especially in the upper part of the palaeosol, and consist of the so far endemic *Pseudidyla martingrossi* Harzhauser et al. 2008 and *Pleurodonte michalkovaci* Binder and Harzhauser, 2008, and 13 additional species of predominantly terrestrial shell bearing pulmonata (including only two fragments of two different aquatic taxa), and slugs (Harzhauser et al. 2008). While the large shells of *Pleurodonte michalkovaci* (diameter up to 3 cm) are heavily crushed due to lithostatic pressure (GPIT/GA/5044; Fig. 2c), the smaller (up to 5 mm high) gastropods, such as *Pseudidyla*, or isolated nuclei of different species, are almost uncrushed. Most likely, the higher clay content in the upper part of the palaeosol in contrast to the lower part, and the therefore resulting higher degree of compaction during diagenesis, caused crushing of the large, fragile shells. Apparently, there

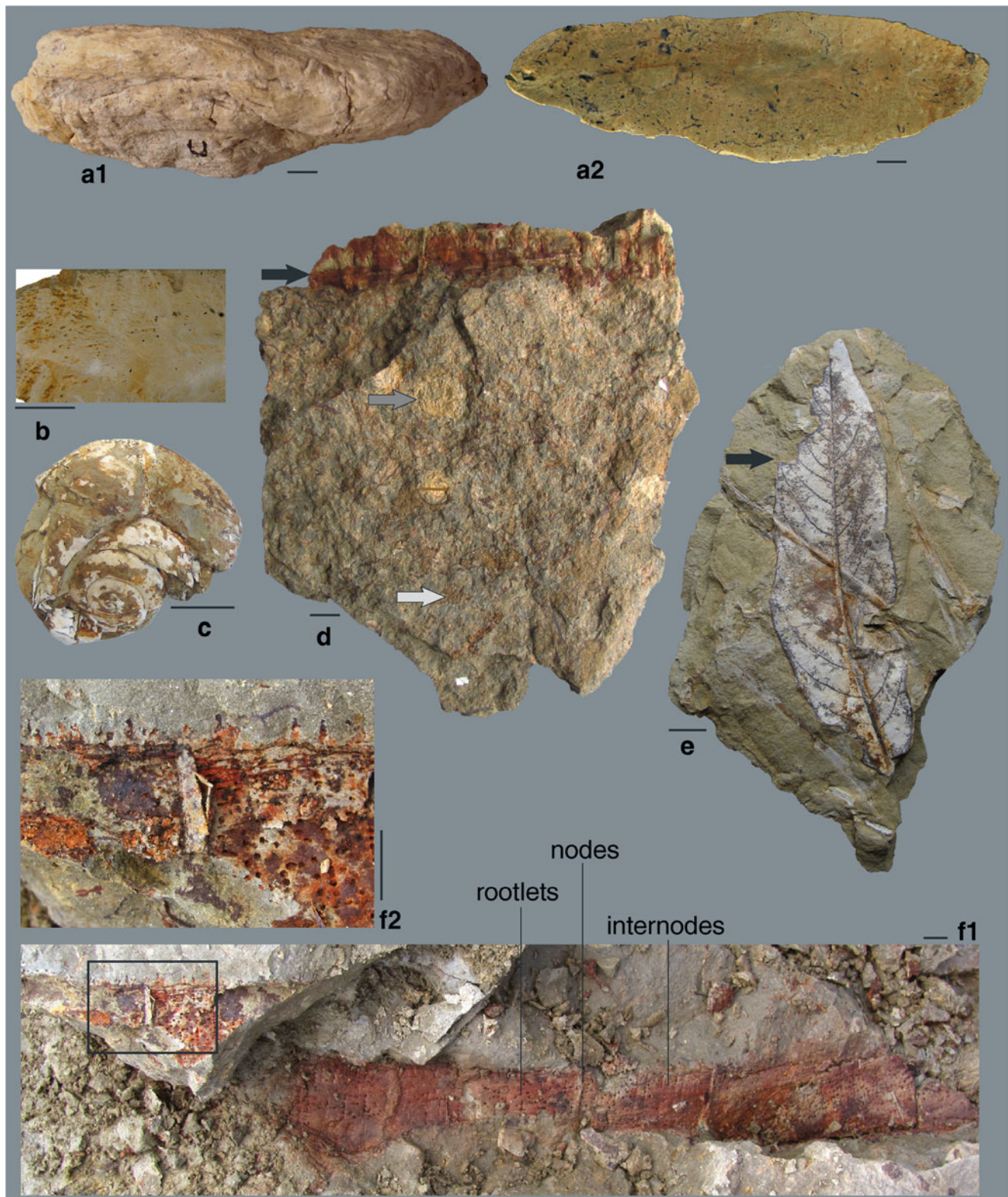


Fig. 2 Preservation of plants and invertebrates at Gratkorn locality: **a** microbialite in side view (1) and in transversal section (2; GPIT/LI/736), **b** thin section of (a) with laminar structures, **c** diagenetically crushed shell of *Pleurodonte michalkovaci* (GPIT/GA/5044), **d** horizontal surface of a sample from the upper part of the soil layer with a fossil root (dark

arrow), back-filled burrows (grey arrow) and sand lenses (white arrow; GPIT/IC/253), **e** leaf of *Salix*, showing signs of margin feeding by insects (leaf-layers approx. 15 cm above the top of palaeosol; GPIT/PL/761), **f** horizontal rhizome of Poales gen. et sp. indet. (1) and detail with rootlets and node (2); scale bar 1 cm

is no gastropod record from the lower part of palaeosol, as it represents a deeper horizon of the whole palaeosol and thus was not accessible for gastropods. Frequent findings of the more compact slug shells, attributed to *Testacella schuetti* Schlickum 1967 and *Limax* sp., do not show signs of compression in contrast to the pulmonate shells. Furthermore, there are no indications for prolonged transportation observed in the gastropod record, such as fragmentation (e.g. Hanley and Flores 1987).

The level of recrystallisation in gastropod shells is very low, as XRD analysis tested primary aragonitic shell composition for the surface of *Pseudidyla martingrossi* and *Pleurodonte michalkovaci*. The mineralogical composition of slug shells, such as *Limax* sp., consists in calcite crystals similar the extant *Limax maxima* (Furbish and Furbish 1984). Unfortunately, information on the shell structure and mineralogy of extant taxa of this genus is rather scarce (Tompa 1980) and interspecies differences in crystallite sizes rather than recrystallisation can therefore not be excluded for the slug shells at Gratkorn. In any case, primary carbonate (aragonitic) shell preservation of other gastropod shells at Gratkorn indicates a low level of diagenetic recrystallisation, and therefore makes a secondary decalcification of the palaeosol unlikely, leading to the interpretation of a primarily carbonate-depleted sediment according to bedrocks exposed in the source area.

Arthropods and ichnology

The arthropod fauna from Gratkorn consists of a thin-shelled limnic ostracod fauna (11 species; Gross 2008), in freshwater crabs of the genus *Potamon* (Klaus and Gross 2010) and in a very few land-living arthropods, all preserved in the lacustrine siltstones and marls above the palaeosol. Articulated terrestrial arthropods are preserved as brownish impressions in the leaf-rich, laminated siltstones up to 1 m above the palaeosol. So far, they comprise one woodlouse (Oniscidea) and one shieldbug (Pentatomoidea) (undescribed). Signs of insect feeding (margin feeding) have been observed on a few leaves, but cannot be assigned to specific taxa (GPIT/PL/761; Fig. 2e). Skeletisation and other kinds of feeding marks on leaves are not clear enough to be classified in detail.

Although in the palaeosol itself no body fossils of insects are preserved, abundant ichnofossils have been recorded and classified as fodichnia and domichnia of different species (nomenclature after Seilacher 1964). Fodichnia, in terms of scavenging marks, were observed on some vertebrate specimens, such as, e.g. on the root of a rhinocerotid tooth (UMJGP 203459; Fig. 3d), and indicate the presence of osteophagous insects. The marks on the tooth root are similar in size and orientation to those described by Fejfar and Kaiser (2005) and interpreted as gnawing marks of termites, but strongly differ from those observed in the Pliocene of

Tanzania and the Holocene of South Africa, as the scratches are not as strictly concentric in the former (for comparison, see figures in Fejfar and Kaiser 2005; Backwell et al. 2012). Given a record of termites in slightly younger sediments from the Styrian Basin (Lower Pannonian, 11.3 Ma; Engel and Gross 2009), the presence of termites damage does not seem unlikely for Gratkorn, but we can only attribute the scavenging marks to termites with reservations. An additional indication of the presence of social insects is given by sand-filled burrows of a few millimeters to 3 cm in diameter, where the sediment is oxidized (Fig. 2d; light grey arrow). The burrows are reticular and thickened in the parts where they meet. Therefore, they are interpreted as domichnia, similar in shape to different kinds of social insect burrows (e.g. ants or termites), but, due to the high variability and the few descriptions of comparable extant structures available (Tschinkel 2003), a more detailed classification is not possible.

Other kinds of bioturbation, again representing fodichnia, consist of vertical back-filled burrows up to 1.5 cm in diameter (Fig. 2d; dark grey arrow). As only cross-sections of burrows are preserved and no chambers are known up to now, a designation to a certain ichnogenus is limited. However, due to their morphology, they could be interpreted as traces of deposit-feeding soil invertebrates, like, e.g. beetles and cicada (Hembree and Hasiotis 2008 and citations therein). They correspond well in size and shape to *Beaconites kytosichnus*, an ichnogenus emended by Hembree and Hasiotis (2008) for burrows observed in a Miocene palaeosol from Colorado in sandy siltstones with rhizolites. A designation to this ichnogenus can be given only tentatively, as the diagnostic cocoon-bearing chamber is missing and therefore a distinction from other ichnogenera like *Taenadium*, *Muensteria*, and *Anchorichnus* is almost impossible.

Large mammal taphonomy

Overview

Vertebrate findings are mostly restricted to the palaeosol itself and occur only sporadically in the overlying lacustrine marls. They consist of large and small mammals as well as birds, reptiles, amphibians, and scarce remains of fishes (fishes only in the lacustrine marls; for detailed faunal composition, see Gross et al. 2011; Aiglstorfer et al. 2014a, b, c, d, this issue; Böhme and Vasilyan 2014, this issue; Göhlich and Gross 2014, this issue; Prieto et al. 2014, this issue; Van der Made et al. 2014, this issue). Large mammals comprise the proboscidean *Deinotherium levius* vel *giganteum*, three rhinocerotid species, *Aceratherium* sp., *Brachypotherium brachypus*, *Lartetotherium sansaniense*, and the chalicothere *Chalicotherium goldfussi*, while equids are only recorded by few bones of *Anchitherium* sp.. Most abundant are ruminants, with the most frequent species *Euprox fircatus* and the second



Fig. 3 Preservation of large mammal remains at Gratkorn locality (*scale bar* 1 cm): **a**,2 modern analogue: left humerus of *Capreolus capreolus* (extant) showing clear signs of gnawing by *Vulpes vulpes* and **b**,2 left humerus of *Euprox furcatus* (GPIT/MA/2418) showing similar biting marks; **c** distal fragment of ruminant right femur with tooth puncture (UMJGP 210695), note the iron oxide crust on surface, **d**1,2 *Lartetotherium sansaniense* left m/1 (UMJGP 203459): insect bioerosion marks on the root of tooth and detail with redrawing of marks, **e** bone fragment (GPIT/MA/4519) with clear signs of digestion such as dissolution of the surface (**e2**) but still showing the structure of spongiosa inside (**e1**), **f** *Listriodon splendens* right M2/(GPIT/MA/2757), 1 broken into several pieces, and 2 after preparation, **g** unidentified long bone (GPIT/MA/3852) heavily fractured by trampling, **h** fragment of deinothere ?scapula (UMJGP 204103) with gnawing marks by a large carnivore, **i** semiarticulated vertebral column and pelvis? of ruminant (UMJGP 210804; *scale bar* 1 cm)

most frequent *Dorcatherium navi*. The bovid *Tethytragus* sp., the moschid *Hispanomeryx* sp., and a large palaeomerycid are rare. The ‘smallest’ large mammal, the moschid *Micromeryx flourensianus*, is recorded with six specimens. Two different species of suids are part of the Gratkorn large mammal community: the more bunodont *Parachleuastochoerus steinheimensis*, and the more lophodont *Listriodon splendens*.

Distribution, disarticulation and decomposition of skeletal elements

Though assignment to different levels of the palaeosol is restricted due to the gradual change from the lower to the upper part, and due to strong neotectonic activities (represented by frequent slickensides of normal faults; Gross et al. 2011) resulting in a strong unevenness of the palaeosol, field experience tentatively allows the following observation on the abundance of certain taxa in single parts of the soil: partly articulated/associated fossorial herpetofauna (Böhme and Vasilyan 2014, this issue) and small mammals (Prieto et al. 2014, this issue) are restricted to the upper part of the palaeosol, and cervids are more abundant therein, while suids and heavyweight large mammals are more frequent in the lower part. Nevertheless, all findings must be considered to be deposited in a short time span, maximally several decades, as, for example bone fragments from the same skeletal element of a single individual were excavated in different horizons of the palaeosol. Trampling must be considered a very important burial, as well as fracturing mechanism for large mammal bones.

Large mammal remains are not randomly distributed in the palaeosol but locally concentrated (density illustrated on metre scale in Fig. 4). While excavation campaigns in 2011 and 2012 recovered several jaws of ruminants, during the campaign in 2010 only a very few large mammal bones and jaws were detected, though a similar-sized area was excavated. Large mammal remains are mostly

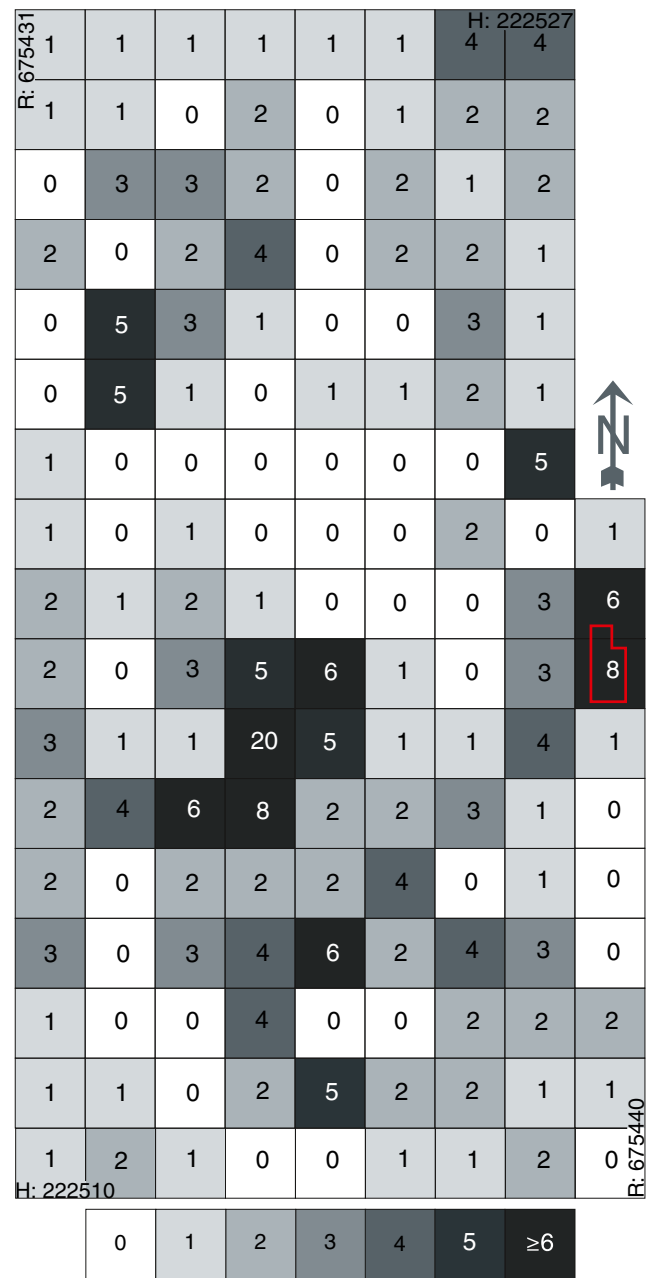


Fig. 4 Excavation map of campaigns 2011 and 2012 with additional data from 2013 showing the heterogeneous concentration of large mammal specimen per square metre. Numbers indicate the number of objects excavated; coordinates are in Austrian Grid (BMN M34–GK), red line shows outline of Fig. 5

disarticulated. Only one partial skeleton of *Deinotherium levius* vel *giganteum* (Aiglstorfer et al. 2014b, this issue), and some postcranial ruminant material (UMJGP 210804; Fig. 3i) are partially articulated. Assuming a dislocation of carcasses by carnivores, this would rather point to scavengers than to predators (Palmqvist and Arribas 2001). Palmqvist and Arribas (2001) based their distinction between predators (leopards) and scavengers (hyaenas) on data generated from recent ecosystems. They characterised

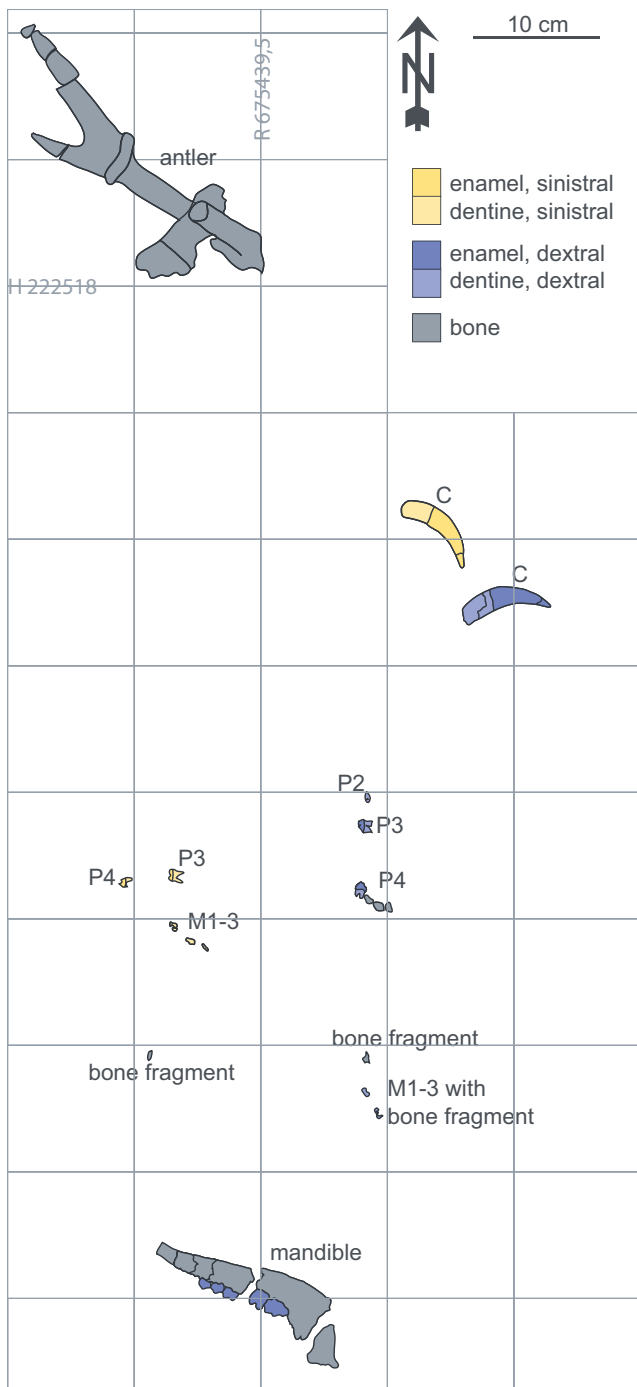


Fig. 5 Detail of excavation map of the campaign 2012 showing fragments of the skull of one individual of *Euprox furcatus* scattered over a large surface due to trampling (antler UMJGP 210955; skull fragments and teeth GPIT/MA/2736)

primary assemblages (collected by predators) as rich in articulations, and secondary assemblages (collected by scavengers) as poor in articulations, except of metapodials and vertebra. Such a secondary assemblage corresponds to the record from Gratkorn (Fig. 3i). Rough assemblages of individuals are more common, and in many cases skull

fragments or tooth rows, especially in ruminants, were found in relative proximity and are clearly assignable to single individuals (Fig. 5; see also Gross et al. 2011). Long bones are commonly fractured into several splinters by longitudinal and transverse as well as helical fractures in a single specimen (nomenclature after Haynes 1983). Long bone fragments, which were excavated in adjacency, show perfect fitting without any signs of abrasion or erosion on the fracture surface (GPIT/MA/3852; Fig. 3g). Heavy breakage of bones could be explained by the following mechanisms: trampling, scavenging, weathering, and tectonics. Trampling by larger herbivores shortly after deposition is often observed in modern large mammal assemblages. Lyman (1994) states that breakage of bones by trampling is more likely after some weathering when the bone is no longer so durable, and that fitting of contiguous fragments, as observed in Gratkorn, would indicate trampling rather than breakage prior to final deposition. Furthermore, dipping of bones (typically for trampling; Shipman 1981; Haynes 1983; Badiola et al. 2009) can be observed for several long bone fragments at Gratkorn. In Fig. 3g, a large mammal long bone (presumably a ruminant) is shown, broken into splinters with clear dislocation of few centimetres and dipping fragments. Another biotic factor for strong fragmentation is gnawing and scavenging by carnivores. Some bone crushing possibly results from sediment compaction, and in other cases neotectonics lead to vertical movements up to 10 cm (see, e.g. fig. 5c in Gross et al. 2011).

Different degrees of weathering stages (Behrensmeyer 1978) can be observed in the large mammal record from Gratkorn, but are difficult to quantify as in many cases diagenetic iron hydroxide incrustations and diagenetic alteration overprint the primary weathering stage. Those impregnations on bones and splinters of different large mammal remains can be up to 1 mm thick. The partial skeleton of *Deinotherium levius* vel *giganteum* comprises many bones, which are strongly weathered (weathering stage 5; after Behrensmeyer 1978) and often the bone compacta is not preserved, but only bone spongiosa. It shows clear signs of a prolonged exposure, such as fragmentation on the surface and scavenging of larger carnivores (see discussion below; Fig. 3h; and Aiglstorfer et al. 2014b, this issue). This could be explained by the size of the bones, which are much larger than in all other species from Gratkorn, and therefore the skeleton was probably not covered so soon and bones not dislocated as deep into the palaeosol as observed in other specimens. This is well in accordance with recent decomposition data in modern elephants (Coe 1978; Conybeare and Haynes 1984; see discussion in Aiglstorfer et al. 2014b, this issue). Furthermore, the deinotherium remains are sticking out over the top of the palaeosol and many remains were recovered from the uppermost part of it, which led to longer exposure

near or on the surface and therefore stronger weathering during early diagenesis. Such boundaries between lithologies with different fluid flow ratios often provide ideal conditions for groundwater permeability. Such diagenetic fluids influence preservation of the Gratkorn large mammal remains (at least near or on the surface) to a certain degree as, e.g. shown by the iron hydroxide incrustation described above (Fig. 3b, g, h).

Other remains, for example some ruminant long bones, are fractured but still possess a smooth surface and do not show any signs of, e.g. flaking or chemical weathering (weathering stage 0 or 1; after Behrensmeyer 1978). Different degrees of weathering stages in the Gratkorn assemblage indicate that the faunal assemblage did not result from a mass mortality, but rather from accumulation over some years or decades (Behrensmeyer 1978).

Besides fracturing of bones, teeth are also disrupted (e.g. M2 dex. of the suid *Listriodon splendens* GPIT/MA/2757; Fig. 3f), with splinters found clearly distant from each other (some up to several decimetres) still showing perfect fittings. This is more likely for teeth that are broken by trampling, as weathered, splitting teeth would be more likely to lose small pieces that would prevent perfect re-fitting (A.K. Behrensmeyer, personal communication). Fracturing of teeth can be observed at Gratkorn in robust teeth with thick enamel (e.g. molars of *Listriodon splendens*) and more fragile teeth with thinner enamel, as, e.g. in cervids. While tooth fragmentation in the more fragile teeth can easily result from sediment compaction (comparable to preservation of gastropod shells described above) and trampling, tooth disruption of, e.g., suid molars is more likely to result from weathering and trampling. Tooth splitting when desiccating at the surface was described by Behrensmeyer (1978) for extant mammal remains of the Amboseli basin (Kenya). As she observed differences in weathering more dependent on the individual morphology and characteristics of the tooth (eruption, stage of wear, enamel thickness) than on surface exposure and climatic conditions, she stated that weathering stages are not as applicable to teeth as they are to bones. Keeping in mind that molars of *Listriodon splendens* possess a rather thick enamel, and including observations of longitudinal tooth splitting on a camel skeleton in Abu Dhabi (Andrews and Whybrow 2005) it seems likely, that longer surface exposure and increased aridity (low absolute humidity; as commonly observed in desertic environments; M. Böhme personal observation) might have enhanced splitting of the suid teeth. A peculiarity of the Gratkorn site is the frequent occurrence of transversal fragmentation of teeth besides longitudinal fragmentation (Fig. 3f), which cannot be explained by long surface exposure or desiccation, but probably by neotectonic activities (see dislocation of the lower part of tooth in finding position in Fig. 3f).

Current alignment of long bones, size sorting or abrasion was not observed in bones from the Gratkorn locality. Small and large mammal remains as well as small and large bone

splinters are preserved in vertical as well as horizontal adjacency. A prolonged transportation (e.g. fluvial, see below) of bones or teeth after skeletisation and disarticulation of the animal can be excluded due to the described perfect fittings of fragments and the lack of any indications of transport (see also discussion in Badiola et al. 2009).

Bioerosion

Signs of bioerosion by invertebrates and vertebrates are present on many large mammal remains from Gratkorn, and comprise insect osteophagy, scavenging of different kinds and small mammal gnawings. Bioerosion by insects was observed in a few cases, and is possibly attributed to termites (see “Arthropods and ichnology”). Small mammal gnawing marks of the ichnogenus *Machinus* are very frequent on many large mammal bones as well as on turtle shell fragments (Gross et al. 2011). As a description of these trace fossils is in progress, this topic will not be discussed in detail here.

As mentioned above, gnawing and scavenging by carnivores plays a major role in the fracturing and fragmentation of long bones. The preferred accumulation of tooth material in comparison to long bones or axial skeleton elements could be explained by the general consumption sequence (e.g. discussion in Lyman 1994) and enhanced trampling. While postcranial flesh is consumed first, mandible and maxilla flesh are often last to be consumed by carnivores (Blumenshine 1987; Lyman 1994). Most large mammal long bones discovered comprise distal or proximal epiphyses with most of the shaft missing. Most of the femora excavated comprise more or less only the distal articulation. Extensive marrow consumption could explain this kind of fragmentation and would rather point to an accumulation by scavengers than by predators (Palmqvist and Arribas 2001). In fact, in the consumption sequence of marrow by Blumenshine (1987), femora are consumed first, followed by most long bones, and last are pulps of the skeletal elements (especially skull and mandible). On a humerus of the cervid *Euprox furcatus* (GPIT/MA/2418; Fig. 3b), bite marks (puncture marks) at the proximal epiphysis can be observed. Similar bite marks by *Vulpes vulpes* can be observed on a humerus of the extant *Capreolus capreolus* (Fig. 3a) and indicate that a medium-sized carnivore was responsible for some of the bite marks from Gratkorn. Bite marks on the distal fragment of a ruminant femur (UMJGP210695; Fig. 3c) fit well to size and morphology of the tricuspid P4 of an yet undescribed carnivore discovered at Gratkorn locality. Besides bite marks, chewing marks of an unknown larger carnivore can be observed on a fragment of the scapula of *Deinotherium levius vel giganteum* (UMJGP 204103; Fig. 3h).

Only one bone fragment from Gratkorn could be interpreted as digested (GPIT/MA/4519; Fig. 3e). Because of the strong alteration of bony material and the high but irregular degree of “surface rounding” on this specimen, we

consider it to represent a coprolite or a regurgitated bone (in any case, a partially digested bone fragment). This interpretation is supported by the visible damage to the microstructure of spongiosal bone material in a cross-section of the specimen (Fig. 3e1). Another specimen with evidence of rounding could be explained by gnawing of micromammals and scavengers. One single phosphatic coprolite (Hyaenidae? UMJGP 209210) has been excavated has so far (Gross et al. 2011). Considering Thulborn (1991) and literature cited therein, preservation of coprolites in a palaeosol is most probably restricted to at least temporarily arid climates. Humid conditions would quickly destroy coprolites. The reconstructed seasonality and precipitation ratios of 486 ± 252 mm/year

(Gross et al. 2011) could well favour the preservation of coprolites, assuming a burial of this coprolite prior to the wet season. As there are no visible septaria-like cracks, the assumption of a rapid covering is supported and an extended pre burial desiccation of the coprolite itself can be excluded.

Voorhies analysis

A total of 363 out of 700 large mammal remains were analysed in an expanded Voorhies classification (expanded Voorhies groups: I, I-II, II, II-III, III, according to Voorhies 1969 and expanded by Behrensmeyer 1975) for obtaining an estimate of possible fluvial transportation. As the Voorhies classification is limited to anatomically designable objects, undetermined splinters or fragments are not considered (Fig. 6a). Furthermore, according to classifications of Voorhies (1969) and Behrensmeyer (1975), different parts of bones have to be classified into different groups, because of their morphology, e.g. isolated articulation surfaces (if broken off or if resulting from not completely closed symphysis; juveniles) should be classified in a different way than more complete long bones. The results of the analysis, additionally resolving the anatomical position of the specimens analysed are shown in Fig. 6b. As the sample was taken from material discovered during well-documented excavations, we expect this result to be representative for the whole fossil-bearing palaeosol at the Gratkorn site. Although all Voorhies groups are present in the sample, 63 % of bones are attributed to Voorhies group III, which is considered to contain bones resistant to prolonged fluvial transportation, such as teeth, jaw fragments, and astragali. Apparently isolated teeth are heavily over-represented (146 isolated teeth, 30 assignable fragments), and frequently associated with skull fragments or antlers (in ruminants). But there is also a remarkable number of specimens attributed to Voorhies group I (e.g. vertebra, ribs). These elements are considered to be non-resistant to transportation, because of their shape. The Voorhies data gained from Gratkorn are in agreement with data from the

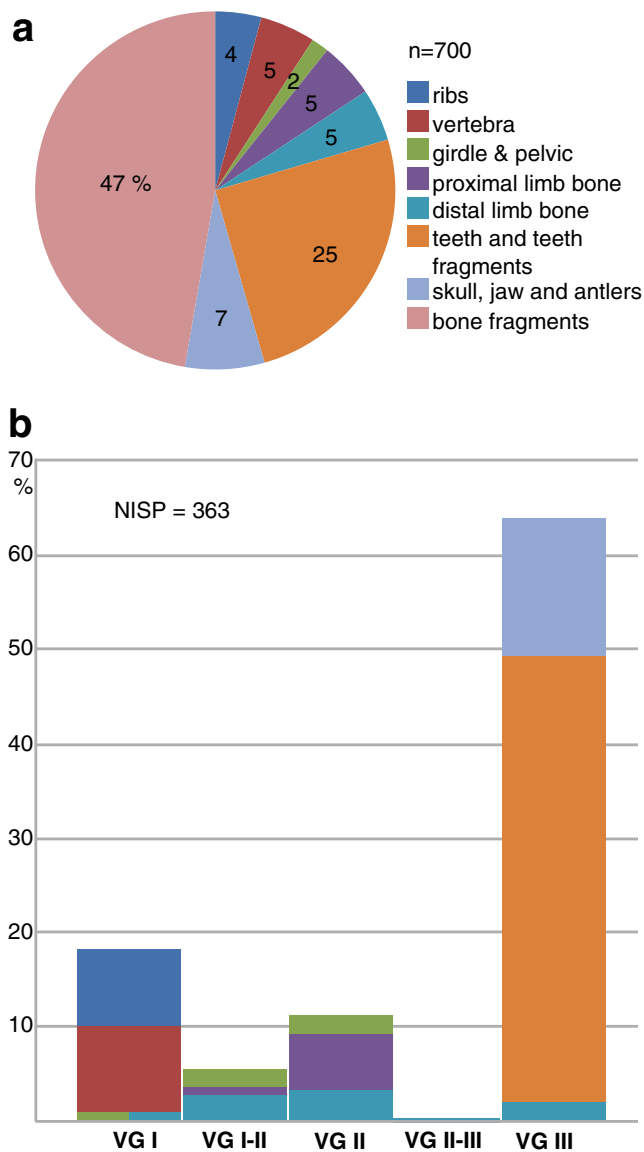


Fig. 6 Distribution of skeletal elements of large mammals. **a** Relative abundance of elements in percent, **b** expanded Voorhies analysis based on a NISP of 363 from all excavation campaigns up to 2012 at the Gratkorn locality; in percent of total amount (colours correspond to anatomical classification in **a**)

Table 2 Expanded Voorhies analysis of large mammal remains from the Gratkorn locality compared with the Zambrana locality (data from Badiola et al. 2009)

Voorhies group	Gratkorn	Zambrana
VG I	18 %	17 %
VG I-II	6 %	4 %
VG II	11 %	7 %
VG II-III	1 %	10 %
VG III	63 %	61.5 %
VG III teeth	48 %	55 %

Data from Zambrana are medium values between samples I and II VG Voorhies group,

Zambrana locality, (late Eocene, Spain; Table 2) described by Badiola et al. (2009). In two different samples from excavations at this site, Badiola et al. (2009) grouped 14 and 20 %, respectively, of the sample to group I and 60 and 63 %, respectively, to group III with a similar overweight of teeth in the samples (225 out of 375 NISP and 210 out of 420 NISP; Badiola et al. 2009, fig. 6). A similar taphonomic pattern for the Gratkorn site as observed in Zambrana can therefore be assumed. As both, elements grouped in Voorhies group I (“no prolonged fluvialite transportation possible”) and III (“prolonged fluvialite transportation possible”), were well represented, a prolonged transportation has to be excluded. Furthermore, there are no signs of rounding by fluvialite transportation, which is in accordance with observations on gastropod shell preservation, sedimentology, and pedogenic features.

Also, the anatomical distribution (Fig. 6a) shows clear similarities to the Zambrana locality: after bone fragments with 47 %, teeth and teeth fragments are the second most abundant group of elements (25 %), while postcranial material is definitively underrepresented with a total of 21 %. The high relative abundance of teeth can possibly be

explained by carnivore behaviour (see discussion above). Comparing different ways of bone collecting by predators and by scavengers, Palmqvist and Arribas (2001) observed a lower ratio of vertebrae and ribs versus girdle and limb bones as typical for scavengers (1:9 in contrast to 1:4 in predators). The almost equalized ratio (1:1.25) observed at Gratkorn would therefore point more to a predator assemblage. As most of the vertebrae and ribs coded in the Voorhies analysis originate from the deinothere skeleton, which is unlikely to be transported by any of the carnivores but most probably died at the place of its deposition (compare to Coe 1978 and excavation map in Aiglstorfer et al. 2014b, this issue), it has to be excluded from this comparison. The ratio (1:8.7) for isolated remains of all the other large herbivorous mammals, excluding the proboscidean, clearly points to collecting by scavengers.

Taxonomic and body mass distribution

Small mammals including rare semiarticulated skeletons are the most common vertebrate remains from the Gratkorn locality. With a MNI of 34, ruminants are the most abundant large mammals (Fig. 7), dominated by the cervid *Euprox furcatus* (16), followed by *Dorcatherium navi* (9) and the small moschid *Micromeryx flourensianus* (6), while additional taxa *?Hispanomeryx*, *Tethytragus* sp. and *Palaeomerycidae* gen. et sp. indet. are only represented by single individuals. Suidae are frequent with at least 7 individuals. Carnivores are rare with only 3 MNI (6 % of all large mammals). Perissodactyla (4) and the only proboscidean *Deinotherium levius* vel *giganteum* (2) are less common. This distribution corresponds to an accumulation of the remains by scavengers, as does the generally wide range of body mass and the high diversity of the species (Palmqvist and Arribas 2001). Besides ecological considerations (Aiglstorfer et al. 2014c, this issue), the abundance of small mammals and the rarity of specimens with a body mass of more than 1,000 kg (Fig. 7a) excludes sorting by fluvialite transport and emphasises the assumption of a more or less autochthonous taphocoenosis (Gross et al. 2011). In a regime dominated by fluvial transportation, one would expect to find a distinct abundance of species with large body mass in comparison to low or medium weight species (Behrensmeier 1988; see also data for the fluvialite-dominated Eppelsheim Formation described in Sommer 2007).

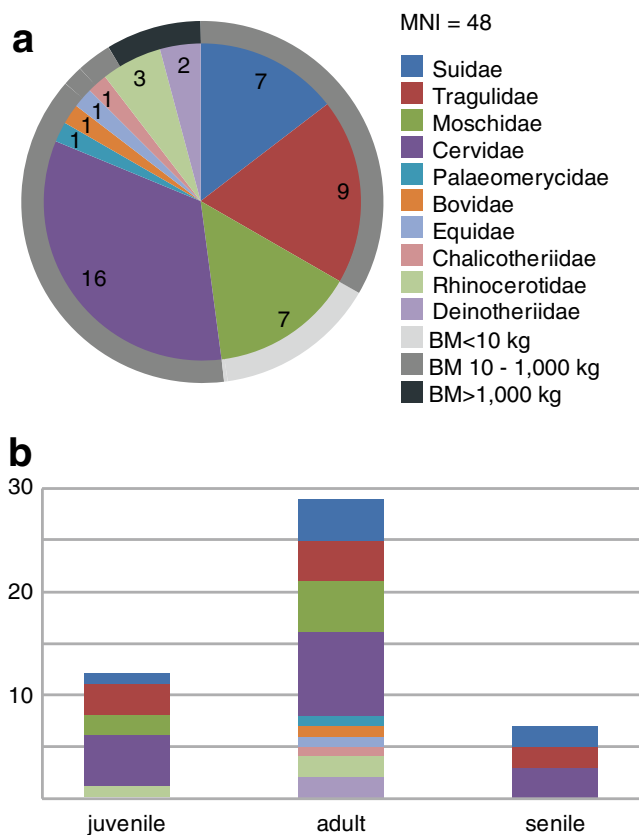


Fig. 7 Faunal composition of the Gratkorn large mammal taphocoenosis: **a** MNI of herbivore large mammals on the family level based on the number of similar anatomical elements and tooth enamel consumption (body mass, BM, following categories given in Costeur et al. 2013), **b** age model of large mammals based on enamel consumption (juvenile: deciduous dentition; adult: permanent dentition, senile: trigonid of m1 completely worn) and apophyseal growth (colours correspond to Fig. 8a)

Age profile

Large mammal specimens from Gratkorn show a clear dominance of (prime) adult specimens (MNI=29; 60 %), while juvenile specimens are less frequent (MNI=12; 25 %) and senile ones are rarest (MNI=7; 15 %). Though we are well

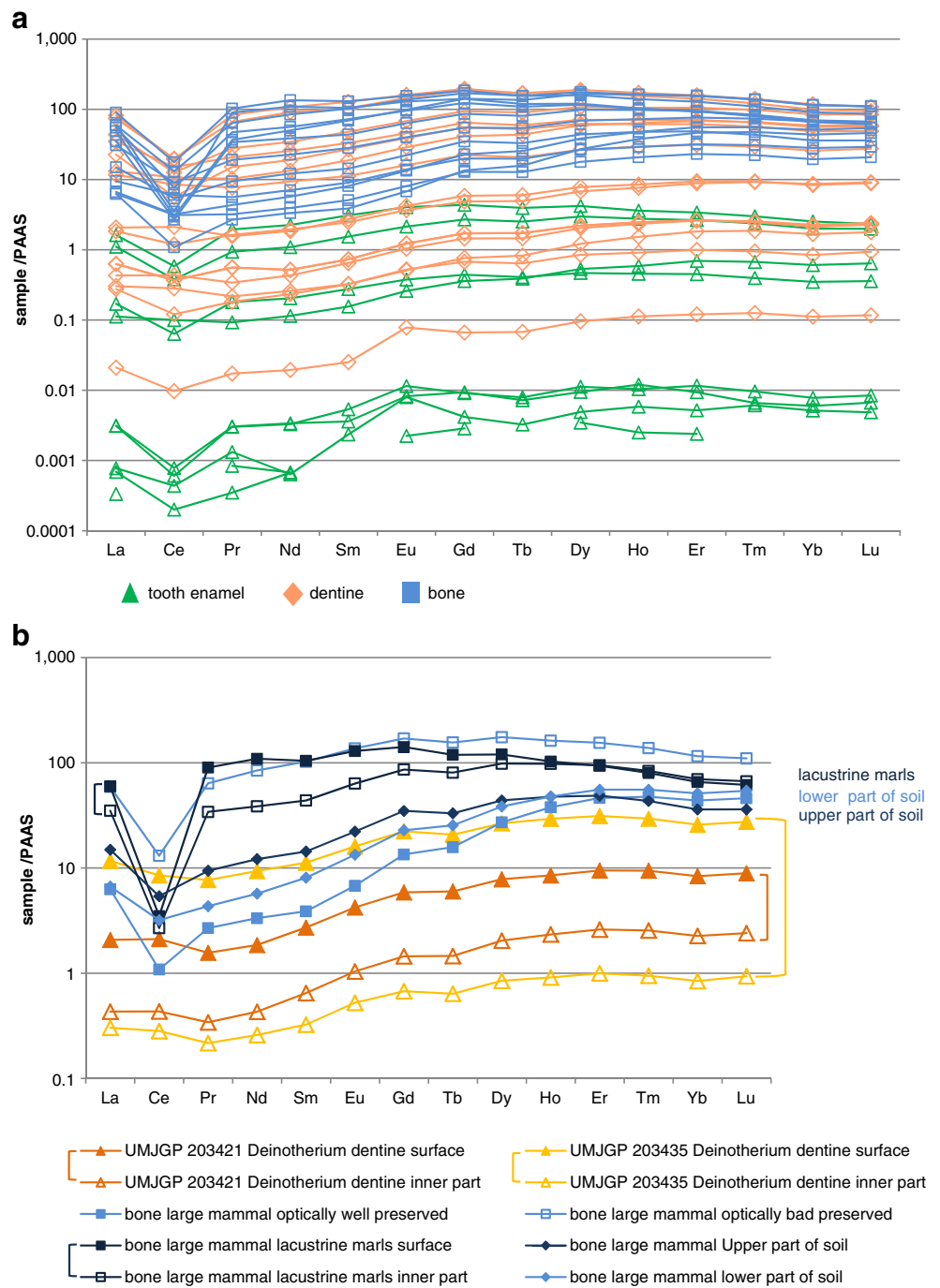
aware that these numbers are far from statistical significance, and that interpretations on age–frequency distribution are speculative to a certain degree (Lyman 1994 and references therein), the age profile from Gratkorn still allows some interpretations. Following Lyman (1994) and references therein, two basic types of mortality pattern can be distinguished. An attritional/normal mortality pattern is U-shaped, comprising an overrepresentation of juvenile and senile specimens, which are more susceptible to hazards than prime adults. A catastrophic/mass mortality pattern is L-shaped representing the age profile of the live community with fewer senile specimens. Surprisingly, the pattern observed at Gratkorn does not fit to the attritional/normal mortality one would expect for a site where different populations of large mammals meet for drinking or feeding, and where young and inexperienced or old individuals are more likely to become the prey of cursorial predators or prone to other hazards. The Gratkorn assemblage in contrast shows an L-shaped pattern (in the sense of Lyman 1994 and references therein), with a clear dominance of prime individuals. Such a pattern could be observed as a result of mass mortality (Lyman 1994). This interpretation is not suitable for Gratkorn, as we do not have any sedimentological signs for desiccation or flooding, as should be expected in such a case. Following Stiner (1990), an L-shaped pattern could also be caused by ambush predators such as Felidae. Even though neither Felidae nor Barbooufelidae have been recorded from Gratkorn or from other Sarmatian localities of the Central Paratethys realm (Morlo 2006), their presence in this ecosystem is possible, as there is a record from Atzelsdorf (Austria; Nagel 2009) and from different localities in the North Alpine Foreland Basin (Morlo 2006). An L-shaped pattern can also be explained by collecting by scavengers (secondary assemblage) to which corresponds the level of disarticulation and the anatomical distribution of skeletal elements of prey animals observed at Gratkorn (Palmqvist and Arribas 2001).

REE analysis

During lifetime, bones show very low absolute contents of rare earth elements (REE; levels of ~0.1 ppm or even in the range of ppb; Tütken 2003; Trueman 2007), but a rapid post mortem incorporation is observed (e.g. ~1,000 ppm for fish teeth younger than 10,000 years; Trueman 2007). REE are therefore considered a useful tool for taphonomical considerations (Trueman 2007). A strong enrichment in total REE values generally points to a stronger diagenetic alteration of the original tissue, while a lower REE content indicates minor diagenetic alteration. The vertebrate remains from Gratkorn show total REE contents ranging from below the detection limit (0.07 ppm) to 13,484 ppm, with bones (values between 989 and 13,484 ppm) and dentine (values between 4 and 12,510 ppm) comprising, in general, higher contents than enamel [values from below detection limit (0.07 ppm) up to 284 ppm; Online resource 1]. This shows lower

diagenetic alteration for tooth enamel than for dentine and bone. The shapes of REE distribution patterns have often been used for estimations of the degree and time of diagenetic alteration of vertebrate remains (see, e.g. Trueman 2007; Badiola et al. 2009; Rogers et al. 2010) with a flat pattern [no considerable medium-sized rare earth elements (MREE) enrichment] indicating weak or early diagenesis (Badiola et al. 2009), while a bell-shaped pattern would imply more extensive or late diagenesis (Reynard et al. 1999). However, recent works on REE contents in fossil bones and teeth (see, e.g. Kocsis et al. 2010; Herwartz et al. 2013; Trueman 2013) have shown a more complex process of REE uptake, fractionation, and protracted content alteration, and question the assumption that recrystallisation can be more or less synonymised with a late diagenetic alteration. Both adsorption and recrystallisation could represent early and late diagenetic processes (Herwartz et al. 2013). In any case, all samples from Gratkorn show flat REE distribution patterns and MREE enrichment is generally poor (Fig. 8a), indicating a minor degree of recrystallisation. Intrabone and intradentine fractionation from the surface (more enriched in REE) to inner parts (less enriched in REE) can be observed for the Gratkorn specimens (Fig. 8b; Online resource 1; fitting well to observations of Tütken et al. 2008; Herwartz et al. 2013) and indicate a chemically less altered preservation of the inner parts of skeletal tissues than on the surface. Optically categorised “well preserved bone” and “badly preserved bone” differ in total REE amounts, being respectively less (1,014 ppm) and more (10,025 ppm) enriched in REE contents, and encompass all values for the bones of different levels (Fig. 8b). Upper and lower parts of soil comprise quite similar values, thus re-enforcing the assumption of a generally “uniform” history for the vertebrate-bearing palaeosol. Trueman et al. (2006) and Trueman (2013) showed that REE composition still preserves broadly environment-specific REE patterns, implying that the REE composition retains the early diagenetic signal to a considerable degree and is not significantly overprinted by late diagenesis (see discussions in Kocsis et al. 2010 and Herwartz et al. 2013). With shale-normalised ratios ranging between 0.337 and 1.6198 for La/Sm and between 0.1302 and 0.9903 for La/Yb (Online resource 1), all values are well within the range of “terrestrial samples” (Trueman et al. 2006; Herwartz et al. 2013), and in general plot with the pattern described for soils by Trueman (2013). Most specimens comprise a negative Ce anomaly, which is often used to evaluate redox conditions in REE studies of fossil bones and teeth (e.g. Metzger et al. 2004; Domingo et al. 2011). Herwartz et al. (2013), however, observed that only a few bones in their study comprised Ce anomalies actually related to redox conditions, and further observed an intrabone shift from a negative to a positive Ce anomaly. The biogenic apatite from Gratkorn mostly displays negative Ce anomalies and does not show intrabone or intradentine inverse of anomalies, but a decreasing negative anomaly can be observed in one bone from the outer surface to the inner part of the cortex (Fig. 8b), well in agreement with the

Fig. 8 Distribution of rare earth elements (REE) of fossil bone, dentine, and enamel from Gratkorn (for details, see Online resource 1): **a** total distribution patterns for tooth enamel, dentine and bones, **b** distribution pattern of different bone samples from different parts of the vertebrate-bearing palaeosol and from different parts of one sample (intradentine and intrabone sampling indicated with brackets)



observations of Herwartz et al. (2013), which could be explained by changing fluid composition during diagenesis.

Conclusions

Almost all vertebrate and most invertebrate remains originate from one palaeosol layer, and the community preserved is considered to be more or less contemporarily deposited and therefore representing an autochthonous taphocoenosis.

Bioturbation, roots, and rhizomes emphasise the interpretation of the fossil-bearing horizon as autochthonous palaeosol, as does the diverse, rich, and predominantly terrestrial gastropod fauna. The general grade of diagenetic alteration is low, as shown by primary aragonitic gastropod shells and the REE pattern in enamel, dentine, and bones. Therefore, especially enamel is very likely to have preserved in vivo signals for isotopic measurements (Aiglstorfer et al. 2014a, this issue). Taphonomical considerations on small mammals need to be treated independently as completely different mechanisms,

e.g. predation by birds (Gross et al. 2011) is of importance. The large mammal age profile from Gratkorn could be explained by mass mortality or the accumulation by scavengers. However, a mass mortality community can be excluded due to the following observations: (1) different weathering stages, (2) inhomogeneous dispersal inside the vertebrate-bearing palaeosol, and (3) anatomical separation (except of the proboscidean partial skeleton). Fluvial transport of bones and teeth can be excluded, as there is no sign of abrasion, no alignment of long bones, no size sorting, and bone fragments of individual bones are in close proximity. Furthermore, the Voorhies analysis showed a clearly bimodal distribution including groups I and III. Nevertheless, the level of disarticulation is high, supposedly caused by predation, scavenging, trampling, and bioerosion, together with post-depositional neotectonics (simple faults on slickensides). The accumulation of large herbivorous mammal remains most likely represents a secondary assemblage, transported by scavengers, as indicated by a low ratio of vertebrae and ribs in comparison to girdle and limb bones, a scarcity of diaphyses and completely preserved long bones, a low MNI for carnivores, a low proportion of juvenile specimens, a high species diversity, and a wide range in bodysize (Palmqvist and Arribas 2001). Furthermore, there are different signs of gnawing and bite marks observed, confirming activity of carnivores and osteophagy by small mammals and insects.

Acknowledgements Dr. Kerstin Drost (Tübingen University) is thanked for REE analysis, Dipl. Min. Melanie Keuper and Dr. Christoph Berthold for the X-ray microdiffraction analysis, Sabine Kötter for catching extant *Limax*, Henrik Stöhr for preparation (all Tübingen University), Helmut Reindl (Gratkorn) and the participants in all excavation campaigns from UMJGP Graz, Ludwig-Maximilians-Universität Munich and Eberhard Karls Universität Tübingen for their hard work in the field. The municipal administration of the town of Gratkorn is thanked for continuous support of the excavations. We furthermore want to thank Achim G. Reisdorf (University of Basel) and Prof. Dr. Anna Kay Behrensmeyer (NMNH, Washington) whose reviews helped to seriously improve the content and English spelling of an earlier version of this manuscript.

References

- Aiglstorfer M, Bocherens H, Böhme M (2014a) Large mammal ecology in the late Middle Miocene Gratkorn locality (Austria). In: Böhme M, Gross M, Prieto J (eds) The Sarmatian vertebrate locality Gratkorn, Styrian Basin. Palaeobio Palaeoenv 94(1). doi:10.1007/s12549-013-0145-5
- Aiglstorfer M, Göhlich UB, Böhme M, Gross M (2014b) A partial skeleton of *Deinotherium* (Proboscidea, Mammalia) from the late Middle Miocene Gratkorn locality (Austria). In: Böhme M, Gross M, Prieto J (eds) The Sarmatian vertebrate locality Gratkorn, Styrian Basin. Palaeobio Palaeoenv 94(1). doi:10.1007/s12549-013-0140-x
- Aiglstorfer M, Heissig K, Böhme M (2014c) *Perissodactyla* from the late Middle Miocene Gratkorn locality (Austria). In: Böhme M, Gross M, Prieto J (eds) The Sarmatian vertebrate locality Gratkorn, Styrian Basin. Palaeobio Palaeoenv 94(1). doi:10.1007/s12549-013-0138-4
- Aiglstorfer M, Rössner GE, Böhme M (2014d) *Dorcatherium nauai* and pecoran ruminants from the late Middle Miocene Gratkorn locality (Austria). In: Böhme M, Gross M, Prieto J (eds) The Sarmatian vertebrate locality Gratkorn, Styrian Basin. Palaeobio Palaeoenv 94(1). doi:10.1007/s12549-013-0141-9
- Andrews P, Whybrow P (2005) Taphonomic observations on a camel skeleton in a desert environment in Abu Dhabi. Palaeontol Electron 8(1):1–17
- Backwell LR, Parkinson AH, Roberts EM, d'Errico F, Huchet J-B (2012) Criteria for identifying bone modification by termites in the fossil record. Palaeogeogr Palaeoclimatol Palaeoecol 337–338:72–87
- Badiola A, Berreteaga A, Pereda-Suberbiola X, Elorza J, Astibia H, Etxebarria N (2009) Taphonomy of vertebrate fossil assemblages from swampy circum-lake environments: an example from the Late Eocene of Zambrana (Iberian Peninsula). Palaios 24:522–534
- Behrensmeyer AK (1975) The taphonomy and paleoecology of Plio-Pleistocene vertebrate assemblages east of Lake Rudolf, Kenya. Bull Mus Comp Zool 146:473–578
- Behrensmeyer AK (1978) Taphonomic and ecologic information from bone weathering. Paleobiology 4(2):150–162
- Behrensmeyer AK (1988) Vertebrate preservation in fluvial channels. Palaeogeogr Palaeoclimatol Palaeoecol 63(1–3):183–199. doi:10.1016/0031-0182(88)90096-X
- Behrensmeyer AK (1991) Terrestrial vertebrate accumulations. In: Allison PA, Briggs DE (eds) Taphonomy: Releasing the data locked in the fossil record. Plenum Press, New York, pp 291–335
- Behrensmeyer AK, Kidwell SM (1985) Taphonomy's contributions to paleobiology. Paleobiology 11(1):105–119
- Berthold C, Bjeoumikhov A, Brügemann L (2009) Fast XRD² Microdiffraction with Focusing X-Ray Microlenses. Part Part Syst Charact 26:107–111
- Bhatia SB, Soulié-Marsche I, Gemayel P (1998) Late Oligocene and Early Pleistocene charophyte floras of the Hirpur Formation, Karewa Group, India. N Jb Geol Paläont, Abh 210(2):185–209
- Blumenschine RJ (1987) Carcass consumption sequences and the archaeological distinction of scavenging and hunting. J Hum Evol 15:639–659
- Böhme M, Ilg A, Winkelhofer M (2008) Late Miocene “washhouse” climate in Europe. Earth Planet Sci Lett 275(3–4):393–401
- Böhme M, Winkelhofer M, Ilg A (2011) Miocene precipitation in Europe: temporal trends and spatial gradients. Palaeogeogr Palaeoclimatol Palaeoecol 304:212–218
- Böhme M, Vasilyan D (2014) Ectothermic vertebrates from the late Middle Miocene of Gratkorn (Austria, Styria). In: Böhme M, Gross M, Prieto J (eds) The Sarmatian vertebrate locality Gratkorn, Styrian Basin. Palaeobio Palaeoenv 94(1). doi:10.1007/s12549-013-0143-7
- Coe M (1978) The decomposition of elephant carcasses in the Tsavo (East) National Park, Kenya. J Arid Environ 1:71–86
- Conybeare A, Haynes G (1984) Observations on elephant mortality and bones in Water Holes. Quat Res 22:189–200
- Costeur L, Maridet O, Montuire S, Legendre S (2013) Evidence of northern Turolian savanna-woodland from the Dorn-Dürkheim 1 fauna (Germany). Palaeobio Palaeoenv 93(2):259–275. doi:10.1007/s12549-013-0116-x
- Domingo MS, Domingo L, Sánchez IM, Alberdi MT, Azanza B, Morales J (2011) New insights on the taphonomy of the exceptional mammalian fossil sites of Cerro de los Batallones (Late Miocene, Spain) based on rare earth element geochemistry. Palaios 26:55–65
- Engel MS, Gross M (2009) A giant termite from the Late Miocene of Styria, Austria (Isoptera). Naturwissenschaften 96:289–295
- Fejfar O, Kaiser TM (2005) Insect bone-modification and paleoecology of oligocene mammal-bearing sites in the Doupov Mountains, Northwestern Bohemia. Palaeontol Electron 8(1):11p
- Flügel HW, Nowotny A, Gross M (2011) Geologische Karte 1:50.000, Blatt 164 Graz. 1 Blatt. Geologische Bundesanstalt, Wien

- Furbish DR, Furbish WJ (1984) Structure, Crystallography, and morphogenesis of the cryptic shell of the terrestrial slug *Limax maximus* (Mollusca, Gastropoda). *J Morphol* 180:195–211
- Gerdes G (2007) Structures left by modern microbial mats in their host sediments. In: Schieber J, Bose PK, Eriksson PG, Banerjee, S, Sarkar S, Altermann W, Catuneau, O. (eds) Atlas of microbial mat features preserved within the clastic rock record. Elsevier, Amsterdam, pp 5–38
- Göhlich UB, Gross M (2014) The Sarmatian (late Middle Miocene) avian fauna from Gratkorn, Austria. In: Böhme M, Gross M, Prieto J (eds) The Sarmatian vertebrate locality Gratkorn, Styrian Basin. *Palaeobio Palaeoenv* 94(1). doi:10.1007/s12549-013-0139-3
- Gross M (2008) A limnic ostracod fauna from the surroundings of the Central Paratethys (late Middle Miocene/early Late Miocene; Styrian Basin; Austria). *Palaeogeogr Palaeoclimatol Palaeoecol* 264(3–4):263–276
- Gross M, Böhme M, Prieto J (2011) Gratkorn: A benchmark locality for the continental Sarmatian s.str. of the Central Paratethys. *Int J Earth Sci (Geol Rundsch)* 100(8):1895–1913. doi:10.1007/s00531-010-0615-1
- Gross M, Böhme M, Havlik P, Aiglstorfer M (2014) The late Middle Miocene (Sarmatian s.str.) fossil site Gratkorn - the first decade of research, geology, stratigraphy and vertebrate fauna. In: Böhme M, Gross M, Prieto J (eds) The Sarmatian vertebrate locality Gratkorn, Styrian Basin. *Palaeobio Palaeoenv* 94(1). doi:10.1007/s12549-013-0149-1
- Hanley JH, Flores RM (1987) Taphonomy and paleoecology of nonmarine mollusca: Indicators of alluvial plain lacustrine sedimentation, upper part of the Tongue River Member, Fort Union Formation (Paleocene), Northern Powder River Basin, Wyoming and Montana. *Palaios* 1987(2):479–496
- Harzhauser M, Gross M, Binder H (2008) Biostratigraphy of Middle Miocene (Sarmatian) wetland systems in an Eastern Alpine intramontane basin (Gratkorn Basin, Austria): the terrestrial gastropod approach. *Geol Carpathica* 59(1):45–58
- Haynes G (1983) Archaeology frequencies of spiral and green-bone fractures on ungulate limb bones in modern surface assemblages. *Am Antiq* 48(1):102–114
- Hembree DI, Hasiotis ST (2008) Miocene vertebrate and invertebrate burrows defining compound paleosols in the Pawnee Creek Formation, Colorado, U.S.A. *Palaeogeogr Palaeoclimatol Palaeoecol* 270(3–4):349–365. doi:10.1016/j.palaeo.2008.07.019
- Herwartz D, Tütken T, Jochum KP, Sander PM (2013) Rare earth element systematics of fossil bone revealed by LA-ICPMS analysis. *Geochim Cosmochim Acta* 103:161–183
- Klaus S, Gross M (2010) Synopsis of the fossil freshwater crabs of Europe (Brachyura:Potamoidea: Potamidae). *N Jb Geol Paläont, Abh* 256(1):39–59
- Kocsis L, Trueman CN, Palmer MR (2010) Protracted diagenetic alteration of REE contents in fossil bioapatites: Direct evidence from Lu–Hf isotope systematics. *Geochim Cosmochim Acta* 74(21):6077–6092. doi:10.1016/j.gca.2010.08.007
- Kohn MJ, Schoeninger MJ, Barker WB (1999) Altered states: effects of diagenesis on fossil tooth chemistry. *Geochim Cosmochim Acta* 63:2737–2747
- Lyman RL (1994) Vertebrate taphonomy. Cambridge Manuals in Archaeology. Cambridge University Press, Cambridge
- Martin, RE (1999) Taphonomy: A process approach. Cambridge Paleobiology Series 4. Cambridge University Press, Cambridge
- Merceron G, Costeur L, Maridet O, Ramdarshan A, Göhlich UB (2012) Multi-proxy approach detects heterogeneous habitats for primates during the Miocene climatic optimum in Central Europe. *J Hum Ev* 63(1):150–161. doi:10.1016/j.jhevol.2012.04.006
- Metzger CA, Terry DO, Grandstaff DE (2004) Effect of paleosol formation on rare earth element signatures in fossil bone. *Geology* 32(6):497–500. doi:10.1130/g20376.1
- Morlo M (2006) New remains of Barbourfelidae (Mammalia, Carnivora) from the Miocene of Southern Germany: implications for the history of barbourfelid migrations. *Beitr Paläont* 30:339–346
- Nagel D (2009) The early Vallesian vertebrates of Atzelsdorf (Late Miocene, Austria). 10. Carnivora Ann Nathist Mus Wien A Mineral Petrol Geol Palaeontol Archaeozool Anthropol Praehist 111(A):605–618
- Palmqvist P, Arribas A (2001) Taphonomic decoding of the paleobiological information locked in a lower Pleistocene assemblage of large mammals. *Paleobiology* 27(3):512–530. doi:10.1666/0094-8373(2001)027<0512:tdotpi>2.0.co;2
- Poole JH (1996) The African elephant. In: Kangwana K (ed) Studying elephants. African Wildlife Foundation Technical Handbook Series 7:1–8
- Prieto J, Angelone C, Casanovas-Vilar I, Gross M, Hír J, Hoek Ostende LW van den, Maul LC, Vasilyan D (2014) The small mammals from Gratkorn: an overview. In: Böhme M, Gross M, Prieto J (eds) The Sarmatian vertebrate locality Gratkorn, Styrian Basin. *Palaeobio Palaeoenv* 94(1). doi:10.1007/s12549-013-0147-3
- Reynard B, Lécuyer C, Grandjean P (1999) Crystal-chemical controls on rare-earth element concentrations in fossil biogenic apatites and implications for paleoenvironmental reconstructions. *Chem Geol* 155(3–4):233–241. doi:10.1016/S0009-2541(98)00169-7
- Rink WJ, Schwarcz HP (1955) Tests for diagenesis in tooth enamel: ESR dating signals and carbonate contents. *J Archaeol Sci* 22(2):251–255. doi:10.1006/jasc.1995.0026
- Rogers RR, Fricke HC, Addona V, Canavan RR, Dwyer CN, Harwood CL, Koenig AE, Murray R, Thole JT, Williams J (2010) Using laser ablation-inductively coupled plasma-mass spectrometry (LA-ICP-MS) to explore geochemical taphonomy of vertebrate fossils in the Upper Cretaceous Two Medicine and Judith River Formations of Montana. *Palaios* 25(3):183–195. doi:10.2110/palo.2009.p09-084r
- Seilacher A (1964) Sedimentological classification and nomenclature of trace fossils. *Sedimentology* 3:253–256
- Shipman P (1981) Life history of a fossil; An introduction to taphonomy and paleoecology. Harvard University Press, Cambridge
- Sommer J (2007) Sedimentologie, Taphonomie und Paläoökologie der miozänen Dinotheriensande von Eppelsheim/Rheinhessen. Johann Wolfgang Goethe-Universität, Frankfurt am Main
- Stiner MC (1990) The use of mortality patterns in archaeological studies of hominid predatory adaptations. *J Anthropol Archaeol* 9:305–351
- Taylor SR, McLennan SM (1985) The continental crust: its composition and evolution. Blackwell, Oxford
- Thulborn EA (1991) Morphology, preservation and palaeobiological significance of dinosaur coprolites. *Palaeogeogr Palaeoclimatol Palaeoecol* 83(4):341–366. doi:10.1016/0031-0182(91)90060-5
- Tompa AS (1980) A comparative study of the ultrastructure and mineralogy of calcified land snail eggs (Pulmonata: Stylommatophora). *J Morphol* 150:861–888
- Trueman C (2007) Trace element geochemistry of bonebeds. In: Rogers RR, Eberth DA, Fiorillo AR (eds) Bonebeds: Genesis, analysis, and paleobiological significance. The University of Chicago Press, Chicago, pp 397–435
- Trueman CN (2013) Chemical taphonomy of biomineralized tissues. *Palaeontology* 56(3):475–486. doi:10.1111/pala.12041
- Trueman CN, Behrensmeier AK, Potts R, Tuross N (2006) High-resolution records of location and stratigraphic provenance from the rare earth element composition of fossil bones. *Geochim Cosmochim Acta* 70(17):4343–4355. doi:10.1016/j.gca.2006.06.1556
- Tschinkel WR (2003) Subterranean ant nests: trace fossils past and future? *Palaeogeogr Palaeoclimatol Palaeoecol* 192:321–333
- Tütken T (2003) Die Bedeutung der Knochenfrühdigenese für die Erhaltungsfähigkeit in vivo erworbener Element- und Isotopenzusammensetzungen in fossilen Knochen. Eberhard Karls Universität, Tübingen

- Tütken T, Vennemann TW, Pfretzschner HU (2008) Early diagenesis of bone and tooth apatite in fluvial and marine settings: Constraints from combined oxygen isotope, nitrogen and REE analysis. *Palaeogeogr Palaeoclimatol Palaeoecol* 266(3–4):254–268. doi:[10.1016/j.palaeo.2008.03.037](https://doi.org/10.1016/j.palaeo.2008.03.037)
- van der Made J, Prieto J, Aiglstorfer M, Böhme M, Gross M (2014) Taxonomic study of the pigs (Suidae, Mammalia) from the late Middle Miocene of Gratkorn (Austria, Styria). In: Böhme M, Gross M, Prieto J (eds) *The Sarmatian vertebrate locality Gratkorn, Styrian Basin*. *Palaeobio Palaeoenv* 94(1). (in press)
- Voorhies MR (1969) Taphonomy and population dynamics of an early Pliocene vertebrate fauna, Knox County, Nebraska. *Contributions to Geology University of Wyoming Special Paper* 1:69

			19/PAAS	30,8409	9,0640	19,0792	22,6802	28,1962	40,0669	54,9396	54,0792	69,0411	72,4840	76,3231	73,7125	67,2076	66,5790	684,2934	0,4589	1,0938	3,4399
--	--	--	---------	---------	--------	---------	---------	---------	---------	---------	---------	---------	---------	---------	---------	---------	---------	-----------------	--------	--------	--------

Publication #5

Aiglstorfer M, Bocherens H, Böhme M. (2014) Large Mammal Ecology in the late Middle Miocene locality Gratkorn (Austria). *Palaeobiodiversity and Palaeoenvironments* 94, 189-213.

Own contribution:	
Scientific ideas (%)	80
Data generation (%)	100
Analysis and Interpretation (%)	90
Paper writing (%)	95

Large mammal ecology in the late Middle Miocene Gratkorn locality (Austria)

Manuela Aiglstorfer · Hervé Bocherens ·
Madelaine Böhme

Received: 24 September 2013 / Revised: 26 November 2013 / Accepted: 16 December 2013 / Published online: 18 February 2014
© Senckenberg Gesellschaft für Naturforschung and Springer-Verlag Berlin Heidelberg 2014

Abstract $\delta^{18}\text{O}_{\text{CO}_3}$, $\delta^{13}\text{C}$ and $^{87}\text{Sr}/^{86}\text{Sr}$ measurements were performed on tooth enamel of several species to gain information on the diet and mobility of herbivorous large mammals from Gratkorn (Austria; late Sarmatian sensu stricto; 12.2–12.0 Ma). Except for the tragulid *Dorcatherium naui*, which was most likely frugivorous to a certain degree, the mean values and the total ranges of $\delta^{13}\text{C}$ and $\delta^{18}\text{O}$ of the large mammal taxa are typical for an exclusively C_3 vegetation diet and point to predominantly browsing in mesic/woodland environments. Occupation of different ecological niches is indicated by variation in $\delta^{18}\text{O}$ and $\delta^{13}\text{C}$ among the taxa, and could be shown to be typical for the species by comparison with other Miocene localities from different areas and ages. The small moschid *Micromeryx flourensianus* might have occasionally fed on fruits. The cervid *Euprox furcatus* represents a typical subcanopy browsing taxon. The proboscidean *Deinotherium levius* vel *giganteum* browsed on canopy plants in the higher parts of an exclusively C_3 vegetation as did the bovid *Tethytragus* sp.. Generally higher values for $\delta^{18}\text{O}$ and $\delta^{13}\text{C}$ of *Lartetotherium sansaniense* indicate feeding in a more open environment. Different ecological niches can be reconstructed for the two suids. While *Listriodon splendens* was a browsing taxon with a considerable input of fruits and maybe some grass in its diet, *Parachleuastochoerus steinheimensis* might have included roots. Distinct differences in $^{87}\text{Sr}/^{86}\text{Sr}$ values indicate that most of the larger mammals (*Deinotherium levius* vel *giganteum*, *Parachleuastochoerus steinheimensis*, *Euprox furcatus*, *Lartetotherium sansaniense* and to a minor degree

maybe *Listriodon splendens*) were not permanent residents of the area around Gratkorn but rather inhabited a wider area, most likely including the Styrian Basin and the higher altitudes of the Eastern Alps' palaeozoic basement.

Keywords Oxygen · Carbon · Strontium · Isotope · Enamel · Diet · Niche partitioning · Central Europe · Paratethys

Introduction

The Gratkorn locality (St. Stefan clay pit) is located 10 km NNW of Graz (Styria, Austria). The fossil-bearing palaeosol of late Middle Miocene age (late Sarmatian sensu stricto; 12.2–12.0 Ma; Gross et al. 2011) houses abundant small and large mammal fossils and is one of the richest vertebrate localities (the richest for the Paratethys realm) of this time period recorded so far. All mammalian fossils originate from a single fine-grained clastic soil layer (55 cm in total thickness; Gross et al. 2011; 2014, this issue), interpreted as a floodplain palaeosol (Gross et al. 2011). The uniformity of the palaeosol (without distinct soil horizons), the preservation of vertebrate and invertebrate remains and even coprolites point to a rather rapid accumulation and short time of soil formation (10^1 – 10^2 years; Gross et al. 2011; Havlik et al. 2014, this issue). Alternating wet and dry periods have been reconstructed based on lithology and fossil content (Gross et al. 2011; 2014, this issue) and on relict bedding, intense mottling, and drab colouring in the upper part of the palaeosol. All these features indicate an increase in hydromorphic conditions from the lower to the upper part of the soil. Due to the fast deposition of the palaeosol and the lack of any indications for reworking of the fossil content (flora and fauna), all the components of the excavated assemblage, including plants and animals, are considered to be contemporaneous and accumulated within a few decades (see also Havlik et al. 2014, this issue for further discussion). Palaeoclimatic reconstructions based on pedogenic features and the faunal composition

This article is a contribution to the special issue “The Sarmatian vertebrate locality Gratkorn, Styrian Basin.”

M. Aiglstorfer (✉) · H. Bocherens · M. Böhme
Department for Geosciences, Eberhard Karls Universität Tübingen,
Sigwartstraße 10, 72076 Tübingen, Germany
e-mail: manuela.aiglstorfer@senckenberg.de

M. Aiglstorfer · M. Böhme
Senckenberg Center for Human Evolution and Palaeoenvironment
(HEP), Sigwartstraße 10, 72076 Tübingen, Germany

of ectothermic vertebrates indicate a semi-arid, subtropical climate with distinct seasonality, a mean annual precipitation (MAP) of 486 ± 252 mm, and a mean annual temperature (MAT) of ~ 15 °C (Gross et al. 2011).

Although scientific analysis of the fossil flora from the Gratkorn locality is still in progress, it can already be said that medium-sized hackberry trees grew frequently in the area due to the high abundance of *Celtis* endocarps, especially in the upper part of the palaeosol. Besides large mammals, a quite diverse ectothermic vertebrate fauna, a few bird remains, and a rich and diverse small mammal fauna (for faunal lists, see Gross et al. 2011; Böhme and Vasilyan 2014, this issue; Göhlich and Gross 2014, this issue; Prieto et al. 2014, this issue) have been excavated at Gratkorn. Herbivorous large mammal taxa are represented by small body sizes of less than 10 kg (Moschidae: *Micromeryx flourensianus* and ?*Hispanomeryx* sp.) up to large species, such as, e.g. the proboscidean *Deinotherium levius vel giganteum* (Aiglstorfer et al. 2014a, this issue), and three rhinocerotid species, *Aceratherium* sp., *Brachypotherium brachypus* and *Lartetotherium sansaniense*, which can reach more than 1000 kg in weight (Aiglstorfer et al. 2014b, this issue). Since skeletal material of *Brachypotherium brachypus* comprises only postcranial elements and *Aceratherium* sp. is only represented by a deciduous premolar, isotopic measurements of rhinocerotids could be gained only for *Lartetotherium sansaniense*. The chalicothere *Chalicotherium goldfussi* and the equid *Anchitherium* sp. are further faunal elements of the Gratkorn assemblage (Aiglstorfer et al. 2014b, this issue), but could not be measured due to scarcity of material or total lack of dental material. Suidae are represented in Gratkorn by two species, the more bunodont *Parachleuastochoerus steinheimensis*, and the more lophodont *Listriodon splendens* (van der Made et al. 2014). Ruminants are the most abundant large mammals, and are represented by the cervid *Euprox furcatus* (most frequent species), the tragulid *Dorcatherium nauii* (second most frequent species), the above-mentioned two Moschidae, a large palaeomerycid (which is represented only by a single bone), and by the bovid *Tethyragus* sp. (so far recorded with only one individual; Aiglstorfer et al. 2014c, this issue).

Stable isotopes as indicator for ecology

Carbon isotopes

The carbon isotope ratio ($^{12}\text{C}/^{13}\text{C}$) of vertebrate fossils yields information about the diet and ecology of animals, since differences in isotopic compositions of diet are incorporated into body tissues (DeNiro and Epstein 1978; Tütken and Vennemann 2009; Ecker et al. 2013). Dental enamel proved to be an ideal tissue for this investigation as it is less susceptible to diagenetic alteration than bone or dentine (Koch et al. 1997; Bocherens and Sen 1998; Lee-Thorp and Sponheimer

2003; Tütken et al. 2006; Domingo et al. 2009, 2012; Tütken and Vennemann 2009; Bocherens et al. 2011a).

Plant carbon isotope compositions vary due to different photosynthetic pathways for atmospheric CO_2 assimilation. While today, most trees, shrubs, and “cool-season growing” grasses fix CO_2 by forming a 3-carbon molecule, therefore termed C_3 plants, C_4 plants, representing most of “warm-season growing” grasses and sedges in warm and/or more arid habitats, fix CO_2 in a 4-carbon molecule (Ehleringer and Cerling 2002; Tipple and Pagani 2007). In modern plant tissues, a different $\delta^{13}\text{C}$ value is observed for C_3 (-36 to -22 ‰) and C_4 plants (-17 to -9 ‰; Bocherens et al. 1993; Tipple and Pagani 2007; Domingo et al. 2012; all $\delta^{13}\text{C}$ and $\delta^{18}\text{O}$ values are reported relative to the Vienna Pee Dee Belemnite, V-PDB, standard, if not given otherwise). A third photosynthetic pathway, the crassulacean acid metabolism (CAM; common in desert succulents, tropical epiphytes, and aquatic plants) is characterised by fixation of CO_2 at nighttime. It is rarer (6 % of terrestrial and 6 % of aquatic plants; Keeley and Rundel 2003) and often corresponds to environments in climatically stressful conditions, such as increased aridity (Tütken 2011). Their $\delta^{13}\text{C}$ values show a wider range (-30 to -11 ‰) and overlap with values for C_3 and C_4 plants (Tütken 2011). CAM plants usually comprise only a marginal biomass in ecosystems and do not represent the expected food plants for the herbivorous large mammal taxa sampled for this publication.

Herbivores incorporate the ingested plant carbon in their mineralised skeletal and dental tissues, such as bone, dentine and tooth enamel (DeNiro and Epstein 1978; Tütken and Vennemann 2009; Ecker et al. 2013). Carbonate isotope ratios in enamel of herbivores can thus be used to reconstruct the proportion of C_3 or C_4 plants in their diet. An average $\Delta^{13}\text{C}_{\text{enamel-diet}}$ enrichment factor of 14.1 ± 0.5 ‰ was observed by Cerling and Harris (1999) for large ruminants (with a total range of 12.6–14.7 ‰). They stated that non-ruminant ungulates give similar values and they did not find a significant difference among taxa. For the sampled rhinocerotids, they observed 14.4 ± 1.6 ‰. In an experiment with controlled diets, Passey et al. (2005) showed that digestive physiology considerably influences the enrichment factor as they measured a factor of 14.6 ± 0.7 ‰ for domestic cattle (ruminant digestion) and a factor of 13.3 ± 0.3 ‰ for pigs (non-ruminant digestion). Since it cannot be estimated whether the digestive physiology of ruminants from Gratkorn is comparable to modern representatives (see differences in digestive physiology of modern Tragulidae and Pecora; Rössner 2007), the average $\Delta^{13}\text{C}_{\text{enamel-diet}}$ enrichment factor of 14.1 ± 0.5 ‰ after Cerling and Harris (1999) has been applied to the herbivorous large mammals from Gratkorn, comparable to other works dealing with Miocene herbivorous large mammals (Domingo et al. 2009, 2012; Tütken and Vennemann 2009; Merceron et al. 2013).

In modern large mammal faunas, pure C_3 consumers exhibit a range of -22 to -8 ‰, mixed feeders a range of -8 to -3 ‰, and pure C_4 feeders a range of -3 to $+5$ ‰ in $\delta^{13}\text{C}$ for

enamel (Cerling et al. 1997a, b; Domingo et al. 2012). For pure C₃ feeders, Domingo et al. (2012) estimated the ranges for the different habitats, closed canopy (−22 to −16 ‰), mesic/woodland (−16 to −11 ‰) and open/arid (−11 to −8 ‰). However, when dealing with fossil taxa, variations of δ¹³C for the atmospheric CO₂ have to be taken into consideration. Modern atmospheric CO₂ (δ¹³C_{CO2} = −8 ‰) is depleted in ¹³C compared with preindustrial CO₂ (δ¹³C = −6.5‰), due to the fossil-fuel burning of ¹²C-rich hydrocarbons (Friedli et al. 1986). Tipple et al. (2010) reconstructed variations in the δ¹³C value of the atmospheric CO₂ for the Cenozoic based on isotopic data derived from benthic foraminifera. Following their measurements, a δ¹³C value of about −6 ‰ can be estimated for the latest Middle Miocene CO₂ (12 Ma; 2 ‰ higher than in the modern atmosphere). Late Middle Miocene C₃ feeders are thus expected to have δ¹³C values ranging from −20 to −6 ‰, with −20 to −14 ‰ for feeding in closed canopy, −14 to −9 ‰ in mesic/woodland environment, and −9 to −6 ‰ in more open/arid C₃ vegetation. Values between −6 and −1 ‰ and between −1 and +7 ‰ are expected for mixed feeders and pure C₄ feeders, respectively (Domingo et al. 2012).

Although the existence of C₄ grasses has been documented at least for southwestern Europe since the Early Oligocene (Urban et al. 2010), C₃ plants represent the dominant vegetation in Europe during the Miocene and no noteworthy C₄ grasslands evolved until the Late Miocene (Cerling et al. 1993; Tütken and Vennemann 2009). Though small amounts of C₄ vegetation cannot be completely ruled out for the Miocene of Europe, isotopic values measured on Late Miocene *Hippotherium* specimens from Central Europe and herbivorous large mammals from the Iberian Peninsula showed a pure C₃ plant diet for these animals (Domingo et al. 2013; Tütken et al. 2013). The same taxa or closely related ones are known to have consumed C₄ plants when they were available (see Nelson 2007; Badgley et al. 2008; Passey et al. 2009; Bocherens et al. 2011a).

Oxygen Isotopes

Variations in the oxygen isotope ratio (¹⁶O/¹⁸O) in skeletal and dental tissues are in equilibrium with the body water and thus record the in vivo signal of the animal (Longinelli 1984). Oxygen isotope values of the body water are mostly influenced by the composition of the drinking water (meteoric water (δ¹⁸O_{H2O})), and the drinking behaviour of the animal (Longinelli 1984; Luz et al. 1984; Kohn 1996; Kohn et al. 1996; Bocherens et al. 1996; Tütken et al. 2006; Levin et al. 2006; Clementz et al. 2008). While, for example, δ¹⁸O values of terrestrial obligate drinkers mainly depend on the values of the surface water, drought-tolerant species have usually less negative values as they gain more water from leaves, fruits, and seeds, which are more enriched in ¹⁸O (Kohn 1996; Kohn et al. 1996). Plant roots and stems usually display similar values as meteoric water (Tütken and Vennemann 2009).

In contrast to terrestrial animals, aquatic animals have generally lower values in δ¹⁸O (Bocherens et al. 1996; Clementz et al. 2008). The δ¹⁸O_{H2O} value of meteoric water is influenced by climatic conditions, such as air temperature, degree of aridity (amount of precipitation vs. evaporation), seasonality of precipitation, or the trajectories of storms, as well as by geographic conditions, for example latitude or distance from the source area (continental effect) (Dansgaard 1964; Rozanski et al. 1993; Higgins and MacFadden 2004; Levin et al. 2006). Thus, δ¹⁸O values preserved in fossil enamel help to reconstruct climatic conditions as well as infer information concerning animal ecology. Because tooth mineralisation is a progressive process, variations in climatic conditions can be recorded along the growth axis of the tooth and thus high crowned teeth can give information on seasonal variations (Kohn 2004; MacFadden and Higgins 2004; Nelson 2005; van Dam and Reichert 2009; Zin-Maung-Maung-Thein et al. 2011; Tütken et al. 2013).

The δ¹⁸O value of the ingested water is incorporated in the mineral phase of bones and teeth and mostly bound on phosphate (PO₄^{3−}) and carbonate (CO₃^{2−}) ions, with the greater amount being incorporated in phosphate, as carbonate comprises only 2–4 wt.% of the mineral phase (Tütken and Vennemann 2009). While the PO₄ component is less susceptible to inorganic diagenetic alteration than the CO₃ component, the latter suffers less from microbially-mediated isotopic exchange (Domingo et al. 2013). As the δ¹⁸O values of the phosphate and carbonate components are correlated and exhibit an equilibrium offset of about 8.5 ‰, both are usable for reconstruction of the in vivo signal of animals (Iacumin et al. 1996).

⁸⁷Sr/⁸⁶Sr: Indicator of migration

In addition to δ¹⁸O and δ¹³C values, the strontium isotope composition (⁸⁷Sr/⁸⁶Sr ratio) of diet and drinking water is incorporated in the skeletal and dental tissues of animals (Hoppe et al. 1999; Maurer et al. 2012). Since this ratio is constant and does not change up the food chain, it reflects the bioavailable ⁸⁷Sr/⁸⁶Sr in the animal's habitat (Blum et al. 2000; Bentley 2006). This value depends on the ⁸⁷Sr/⁸⁶Sr ratios in bioavailable strontium of the underlying bedrocks. The latter is mainly influenced by the primary Rb concentration, respectively the Rb/Sr ratio, as well as the age of the rock (Tütken 2010). Thus, older and Rb-enriched bedrocks display higher ⁸⁷Sr/⁸⁶Sr ratios (Bentley 2006; Tütken 2010). However, differences from bedrock to bioavailable ratios can be observed for example due to residual clay minerals with higher Rb/Sr and ⁸⁷Sr/⁸⁶Sr than the underlying bedrock (Cooke et al. 2001; Tütken et al. 2011), complicating the reconstruction of provenance with ⁸⁷Sr/⁸⁶Sr ratios. In any case the ratio is still related to the underlying rock, though sometimes in a more complex way (Maurer et al. 2012) and thus still enables reconstruction of provenance or possible migration of the animal (Tütken and Vennemann 2009; Maurer et al.

2012). The latter is possible as tooth enamel grows progressively and therefore incorporates variations in isotopic composition, as mentioned above. While large mammals can undertake long-distance migrations (Hoppe et al. 1999; Tütken and Vennemann 2009; Maurer et al. 2012), small mammals and invertebrates display only small individual travel distances (Porder et al. 2003) and are thus more likely to represent the local bioavailable $^{87}\text{Sr}/^{86}\text{Sr}$ values. Hence, small mammals are often used to determine the local $^{87}\text{Sr}/^{86}\text{Sr}$ ratios (see Bentley 2006 and references therein).

Institutional Abbreviations

GPIT	Paläontologische Sammlung der Universität Tübingen, Tübingen, Germany
IGM	Montanuniversität Leoben, Leoben, Austria
NHMW	Naturhistorisches Museum Wien, Vienna, Austria
UMJGP	Universalmuseum Joanneum, Graz, Austria

Material

We analysed the carbonate component of 14 bulk enamel samples of large mammal teeth (*Parachleuastochoerus steinheimensis*, *Listriodon splendens*, *Dorcatherium nauai*, *Euprox furcatus*, *Micromeryx flourensianus*, *Tethytragus* sp.; see Appendix 1), three bulk samples of whole small mammal teeth (cheek teeth of *Schizogalerix voesendorfensis* and *Prolagus oeningensis* and incisors of indeterminate small mammals) and 21 serial samples of *Deinotherium levius* vel *giganteum* and *Lartetotherium sansaniense* for $\delta^{18}\text{O}_{\text{CO}_3}$ and $\delta^{13}\text{C}$. Due to scarcity of material, the second moschid *?Hispanomeryx* sp. was not measured. To avoid milk suckling and weaning signals, M3s (upper third molars) or m3s (lower third molars) were sampled for large mammals, if possible. Additionally, gastropods (*Pseudidyla martingrossi*, *Limax* sp., *Pleurodonte michalkovaci*, *Testacella schuetti*, and opercula of indetermined gastropods), plant remains (*Celtis* endocarps), soil samples (random and samples from upper and lower parts), and a microbialite (originating from the uppermost part of the palaeosol; see Havlik et al. 2014, this issue for details) were analysed. Strontium isotope composition ($^{87}\text{Sr}/^{86}\text{Sr}$) was measured on enamel samples of *Listriodon splendens*, *Parachleuastochoerus steinheimensis*, *Dorcatherium nauai*, *Euprox furcatus*, *Tethytragus* sp., *Lartetotherium sansaniense*, *Deinotherium levius* vel *giganteum*, *Schizogalerix voesendorfensis*, *Prolagus oeningensis*, *Limax* sp., *Pleurodonte michalkovaci*, and the microbialite from Gratkorn. All material is housed at GPIT and UMJGP.

Large mammal enamel values ($\delta^{18}\text{O}_{\text{CO}_3}$ and $\delta^{13}\text{C}_{\text{CO}_3}$) are compared with values from Middle Miocene localities from Austria, Germany, and Spain.

The following taxa were sampled for direct comparison at the IGM, UMJGP, and NHMW (for detailed information, see Appendix 2):

- *Dorcatherium crassum*, *Dorcatherium vindebonense* (tragulids), and *Hoploaceratherium* sp. (rhinocerotid) from the early Middle Miocene locality of Göriach (Austria; $\sim 14.5 \text{ Ma} \pm 0.3 \text{ Ma}$);
- *Heteroprox larteti* (cervid) and *Prodeinotherium bavaricum* (deinothere) from the early Middle Miocene locality of Seegraben (Austria; 14.8 Ma);
- *Deinotherium* sp. from the late Middle Miocene localities of Türkenschanze (Austria; 12.6 Ma) and Trössing near Gnas (Austria; 12.7–11.6 Ma);
- *Brachypotherium* (?) from Trössing near Gnas;
- *Deinotherium* from the locality of Bruck an der Leitha (Austria; assumably early Sarmatian; 12.7–12.2 Ma) and from the Miocene localities of Wolfau (Austria; early Late Miocene) and Mödling (Austria; Miocene);
- *Brachypotherium* sp. from the Miocene locality of Eichkogel near Mödling (Austria).

Furthermore, comparison data could be gained from the literature for the following taxa and localities:

- Sandelzhausen (Germany; 15.2–15.1 Ma; from Tütken and Vennemann 2009): *Lartetotherium sansaniense*, *Heteroprox eggeri* (cervid), *Gomphotherium subtapiroideum* (proboscidean), *Plesiaceratherium fahlbuschi* and *Prosantorhinus germanicus* (both rhinocerotids);
- Somosaguas (Spain; 14.1–13.8 Ma; from Domingo et al. 2009): *Gomphotherium angustidens* (proboscidean), *Conohyus simorreensis* (suid), and indetermined ruminants;
- Steinheim a. A. (am Albuch; Germany; Middle Miocene; 13.8–13.7 Ma; from Tütken et al. 2006): *Parachleuastochoerus steinheimensis*, *Listriodon splendens*, *Euprox* vel *Heteroprox*, *Micromeryx flourensianus*, *Gomphotherium steinheimense* (proboscidean), *Lartetotherium sansaniense*, *Brachypotherium brachypus*, *Alicornops simorreensis* (rhinocerotid) and *Aceratherium* sp.;
- Paracuellos 5 (Spain; Middle Miocene; 13.7–13.6 Ma; from Domingo et al. 2012): *Gomphotherium angustidens*, *Listriodon splendens*;
- Puente de Vallecas (Spain; Middle Miocene; 13.7–13.6 Ma; from Domingo et al. 2012): *Heteroprox moralesi* (cervid);
- Paracuellos 3 (Spain; Middle Miocene; 13.4–13.0 Ma; from Domingo et al. 2012): *Listriodon splendens* and *Tethytragus langai* (bovid).

Methods

C and O isotope measurements of the carbonate component of hydroxyapatite

Samples were obtained by hand drilling with a diamond-tipped dental burr on Dremel 10.8 V and Emax EVOLUTION and by crushing with a steel mortar and pestle. Prior to enamel sampling, the outer surface of the teeth was abraded by hand drilling to minimise effects of diagenetic alteration. Invertebrate samples were optically checked for contamination and cleaned with deionized water prior to crushing. Parts with stronger coloration and visible cracks were avoided to minimise contamination. Isotope analysis was done using 5–15 mg (depending on tooth size and fragility) enamel powder. Prior to analysis of carbon and oxygen isotopes, all enamel and dentine samples were chemically pretreated with 2 % NaOCl (24 h) and 0.1 M Ca-Acetate acetic acid buffer solution (24 h) in order to remove organics and diagenetic carbonate (Bocherens et al. 1996). Soil samples, invertebrates, and microbialite were pretreated with 2 % NaOCl (24 h). Samples were rinsed with deionised water after each chemical treatment. About 2–3 mg of powder were used for C and O analyses and measurement of CaCO₃ content (wt. %; ± 10 %). This was performed at 70 °C with a Gasbench II connected to a Finnigan MAT 252 gas mass spectrometer, at the Department of Geosciences of the University of Tübingen (Germany). The measured O and C isotopic compositions were calibrated using the standards NBS-18 ($\delta^{18}\text{O} = -22.96 \text{‰}$, $\delta^{13}\text{C} = -5.00 \text{‰}$ V-PDB) and the NBS-19 ($\delta^{18}\text{O} = -2.20 \text{‰}$, $\delta^{13}\text{C} = 1.95 \text{‰}$ V-PDB), with a reproducibility of ± 0.1 ‰ ($\delta^{13}\text{C}$) and ± 0.2 ‰ ($\delta^{18}\text{O}$). Following Bocherens et al. (2011b), isotopic measurements are expressed as δ (delta) values in ‰, as follows: $\delta^Y X = (R_{\text{sample}}/R_{\text{standard}} - 1) \times 1,000$, where X is C or O and Y is the mass number 13 or 18, and R is the isotopic ratio $^{13}\text{C}/^{12}\text{C}$ and $^{18}\text{O}/^{16}\text{O}$, respectively. The δ values are quoted in reference to international standards: Vienna Pee Dee Belemnite (V-PDB) for carbon and oxygen, furthermore, for oxygen Vienna Standard Mean Ocean Water (V-SMOW). In general, if not noted otherwise, V-PDB values are used. If $\delta^{18}\text{O}$ values measured in V-PDB were converted to V-SMOW, this was accomplished using the following formula: $\delta^{18}\text{O}$ (V-SMOW) = [$\delta^{18}\text{O}$ (V-PDB) × 1.03086] + 30.86.

Due to the small number of samples, maximum and minimum values are given in figures instead of standard deviations. Accordingly, to allow comparison, literature data are plotted with mean values and total ranges instead of standard deviations.

$^{87}\text{Sr}/^{86}\text{Sr}$ of the carbonate in the hydroxyapatite

A representative amount of the samples analysed for C and O was selected for $^{87}\text{Sr}/^{86}\text{Sr}$ analysis. Furthermore, three samples of each of the serially sampled teeth of *Lartetotherium sansaniense* and

Deinotherium levius vel *giganteum* (where possible maxima and minima in $\delta^{18}\text{O}$) were chosen. For $^{87}\text{Sr}/^{86}\text{Sr}$ analysis, 1–10 mg of pretreated enamel powder were prepared in a clean laboratory. Isotope ratio measurements were performed on the Finnigan MAT 262 TIMS located at the Isotope Geochemistry Group of the University of Tübingen (Germany). Sample material was weighed into Savillex® Teflon beakers, dissolved with 0.5 ml HCl_{conc.} in closed beakers on a hot plate at 80 °C overnight and subsequently dried down. Samples were then redissolved in 2.5 M HCl for the separation of Sr by conventional ion exchange chromatography using quartz glass columns filled with BioRad AG 50 W-X12 (200–400 mesh). Subsequent purification of Sr was achieved in microcolumns filled with Eichrom® Sr-spec resin using the HNO₃–H₂O technique. Sr separates were loaded with a Ta-activator on Re single filaments and isotope ratio measurements were performed in dynamic mode. Analytical mass fractionation was corrected using a $^{88}\text{Sr}/^{86}\text{Sr}$ ratio of 8.375209 and exponential law. External reproducibility for NBS SRM 987 ($n=18$) is 0.710254 ± 20 (2sd) for the $^{87}\text{Sr}/^{86}\text{Sr}$ ratio. Total procedural blank (chemistry and loading) was <1,475 pg contributing <1.5 % to the total Sr and thus negligible.

Results and discussion

Sediment, plant, and invertebrate fossils

Sediment samples from different parts of the palaeosol were measured as an indicator for the degree of alteration in dentine and bone of mammals. The samples showed a very wide range for both $\delta^{18}\text{O}$ and $\delta^{13}\text{C}$ (Fig. 1), probably originating from the strong heterogeneity of the different components of the clastic sediment with little carbonate cement. Similar discrepancies between sediment and diagenetically altered dentine were observed recently for the locality of Höwenegg (Tütken et al. 2013, supplementary data). Furthermore, the low CaCO₃ content (0.08–0.46 wt.%; Appendix 1) hinders reliable measurements. The microbialite shows lower values for $\delta^{13}\text{C}$ in comparison to the upper part of the palaeosol, representing its host sediment. As biological fractionation produces such negative shifts (Breitbart et al. 2009), the values tentatively confirm the assumption of biogenic (bacterial) build up (see also Havlik et al. 2014, this issue).

Due to assumed strong diagenetic alteration (bad preservation already optically observable; soft, crumbly, high porosity, and rich brownish colour), *Celtis* endocarps were also measured for $\delta^{18}\text{O}$ and $\delta^{13}\text{C}$ to be used as an indicator for the degree of alteration in dentine and bone of mammals. The endocarps showed the highest $\delta^{18}\text{O}$ values measured for the locality and were clearly distinct from all values measured for large and small mammals (Fig. 1). As diagenetic alteration can be a long-term process and even REE uptake does not necessarily have to be restricted to early diagenesis (Herwartz et al. 2011 and 2013), these high values in *Celtis* endocarps could be explained by later (perhaps modern)

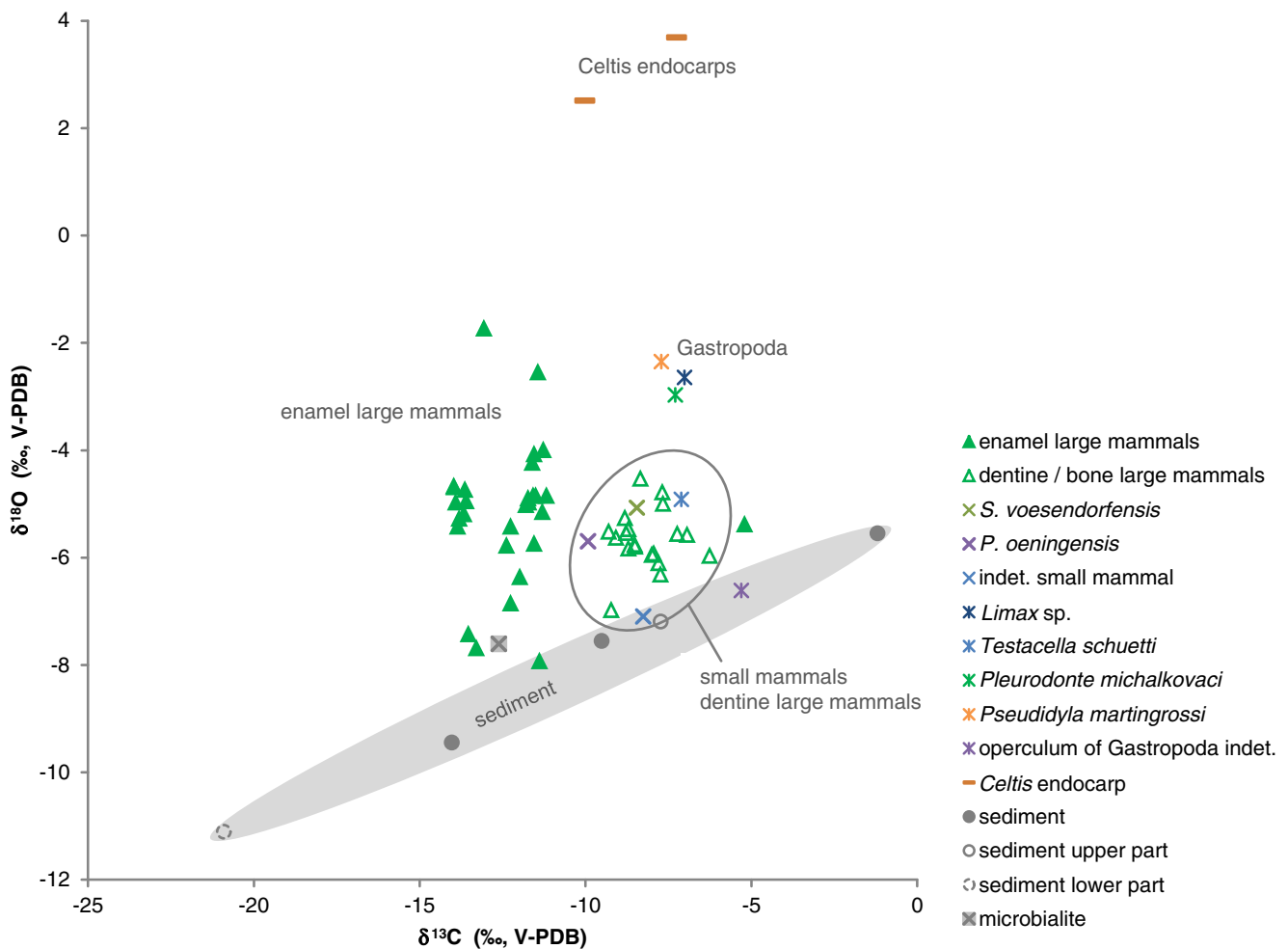


Fig. 1 $\delta^{18}\text{O}_{\text{CO}_3}$ (‰ V-PDB) versus $\delta^{13}\text{C}$ (‰ V-PDB) for large mammals (enamel, dentine and bone), small mammals (complete teeth), terrestrial gastropods, *Celtis* endocarps, sediment samples and a microbialite from the Gratkorn locality

diagenetic alteration, to which the fruits are more susceptible as they represent a system more easily accessible for diagenetic fluids due to their bad preservation and higher porosity.

Recrystallisation of gastropod shells of *Pseudidyla martingrossi* and *Pleurodonte michalkovaci* during diagenesis is unlikely as they still possess an aragonitic shell composition (Havlik et al. 2014, this issue). Rudimental shells of the slug *Limax* sp. showed calcite crystals. As the mineralogy of extant species of *Limax* is not fully understood, it cannot be verified whether or not the slug shells from Gratkorn are recrystallised (Havlik et al. 2014, this issue). Therefore, $\delta^{18}\text{O}$ and $\delta^{13}\text{C}$ values of *Pseudidyla martingrossi* and *Pleurodonte michalkovaci* are considered more reliable in preservation of the in vivo signals. *Pseudidyla martingrossi*, *Pleurodonte michalkovaci*, and *Limax* sp. showed similar $\delta^{18}\text{O}$ and $\delta^{13}\text{C}$ values, but distinctly higher $\delta^{18}\text{O}$ than small mammal whole teeth, large mammal dentine, other gastropod remains (*Testacella schuetti*, opercula of indeterminate gastropod), and sediment (Fig. 1). As little isotopic exchange can be assumed for the non-recrystallised *Pseudidyla martingrossi* and *Pleurodonte michalkovaci*, and the values clearly differ from tissues affected by

diagenetic alteration (small mammal whole teeth and large mammal dentine), the values for *Pseudidyla martingrossi*, *Pleurodonte michalkovaci*, and *Limax* sp. are considered in vivo signals and fit well with the observations of Yapp (1979), who showed that modern land snails are enriched in ^{18}O in comparison to meteoric water. As point and interval of time of gastropod shell mineralisation depends on many climate variables, for example, seasonality (Yanes et al. 2009), more measurements and a reliable correlation in behaviour and habitat to modern relatives is needed to gain further information. Food preference in terms of C_3 and C_4 plant diet also cannot be easily reconstructed, due for example to changes in metabolic rates (Balakrishnan and Yapp 2004).

Preservation of vertebrate remains

For small mammals, only bulk samples of enamel and dentine could be gained due to the thin enamel cover in comparison to large mammals. The authors are well aware that small mammal $\delta^{13}\text{C}$ and $\delta^{18}\text{O}_{\text{CO}_3}$ values are more likely to be significantly biased by diagenetic alteration. The measured small mammal

values are therefore not used here for ecological interpretations, but as indicators for diagenetic alteration of bone and dentine of large mammals. Small mammal $\delta^{13}\text{C}$ and $\delta^{18}\text{O}_{\text{CO}_3}$ values are well in accordance with bone and dentine of large mammals. Most likely both suffered from stronger isotopic exchange during their early taphonomic history, as is also indicated by the stronger influence of early diagenesis on the REE pattern (Trueman et al. 2006; Trueman 2013; for discussion, see also Havlik et al. 2014, this issue). $^{87}\text{Sr}/^{86}\text{Sr}$ ratios of small mammals are well suited to reconstruct the local $^{87}\text{Sr}/^{86}\text{Sr}$ ratios in bioavailable strontium during formation of the palaeosol.

The total carbonate content in large mammal enamel sampled for this work ranged between 4 and 6 % (Appendix 1) for all measured samples and thus presented the same proportions as expected in fresh, unaltered ungulate enamel (Rink and Schwarcz 1995; Julien et al. 2012). Hence, there are no signs of recrystallisation that would have led to unusually low carbonate values or of contamination by exogenous carbonate, which would be indicated by high values (Koch et al. 1997; Ecker et al. 2013). Furthermore, CaCO_3 content did not show any correlation with either $\delta^{18}\text{O}$ or $\delta^{13}\text{C}$ values in the measured samples. Moreover, large mammal enamel $\delta^{18}\text{O}$ and $\delta^{13}\text{C}$ values are distinct from corresponding measurements of dentine and bone, which clearly overlap with small mammals and invertebrates (Fig. 1), indicating to a certain degree a diagenetic alteration of dentine and bone.

Total REE contents (Havlik et al. 2014, this issue) of vertebrate enamel range from below detection limit (0.07 ppm) up to 284 ppm comprising in general lower values than bone (values between 988 and 13,484 ppm) and dentine (values between 4 and 12,510 ppm). Except for two higher values in ruminants, *Tethyragus* sp. (GPIT/MA/2753: 172.34 ppm) and *Euprox furcatus* (GPIT/MA/2414: 284.42 ppm), enamel REE values were below 30 ppm and therefore indicate that tooth enamel from Gratkorn was not affected by extensive diagenetic alteration (see also discussions in Domingo et al. 2009; Havlik et al. 2014, this issue). The higher values for the two ruminant specimens could be explained by the enamel of ruminants being much thinner and more fragile and therefore more susceptible to diagenetic alteration in comparison to Rhinocerotidae and Deinotheriidae. In the case of *Euprox furcatus* (GPIT/MA/2414), the sampled tooth is a non-erupted molar and thus incomplete mineralisation could explain a higher degree of REE uptake. An incisor of a small mammal with very thin enamel (REE content of 0.079 ppm) and another ruminant, *Dorcatherium naui* (REE content of 0.5281 ppm), showed only small total REE contents. Diagenetic alteration and REE uptake thus seems to be more complex, as also observed by Herwartz et al. (2013). Due to a clear distinction of enamel and dentine/bone values for all measured *Euprox furcatus* and *Tethyragus* sp. and the inconspicuous carbonate content, enamel samples measured from these species are still considered to have retained biogenic $\delta^{18}\text{O}$ and $\delta^{13}\text{C}$ values.

In general, values of $\delta^{18}\text{O}_{\text{CO}_3}$ have to be considered less reliable than $\delta^{13}\text{C}$ values. Two teeth of one individual of

Dorcatherium naui (UMJGP 204662, m3 dex. and UMJGP 204665, m3 sin.) yielded a difference of 1.15 ‰ for $\delta^{18}\text{O}_{\text{CO}_3}$, while the offset in $\delta^{13}\text{C}$ was only 0.03 ‰. As teeth of Middle Miocene ruminants are smaller and possess thinner enamel than, e.g. Late Miocene bovids or than proboscideans, teeth cannot always be sampled at exactly the same tooth element in order to gain the necessary sample amount. The offset of $^{18}\text{O}_{\text{CO}_3}$ might thus result from a different amount of powder from trigonid or talonid and therefore average different mineralisation phases (see, e.g. different mineralisation phases for different conids in Avishai et al. 2004).

Diet of large mammals ($\delta^{18}\text{O}$ and $\delta^{13}\text{C}$)

Except for the tragulid *Dorcatherium naui* ($\delta^{13}\text{C}$: min -11.8 ‰, mean -9.9 ‰, max -5.2 ‰), which was most likely a frugivore to a certain degree, the $\delta^{13}\text{C}$ values of enamel of the other herbivorous large mammal teeth displayed a range from -14 to -11.2 ‰ and a mean value of -12.4 ‰ (Fig. 2). They are well within the range of Miocene large mammalian herbivores predominantly feeding in a mesic/woodland environment of a pure C_3 ecosystem, where a range from -14 to -9 ‰ is expected (Domingo et al. 2012). None of the taxa derived its diet from closed-canopy conditions, as Miocene herbivores feeding in closed canopy conditions should have $\delta^{13}\text{C}$ values lower than -15 – -14 ‰ (Tütken and Vennemann 2009; Domingo et al. 2012). Different values for $\delta^{18}\text{O}$ and $\delta^{13}\text{C}$ indicate different ecological niches among the large mammals from Gratkorn. The data fit well with a late Middle Miocene faunal assemblage from this area and are well in accordance with other Middle Miocene large mammal communities from Europe (see, e.g. Tütken et al. 2006; Tütken and Vennemann 2009; Domingo et al. 2009, 2012).

Ruminantia

Euprox furcatus

The cervid *Euprox furcatus* generally shows lower values for $\delta^{13}\text{C}$ (min: -13.6 ‰, mean: -12.9 ‰, max: -12 ‰; $n=5$) and $\delta^{18}\text{O}$ (min: -7.7 ‰, mean: -6.7 ‰, max: -5 ‰; $n=5$) in comparison to other taxa from Gratkorn, overlapping with the values of *M. flourensianus* and the lower value of *Listriodon splendens* (Fig. 2). The $\delta^{13}\text{C}$ values of *Euprox furcatus* fit well with feeding in a more closed, forested C_3 environment, and the lower values for both $\delta^{13}\text{C}$ and $\delta^{18}\text{O}$ to an ecological niche comprising mostly subcanopy diet. Besides inhabiting an environment with less evaporation, the low $\delta^{18}\text{O}$ values for *Euprox furcatus* in comparison to other large mammals could also indicate an obligate drinking behaviour (Kohn 1996; Kohn et al. 1996). So far, no isotopic measurements have been carried out on well-determined material of *Euprox furcatus*. The Middle Miocene locality of Steinheim, while yielding rich material of the species, also houses, besides *Euprox furcatus*, a similar-sized cervid, *Heteroprox larteti*,

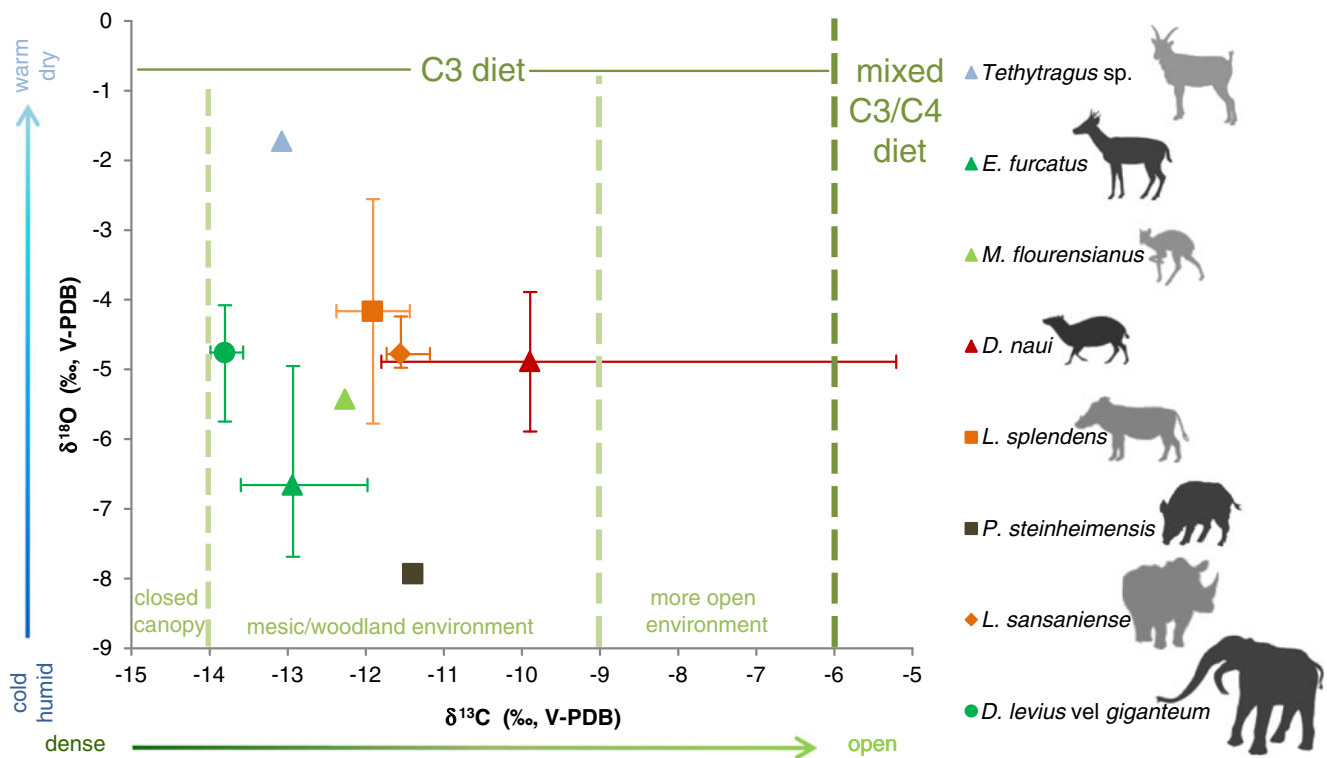


Fig. 2 Mean values with total range of $\delta^{18}\text{O}_{\text{CO}_3}$ (‰ V-PDB) versus $\delta^{13}\text{C}$ (‰ V-PDB) for large mammals (enamel) from the Gratkorn locality with designated niches (after Domingo et al. 2012) in a predominantly C_3

vegetation. Trends from dense and cold/humid environment to more open and warm/dry environment are indicated

which cannot be distinguished from the former on isolated dental material alone, and thus isotopic investigations on the locality only allowed a measurement of mixed material (*Euprox* vel *Heteroprox*; Tütken et al. 2006). Comparing measurements of the genus *Heteroprox* and indeterminate ruminants from other localities (Sandelzhausen, Seegraben, Somosaguas, and Puente de Vallecas; data from Tütken et al. 2006; Domingo et al. 2009, 2012; and own measurements) with the data from Gratkorn (Fig. 3a), it can be observed that *Euprox furcatus* shows the lowest values, while *Heteroprox* seems to be more enriched in both ^{18}O and ^{13}C . This could be explained by less browsing in subcanopy environment by the latter in comparison to *Euprox furcatus* but a higher degree of mixed feeding. Merceron et al. (2012) also observed a high degree of grazing in *Heteroprox* from Austria and Slovakia. However, occupation of different ecological niches is also dependent on the ecological conditions and the number of co-occurring species, as was shown in the study of DeMiguel et al. (2011) on the microwear of ruminants in Middle Miocene deposits of Central Spain. This might also explain the classification of *Heteroprox larteti* as a browser in Middle Miocene localities from the NAFB (North Alpine Foreland Basin; Kaiser and Rössner 2007), as it co-occurred with another cervid, *Dicrocerus elegans*, which was classified in their investigation as a mixed feeder. Although a certain degree of variability concerning the degree of mixed feeding in different ruminant assemblages can be expected, DeMiguel et al. (2011) observed a higher intake of grass and

tough vegetation in *Heteroprox larteti* than in *Euprox furcatus* at a locality where both co-occurred. So far, there is not enough data to define clearly distinct ecological niches for *Euprox furcatus* (subcanopy browser) and *Heteroprox* ssp. (more open environment mixed feeder). However, the results from Gratkorn and literature data (Tütken et al. 2006; DeMiguel et al. 2011; Domingo et al. 2012), indicate that the interpretation of *Euprox furcatus* as an inhabitant of drier environments by Thenius (1950) is less likely. *Euprox furcatus* rather represents a subcanopy browser and, in the case of co-occurrence with *Heteroprox larteti*, might have displayed a lower degree of mixed feeding than the latter.

Micromeryx flourensianus

A pure C_3 browsing diet can be assumed for the small moschid *Micromeryx flourensianus* ($\delta^{13}\text{C} = -12.3$ ‰; $\delta^{18}\text{O} = -5.4$ ‰; Fig. 2), possibly with slight enrichment by fruits and seeds, resulting in the slightly higher values for $\delta^{13}\text{C}$ and $\delta^{18}\text{O}$ in comparison to most of the cervids (Tütken and Vennemann 2009). However, because the isotopic data of *Micromeryx flourensianus* from Gratkorn were measured on only one individual, speculations on diet are rather limited. Merceron et al. (2007) and Merceron (2009) reconstructed a browsing diet (with some affinities to mixed feeding) with a significant intake of fruits and seeds for *Micromeryx*

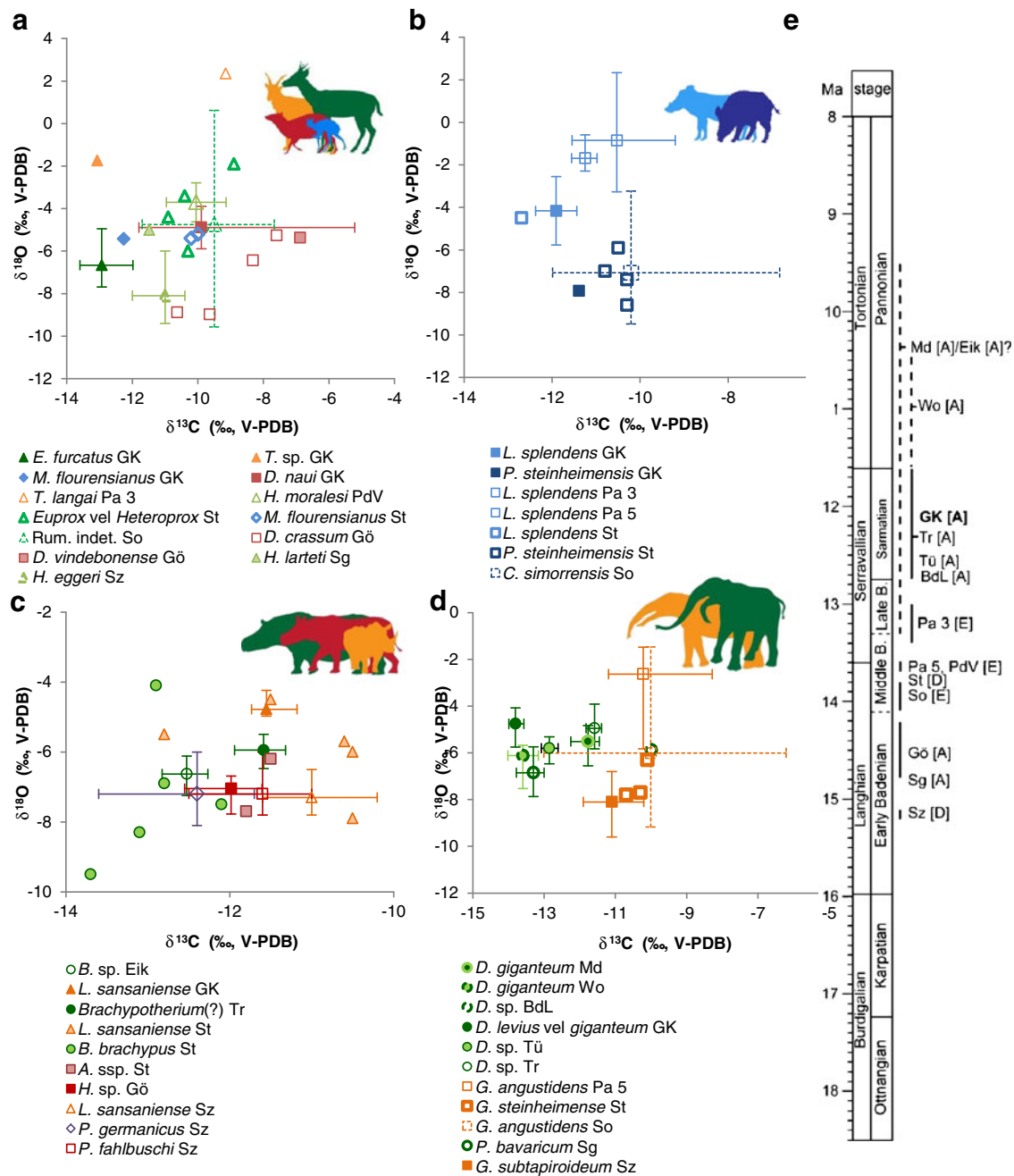


Fig. 3 Mean values with total range of $\delta^{18}\text{O}_{\text{CO}_3}$ (‰ V-PDB) versus $\delta^{13}\text{C}$ (‰ V-PDB) for large mammals (enamel) from the Gratkorn locality in comparison with data from other Miocene localities (GK Gratkorn (own measurements); Pa 3 Paracuellos 3 (from Domingo et al. 2012); PdV Puente de Vallecas (from Domingo et al. 2012); St Steinheim a. A. (from Tütken et al. 2006); So Somosaguas (from Domingo et al. 2009); Gö Görriach (own measurements); Sg Seegraben (own measurements); Sz Sandelzhausen (from Tütken and Vennemann 2009); Pa 5 Paracuellos 5 (from Domingo et al. 2012); Eik Eichkogel (own measurement); Tr Trössing (own measurements); Md Mödling (own measurements);

Wolfau (own measurements); BdL Bruck an der Leitha (own measurements)). **a** Ruminantia (*E. Euprox*; *T. Tethytragus*; *M. Micromeryx*; *D. Dorcatherium*; *H. Heteroprox*; Rum. Ruminantia); **b** Suidae (*L. L. Listriodon*; *P. Parachleuastochoerus*; *C. Conohyus*); **c** Rhinocerotidae (*B. Brachypotherium*; *L. Lartetotherium*; *A. Aceratherium*; ssp. several species; *H. Hoploaceratherium*; *P. germanicus* *Prosantorhinus germanicus*; *P. fahlbuschi* *Plesiaceratherium fahlbuschi*); **d** Proboscidea (*D. Deinotherium*; *G. Gomphotherium*; *P. Prodeinotherium*); **e** Stratigraphic age of different localities (A Austria, D Germany, E Spain, B Badenian)

flourensianus from Rudabanya and Atzelsdorf (both Late Miocene). Isotopic data for *Micromeryx flourensianus* from Steinheim (Tütken et al. 2006) are well in accordance with the measurements from Gratkorn (even more enriched in

^{13}C ; Fig. 3a). So far, isotopic data and microwear therefore indicate a generally C_3 browsing diet for the small moschid *Micromeryx flourensianus* with considerable intake of fruits or seeds and occasional grazing.

Tethytragus sp.

With a $\delta^{13}\text{C}$ value of -13.1‰ , a pure C_3 browsing diet can be assumed for *Tethytragus* sp.. It shows the highest value for $\delta^{18}\text{O}$ (-1.7‰) observed in the large mammal fauna of the locality (Fig. 2). In spite of the high REE content in this sample, and the fact that the CO_3 component is more susceptible to diagenetic alteration, the value is still considered to reflect a biological signal. The CaCO_3 content is not significantly higher than in other samples recorded, and the $\delta^{18}\text{O}$ value is not shifted in the direction of dentine and sediment samples, as would be expected when a considerable bias through diagenetic alteration has occurred. The higher values for $\delta^{18}\text{O}$ but similar values for $\delta^{13}\text{C}$ in comparison with other ruminants from Gratkorn could result from feeding on top canopy plants exposed to higher evaporation, as was reconstructed, for example, for *Giraffokeryx* (Giraffidae) from Paşalar by Bocherens and Sen (1998) or for *Germanomeryx* (Palaeomerycidae) from Sandelzhausen by Tütken and Vennemann (2009). Other isotopic measurements for the same genus (Domingo et al. 2012) also showed high $\delta^{18}\text{O}$ values and are well in accordance with the data from Gratkorn (Fig. 3a). Although small in body size in comparison to *Giraffokeryx* and *Germanomeryx*, feeding on top canopy plants could have been possible for *Tethytragus* due to a caprine-like postcranial adaptation enabling climbing and tree/rock-jumping to a certain degree (for further discussion, see Aiglstorfer et al. 2014c, this issue). Köhler (1993) could show adaptation to mountainous areas for *Tethytragus koehlerae* from the Turkish locality of Çandır (Middle Miocene). Micro- and mesowear analysis on *Tethytragus* from the Middle Miocene of Central Spain display different degrees of mixed feeding and grazing in their diet and even inconsistency between the two different methods in one population was observed (DeMiguel et al. 2011). As microwear is affected by the so-called “last-supper-effect” (Grine 1986), the diet of *Tethytragus koehlerae* might also depend on seasonal variations, which could also have been the case at Gratkorn.

Dorcatherium nauii

So far, no isotopic measurements have been published on Miocene Tragulidae of Europe. The high $\delta^{13}\text{C}$ values of -11.8 to -5.2‰ with a mean of -9.9‰ ($n=4$) for the tragulid *Dorcatherium nauii* were thus quite unexpected, as modern Tragulidae inhabit the undergrowth of forested environments (Rössner 2007), and other species of the genus, like *Dorcatherium crassum*, have been considered as indicators for wetland conditions. Therefore, one would have expected $\delta^{13}\text{C}$ and $\delta^{18}\text{O}$ values typical for closed canopy or at least subcanopy feeding in a more humid environment for *Dorcatherium nauii* from Gratkorn. In contrast to this expectation, this taxon yielded $\delta^{13}\text{C}$ values clearly higher than for all other large mammals from the locality (Fig. 2). $\delta^{18}\text{O}$ values are instead only slightly higher than in cervids (min: -5.4‰ , mean: -4.9‰ , max: -4‰). These values can be explained by a certain

amount of mixed feeding (leaves and grass) or by ingestion of a considerable amount of fruit. In investigations on a modern large mammal assemblage from the Ituri Forest (Democratic Republic of Congo), tragulids showed higher values for $\delta^{13}\text{C}$ but similar ones for $\delta^{18}\text{O}$, and nested well within canopy frugivores (Cerling et al. 2004). Moreover, Codron et al. (2005) could show that tree fruits were significantly ^{13}C -enriched, by about 1.5–2 ‰ on average, compared to tree leaves. The mean enrichment of 3 ‰ for $\delta^{13}\text{C}$ observed at Gratkorn is slightly higher but would still fit well with the ingestion of a considerable amount of fruit by *Dorcatherium nauii*. However, an exclusively frugivore diet for the species cannot be assumed, as the climate (seasonality, MAP of 486 ± 252 mm, and MAT of $\sim 15\text{°C}$; Gross et al. 2011) makes an all-year fruit supply for the area around Gratkorn most unlikely. Today, the fruit supply is not high enough even in evergreen forests for a strictly frugivore feeding of terrestrial frugivores all year (Smythe 1986). The assumption of Sponheimer and Lee-Thorp (2001) that frugivores should be more depleted in ^{18}O than folivores can only be sustained under the presumption that the animals fed from the same plant/tree, since besides intraspecific differences (leaves vs. fruits), interspecific differences were also observed in the enrichment in ^{18}O by Dunbar and Wilson (1983). As it is most likely that the leaf-browsing cervid *Euprox furcatus* and the browsing and facultative frugivorous tragulid *Dorcatherium nauii* did not feed exclusively on the same plants, the different values in $\delta^{13}\text{C}$ and the similar values in $\delta^{18}\text{O}$ fit well with the proposed differences in ecological niches. Measurements on other species of the genus, *D. crassum* and *D. vindebonense*, from an intramontane basin (early Middle Miocene locality of Göriach; Austria; $\sim 14.5\text{ Ma} \pm 0.3\text{ Ma}$) also showed generally slightly higher $\delta^{13}\text{C}$ values than other ruminants (Fig. 3a), which could also result from ingestion of a considerable amount of fruits. Furthermore, works based on microwear analyses reconstructed a frugivore browsing diet for *D. nauii* from the Late Miocene locality of Atzelsdorf (Austria; 11.1 Ma; Merceron 2009) and for *Dorcatherium crassum* from Göriach and other Austrian intramontane basins (Merceron et al. 2012), while *Dorcatherium vindebonense* was termed a generalist, comparable to the modern red deer by Merceron et al. (2012). As we cannot exclude a certain amount of mixed feeding (browsing and grazing on C_3 vegetation) from our measurements at the locality of Göriach, and as $\delta^{18}\text{O}$ values of the different specimens from the locality show quite a wide range, occupation of more diverse ecological niches among the different *Dorcatherium* specimens with a considerable amount of C_3 grass ingestion do not seem unlikely.

Since there is so far no evidence for the existence of a relevant amount of grass in the vegetation of Gratkorn, and keeping in mind the observations of Merceron (2009), we assume fruit ingestion rather than grazing to be more likely for *Dorcatherium nauii* from Gratkorn. In addition, the morphology of the species' incisor arcade rather points to ingestion of fruits to a certain degree more than to grazing (for further discussion, see Aiglstorfer et al. 2014c, this issue). On the other

hand, a mixed diet was reconstructed for *Dorcatherium guntianum* from the NAFB by Kaiser and Rössner (2007). It is, together with *Dorcatherium naui*, part of a phylogenetic lineage differing from the more bunodont *Dorcatherium crassum* by more selenodont and higher crowned teeth (for further discussion, see Aiglstorfer et al. 2014c, this issue). Ungar et al. (2012) also observed mixed feeding for Early Miocene Tragulidae from Africa. In summary, for the moment, we therefore consider *Dorcatherium naui* from Gratkorn a browser with facultative frugivory, but we cannot completely rule out a certain amount of mixed feeding.

In addition to different diets, different digestion systems between *Dorcatherium* and higher ruminants could also explain differences in isotopic ratios. In modern tragulids, for example, the rumen, where fermentation takes place in symbiosis with bacteria, is relatively small compared to more derived ruminants (Rössner 2007). Slightly higher $\delta^{18}\text{O}$ values could furthermore be triggered by less dependency on drinking than observed in the obligate drinker *Euprox furcatus*. Modern tragulids have the lowest water intake of modern ruminants in the tropics (Rössner 2007).

Suidae

Listriodon splendens (min: -12.4‰ , mean: -11.9‰ , max: -11.4‰ ; $n=2$) and *Parachleuastochoerus steinheimensis* (-11.4‰) show similar values for $\delta^{13}\text{C}$, well in accordance with other browsing taxa. In contrast to $\delta^{13}\text{C}$, $\delta^{18}\text{O}$ values of *Listriodon splendens* (min: -5.8‰ , mean: -4.2‰ , max: -2.6‰ ; $n=2$) and of *Parachleuastochoerus steinheimensis* (-7.9‰) are quite distinct (Fig. 2). Because of the Tapir-like lophodont dentition, *Listriodon splendens* has been traditionally considered a specialised folivore (van der Made 1996). Isotopic measurements from Gratkorn fit well within this ecological niche and higher values in $\delta^{18}\text{O}$ indicate a certain amount of mixed feeding or ingestion of maybe upper canopy fruit, more enriched in ^{18}O (Nelson 2007). This is well in accordance with ecological interpretations based on morphology by van der Made et al. (2014). The distinctly lower $\delta^{18}\text{O}$ values, but similar $\delta^{13}\text{C}$ values in *Parachleuastochoerus steinheimensis* from Gratkorn, could be explained by digging for roots, as these are depleted in $\delta^{18}\text{O}$ in comparison to leaves, while $\delta^{13}\text{C}$ values are similar (Sponheimer and Lee-Thorp 2001). While incisor and general jaw morphology makes consumption of roots for the genus *Listriodon* unlikely (van der Made 1996 and references therein; van der Made et al. 2014), for the subfamily Tetraconodontinae, to which *Parachleuastochoerus* is assigned, a certain amount of root consumption is assumed due to dental morphology (Hünemann 1999; van der Made et al. 2014). Comparing isotopic measurements from Gratkorn with literature data from other Miocene localities (Tütken et al. 2006; Domingo et al. 2009, 2012; Fig. 3b) different ecological niches for *Listriodon splendens* and for tetraconodontid suids (*Parachleuastochoerus*

steinheimense and *Conohyus simorreensis*) are verified and seem to be rather independent from climate and stratigraphic level. While *Listriodon splendens* plots well in a mostly browsing diet with occasional input of fruits or grass, $\delta^{18}\text{O}$ values in tetraconodontid suids are usually more negative, indicating a considerable amount of rooting in their diet.

Perissodactyla

Lartetotherium sansaniense

The $\delta^{13}\text{C}$ values of the rhinocerotid *Lartetotherium sansaniense* (min: -11.7‰ , mean: -11.6‰ , max: -11.2‰) are slightly higher than in the cervid *Euprox furcatus* or the proboscidean *Deinotherium*, though still nesting well within the range expected for feeding in a mesic/woodland C_3 -dominated environment (Fig. 2). Tütken et al. (2006) and Tütken and Vennemann (2009) observed higher $\delta^{13}\text{C}$ values for *Lartetotherium sansaniense* from Sandelzhausen and Steinheim a. A. in comparison to other rhino taxa, and therefore assumed feeding in more open environment for the species. This is well in accordance with the $\delta^{13}\text{C}$ values and the slightly higher $\delta^{18}\text{O}$ values (min: -5‰ , mean: -4.8‰ , max: -4.2‰) in comparison to other taxa observed in *Lartetotherium sansaniense* from the Gratkorn locality. Comparing different values for Miocene Rhinocerotidae from literature and our own measurements (Fig. 3c), it can be observed that, independently of age and climate, *Lartetotherium sansaniense* usually shows higher values for $\delta^{13}\text{C}$ and also frequently for $\delta^{18}\text{O}$ than other Rhinocerotidae. The two teleoceratini, the large rhinocerotid *Brachypotherium* from Steinheim a. A. (data from Tütken et al. 2006) and Eichkogel (own measurements) and the smaller *Prosantorhinus germanicus* from Sandelzhausen (data from Tütken and Vennemann 2009), generally display lower $\delta^{13}\text{C}$ values. The high $\delta^{13}\text{C}$ values for *Brachypotherium* (?) from Trössing could also be explained by a wrong taxonomic identification of the specimen, as it comprises only fragments which cannot be identified with certainty. Aceratini (*Plesiaceratherium fahlbuschi*, *Hoploaceratherium* sp., *Aceratherium* ssp. (including *Alicornops simorreense*); Fig. 3c; data from Tütken et al. 2006; Tütken and Vennemann 2009; own measurements) display values inbetween the other two groups. Though we are well aware that more data are needed to reconstruct ecological adaptations for the different rhinocerotid genera and species, the data presented here already indicate different ecological niches with *Brachypotherium* and other teleoceratini feeding in a more closed mesic/woodland environment (also fitting well to the graviportal gait and limb shortening; Heissig 1999), while *Lartetotherium sansaniense* was feeding in more open environment and aceratini occupied niches inbetween, which is also well in accordance with other considerations on the ecology of the different taxa (Heissig 1999; Bentaleb et al. 2006; Tütken and Vennemann 2009).

Since serial sampling of rhinocerotid teeth has proved to be an indicator for seasonal variability (MacFadden and Higgins 2004; Zin-Maung-Maung-Thein et al. 2011), the fragmented lower second molar (m2) was sampled along the axis of the tooth from the base of enamel to occlusal surface (height about 2 cm; Fig. 4a). Unfortunately, both intra-tooth ranges, $\Delta^{13}\text{C}$ (0.5) and $\Delta^{18}\text{O}$ (0.8), are too small to infer any seasonality and $^{87}\text{Sr}/^{86}\text{Sr}$ values do not show any significant variations. Since a clear seasonality for the region around Gratkorn is indicated by sedimentology and ectothermic vertebrates (Gross et al. 2011), and by serial measurements on *Deinotherium levius* vel *giganteum* (see discussion below), the height of the tooth fragment might be too short to represent a time interval recording seasonal variation.

Proboscidea

Deinotherium levius vel *giganteum*

Values for $\delta^{13}\text{C}$ for *Deinotherium levius* vel *giganteum* are the most negative among the large mammals from Gratkorn (min: -14‰ , mean: -13.8‰ , max: -13.6‰), but are still clearly in the range for a C_3 -dominated mesic/woodland environment. $\delta^{18}\text{O}$ values are generally higher (min: -5.8‰ , mean: -4.8‰ , max: -4.1‰) than for the cervid *Euprox furcatus*, but overlap more with *Listriodon splendens* and *Dorcatherium nauti*. The data fit well with browsing on top canopy leaves (Bocherens and Sen 1998).

Comparing the values for $\delta^{13}\text{C}$ and $\delta^{18}\text{O}$ of *Deinotherium levius* vel *giganteum* from Gratkorn with other measurements on Proboscidea from different Miocene localities of different stratigraphic levels (see “Material” for details), it can be observed that they nest well among the deinotheriidae (Fig. 3d), which generally show values typical for browsing in a C_3 dominated mesic/woodland environment. Only one deinotherid from Bruck an der Leitha (Austria, early Sarmatian) displayed higher $\delta^{13}\text{C}$ values, which could result from feeding in a more open environment. In contrast, Gomphotheres (data from Tütken and Vennemann 2009; Domingo et al. 2009, 2012) usually show higher $\delta^{13}\text{C}$ values, indicating a higher degree of mixed feeding and feeding in a more open environment, though still in C_3 -dominated vegetation. Harris (1996) also described strict feeding on C_3 vegetation for African deinotheres through their evolutionary history, while other proboscideans like gomphotheres switched from C_3 to C_4 during the Late Miocene (Harris 1996; Huttunen 2000; Lister 2013). Although this change seems not to have taken place in Europe (Domingo et al. 2013), clearly different ecological niches for deinotheres (browsing in mesic/woodland environment) and gomphotheres (mixed feeding in more open environment) can be observed, fitting well to the lophodont Tapir-like dentition in deinotheres in contrast to a more bunodont dentition in gomphotheres.

Along the axis of two fragmented teeth, a series of samples was measured for $\delta^{18}\text{O}$ and $\delta^{13}\text{C}$ to check for seasonal variation

(Fig. 4b). The teeth are a lower fourth premolar (p4; at least 3/4 of the original tooth crown height preserved) and a fragment of an unidentified molar (Mx/mx; at least 1/2 of the original tooth crown height preserved; due to enamel thickness, affiliation to a premolar is less likely). From general taphonomy (Aiglstorfer et al. 2014a, this issue; Havlik et al. 2014, this issue), finding position, and preservation of the two teeth, they most likely belong to one individual. However, since the tooth position of the molar cannot be determined, the sequence of mineralisation and eruption of the two teeth cannot be given. As tooth formation in the genus *Deinotherium* extends over at least 1.5 years (Macho et al. 2003), a record of at least two seasons was expected for each tooth. $\delta^{13}\text{C}$ values are quite constant and show little variation [intra-tooth range: $\Delta^{13}\text{C}$ (p4)=0.4; $\Delta^{13}\text{C}$ (Mx/mx)=0.4]. In contrast, both teeth (Fig. 4b) exhibit one clear maximum (p4: -4.1‰ , Mx/mx: -4.1‰) and one clear minimum (p4: -5.8‰ , mx/Mx: -5.7‰) each for $\delta^{18}\text{O}$ and intra-tooth ranges of 1.7 [$\Delta^{18}\text{O}$ (p4)] and 1.6 [$\Delta^{18}\text{O}$ (Mx/mx)].

Similar variations in $\delta^{13}\text{C}$, were observed in plant material from two localities in North America, comprising one cold desert biome (MAT 8 °C; MAP 290 mm; main precipitation in winter, spring/autumn) and one desert scrub to grassland (MAT 17 °C; MAP 300 mm; main precipitation in summer) and attributed to water stress and senescent leaves of plants by Hoppe et al. (2004). Considering additional dampening of diet $\delta^{13}\text{C}$ values due to enamel maturation in herbivores (Passey and Cerling 2002), seasonality in $\delta^{13}\text{C}$ values of the diet could thus be expected. Unfortunately, the $\delta^{13}\text{C}$ values display no clear seasonal pattern and are not concordant with the stronger and seasonal variation of $\delta^{18}\text{O}$, implying no seasonal diet change for *Deinotherium levius* vel *giganteum* but would fit to a more generalistic and unselective feeding strategy (Tütken and Vennemann 2009). However, the generally quite low $\delta^{13}\text{C}$ values point to an exclusively browsing diet. In order to ascertain if $\delta^{18}\text{O}$ variation was induced by seasonality of the local climate or seasonal migration of the animal, $^{87}\text{Sr}/^{86}\text{Sr}$ measurements were accomplished on the samples displaying maxima and minima for $\delta^{18}\text{O}$. Though $^{87}\text{Sr}/^{86}\text{Sr}$ values differ distinctly from the local fauna (see discussion below), no significant intra-tooth variation could be observed and thus $\delta^{18}\text{O}$ variation more likely represents seasonality than extensive migration of the animal at the time of enamel mineralisation. As each tooth displays one maximum (summer) and one minimum (winter), a 1-year cycle would be recorded by combining the two patterns, under the assumption that both teeth belong to the same individual.

Provenance analysis ($^{87}\text{Sr}/^{86}\text{Sr}$)

As mentioned above, $^{87}\text{Sr}/^{86}\text{Sr}$ values of fossil bones and teeth are useful to detect the provenance of different faunal elements in a taphocoenosis. Small mammals as well as invertebrates more likely represent the locally bioavailable $^{87}\text{Sr}/^{86}\text{Sr}$ ratio (Hoppe

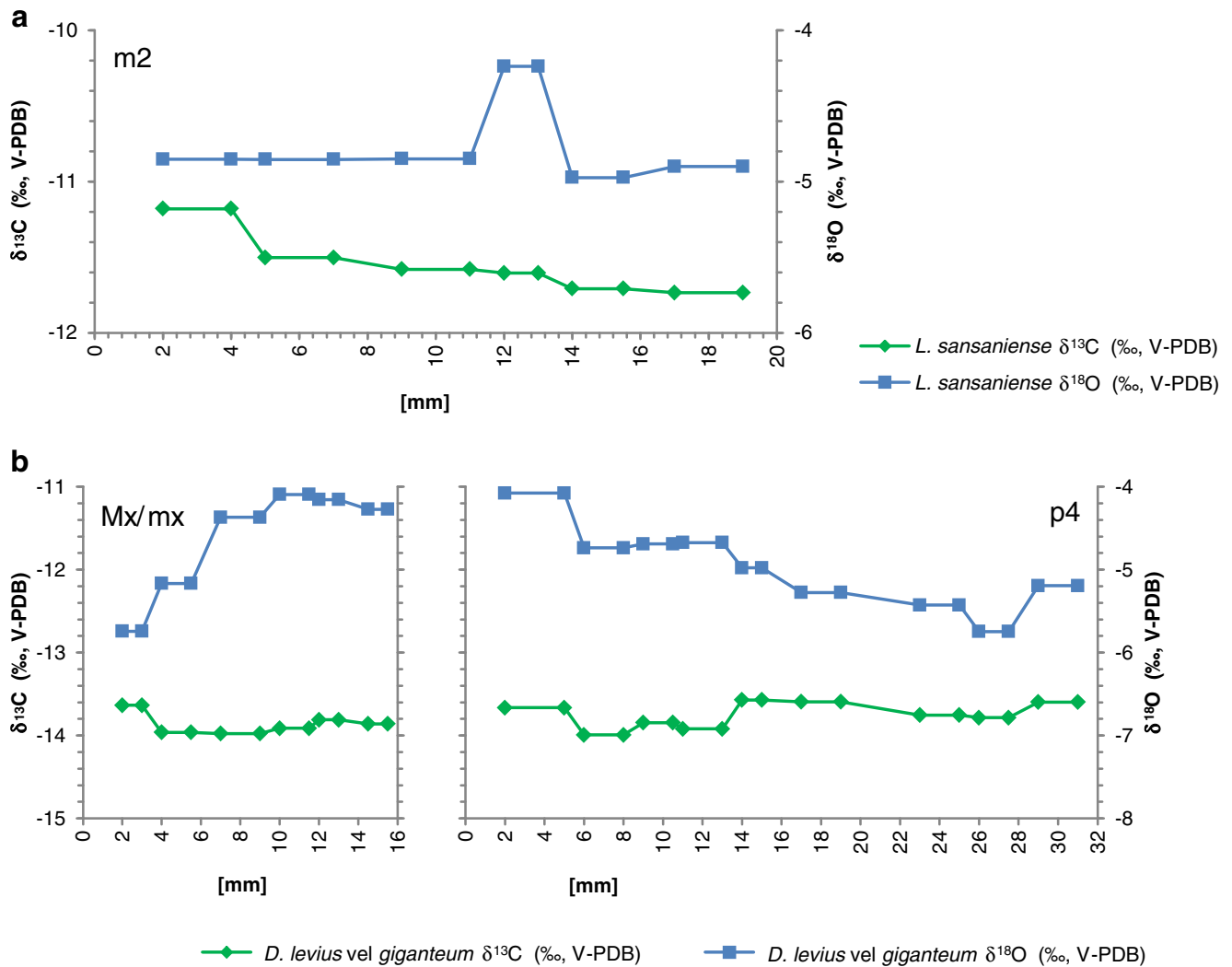


Fig. 4 Serial values of $\delta^{13}\text{C}$ (‰ V-PDB) and $\delta^{18}\text{O}_{\text{CO}_3}$ (‰ V-PDB) along the tooth crown axis from base (0 mm) to occlusal surface of the lower second molar of *Lartetotherium sansaniense* from Gratkorn (**a**), and of the

unidentified molar and the lower fourth premolar of *Deinotherium levius vel giganteum* from Gratkorn (**b**)

et al. 1999; Bentley 2006; Tütken and Vennemann 2009; Maurer et al. 2012). Although Maurer et al. (2012) observed that modern snail shells can be biased concerning the locally bioavailable $^{87}\text{Sr}/^{86}\text{Sr}$ ratio, at Gratkorn they are well in accordance with the small mammals and the microbialite, and thus represent the local signal, which is on average 0.711232 and ranges from 0.711031 to 0.711366 (Fig. 5). Among the large mammals, only *Tethytragus* sp. ($^{87}\text{Sr}/^{86}\text{Sr}$: 0.711472) and *Dorcatherium naui* ($^{87}\text{Sr}/^{86}\text{Sr}$: 0.711261) did not show significant differences from the local ratio and are interpreted as more or less permanent residents of the area around Gratkorn. Although small mammal samples suffered from a considerable diagenetic overprint, we still consider their $^{87}\text{Sr}/^{86}\text{Sr}$ ratio as a local signal of the Gratkorn locality representative for the time of sediment deposition (including early diagenesis). Small mammals, microbialite, gastropods, *Tethytragus* sp. and *Dorcatherium naui* are well in agreement concerning their $^{87}\text{Sr}/^{86}\text{Sr}$ ratios. It could be argued that the

sample of *Tethytragus* sp. with its high REE content might also have been influenced by diagenesis. However, its $\delta^{18}\text{O}$ and $\delta^{13}\text{C}$ values are not shifted in the direction of the small mammals, as would be expected in a case of strong alteration. Furthermore, the non-recrystallised gastropod, *Pleurodonte michalkovaci*, and the sample of *Dorcatherium naui*, are less likely to be considerably influenced by diagenesis (as mentioned above) and show similar values for $^{87}\text{Sr}/^{86}\text{Sr}$.

The suid *Listriodon splendens* (0.710888) and the rhinocerotid *Lartetotherium sansaniense* (mean $^{87}\text{Sr}/^{86}\text{Sr}$ =0.710633) showed slightly lower values, while $^{87}\text{Sr}/^{86}\text{Sr}$ values for *Euprox furcatus* ($^{87}\text{Sr}/^{86}\text{Sr}$ =0.710249) and *Deinotherium levius vel giganteum* (mean $^{87}\text{Sr}/^{86}\text{Sr}$ (p4)=0.709271 and mean $^{87}\text{Sr}/^{86}\text{Sr}$ (Mx/mx)=0.709234) are considerably shifted to lower values. These taxa ingested food and water in areas where $^{87}\text{Sr}/^{86}\text{Sr}$ ratios of bioavailable strontium were lower. The values are shifted in the direction of marine carbonates (Fig. 5), which in general show

values from 0.7076 to 0.7092 depending on the composition of the sea water and the age (McArthur et al. 2001; Tütken 2010). Increased total Sr content (Appendix 1) in contrast to other species might have biased the $^{87}\text{Sr}/^{86}\text{Sr}$ value for *Deinotherium levius* vel *giganteum* to a certain degree, but as no correlation can be observed between $^{87}\text{Sr}/^{86}\text{Sr}$ values and Sr content, taking into consideration the other large mammals, the decreased value for *Deinotherium levius* vel *giganteum* is still considered reliable, but treated with caution. $^{87}\text{Sr}/^{86}\text{Sr}$ values for Badenian to early Sarmatian (16–12.2 Ma) marine shark teeth and foraminifera from the nearby shallow marine Vienna Basin showed values from 0.708741 to 0.708893 (Hagmaier 2002; Kocsis et al. 2009), while late Karpatian to early Badenian localities from the more open Pannonian basin showed values of 0.708814 and 0.708895 (Kocsis et al. 2009). The Gratkorn locality is located in a satellite basin of the Styrian basin (Gross et al. 2011). As the latter was connected to both the more open Pannonian Basin and the shallower Vienna Basin during marine sedimentation in Badenian and early Sarmatian times, similar values are thus expected for the Styrian Basin. Due to a marginal marine situation at this time for the area south of Gratkorn, an enhanced terrestrial clastic sediment

input could have shifted the normal marine ratios to higher values. A terrestrial influence is documented by early Sarmatian marine pelites with intercalated gravels and sands in a drill core less than 20 km south of Gratkorn (Gross et al. 2007). Thus, *Euprox furcatus* and occasionally also *Listriodon splendens* and *Lartetotherium sansaniense* could have ingested food and water in areas where bioavailable $^{87}\text{Sr}/^{86}\text{Sr}$ resulted from these underlying bedrocks, while *Deinotherium levius* vel *giganteum* could have inhabited areas in the Styrian Basin with underlying marine sediments showing less terrestrial input.

In contrast to all other species, $^{87}\text{Sr}/^{86}\text{Sr}$ values (0.712732) for *Parachleuastochoerus steinheimensis* are distinctly higher than the local mean. Therefore, a different habitat is assumed for this species, with bedrocks yielding much higher $^{87}\text{Sr}/^{86}\text{Sr}$ values in bioavailable strontium than can be observed in Gratkorn. The Gratkorn locality is in close vicinity to the Eastern Alpine Mountain Chain, which consists to a considerable extent of Palaeozoic felsic magmatites and metamorphites. Palaeozoic granites and mica schists display higher $^{87}\text{Sr}/^{86}\text{Sr}$ values (Bentley 2006; Tütken 2010) and thus could be a possible bedrock for the habitat of *Parachleuastochoerus steinheimensis*.

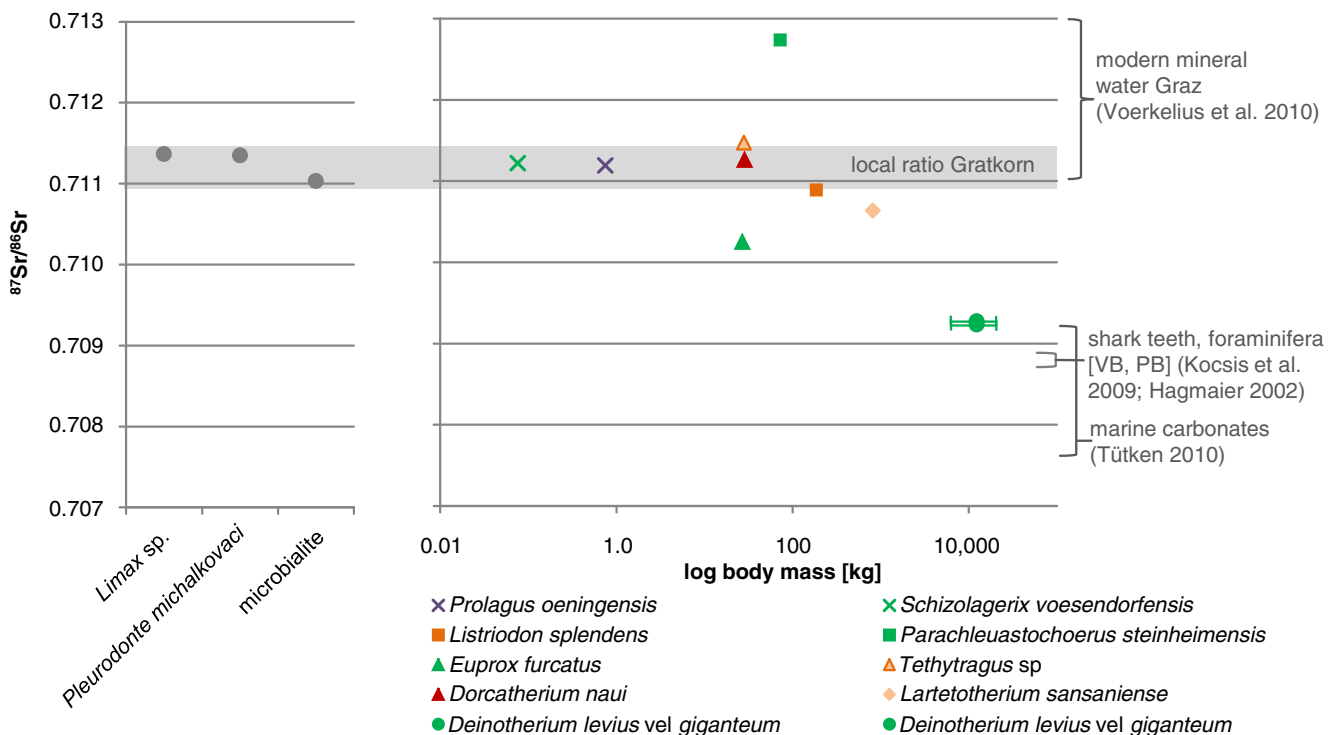


Fig. 5 $^{87}\text{Sr}/^{86}\text{Sr}$ isotope compositions from Gratkorn versus body mass (mammals only). Gastropods, the microbialite and small mammals (complete teeth) represent the local ratio for the locality. Most of the large mammals (enamel), especially with larger body mass, show different values from the local ratio due to migration (maybe provoked by limitation of available biomass at the locality). The values are compared to the modern natural mineral water values from Graz (data from Voerkelius et al. 2010), to the range for marine carbonates in general (data from Tütken 2010) and to ratios from measurements on shark teeth and foraminifera from late Karpatian to early Sarmatian sediments from

Austria (Bad Vöslau, Leithakalk, Siebenhirten) and Hungary (Danitzpuszta and Himesháza) (data from Kocsis et al. 2009; Hagmaier 2002; VB Vienna Basin; PB Pannonian Basin). Bodymass estimations follow Aiglstorfer et al. (2014c, this issue) for ruminants; Costeur et al. (2012) for *Listriodon splendens* and *Prolagus oeningensis*; Aiglstorfer et al. (2014a, this issue, and citations therein) for *Deinotherium levius* vel *giganteum*; and Fortelius (2013 (NOW database)) for *Parachleuastochoerus steinheimensis*; and is oriented for *Schizolagerix voesendorfensis* on the value for *Schizolagerix* sp. given by Merceron et al. (2012)

Summing up, no detailed migrational history can be reconstructed from $^{87}\text{Sr}/^{86}\text{Sr}$ ratios of the large mammals from Gratkorn due to limited data. However, it can be observed that, besides the more or less local residents *Tethytragus* sp. and *Dorcatherium nauti*, the other large mammals, *Listriodon splendens* (only to a minor degree), *Lartetotherium sansaniense*, *Euprox furcatus*, *Deinotherium levius vel giganteum*, and *Parachleuastochoerus steinheimensis*, lived in areas with lower or higher $^{87}\text{Sr}/^{86}\text{Sr}$ ratios in bioavailable strontium, at least temporarily. Especially the larger herbivores, such as the proboscidean or the rhinocerotids (see Fig. 5 for bodymasses), were dependent on a large amount of daily food supply. A limitation in available biomass (at least during some seasons) at the Gratkorn locality might be an explanation for migration of the larger mammals. However, for small mammals and the maybe better adapted *Dorcatherium nauti* and *Tethytragus* sp., food supply could have been enough during all seasons. With slightly higher values, the latter might have occasionally fed on bedrocks with higher values as well.

Conclusions

In summary, the herbivorous large mammals from Gratkorn were feeding on an exclusively C_3 vegetation and predominantly browsing in mesic/woodland environments. The isotope data of large mammal enamel presented here (for some taxa, comprising the first isotope data so far) indicate occupation of different ecological niches. Since the data from Gratkorn are well in accordance with measurements from other Miocene localities from different stratigraphic levels and with different climatic conditions (Tütken et al. 2006; Domingo et al. 2009, 2012; Tütken and Vennemann 2009,) relatively stable ecological niches can be reconstructed for some taxa.

Significantly higher $\delta^{13}\text{C}$ values in *Dorcatherium nauti* than displayed by the rest of the large mammal fauna from Gratkorn point to an ingestion of more fruits in its diet. The small moschid *Micromeryx flourensianus* could also have ingested fruits from time to time. The cervid *Euprox furcatus* represents a typical subcanopy browser and thus preferably occupied a different niche than the cervid *Heteroprox* (not recorded at Gratkorn), which was more adapted to an open environment. In spite of its small size, the bovid *Tethytragus* sp. represents a canopy browser (with a possibly caprine-like postcranial adaptation). The proboscidean *Deinotherium levius vel giganteum* browsed on canopy plants in the higher parts of an exclusively C_3 vegetation, in contrast to the more bunodont proboscidean *Gomphotherium*, which has not so far been recorded from Gratkorn, and exhibited a more mixed feeding diet. The latter proboscidean genus is recorded for Austria at the time of the Gratkorn locality. Its absence from the mammal assemblage from Gratkorn could thus have ecological reasons. Generally higher values for $\delta^{18}\text{O}$ and $\delta^{13}\text{C}$ in *Lartetotherium sansaniense*

indicate feeding in more open environments, as has also been observed for other localities (Tütken et al. 2006; Tütken and Vennemann 2009). *Listriodon splendens* was a typical browsing taxon with considerable input of fruits and maybe some grass in its diet, while the other suid from Gratkorn, *Parachleuastochoerus steinheimensis*, showed a certain degree of rooting as part of its diet. These different ecological niches for Listriodontinae and Tetraconodontinae seem to be quite stable, as similar values can be observed for different localities with different stratigraphic ages. Serial measurements on the teeth of *Deinotherium levius vel giganteum* show a seasonal variation at this time for the wider area around Gratkorn, fitting well to sedimentology and climate reconstructions based on ectothermic vertebrates from the Gratkorn locality itself (Gross et al. 2011; Böhme and Vasilyan 2014, this issue). Distinct differences in $^{87}\text{Sr}/^{86}\text{Sr}$ values indicate that not all large mammals were permanent residents of the area around Gratkorn, but inhabited a wider area, most likely including the Styrian Basin and the palaeozoic and metamorphic basement in the Eastern Alps. Biomass at the locality itself was most likely limited, and thus maybe not enough food was available for the largest herbivores during all seasons. Therefore, it can be assumed that the largest mammals were migrating to a certain degree.

We can reconstruct for the wider area around the Gratkorn locality an ecosystem with predominantly C_3 vegetation in a semi-arid, subtropical climate with distinct seasonality and too little precipitation for a closed canopy woodland. It provided enough diversity in plant resources to allow occupation of different niches, from subcanopy browsing and rooting to top canopy browsing, plus a certain degree of frugivory and mixed feeding for diverse large mammals. This or similar organisation patterns can be observed in other European Miocene localities (Tütken et al. 2006; Tütken and Vennemann 2009; Domingo et al. 2009, 2012), and seem to be affected only to a minor degree by climatic conditions but rather represent a typical niche partitioning of large mammals in a Middle Miocene ecosystem.

Acknowledgements P. Havlik (GPIT) is thanked for helpful discussions, proof reading of the manuscript and allowing the sampling of collection material. M. Gross (UMJGP), G. Scharf (IGM), U. Göhlich (NHMW) are thanked for access to collections and for allowing sampling of collection material. H. Reindl (UMJGP) is thanked for the help in the search for comparison material. I. Fritz, R. Niederl, F. Gitter, and N. Winkler (all UMJGP) are thanked for all the help during visits at the collection of the Joanneum, Graz. B. Steinhilber, I. Kleinhans, and E. Reitter (all three: Working Group Isotope Geochemistry, Eberhard Karls Universität Tübingen) are thanked for analyses of samples. Furthermore, D. Drucker, C. Wissing, M. Diaz-Zorita Bonilla (all Working Group Biogeology, Eberhard Karls Universität Tübingen), and T. Tütken (Johannes Gutenberg Universität Mainz) are thanked for helpful discussions. We want to thank two anonymous reviewers for the helpful comments and correction of the English which greatly helped to improve the quality of this publication. And last but not least, the authors want to thank the students and volunteers from Graz, Munich and Tübingen for the good work in the excavations from 2005 to 2013.

Appendix 1 Data from the Gratkorn locality

Table 1 $\delta^{13}\text{C}$ V-PDB (‰), $\delta^{18}\text{O}_{\text{CO}_3}$ V-PDB (‰) and $\delta^{18}\text{O}_{\text{CO}_3}$ V-SMOW (‰), CaCO_3 content (wt %), $^{87}\text{Sr}/^{86}\text{Sr}$ ratio of tooth enamel, dentine, and bone samples of small and large mammals and of invertebrates and soil samples from the Gratkorn locality

Sample	Specimen	Species	Tooth position	Tissue	$\delta^{13}\text{C}$ V-PDB (‰)	$\delta^{18}\text{O}$ V-PDB (‰)	$\delta^{18}\text{O}$ V-SMOW (‰)	CaCO_3 (wt %)	$^{87}\text{Sr}/^{86}\text{Sr}$	SD	Sr content (ppm) from Havlik et al., this issue
MA- 1e	UMJGP 203427	<i>Listriodon splendens</i>	m3	Enamel	-12.4	-5.8	24.9	3.52			
MA- 312	GPIT/MA/02757	<i>Listriodon splendens</i>	M3	Enamel	-11.4	-2.6	28.2	3.48	0.710888000	0.000009	168
MA- 2e	UMJGP 204652	<i>Parachleuastochoerus steinheimensis</i>	m3	Enamel	-11.4	-7.9	22.7	3.12			
MA- 332	UMJGP 204652	<i>Parachleuastochoerus steinheimensis</i>	m3	Enamel					0.712732000	0.000010	
MA- 5e	UMJGP 204665	<i>Dorcatherium navi</i>	m3	Enamel	-11.3	-4.0	26.7	3.32			
MA- 6e	UMJGP 204662	<i>Dorcatherium navi</i>	m3	Enamel	-11.3	-5.2	25.6	2.03			
MA- 7e	UMJGP 204109	<i>Dorcatherium navi</i>	m3	Enamel	-11.8	-5.0	25.7	4.60	0.711261000	0.000010	227
MA- 88	UMJGP 210694	<i>Dorcatherium navi</i>	m3	Enamel	-5.2	-5.4	25.3	3.58			
MA- 3e	UMJGP 204711	<i>Euprox.furcatus</i>	m3	Enamel	-13.3	-7.7	22.9	4.30	0.710249000	0.000009	313
MA- 4e	UMJGP 204713	<i>Euprox.furcatus</i>	m3	Enamel	-13.5	-7.4	23.2	3.00			
MA- 308	GPIT/MA/2386	<i>Euprox.furcatus</i>	m3	Enamel	-12.0	-6.4	24.3	3.95			
MA- 314	GPIT/MA/02739	<i>Euprox.furcatus</i>	M3	Enamel	-13.6	-5.0	25.8	3.09			
MA- 317	GPIT/MA/02393	<i>Euprox.furcatus</i>	m3	Enamel	-12.3	-6.9	23.8	4.25			
MA- 89	UMJGP 204685	<i>Micromeryx flourensianus</i>	m3	Enamel	-12.3	-5.4	25.3	4.43			
MA- 325	GPIT/MA/02753	<i>Tethyragus</i> sp.	M2?	Enamel	-13.1	-1.7	29.1	4.79	0.711472000	0.000009	145
MA- 67	UMJGP 203459	<i>Lartetotherium sansaniense</i>	m2 - base	Enamel	-11.2	-4.9	25.9	3.63	0.710517000	0.000009	136 (measured on fragment of tooth)
MA- 68	UMJGP 203459	<i>Lartetotherium sansaniense</i>	m2 - 2	Enamel	-11.5	-4.9	25.9	2.30			
MA- 69	UMJGP 203459	<i>Lartetotherium sansaniense</i>	m2 - 3	Enamel	-11.6	-4.8	25.9	2.71			
MA- 70	UMJGP 203459	<i>Lartetotherium sansaniense</i>	m2 - 4	Enamel	-11.6	-4.2	26.5	2.95	0.710700000	0.000009	
MA- 71	UMJGP 203459	<i>Lartetotherium sansaniense</i>	m2 - 5	Enamel	-11.7	-5.0	25.7	2.01			
MA- 72	UMJGP 203459	<i>Lartetotherium sansaniense</i>	m2 - tip	Enamel	-11.7	-4.9	25.8	2.29	0.710684000	0.000009	
MA- 73	UMJGP 203421	<i>Deinotherium levius</i> vel <i>giganteum</i>	Mx/mx - base	Enamel	-13.6	-5.7	24.9	4.28	0.709233000	0.000010	
MA- 74	UMJGP 203421	<i>Deinotherium levius</i> vel <i>giganteum</i>	Mx/mx-2	Enamel	-14.0	-5.2	25.5	3.76			
MA- 75	UMJGP 203421	<i>Deinotherium levius</i> vel <i>giganteum</i>	Mx/mx-3	Enamel	-14.0	-4.4	26.4	3.67			

Table 1 (continued)

Sample	Specimen	Species	Tooth position	Tissue	$\delta^{13}\text{C}$ V-PDB (‰)	$\delta^{18}\text{O}$ V-PDB (‰)	$\delta^{18}\text{O}$ V-SMOW (‰)	CaCO_3 (wt. %)	$^{87}\text{Sr}/^{86}\text{Sr}$	SD	Sr content (ppm) from Havlik et al., this issue
MA- 76	UMJGP 203421	<i>Deinotherium levius</i> vel <i>giganteum</i>	Mx/mx-4	Enamel	-13.9	-4.1	26.6	3.64	0.709222000	0.000012	
MA- 77	UMJGP 203421	<i>Deinotherium levius</i> vel <i>giganteum</i>	Mx/mx-5	Enamel	-13.8	-4.2	26.6	2.32			
MA- 78	UMJGP 203421	<i>Deinotherium levius</i> vel <i>giganteum</i>	Mx/mx - tip	Enamel	-13.9	-4.3	26.5	2.38	0.709247000	0.000009	
MA- 79	UMJGP 203435	<i>Deinotherium levius</i> vel <i>giganteum</i>	p4 - base	Enamel	-13.7	-4.1	26.7	2.77	0.709277000	0.000010	2,536 (measured on fragment of tooth)
MA- 80	UMJGP 203435	<i>Deinotherium levius</i> vel <i>giganteum</i>	p4 - 2	Enamel	-14.0	-4.7	26.0	2.31			
MA- 81	UMJGP 203435	<i>Deinotherium levius</i> vel <i>giganteum</i>	p4 - 3	Enamel	-13.8	-4.7	26.0	3.29			
MA- 82	UMJGP 203435	<i>Deinotherium levius</i> vel <i>giganteum</i>	p4 - 4	Enamel	-13.9	-4.7	26.0	3.36			
MA- 83	UMJGP 203435	<i>Deinotherium levius</i> vel <i>giganteum</i>	p4 - 5	Enamel	-13.6	-5.0	25.7	3.75	0.709262000	0.000011	
MA- 84	UMJGP 203435	<i>Deinotherium levius</i> vel <i>giganteum</i>	p4 - 6	Enamel	-13.6	-5.3	25.4	3.78			
MA- 85	UMJGP 203435	<i>Deinotherium levius</i> vel <i>giganteum</i>	p4 - 7	Enamel	-13.8	-5.4	25.3	2.35			
MA- 86	UMJGP 203435	<i>Deinotherium levius</i> vel <i>giganteum</i>	p4 - 8	Enamel	-13.8	-5.8	24.9	2.20	0.709276000	0.000009	
MA- 87	UMJGP 203435	<i>Deinotherium levius</i> vel <i>giganteum</i>	p4 - tip	Enamel	-13.6	-5.2	25.5	2.72			
MA- 323	No number	<i>Schizogalerix voesendorffensis</i>	Cheek teeth	Dentine/enamel	-8.5	-5.1	25.6	4.58	0.711218000	0.000009	
MA- 324	No number	<i>Prolagus oeningensis</i>	Cheek teeth	Dentine/enamel	-9.9	-5.7	25.0	4.70	0.711193000	0.000010	
MA- 327	No number	Undetermined small mammal	Incisor	Dentine/enamel	-8.3	-7.1	23.5	5.47			
MA- 178	No number	<i>Pseudidyla martingrossi</i>	Shell	Shell	-7.7	-2.4	28.4	98.96			
MA- 179	No number	<i>Limax</i> sp.	Shell	Shell	-7.0	-2.6	28.1	92.52	0.711366000	0.000024	
MA- 180	No number	<i>Pleurodonite michalkovaci</i>	Shell	Shell	-7.3	-3.0	27.8	101.12	0.711350000	0.000009	
MA- 182	No number	<i>Testacella schuetti</i>	Shell	Shell	-7.1	-4.9	25.8	95.41			
MA- 183	No number	Operculum of indetermined gastropoda			-5.3	-6.6	24.0	100.63			
MA- 176	No number	<i>Celtis</i> sp.	Endocarb	Endocarb	-7.3	3.7	34.8	97.35			
MA- 177	No number	<i>Celtis</i> sp.	Endocarb	Endocarb	-10.0	2.5	33.5	97.35			
MA- 320	No number	Microbialite	Carbonate	Carbonate	-12.6	-7.6	23.0	85.24	0.711031000	0.000011	
MA- 307	From UMJGP 210694	Sediment	Sediment	Sediment	-1.2	-5.6	25.1	0.46			

Table 1 (continued)

Sample	Specimen	Species	Tooth position	Tissue	$\delta^{13}\text{C}$ V-PDB (‰)	$\delta^{18}\text{O}$ V-PDB (‰)	$\delta^{18}\text{O}$ V-SMOW (‰)	CaCO_3 (wt. %)	$^{87}\text{Sr}/^{86}\text{Sr}$	SD	Sr content (ppm) from Havlik et al., this issue
MA-311	From GPIT/MA/2386	Sediment		Sediment	-9.5	-7.6	23.1	0.16			
MA-316	From GPIT/MA/02739	Sediment		Sediment	-14.0	-9.4	21.1	0.13			
MA-321	From G 105/12	Soil upper part/leave		Sediment	-7.7	-7.2	23.4	0.08			
MA-322	From GPIT/MA/02757	Soil lower part		Sediment	-20.9	-11.1	19.4	0.23			
MA-1w	UMJGP 203427	<i>Listriodon splendens</i>	m3 root	Dentine	-7.2	-5.6	25.1	5.91			
MA-2k	UMJGP 204652	<i>Parachleuastochoerus steinheimensis</i>	Dentary	Bone	-9.2	-7.0	23.7	5.46			
MA-5w	UMJGP 204665	<i>Dorcatherium navi</i>	m3 root	Dentine	-8.7	-5.8	24.8	6.60			
MA-5k	UMJGP 204665	<i>Dorcatherium navi</i>	Dentary	Bone	-8.5	-5.8	24.9	7.14			
MA-6w	UMJGP 204662	<i>Dorcatherium navi</i>	m3 root	Dentine	-8.8	-5.5	25.1	3.91			
MA-6k	UMJGP 204662	<i>Dorcatherium navi</i>	Dentary	Bone	-8.5	-5.8	24.9	6.90			
MA-168	UMJGP 204109	<i>Dorcatherium navi</i>	m2 root	Dentine	-7.9	-5.9	24.8	4.05			
MA-306	UMJGP 210694	<i>Dorcatherium navi</i>	m3 root	Dentine	-6.3	-6.0	24.7	4.47			
MA-4w	UMJGP 204713	<i>Euprox furcatus</i>	m3 root	Dentine	-9.3	-5.5	25.2	6.33			
MA-167	UMJGP 204711	<i>Euprox furcatus</i>	m3 root	Dentine	-9.1	-5.6	25.1	5.26			
MA-328	UMJGP 204685	<i>Micromeryx flourensianus</i>	Dentary	Bone	-8.8	-5.3	25.4	5.90			
MA-169	UMJGP 203459	<i>Larietotherium sansaniense</i>	m2	Dentine	-6.9	-5.6	25.1	4.98			
MA-170	UMJGP 203435	<i>Deinotherium levius</i> vel <i>giganteum</i>	p4	Dentine	-7.8	-6.1	24.6	5.63			
MA-171	UMJGP 203421	<i>Deinotherium levius</i> vel <i>giganteum</i>	Mx/mx	Dentine	-8.0	-6.0	24.7	5.13	0.710284000	0.000010	
MA-313	GPIT/MA/02757	<i>Listriodon splendens</i>	M3	Dentine	-7.7	-4.8	25.9	4.33			
MA-315	GPIT/MA/02739	<i>Euprox furcatus</i>	Maxilla	Bone	-7.7	-5.0	25.7	4.83			
MA-319	GPIT/MA/02393	<i>Euprox furcatus</i>	Dentary	Bone	-8.7	-5.5	25.2	4.20			
MA-326	GPIT/MA/02753	<i>Tethyragus</i> sp.	M2?	Dentine	-8.3	-4.5	26.2	4.69			

Appendix 2 Comparison data from Austrian localities

Table 2 $\delta^{13}\text{C}$ V-PDB (‰), $\delta^{18}\text{O}_{\text{CO}_3}$ V-PDB (‰) and $\delta^{18}\text{O}_{\text{CO}_3}$ V-SMOW (‰) values and CaCO_3 content (wt %) of tooth enamel, dentine, and bone samples of large mammals from several Austrian localities used as comparison data

Sample	Specimen	Species	Tooth position	Tissue	$\delta^{13}\text{C}$ V-PDB (‰)	$\delta^{18}\text{O}$ V-PDB (‰)	$\delta^{18}\text{O}$ V-SMOW (‰)	CaCO_3 (wt. %)	Kind of site	Age (Ma)	Locality
MA- 8	IGM 6025	<i>Dorcatherium crassum</i>	m3	Enamel	-9.6	-9.0	21.6	3.31	Intramontane	~14.5	Göriach
MA- 27	UMJGP 1942	<i>Dorcatherium crassum</i>	m3	Enamel	-8.3	-6.4	24.2	2.12	Intramontane	~14.5	Göriach
MA- 28	UMJGP 3787	<i>Dorcatherium crassum</i>	m3	Enamel	-7.6	-5.3	25.4	2.31	Intramontane	~14.5	Göriach
MA- 287	UMJGP 1952	<i>Dorcatherium crassum</i>	m3	Enamel	-10.6	-8.9	21.7	3.88	Intramontane	~14.5	Göriach
MA- 30	UMJGP 1918	<i>Dorcatherium vindebonense</i>	m3	Enamel	-6.9	-5.4	25.3	3.05	Intramontane	~14.5	Göriach
MA- 288	UMJGP 56886	<i>Heteroprox larteti</i>	M3	Enamel	-11.5	-5.0	25.7	2.85	Intramontane	14.8	Seegraben
MA- 9	IGM 89	<i>Prodeinotherium bavaricum</i>	Mx/mx - base	Enamel	-13.8	-7.5	23.1	4.21	Intramontane	14.8	Seegraben
MA- 10	IGM 89	<i>Prodeinotherium bavaricum</i>	Mx/mx-2	Enamel	-13.3	-5.7	24.9	2.76	Intramontane	14.8	Seegraben
MA- 11	IGM 89	<i>Prodeinotherium bavaricum</i>	Mx/mx-3	Enamel	-13.1	-6.7	24.0	2.70	Intramontane	14.8	Seegraben
MA- 12	IGM 89	<i>Prodeinotherium bavaricum</i>	Mx/mx-4	Enamel	-13.0	-7.1	23.5	2.56	Intramontane	14.8	Seegraben
MA- 13	IGM 89	<i>Prodeinotherium bavaricum</i>	Mx/mx-5	Enamel	-13.7	-7.9	22.8	3.56	Intramontane	14.8	Seegraben
MA- 14	IGM 89	<i>Prodeinotherium bavaricum</i>	Mx/mx-6	Enamel	-13.1	-6.3	24.4	4.03	Intramontane	14.8	Seegraben
MA- 15	IGM 89	<i>Prodeinotherium bavaricum</i>	Mx/mx - tip	Enamel	-13.1	-6.8	23.9	4.18	Intramontane	14.8	Seegraben
MA- 226	NHMW 1872 V 11	<i>Deinotherium</i> sp.	Px - base	Enamel	-12.8	-5.9	24.8	3.59	Vienna Basin	12.6	Türkenschanze
MA- 227	NHMW 1872 V 11	<i>Deinotherium</i> sp.	Px-2	Enamel	-13.0	-5.8	24.9	3.39	Vienna Basin	12.6	Türkenschanze
MA- 228	NHMW 1872 V 11	<i>Deinotherium</i> sp.	Px-3	Enamel	-13.0	-5.7	24.9	3.37	Vienna Basin	12.6	Türkenschanze
MA- 229	NHMW 1872 V 11	<i>Deinotherium</i> sp.	Px-4	Enamel	-12.8	-5.3	25.4	3.32	Vienna Basin	12.6	Türkenschanze
MA- 230	NHMW 1872 V 11	<i>Deinotherium</i> sp.	Px-5	Enamel	-13.1	-6.5	24.2	2.95	Vienna Basin	12.6	Türkenschanze
MA- 231	NHMW 1872 V 11	<i>Deinotherium</i> sp.	Px-6	Enamel	-12.6	-5.8	24.9	3.11	Vienna Basin	12.6	Türkenschanze
MA- 232	NHMW 1872 V 11	<i>Deinotherium</i> sp.	Px - tip	Enamel	-12.7	-5.6	25.1	3.08	Vienna Basin	12.6	Türkenschanze
MA- 95	UMJGP 50165	<i>Deinotherium</i> sp.	Mx/mx - base	Enamel	-11.5	-4.3	26.4	3.30	Styrian Basin	12.7–11.6	Trössing near Gnas
MA- 96	UMJGP 50165	<i>Deinotherium</i> sp.	Mx/mx-2	Enamel	-11.5	-3.9	26.8	2.99	Styrian Basin	12.7–11.6	Trössing near Gnas
MA- 97	UMJGP 50165	<i>Deinotherium</i> sp.	Mx/mx-3	Enamel	-11.8	-4.3	26.5	2.82	Styrian Basin	12.7–11.6	Trössing near Gnas
MA- 98	UMJGP 50165	<i>Deinotherium</i> sp.	Mx/mx-4	Enamel	-11.8	-5.2	25.5	2.73	Styrian Basin	12.7–11.6	Trössing near Gnas
MA- 99	UMJGP 50165	<i>Deinotherium</i> sp.	Mx/mx-5	Enamel	-11.7	-5.5	25.2	3.06	Styrian Basin	12.7–11.10	Trössing near Gnas
MA- 100	UMJGP 50165	<i>Deinotherium</i> sp.	Mx/mx-6	Enamel	-11.6	-5.6	25.1	3.02	Styrian Basin	12.7–11.10	Trössing near Gnas

Table 2 (continued)

Sample	Specimen	Species	Tooth position	Tissue	$\delta^{13}\text{C}$ V-PDB (‰)	$\delta^{18}\text{O}$ V-PDB (‰)	$\delta^{18}\text{O}$ V-SMOW (‰)	CaCO_3 (wt. %)	Kind of site	Age (Ma)	Locality
MA-101	UMJGP 50165	<i>Deinotherium</i> sp.	Mx/mx-7	Enamel	-11.5	-5.2	25.5	3.17	Styrian Basin	12.7–11.10	Trössing near Gnas
MA-102	UMJGP 50165	<i>Deinotherium</i> sp.	Mx/mx-8	Enamel	-11.5	-5.0	25.7	3.29	Styrian Basin	12.7–11.10	Trössing near Gnas
MA-103	UMJGP 50165	<i>Deinotherium</i> sp.	Mx/mx-9	Enamel	-11.5	-5.8	24.9	3.01	Styrian Basin	12.7–11.10	Trössing near Gnas
MA-104	UMJGP 50165	<i>Deinotherium</i> sp.	Mx/mx - tip	Enamel	-11.4	-4.7	26.0	3.66	Styrian Basin	12.7–11.10	Trössing near Gnas
MA-215	NHMW 2000z0024/0000	<i>Deinotherium giganteum</i>	M2?	Enamel	-10.0	-5.9	24.8	3.79	Vienna Basin	12.7–12.2	Bruck a.d. Leitha
MA-31	UMJGP 45.816	<i>Deinotherium giganteum</i>	Mx/mx - base	Enamel	-14.0	-6.2	24.5	2.83	Styrian Basin	Early Late Miocene	Wolfa
MA-32	UMJGP 45.816	<i>Deinotherium giganteum</i>	Mx/mx-2	Enamel	-14.0	-5.7	25.0	3.03	Styrian Basin	Early Late Miocene	Wolfa
MA-33	UMJGP 45.816	<i>Deinotherium giganteum</i>	Mx/mx-3	Enamel	-13.3	-5.1	25.6	1.63	Styrian Basin	Early Late Miocene	Wolfa
MA-34	UMJGP 45.816	<i>Deinotherium giganteum</i>	Mx/mx-4	Enamel	-13.2	-7.5	23.1	3.48	Styrian Basin	Early Late Miocene	Wolfa
MA-35	UMJGP 45.816	<i>Deinotherium giganteum</i>	Mx/mx-5	Enamel	-13.6	-6.1	24.5	1.65	Styrian Basin	Early Late Miocene	Wolfa
MA-36	UMJGP 45.816	<i>Deinotherium giganteum</i>	Mx/mx - tip	Enamel	-13.6	-6.0	24.7	1.61	Styrian Basin	Early Late Miocene	Wolfa
MA-234	NHMW 1898	<i>Deinotherium giganteum</i>	M2? - base	Enamel	-12.2	-4.8	25.9	3.17	Vienna Basin	Miocene	Mödling
MA-235	NHMW 1898	<i>Deinotherium giganteum</i>	M2? - 2	Enamel	-11.8	-5.0	25.7	3.18	Vienna Basin	Miocene	Mödling
MA-236	NHMW 1898	<i>Deinotherium giganteum</i>	M2? - 3	Enamel	-12.3	-6.2	24.5	3.07	Vienna Basin	Miocene	Mödling
MA-237	NHMW 1898	<i>Deinotherium giganteum</i>	M2? - 4	Enamel	-12.0	-5.0	25.7	2.91	Vienna Basin	Miocene	Mödling
MA-238	NHMW 1898	<i>Deinotherium giganteum</i>	M2? - 5	Enamel	-11.5	-5.2	25.5	2.78	Vienna Basin	Miocene	Mödling
MA-239	NHMW 1898	<i>Deinotherium giganteum</i>	M2? - 6	Enamel	-11.9	-6.6	24.1	2.78	Vienna Basin	Miocene	Mödling
MA-240	NHMW 1898	<i>Deinotherium giganteum</i>	M2? - 7	Enamel	-11.7	-6.1	24.6	2.70	Vienna Basin	Miocene	Mödling
MA-241	NHMW 1898	<i>Deinotherium giganteum</i>	M2? - 8	Enamel	-11.4	-5.5	25.2	2.69	Vienna Basin	Miocene	Mödling
MA-242	NHMW 1898	<i>Deinotherium giganteum</i>	M2? - 9	Enamel	-11.6	-5.2	25.5	2.81	Vienna Basin	Miocene	Mödling
MA-243	NHMW 1898	<i>Deinotherium giganteum</i>	M2? - 10	Enamel	-11.5	-5.4	25.3	2.91	Vienna Basin	Miocene	Mödling
MA-244	NHMW 1898	<i>Deinotherium giganteum</i>	M2? - tip	Enamel	-11.7	-5.7	25.0	3.13	Vienna Basin	Miocene	Mödling
MA-23	IGM 3439	<i>Hoploacatherium</i> sp.	Mx/mx - base	Enamel	-11.8	-6.7	24.0	3.42	Intramontane	~14.5	Göriach
MA-24	IGM 3439	<i>Hoploacatherium</i> sp.	Mx/mx-2	Enamel	-11.6	-6.7	24.0	2.67	Intramontane	~14.5	Göriach
MA-25	IGM 3439	<i>Hoploacatherium</i> sp.	Mx/mx-3	Enamel	-12.0	-7.8	22.8	1.95	Intramontane	~14.5	Göriach
MA-26	IGM 3439	<i>Hoploacatherium</i> sp.	Mx/mx - tip	Enamel	-12.5	-7.0	23.6	2.54	Intramontane	~14.5	Göriach
MA-116	UMJGP 50178	<i>Brachyotherium</i> (?)	Mx/mx - base	Enamel	-11.9	-5.5	25.2	3.66	Styrian Basin	12.7–11.6	Trössing near Gnas
MA-117	UMJGP 50178	<i>Brachyotherium</i> (?)	Mx/mx-2	Enamel	-11.8	-5.5	25.2	3.22	Styrian Basin	12.7–11.6	Trössing near Gnas
MA-118	UMJGP 50178	<i>Brachyotherium</i> (?)	Mx/mx-3	Enamel	-11.8	-6.2	24.5	3.07	Styrian Basin	12.7–11.6	Trössing near Gnas
MA-119	UMJGP 50178	<i>Brachyotherium</i> (?)	Mx/mx-4	Enamel	-11.7	-6.5	24.2	2.87	Styrian Basin	12.7–11.6	Trössing near Gnas
MA-120	UMJGP 50178	<i>Brachyotherium</i> (?)	Mx/mx-5	Enamel	-11.6	-5.9	24.8	2.79	Styrian Basin	12.7–11.6	Trössing near Gnas
MA-121	UMJGP 50178	<i>Brachyotherium</i> (?)	Mx/mx-6	Enamel	-11.4	-5.9	24.8	2.87	Styrian Basin	12.7–11.6	Trössing near Gnas
MA-122	UMJGP 50178	<i>Brachyotherium</i> (?)	Mx/mx-7	Enamel	-11.4	-5.6	25.1	2.84	Styrian Basin	12.7–11.6	Trössing near Gnas
MA-123	UMJGP 50178	<i>Brachyotherium</i> (?)	Mx/mx-8	Enamel	-11.3	-5.9	24.8	2.87	Styrian Basin	12.7–11.6	Trössing near Gnas

Table 2 (continued)

Sample	Specimen	Species	Tooth position	Tissue	$\delta^{13}\text{C V-PDB}$ (‰)	$\delta^{18}\text{O V-PDB}$ (‰)	$\delta^{18}\text{O V-SMOW}$ (‰)	CaCO_3 (wt. %)	Kind of site	Age (Ma)	Locality
MA-124	UMJGP 50178	<i>Brachypotherium</i> (?)	Mx/mx-9	Enamel	-11.5	-6.4	24.3	2.86	Styrian Basin	12.7–11.6	Trössing near Gnas
MA-125	UMJGP 50178	<i>Brachypotherium</i> (?)	Mx/mx - tip	Enamel	-11.4	-6.1	24.6	3.05	Styrian Basin	12.7–11.6	Trössing near Gnas
MA-217	NHMW 1954/74	<i>Brachypotherium</i> sp.	Mx - tip	Enamel	-12.6	-6.2	24.5	3.18	Vienna Basin	Miocene	Eichkogel near Mödling
MA-218	NHMW 1954/74	<i>Brachypotherium</i> sp.	Mx-2	Enamel	-12.7	-7.0	23.6	3.00	Vienna Basin	Miocene	Eichkogel near Mödling
MA-219	NHMW 1954/74	<i>Brachypotherium</i> sp.	Mx-3	Enamel	-12.4	-7.2	23.4	2.93	Vienna Basin	Miocene	Eichkogel near Mödling
MA-220	NHMW 1954/74	<i>Brachypotherium</i> sp.	Mx-4	Enamel	-12.3	-7.2	23.4	2.57	Vienna Basin	Miocene	Eichkogel near Mödling
MA-221	NHMW 1954/74	<i>Brachypotherium</i> sp.	Mx-5	Enamel	-12.3	-6.6	24.1	2.68	Vienna Basin	Miocene	Eichkogel near Mödling
MA-222	NHMW 1954/74	<i>Brachypotherium</i> sp.	Mx-6	Enamel	-12.5	-6.3	24.3	3.18	Vienna Basin	Miocene	Eichkogel near Mödling
MA-223	NHMW 1954/74	<i>Brachypotherium</i> sp.	Mx-7	Enamel	-12.7	-6.1	24.6	3.22	Vienna Basin	Miocene	Eichkogel near Mödling
MA-224	NHMW 1954/74	<i>Brachypotherium</i> sp.	Mx - base	Enamel	-12.8	-6.3	24.4	3.77	Vienna Basin	Miocene	Eichkogel near Mödling
MA-286	UMJGP 1942	<i>Dorcatherium crassum</i>	m3 root	Dentine	-7.4	-7.5	23.1	5.78	Intramontane	~14.5	Göriach
MA-283	UMJGP 3787	<i>Dorcatherium crassum</i>	Bone	Bone	-4.2	-7.7	22.9	6.12	Intramontane	~14.5	Göriach
MA-285	UMJGP 1952	<i>Dorcatherium crassum</i>	m3 root	Dentine	-8.6	-7.7	22.9	5.51	Intramontane	~14.5	Göriach
MA-284	UMJGP 56886	<i>Heteroprox larteti</i>	Bone	Bone	-11.4	-9.4	21.2	6.27	Intramontane	14.8	Seegraben
MA-282	UMJGP 45.816	<i>Deinotherium</i>	Mx/mx	Dentine	-10.4	-7.4	23.2	5.57	Styrian Basin	Early Late Miocene	Wolfau
MA-279	UMJGP 50165	<i>Deinotherium</i>	Mx/mx	Dentine	-11.7	-5.9	24.8	5.23	Styrian Basin	12.7–11.6	Trössing near Gnas
MA-216	NHMW 2000z0024/0000	<i>Deinotherium</i> sp.	M2?	Dentine	-7.7	-5.8	24.9	5.16	Vienna Basin	12.7–12.2	Bruck a.d. Leitha
MA-233	NHMW 1872 V 11	<i>Deinotherium</i> sp.	Px	Dentine	-11.6	-4.7	26.0	5.13	Vienna Basin	12.6	Türkenschanze
MA-245	NHMW 1898	<i>Deinotherium giganteum</i>	M2?	Dentine	-11.9	-5.8	24.9	6.36	Vienna Basin	Miocene	Mödling
MA-276	UMJGP 50178	<i>Brachypotherium</i> (?)	Mx/mx	Dentine	-10.4	-6.0	24.7	5.42	Styrian Basin	12.7–11.6	Trössing near Gnas
MA-225	NHMW 1954/74	<i>Brachypotherium</i> sp.	Mx	Dentine	-12.6	-6.7	24.0	6.14	Vienna Basin	Miocene	Eichkogel near Mödling

References

- Aiglstorfer M, Göhlich UB, Böhme M, Gross M (2014a) A partial skeleton of *Deinotherium* (Proboscidea, Mammalia) from the late Middle Miocene Gratkorn locality (Austria). In: Böhme M, Gross M, Prieto J (eds) The Sarmatian vertebrate locality Gratkorn, Styrian Basin. *Palaeobio Palaeoenv* 94(1). doi:10.1007/s12549-013-0140-x
- Aiglstorfer M, Heissig K, Böhme M (2014b) *Perissodactyla* from the late Middle Miocene Gratkorn locality (Austria). In: Böhme M, Gross M, Prieto J (eds) The Sarmatian vertebrate locality Gratkorn, Styrian Basin. *Palaeobio Palaeoenv* 94(1). doi:10.1007/s12549-013-0138-4
- Aiglstorfer M, Rössner GE, Böhme M (2014c) *Dorcatherium naudi* and pecoran ruminants from the late Middle Miocene Gratkorn locality (Austria). In: Böhme M, Gross M, Prieto J (eds) The Sarmatian vertebrate locality Gratkorn, Styrian Basin. *Palaeobio Palaeoenv* 94(1). doi:10.1007/s12549-013-0141-9
- Avishai G, Müller R, Gabet Y, Bab I, Zilberman U, Smith P (2004) New approach to quantifying developmental variation in the dentition using serial microtomographic imaging. *Microsc Res Tech* 65: 263–269
- Badgley C, Barry JC, Morgan ME, Nelson SV, Behrensmeyer AK, Cerling TE, Pilbeam D (2008) Ecological changes in Miocene mammalian record show impact of prolonged climatic forcing. *Proc Natl Acad Sci USA* 105(34):12145–12149. doi:10.1073/pnas.0805592105
- Balakrishnan M, Yapp CJ (2004) Flux balance models for the oxygen and carbon isotope compositions of land snail shells. *Geochim Cosmochim Acta* 68(9):2007–2024. doi:10.1016/j.gca.2003.10.027
- Bentaleb I, Langlois C, Martin C, Iacumin P, Carré M, Antoine P-O, Duranthon F, Moussa I, Jaeger J-J, Barrett N, Kandorp R (2006) Rhinocerotid tooth enamel $^{18}\text{O}/^{16}\text{O}$ variability between 23 and 12 Ma in southwestern France. *CR Geol* 338(3):172–179. doi:10.1016/j.crte.2005.11.007
- Bentley AR (2006) Strontium isotopes from the earth to the archaeological skeleton: a review. *J Archaeol Method Theory* 13(3):135–187. doi:10.1007/s10816-006-9009-x
- Blum JD, Taliaferro EH, Weisse MT, Holmes RT (2000) Changes in Sr/Ca, Ba/Ca and $^{87}\text{Sr}/^{86}\text{Sr}$ ratios between trophic levels in two forest ecosystems in the northeastern U.S.A. *Biogeochemistry* 49(1):87–101. doi:10.2307/1469413
- Bocherens H, Sen S (1998) Pliocene vertebrate locality Çalta, Ankara, Turkey. 11. Isotopic investigation. *Geodiversitas* 20(3):487–495
- Bocherens H, Friis EM, Mariotti A, Pedersen KR (1993) Carbon isotopic abundances in Mesozoic and Cenozoic fossil plants: Palaeoecological implications. *Lethaia* 26:347–358
- Bocherens H, Koch PL, Mariotti A, Geraads D, Jaeger J-J (1996) Isotopic biogeochemistry (^{13}C , ^{18}O) of mammalian enamel from African Pleistocene hominid sites. *Palaio* 11:306–318
- Bocherens H, Sandrock O, Kullmer O, Schrenk F (2011a) Hominin palaeoecology in Late Pliocene Malawi: Insights from isotopes (^{13}C , ^{18}O) in mammal teeth. *S Afr J Sci* 107(3/4):95–100
- Bocherens H, Stiller M, Hobson KA, Pacher M, Rabeder G, Burns JA, Tütken T, Hofreiter M (2011b) Niche partitioning between two sympatric genetically distinct cave bears (*Ursus spelaeus* and *Ursus ingressus*) and brown bear (*Ursus arctos*) from Austria: Isotopic evidence from fossil bones. *Quat Int* 245(2):238–248. doi:10.1016/j.quaint.2010.12.020
- Böhme M, Vasilyan D (2014) Ectothermic vertebrates from the late Middle Miocene of Gratkorn (Austria, Styria). In: Böhme M, Gross M, Prieto J (eds) The Sarmatian vertebrate locality Gratkorn, Styrian Basin. *Palaeobio Palaeoenv* 94(1). doi:10.1007/s12549-013-0143-7
- Breitbart M, Hoare A, Nitti A, Siefert J, Haynes M, Dinsdale E, Edwards R, Souza V, Rohwer F, Hollander D (2009) Metagenomic and stable isotopic analyses of modern freshwater microbialites in Cuatro Ciénegas, Mexico. *Environ Microbiol* 11(1):16–34. doi:10.1111/j.1462-2920.2008.01725.x
- Cerling TE, Harris MJ (1999) Carbon isotope fractionation between diet and bioapatite in ungulate mammals and implications for ecological and paleoecological studies. *Oecologia* 120:347–363
- Cerling TE, Wang Y, Quade J (1993) Expansion of C_4 ecosystems as an indicator of global ecological change in the late Miocene. *Letter to Nature* 361:344–345
- Cerling TE, Harris JM, MacFadden BJ, Leakey MG, Quade J, Eisenmann V, Ehleringer JR (1997a) Global vegetation change through the Miocene/Pliocene boundary. *Nature* 389(6647):153–158
- Cerling TE, Harris MJ, Ambrose SH, Leakey MG, Solounias N (1997b) Dietary and environmental reconstruction with stable isotope analyses of herbivore tooth enamel from the Miocene locality of Fort Terman, Kenya. *J Hum Evol* 33:635–650
- Cerling T, Hart J, Hart T (2004) Stable isotope ecology in the Ituri Forest. *Oecologia* 138(1):5–12. doi:10.1007/s00442-003-1375-4
- Clementz MT, Holroyd PA, Koch PL (2008) Identifying aquatic habits of herbivorous mammals through stable isotope analysis. *Palaio* 23(9):574–585. doi:10.2110/palo.2007.p07-054r
- Codron D, Codron J, Lee-Thorp J, Sponheimer M, de Ruiter D (2005) Animal diets in the Waterberg based on stable isotopic composition of faeces. *S Afr J Wildl Res* 35(1):43–52
- Cooke MJ, Stern LA (2001) Banner JL (2001) The strontium isotope composition of fossil hackberry seed carbonate and tooth enamel as a potential record of soil erosion. Paper presented at the American Geophysical Union, Fall Meeting
- Costeur L, Guérin C, Maridet O (2012) Paléoécologie et paléoenvironnement du site miocène de Sansan. In: Peigné S, Sen S (eds) Mammifères de Sansan, vol 203, *Mem Mus Natl Hist Nat.*, pp 661–693
- Dansgaard W (1964) Stable isotopes in precipitation. *Tellus* 16:436–468
- DeMiguel D, Azanza B, Morales J (2011) Paleoenvironments and paleoclimate of the Middle Miocene of central Spain: A reconstruction from dental wear of ruminants. *Palaeogeogr Palaeoclimatol Palaeoecol* 302(3–4):452–463. doi:10.1016/j.palaeo.2011.02.005
- DeNiro MJ, Epstein S (1978) Influence of diet on the distribution of carbon isotopes in animals. *Geochim Cosmochim Acta* 42:495–506
- Domingo L, Cuevas-González J, Grimes ST, Hernández Fernández M, López-Martínez N (2009) Multiproxy reconstruction of the palaeoclimate and palaeoenvironment of the Middle Miocene Somosaguas site (Madrid, Spain) using herbivore dental enamel. *Palaeogeogr Palaeoclimatol Palaeoecol* 272(1–2):53–68. doi:10.1016/j.palaeo.2008.11.006
- Domingo L, Koch PL, Grimes ST, Morales J, López-Martínez N (2012) Isotopic paleoecology of mammals and the Middle Miocene Cooling event in the Madrid Basin (Spain). *Palaeogeogr Palaeoclimatol Palaeoecol* 339–341:98–113. doi:10.1016/j.palaeo.2012.04.026
- Domingo L, Koch PL, Hernández Fernández M, Fox DL, Domingo MS, Alberdi MT (2013) Late neogene and early quaternary paleoenvironmental and paleoclimatic conditions in southwestern Europe: isotopic analyses on mammalian taxa. *PLoS ONE* 8(5): e63739
- Dunbar J, Wilson AT (1983) Oxygen and hydrogen isotopes in fruit and vegetable juices. *Plant Physiol* 72:725–727
- Ecker M, Bocherens H, Julien M-A, Rivals F, Raynal J-P, Moncel M-H (2013) Middle Pleistocene ecology and Neanderthal subsistence: Insights from stable isotope analyses in Payre (Ardèche, southeastern France). *J Hum Evol* 65(4):363–373. doi:10.1016/j.jhevol.2013.06.013
- Ehleringer JR, Cerling TE (2002) C_3 and C_4 photosynthesis. In: Mooney HA, Canadell JG (eds) *Encyclopedia of global environmental change, vol 2, The Earth system: biological and ecological dimensions of global environmental change.* John Wiley, Chichester, pp 186–190
- Fortelius M (2013) New and old worlds database of fossil mammals (NOW). dataset downloaded Sep. 22, 2013. University of Helsinki. <http://www.helsinki.fi/science/now/>

- Friedli H, Lotscher H, Oeschger H, Siegenthaler U, Stauver B (1986) Ice core record of the $^{13}\text{C}/^{12}\text{C}$ ratio of atmospheric CO_2 in the past two centuries. *Nature* 324:237–238
- Göhlich UB, Gross M (2014) The Sarmatian (late Middle Miocene) avian fauna from Gratkorn, Austria. In: Böhme M, Gross M, Prieto J (eds) The Sarmatian vertebrate locality Gratkorn, Styrian Basin. *Palaeobio Palaeoenv* 94(1). doi:10.1007/s12549-013-0139-3
- Grine FE (1986) Dental evidence for dietary differences in *Australopithecus* and *Paranthropus*: a quantitative analysis of permanent molar microwear. *J Hum Evol* 15:783–822
- Gross M, Harzhauser M, Mandic O, Piller WE, Rögl F (2007) A stratigraphic enigma: the age of the Neogene deposits of Graz (Styrian Basin; Austria). *Joanna* 9:195–220
- Gross M, Böhme M, Prieto J (2011) Gratkorn: A benchmark locality for the continental Sarmatian s.str. of the Central Paratethys. *Int J Earth Sci (Geol Rundsch)* 100(8):1895–1913. doi:10.1007/s00531-010-0615-1
- Gross M, Böhme M, Havlik P, Aiglstorfer M, (2014) The late Middle Miocene (Sarmatian s.str.) fossil site Gratkorn - the first decade of research, geology, stratigraphy and vertebrate fauna. In: Böhme M, Gross M, Prieto J (eds) The Sarmatian vertebrate locality Gratkorn, Styrian Basin. *Palaeobio Palaeoenv* 94(1). doi:10.1007/s12549-013-0149-1
- Hagmaier M (2002) Isotopie (C, O und Sr) von Foraminiferen der zentralen nördlichen Paratethys (Bayerische Molasse, Wiener Becken) im Miozän als paläozooanographische Proxies. Eberhard Karls Universität Tübingen, Tübingen
- Harris JM (1996) Isotopic changes in the diet of African Proboscideans. *J Vertebr Paleontol* 16(40A)
- Havlik P, Aiglstorfer M, Beckman A, Gross M, Böhme M (2014) Taphonomical and ichnological considerations on the late Middle Miocene Gratkorn locality (Styria, Austria) with focus on large mammal taphonomy. In: Böhme M, Gross M, Prieto J (eds) The Sarmatian vertebrate locality Gratkorn, Styrian Basin. *Palaeobio Palaeoenv* 94(1). doi:10.1007/s12549-013-0142-8
- Heissig K (1999) Family rhinocerotidae. In: Rössner GE, Heissig K (eds) Land mammals of Europe. Verlag Dr. Friedrich Pfeil, München, pp 175–188
- Herwartz D, Tütken T, Münker C, Jochum CP, Stoll B, Sander PM (2011) Timescales and mechanisms of REE and Hf uptake in fossil bones. *Geochim Cosmochim Acta* 75:82–105
- Herwartz D, Tütken T, Jochum KP, Sander PM (2013) Rare earth element systematics of fossil bone revealed by LA-ICPMS analysis. *Geochim Cosmochim Acta* 103:161–183
- Higgins P, MacFadden BJ (2004) “Amount Effect” recorded in oxygen isotopes of Late Glacial horse (Equus) and bison (Bison) teeth from the Sonoran and Chihuahuan deserts, southwestern United States. *Palaeogeogr Palaeoclimatol Palaeoecol* 206(3–4):337–353. doi:10.1016/j.palaeo.2004.01.011
- Hoppe KA, Koch PL, Carlson RW, Webb SD (1999) Tracking mammoths and mastodons: Reconstruction of migratory behavior using strontium isotope ratios. *Geology* 27(5):439–442. doi:10.1130/0091-7613(1999)027<0439:tmamro>2.3.co;2
- Hoppe KA, Amundson R, Vavra M, McClaran MP, Anderson DL (2004) Isotopic analysis of tooth enamel carbonate from modern North American feral horses: implications for paleoenvironmental reconstructions. *Palaeogeogr Palaeoclimatol Palaeoecol* 203(3–4):299–311. doi:10.1016/S0031-0182(03)00688-6
- Hünemann KA (1999) Superfamily Suidae. In: Rössner GE, Heissig K (eds) Land mammals of Europe. Verlag Dr. Friedrich Pfeil, München, pp 209–216
- Huttunen KJ (2000) Deinotheriidae (Proboscidea, Mammalia) of the Miocene of Lower Austria, Burgenland and Czech Republic: systematics, odontology and osteology. PhD thesis. Universität Wien, Vienna
- Iacumin P, Bocherens H, Mariotti A, Longinelli A (1996) Oxygen isotope analyses of co-existing carbonate and phosphate in biogenic apatite: a way to monitor diagenetic alteration of bone phosphate? *Earth Planet Sci Lett* 142(1–2):1–6. doi:10.1016/0012-821X(96)00093-3
- Julien M-A, Bocherens H, Burke A, Drucker DG, Patou-Mathis M, Krotova O, Péan S (2012) Were European steppe bison migratory? ^{18}O , ^{13}C and Sr intra-tooth isotopic variations applied to a palaeoethological reconstruction. *Quat Int* 271:106–119. doi:10.1016/j.quaint.2012.06.011
- Kaiser TM, Rössner GE (2007) Dietary resource partitioning in ruminant communities of Miocene wetland and karst palaeoenvironments in Southern Germany. *Palaeogeogr Palaeoclimatol Palaeoecol* 252(3–4):424–439. doi:10.1016/j.palaeo.2007.04.013
- Keeley J, Rundel P (2003) Evolution of CAM and C_4 carbon-concentrating mechanisms. *Int J Plant Sci* 164(Suppl 3):S55–S77
- Koch PL, Tuross N, Fogel ML (1997) The effects of sample treatment and diagenesis on the isotopic integrity of carbonate in biogenic hydroxylapatite. *J Archaeol Sci* 24:417–429
- Kocsis L, Vennemann TW, Hegner E, Fontignie D, Tütken T (2009) Constraints on Miocene oceanography and climate in the Western and Central Paratethys: O-, Sr-, and Nd-isotope compositions of marine fish and mammal remains. *Palaeogeogr Palaeoclimatol Palaeoecol* 271(1–2):117–129. doi:10.1016/j.palaeo.2008.10.003
- Köhler M (1993) Skeleton and habitat of recent and fossil ruminants. *Münchner Geowiss Abh* 25:87
- Kohn MJ (1996) Predicting animal $\delta^{18}\text{O}$: Accounting for diet and physiological adaptation. *Geochim Cosmochim Acta* 60(23):4811–4829. doi:10.1016/S0016-7037(96)00240-2
- Kohn MJ (2004) Comment: tooth enamel mineralization in ungulates: implications for recovering a primary isotopic time-series, by B. H. Passey and T. E. Cerling (2002). *Geochim Cosmochim Acta* 68(2): 403–405. doi:10.1016/S0016-7037(03)00443-5
- Kohn MJ, Schoeninger MJ, Valley JW (1996) Herbivore tooth oxygen isotope compositions: Effects of diet and physiology. *Geochim Cosmochim Acta* 60(20):3889–3896. doi:10.1016/0016-7037(96)00248-7
- Lee-Thorp J, Sponheimer M (2003) Three case studies used to reassess the reliability of fossil bone and enamel isotope signals for paleodietary studies. *J Anthropol Archaeol* 22(3):208–216. doi:10.1016/S0278-4165(03)00035-7
- Levin NE, Cerling TE, Passey BH, Harris JM, Ehleringer JR (2006) A stable isotope aridity index for terrestrial environments. *Proc Natl Acad Sci USA* 103(30):11201–11205. doi:10.1073/pnas.0604719103
- Lister AM (2013) The role of behaviour in adaptive morphological evolution of African proboscideans. *Nature* 500(7462):331–334. doi:10.1038/nature12275, <http://www.nature.com/nature/journal/v500/n7462/abs/nature12275.html#supplementary-information>
- Longinelli A (1984) Oxygen isotopes in mammal bone phosphate: A new tool for paleohydrological and paleoclimatological research? *Geochim Cosmochim Acta* 48(2):385–390. doi:10.1016/0016-7037(84)90259-X
- Luz B, Kolodny Y, Horowitz M (1984) Fractionation of oxygen isotopes between mammalian bone-phosphate and environmental drinking water. *Geochim Cosmochim Acta* 48(8):1689–1693. doi:10.1016/0016-7037(84)90338-7
- MacFadden B, Higgins P (2004) Ancient ecology of 15-million-year-old browsing mammals within C_3 plant communities from Panama. *Oecologia* 140(1):169–182. doi:10.1007/s00442-004-1571-x
- Macho GA, Leakey MG, Williamson DK, Jiang Y (2003) Palaeoenvironmental reconstruction: evidence for seasonality at Allia Bay, Kenya, at 3.9 million years. *Palaeogeogr Palaeoclimatol Palaeoecol* 199(1–2):17–30. doi:10.1016/S0031-0182(03)00483-8
- Made J van der (1996) Listriodontinae (Suidae, Mammalia), their evolution, systematics and distribution in time and space. *Contrib Tert Quatern Geo* 33:1–160
- Made J van der, Prieto J, Aiglstorfer M, Böhme M, Gross M (2014) Taxonomic study of the pigs (Suidae, Mammalia) from the late Middle Miocene of Gratkorn (Austria, Styria). In: Böhme M, Gross M, Prieto J (eds) The Sarmatian vertebrate locality Gratkorn,

- Styrian Basin. *Palaeobio Palaeoenv* 94(1). doi:10.1007/s12549-014-0152-1
- Maurer A-F, Galer SJG, Knipper C, Beierlein L, Nunn EV, Peters D, Tütken T, Alt KW, Schöne BR (2012) Bioavailable $^{87}\text{Sr}/^{86}\text{Sr}$ in different environmental samples — Effects of anthropogenic contamination and implications for isoscapes in past migration studies. *Sci Total Environ* 433:216–229. doi:10.1016/j.scitotenv.2012.06.046
- McArthur JM, Howarth RJ, Bailey TR (2001) Strontium isotope stratigraphy: LOWESS Version 3: best fit to the marine Sr-isotope curve for 0–509 Ma and accompanying lookup table for deriving numerical age. *J Geol* 109:155–170
- Merceron G (2009) The early Vallesian vertebrates of Atzelsdorf (Late Miocene, Austria) 13. Dental wear patterns of herbivorous ungulates as ecological indicators. *Ann Nat Hist Mus Wien* 111A: 647–660
- Merceron G, Schulz E, Kordos L, Kaiser TM (2007) Palaeoenvironment of *Dryopithecus brancai* at Rudabánya, Hungary: evidence from dental meso- and micro-wear analyses of large vegetarian mammals. *J Hum Evol* 53(4):331–349. doi:10.1016/j.jhevol.2007.04.008
- Merceron G, Costeur L, Maridet O, Ramdarshan A, Göhlich UB (2012) Multi-proxy approach detects heterogeneous habitats for primates during the Miocene climatic optimum in Central Europe. *J Hum Evol* 63(1):150–161. doi:10.1016/j.jhevol.2012.04.006
- Merceron G, Kostopoulos DS, Ld B, Fourel F, Koufos GD, Lécuyer C, Martineau F (2013) Stable isotope ecology of Miocene bovids from northern Greece and the ape/monkey turnover in the Balkans. *J Hum Evol* 65(2):185–198. doi:10.1016/j.jhevol.2013.05.003
- Nelson SV (2005) Paleoseasonality inferred from equid teeth and intra-tooth isotopic variability. *Palaeogeogr Palaeoclimatol Palaeoecol* 222(1–2):122–144. doi:10.1016/j.palaeo.2005.03.012
- Nelson SV (2007) Isotopic reconstructions of habitat change surrounding the extinction of *Sivapithecus*, a Miocene hominoid, in the Siwalik Group of Pakistan. *Palaeogeogr Palaeoclimatol Palaeoecol* 243(1–2):204–222. doi:10.1016/j.palaeo.2006.07.017
- Passey BH, Cerling TE (2002) Tooth enamel mineralization in ungulates: implications for recovering a primary isotopic time-series. *Geochim Cosmochim Acta* 66(18):3225–3234. doi:10.1016/S0016-7037(02)00933-X
- Passey BJ, Robinson TF, Ayliffe LK, Cerling TE, Sponheimer M, Dearing MD, Roeder BL, Ehleringer JR (2005) Carbon isotope fractionation between diet, breath CO_2 , and bioapatite in different mammals. *J Archaeol Sci* 32:1459–1470
- Passey BH, Ayliffe LK, Kaakinen A, Zhang Z, Eronen JT, Zhu Y, Zhou L, Cerling TE, Fortelius M (2009) Strengthened East Asian summer monsoons during a period of high-latitude warmth? Isotopic evidence from Mio-Pliocene fossil mammals and soil carbonates from northern China. *Earth Planet Sci Lett* 277(3–4):443–452. doi:10.1016/j.epsl.2008.11.008
- Porder S, Paytan A, Hadly EA (2003) Mapping the origin of faunal assemblages using strontium isotopes. *Paleobiology* 29(2):197–204. doi:10.1666/0094-8373(2003)029<0197:mt00fa>2.0.co;2
- Prieto J, Angelone C, Casanovas-Vilar I, Gross M, Hir J, van der Hoek Ostende L, Maul LC, Vasilyan D (2014) The small mammals from Gratkorn: an overview. In: Böhme M, Gross M, Prieto J (eds) The Sarmatian vertebrate locality Gratkorn, Styrian Basin. *Palaeobio Palaeoenv* 94(1). doi:10.1007/s12549-013-0147-3
- Rink WJ, Schwarcz HP (1995) Tests for diagenesis in tooth enamel: ESR dating signals and carbonate contents. *J Archaeol Sci* 22(2):251–255. doi:10.1006/jasc.1995.0026
- Rössner GE (2007) Family Tragulidae. In: Prothero DR, Foss SE (eds) *The evolution of artiodactyls*. The Johns Hopkins University Press, Baltimore, pp 213–220
- Rozanski K, Araguás-Araguás L, Gonfiantini R (1993) Isotopic patterns in modern global precipitation. *Climate change in continental isotopic records*. American Geophysical Union, In, pp 1–36. doi:10.1029/GM078p0001
- Smythe N (1986) Competition and resource partitioning in the guild of neotropical terrestrial frugivorous mammals. *Annu Rev Ecol Syst* 17:169–188
- Sponheimer M, Lee-Thorp J (2001) The oxygen isotope composition of mammalian enamel carbonate from Morea Estate, South Africa. *Oecologia* 126(2):153–157. doi:10.1007/s004420000498
- Thenius E (1950) Die tertiären Lagomeryciden und Cerviden der Steiermark. *Sitzungsber Österr Akad Wiss Math-Nat wiss Kl* 159:219–254
- Tipple BJ, Pagani M (2007) The early origins of terrestrial C_4 photosynthesis. *Annu Rev Earth Planet Sci* 35:435–461
- Tipple BJ, Meyers SR, Pagani M (2010) Carbon isotope ratio of Cenozoic CO_2 : A comparative evaluation of available geochemical proxies. *Paleoceanography* 25(3), PA3202. doi:10.1029/2009pa001851
- Trueman CN (2013) Chemical taphonomy of biomineralized tissues. *Palaeontology* 56(3):475–486. doi:10.1111/pala.12041
- Trueman CN, Behrensmeyer AK, Potts R, Tuross N (2006) High-resolution records of location and stratigraphic provenance from the rare earth element composition of fossil bones. *Geochim Cosmochim Acta* 70(17):4343–4355. doi:10.1016/j.gca.2006.06.1556
- Tütken T (2010) Die Isotopenanalyse fossiler Skelettreste – Bestimmung der Herkunft und Mobilität von Menschen und Tieren. In: Meller H, Alt KW (eds) *Anthropologie, Isotopie und DNA – biografische Annäherung an namenlose vorgeschichtliche Skelette*. Tagungsband 2. Mitteldeutscher Archäologentag, vol 3. Tagungen des Landesmuseums für Vorgeschichte, Halle, pp 33–51
- Tütken T (2011) 4. The diet of sauropod dinosaurs: implications of carbon isotope analysis on teeth, bones, and plants. In: Klein N, Remes K, Gee CT, Sander MP (eds) *Biology of the sauropod dinosaurs: understanding the life of giants*. Indiana University Press, Bloomington and Indianapolis, pp 57–79
- Tütken T, Vennemann T (2009) Stable isotope ecology of Miocene large mammals from Sandelzhausen, southern Germany. *Paläontol Z* 83(1):207–226. doi:10.1007/s12542-009-0011-y
- Tütken T, Vennemann TW, Janz H, Heizmann EPJ (2006) Palaeoenvironment and palaeoclimate of the Middle Miocene lake in the Steinheim basin, SW Germany: A reconstruction from C, O, and Sr isotopes of fossil remains. *Palaeogeogr Palaeoclimatol Palaeoecol* 241(3–4):457–491. doi:10.1016/j.palaeo.2006.04.007
- Tütken T, Vennemann TW, Pfretzschner H-U (2011) Nd and Sr isotope compositions in modern and fossil bones – Proxies for vertebrate provenance and taphonomy. *Geochim Cosmochim Acta* 75(20): 5951–5970. doi:10.1016/j.gca.2011.07.024
- Tütken T, Kaiser TM, Vennemann T, Merceron G (2013) Opportunistic feeding strategy for the earliest old world hypsodont equids: evidence from stable isotope and dental wear proxies. *PLoS ONE* 8(9): e74463
- Ungar PS, Scott JR, Curran SC, Dunsworth HM, Harcourt-Smith WEH, Lehmann T, Manthi FK, McNulty KP (2012) Early Neogene environments in East Africa: Evidence from dental microwear of tragulids. *Palaeogeogr Palaeoclimatol Palaeoecol* 342–343:84–96. doi:10.1016/j.palaeo.2012.05.005
- Urban MA, Nelson DM, Jiménez-Moreno G, Châteauneuf J-J, Pearson A, Hu FS (2010) Isotopic evidence of C_4 grasses in southwestern Europe during the Early Oligocene–Middle Miocene. *Geology* 38(12):1091–1094. doi:10.1130/g31117.1
- van Dam JA, Reichart GJ (2009) Oxygen and carbon isotope signatures in late Neogene horse teeth from Spain and application as temperature and seasonality proxies. *Palaeogeogr Palaeoclimatol Palaeoecol* 274(1–2):64–81. doi:10.1016/j.palaeo.2008.12.022
- Voerkelius S, Lorenz GD, Rummel S, Quélet CR, Heiss G, Baxter M, Brach-Papa C, Deters-Itzelsberger P, Hoelzl S, Hoogewerff J, Ponzevera E, Van Bockstaele M, Ueckermann H (2010)

- Strontium isotopic signatures of natural mineral waters, the reference to a simple geological map and its potential for authentication of food. *Food Chem* 118(4):933–940. doi:[10.1016/j.foodchem.2009.04.125](https://doi.org/10.1016/j.foodchem.2009.04.125)
- Yanes Y, Romanek CS, Delgado A, Brant HA, Noakes JE, Alonso MR, Ibáñez M (2009) Oxygen and carbon stable isotopes of modern land snail shells as environmental indicators from a low-latitude oceanic island. *Geochim Cosmochim Acta* 73(14):4077–4099. doi:[10.1016/j.gca.2009.04.021](https://doi.org/10.1016/j.gca.2009.04.021)
- Yapp CJ (1979) Oxygen and carbon isotope measurements of land snail shell carbonate. *Geochim Cosmochim Acta* 43(4):629–635. doi:[10.1016/0016-7037\(79\)90170-4](https://doi.org/10.1016/0016-7037(79)90170-4)
- Zin Maung Maung T, Takai M, Uno H, Wynn JG, Egi N, Tsubamoto T, Thaug H, Aung Naing S, Maung M, Nishimura T, Yoneda M (2011) Stable isotope analysis of the tooth enamel of Chaingzauk mammalian fauna (late Neogene, Myanmar) and its implication to paleoenvironment and paleogeography. *Palaeogeogr Palaeoclimatol Palaeoecol* 300(1–4):11–22. doi:[10.1016/j.palaeo.2010.11.016](https://doi.org/10.1016/j.palaeo.2010.11.016)

Curriculum Vitae

Name: Manuela Ottilie Aiglstorfer

Geburtsdaten: 10.11.1981 in Nördlingen

09/1988 – 07/1992 Grundschule Amerdingen

09/1992 – 06/2001 Theodor-Heuss-Gymnasium Nördlingen

Abschluss: Allgemeine Hochschulreife

10/2002 – 09/2008 Studium der Geologie und Paläontologie an der Ludwig-Maximilian Universität München

Studienschwerpunkte: Paläontologie, Sedimentologie, Fernerkundung

Diplomarbeit: The Upper Jurassic Metriorhynchidae at the Bayerische Staatssammlung für Paläontologie und Geologie

Diplomkartierung: Fazies-Kartierung im Toarcium der weiteren Umgebung von Mistelgau (Oberfranken)

11/2008-02/2009 Anstellung als wissenschaftliche Hilfskraft an der Technischen Universität

München und an der Bayerischen Staatssammlung für Paläontologie im

Rahmen von Drittmittelprojekten

02/2009-08/2009 freiberufliche Tätigkeit im Rahmen des LfU-Projektes

„Informationsoffensive oberflächennahe Geothermie 2008-

2011“ Geologische Karte von Bayern 1 : 25 000, Blatt 8228

Wildpoldsried

12/2010-04/2011 Neugestaltung und konzeptionelle Ausarbeitung der Ausstellungsräume der

Paläontologischen Sammlung der Universität Tübingen mit Schwerpunkt auf

Illustrationen und Beschilderung

12/2009-05/2014 Wissenschaftliche Mitarbeiterin (E13/2) in der Arbeitsgruppe Terrestrische

Paläoklimatologie am Senckenberg Center for Human Evolution and

Palaeoenvironment (HEP) Tübingen (Kooperation zwischen der Senckenberg

Gesellschaft für Naturforschung und der Eberhard Karls Universität Tübingen)

12/2009-05/2014 Promotion zum Thema „Herbivorous large mammals from the late Middle

Miocene Gratkorn locality (Styria, Austria) - Taxonomic Assignment and

Ecological Interpretation based on Stable Isotope Analyses ($\delta^{18}\text{O}_{\text{CO}_3}$, $\delta^{13}\text{C}$)”

an der Eberhard Karls Universität Tübingen